ORNL-3350
Special
FILE COPY
#305

OAK RIDGE NATIONAL LABORATORY 1962

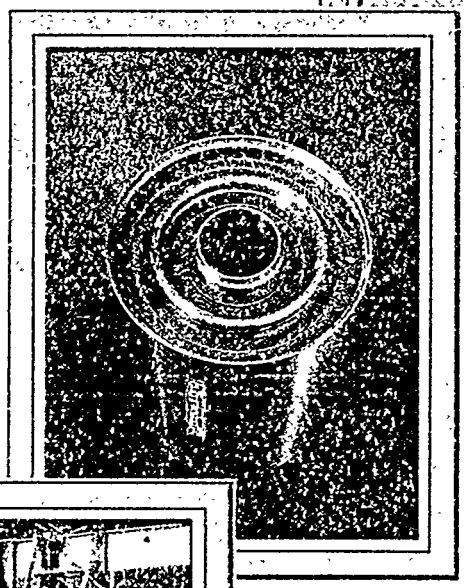

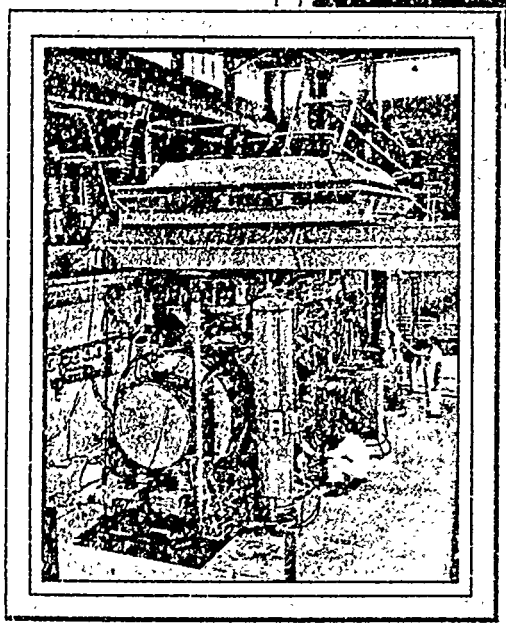

ChemRisk Document No. 305

OAK RIDGE NATIONAL LABORATORY
OPERATED BY UNION CARBIDE CORPORATION • FOR THE U.S. ATOMIC ENERGY COMMISSION

ABOUT THE COVER

Top: Antibody-synthesizing plasma cells in mitosis; part of a study linking protein synthesis with transfer of nuclear information.

Center: Fuel element for the High-Flux Isotope Reactor. The element, 24 inches long and 17 inches in diameter, contains two concentric rings of enriched-U^{235} fuel plates. The hollow center of the element can hold 31 target rods encasing heavy elements which will be bombarded by neutrons to produce research quantities of transplutonium isotopes – principally americium, curium, and californium. The HFIR will generate a thermal-neutron flux higher than that of any other reactor in the United States.

Bottom: The DCX-2 apparatus, in which a hot, dense plasma is generated by the injection and dissociation of 600-kev hydrogen molecular ions in a magnetic-mirror field. The molecular ions are given a long path length in the magnetic field, and the ion-pumping action of the plasma maintains the necessary vacuum.

OAK RIDGE NATIONAL LABORATORY

operated by

UNION CARBIDE CORPORATION

for the

U. S. ATOMIC ENERGY COMMISSION

LEGAL NOTICE

This report was prepared as an account of Government sponsored work. Neither the United States, nor the Commission, nor any person acting on behalf of the Commission:

A. Makes any warranty or representation, expressed or implied, with respect to the accuracy, completeness, or usefulness of the information contained in this report, or that the use of any information, apparatus, method, or process disclosed in this report may not infringe privately owned rights; or

B. Assumes any liabilities with respect to the use of, or for damages resulting from the use of any information, apparatus, method, or process disclosed in this report.

As used in the above, "person acting on behalf of the Commission" includes any employee or contractor of the Commission, or employee of such contractor, to the extent that such employee or contractor of the Commission, or employee of such contractor prepares, disseminates, or provides access to, any information pursuant to his employment or contract with the Commission, or his employment with such contractor.

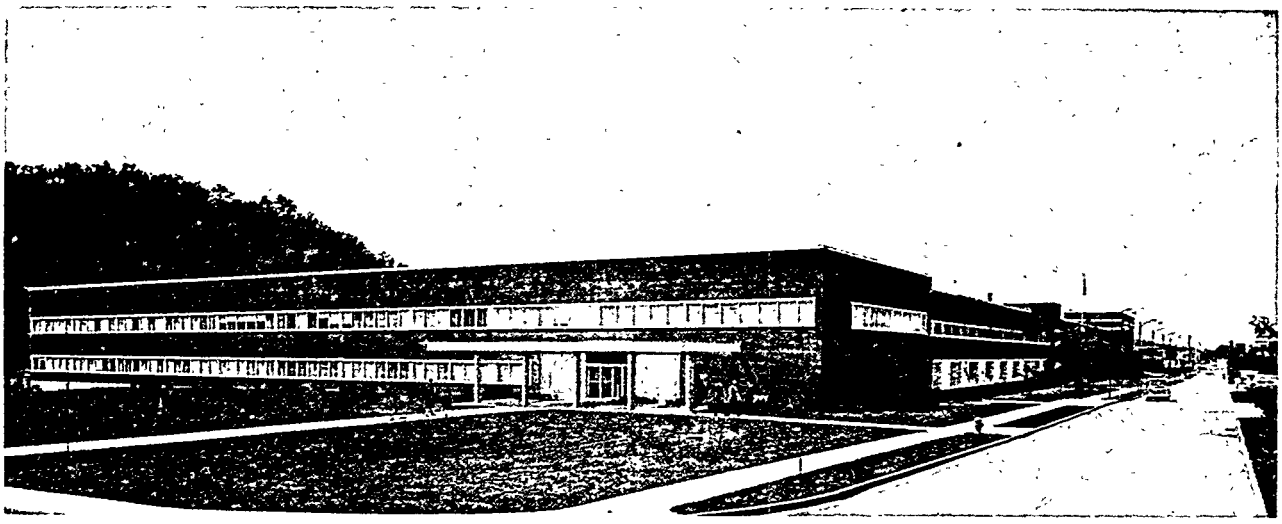

Central Research Building at Oak Ridge National Laboratory.

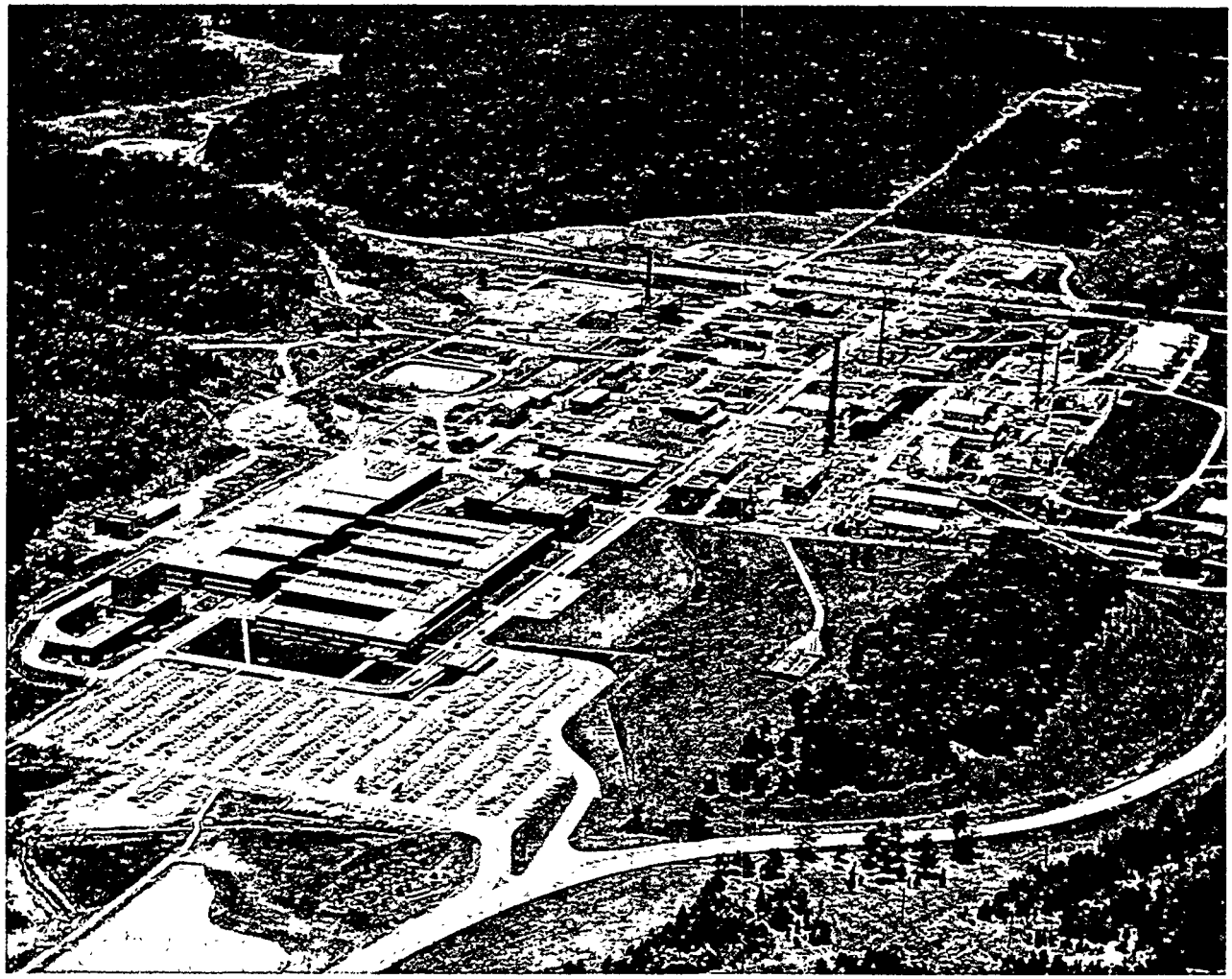

The X-10 Area, which contains most of the buildings of Oak Ridge National Laboratory.

Foreword

The Oak Ridge National Laboratory investigates science on so large a scale that no single document can do full justice to its many scientific and technical achievements. The work of Oak Ridge National Laboratory has therefore been mainly communicated to the scientific world through specialized, traditional channels such as scientific papers, divisional reports, and speeches. These means of communication are useful to the specialist who wishes to find out how Oak Ridge adds in detail to a scientific field, but they fail to convey certain essential qualities of science at Oak Ridge National Laboratory – its scale, its variety, and its professionalism. Moreover, they do not do full justice to the massive support given to our scientists and engineers by the devoted administrators, craftsmen, and service people at ORNL.

This report is the first of an annual series intended to present a global view of the Laboratory's achievements. I believe that the series of yearly summaries will eventually constitute a scientific and organizational history of ORNL that will be interesting to the general scientific public, as well as a source of pride to the members of the staff who have contributed so effectively to the activities of the Laboratory.

Alvin M. Weinberg

Alvin M. Weinberg

July 1, 1963

A Historical Note

Early in 1943, the Oak Ridge National Laboratory – then known as Clinton Laboratories – was organized under the University of Chicago Metallurgical Project. Its objectives were to develop a plutonium separation process for Hanford, to produce gram quantities of plutonium, to train people for operating the Hanford plutonium plant, and to evaluate the health hazards associated with radioactivity.

The original plant, which cost about $13,000,000, comprised unique facilities, including the first forced-air-cooled nuclear reactor ever built and special pilot-plant and research buildings and equipment. At the wartime peak 1515 people – most of them scientists, engineers, and highly skilled technicians – operated the Laboratory.

A. M. Weinberg, Laboratory Director

J. A. Swartout, Deputy Director

H. G. MacPherson, Associate Director

ASSISTANT DIRECTORS

G. E. Boyd
R. W. Johnson
W. H. Jordan
M. E. Ramsey
A. H. Snell

F. R. Bruce, Assistant Deputy Director

With the attainment of its early objectives and with the proven capabilities of its unique facilities, the Laboratory gained impetus to help it become one of the great nuclear research and development centers of the world.

In 1948 the Laboratory, in keeping with its new designation as a permanent national laboratory, was assigned a course of fundamental research and engineering development central to the reactor development program of the Atomic Energy Commission. Projects came to range from basic studies in physics, chemistry, metallurgy, and biology to reactor and chemical technology, isotope production, and health protection, and more recently to controlled thermonuclear research.

Chemical research and development activities at ORNL, which are centered around nuclear reactors, include all phases of nuclear energy technology from raw materials processing to the recovery of uranium from spent reactor fuel and the safe disposal of waste.

Major reactors being developed include the molten-salt-fueled and the gas-cooled. ORNL designed and built the forerunner of a number of pool-type research reactors. The Materials Testing Reactor, now in operation at the National Reactor Testing Station in Idaho, was also designed here. The High-Flux Isotope Reactor, which will produce a very large number of neutrons for the transmutation of elements, is now under construction at the Laboratory. In operation at ORNL, in addition to the Graphite Reactor constructed in 1943, are the Low-Intensity Testing Reactor, the original "Swimming Pool" Reactor, the Tower Shielding Facility, and the Oak Ridge Research Reactor.

Oak Ridge National Laboratory is the world's chief source of stable and radioactive isotopes. ORNL is also a nuclear education center for academic, industrial, and government representatives.

By 1962, the Laboratory had expanded until the value of the plant was set at $119,000,000, and about 4300 people were at work in the 24 research and service divisions.

PROGRAM	COST
04 REACTOR DEVELOPMENT	$34,960,000
05 PHYSICAL RESEARCH	22,948,000
06 BIOLOGY AND MEDICINE	6,957,000
08 ISOTOPE DEVELOPMENT	1,497,000

PROGRAM	COST
02 SPECIAL NUCLEAR MATERIALS	$465,000
07 TRAINING, EDUCATION, AND INFORMATION	364,000
TOTAL	$ 67,191,000

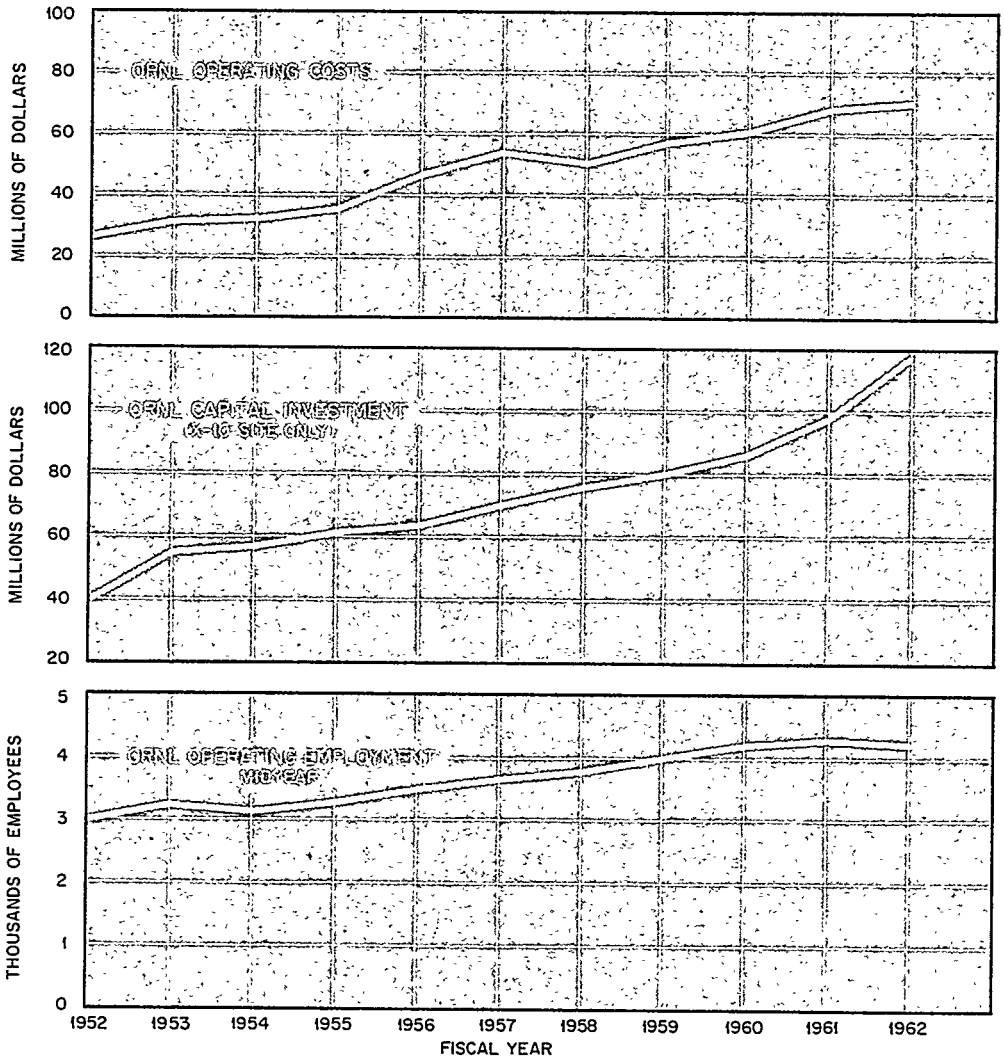

About This Report

This report is a summary of important goals and the progress toward them at Oak Ridge National Laboratory during fiscal year 1962. These activities touch on most areas of interest to the Atomic Energy Commission. They include reactor development, reactor fuel processing, radioactive waste disposal, physics, mathematics, chemistry, metallurgy, solid-state physics, controlled thermonuclear research, biology, medicine, health physics, training and education, and radioisotope and stable isotope research, development, and production.

Details of the work are not included here but may be obtained from the progress and topical reports issued by ORNL.

Contents

Foreword iv

A Historical Note v

About This Report vii

REACTOR DEVELOPMENT

Gas-Cooled Reactor Program 3
- Introduction 3
- Experimental Gas-Cooled Reactor 3
- Advanced Gas-Cooled Reactor Design and Analysis 13
- Pebble-Bed Reactor Experiment Design and Analysis 17
- Irradiation Experiments 21
- Reactor Materials and Components 24

Thorium Utilization Program 34
- Introduction 34
- Thorium Fuel-Cycle Development 35
- Thorium Reactor Evaluation 36
- Behavior of Thoria Pellets and Powders Under Irradiation 37
- Testing of Thoria-Suspension Fuels 37
- Homogeneous Reactor Experiment No. 2: Some Metallographic Results and Recovery of D_2O and Fuel 38
- Chemistry and Phase Relationships of Thoria-Urania Solid Fuels 39
- Properties of Flocculated Thoria Slurries at High Rates of Shear 39

Molten-Salt Reactor Program 40
- Introduction 40
- Design and Construction of the MSRE 40
- INOR-8, an Alloy Important to the MSRE 42
- Compatibility of the Molten-Salt Fuel and the Graphite Moderator 43
- Mechanical Components 43

Nuclear Safety Program 50
- Out-of-Pile Fission-Product Release 50
- In-Pile Fission-Product Release 50
- Characterization of Released Fission Products 50

High-Temperature Materials Development 51
- Corrosion of Metallic Components by Molten or Boiling Alkali Metals 51
- Oxidation of Columbium and Columbium-Base Alloys 52
- High-Temperature Evaporation of Metals in Vacuum 54
- Protective Atmospheres for Refractory Metals at High Temperatures 54
- Stability of Refractory Alloys During Service 54
- Joining of Refractory Metals by Brazing 55

Engineering Science: Heat Transfer 56
- Fundamental Heat Transfer and Fluid Mechanics 56
- Heat Transfer and Coolant Technology 58

High-Flux Isotope Reactor 64
Introduction 64
Project Status 64
Description of the HFIR 65
Experimental Program 72

Army Power Reactors 76
Dispersion-Fuel-Element Development 76
Control-Rod Development 80

Maritime Reactors Program 82
Pressurized-Water Reactor Chemistry 82
In-Place Testing of NS "Savannah" Iodine Adsorbers 83
NS "Savannah" Shield Evaluation 84

Nuclear Technology and General Support 87
Radiation Damage: Advanced Engineering and Development 87
Basic Reactor Physics 87
Radiation Shielding 93
Advanced Test Reactor Corrosion Program 100
Contributions of Metals and Ceramics Division to Reactor Development 100
Power Reactor Fuel Processing 101
Dissolver Solution Analysis 108
Polarography in Acidic Fluoride Systems 109
Absorption Spectrophotometric Studies of the Polymerization and Depolymerization of Quadrivalent Plutonium 109
Reactor Controls Development 110
Process Control 114

Waste Treatment and Disposal 115
Waste Treatment 115
Waste Disposal 120

PHYSICAL RESEARCH

Physics and Mathematics Research 131
Magnetic Properties of the Heavy Rare-Earth Metals 131
Proton Helicity Experiment 131
Superconducting Magnets 131
Theory of Nuclear Reactions 132
Stable Rare-Gas Organic Molecular Ions 132
Capture Cross Section of Tin Isotopes 133
Electronuclear Research 133
The Oak Ridge Isochronous Cyclotron 133
Studies of Nuclear Structure 135
Nucleon Tunneling 136
Studies of Direct Nuclear Reactions 138
ORNL Cyclotron Analogue 138
Superconductors for Magnets 138

Chemistry Research 141
Radiation Chemistry of Organic Materials: High Polymers 141
Quantitative DC Derivative Controlled-Potential Polarography 141
Spectrophotometric Study of Solutions at Elevated Temperatures and Pressures 142

Chronopotentiometry 143
Coulometric Instrumentation 143
Flame Spectrophotometer 143
Effects of Radiation on Analytical Methods 143
Molten-Salt Spectrophotometry 144
Nuclear Methods of Chemical Analysis 145
Solvent Extraction Research 145
Preparation of Research Materials 149
Radiation Effects on Catalysts 150
Cation Exchange at Ultrahigh Ionic Strength 150
Neutron Diffraction 150
A Precise Measurement of the Longitudinal Polarization of Beta Particles Following the Decay of Phosphorus-32 151
Capture-to-Fission Ratio in Uranium-233 for Epithermal Neutrons 152
Solutions of Metals in Molten Salts 152
The Differential Method for Measuring Isotope Effects 153
Separation of Nitrogen Isotopes 153
Effects of Reactor Radiations on Zircaloy-2 Corrosion in High-Temperature Aqueous Environments 153
Electrochemical Study of Zircaloy-2 Corrosion at Elevated Temperatures 154
Behavior of Molten-Salt Mixtures 155
Densities of Complex Fluorides 155
Crystal-Structure Determinations 156
Electrical Conductance of Aqueous Solutions at High Temperatures and Pressures 156
Phase Equilibria in High-Temperature Aqueous Systems 156
High-Temperature Acidity Measurements: U(VI) and Th(IV) Hydrolysis 157
Gas-Solubility Studies 157
Chemical Applications of Nuclear Explosions 157
Chemical Processing of Transuranium Elements 159

Metallurgy and Materials Research 162
Introduction 162
Support for Laboratory Programs 162
Research on Properties of Materials 162
Fabrication Research and Development 168
Evaluation of Properties of Materials 171
Compatibility of Materials and Environment 176
Fundamental Investigation of Radiation Effects in Solids 179

Controlled Thermonuclear Research 182
DCX-1 182
DCX-2 186
Radio-Frequency Heating 186
Plasma Physics and Other Research 186

Reactor Operations 190
Detection of Boiling in the ORR 190
Development of a Method for Annealing the ORNL Graphite Reactor 191
Training of Off-Site Personnel in Reactor Operations 192

BIOLOGY AND MEDICINE

Biology 195
Educational and Training Programs of the ORNL Biology Division, 1947–1961 195
Genetic and Cytogenetic Studies 195
Mammalian Cytogenetics 198
Genetic and Developmental Effects of Radiation in Mice 200
Studies of Late Somatic Effects of Radiation 202
Experimental Treatment of Radiation Injury and the Physiology of Blood-Forming Organs 203
Comparison of Ionizing Radiation and Radiomimetic Chemicals 204
Genetics and Physiology of Hemoglobin Synthesis 204
Radiation Microbiology 205
Function of the Cell Nucleus 206
Protein Synthesis 206
Nucleic Acid Research 208
Messenger RNA 208
The Primary Acts in Photosynthesis 208
New Genetic Strains of Photosynthetic Bacteria 209
Ultraviolet Studies 209
Electron-Spin and Nuclear Magnetic Resonance Studies 210
Auxin Actions on Cell Division and Expansion 211
Environmental Research 213
Radiation Ecology 213
Health Physics and Instrumentation 218
Contamination Control 218
Estimation of Internal Dose 218
Electron Interactions with Water Vapor 221
Simulated Fallout Area 224
Absorption and Reemission of Energy from Electrons Collectively Excited by Ionizing Radiation 224
Models for the Study of Radiation-Induced Cancers 224
Health Physics Research Reactor and the Japanese Dosimetry Problem 225
Basic Instrumentation: Research on Semiconductors as Detectors of Nuclear Particles 225
Electronics 226

ISOTOPE DEVELOPMENT PROGRAM

Uses of Radioisotopes in Analytical Chemistry 229
Neutron-Activation-Analysis Research 229
Fission Product Recovery 230
Isotopes Development Center 231
Introduction 231
Radioisotopes 232
Electromagnetic Separations 235

TRAINING AND EDUCATION PROGRAM

International Programs in Reactor Technology 241

Other Educational Programs 241
ASEE-AEC Basic Summer Institute 241
Summer Institute for Physics Teachers 242
Training Program for Reactor Safeguard Specialists 242

SERVICE AND OPERATING DIVISIONS

Engineering and Mechanical Services 245
Special Projects and New Developments 245

Inspection Engineering 254

Technical Information 255

Health Services 262

REACTOR DEVELOPMENT

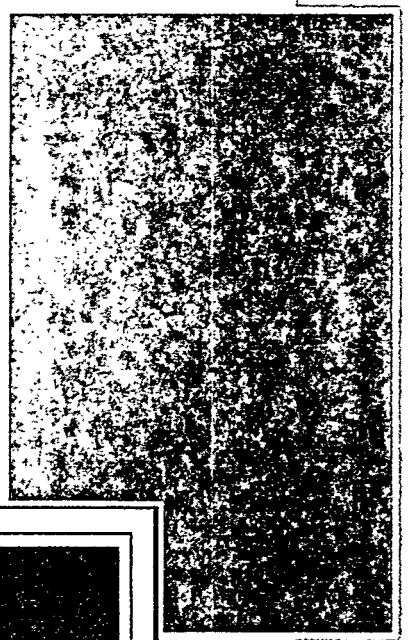

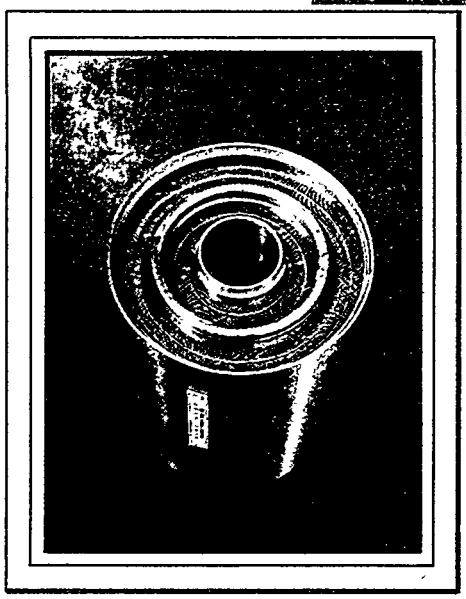

Gas-Cooled Reactor Program

INTRODUCTION

The gas-cooled reactor program involves work on three reactor types: the Experimental Gas-Cooled Reactor (EGCR), the advanced gas-cooled reactor, and the Pebble-Bed Reactor. Work on the EGCR consists of investigations in support of the design and construction of this power-producing facility on the Oak Ridge Area for the AEC by Allis-Chalmers Manufacturing Company and Kaiser Engineers. This helium-cooled, graphite-moderated, experimental reactor is to be fueled with enriched UO_2 clad with stainless steel and will have a net design electrical power output of approximately 25 Mw. The facility is to be operated by the Tennessee Valley Authority.

Design studies for the advanced gas-cooled reactor are based on the technology previously embodied in the GCR-2 study completed in 1958 as a design basis for the EGCR. The concept now being studied consists of a helium-cooled, graphite-moderated reactor (GCR-3) designed to use clad fuel and to have an electrical power output of 750 Mw.

General studies of the pebble-bed type of reactor have culminated in developmental work on a 5-Mw Pebble-Bed Reactor Experiment (PBRE). The unique feature of the pebble-bed reactor concept is the formation of the core from a bed of randomly packed spherical fuel elements. Graphite is used as the primary sphere material; the fissile and fertile materials are refractory compounds of low-cross-section elements, and helium is the coolant.

EXPERIMENTAL GAS-COOLED REACTOR

Core Physics

Physics analyses of the EGCR included specification of the fuel enrichment, analysis of reactivity worth of control rods, and determination of power distributions. Experimental confirmation of the physics analyses was obtained with the Hanford Physical Constants Test Reactor.

Existing techniques were improved and extended for these analyses. Methods for analyzing the fast effect, that is, fast fission in U^{238}, were extended to permit analysis of rod-bundle fuel elements. Previously accepted correlations of neutron temperature and moderator temperature and the treatment of the thermal-neutron spectrum in a reactor were modified and improved. A family of useful digital-computer programs for computing spectra and averaging cross sections was developed and utilized.

In connection with the hazards evaluation for the EGCR, the reactivity of the reactor was calculated in several abnormal situations, with the fuel having its maximum (i.e., initial) reactivity. In a postulated fuel-meltdown accident, the multiplication factor was calculated as a function of the height in the fuel channel over which the UO_2 was assumed to be distributed following melting of the stainless steel cladding and support spiders. The calculations showed that, if the stainless steel drained away completely, the core would probably be critical at room temperature, even with all control rods inserted. If the stainless steel were mixed with the UO_2, the reactor would be in the shutdown condition at room temperature with the control rods inserted. In both instances, the core would be supercritical without the control rods.

The effect of overheating of the core support plate might be to allow the plate to sag and the core to fall away from the control rods, which are supported from above. The multiplication factor was calculated as a function of the amount of sag, and it was found that approximately 3 feet of sag would be required before the core would be critical at room temperature.

Various calculations were performed in connection with planning for the commissioning program of the EGCR. These included calculations of fission-chamber response during initial core loading, source requirements, and effect of control-rod-drive speed on the feasibility of various reactivity measurements.

Fuel-Element Design and Fabrication

The fuel elements to be used in the EGCR were designed, and methods for their fabrication were specified and tested. The fuel assemblies for the EGCR consist of a seven-element cluster of UO_2 pellets clad with 0.020-inch-thick type 304 stainless steel. The cluster is supported within a 1-inch-thick graphite sleeve that has an outside diameter of 5 inches, an inside diameter of 3 inches, and a stacked length of 29 inches. The UO_2 pellets are 0.707 inch in outer diameter by 0.323 inch in inner diameter by 0.740 inch long. The hollow center in the pellets serves to reduce the central temperatures that would exist for solid pellets and to provide space for fission-gas buildup within the elements. The design lifetime of the elements is conservatively set at 10,000 Mwd per metric ton. The nominal peak operating temperature of the stainless steel cladding is about 1500°F.

The assemblies are being fabricated by Westinghouse Electric Corporation at a cost of $55 per kilogram of contained uranium metal. Fabrication of the UO_2 pellets is complete, and all other components are available. Procedures were reviewed and approved for the control of moisture content in the UO_2, welding and radiographic examination of end closures on the fuel elements, the welding of end caps to the spiders, and the copper brazing of mid-plane spacers to the fuel-element tubes. Approximately 25% of the fuel elements are loaded, and the assemblies are being constructed.

Operating plans for the EGCR require that four selected channels each contain a group of fuel assemblies that are mechanically joined together and that contain numerous thermocouples to monitor the temperatures of the fuel, cladding, coolant, and graphite sleeves. Fabrication techniques were therefore developed for installing swaged Chromel vs Alumel thermocouples on the inner surfaces of the fuel-element tubes. The thermocouples were held in place by a mandrel while being copper brazed to the inner surface. As many as four thermocouples were attached to a single capsule by this method. Several such capsules were prepared and successfully tested by irradiation in the ORR poolside facility and in GCR-ORR loop No. 1. The design of instrumental fuel assemblies was based on these studies. Each stringer or column is about 42 feet long and contains 17 thermocouples that will measure the temperature of the coolant, the fuel-element cladding, and the UO_2 central region. The top dummy assembly includes a venturi section to measure the channel flow. The instrumentation is arranged to provide data on the effective thermal conductivity of the fuel, heat transfer coefficient, and gas temperature asymmetries within the fuel-element cluster. The gas temperature, combined with the flow measurement, will give a heat balance for the instrumented channel.

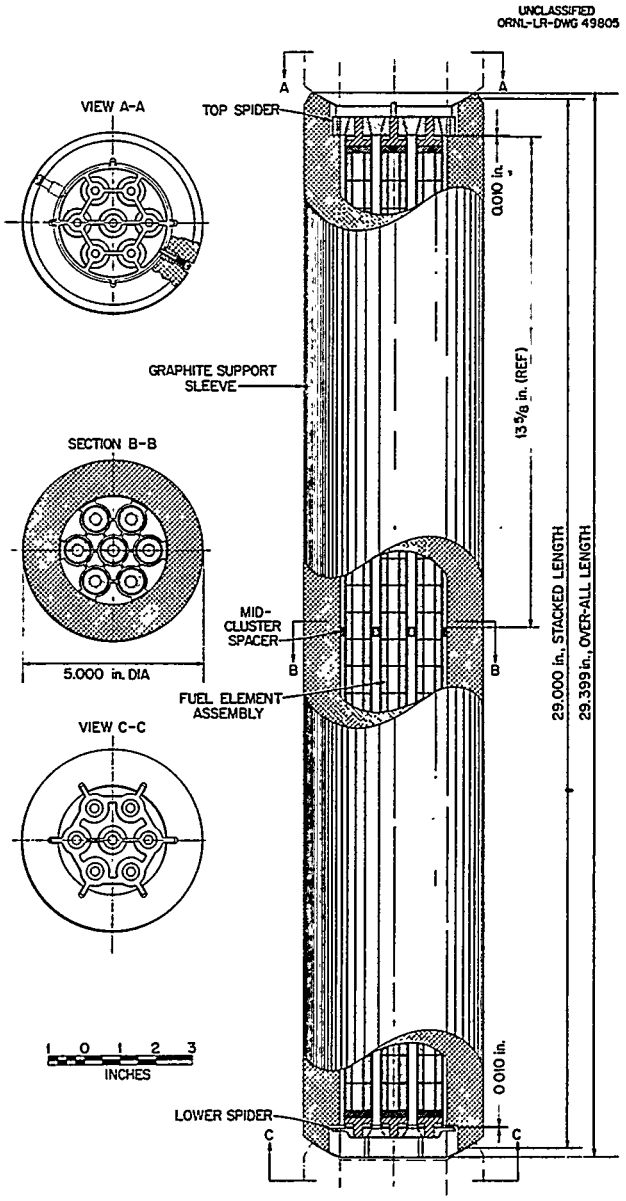

EGCR title II fuel-element assembly.

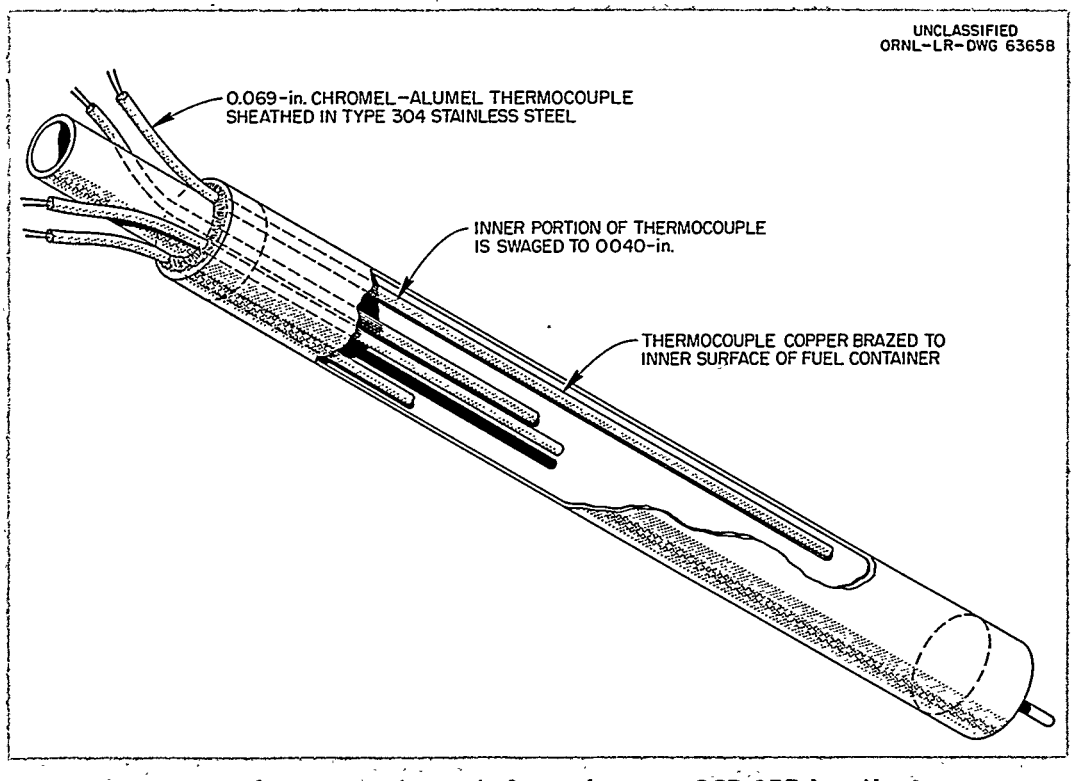

Diagram of instrumented capsule for irradiation in GCR-ORR loop No. 1.

The dimensional behavior of the fuel elements was investigated because differences in the mechanical properties of the cladding and the fuel pellets and the existence of the hollow center creates uncertainties in predictions. An apparatus was designed to simulate the thermal conditions during service, and was used for studying fuel elements both with a radial gap between the cladding and the fuel pellet and with the cladding collapsed onto the pellet by external pressure. An element that contained a radial gap between the cladding and the fuel pellet was found to respond to thermal cycling in the same manner that the individual components would react if subjected to the same thermal conditions and tested separately. When no radial gap existed between the fuel and the cladding, the behavior during thermal cycling was found to be a function of the fuel temperature, cladding temperature, and the external pressure. Under such conditions plastic axial strains were

UNCLASSIFIED
ORNL-LR-DWG 63653R

THERMOCOUPLE SCHEDULE		
TE NO.	FUEL SECTION NO.	LOCATION
1	3	GAS
2	3	GAS
3	3	CLAD ELEMENT, 3-1
4	3	CLAD ELEMENT, 3-2
5	3	CENTRAL ELEMENT, 3-2
6	3	CLAD ELEMENT, 3-2
7	5	GAS
8	3	GAS
9	5	GAS
10	4	CLAD ELEMENT, 4-5
11	3	GRAPHITE
12	4	CENTRAL ELEMENT, 4-5
13	4	CLAD ELEMENT, 4-5
14	3	GAS
15	3	GAS
16	VENTURI	GAS EXIT
17	VENTURI	GAS EXIT
18	SHIELD PLUG	CONCRETE

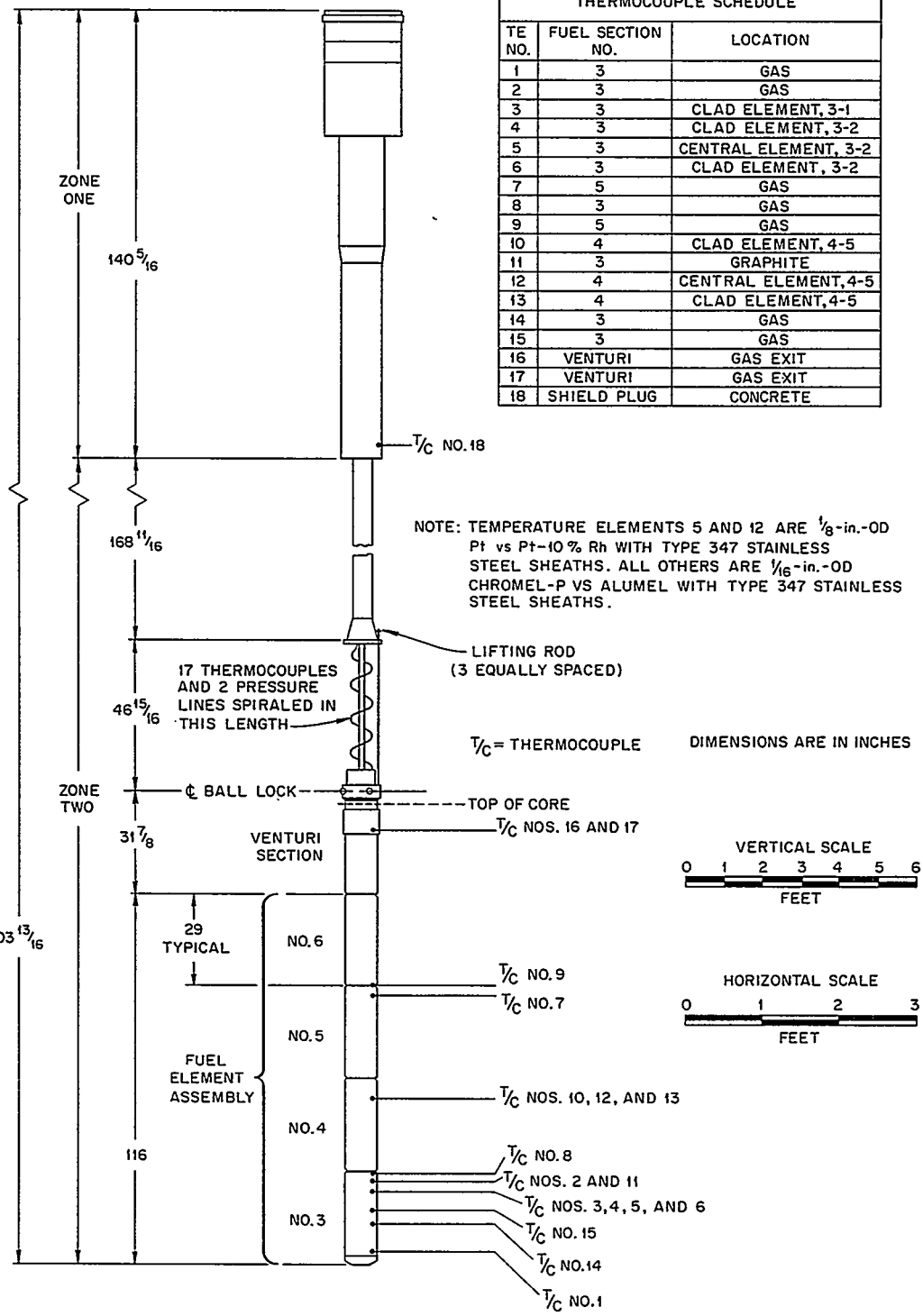

EGCR instrumented fuel assembly.

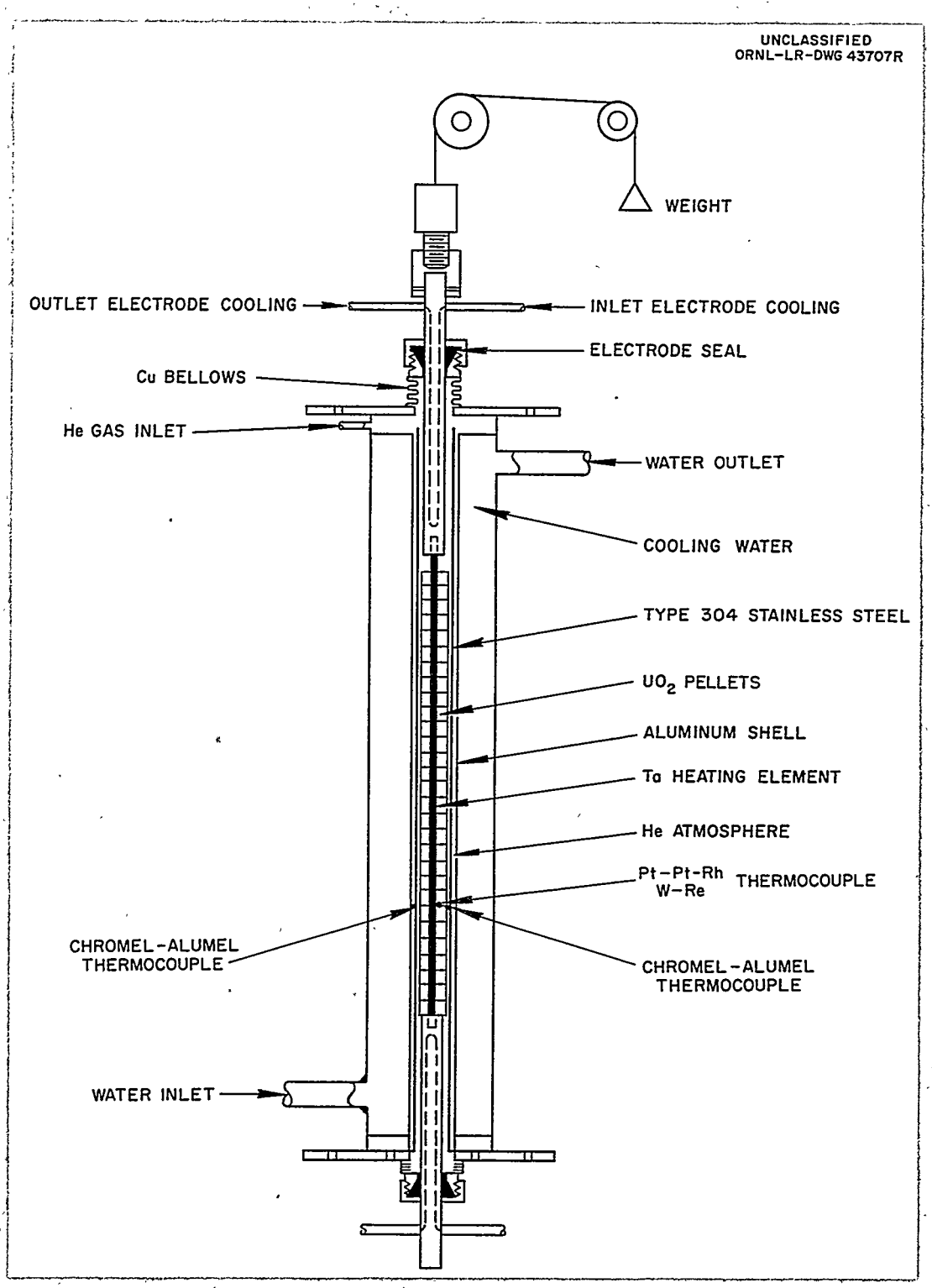

Apparatus for studying the dimensional stability and mechanical behavior of UO_2 pellets in a simulated EGCR fuel element.

induced in the cladding during cycling; therefore methods were developed for predicting the amount of strain for a given set of conditions.

During this extensive series of thermal cycling tests, severe deformations were induced in the cladding without a single failure, and fracture of the fuel pellets occurred without significant redistribution of the fuel. It was therefore predicted that the EGCR fuel elements will operate satisfactorily under the proposed service conditions.

Prototype EGCR fuel elements were irradiated to burnups of 1000 to 3000 Mwd per metric ton of uranium, and postirradiation examinations indicated good radiation stability. Although the hollow fuel pellets frequently cracked into more than four pieces, no significant fuel shifting occurred. Micrometer measurements of the fuel pellets and cladding showed no consistent dimensional changes other than collapse of the stainless steel cladding onto the fuel pellets in the higher temperature irradiations. Circumferential cladding ridges at UO_2 pellet-to-pellet interfaces appeared that were similar to those found after out-of-pile thermal cycling tests. Metallographic examination of these ridges showed the formation of voids and sigma-phase material as a result of the localized high-strain rates at elevated temperatures. Although small bits of UO_2 were embedded in the stainless steel in these areas, no reaction was apparent.

Fission-gas release during the irradiation of bulk UO_2 was found to be a function of UO_2 density, stoichiometry, and temperature. Significant quantities of impurities, such as carbon and nitrogen, are thought to have measurable effects also. No definite change in fission-gas release with increased burnup was observed up to 2 atomic percent uranium fission. For UO_2 meeting EGCR specifications, fission-gas release has varied from about 0.1% at 1700° F to about 10% at 3000° F. In EGCR prototype fuel-element tests, where the burnup was about 0.2 atomic percent U and the fuel temperature varied from about 1500° F at the outer surface to about 2500° F at the inner surface, approximately 1% of the fission gas was released from the UO_2.

Control-Rod Design

The design of the control rods for the EGCR was developed. The control rods are 20 feet long, $3\frac{1}{4}$ inches in outside diameter, and have an absorber length of 15 feet. The rods are made in 5-foot-long absorber segments that are supported by a central stainless steel rod. The central support rod is flexible enough to ensure entry of the control rod into the core even if the control-rod channels are not straight. Each of the 5-foot-long absorber segments is made up of annular rings of hot-pressed boron carbide, each 3 inches high. The boron carbide is encased in copper-plated stainless steel tubing. Each segment is vented to the primary coolant system through stainless steel filters. The design life of the rods is greater than 20 years. These rods are being procured from Dresser Industries.

Heat Transfer Analyses

Fuel Assembly Heat Transfer. – Heat transfer was examined in an apparatus consisting of two electrically heated full-scale fuel-element clusters. Circumferential surface temperature distributions were obtained as a function of axial distance for all seven tubes of the downstream cluster for the following conditions: (1) uniform heat generation, downstream cluster only; (2) downstream cluster only heated, with the central-tube power decreased by approximately 25%; (3) both clusters uniformly heated; and (4) both clusters heated, with the power in the central tubes decreased by approximately 25%.

For the condition of uniform heat generation in the downstream cluster only, typical temperature measurements indicated that, in the upstream half of the cluster, circumferential temperature variations of approximately 15° F exist around each of the six peripheral tubes, with the highest surface temperatures adjacent to the channel wall. In the downstream half of the cluster, however, the highest surface temperatures on the peripheral tubes were adjacent to the central tube. In this region the diametral temperature variations were approximately 10° F, decreasing with increasing distance from the midcluster spacer. Hence, it was conjectured that, given sufficient additional unobstructed channel, the profiles would again revert to the upstream pattern. Central tube profiles showed significantly less circumferential variation (a maximum of 3° F) than observed for the peripheral tubes; the influence of the spacer and spider ribs

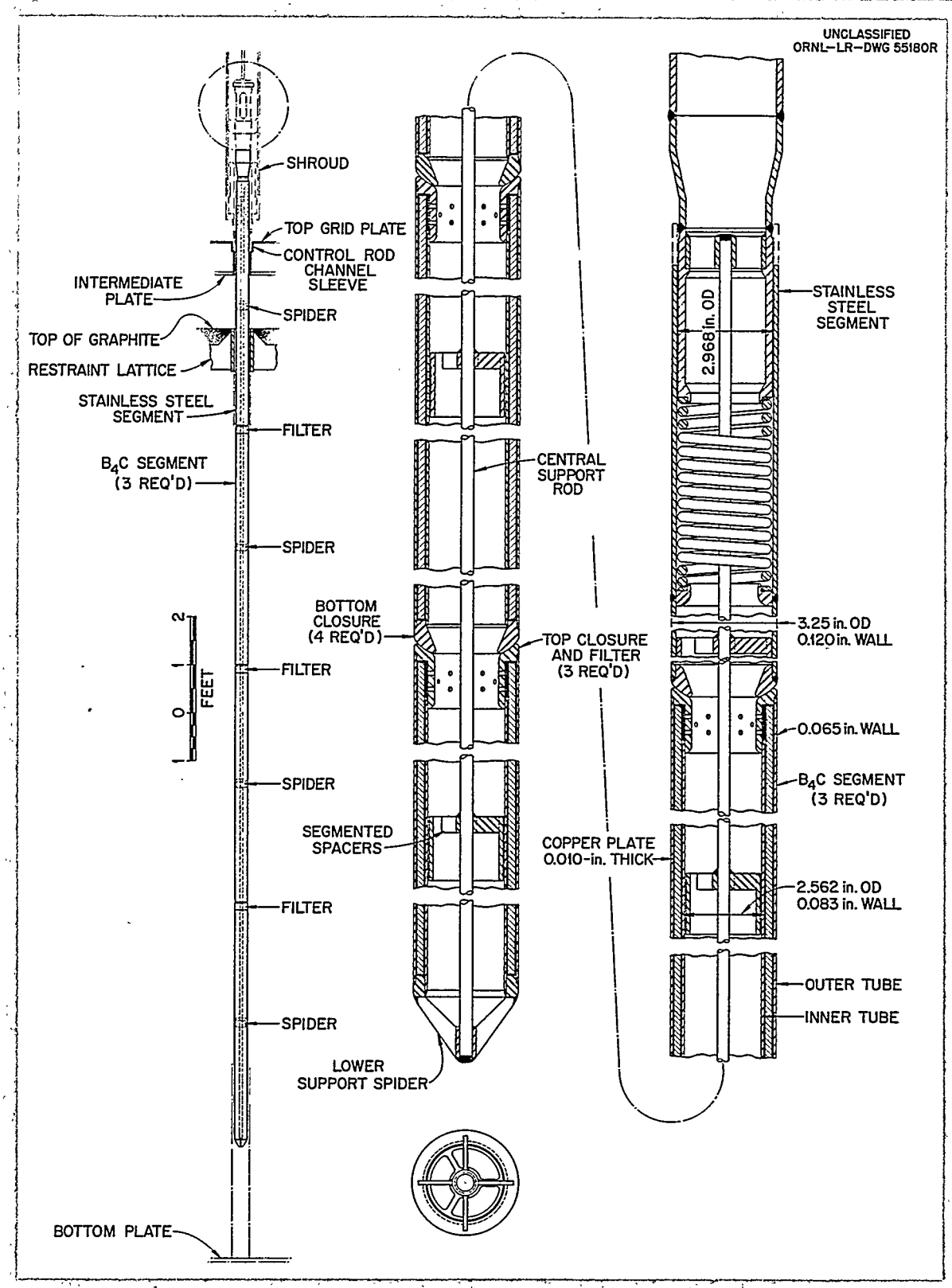

EGCR control rod.

was detectable. The gross thermal performance was similar for the two halves of the cluster.

With a 25% power reduction in the central tube of the downstream cluster (simulating the effects of self-shielding in the reactor), mean surface temperatures for the central tube were approximately 15% below those attained in the uniform power investigation, and the maximum circumferential temperature differences were 25% below the previously obtained values.

With both clusters uniformly heated, interpretation of the circumferential temperature profiles suggested that a form of "hot-streaking" existed, with the end spiders effecting (through mixing) little equalization in temperature of the gas flowing in the inner and outer flow regions of the channel.

The effect of reduced central-tube power on either the axial-mean or the circumferential temperature distributions was found to be small for both the one- and two-heated-cluster situations. The presence of the cooler central tube and decreased total heat input resulted in lower minimum surface temperatures.

Adjusted values of the Nusselt modulus at the exit end of the test cluster differed between experiments by less than 3%. No significant effect of nonuniform inlet gas temperature was observed. A comparison of these data with a correlation developed from earlier experiments showed a disagreement of less than 11%.

Velocity Profile in Fuel Assemblies. – The accumulation of data for delineating the velocity field in the downstream cluster of two seven-tube clusters as a function of relative cluster orientation was completed. The influence of spiders and cluster orientation was most noticeable just downstream of the cluster inlet. The effects of cluster orientation appeared to be negligible downstream of the midcluster spacer, the velocity distribution being controlled by the midcluster spacer configuration and the general cross-sectional geometry of the flow channel.

Pressure Drop Through Fuel Assemblies. – The contribution of the support spiders and midcluster spacers to the pressure loss in the EGCR fuel assemblies was studied. In the Reynolds modulus range of interest, these pressure-loss coefficients were found to be essentially constant: 0.43 for the spider pair and 0.34 for the midcluster spacer. These values were in agreement with calculated values.

The influence of "roughened" surfaces on the pressure loss was investigated. A 0.006-inch-diameter wire spirally wrapped at a pitch of 0.060 inch on all seven tubes constituted the roughness. It was observed that the Blasius friction factor at a Reynolds modulus of approximately 50,000 was about three times greater than the value associated with flow through smooth tubes and corresponded closely to the Nikuradse curve for surfaces having a tube-radius to roughness-height ratio of 15. In this experiment the roughness ratio, based on equivalent channel diameter and twice the wire diameter, was 50; thus the data fall significantly above predicted values. The pressure-loss coefficients associated with midcluster spacers and the end spiders were somewhat less than those previously observed in the smooth-tube experiments. It is suggested, in analogy with results for a single sphere with a tripping wire on its surface, that the wires influence the boundary-layer flow on the surface of the spiders and spacers sufficiently to effect early transition to the low-drag condition.

Flow Tests of Top and Bottom Dummy Fuel Assemblies. – Airflow tests were carried out on the EGCR top and bottom dummy fuel assemblies to determine flow distributions in their passages and to determine performance of associated fixed and variable orifices. Relatively inexpensive changes in size were recommended to permit the full range of gas flow distributions required.

Stress Analyses

Pressure Vessel. – An experimental stress analysis was made of the top head of the EGCR pressure vessel through the use of a strain-gaged aluminum model. The experimental results were correlated and were transformed into quantities applicable to the full-scale vessel. Methods were developed for obtaining complete stress distributions along a nozzle from the strain-gage data. Thus the maximum stresses in the nozzles caused by an internal pressure loading and by other design loadings were determined. Experimental results were compared with theoretical results to examine the applicability and accuracy of simple analytical models for use in predicting stresses.

The stress profiles along the nozzles were obtained for each separate loading so that the total

stresses could be determined for any combination of loads given by the design specifications. Experimental stresses in the spherical head were compared with nozzle stresses, and it was concluded that for a particular type of loading, the maximum stresses always occur in the nozzles. For certain combinations of localized and pressure loadings, the maximum stress may occur in the head; however, for critical design loadings this is not true.

Structural evaluation of the upper head of the vessel, including the nozzles, was made with procedures outlined in the Navy Code (*Tentative Structural Design Basis for Reactor Pressure Vessels and Directly Associated Components,* PB 151987, Dec. 1, 1958, revision, Department of Commerce, Office of Technical Services). On the basis of the available data, the entire design was found to be adequate.

A three-dimensional photoelastic model of the top head and adjacent cylindrical portion of the EGCR pressure vessel was also made and examined. The purpose of this study was to augment the strain-gage data and to provide detailed information regarding stress distributions throughout the head region. The photoelastic analysis thus provided data for making comparisons with the strain-gage results and the curves derived from them. Complete experimental distributions were obtained for the shell and thicker nozzles in the head. Time-edge effects and possible other factors adversely affected the results for the thin cluster nozzles, however, and precluded the use of the photoelastic data for these components. The data obtained verified the conclusions set forth in the strain-gage study regarding structural integrity of the prototype vessel. The most significant conclusion is that the maximum stresses are in the nozzles and that the design of the upper head of the pressure vessel is adequate for the design loading conditions.

Graphite Columns. — The IBM 7090 computing-machine program for calculating irradiation-induced stresses in graphite and thermal stresses in solid bodies was improved and modified so that it could be set up for routine analyses. Two-dimensional stress analyses can now be made for bodies with arbitrary temperature or irradiation-exposure distributions. As originally prepared, the program consisted of a series of separate codes that were run sequentially, with the use of each one being almost independent of the preceding code. The

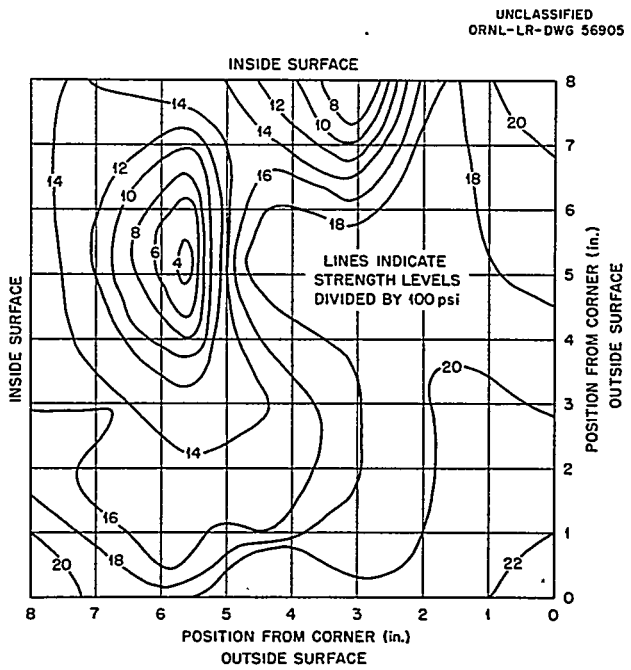

Variation of axial tensile strength across one quarter of an 18 × 18 in. block of AGOT graphite.

method employed for solving large-order systems of equations was based on taking an initial approximate solution and applying extrapolation and iteration techniques. The setup and computational time for a given problem was inordinately long. Programs for transposing and solving large systems of equations were therefore developed to replace the original method, and the individual codes were combined into one. The time required for solving a given problem was cut to about one-third with the reworked program. Difficult stress analysis problems can now be solved readily, and graphite geometry optimization studies for particular nuclear reactor applications are feasible.

The stress analysis code was consequently used to calculate the steady-state thermal stresses in an EGCR graphite column during fuel-handling operations. The column was assumed to be insulated around the outer periphery, while gas with an inlet temperature of 510°F flowed at the normal rate of 90 pounds per hour through three of the four channels. Gas was assumed to be flowing at a rate of 1400 pounds per hour through the fourth channel in which the fuel-handling operations were assumed to occur. Two gas inlet temperatures, 350 and 510°F, for this channel were used.

Despite the conservatism of the model from the heat transfer standpoint, the stresses for both cases were small and almost equal. The maximum stress for the 510°F inlet temperature case was approximately 150 psi. From these results it was concluded that the refueling operations will not affect the structural integrity of the columns, except possibly during the transient period when the flow rate is instantaneously increased from 90 to 1400 pounds per hour.

The graphite columns in the reactor will initially be under compressive loading, but after the reactor goes critical the columns will undergo radiation-induced shrinkage, and because of variations in neutron flux in the reactor, bending strains will be forced into the graphite columns. Specimens of AGOT graphite from three blocks were therefore examined, using incrementally loaded short-time tensile, short-time bending, and creep tests under compressive, tensile, and bending loads. The results showed that the mechanical properties of graphite are not affected by temperatures in the range 75 to 1100°F, and therefore the fracture stresses and strains are not temperature dependent. The fracture stresses calculated on the basis of elasticity theory for bending are greater than the experimental fracture stresses under tensile loads; however, the fracture strains are very similar. Some initial creep was detected, but the creep rate quickly decreased to less than 5×10^{-9} inch per inch per hour.

The mechanical properties vary widely, and the mechanical anisotropy is difficult to predict. It is apparent that the strength variation across the graphite block increases with the section size of the block. Because of the low ductility of graphite, it will not be expected to sustain the tensile strains produced by the variable radiation dose during reactor operation without fracturing. Fracturing may not occur, however, if the radiation-induced shrinkage is either inhibited or stopped by the occurrence of stress, or if the effects of radiation enable the graphite to sustain greater tensile strains before fracturing.

Through-Tubes for Experimental Loops. – The experimental loop through-tubes pass through the reactor coolant outlet plenum, the core region, and the bottom gas plenum. Consequently, they may be exposed to gas at 1200°F, since the reactor is to be capable of operating with this coolant outlet temperature. In order to establish the collapse characteristics of the tubes when subjected to external pressure at 1200°F, an experimental study is being conducted. The experiments include instantaneous and time-dependent collapse tests for obtaining correlations between pressure and time to collapse. The major portion of the work is being done on models, but specimens having dimensions near those of the reactor tubing are also being tested.

The dimensions chosen for the larger specimens are: outside diameters of 4.0 and 8.0 inches and wall thicknesses of 0.12 and 0.25 inch, respectively. The lengths of the through-tubes in the reactor are great enough to be considered infinite from the collapse standpoint. The specimen lengths were therefore chosen to obtain collapse behavior corresponding to tubes of infinite length.

A series of tests was completed on five 8.0-inch-outside-diameter units and five 4.0-inch-outside-diameter tubes. All the specimens were made of type 304 stainless steel, except two 4.0-inch-outside-diameter units made of type 347 stainless steel.

Results of the tests on the large specimens show that the initial out-of-roundness in commercial tubing plays an important role in establishing the collapse configuration. The tubes tested collapsed into shapes which exaggerated the original variations from a circular shape. In order to evaluate the effect of initial out-of-roundness analytically, a method was developed for predicting the instantaneous-collapse and creep-buckling characteristics of out-of-round tubes subjected to external pressure. The critical pressure and the deformation of a tube at the instant of impending collapse may be determined by this method. The analytical model was used to calculate the instantaneous and time-dependent collapse pressures for the 8.0-inch-outside-diameter specimens. The instantaneous-collapse pressures thus determined agreed closely with the experimental values, but the time-dependent collapse predictions were found to increase in conservatism with time.

Component Development and Testing

Control-Rod-Drive Mechanism. – A facility was constructed for performance-acceptance testing of the EGCR prototype control-rod-drive mechanism. Tests will be conducted in accordance with EGCR project specifications in a controlled helium

environment simulating reactor conditions of temperature, pressure, coolant flow, helium purity, and physical configuration of control-rod nozzle and core channel. Delivery of the prototype EGCR mechanism to ORNL for testing is expected in October 1962.

Blowers and Shaft Seals. – Studies were made of various problems involved in the construction and operation of the main blowers and vessel cooling compressors for the EGCR. The resolution of problems in fabricating, welding, and inspecting the casings received special emphasis. Procedures were developed that permitted the fabrication of the casings to proceed at a more rapid pace. Virtually all other parts of the EGCR blowers and vessel cooling compressors were completed. Modifications were made to the monitoring, control instrumentation, and seal water systems to improve reliability.

Dissimilar-Metal Joints. – Welding procedures were developed for joining type 304 stainless steel to ASTM A-387, grade D, steel and to ASTM A-212, grade B, carbon steel. Large ducts of these materials will be subjected to cyclic service in the EGCR, and joints between them will develop severe stresses because of differential thermal expansion. A newly developed commercial nickel-base welding rod (BP-85) was used in the development of the welding procedures. Extensive tests of large welded specimens showed that the joints will perform satisfactorily.

Methods were developed for fabricating the joints where the stainless steel burst-slug-detection tubes and stainless-steel-clad thermocouples penetrate the carbon steel pressure shell of the EGCR. Both types of penetrations require the welding of relatively thin-walled components to thicker members under very limited accessibility. Suitable joint designs were developed, and fabrication and inspection procecures were established in the construction of prototype demonstration assemblies. Conventional welding and brazing equipment and joining procedures were used throughout.

Experimental Loops. – The preliminary designs were prepared for two EGCR in-pile loops. The loops are designed for the irradiation of 1500-kilowatt fuel samples operating at a coolant pressure of 1000 psi and an outlet temperature of 1050° F. The loops are designed to operate with helium or carbon dioxide as the coolant. A preliminary design analysis was also made for a hydrogen-cooled loop. The analysis was based on a coolant pressure of 300 psi and for a 500-kilowatt fuel sample. The loop piping to be installed within the reactor biological shield was fabricated and was delivered to the EGCR site; the upper and lower reactor-vessel loop nozzles are nearing completion.

Mechanical joints suitable for use in the loops were procured and were subjected to tests at representative operating conditions. These joints feature a double seal with a high-pressure helium interspace to prevent any leakage of loop helium to the atmosphere. Four large commercial valves with various body and stem seal configurations are being tested at temperatures and pressures to which they would be exposed in the loop application. Seat and stem seal leakages are measured in these tests as a function of temperature and pressure cycles and during a program of open-close cycling.

A special loop-orifice configuration was tested. This orifice is required in the annulus between the through-tube and the moderator graphite support plate to control helium flow between the through-tube and the moderator graphite. Since theoretical prediction of the performance of this device was unreliable, a test on the actual geometry was required to prove that the device would operate satisfactorily.

A test was conducted to determine the appropriate hard-facing material for the journal bearing in the lower T section of the loop installation. This bearing must operate unlubricated in dry helium for the life of the reactor to accommodate differential thermal growth between the through-tube and the reactor pressure vessel. Candidate materials were tested in an environment simulating the reactor application, and a suitable material was chosen.

ADVANCED GAS-COOLED REACTOR DESIGN AND ANALYSIS

System Analysis

The economic gains that might be associated with foreseeable improvements in metal-clad and all-ceramic fuels, as well as reactor component performance, were studied. In connection with

these studies, preliminary designs were prepared for integrated core and steam-generator units based on a new type of axial-tube steam generator.

Machine codes were developed for studying steam generators with flow either parallel to or across the tubes. A parametric study made with the use of these codes indicated that the size and cost of steam generators for use with gas-cooled reactors could be reduced by increasing the gas system pressure and temperature. Steam power plants were found to be economically favorable in comparison with gas turbine plants for use with ceramic-fueled and -moderated gas-cooled reactor plants.

For high-temperature ceramic-fueled reactors – that is, fuel in a graphite or BeO matrix – analyses were made of the limiting power-density capabilities, the effect of graphite and BeO reflectors on core performance and on the neutron damage to pressure vessels, the effect of specific power on the neutron economy, the breeding potential of two-region and multiregion cores, and fuel cycle characteristics as a function of fuel composition for U^{235}-Th-U^{233} systems. An appraisal was made of fission-product poisoning as a function of fuel burnup and of the fraction of epithermal fissions.

GCR-3 Design

A design is being developed for a large-scale gas-cooled reactor power plant. The reactor is designated GCR-3 because it is an advanced concept that is an outgrowth of the GCR-2 design completed in 1958. It utilizes clad fuel, it is cooled with helium, and it has a design electrical power output of 750 Mw. The information obtained from the EGCR research and development program and the subsidiary design and component studies carried out during the past three years is being utilized as the basis for this advanced design. An attempt is being made in the design study to find the problem areas and to determine the ways in which operation of the EGCR can contribute to solution of the problems.

Following the current trend toward large turbine-generator units in conventional steam power plants, the size of the reference plant was selected to utilize a turbine with electrical output in the range 650 to 750 Mw. Subsequent cycle analyses showed that the GCR-3 is capable of a design net electrical power output of approximately 750 Mw from 2000 Mw of thermal energy. Preliminary design layouts of the reactor vessel and core are based on refueling the reactor after shutdown, but on-stream fueling will be considered.

Preliminary data for the GCR-3 design are presented below:

Reactor thermal power	1910 Mw
Net electrical power	766 Mw
Helium conditions	
Pressure	400 psia
Temperature	550–1150°F
Steam conditions	
Throttle pressure	2415 psia
Throttle temperature	950°F
Reheat temperature	1000°F
Feed-water temperature	450°F
Net thermal efficiency	40%

Preliminary designs were prepared of the core graphite, peripheral restraint system, and core support structure. The graphite is entirely replaceable; so irradiation-induced dimensional changes will not influence operation or change the useful lifetime of the reactor. The graphite moderator pieces may be replaced singly, and thus quasi-continuous replacement is possible. In order to obtain maximum useful lifetimes from the moderator graphite pieces, they may also be shifted from place to place within the core region. When the useful life of a moderator cylinder expires, the unit will be removed from the reactor and replaced.

The graphite stack is a right-circular cylinder with a diameter of 31 feet 9 inches and a height of 24 feet. This stack is designed to withstand seismic disturbances with maximum accelerations in horizontal and vertical directions equal to approximately 10 and 5%, respectively, of the acceleration from gravity. A peripheral restraint system is provided to bind the core into a stable structural unit during reactor operation, allow for removal of graphite pieces during reactor shutdowns, and transmit the seismic loads from the core to the pressure vessel. The major requirements of the core support structure are that it be rigid enough to carry the weight of the graphite stack and fuel elements without exceeding the allowable deflection, that it be proportioned so that the stresses will be low enough to avoid

the possibility of fracture because of brittleness resulting from neutron exposure of the steel, and that it not obstruct coolant gas flow to the fuel channels.

On the basis of a fast-neutron flux distribution for a single fuel channel producing power at a rate equal to the average in the GCR-3 core, a sleeve 0.75 inch thick, 4.94 inches in inside diameter, and 6.44 inches in outside diameter was tentatively chosen for the fuel element. The use of this sleeve yields maximum stresses in the moderator graphite that are approximately 30% of those that would exist in the graphite if the sleeve and block were built integrally. Thus the effective lifetime for the graphite may be increased by a factor of 3.

The moderator blocks are hexagonal cylinders with axial keys and slots machined on the outer surfaces. These keys and slots are used to interlock adjacent units and impart structural unity to the core. There is one channel through the center of each moderator block, and the channels are on a triangular pattern in the assembled graphite stack. The cylinders are 9.4 inches across the flats and 10 feet 6 inches long. The arrangement of moderator cylinders in the core eliminates continuous horizontal cutting planes through the core in an effort to obtain maximum stability against seismic forces.

The reflector region is made up of monolithic graphite columns 24 feet long, approximately 1.5 feet in radial thickness, and 2 feet wide. There is a row of solid hexagonal cylinders between the reflector columns and the moderator cylinders. The solid hexagonal cylinders are subject to large fast-neutron flux gradients at the edge of the core and serve to protect the reflector columns from induced bowing deformation. After a cylinder has received a specified exposure in one position, it

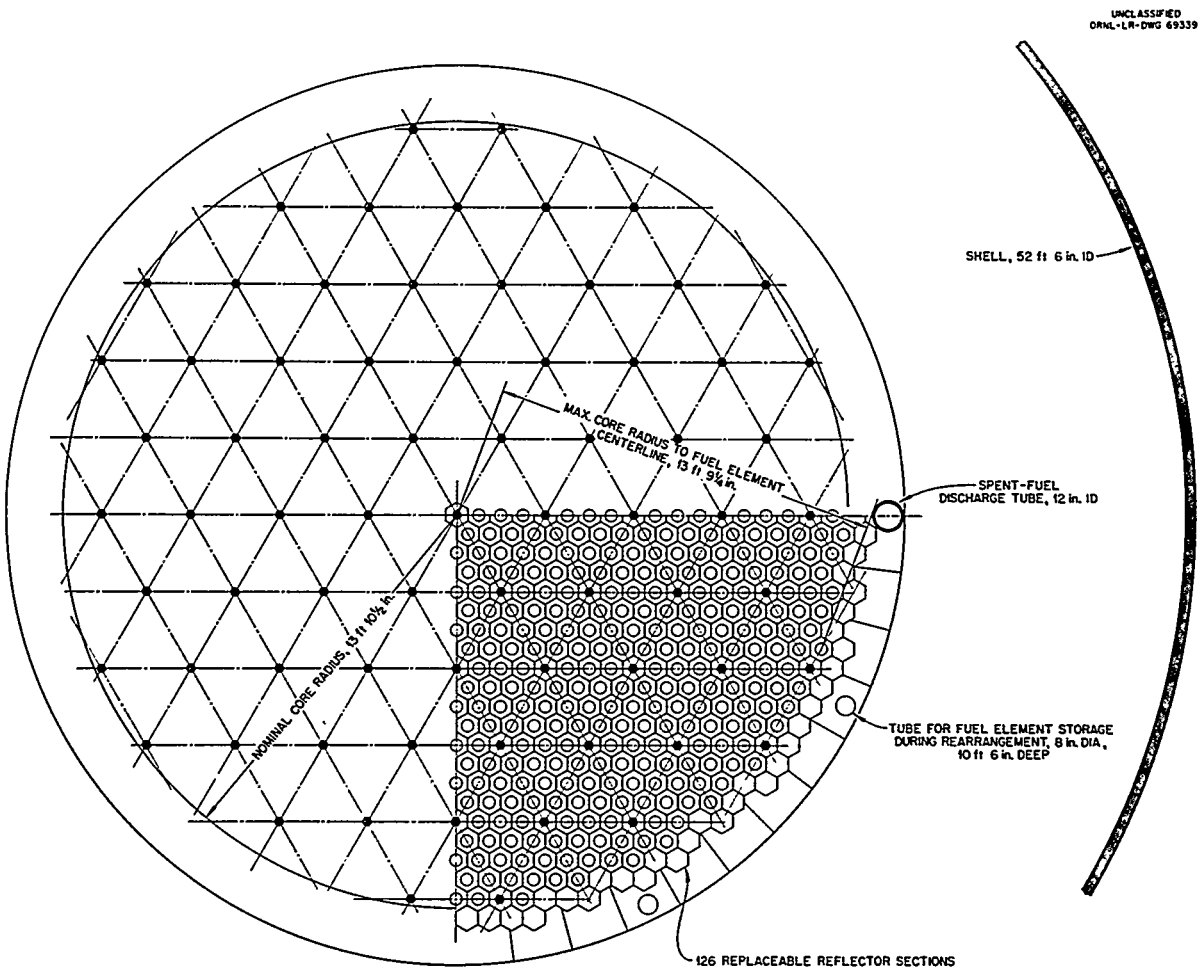

Horizontal cross section of GCR-3 core.

may be moved across the graphite stack, where the induced bowing strains will tend to reverse the previous deformation.

Several concepts for restraint bands were examined, and two were selected for further study. Both utilize the differences in thermal expansion between Invar and type 304 stainless steel to control the expansion of the bands as desired. One design is such that the circumference of the band will not change in going from room temperature to 1200°F. The other design gives a band that decreases in circumference as the temperature is increased. With either design the band offers no restraint at room temperature but becomes tight around the stack at operating temperatures.

The graphite stack rests on a segmented flat plate 2 inches thick that is mounted on a grid structure. Three sets of parallel beams are used for this grid structure to form a triangular pattern with openings matching the channels through the core. The grid members tentatively selected are made of type A212, grade B, carbon steel plates. The beams are 1.5 inches thick and 36 inches deep, and they are supported near the circular outer boundary of the structure by a short cylindrical skirt 170 inches in radius. The 1.5-inch-thick, 24-inch-high skirt transmits the weight of the core to the pressure vessel and supporting structure. This cylinder may also serve as a portion of the structure for separating the reactor inlet and outlet gases.

GCR-3 Physics

Calculations were made to determine the physics characteristics of the GCR-3 as a function of lattice parameters and fuel enrichment. The fuel element is a seven-rod cluster of UO_2 pellets, 0.97 inch in outside diameter and 0.74 inch in inside diameter, in stainless steel cans with an effective thickness of 0.016 inch. Fuel-cycle costs approach a minimum for a triangular lattice pitch of about $10\frac{1}{4}$ inches, but allowance for capital costs will undoubtedly result in a smaller pitch. With respect to fuel enrichment, no minimum was found for enrichments up to 4% U^{235}; however, the corresponding fuel exposures are very high (> 40,000 Mwd per metric ton). With exposures of about 25,000 Mwd per metric ton, fuel costs of around 1.6 mills/kwhr (electrical) appear possible, and the required enrichment does not exceed 3%.

Core lifetime and fuel-cycle cost analyses were made with beryllium substituted for the stainless steel cladding on the fuel elements. All factors relating to the thermal performance were assumed to remain the same; so the calculations were only approximate. Fuel fabrication cost, lattice pitch, and enrichment were chosen as variables. Lifetimes comparable to those for the steel-clad elements were obtained with fuel enrichments that were lower by approximately 1% (i.e., 1.5% instead of 2.5%). If there were no metallurgical limitation on the attainable exposure, the beryllium-clad elements could cost three or four times as much as steel-clad elements and yet have lower fuel-cycle costs. If the exposure were limited to 20,000 Mwd per metric ton of uranium, the fuel fabrication cost could not be as much as three times that of steel-clad elements.

The spatial distribution of the neutron flux in the 0.18- to 10-Mev range was calculated for the GCR-3 lattice cell, since it is believed that the dimensional changes in graphite which result from neutron irradiation are produced primarily by neutrons in this energy range. Compared with the analogous results for the EGCR, the fluxes are higher by approximately a factor of 3 because of the higher fuel ratings in the GCR-3; however, the larger channel diameter in the GCR-3 results in a somewhat fractional variation of the flux in the graphite. The average neutron flux above 0.18 Mev varies from 3.46×10^{13} neutrons cm^{-2} sec^{-1} at the inner surface of the fuel channel to 2.76×10^{13} neutrons cm^{-2} sec^{-1} at the outer surface of a cell column.

GCR-3 Fuel-Element Development

The fuel-element designs are based on a seven-element cluster of clad UO_2 pellets. The cluster is supported in a graphite sleeve, and the elements have roughened surfaces to improve their heat transfer characteristics. The possible use of the EGCR as a test bed for these elements is being studied.

Calculations are under way to examine the problems associated with a transition of the EGCR fuel loading from the design elements to the advanced clad elements of the GCR-3. The transition would begin with the testing of a few elements in the open core and would lead to operation with a full loading of GCR-3 type elements. Because of

the higher power per channel, the core would generate its full rated power of 84.3 Mw with fuel elements in only 72 of the 232 fuel channels.

PEBBLE-BED REACTOR EXPERIMENT DESIGN AND ANALYSIS

System-Design Studies

A preliminary design of a system for testing the concept of a reactor core formed from a bed of spherical fuel elements was developed. In such a reactor it will be relatively simple to refuel during operation at power. Fuel can be added by dropping elements on the top of the core and can be removed by permitting gravity flow through an opening at the bottom. The use of graphite as the fuel matrix and helium as the coolant will permit operation at high temperatures with good neutron economy.

The 5-Mw (thermal) PBRE is designed for investigating the thermal characteristics of the nuclearly heated bed of fueled-graphite balls and the performance of an on-stream fuel-handling system. The core will be a 2½-foot-diameter by 4-foot-tall cylinder containing approximately 12,000 fuel balls 1½ inches in diameter. Helium coolant at 500 psia will enter the steam generator at temperatures up to 1400° F, the present level of interest for power generation with a steam cycle. It will be possible, however, to operate the core with helium temperatures up to 2000° F, and perhaps higher, by mixing the hot gas with colder helium at the core exit. This procedure will permit use of the PBRE for testing core materials at conditions of interest for high-temperature process-heat applications.

Conceptual designs were made for the primary coolant pressure envelope and for the graphite reflector structure. The pressure envelope was selected to provide a reliable system requiring a minimum of research and development work and to minimize the number of auxiliary coolant systems required. The entire envelope is swept by the primary coolant gas at the core inlet temperature (550° F), thus allowing for the use of carbon steel and isolating the system from thermal transients caused by changes in reactor operating conditions. The system layout provides for maintenance of each component, and the system will withstand expected seismic loadings without suffering damage. The relative positions of the steam generator and reactor core were chosen on the basis of free-convection cooling requirements during emergency conditions.

The primary coolant system for the PBRE consists of the reactor vessel and steam generator connected by concentric ducts. Helium emerging from the top of the core flows through the central duct to the heat exchanger, passes through the heat exchanger, and then flows from the heat exchanger to the blower through long flexible piping. From the blower it passes back through the heat exchanger and through the annular region of the concentric ducts to the reactor. Inside the reactor vessel the cool helium passes downward between a liner and the vessel wall to again enter the core at the bottom.

A stainless steel shell (or liner) is used inside the pressure vessel to separate the cool return gas (550° F) from the hot gas (1250° F) leaving the reactor core. The liner surfaces exposed to hot gas are covered with reflective insulation. The

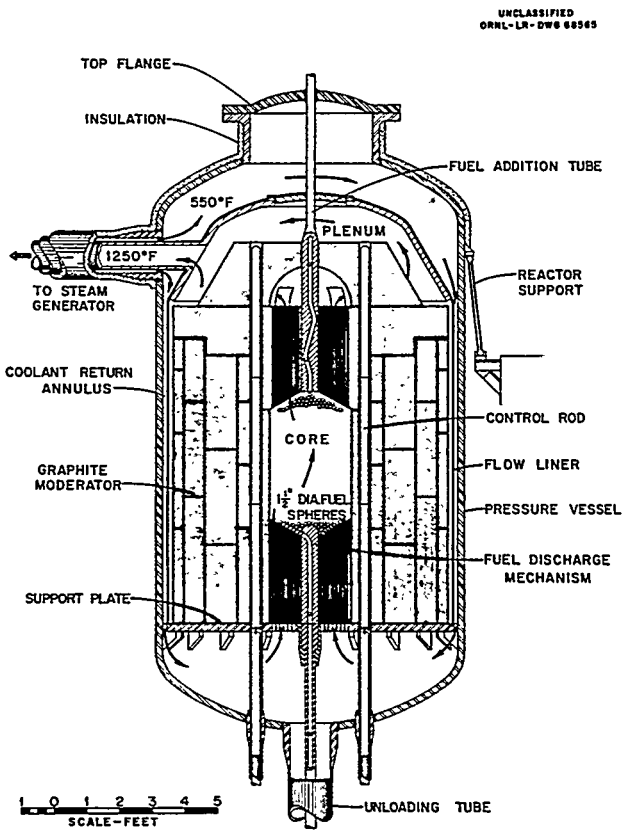

Cross-sectional view of PBRE.

flow distribution obtained by returning the cool gas into the plenum between the pressure vessel and the liner dome should provide uniform cooling for the support region and cylindrical sides of the vessel.

The pressure vessel, steam generator shell, and the outer member of the concentric ducts are carbon steel. The central member of the concentric ducts is stainless steel with 1 inch of reflective insulation on its inner surface. A slip joint will be used to accommodate the difference in axial thermal expansion of the two ducts. The differences in vertical displacements of the two ends of the inner duct will be accommodated by bellows joints.

The reactor pressure vessel is cylindrical, with torispherical heads. The concentric piping ties into the cylindrical portion of the vessel. One fuel-removal and four control-rod-drive nozzles are located in the bottom head. The top head of the vessel has a single large nozzle, and below it is a bolted opening in the metal liner; removal of both closures provides access to the core.

The pressure vessel is supported in a horizontal plane through the gas inlet nozzle by a structure similar to that used on the British AGR. Lugs on the vessel rest on flat-plate columns with cylindrical ends which, in turn, bear on structural members attached to the adjacent biological shielding. These columns can rotate to accommodate the radial expansion of the vessel. Lateral translation of the columns is prevented by side plates that restrain the cylindrical ends, and slippage on the bearing surfaces is prevented by a gear-tooth arrangement.

A flexible support system for the steam generator is provided to accommodate the lateral movements caused by thermal expansion of piping between the steam generator and the reactor vessel, the radial expansion of the pressure vessel, and the radial expansion of the steam generator. The support system consists of six beam columns sized so that only a small force is required for the necessary displacement. This support system has an advantage over more conventional systems in that no maintenance is required.

The fuel bed or core of the reactor is surrounded by a graphite reflector with a minimum reflector thickness of 3 feet. This results in a cylindrical graphite structure with an outside diameter of 8.5 feet and a height of 10 feet. The graphite regions immediately above and below the fuel cavity are designed with passages for coolant flow through the bed. An additional graphite structure is mounted on top of the reflector. This structure forms a cavity for collecting the hot gas from the core. Core exit gas flows from the cavity into the upper plenum by way of four passages through the graphite.

Shrinkage of graphite from fast-neutron irradiation will occur at the temperatures in the PBRE. Uneven shrinkage from flux gradients may result in severe stresses and possible cracking in the reflector. Consequently, provision is made for replacement of the graphite structure by passing blocks through the access nozzle at the top of the vessel. Therefore the dimensions of the pieces used to make up the reflector region are limited by the size of the top access nozzle.

Where applicable, the reactor pressure vessel was designed and evaluated in accordance with the ASME and Navy pressure vessels codes. The basic dimensions of the vessel were determined in accordance with the ASME code. The discontinuity stresses in the vicinity of the head-to-cylinder junction and in the nozzle attachment regions were then determined and evaluated in accordance with the Navy code. In addition, the combined effects of all stresses, including thermal, were evaluated in terms of resistance to fatigue.

An analysis of the stresses from vertical misalignment of the pressure vessel relative to the steam generator indicated that only a small amount of misalignment can be tolerated. The pressure vessel liner and the core support plate were also examined. The primary coolant gas on the outside of the liner will be at a higher pressure than the gas on the inside of the liner; therefore the resistance of the component to collapse from external pressure was of interest. Also, the effects of differential thermal expansion between the liner and core support plate were evaluated. The stresses in the perforated plate which supports the core and reflector were determined and assessed for normal operating conditions.

The pressure vessel support system consists of 11 vertical plates which act as columns to support the weight of the pressure vessel and its contents. The plates were designed with cognizance being taken of the critical load for the plates, the bearing-type contact stresses on the ends of the plates, and the maximum forces from seismic loads. In addition, the stresses induced in the pressure vessel from bending caused by

the upward thrust of the support plates were determined and evaluated.

The steam generator support system, which consists of beam columns with small moments of inertia corresponding to the desired direction of motion, allows the steam generator to move freely in a single horizontal direction and thus accommodate the thermal expansion in the system. In order to properly design a support system of the type proposed, relations between the axial load on each column, the critical axial load, the lateral load, and the relative lateral and axial displacements of the ends of a beam column must be known. These relations were developed and the support system was evaluated.

The rapid decay of the radial fast-neutron flux in the inner portion of the graphite reflector will produce significant differential radiation shrinkage in the reflector, and it is assumed that the induced strains will cause failure after some exposure interval. This interval depends on the graphite configuration and on the ability of the graphite to withstand deformation without rupture. In order to evaluate the possibility of using removable graphite sleeves for the inner portion of the reflector (immediately adjacent to the core), an anisotropic elastic analysis was used to calculate the shrinkage stresses and the associated strains in several cylindrical sleeves of various thicknesses. The average expected lifetimes of the cylinders before cracking were found to range from 25 weeks for a 12-inch-thick cylinder to 77 weeks weeks for a 2-inch-thick cylinder, based on properties for EGCR-type graphite and full-power operation. Solid sleeves have the advantage that radial gas leakage from the fuel bed is eliminated; however, lifetimes greater than those estimated for continuous cylinders are desirable. Therefore studies are being made of other geometric configurations in order to determine the best design of graphite bodies for the PBRE reflector, as measured by the calculated lifetime before cracking.

Since cylindrical graphite bodies with small diameters may be useful for reflector structures above the core of the pebble-bed reactor, the irradiation-induced stresses in solid cylinders were also studied. Equations were derived, and a closed-form solution was obtained for a cylinder subjected to irradiation exposure that varies only with distance along the axis of the cylinder. Thus another means for studying irradiation-induced stresses is available for use in graphite geometry studies.

Reactor-Physics Analyses

The effects of various factors on attainable fuel exposure and on fuel cycle costs were evaluated for large, high-temperature, homogeneous, graphite reactors. These included initial fuel composition, neutron leakage, recycle of discharged uranium, and possible variations in the basic cost factors employed in estimating fuel costs. The necessary data for computing the thermal-neutron spectrum as a function of position in the PBRE were assembled, and preliminary calculations were made. Temperature coefficients of reactivity and the power density distribution are being determined precisely.

Engineering Studies

Fuel-Bed Void Fraction and Velocity Distribution. – Data on the characteristics of spherical-particle packed beds were compiled. A preliminary evaluation indicated that the mean bed void fraction for the PBRE reference design core could be estimated only to within ±15% (0.375 ± 0.055). No data exist on the velocity distribution within beds, and the currently accepted procedure of traversing the exit face of a bed to obtain the velocity distribution contains some inherent shortcomings. A comparison of experimental and calculated velocity profiles shows a greater maximum-to-minimum velocity difference for the experimental results.

An extensive examination of the technical literature in regard to the pressure loss associated with flow through a randomly packed sphere bed indicated a lack of agreement as to the functional form of the dependence of the friction factor on the Reynolds modulus and the void fraction. A critical evaluation of the available data led to the conclusion that an empirical equation was adequate (±25%) for predicting the friction factor over the complete range of PBRE interest.

A full-scale model of the PBRE core region consisting of a Plexiglas vessel and unfueled graphite spheres was constructed. This mockup will be used to investigate such gross characteristics of the PBRE as average axial void distribution, exit-face velocity profiles, average axial and

radial turbulent diffusivities, and incipient-levitation velocity. Preliminary results for the void fraction (obtained by filling the model with known volumes of water and measuring the height attained) suggested a value of 0.395 for the average axial void fraction.

Fuel-Bed Thermal Structure. – A study of the local thermal structure in the interior of spaced-sphere beds was instituted. Because of its inherent simplicity, a mass-transfer technique using water-soluble benzoic acid spheres was selected. To provide a basis for interpreting later results for random beds and to establish the experimental procedure, initial experiments involved isolated spheres and single active spheres within regular packings. The isolated-sphere data were found to compare favorably with the results of other investigators on heat and mass transfer from single spheres; it was concluded that the technique of preparing spheres yielded reproducible surface properties and that the method of determining mass-transfer rates from dimensional changes was reliable. Preliminary measurements of the local variation in mass transfer from a sphere at the center of a cubic array yielded profiles which differed significantly from those observed for isolated spheres; a qualitative explanation based on reasonable conjectures as to the flow through a cubic array was advanced. It was established that the mass transfer was essentially zero at the contact points. An increase in the magnitude of the Sherwood modulus observed in the cubic-array experiment over that found with isolated spheres was ascribed to an increased turbulence level.

Fuel-Element Flow Through Core. – It is desired, if possible, to have a ball flow pattern through the PBRE core such that uniform burnup of fuel is achieved. The PBRE thermal flux is peaked near the reflector; so a slightly higher fuel-element velocity is desired at the periphery of the core. A plastic model of the PBRE core, scaled to simulate fuel elements with glass marbles, was operated. This model showed that flow down the cylindrical portion of the core was nearly pistonlike; however, movement of marbles at the periphery of the core was 15% slower than the overall average. A full-scale model equipped with a blower will be used to check the effect of operating at near-fluidized conditions on the fuel-element velocity distribution.

Fuel Handling

A system was developed for charging, discharging, and recycling fuel and inert balls. Mock-ups of portions of this system were constructed and operated.

A scale-model fuel-element-unloading machine satisfactorily removed $\frac{5}{8}$-inch glass marbles from a plastic model of the PBRE core. The discharge device is a rotating dome that protrudes into the conical bottom of the core. The rotating dome removes spheres symmetrically about the axis of the bed and collimates them for entry into the valve lock manifold.

Test valves that will serve as locks for passing balls between ambient pressures and reactor pressure are being procured for testing. The types of valves being considered are gate valves and ball valves.

From the discharge valve manifold, the balls roll by gravity to a fuel-element classifier. A model classifier, consisting of two rotating drums mounted at a small angle to each other, removed chips and classified marbles according to size. A unit of this type will be required in the fuel-handling system to remove chips and grossly chipped spheres and to separate small inert spheres from the fuel.

The classified fuel elements will need to be inspected for sphericity, cracks, and fuel burnup. Components and instruments for this service are undefined as yet. Fuel elements may then be stored in two noncritical helical trays, each having a storage capability of 12,000 fuel or inert elements. An unloading mechanism for removing spheres from such trays in single file was tested.

A pneumatic lift of the type proposed for transferring fuel elements from the storage system to the valve locks above the core was tested successfully. The ability to cushion a ball falling in a vertical pipe by passing air up the pipe was demonstrated. There are several places in the PBRE where cushioning will be necessary to prevent damage to the fuel elements.

A ball counter was developed that will monitor the movement of fuel elements through a pipe. No penetration into the system is necessary, since the unit consists of a differential transformer wound around the pipe, an oscillator-amplifier, and an electronic counter.

Fission-Product Transport and Deposition. – An experimental program was initiated for studying

fission-product deposition problems in gas-cooled reactors. Irradiated fuel samples were annealed in an out-of-pile furnace, and the fission products released were analyzed. For specimen temperatures up to 2000°C the following species were released: Ba^{140}, Te^{132}, Zr^{95}, Cs^{137}, Ru^{103}, Sr^{89}, I^{131}, and Nd^{147}. Samples of different materials with surface conditions typically found in reactors were inserted into several fuel irradiation sweep capsules in order to study the affinity of fission products for various surfaces.

Graphite Oxidation and Mass Transfer. – A loop for studying the mechanisms of graphite oxidation and mass transport was assembled and put into operation. This loop will accommodate graphite specimens of the size of PBRE fuel balls that can be heated to 2000°F and exposed to helium of varying degrees of impurity. A cooler is provided in which carbon mass-transport experiments can be carried out.

IRRADIATION EXPERIMENTS

Capsule Irradiations in LITR, MTR, ETR, and ORR

Fuel-capsule irradiations were carried out in support of EGCR and advanced fuel-element design studies. Beryllium-clad uranium dioxide pellets and all-ceramic fuels were irradiated. Equipment modifications were made that included installation of thermocouples at the center of hollow fuel pellets in EGCR prototype-size capsules, testing of thermocouples attached to the inner surface of stainless-steel-clad elements, and improvement of facilities for the continuous sweep of fission gases to sampling stations. Equipment was developed for adjusting the position of ORR poolside capsules to vary the neutron flux as desired. Cadmium shutters were provided for thermal cycling. External pressurization of the fuel element up to 850 psi was provided, along with a periodic helium sweep to observe cladding failures. Twelve capsules were irradiated in the LITR (Low Intensity Test Reactor), 20 in the ORR (Oak Ridge Research Reactor), and 14 in the ETR (Engineering Test Reactor). Some of the capsules are undergoing long-term irradiation. Four fueled-graphite assemblies were irradiated at the MTR (Materials Testing Reactor).

Irradiated specimens were examined at the General Electric Company's Vallecitos Laboratory and in hot cells at ORNL. Dimensional measurements, density determinations, burnup calculations and analyses, gamma scans, and metallographic examinations of fuel and capsule material provided

ORR poolside irradiation facility.

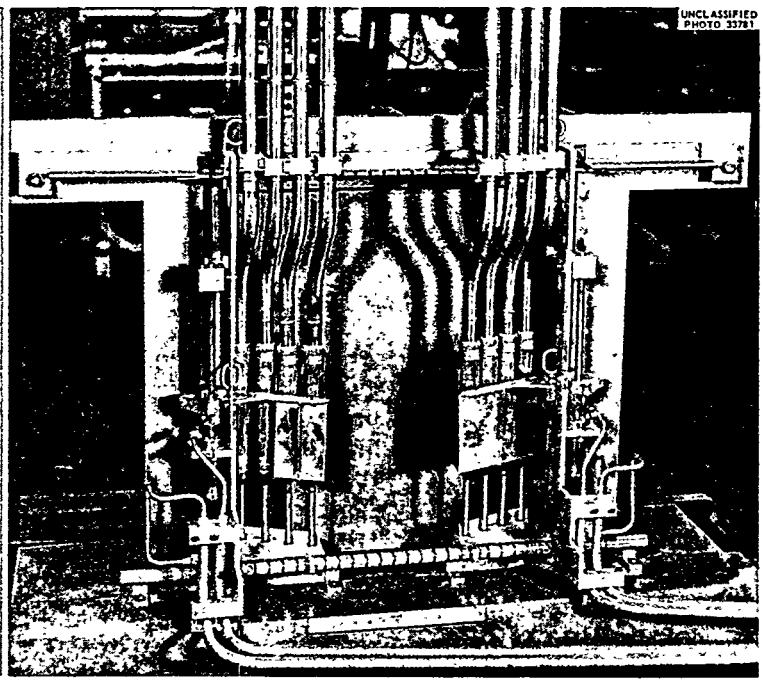

data of importance in reactor design. Fission-gas-release experiments provided information on pressure buildup in clad fuel elements and on contamination of coolants in systems with unclad ceramic fuel elements.

Fuel-Element Irradiations in Gas-Cooled ORR In-Pile Loop No. 1

Construction of gas-cooled ORR in-pile loop No. 1 was completed. This loop accommodates a single clad fuel element up to 18 inches long and 1 inch in diameter. Helium at 300 psi and at temperatures up to 1400°F is used as the coolant, but carbon dioxide can be used at lower temperatures if desired. There is complete double containment of the loop, and it can be decontaminated. Therefore tests can be run at near-failure conditions; however, operation with fission-product contaminants in the coolant is not anticipated. Fuel elements with heat ratings up to 70,000 Btu hr^{-1} ft^{-1} can be accommodated. Performance has exceeded the design requirements in all respects.

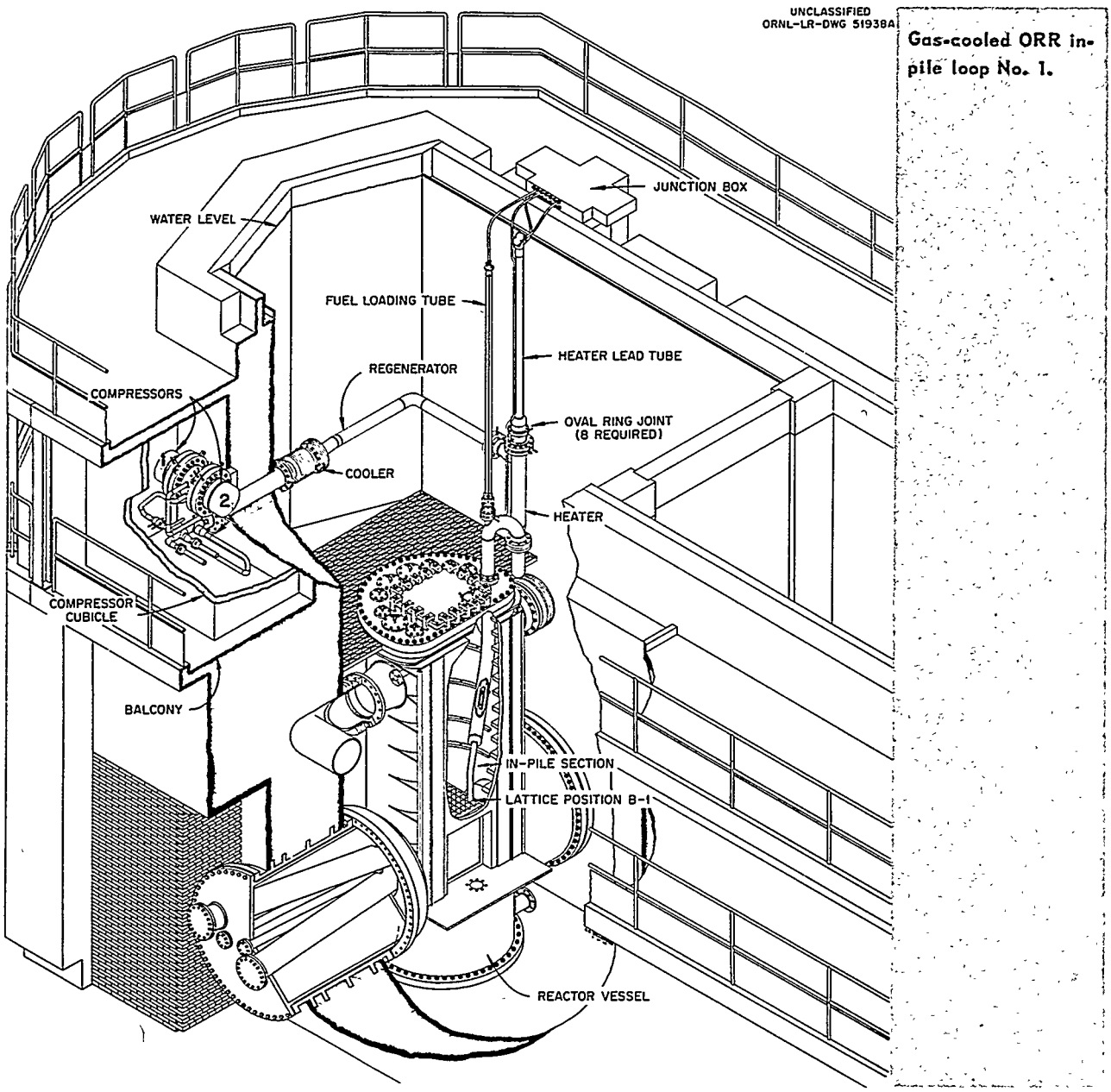

Gas-cooled ORR in-pile loop No. 1.

UNCLASSIFIED
ORNL-LR-DWG-52934-B

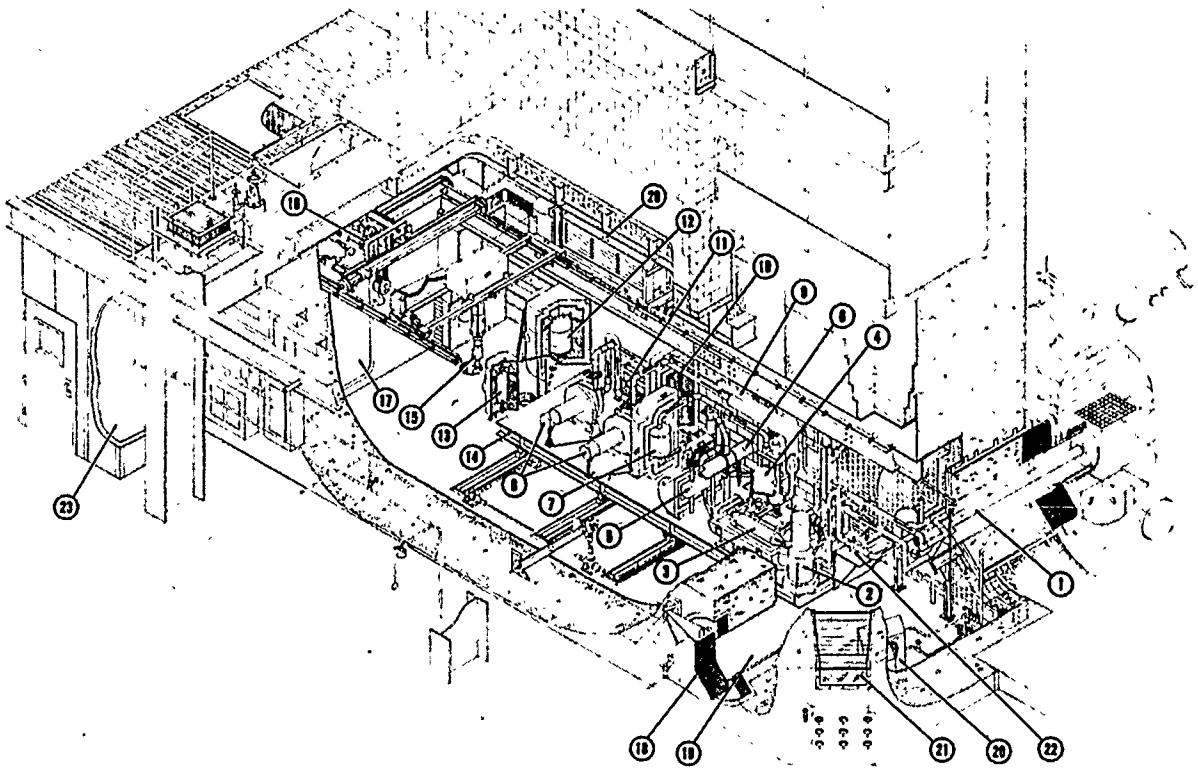

1. FUEL TEST TUBE
2. HEATER
3. REGENERATER
4. EVAPORATOR BY-PASS VALVE
5. EVAPORATOR
6. CONDENSER
7. FILTER
8. COMPRESSORS
9. SHELL COOLANT STREAM
10. CuO BED
11. SIDE STREAM COOLER
12. SIDE STREAM CARBON TRAP
13. MOLECULAR SIEVE
14. MOVABLE RACK
15. REMOTE MANIPULATOR
16. 5-TON CRANE
17. PERSONNEL ACCESS DOOR
18. EXTERNAL SHIELD DOOR
19. TEST PLUG REMOVAL SLEEVE
20. SPACE COOLERS
21. VIEWING WINDOW
22. MARMON SEAL FLANGE
23. AIR LOCK

Gas-cooled ORR in-pile loop No. 2.

Helium leakage was a problem initially, but this has been corrected.

The current test program involves evaluation of EGCR fuel elements of the type to be utilized in instrumented fuel assemblies. In these elements, sheathed thermocouples are attached to the inner surface of the fuel cladding and are installed in the center of the hollow uranium dioxide pellets to measure the maximum temperature of the uranium dioxide. Three elements have been irradiated. In addition, two sets of Charpy V-notch impact and tensile-test specimens of EGCR pressure-vessel steel and weld metal were exposed to a fast-neutron dose of about 10^{20} neutrons/cm^2 during loop shakedown operations. These specimens and the irradiated fuel elements are being examined.

Design and Construction of Gas-Cooled ORR In-Pile Loop No. 2

A facility is being constructed for development testing of unclad fuel elements. It will be used to study fuel-element stability, characteristics of fission-product release and deposition, purification of the coolant, engineering problems of a fission-product-laden, high-temperature, helium-circulating system, and decontamination and maintenance of system hardware. The facility consists of a shielded airtight cell adjacent to the large HS beam hole of the ORR. This cell contains a circulating-gas system in which representative unclad fuel elements may be exposed to radiation while being maintained within the range of typical reactor operating conditions.

Construction of the facility is nearly complete, and instruments and equipment are being tested. The main loop components, including the in-pile piping section, were tested out-of-pile in a component-testing loop to obtain information on heat exchanger performance, pressure drops, and other operating characteristics. The loop was analyzed on the analog computer, and various normal and abnormal operating and control situations were investigated. Parts are being fabricated for the first experiment, in which the operation of the loop will be calibrated at fission powers of a few watts. The second experiment, in which PBRE-type fueled graphite spheres are to be tested, is being designed.

Filters proposed for use in the main gas stream were tested, as-received and after representative thermal cycling, to determine filtering efficiency and pressure drop. A special check valve for the loop was performance-tested, and tests were run on the compressor to determine its resistance to gas flow when inoperative with the impeller both stalled and free to rotate.

REACTOR MATERIALS AND COMPONENTS

Coated-Particle Fuel Elements

Pyrolytic-carbon-coated uranium carbide and uranium-thorium carbide particles were evaluated as fuel materials for helium-cooled reactors. Metallographic techniques were developed for examination of such particles and examination of graphite-matrix fuel elements containing coated particles. In general, the particles evaluated met a preliminary requirement for surface contamination of less than 0.005% of the contained fuel. Leaching with 8 *M* nitric acid only reduced the exposed fuel, as determined by alpha counting, while thermal cycling to 1500°C usually caused an increase in the leachable fuel and surface contamination.

Techniques for contact microradiography of the particles were developed to permit evaluation of various features (size and presence, and migration) of the fuel particle and coating. Coating thickness and uniformity can be readily measured, and the presence of unfueled particles and uranium migration into the coating can be detected. This evaluation method also gives an indication of the surface condition of the fuel particle and the integrity of the coatings.

In an extensive series of neutron-activation tests, the as-received particles exhibited good fission-gas retention properties at temperatures less than 1500°C. The behavior at higher temperatures suggested that uranium migrated into the carbon coatings and that coatings cracked either at temperature or after cooling to room temperature. Indications are that these processes are dependent on the microstructure of the carbon coatings.

Cylindrical bodies of fueled graphite consisting of dispersions of coated fuel particles in a graphite matrix were obtained from two vendors and tested extensively. Leaching and neutron-activation tests indicated that some phases of the fabrication procedures could damage the particles in such a way as to adversely affect fission-product

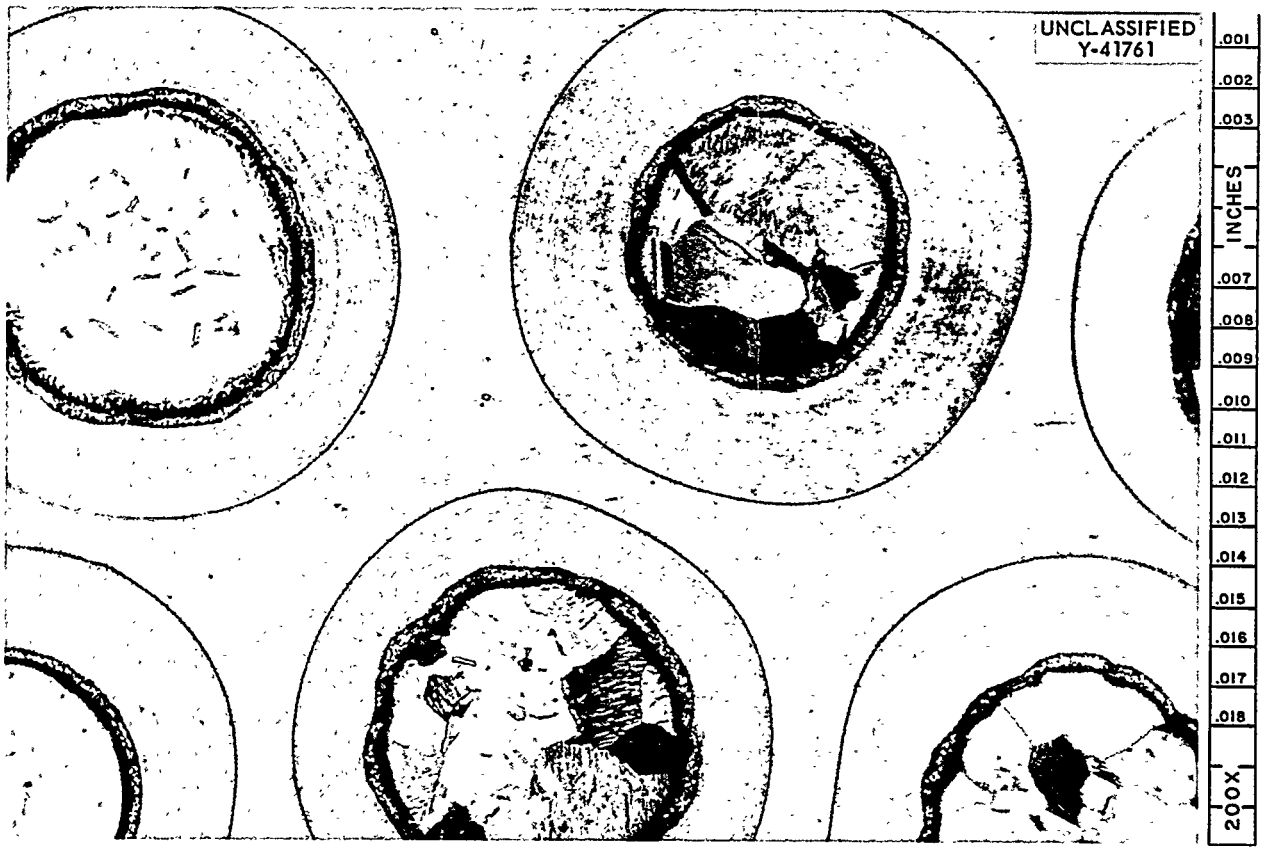

Pyrolytic-carbon-coated UC_2 particles showing laminar structure of the coating and UC platelets in the particle at left. Etchant: CH_3COOH, HNO_3, H_2O, 1:1:1. 200X.

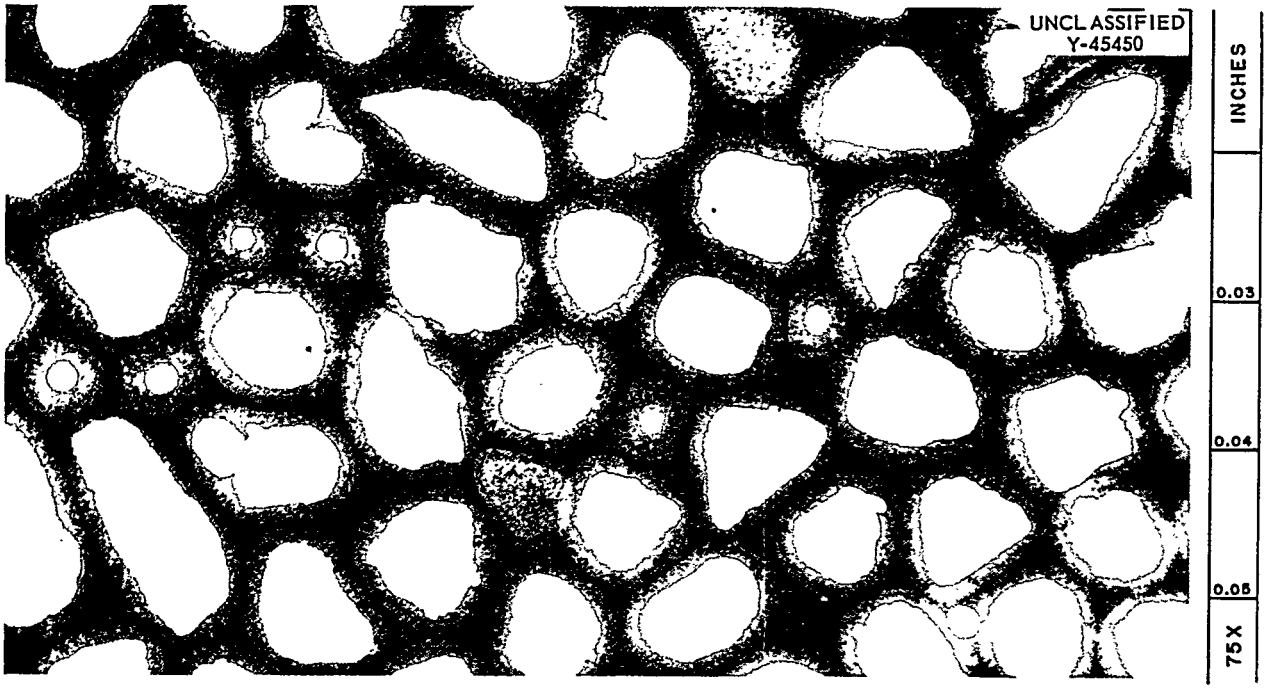

Microradiograph of particles showing variation in size and presence of unfueled particles.

retention. A series of tests on several batches of fueled bodies showed, however, that properly controlled fabrication processes produced satisfactory fueled-graphite bodies. A specification defining the properties of fueled-graphite spheres was thus developed and is being used in procuring prototype PBRE fuel elements for testing.

The fission products other than Xe^{133} that are released from fueled graphite were identified and measured in a separate series of neutron-activation tests. Fueled-graphite elements were lightly irradiated and heat treated, and the released fission products were collected on a metallic deposition tube near the specimen. The major species released at temperatures up to 1200°C were I^{131}, Te^{132}, and Ag^{111}. The fractions of iodine and tellurium that were released were approximately the same as the fraction of Xe^{133} released, but the silver isotope was detected in much greater amounts. Apparently Ag^{111} diffuses readily through the coatings at 1000 to 1200°C. The release of Ba^{140} by a similar mechanism was observed at temperatures greater than 1400°C.

Irradiation tests in both static and sweep capsules were performed in which burnups as high as 15 atomic percent of the uranium were achieved at temperatures between 1500 and 2600°F. It was observed that some cracking of the pyrolytic-carbon coatings occurred during irradiation; however, acceptable fission-gas retention with respect to the PBRE was observed in tests at the lower temperatures. Cracking of the coatings was attributed to the combined effects of swelling of the fuel particles, uranium migration, radiation-induced shrinkage of the coatings, and pressure buildup of fission gases within the coated particles. The relative importance of each of these processes is not yet known.

A series of experiments was conducted in the MTR on uncoated uranium carbide dispersed in graphite. Internal temperatures of 2500°F were obtained during irradiation at burnups of up to 21 atomic percent uranium. In general, the fuel cylinders showed a 4% decrease in diameter and a 3% increase in length. Microexamination of the fuel particles showed that void formation occurred at 3.5 atomic percent burnup of the uranium and increased with longer burnup. At 21% burnup, the fuel had spheroidized and had started to diffuse through the graphite matrix.

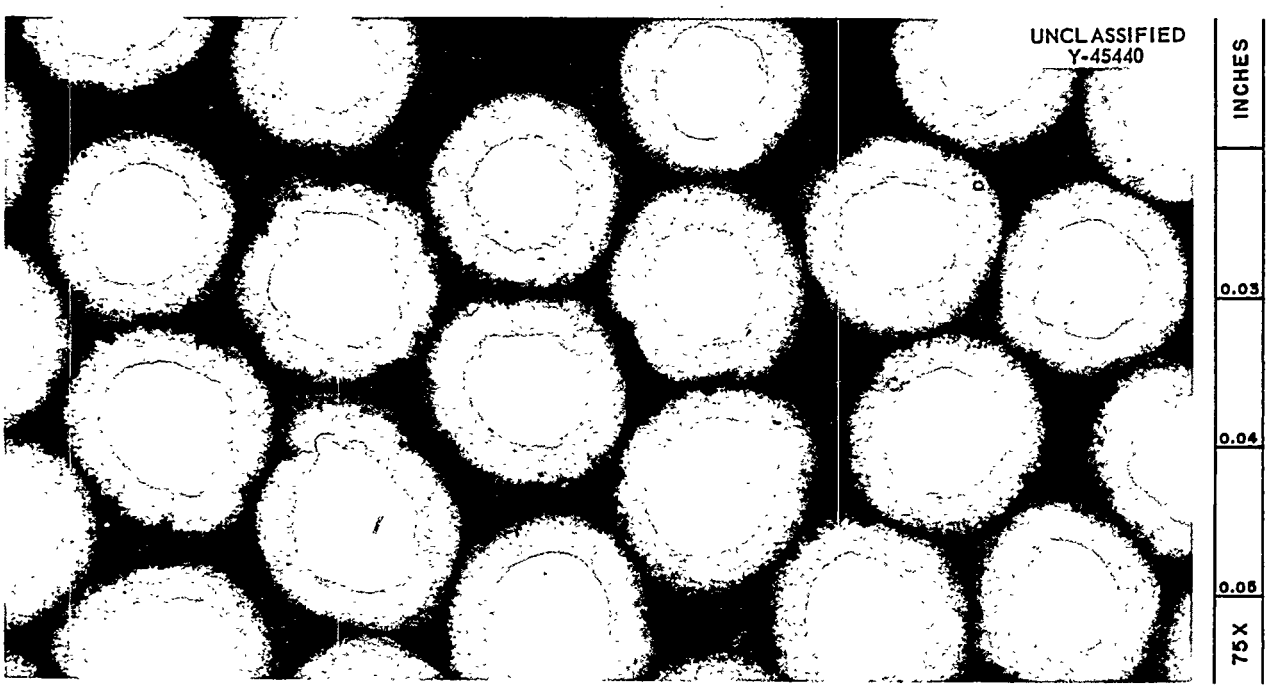

Microradiograph of particles showing migration of uranium into coatings.

Beryllium as Fuel-Element Cladding Material

In the process of evaluating beryllium for use as a cladding material in gas-cooled reactors, various aspects of the technology of beryllium were studied. Batches of smooth-walled tubing were procured from all domestic and foreign sources for evaluation and testing. In addition, a supply of finned tubing was obtained as the product of a fabrication subcontract. This tubing is approximately 0.5 inch in inside diameter, with a 0.040-inch minimum wall thickness, and has 12 equally spaced helical fins.

Nondestructive inspection techniques were developed for comparing the quality of the tubing and for ensuring the integrity of test specimens. Low-voltage radiography utilizing bare-film exposure techniques and a helium-atmosphere couple was found to be the most useful examination. The presence of pits of the inner surface or contamination from foreign materials was readily detected by such inspection. An eddy-current procedure with an internal bobbin coil was developed for detecting cracks in the finned tubing. The more conventional liquid-penetrant and ultrasonic techniques were adapted to supplement the radiographic inspection.

Joint designs and welding procedures were developed for the fabrication of test specimens and irradiation capsules. The shear strengths of end-cap welds were determined for several different kinds of tubing at room and elevated temperature. A conventional tensile machine equipped with a special fixture (see photograph) was used.

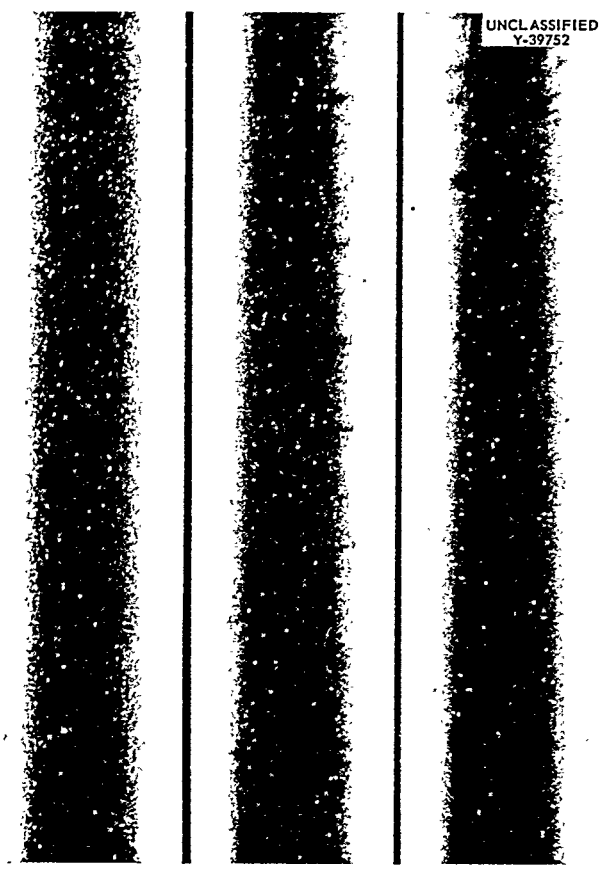

Radiograph of beryllium tubing showing pits and high-density material.

Positive print from low-voltage radiograph of finned beryllium tube.

The edge-welded sample was placed in the fixture, and the end cap was pushed out of the fixed tube through shearing of the weld. Results of tests at room temperature and at 600°C are summarized in the following table. It may be seen that the welds in all types of tubing exhibited similar strengths at both temperatures, even though radiographic examination had shown that the welds in most of the extruded tubing contained some pores.

Changes in the mechanical and physical properties of beryllium occur upon neutron irradiation and may be attributed to the displacements produced by energetic neutrons or to the products from the $(n,2n)$ and (n,α) reactions with beryllium and the effects produced by agglomeration of the gases produced by these transmutations. In order to study the effects of the changes, a program of irradiations was conducted in which beryllium specimens of various chemical compositions and fabrication histories were exposed at temperatures between 50 and 780°C. Postirradiation bend tests and hardness measurements were made, and the density decreases during the irradiations were determined. These data were compared with those obtained by postirradiation annealing of specimens irradiated at 50°C. Small tubular specimens were pressurized and were irradiated at temperatures between 500 and 700°C, and tests indicated that slight hardening occurred upon irradiation or postirradiation annealing at temperatures below 600°C. Dimensional measurements showed that beryllium swells more than 1% when irradiated to a fast (> 1 Mev) neutron exposure of 3.6×10^{20} neutrons per square centimeter. No significant swelling occurred during irradiation at lower temperatures or for lower exposures. Several in-pile stress-rupture experiments were run, and it was found that data obtained at 600°C could be represented by the equation

$$\Delta_{100} = 5.37 \times 10^{-14} \phi_I^{0.628} ,$$

where Δ_{100} is the fractional decrease in 100-hour rupture strength after an exposure of ϕ_I neutrons per square centimeter. Additional tests at 520°C showed that exposures as high as 3.4×10^{20} neutrons per square centimeter had little effect on the time to rupture at this temperature.

The reactions of beryllium with potential coolants were also studied. The rate of reaction with wet and dry CO_2 was found to be parabolic in the temperature range 550 to 720°C for times up to

UNCLASSIFIED
PHOTO 55466

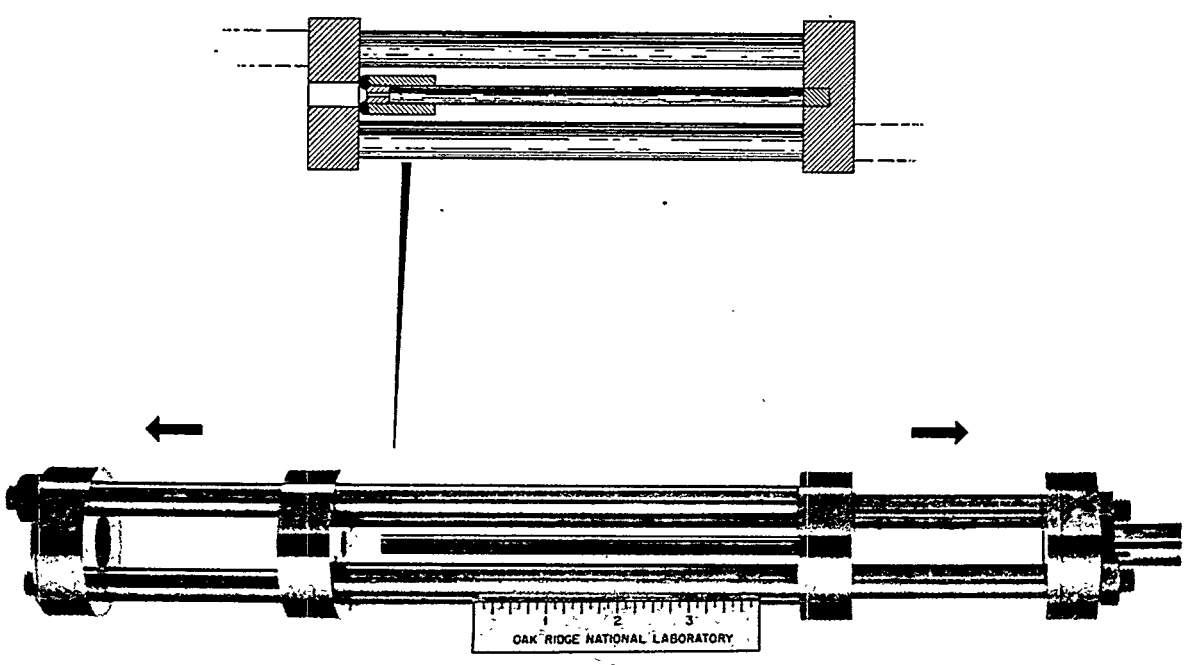

Shear testing equipment.

1000 hours. At 725°C, a "breakaway" reaction was observed in wet CO_2 after 60 to 70 hours. The reaction products were found to be BeO and Be_2C, and the amount of both increased with time and temperature.

The reaction between beryllium, which contains carbon as an impurity, and wet helium was initially rapid, but a protective oxide soon formed on the beryllium that was similar to that formed in dry CO_2. This behavior is believed to be associated with decarburization during the early stages of the test. The products of the reaction of beryllium with water vapor were BeO and hydrogen gas. Methane was found to be a reaction product when Be_2C was exposed to water vapor or hydrogen.

Results of Room- and Elevated-Temperature Shear Tests on End-Cap Welds in Beryllium Tubes

Tube Fabrication Method	Ultimate Shear Strength at Room Temperature[a] (psi)	Ultimate Shear Strength at 600°C (psi)
Machined from hot-pressed rod (low carbon content)	25,700	10,100
Machined from hot-pressed rod (high carbon content)	27,700	10,600
Machined from hot-extruded rod	24,400	16,200
Machined from warm-extruded rod	26,000	10,800
Warm-extruded to size	22,300	9,500
Hot-impact-extruded to size	24,400	11,700
Hot-extruded to size	21,700	12,900
Extruded to size	20,900	10,300

[a]All values are the average of values from two tests.

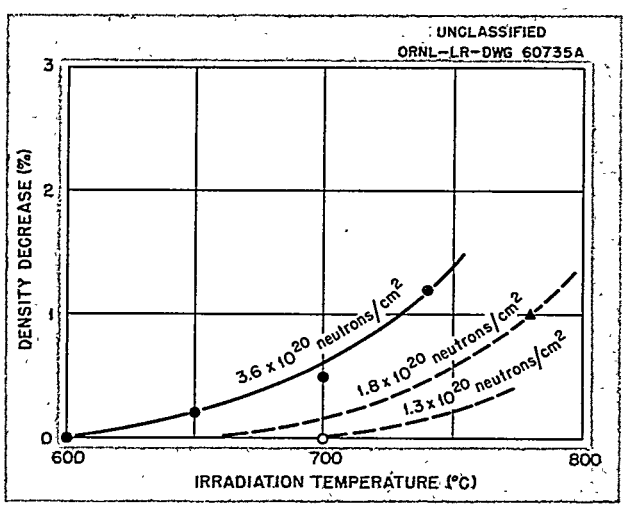

Swelling of beryllium under irradiation at elevated temperatures.

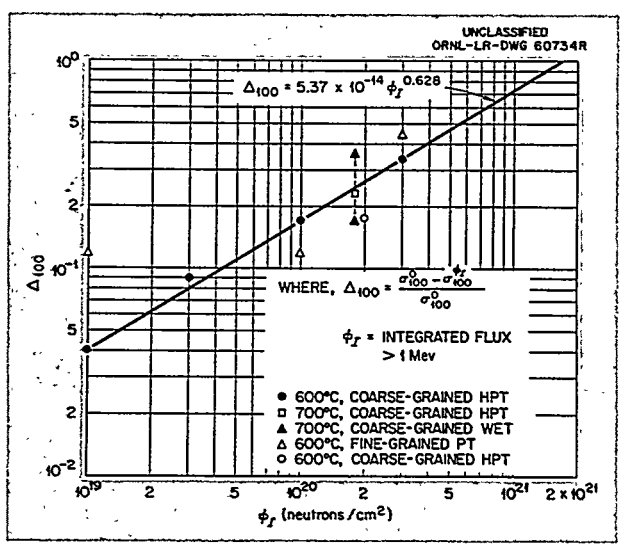

Effect of irradiation on the stress-rupture properties of beryllium.

A series of tests was also run in static, dry CO_2 at 750°C on a Be–0.5 weight percent Ba alloy. This alloy was prepared for testing because of the excellent high-temperature stability of barium carbonate, which could stabilize the protective oxide film on the alloy at a relatively low partial pressure of CO_2. Three tests were run at CO_2 pressures of 6, 50, and 570 millimeters of mercury, respectively. Reaction rate curves determined from weight-gain data indicated that the reaction was pressure-dependent; that is, the highest reaction rates occurred at the lowest pressure.

Two simulated beryllium fuel elements consisting of hollow UO_2 pellets clad with the finned tubing were fabricated and were tested to failure by thermal cycling out-of-pile. A radial temperature gradient between 200 and 440°F was established during cycling. No permanent axial deformation of the beryllium was detected after testing; however, the beryllium tubing had cracked both circumferentially and axially. The axial cracking apparently resulted from the concentration of stresses between the fins.

Fueled Beryllium Oxide

Samples of UO_2-BeO (30-70 volume percent) were irradiated at temperatures up to 2200°F in the LITR. The material showed dimensional increases of up to 3½% at burnups of 3×10^{20} fissions/cm^3. Fission-gas release of 0.3% was measured, based on Kr^{85}. This material contained very fine grains, about 1 micron in diameter. Beryllium oxide specimens containing the dioxides of thorium and uranium were irradiated under comparable conditions. The swelling was reduced to a maximum of 2.2%, and the krypton-gas release was less (0.09%). The volume percentages of UO_2, ThO_2, and BeO in this material were 13, 17, and 70, and it had a larger grain size (25 microns).

Beryllium Oxide Moderators

The attractive nuclear properties of beryllium oxide and its general excellence as a high-temperature ceramic recommend its consideration as a reactor moderator or reflector, but its satisfactory and economical use requires that it withstand very high integrated neutron doses. Irradiation experiments were completed that showed severe damage to beryllium oxide bodies irradiated to fast (>1 Mev) neutron dosages of 10^{21} neutrons per square centimeter. The specimens disintegrated to powder on such irradiated at 110°C and fractured upon irradiation at temperatures up to 950°C; that is, damage decreased with an increase in irradiation temperature. Presumably, some of the damage is reduced by annealing at higher temperatures during reactor operation. Further examination of irradiated specimens showed changes in linear dimensions, anisotropic lattice expansion, and retention of fission gas within the specimen. Experiments are now in progress to determine specific mechanisms of the observed damage and to establish optimum fabrication and operating conditions for successful operation of reactors moderated with beryllium oxide.

Fission-Gas Release from UO_2 During Irradiation

Thin-plate samples of UO_2 were irradiated in order to study fission-gas release during irradiation. Quantitative release rates were obtained for I^{133}, I^{135}, Xe^{133}, Xe^{135}, Kr^{85m}, Kr^{88}, and Kr^{87}.

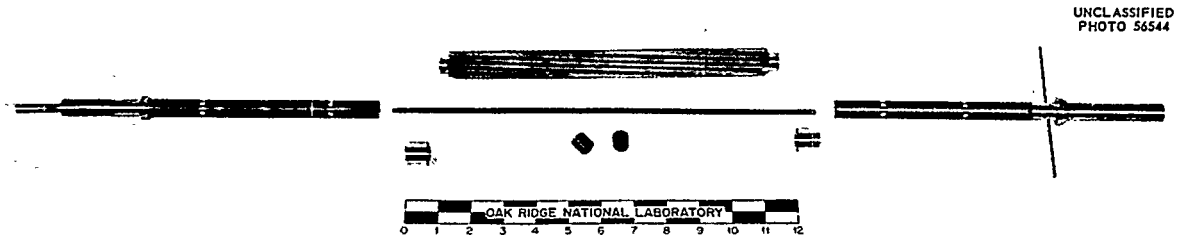

Components of simulated beryllium-clad fuel element.

Beryllium oxide containing 30 vol % UO_2 incorporated as submicronsize particles. Cold-pressed and sintered for 1 hour in argon and 30 minutes in hydrogen at 1750°C.

When the temperature of the UO_2 is increased during irradiation, fission gas is released in an abrupt burst for a short time. In part, this is due to a change in concentration gradient with temperature that makes excess gas available; however, more gas is released than would be expected from concentration-gradient changes, and the burst process is not reversible. Also, some specimens released fission gas in an abrupt burst when the temperature was lowered. The temperature dependence for fission-gas release was measured, and diffusion coefficients were calculated.

A method was found to prevent the in-pile oxidation of the UO_2 by the use of a reducing sweep gas. A new method of flux measurement, by argon activation, was developed. The ratio in which various isotopes were released was discovered to be characteristic of the release mechanism. The electrical conductivity and thermoelectric power of UO_2 were measured during irradiation.

Pressure-Vessel Steel

Accelerated irradiation tests of samples at high fluxes in materials testing reactors and surveillance tests on samples irradiated at low fluxes at regions close to the pressure vessels of operating power reactors are being used to study the effects of irradiation on the brittle fracture of pressure-vessel steel. An experiment was completed in which Charpy V-notch specimens were irradiated at 90 to 130°F in the ORR to fast (>1 Mev) neutron doses of 9×10^{18} neutrons/cm^2. The specimens were ASTM A-212, grade B, carbon-silicon steel. One group of samples was representative of the base material. A second group of samples was given a synthetic heat treatment to reproduce the properties of the metal in the heat-affected zone adjacent to the welds used in the fabrication of a reactor pressure vessel. For both types of samples, the brittle-ductile transition

temperature was increased about 200°F as a result of the irradiation.

One of the first groups of surveillance samples exposed in a power reactor was impact-tested during 1961. The samples were removed from the SM-1 reactor at Fort Belvoir, Virginia, after 16.4 megawatt-years of SM-1 core I life. They were subsize Izod notch-impact samples composed of the ASTM A-212, grade B, steel used for the SM-1 pressure vessel. The exposure temperature was about that of the exit coolant, that is, about 450°F. The samples had been placed on the core support plate in a region of high flux gradient. The observed increases in the brittle-fracture transition temperature ranged from 36 to 138°F, depending upon the precise location of the sample notches. A surveillance program for the EGCR has been planned, and facilities, irradiation capsules, and surveillance samples are being designed and fabricated.

Stress-Rupture Characteristics of Stainless Steel and Inconel During Irradiation

Type 304 stainless steel tube-burst specimens were irradiated in the ORR, while under stress, at temperatures of 1200, 1300, 1400, and 1500°F. The environment was helium inside the tube and a mixture of 90% helium, 8% nitrogen, and 2% oxygen on the outside. The specimens exhibited rupture strengths between 80 and 90% of those obtained in out-of-pile control tests. Postirradiation diameter measurements showed that the diameter increases at rupture were 10 to 50% of those of the control specimens.

Tube-burst tests on specimens fabricated from six special heats of Inconel were also irradiated in the ORR to determine the effect of the boron impurity on the stress-rupture properties during irradiation. The heats contained various amounts of either natural or isotopically enriched boron. A reduction in in-pile time to rupture was noted in all but one case, but the relative change did not follow the trend expected if the B^{10} content was the cause of the reduction in time to rupture. Wide variations in the time to rupture of specimens tested out-of-pile made comparison difficult, and postirradiation metallographic examination gave evidence of nonuniform boron distribution. Postirradiation measurements of the diameter increases at rupture showed these to be very small, averaging only about 15% of corresponding control-specimen diameters.

Gas Content of Graphite

The volume, composition, and rate of release of the gas evolved during the heating of graphite was determined. These data may be used in estimating the extent of attack by corrosive contaminants in the coolant on graphite sleeves and steel cladding of fuel elements in gas-cooled reactors. They are also useful in the design of helium purification systems.

The gas content of the EGCR graphite, as determined by heating to 1800°C, is approximately 0.5 volume of gas per unit volume of graphite. The evolved gas contains about 40 vol % hydrogen and 55 vol % carbon monoxide, with the remainder consisting of nitrogen, carbon dioxide, hydrocarbons, water vapor, and sulfur compounds. When the graphite was heated in the temperature range it will experience in the EGCR (~30 to ~600°C), it evolved about 0.04 volume of gas per volume of graphite. The gas evolved in this temperature range contained (in vol %) CO, 20; CO_2, 15; N_2, 5; hydrocarbons, 20; H_2O, 25; H_2, 5; and sulfur compounds, 10. The sulfur compounds consisted mainly of sulfur dioxide below 600°C.

A linear relationship between the volume of gas evolved and the logarithm of the time of heating exists in the temperature range 300 to 600°C. Each tenfold increase in the heating time releases ~0.001 volume of gas per volume of graphite at 300°C and ~0.006 at 600°C.

Transport of Gases in Porous Media

Advanced gas-cooled reactors are being studied that would operate with unclad fuel elements within porous graphite sleeves through which helium would be bled from the main coolant stream to purge radioactive fission-product gases from the reactor. In such a system it would be essential to minimize back-diffusion of radioactive gas through the sleeve wall against the helium flow. An understanding of diffusive flow of a gas through a porous medium against a forced flow of another gas was therefore needed. This complex problem was examined in a program of theoretical and experimental studies.

The magnitude of diffusive flow with and without forced flow of one component was determined experimentally by careful study of systems in which flowing streams of helium and argon were separated by porous sleeves of graphite. No previous theory of flow satisfactorily explains all the results so obtained; however, a new theoretical treatment of the problem, in which the porous medium is considered a collection of uniformly distributed "dust" particles that are constrained to be stationary, uses rigorous kinetic theory to permit simple derivation of suitable flow equations as special cases of well-known multicomponent mixture equations. Flow equations obtained from this treatment predict the behavior observed experimentally over a wide range of flow conditions and fail only after back-diffusion has been reduced to a minute fraction of its value with no forced flow.

Removal of Radioiodine from Helium at High Temperatures

Radioiodine, a fission product that is especially hazardous because of its volatility and toxicity, must be removed continuously from the coolant of a gas-cooled reactor with unclad fuel elements to minimize contamination of the coolant circuit and to reduce the hazard in the event of a reactor accident. In order to avoid the need for auxiliary heat exchanger equipment, the iodine should be removed at the normal temperature of the reactor coolant. Such a method for removal of radioiodine from helium at elevated temperatures was developed and was tested on a small scale.

Ordinary activated charcoal and silver-plated copper mesh are affective in iodine traps at low temperatures. At temperatures as high as 320°C, however, iodine retention, although significant, is insufficient to permit successful use of these materials. Whetlerite, an activated charcoal impregnated with salts of silver, copper, and chromium, which was developed for use in gas masks, has an efficiency of 99.99+% for removal of radioiodine from helium streams at temperatures as high as 550°C. These high efficiencies persist even at linear flow rates up to 110 feet per minute through a $\frac{1}{4}$-inch-thick bed for at least 200 hours. Use of traps containing this material should markedly reduce difficulties from leakage of radioiodine into the coolant when unclad fuel elements are used in a gas-cooled reactor.

Measurement of Temperatures in Gas-Cooled Reactors

Successful operation of high-temperature reactors will depend, to a considerable degree, on the ability to measure accurately the temperatures within the system. Such ability will become more important as reactor temperatures are increased in future years to afford more efficient operation. Therefore work is in progress on the development of reliable temperature-sensing devices for application under the generally difficult conditions to be encountered in gas-cooled reactors. Of the possible devices, thermocouples appear to be the most suitable. Commercial Chromel-P vs Alumel thermocouples have been used successfully for many years under oxidizing conditions; however, in a mildly oxidizing atmosphere, Chromel-P wires are damaged by selective oxidation of chromium in regions exposed at 700 to 900°C; severe errors in the indicated temperature result. Such oxidation can be prevented by enclosing the wires in a sheath of stainless steel. The sheathed couples must be carefully fabricated, and not all commercial sheathed couples are satisfactory. The problem is considerably lessened by use of less-well-known thermocouple wires of considerably higher chromium content. The use of tungsten, rhenium, and tungsten–rhenium alloy thermocouples at temperatures of interest to advanced gas-cooled reactors is being explored. Experiments in progress will indicate radiation effects on thermocouples, with emphasis on electromotive-force changes resulting from transmutation composition changes.

Noncorrosive Decontamination of Carbon Steel

The use of carbon steel in gas-cooled reactors rather than the stainless steel commonly used in water-cooled reactors has created new problems in decontamination. Decontaminating solutions used in the past for the removal of radioactive fission products to make stainless steel equipment accessible for repair are much too corrosive for carbon steel. Mixtures of oxalate salts and hydrogen peroxide of controlled acidity were therefore developed that are effective decontaminating agents for carbon steel. Corrosion rates are about 0.01 mil per hour. These mixtures are also efficient solvents for uranium dioxide and can therefore be used for the one-solution decontamination of

nuclear reactor components from which irradiated uranium dioxide must be removed. In these solutions, hydrogen peroxide acts as a corrosion inhibitor. Although it was known previously that peroxide under some conditions could inhibit steel corrosion, no extensive use had been made of that property because of its supposed unreliability.

Coolant Gas Purification

Anticipated contaminants of the helium coolant in gas-cooled reactors are (1) nonradioactive gases such as H_2, CO, CO_2, H_2O, and hydrocarbons, (2) particulate matter, and (3) radioactive gases such as xenon and krypton. These contaminants are to be maintained at low levels by continuous purification of at least a portion of the coolant. The proposed method of removing the nonradioactive gaseous contaminants is oxidation followed by sorption of the oxidation products, H_2O and CO_2.

A kinetic study of oxidation of H_2, CO, and CH_4 in helium at low concentrations with a catalytic reaction with oxygen resulted in a design equation based on an empirical correlation of temperature, concentration, and flow rate. A similar study of oxidation in a fixed bed of CuO pellets showed that the rate-controlling mechanism is diffusion of the contaminant gas into the CuO; and the variables temperature, pressure, concentration, and flow rate were correlated based on a mathematical model. A study of cosorption of the oxidation products, H_2O and CO_2, on fixed beds of molecular sieves has shown that the concentration of H_2O and CO_2 can be reduced to <10 parts per million and that the H_2O tends to displace sorbed CO_2. Investigations of particulate size distribution and concentration in gas streams were started with the use of a light-scattering technique.

Thorium Utilization Program

INTRODUCTION

The Thorium Utilization Program, established in 1961 at the Oak Ridge National Laboratory, has as its objective the development of technology associated with the use of thorium instead of U^{238} as the fertile material in thermal and intermediate reactors. Thorium-based fuel systems offer the possibility of reducing nuclear fuel-cycle costs in current-generation reactors by virtue of the attractive nuclear properties of U^{233} compared with plutonium; however, because of the radioactivity of irradiated thorium and U^{233}, recycle of these materials is not possible with existing techniques. A primary part of this program, therefore, is devoted to the development of remote methods of recovering and refabricating fuels for the water, gas, and liquid-metal cooled reactors which constitute the AEC's civilian power reactor program.

A longer-range objective is that of developing reactors capable of achieving conversion ratios of 1.0 or greater, in order to efficiently utilize thorium as a source of energy. Thus the program includes the conceptual design and economics evaluation of advanced thorium reactors which are not otherwise part of the Commission's major reactor

development programs. Basic research in chemistry, physics, metallurgy, and engineering pertinent to the thorium-uranium fuel system is also carried out in support of the overall effort. The results accomplished in FY 1962 are summarized in the following paragraphs.

THORIUM FUEL-CYCLE DEVELOPMENT

For nuclear reactors which use thorium and U^{233}, fuel element fabrication is more difficult and expensive because of the high residual radioactivity associated with U^{233}. A simple, two-step procedure (see reports ORNL TM-53 and ORNL-3225) being developed for manufacturing metal-clad thorium-U^{233} oxide fuel elements consists in preparing irregularly shaped dense particles of ThO_2-UO_2 by the sol-gel process and packing them into a fuel element tube by vibratory compaction. This procedure promises to be simple enough for operation in shielded cells without greatly increasing the cost of fuel element manufacture.

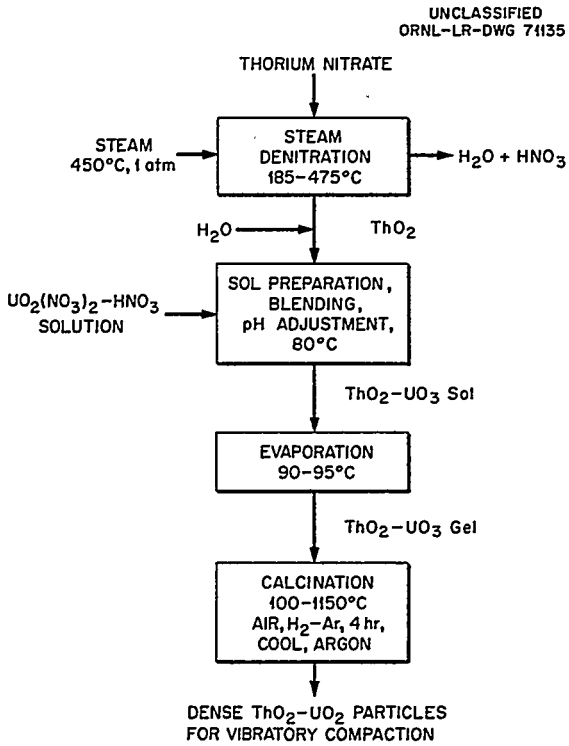

Sol-gel process for ThO_2-UO_2.

Sol-Gel Process

The sol-gel process (ORNL TM-53) was developed to make large, dense particles of ThO_2 or ThO_2-UO_2 suitable for loading into fuel tubes by vibratory compaction, using as starting materials the $Th(NO_3)_4$ and $UO_2(NO_3)_2$ solution products from the Thorex process. The process consists of four simple steps (see flowsheet): the thorium nitrate solution is converted to ThO_2 in a rotary denitrator; this oxide is added to dilute HNO_3 to form a thoria sol [the oxide is added to $UO_2(NO_3)_2$-HNO_3 if mixed oxide is to be made]; the sol is evaporated to form a gel; and the gel is calcined at 1150°C to obtain the final oxide. This oxide has a density >99% of theoretical and can be sized for vibratory-compaction loading of reactor fuel tubes. In the case of the mixed oxide the UO_2 is homogeneously dispersed in the ThO_2.

Process details were completed in laboratory work, and the entire process was demonstrated on a 7-kilogram scale. Steam denitration was successfully demonstrated with product ThO_2 batches of up to 22.5 kilograms, and a 500-gram batch of ThO_2 containing 4% PuO_2 was prepared for irradiation testing. In scouting experiments, large UO_2 particles with a density of about 98% of theoretical were made, but this material has not yet been made in sufficient quantity for vibratory-compaction testing.

Vibratory Compaction

Vibratory-compaction studies included development of procedures for sizing the sol-gel oxide and selecting particle-size distributions and methods for compaction to yield the maximum oxide bulk density. Ternary particle-size distributions containing a coarse, a medium, and a fine fraction can be readily compacted to 8.8 grams/cc in simple, low-cost pneumatic equipment (see ORNL-3225). With a more sophisticated pneumatic device, average bulk densities of 9.0 grams/cc can be reproducibly obtained. Ternary particle-size distribution studies indicated that maximum densities could be obtained over a broad range of size fractions. With appropriate binary particle-size distributions consisting only of a coarse and a fine fraction, densities of 9.0 grams/cc were produced. This suggests that a high yield of useful particles can be readily attained with simplified comminution procedures.

Gamma-scanning procedures were developed which permit evaluation of density variations and absolute density in vibratorily packed fuel rods. Axial density variations of less than 1% can be readily detected, and the precision of measurement is excellent.

Engineering-Scale Demonstration

The sol-gel vibratory-compaction procedure will be applied to the manufacture of a thousand U^{233}-bearing fuel rods in a shielded facility now under construction at ORNL. The remotely operated equipment was designed, and fabrication and procurement are in progress. Operation is expected to begin before the end of 1962.

Irradiation Testing

The irradiation behavior of sol-gel-prepared ThO_2-UO_2 is being studied. Successful exposure of 14 fuel rods at heat ratings of 20,000 to 44,000 Btu hr^{-1} ft^{-1} and burnups of 4,000 to 20,000 Mwd per metric ton were completed. Preliminary results from the postirradiation examination of two specimens exposed at a rating of 44,000 Btu hr^{-1} ft^{-1} to approximately 16,000 Mwd per metric ton showed no significant dimensional changes in the rods and no gross structural changes in the compacted oxide. Sixteen additional tests with higher heat ratings and burnups are in progress, including tests on three specimens containing ThO_2-PuO_2 prepared by the sol-gel process. Two experiments designed to characterize the behavior of vibratorily compacted sol-gel oxide under conditions typical of gas-cooled reactors are in progress. Maximum measured surface and center-line temperatures for the higher-temperature capsule are 1400 and 3700°F, respectively.

Fission-Gas Release

Fission-gas release was lower from the sol-gel-mixed ThO_2-UO_2 than from fused UO_2 powder (see ORNL-3225), as shown by measurements of the fission-gas release rate by a neutron-activation method parameter, D'. The temperature dependence of D' was expressed by the Arrhenius equation, in which an activation energy of 76,000 calories per mole was used. Rapid release of fission gases did not occur below 2200°F for the sol-gel ThO_2-UO_2 oxide or below about 1800°C for sintered UO_2.

THORIUM REACTOR EVALUATION

Uniform bases, procedures, and computer programs for the routine economic evaluation of thorium reactor concepts were developed, and these were applied to the evaluation of promising reactor types. Fuel yields and fuel costs for five thermal breeders were studied previously (see ORNL CF-61-3-9). The capital cost for one of these, the Aqueous Homogeneous Breeder Reactor, was determined in a study conducted jointly with Sargent and Lundy, Engineers (see report SL-1875). In addition, an on-site chemical processing plant (Thorex) for this concept was designed and costed at ORNL (ORNL CF-61-3-9). Using these data as a basis, power costs in a 1000-Mw (electrical) Aqueous Homogeneous Breeder plant are estimated to be 5.3 mills/kwhr, as shown below.

	mills/kwhr
Capital at 14.3%, 80% load factor	3.4
Fuel cycle (including D_2O)	0.9
Operating and maintenance (nominal)	1.0
	5.3

The fuel cost in a near-term, 1000-Mw (electrical), one-region, molten-salt converter reactor (MSCR) was estimated to be 0.8 mill/kwhr. The reactor is a slightly modified, scaled-up version of the Molten-Salt Reactor Experiment, conservatively designed and evaluated on current bases. Spent fuel is processed in a central multipurpose Thorex plant (see *Nuclear Power Plant Cost Evaluation Handbook*) at a rate of 2 cubic feet per day for recovery of uranium and thorium, which are recycled. Carrier salt is discarded in the waste. Ten percent of the circulating fuel is recycled through a sparging chamber for removal of Xe^{135}. Under the conditions, the conversion ratio is 0.93, the specific power is 0.9 Mw (electrical) per kilogram of fissile material, and the thorium exposure is about 40,000 Mwd per ton. Thermal efficiency is 40%, with steam at 1000°F, 2460 psi.

The low fuel cost may be coupled with an attractive capital cost. Pressures in the reactor and intermediate coolant systems are less than 200 psia. Design studies leading to preliminary cost estimation of the reactor plant and energy conversion systems are in progress.

BEHAVIOR OF THORIA PELLETS AND POWDERS UNDER IRRADIATION

The successful use of thorium oxide in a nuclear reactor requires that changes in its properties because of irradiation be predictable. The purpose of the thorium oxide irradiation studies is to determine the behavior of thoria pellets and powders under reactor irradiation both dry and in water.

Pressed and sintered thorium oxide pellets fired at 1650°C showed little damage after being irradiated three months in the ORNL Low-Intensity Test Reactor under D_2O at 250°C, and dry in aluminum capsules under a helium atmosphere to exposures of about 7×10^{16} fissions per gram (see ORNL-3314). The average weight loss as a result of the wet irradiation was 0.4%, and of the dry, <0.05%. Irradiation markedly enhanced the wear resistance of the pellet surfaces, but once the surface layers were removed during the first hour or two of standard spouting-bed tests, the wear rates of the irradiated materials were comparable to those of unirradiated. Irradiation in water also produced a very small increase in void volume and a large number of small pores probably associated with individual fission events. Metallographs of the unirradiated and wet-irradiated pellets showed almost no differences.

Two series of thorium oxide powders fired at 650, 800, 900, 1100, and 1500°C were irradiated dry in aluminum capsules for 16 and 22 months in the LITR to total exposures in both cases of 1.5×10^{18} fissions per gram (see ORNL-3275). The 650, 800, and 900°C-fired oxides became red and sintered into hard, glossy fragments. The 1100°C-fired materials formed off-white chalky plugs, and the 1500°C-fired oxides were blue powders. The specific surface areas of oxide fired at less than 1100°C were markedly decreased by the irradiation, although the estimated maximum temperatures of the powders during irradiation were less than 1000°C. Little or no sintering and only slight particle damage occurred in the 1500°C-fired powders. The sintering probably resulted from recrystallization processes induced by fission-fragment irradiation.

The work is continuing with long-term wet and dry irradiation of a variety of thoria preparations, including fired thoria pellets prepared from pressed powders, fired sol-gel-prepared thoria, and arc-fused thoria. Irradiation exposures will be about 2.5×10^{18} fissions per gram.

TESTING OF THORIA-SUSPENSION FUELS

One of the promising forms in which thorium might be used in a breeder reactor blanket is an aqueous suspension of the oxide. It is desirable to develop information as to the effects of irradiation, especially fissioning, on the properties of such a slurry circulating at high temperatures.

A substantial out-of-pile technology concerning thoria slurries was developed in the Aqueous Homogeneous and Thorium Breeder Reactor programs. In-pile tests conducted before 1962 included one in-pile slurry-loop experiment, operated in a horizontal beam hole of the ORNL Low-Intensity Test Reactor, and a number of capsule experiments. In the loop experiment a D_2O slurry of thorium oxide containing 0.4% uranium-235 oxide was circulated in-pile at 280°C for 2220 hours, with an average neutron flux of 2.6×10^{13}. The uranium simulated an economically reasonable processing level and was added during manufacture rather than being generated by nuclear transformation of thorium to provide accelerated fission-damage effects. It was observed that damage to the thoria particles became substantial as radiation progressed, but slurry-handling problems were not encountered.

In a second in-pile slurry-loop experiment, conducted during the present year, it was desired to irradiate a circulating high-temperature aqueous suspension of pure thoria in order to produce a substantial number of fissions from uranium-233 that had been produced by breeding and to observe the effects of such exposure on the properties of the slurry.

In order to develop the fissions in a shorter time, a higher neutron flux was needed. Consequently, the irradiation was conducted in a horizontal beam hole of the Oak Ridge Research Reactor, using a loop of improved design.

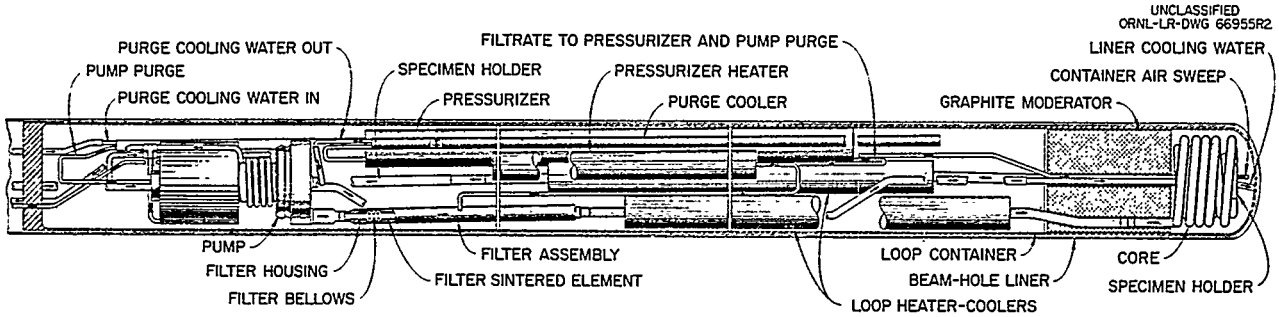

In-pile slurry loop for operation in the Oak Ridge Research Reactor.

The loop was operated in-pile for 2036 hours, 79% of this time being at a neutron flux averaging 1×10^{13} on the entire slurry contents. It is estimated that 0.056% of the thorium atoms were transmuted and that about 1.5×10^{16} fissions were developed per gram of ThO_2. The original concentration of the heavy-water slurry when irradiation began was 937 grams of thorium per liter at 280°C. This was reduced, by sampling during the run, to 847 grams of thorium per liter.

The ability of the slurry to be resuspended after a substantial period of settling was demonstrated when the loop was restarted in-pile after a one-day shutdown for maintenance. No handling problems were encountered with the slurry during the run. No radiolytic gas was observed. Generalized loop corrosion was less than 1 mil per year, as indicated by oxygen gas consumption.

Four slurry samples were taken without difficulty during the irradiation period. Sample concentration agreed well (99, 124, and 103%) with inventory concentrations, indicating maintenance of a satisfactory suspension throughout the run.

Particle-size data on the samples indicated mild degradation. The original thoria had an average diameter of 2.3 microns, with nothing reported below 0.7 micron. Just prior to irradiation (369 hours of circulation) the average diameter was 1.8 to 2.0 microns, with 10% below 0.7 micron. The final sample (2202 hours of circulation) had an average diameter of 1.5 microns, with 21% below 0.7 micron. Operating evidence was also developed for particle breakdown during the final 400 hours of irradiation. The flow rate of filtered water through a sintered-metal filter gradually reduced to 50% of the original value. This may have been caused by a partial plugging of the filter by slurry fines.

The run was terminated when electrical leads to the circulating pump were shorted (outside the loop-containment bulkhead) by water leakage. The loop and its slurry contents were withdrawn from the beam hole and will be examined as hot-cell facilities become available.

No evidence has been developed which would preclude the use of thoria suspensions as a breeder blanket material.

HOMOGENEOUS REACTOR EXPERIMENT NO. 2: SOME METALLOGRAPHIC RESULTS AND RECOVERY OF D_2O AND FUEL

Although operation of the Homogeneous Reactor Experiment No. 2 was discontinued last year, many activities, such as the removal of samples for corrosion information, the recovery of the fuel and heavy water, and the preparation of the reactor system for standby, had to be completed during the past year.

A major accomplishment during the year was the removal of a large portion of the Zircaloy core tank for metallurgical examination. A special cutting torch and manipulator were developed in order to section the core tank at a distance of 20 feet through the small openings in the top of the reactor vessel. About a third of the tank was cut into 78 pieces, of which 56 were removed to a hot cell. At present, six pieces have been replicated with an epoxy film, which was then coated with metal by vapor deposition.

Since the radioactivity did not transfer in the replication process, it was possible to examine the replicas in detail at close range. Many of the remaining 50 parts will be replicated; but on the basis of the examinations completed to date, it can be concluded that the corrosive attack in the upper parts of the core vessel was extremely mild, being no more than a light etching. However, in

the region of the entrance cone, where cooling was shown to be completely inadequate, the attack was extremely severe. As has been previously reported, a hole was formed in the wall of the vessel during an early period of high-power operation. In the vicinity of this hole were seen several areas 1 to 2 inches in diameter which were reduced from the original thickness of 0.385 inch to approximately 0.1 inch.

The fuel solution was processed to remove the heavy water and to recover the enriched uranium. The heavy water was distilled and then run through a mixed-bed resin column. Approximately 10,000 pounds of heavy water was decontaminated sufficiently to return to production channels. The concentrated fuel was solvent-extracted in the Fission Products Pilot Plant, and the enriched uranium was returned to the Y-12 Production Plant.

Except for completing the metallurgical examination of the core parts, Homogeneous Reactor Experiment No. 2 is completed and no further work is planned.

CHEMISTRY AND PHASE RELATIONSHIPS OF THORIA-URANIA SOLID FUELS

This program is primarily concerned with the very complex phase relationships in the system ThO_2-UO_{2+x}-O_2 and the subsystems thereof. The temperature and composition boundaries for the region of stability of the single-phase, fluorite-structure UO_{2+x}-ThO_2 solid solution are of particular interest. Achievements to date have for the most part had to do with either improved techniques for the preparation of pure and/or stoichiometric solids or improvements in methods for identifying and characterizing solid phases.

A very pure, stoichiometric UO_2 was produced by the slow hydrolysis of tetravalent uranium from molten fluorides or chlorides at 800°C. The product had an oxygen-to-uranium ratio of 2.00 ± 0.003, a refractive index of 2.360 ± 0.005, and an x-ray lattice parameter a_0 of 5.472 ± 0.001 angstroms.

The precision of determining refractive indices of such materials has been improved tenfold by employing specially calibrated glasses containing sulfur and selenium for comparisons instead of the usual immersion oils. The discernment of grain boundaries in metallographic examination of solid solutions of UO_2-ThO_2 rich in ThO_2 has been made possible by the development of a suitable etchant. Preliminary experiments indicate that it is possible to detect transitions in the solid phase(s) of the system ThO_2-UO_{2+x}-O_2 by observing discontinuity in the equilibrium oxygen partial pressure as a function of temperature. This technique, supported by metallographic and x-ray characterization of the solids, is being used in a continuing study of the system.

PROPERTIES OF FLOCCULATED THORIA SLURRIES AT HIGH RATES OF SHEAR

Many different suspensions of solids in a liquid carrier tend to flocculate; that is, the individual particles tend to form clumps of particles which constantly break up and re-form under flow conditions. Whereas nonflocculated suspensions have viscous properties very similar to those of the liquid carrier, flocculated suspensions are non-Newtonian and tend to act like paste or jelly.

Aqueous thoria slurries are promising fuels for circulating-fuel and boiling reactors. Thoria slurries normally are flocculated. This implies that they have inferior viscous properties from the standpoint of pumping or heat removal.

Tests, in which measurements were made of the pressure drop of aqueous thoria slurries flowing in tubes of diameters ranging from 0.018 to 1.6 inches and at temperatures up to 280°C, showed that as the shear was increased, the viscosity tended to approach that of a nonflocculated suspension of the same concentration. It was determined also that thoria suspension in turbulent flow had velocity profiles identical to those predicted for Newtonian fluids. It was thus concluded that if these suspensions were circulated through heat exchangers at high rates of shear (velocities of 15 feet per second or greater), they would give up their heat as readily as does water, with a minimum of pumping power required.

The influence of thoria particles on boiling forced-convection heat transfer was investigated in order to provide a basis for the design of metal structures in a slurry reactor. Results for a typical slurry indicate that the heat transfer coefficients are slightly better than those obtained with water, but the burnout heat flux is reduced slightly.

Molten-Salt Reactor Program

INTRODUCTION

The attainment of really low-cost nuclear power may depend on the development of advanced types of power reactors, simply designed, inexpensively built, operable at high temperature in order to utilize the heat efficiently, and fueled with materials that can be made, handled, and processed inexpensively. Molten-salt reactors show promise of fulfilling these requirements. These reactors use molten mixtures of lithium, beryllium, zirconium, uranium, and thorium fluorides, not solid fuel elements. The mixtures are liquid above about 850°F. At 1200°F, the operating temperature of an advanced power reactor, the fuel can be circulated easily through the reactor, through the heat removal equipment, and to the fuel-processing facilities.

Molten-salt reactors were originally proposed as compact power plants for nuclear aircraft, and much of the basic technology was developed under the Aircraft Nuclear Propulsion program. The Molten-Salt Reactor Experiment (MSRE) is now being built to study that technology as it applies to civilian power reactors. The MSRE is a circulating-fuel reactor designed to produce heat at a rate of 10,000 kilowatts and to operate at 1200°F. The major objective of the experiment is to establish that the structural materials and the molten salt will serve reliably in a reactor over long periods. It is also intended to show that this type of fluid-fuel reactor is safe and that there are workable methods for repairing or replacing the components even though they are highly radioactive.

DESIGN AND CONSTRUCTION OF THE MSRE

A drawing of the reactor vessel is shown below. The vessel is 5 feet in diameter by 7½ feet high; it is to be built of INOR-8, a new nickel-base alloy. The reactor core contains 78% graphite and 22% fuel salt, by volume. The salt is composed of 70% lithium fluoride, 23% beryllium fluoride, 5% zirconium fluoride, 1% thorium fluoride, and about 1% uranium tetrafluoride (mole percentages). The graphite is in the form of vertical bars 2 inches square and 5 feet long. It has flow channels for the salt machined along the length of each side of each bar. Three control rods and a channel for irradiating graphite and metal specimens are provided in the center of the core, with access through the top of the vessel.

When the reactor is operated at the design power, fuel will be pumped through the core at 1200 gallons a minute, entering at 1175°F and leaving at 1225°F. The fuel will be circulated outside the reactor vessel through a shell-and-tube heat exchanger, where the heat will be transferred to a coolant salt (66 mole % lithium fluoride and 34 mole % beryllium fluoride), also a molten salt. The coolant will be pumped through the coils of a large radiator over which air will be blown to dissipate the heat to the atmosphere.

A building at ORNL is being modified for the experiment. The reactor will be contained in underground tanks that will be sealed before operation. There will be access through the top of the tanks for maintenance and replacement of equipment when the reactor is not operating. For example, the circulation pumps are expected to be replaced several times and the reactor vessel once or twice during the experiment.

The reactor has been designed, materials have been purchased, and the fabrication of the reactor components by the Y-12 shops of the Union Carbide Nuclear Company is about 30% complete. Site and building modifications are about 70% complete. These modifications are scheduled to be finished in October 1962. Installation of all the reactor equipment is to be completed by July 1963. Prenuclear testing of the reactor is planned for July through December 1963. Nuclear operation should begin with the critical experiments early in 1964.

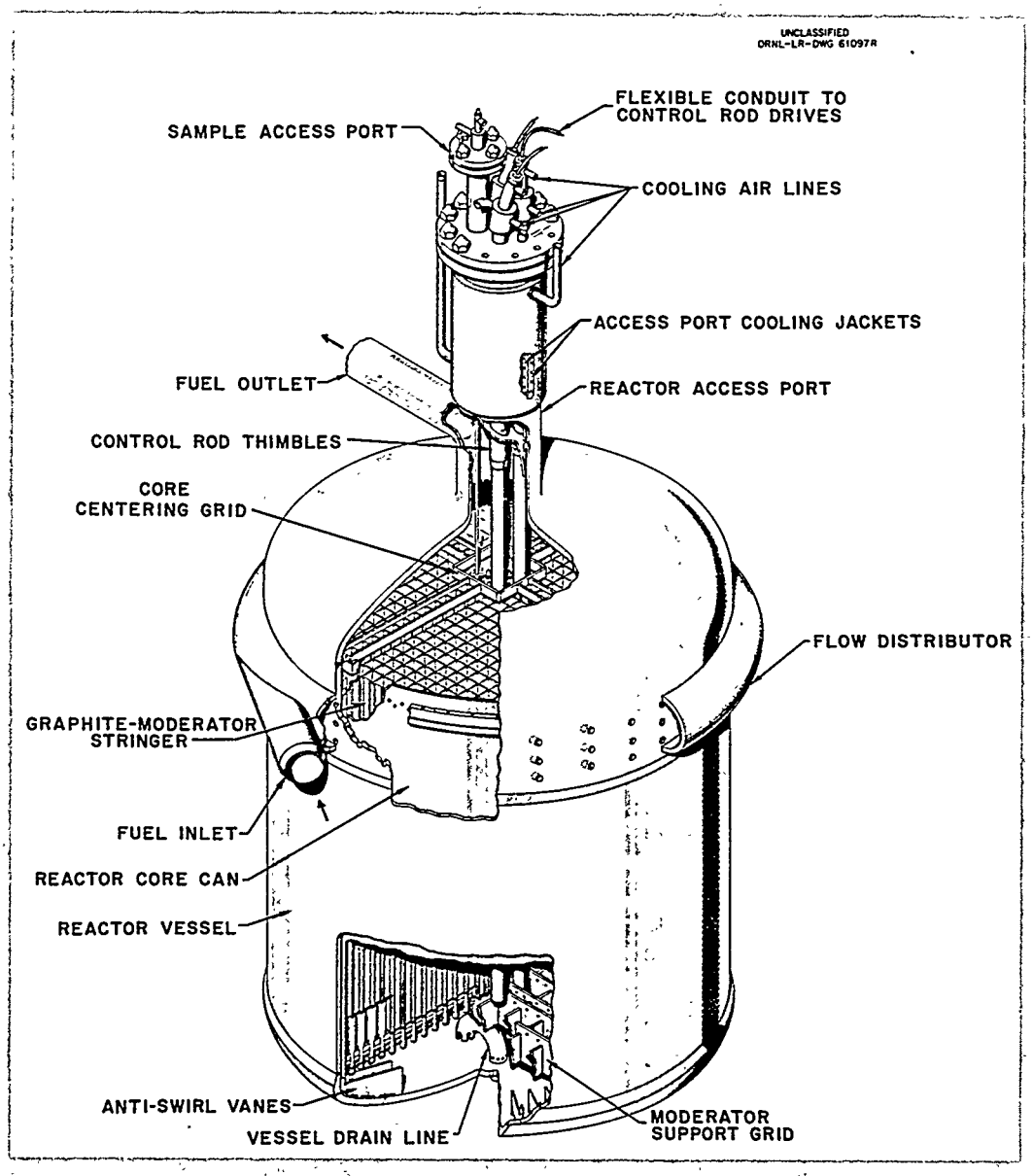

MSRE reactor vessel. It is 7½ feet high and 5 feet in diameter.

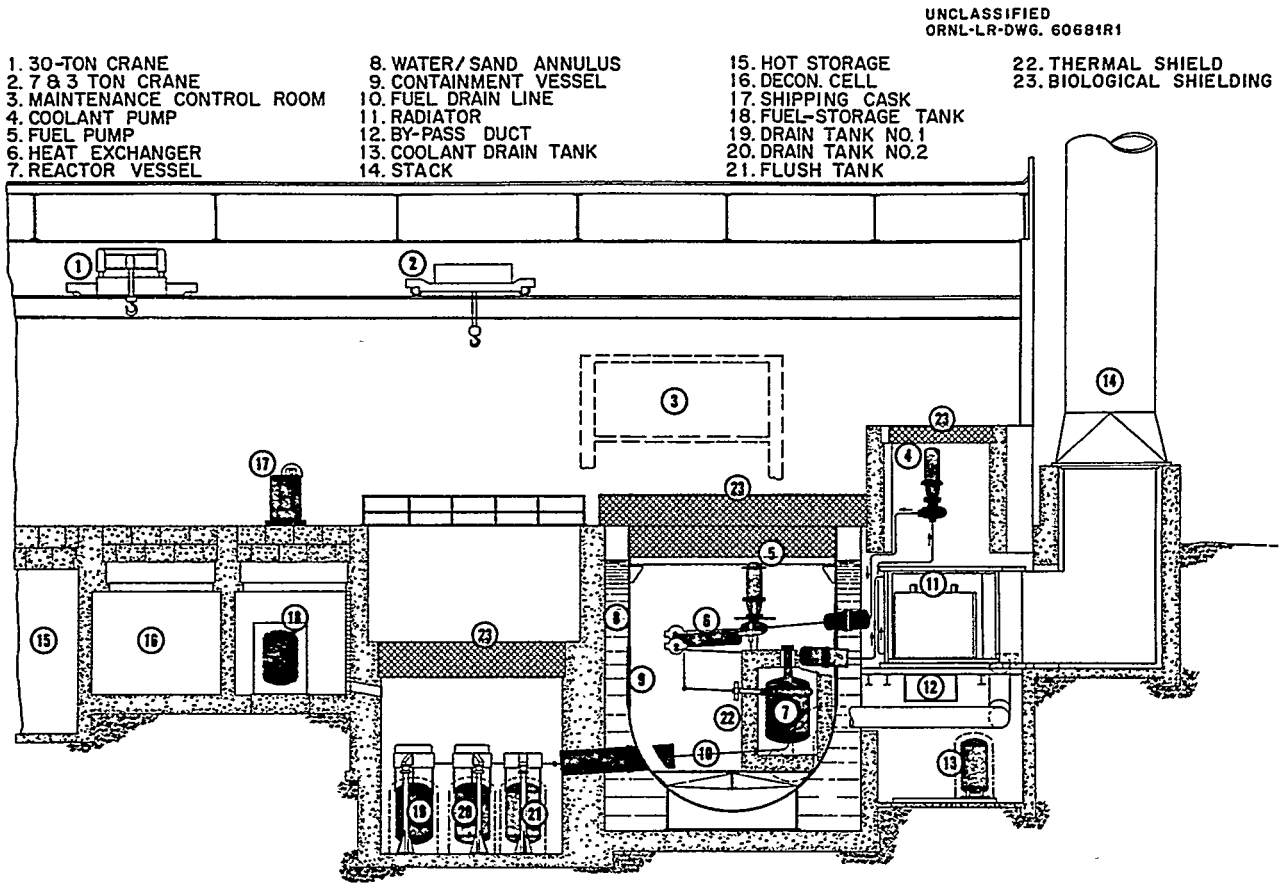

MSRE plant layout, elevation.

INOR-8, AN ALLOY IMPORTANT TO THE MSRE

The MSRE is an advanced reactor that uses new fuel, new materials, and new equipment, and, of course, this calls for a strong research and development program. INOR-8 (called Hastelloy N by the Haynes Stellite Company and Inco No. 608 by the International Nickel Company) is an alloy developed by ORNL to resist corrosion by molten fluorides and to have good strength at high temperature. The composition is tabulated below.

Tests show that INOR-8 corrodes at rates less than 0.001 inch per year in MSRE fuel at 1300°F. Physical and mechanical properties of the alloy have been established, including the stress-rupture and creep strengths necessary for the design of high-temperature equipment. The properties are better than those of austenitic stainless steel for high-temperature service.

Composition of INOR-8

Element	Percentage
Nickel	Balance (~66 to 71)
Molybdenum	15.0 to 18.0
Chromium	6.0 to 8.0
Iron (max)*	5.0
Titanium plus aluminum (max)	0.50
Sulfur (max)	0.02
Manganese (max)	1.0
Silicon (max)	1.0
Copper (max)	0.35
Boron (max)	0.010
Tungsten (max)	0.50
Phosphorus (max)	0.015
Cobalt (max)	0.20
Vanadium (max)	0.5
Carbon	0.04 to 0.08

*Maximal amount.

Sixty-five tons of the new metal has been obtained from the Haynes Stellite Company and the International Nickel Company to specifications that guarantee the weldability of the final product. This metal has been processed by those and other metal processing companies into the plate, sheet, rod, bar stock, pipe, fittings, and tubing that are required to build the reactor.

COMPATIBILITY OF THE MOLTEN-SALT FUEL AND THE GRAPHITE MODERATOR

Promising molten-salt reactors can be designed to operate with the neutron moderation provided by the constituents of the fuel salt itself or with the moderation provided by graphite or beryllium oxide canned in INOR-8, but the reactor with the greatest promise is one which uses unclad graphite for moderator. In building the MSRE, it was decided to attempt a big step forward by using unclad graphite in the core even though greater uncertainties are involved. If difficulties are encountered, the reactor vessel can be replaced with one containing a canned moderator.

An improved grade of graphite is being manufactured by the National Carbon Company. Pores in this graphite will be so small that the fuel cannot penetrate into the interior voids under the reactor operating conditions, provided that the salt does not wet the graphite. Tests in the absence of radiation showed convincingly that molten fluoride mixtures do not normally wet graphite. In addition, no wetting of graphite was observed in in-pile tests in which the materials were exposed to temperatures and power densities much higher than those expected within the reactor and to irradiation dosages which would correspond to more than two years of MSRE operation.

No evidence for chemical reaction of graphite with the fuel mixture has been observed in out-of-pile compatibility tests. However, some in-pile tests at considerably higher temperatures and irradiation levels produced a low concentration of carbon tetrafluoride in the cover gas above the fissioning salt. The liberation of free fluorine (by the decomposition of a fluoride salt in the fuel) along fission-fragment tracks and a subsequent reaction of this fluorine with graphite are believed to account for the formation of the carbon tetrafluoride. The extent of reaction observed was negligible in terms of graphite consumption, and the graphite was not appreciably affected in tests equivalent in fission power to two years of MSRE operation. However, the formation of carbon tetrafluoride represents a potential loss of fluorine from the fluoride salts, and the effect of this loss on the stability of the fuel against precipitation of uranium requires additional study.

Contamination by oxygen (from air or water vapor) of a fuel composed of lithium fluoride, beryllium fluoride, and uranium tetrafluoride causes uranium to precipitate as uranium dioxide. Experiments showed that addition of zirconium fluoride to the MSRE fuel would protect it against contamination by oxygen. When the ratio of zirconium ion to uranium ion is above about 3, the addition of oxygen yields uranium-free zirconium oxide as the insoluble product. This selective precipitation of zirconium oxide indicates that the fuel is being contaminated, but the precipitation of zirconium oxide does not constitute a hazard to the operation.

MECHANICAL COMPONENTS

Successful mechanical operation of the MSRE and of larger molten-salt reactors depends on the development of equipment that will operate for long periods without maintenance and on the development of methods for maintaining the equipment remotely. Such a program of development involves extensive testing and gradual improvement of equipment and methods.

General characteristics of the fluoride salts, the compatibility of graphite and salt, some operating procedures, some full-size MSRE components, and smaller-scale models of other components are being tested in a nonradioactive environment in an engineering test loop. Molten salt is circulated through equipment at 50 gallons a minute, as compared to a flow of 1200 gallons a minute in the MSRE. The engineering test loop operated continuously for 1300 hours in the first run, which was a test of the effects of additions of oxide contaminants on a uranium-free fluoride salt. At the end of the run, it was demonstrated that oxygen could be removed

by treating the molten salt with a mixture of hydrogen and hydrogen fluoride gases in the fuel storage tank. Graphite and additional equipment are being installed in the loop for testing.

Satisfactory operation of the MSRE depends in part on the development of a reliable pump for circulating the fuel and coolant salts. The design of the fuel pump is shown below. The coolant pump is identical, except for minor differences in the impeller, the volute, and the sump tank. The pump is a sump-type centrifugal pump with vertical shaft, overhung impeller, and oil-lubricated bearings. The sump is only partly filled with fuel; the remaining volume is left for the expansion of fuel and is filled with helium. Gaseous fission products will be removed from the fuel by spraying about 4% of the circulating stream into the gas space. Helium will be passed through the gas space to transport the fission products to carbon adsorbers outside the reactor building.

Molten salts have been pumped by similar but smaller pumps for several years. The hydraulic design of the MSRE pumps was tested with water in a full-size plastic model. A prototype has been built and installed in a test loop and is now ready for testing with molten salt.

Heat produced in the MSRE will be dissipated to air in a radiator. The radiator housing has been

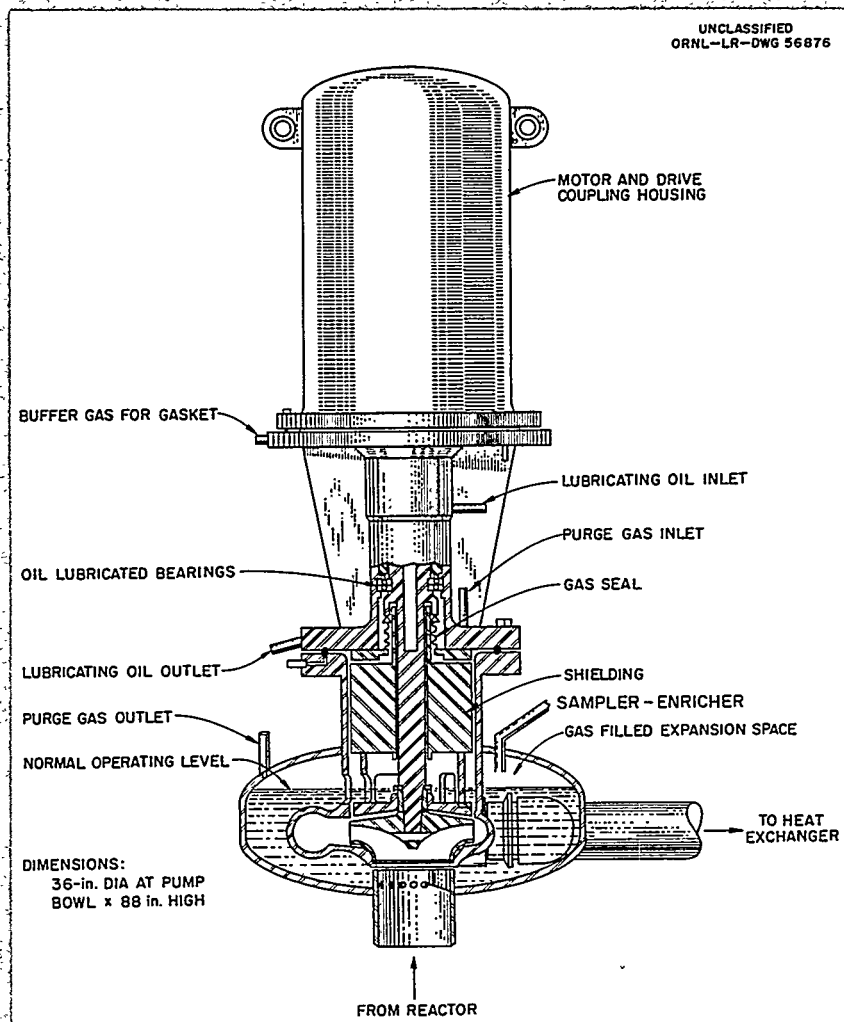

Fuel circulation pump.

built, and work is progressing on the radiator coils and on the mechanisms for operating the doors.

New designs of steam generators are required for later molten-salt power reactors. The principles of a promising type of steam generator will be demonstrated in the drain tanks (tanks that hold the fuel after it is drained from the reactor), where coolers must be provided to remove the heat generated by the radioactive decay of the fission products. Each drain tank will contain 32 bayonet-tube assemblies. Each assembly has a thimble welded into the drain tank and a boiler tube which is inserted into the thimble. In this way two metal walls and a gas space separate the molten salt from contact with water and steam. Further, such an assembly provides a controlled resistance to heat flow, which prevents freezing of salt on the thimble. Three full-size thimbles were tested in a heated tank of salt. When the salt was at 1350°F, 6.3 kilowatts of heat was removed by each tube. The system was undamaged by 31 thermal shocks caused by cold water. Design studies for a large steam generator indicated that the power output could be increased to 250 kilowatts per tube for tubes that are 20 feet long and have a diameter of $1\frac{1}{2}$ inches.

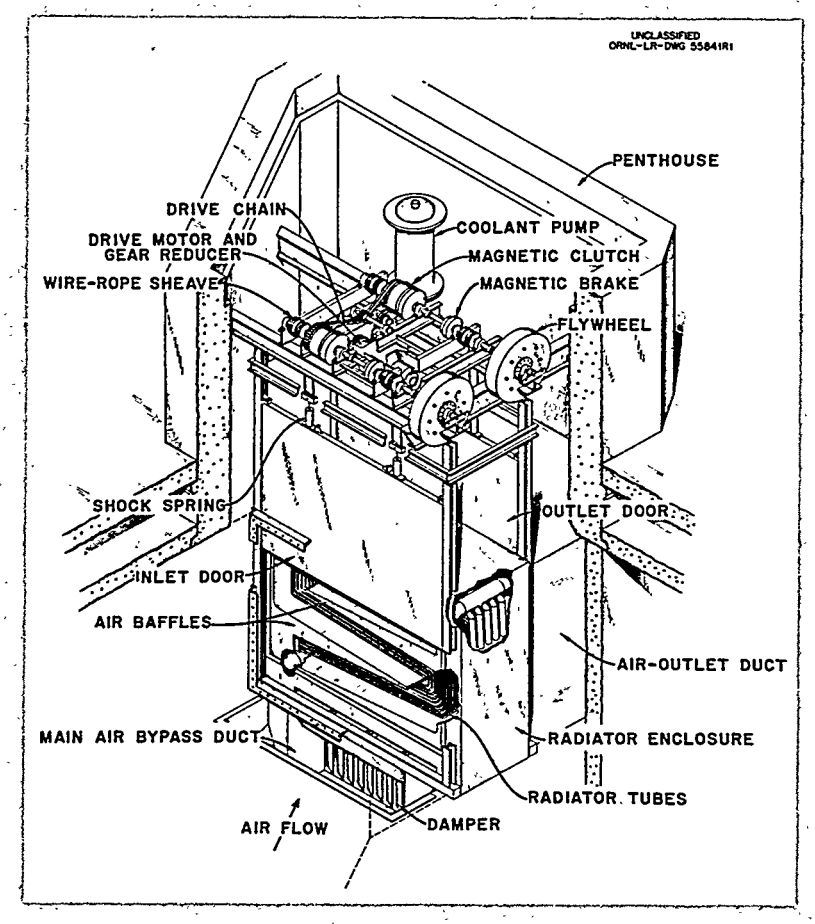

MSRE radiator coil and enclosure.

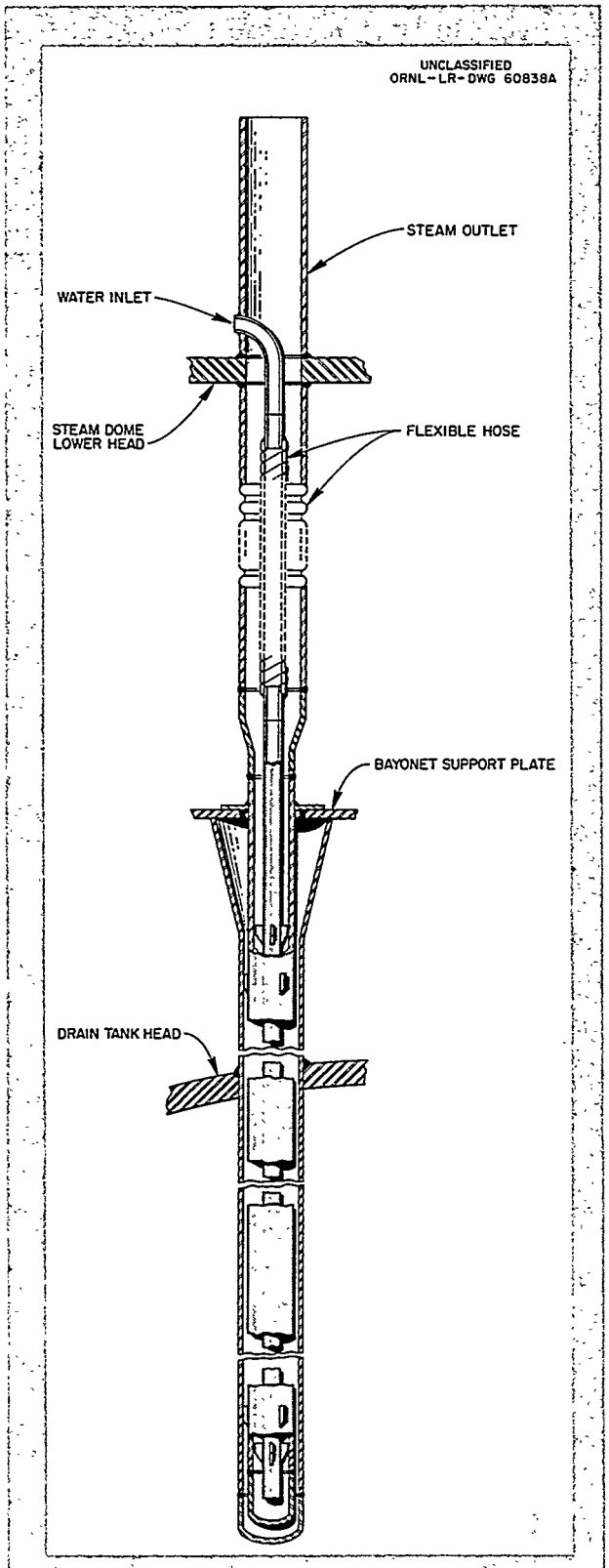

Thimble for containing the bayonet-tube assemblies that cool the molten salt in the drain tank.

Making Pipe Joints Remotely

A major problem of fluid-fuel reactors is that of providing reliable joints which can be used in the remote assembling of equipment and piping. Welded joints are preferred, but methods for remote welding and inspection are not yet developed; so, flanges are used for most applications. Freeze flanges will be used in the 5-inch-diameter pipes which join the pump, heat exchanger, and reactor vessel and the coolant lines to the heat exchanger. The flanges are uninsulated; therefore salt freezes in the gap between the flange faces and provides a seal. Fission-product gases are prevented from escaping by the buffered ring-joint seal. A satisfactory gas seal was difficult to maintain with flanges of early designs because thermal cycling produced permanent distortion of the flanges and the ring. Thermal-cycle tests indicate that the difficulties have been overcome in the final design of MSRE flanges.

A brazing method is being developed for joining some of the smaller pipes. Piping on the equipment to be replaced is cut, the equipment is removed from the cell, and the stubs that remain in place are tapered, all by remotely operated machines. Piping on the new component has specially machined ends, and these ends are fitted with preformed sheets of 82% gold–18% nickel brazing alloy. Simple, expendable induction furnaces are assembled over the parts to be joined; the pieces are placed together and brazed at 1800°F in an inert atmosphere. Equipment for these operations and the joint design are shown below, where the stepwise operations and a completed tapered joint are pictured. Test joints produced in this manner routinely withstand test pressures of 4000 pounds per square inch without leaking. Ultrasonic techniques have been developed for examining the joint nondestructively, and these are being modified for completely remote operation.

Mechanical Disconnects

Several mechanical disconnects have been developed for use in auxiliary lines in the MSRE. They should find application in other systems which require tight joints. The combination ring-joint–Flexitallic flange saves space by manifolding four lines into a single standard ring-joint

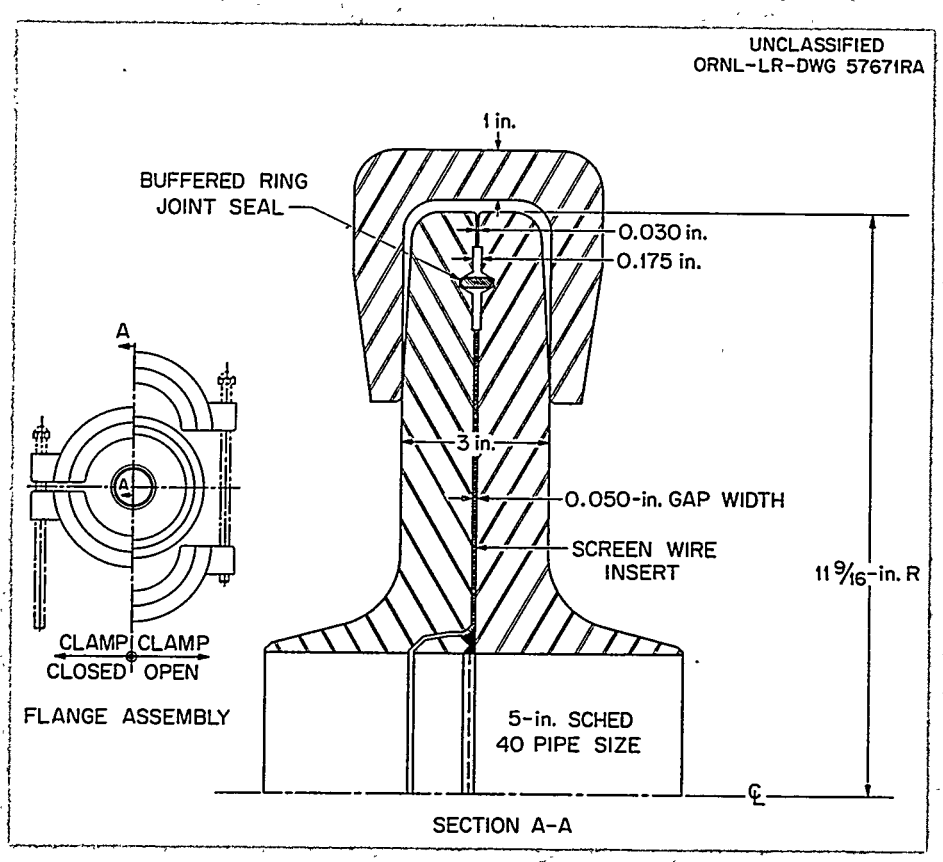

Five-inch molten-salt freeze flange.

flange assembly. In thermal-cycle tests at temperatures to 250°F, the leakage in the outer ring seal was below 0.1 of a standard cubic centimeter of helium per day at a pressure of 500 pounds per square inch, and the leakage between Flexitallic inserts was below 100 cubic centimeters per day.

The ring-joint spring clamp is a double-joint buffer disconnect which was tested at 1200 to 1500°F pipe temperature for over 1000 cycles. Leakage of helium buffer gas from between the double seals was less than 1 cubic centimeter a day. In the yoke-mounted single-cone and dual-seal disconnects, small conical rings are deformed into the rigid blocks. In the dual-seal design, a buffer can be introduced between two seals. These quick disconnects worked well up to 325°F.

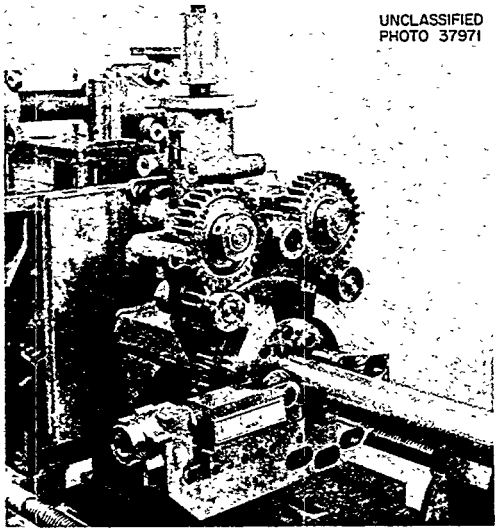

CUTTING THE PIPE

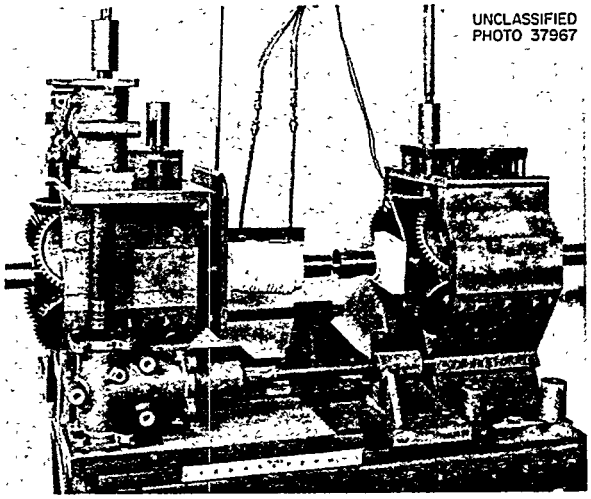

JOINT AND FURNACE READY TO BE ASSEMBLED

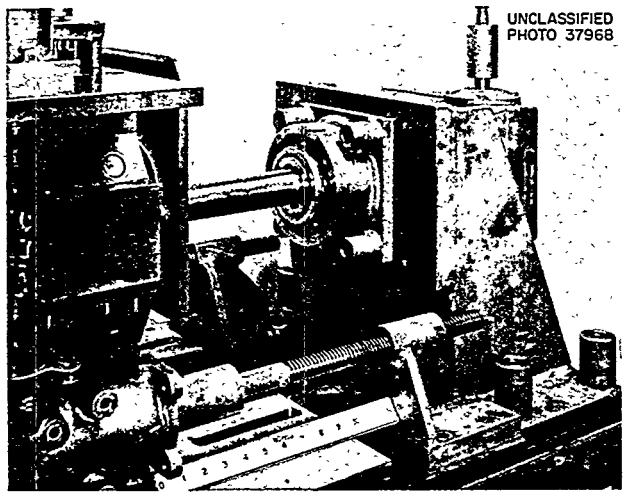

TAPERING THE PIPE

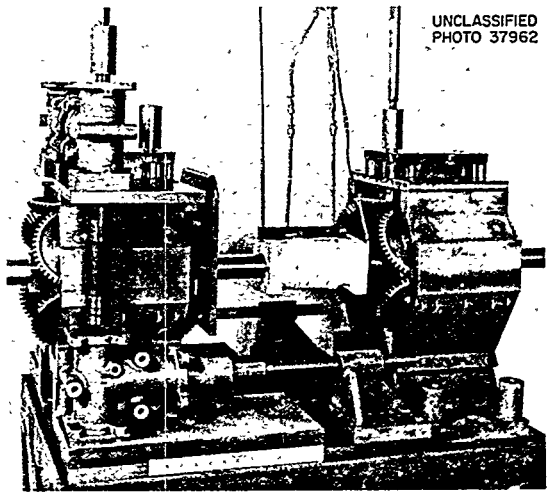

JOINT AND FURNACE ASSEMBLED PREPARATORY TO BRAZING

Equipment for cutting and joining pipe.

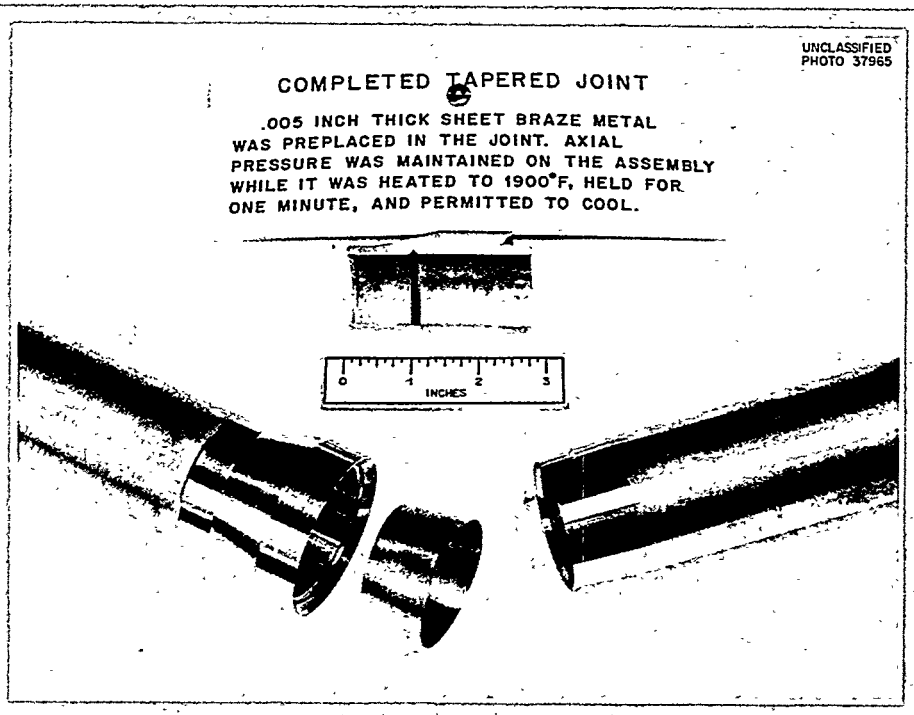

Completed tapered joint.

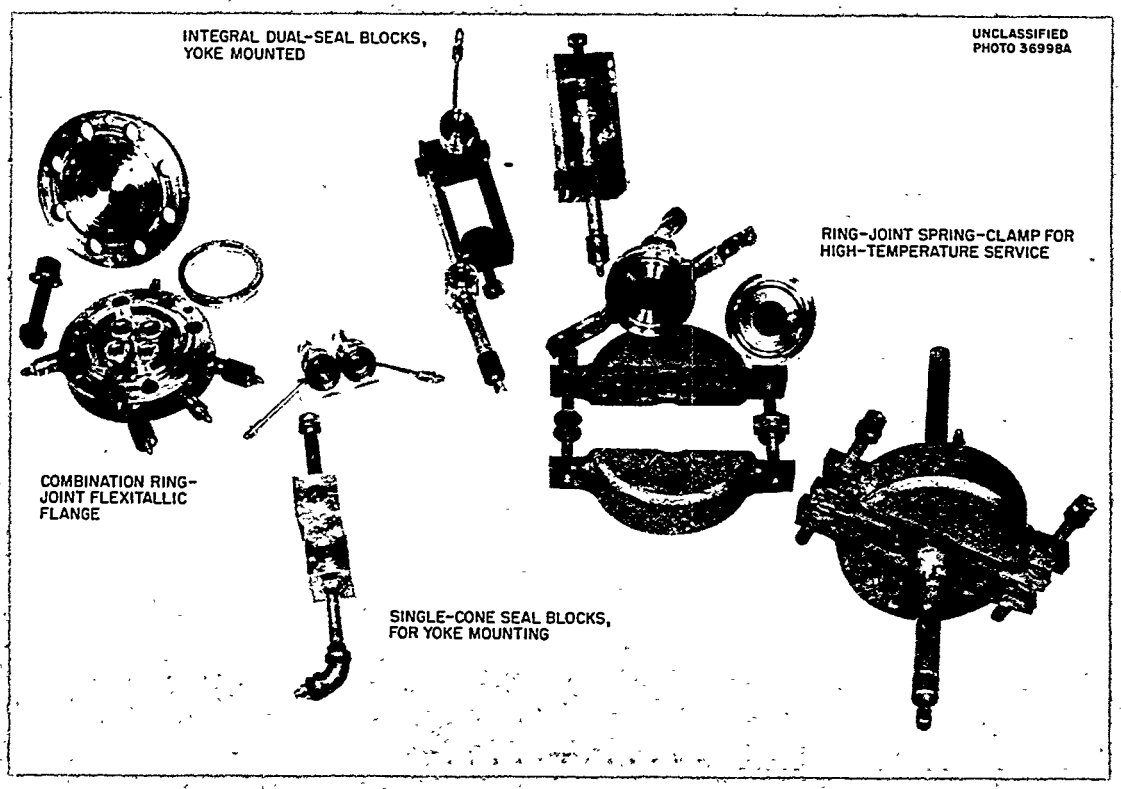

MSRE disconnects. Notice that space is saved by manifolding four pipelines into one assembly (see upper left corner of photograph). Mechanical pipe disconnects are useful in lowering maintenance costs. A variety of disconnects have been developed to fill the needs for different service conditions of temperature, pressure, and process fluids.

Nuclear Safety Program

An important problem now receiving increased attention is the evaluation of the consequences of accidents involving nuclear reactors. The selection of safe reactor sites depends on a realistic evaluation of the possibility of release of toxic fission products following an accident. Furthermore, the cost of the reactor installation is dependent, to a large extent, upon the degree of containment which must be provided to confine the toxic materials in the event of a catastrophe. In studies at ORNL, measurements of both out-of-pile and in-pile release of fission products from uranium dioxide fuels are being carried out, and the characteristics and behavior of the resulting fission-product aerosols are being determined.

OUT-OF-PILE FISSION-PRODUCT RELEASE

In the out-of-pile studies, various fission-product release processes which may occur in UO_2-fueled power reactors as a result of a loss-of-coolant accident were evaluated. On overheating fuel samples in inert atmospheres, a partial release of the volatile fission products was observed only at temperatures above 1400°C. Above 1400°C the volatilized fraction increased uniformly in the following order: tellurium > iodine > xenon-krypton > cesium > ruthenium > strontium. When heated in air, combustion of uranium dioxides takes place, and a larger portion of the volatile fission products are released, as well as small quantities of those having the higher boiling temperatures.

In the most disastrous case (the melting of uranium dioxide), the highest release of the volatile fission products takes place, and appreciable volatilization of such refractory materials as strontium and cerium occurs. Fission-product-bearing uranium oxide aerosols were formed only under the most severe conditions — that is, uranium dioxide melting. Because of the very high release from even trace-irradiated UO_2 on melting, a significant burnup effect could not be detected. A comparison of release rates on oxidizing successively more highly irradiated UO_2 clearly indicated an enhancement factor of 1 to 5 for irradiation levels reaching 11,000 megawatt-days per ton.

IN-PILE FISSION-PRODUCT RELEASE

In experiments designed to simulate reactor accidents more realistically, miniature fuel elements (uranium dioxide) were placed in the ORR and melted or vaporized by fission heat. Temperatures estimated to be above 3300°C (6000°F) were produced. Although most of the fission products were released from the UO_2, the fission-product elements cerium, zirconium, barium, and strontium were almost completely retained in the high-temperature zone, while almost all the volatile fission products and 5% of the ruthenium were released.

CHARACTERIZATION OF RELEASED FISSION PRODUCTS

On examining the vaporized solids released on melting of uranium dioxide, it was shown that almost all the released fission products are associated with the 0.01- to 0.1-micron-size uranium dioxide particles, which form the aerosol. Other than the rare gases, only iodine is significantly depleted in the aerosol particles. A method for further characterizing radioactive materials, based on their diffusion coefficients in gases, was developed. It was found that radioiodine adsorbs on aerosol particles which might be formed during a reactor accident and that these particles are capable of penetrating iodine adsorbers.

High-Temperature Materials Development

CORROSION OF METALLIC COMPONENTS BY MOLTEN OR BOILING ALKALI METALS

Many designs of high-performance nuclear power plants such as those intended for space applications are based on the use of molten or boiling alkali metals for heat transfer or for thermodynamic working fluids. The selection and development of suitable container materials for these unusual high-temperature working fluids is a major problem in the development of such power plants because of the corrosive reactions which may occur between metallic components of the system and molten-alkali metals. Potassium is one of the most attractive of the alkali metals for use as a reactor coolant and thermodynamic working fluid in high-performance nuclear power plants. Consequently, the effect of potassium in both the liquid and vapor states on metallic components has been under study at ORNL.

There are several ways in which molten-alkali metals may attack container metals, including metal solution, erosion, and impurity reactions. Impurities in liquid metals such as oxygen, nitrogen, and carbon may be particularly important since they can alter the mode of attack by changing the surface activity – for example, by changing the wetting nature of the molten alkali – and by introducing chemical reactions involving the impurity itself. In general, the impurities react and stabilize with that constituent which yields the compound having the lowest free energy of formation. Thus, compounds of oxygen, nitrogen, or carbon may be formed on the surface of the container, or constituents of the container may be leached out by the preferential formation of new compounds in the liquid metal.

In a complex power plant system involving the boiling of liquid potassium, the transport of high-velocity vapor, and the condensation of a high-purity liquid, conditions exist for any of several types of corrosion to occur. Thus, in order to identify the rate-controlling processes or mechanisms in each portion of this complex system, much basic information is needed, including the solubility of elemental metals in potassium, velocity effects, and reactions involving impurities.

The investigators at Oak Ridge National Laboratory have used two principal methods for studying corrosion in such a system. One method is called the refluxing-capsule test. In this type of test, specimens of container metals are exposed to potassium which is being boiled, condensed, and reboiled continuously. The purpose is to obtain qualitative information about the corrosion behavior of refractory metals and alloys in contact with refluxing potassium in the range 800 to 1000°C. The apparatus is shown schematically. It consists basically of a metal capsule with sleeve-type specimens located in the condenser region, high-temperature heaters, radiation shields, and a vacuum-containment system. The principal effects evaluated are the influence of condensing rate, exposure time, and test temperature. Columbium alloys have been tested at condensing rates of 5 grams per square inch per minute for test times ranging from 100 to 1000 hours.

A second test method uses a boiling-potassium loop. Sleeve-type insert specimens are positioned in the vapor and subcooled portions of the system. These can be removed for weighing in order to quantitatively measure weight gained or lost as a result of corrosion. In addition, subsize tensile specimens are provided in various regions in order to measure the effect of corrosion on strengths and ductility. Boiling loops of this type have been operated continuously for scheduled times up to 3000 hours. Materials of construction have included nickel-base, iron-base, and cobalt-base alloys.

Corrosion phenomena observed in such loops included mass-transfer of iron, nickel, chromium, and carbon. In mass transfer, the liquid metal dissolves material from the hot portions of the loop and deposits it in cooler regions. The extent

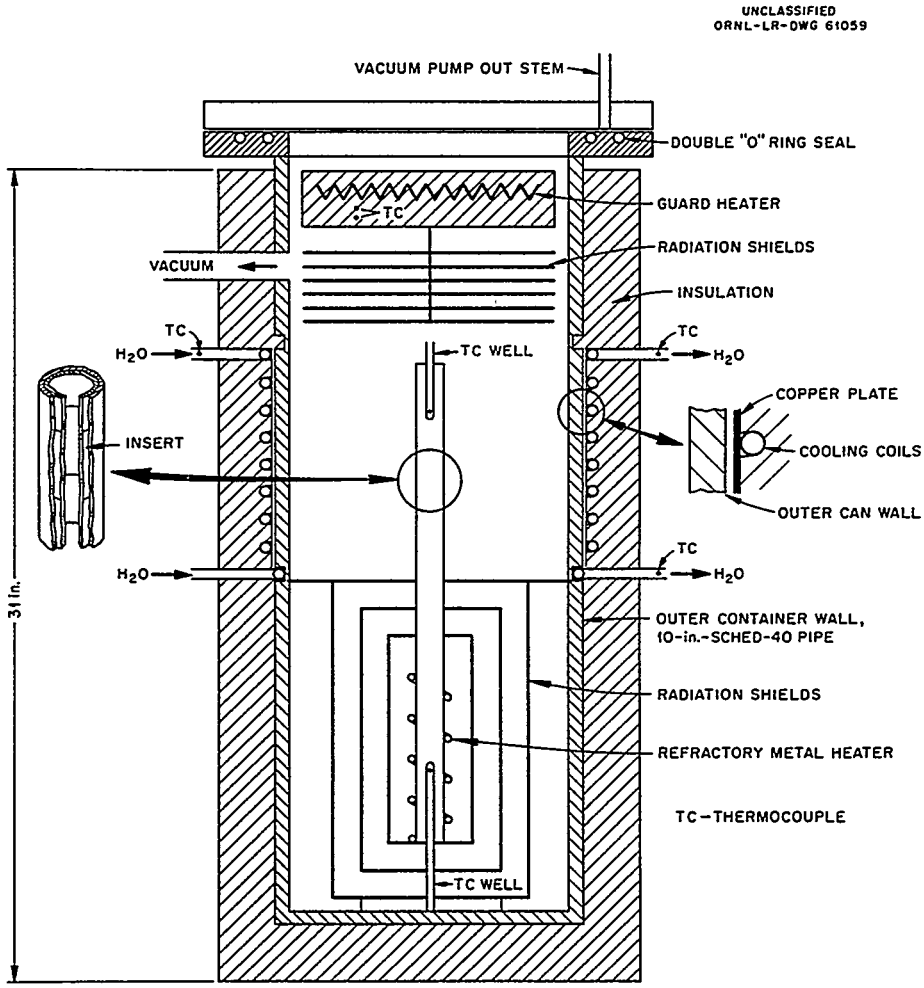

Refluxing capsule for studying the corrosion of metals by potassium.

of mass transfer measured by means of weight changes in recent tests at 1600°F is illustrated in the graph below. Notice that weight losses occur uniformly throughout the region of the loop in which potassium is condensing and that weight gains occur in the regions of the loop in which the potassium is a subcooled liquid.

OXIDATION OF COLUMBIUM AND COLUMBIUM-BASE ALLOYS

The effects of oxygen pressure, temperature, composition of the gaseous atmosphere, and alloying elements on the oxidation rates of columbium and its alloys are being studied at ORNL. This information is needed in the development of oxidation-resistant columbium alloys for use in environments that contain oxygen at very low pressures, near 0.001 millimeter of mercury. A major phase of this research was a study of the oxidation behavior of unalloyed columbium.

The oxidation rate of columbium in oxygen at pressures between 0.00003 and 0.005 millimeter of mercury and in the temperature range of 850 to 1200°C was found to be much less than at atmospheric pressure, lower by factors of 100 to 1000. In spite of these reductions in reaction rate, the metal was severely embrittled after exposures of 5 to 7 hours. Under these test conditions the columbium oxidized in four distinct stages which could be correlated with the formation of solid solutions of oxygen in columbium, followed by

UNCLASSIFIED
ORNL-LR-DWG 47744R2

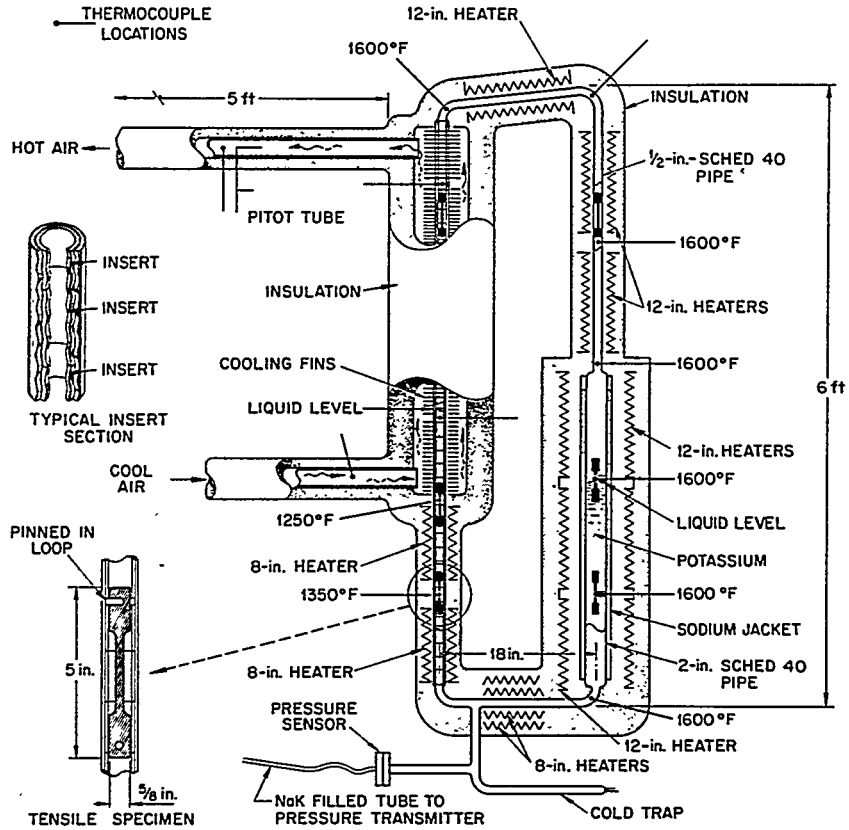

Boiling-potassium loop for studying the corrosion of metals by potassium.

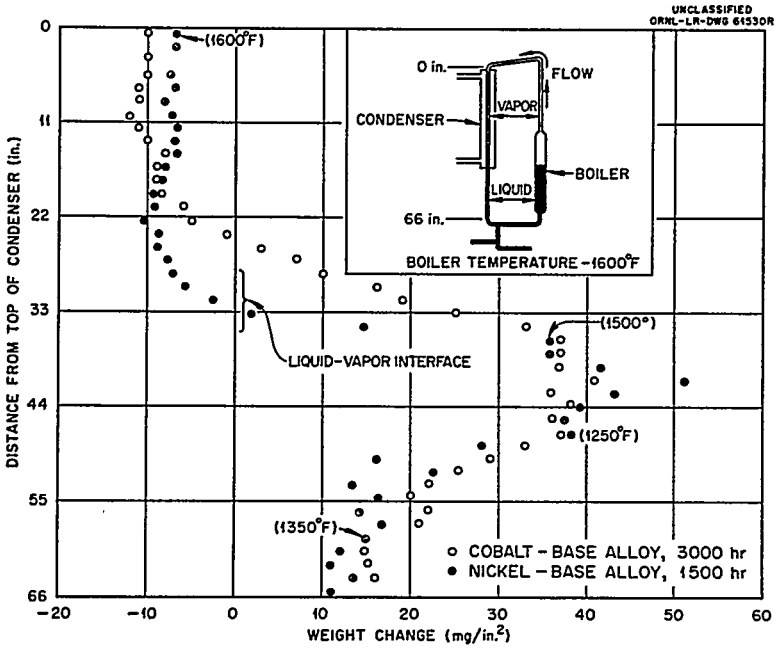

Profile of weight changes of insert specimens in boiling-potassium loop tests.

formation of the columbium oxides: CbO, CbO_2, and Cb_2O_5.

From the rate curves and the nature of the reaction products the events that occurred during each stage were deduced. Solid solutions of oxygen in columbium formed when the rate of oxygen diffusion within the metal was high enough to prevent the buildup of a short gradient of oxygen concentration at the metal surface. Favorable conditions for the formation of solid solutions were, therefore, low oxygen pressure and high temperature. Initially the weight gain was linear with time, but it became parabolic as the solubility limit of oxygen in columbium was approached. The second and third stages were characterized by a parabolic weight gain. During these stages the oxides of columbium increased in concentration, forming a somewhat protective layer of CbO_2 and Cb_2O_5. The fourth stage was characterized by a lessening of the protective nature of the film. The reaction rate became faster, and the weight-gain curve changed to linear.

HIGH-TEMPERATURE EVAPORATION OF METALS IN VACUUM

When hot metals are exposed to the extremely high vacuum of outer space, appreciable evaporation may occur. This will result in the loss of base metal and alloying elements at rates which depend on the temperature, the composition of the alloy, and the absolute pressure. It is therefore important to determine the limiting conditions for which a number of alloys could be useful as structural materials in space.

A number of simple analytical models exist for predicting the rate at which pure metals will vaporize under controlled conditions. However, these theories do not adequately predict the rate at which elements evaporate from complex alloy systems. Experiments were conducted at ORNL for several nickel-, cobalt-, and iron-base alloys in vacuum at temperatures up to 1800°F. Results indicated that there is a preferred sequence in which the constituent elements are released. Carbon, chromium, and manganese are the most volatile elements in these alloys. Below 1600°F, the rate of evaporation from the surface controlled the loss of elements from the alloys. Above 1900°F, the rate of diffusion to the surface limited the rate at which elements were lost. Between these two temperatures, both processes were important in determining the rate of loss by evaporation.

PROTECTIVE ATMOSPHERES FOR REFRACTORY METALS AT HIGH TEMPERATURES

Research and development programs concerned with refractory metals for high-temperature applications face a continual problem of preventing contamination of the active metals. This problem pervades all stages of processing from the initial production of the metal in billet form to the construction and high-temperature operation of a useful device. Although a general grouping of refractory metals according to protective atmosphere is possible, each represents a special problem. As an example, hydrogen is a protective environment for molybdenum and tantalum, but it seriously embrittles columbium. Oak Ridge National Laboratory is investigating gaseous environments and other conditions that can be tolerated by columbium without seriously affecting the finished metal.

Experiments at ORNL indicated that a vacuum of 0.00001 millimeter of mercury provides sufficient protection for columbium if the temperature of the metal does not exceed 1800°F and if the exposure time is not longer than 100 hours. Based on these results it was estimated that equivalent protection would be provided by an inert-gas atmosphere which contained not more than 1 part of active impurity per 100,000,000 parts of inert gas. By use of a closed, circulating gas system in which the gas was continuously purified by hot titanium, an inert-gas environment was achieved which provided protection equivalent to that in the vacuum experiments described above.

STABILITY OF REFRACTORY ALLOYS DURING SERVICE

One important facet of a metallurgical evaluation program is that of determining whether long-time

exposure to high temperatures alters the mechanical properties of an alloy. Changes such as loss of strength or loss of ductility have important significance in the design of components for long operation at high temperatures. ORNL has been studying the stability of refractory alloys under long thermal exposure in order to identify those metals that might be subject to such deterioration and to determine if some solution can be found in specific cases.

Columbium alloyed with 1% zirconium is one alloy which suffers a significant loss of ductility during exposure to certain temperatures. Since significant loss of ductility does not occur in commercially pure columbium, the implication seemed to be that the zirconium was responsible for the aging. With this hypothesis as a focal point, investigations at ORNL revealed the following:

1. Aging occurs when the oxygen content exceeds the limit of its solubility in the alloy.

2. Zirconium reduces the solubility of oxygen in columbium from over 6000 parts per million in pure columbium to about 300 in the alloy.

3. Zirconium oxide was identified as the precipitate that is produced during aging.

4. Overaging treatments can restore the lost ductility.

5. Weldments are as susceptible as the wrought metal to embrittlement.

JOINING OF REFRACTORY METALS BY BRAZING

The favorable high-temperature properties of refractory metals offer an opportunity to more completely utilize the total energy available from nuclear fuels, but there are a number of problems attendant to the use of such metals as structural materials. One problem that requires serious consideration is the joining of a refractory alloy to itself or to other materials. This is being studied at ORNL from the standpoint of developing methods for joining and evaluating the performance of the joints.

One attractive approach is the use of brazing alloys. An evaluation program was conducted here; it included shear tests, fatigue tests, corrosion, and aging studies of various brazing alloys. The study was begun by using columbium as the structural metal. Of the many brazing alloys examined, the zirconium- and titanium-base brazing alloys produced joints with the best strength.

The joining of columbium to iron-base alloys creates additional problems. In addition to the need for a brazing alloy which will wet and flow on both of these metals, some method must be found to avoid the cracking which results from the differences in coefficients of expansion. One solution to the problem of avoiding the high stresses in the joints thus developed is the use of a transition material, one that has an intermediate coefficient of expansion. In the experiments at ORNL, vanadium and iron have shown some promise for this application.

Engineering Science: Heat Transfer

FUNDAMENTAL HEAT TRANSFER AND FLUID MECHANICS

Fundamental investigations into the mechanisms of turbulent momentum and heat transfer are included in the program of engineering research at ORNL. These studies are required to provide a better knowledge of the nature of turbulence both as a basic contribution to the understanding of flow phenomena and in support of advanced reactor heat-transfer and coolant technology.

While much effort, both theoretical and experimental, has been expended in the field of fluid turbulence, there is still little fundamental knowledge of the complex eddy mixing processes which have a dominant effect on the mean velocity profile and on the transport properties of turbulent fluids. For example, the mean surface stresses in a volume element caused by the eddy motion (the so-called Reynolds stresses) which are needed for a solution of the differential equations of turbulent flow are not known. Future progress in this field rests heavily upon accurate measurement of these Reynolds stresses.

To this end, a water loop has been constructed to meet the exacting requirements for successful hot-wire anemometry; the water must contain no particulate contaminants and be nearly gas-free, and extraneous vibrations in both the flow and piping must be damped. These requirements have been accomplished sufficiently that steady hot-wire signals in flowing water have been achieved. Improvements in the wire sensing element are now being made to obtain the required velocity-direction sensitivity.

An improved theory relating the hot-wire signal to the Reynolds stresses has been formulated. It is planned to carry out the measurements in a straight pipe and in converging and diverging geometries.

A fundamental investigation is also under way in which the relationship of fluid turbulence to heat transfer in general, and to the temperature of a fluid-solid heat-transfer interface in particular, is being quantitatively studied. For example, measurements are being made of the random temperature fluctuations at the inside surface of a heated pipe through which a fluid is flowing turbulently; these temperature fluctuations are the result of exchange of heat between the wall and fluid eddies characteristic of flow and are a potential source of fatigue damage. It is known from earlier ORNL studies that thermally induced transient stresses can cause fatigue failure in metals [*Nuclear Sci. and Eng.* 9, 462–74 (1961)].

Significant thermal transients may originate, for example, at the fuel-coolant interface in a nuclear reactor by the mechanism already discussed. In the case of fluid-fuel reactors, the transient structure of turbulent flow, residual hydrodynamic instabilities, and the possibility of adverse temperature profiles are potential sources of temperature oscillations in the fluid which will be felt at the core wall and which will persist to a degree in the fluid leaving the reactor core. The problem is aggravated by the large temperature gradients normal to the bulk flow which may exist in high-temperature, high-performance reactors. The study of fluid turbulence in relation to thermal instabilities is therefore aimed at delineating both the sources of, and important variables influencing, the induced thermal stresses.

Quantitative measurements of instantaneous surface temperatures in a heated 2-inch stainless steel pipe with water in turbulent flow as the fluid have been made (see illustrated test section). "Gun-barrel" type thermocouples which have microsecond thermal response were used as the surface-temperature sensing elements. The pipe was heated by Calrod heaters cast in the 7-inch-OD aluminum jacket as indicated; this construction provided the required uniformity of heat flow at the inner surface of the pipe. Steady flow of water was provided by means of constant-head tanks, thus eliminating the need for a pump, which could

introduce flow instabilities. The geometry was such as to provide 45 diameters of hydrodynamic entrance length and 36 diameters of thermal entrance length. In the future, it is planned to study the effect of decrease in entrance length and of changes in inlet geometry to obtain information which will be of more direct application to design of reactors.

The low-level thermal electromotive forces were amplified by a factor of 10^4 and analyzed by means of an analog filtering device using the techniques of frequency domain analysis developed originally for communications and control engineering problems. This analysis was used to compute the preliminary power spectral density (PSD) of the surface temperature fluctuations plotted below. Here the PSD is a statistical quantity defined as the mean-square fluctuation per unit bandwidth. Note that most of the transient thermal power per unit bandwidth is in the range of frequencies below 5 cycles per second; these low frequency thermal oscillations are believed to be significant from the standpoint of thermal fatigue.

It is intended in the future to study the correlation of surface temperature fluctuations with turbulence

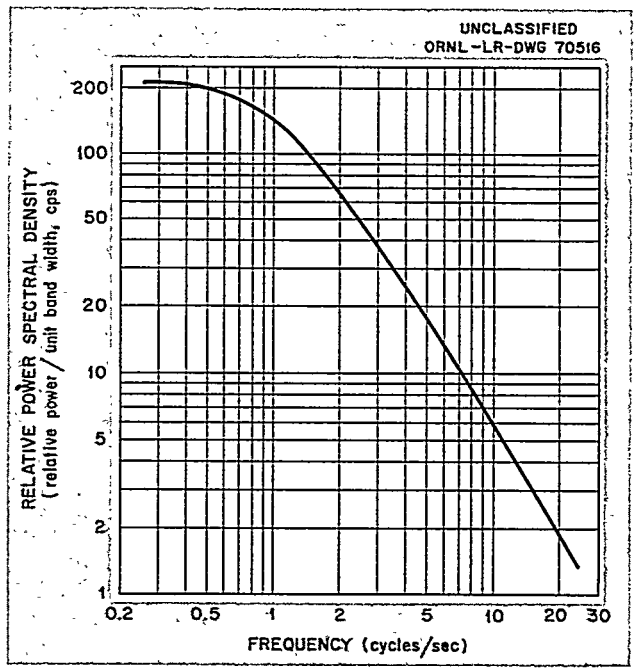

Preliminary power spectral-density analysis of surface thermal instabilities for turbulent flow of water in a 2-in. heated pipe at a Reynolds modulus of 73,000.

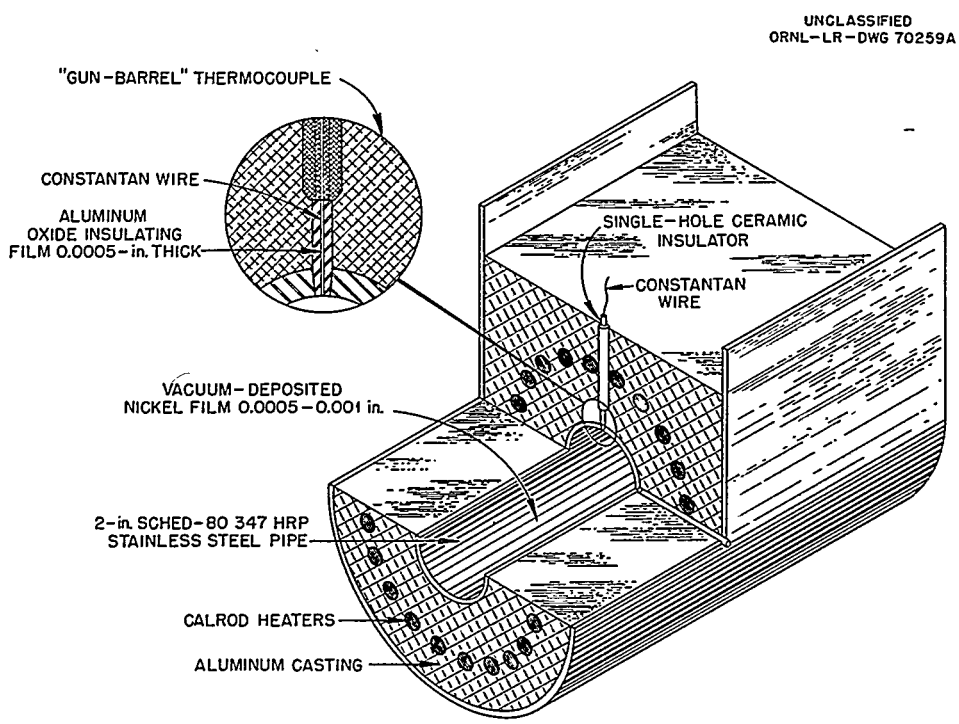

Test section for study of temperature fluctuations at a heat transfer surface. The "gun-barrel" thermocouple provides microsecond thermal response.

in the free stream using the hot-wire anemometry equipment which is currently being employed in the fundamental turbulence research. Such information is needed for a better understanding of the mechanisms involved and as an aid in developing an analytical description.

The techniques developed for measurement of surface temperature fluctuations in single-phase forced-convection heat transfer will be applied also to the case of forced-convection subcooled and saturated boiling, in order to gain knowledge of the local thermal instabilities associated with the boiling process (including potential burnout conditions). Such knowledge is desired not only in relation to the thermal-stress fatigue problem but also as an aid toward a better understanding of boiling heat transfer.

Although the work thus far has been exploratory, sufficient knowledge has been gained to indicate that quantitative measurements of surface thermal transients can be made and that the data can be read out in useful form. It is believed that the results of this study will, in addition to providing information of interest in reactor design, contribute to a better understanding of turbulence in general and of boundary-layer phenomena in particular.

HEAT TRANSFER AND COOLANT TECHNOLOGY

Also included among the engineering-research activities at ORNL are studies of the heat-transfer and hydrodynamic behavior of two-phase systems applicable to advanced reactor technology.

Because of the very high heat-transfer rates attainable with small temperature potentials under nucleate-boiling conditions, there is great interest in this mode of heat removal for high-performance constant-heat-input devices such as nuclear reactors, particle-accelerator targets, microwave-tube anodes, and electromagnets. Since the rate of heat generation in these devices is essentially independent of the rate of heat removal, burnout of the cooled surface may occur if the heat flux exceeds a critical value at which transition occurs from the highly efficient nucleate-boiling mode to the film-boiling mode. In the latter situation, the liquid phase is separated from the cooled surface by a film of vapor of high thermal resistance. The critical or transition heat flux is often termed the "burnout" heat flux.

In order to increase attainable limits of critical heat flux, a swirl-flow boiling technique has been developed and investigated at ORNL during the past four years. This approach, which involves swirling the coolant either by inlet tangential wall slots or full-length and full-diameter twisted tapes, generates a vortex coolant motion within circular passages. Such a fluid motion causes vapor bubbles and heated liquid near the cooled surface to be displaced radially inward by the cooler, denser liquid which moves radially outward under the influence of centrifugal force. The beneficial effects of keeping the wall more nearly vapor-free are evidenced by the attainment of critical heat fluxes as large as 55×10^6 Btu hr^{-1} ft^{-2} – almost three times the energy flux from the surface of the sun. In straight flow at comparable pumping powers, the critical heat flux is approximately 20×10^6 Btu hr^{-1} ft^{-2}, increasing very slowly with increase in pumping power. Early studies were conducted with water and air, and prediction correlations for swirl-flow heat transfer coefficients and friction factors as well as for critical heat flux have been developed.

To gain a more complete understanding of swirl-flow heat transfer, the influence of the thermophysical properties of the coolants on the swirl-flow mechanism is being studied. To this end, a comprehensive study of the high-heat-flux characteristics of pure ethylene glycol was recently conducted. The swirl-flow friction factors determined for this liquid were in reasonable agreement with those predicted by a generalized correlation developed earlier from the water and air data (ASME Paper No. 62-HT-42, to be presented at the Fifth National Heat Transfer Conference, Houston, Texas, August 1962). All ORNL nonboiling swirl-flow heating data (for water and ethylene glycol) were correlated within an average deviation of ±12% with a single expression utilizing the buoyant force per unit volume of boundary-layer liquid. In order to obtain swirl-flow correlations generally applicable to a still broader range of fluid properties, future studies with gaseous helium and liquid mercury are planned.

The current status of swirl-flow heat transfer has also been evaluated. All data available through January 1962 for pressure drop, nonboiling and boiling heat transfer, and burnout were collected and compared on uniform bases. Although more

work is needed to extend the ranges of the variables, to better delineate the mechanisms involved, and to develop more comprehensive correlations, this study clearly shows that heat transfer rates in both the nonboiling and boiling regimes may be considerably augmented with no increase in pumping power by properly swirling the coolant.

Because of the importance of a knowledge of the critical heat flux in a boiling system, a great many equations have been proposed for its prediction. Useful as these correlations have been for specific purposes, most of them are severely limited by (1) their applicability to only a single fluid, usually water, (2) the arbitrary statistical nature of their derivation, which permits no extrapolation, (3) the use of widely variable exponents and "constants" for different regions of the variables, and (4) the relatively small variety of data on which a single correlation is usually based.

In an effort to improve this situation, a new generalized two-termed additive prediction method has been developed at ORNL in which one term represents the boiling contribution to the burnout heat flux in the absence of forced convection and the other the equivalent forced-convection contribution in the absence of boiling. The predictions of this superposition method have been compared with all available experimental data (1263 tests) for burnout with flowing, wetting liquids in the absence of significant net vapor generation. The data compared are for seven fluids in axial, swirl, and cross flow in tubular, rectangular, annular, and rod geometries over very broad ranges of flow conditions: velocities of 0.05 to 174 feet per second, pressures from 4.2 to 3000 psia, subcoolings from 0 to 506°F, centrifugal intensities of 1 to 57,000 *g*'s and burnout heat fluxes from 0.1×10^6 to 37.4×10^6 Btu hr^{-1} ft^{-2}.

When the data which are not entirely representative of burnout under the experimental conditions are excluded, a selected data field of 815 tests remains, for which 95% of the predictions agree with the experimental values within 40%.

In the boiling term of this correlation, the coefficient varies by ±21% about the mean. This variation is believed to be associated with the apparently intrinsic random nature of the boiling process. Though indirect evidence supports this contention, no direct evidence is available, and a series of repetitive pool burnout tests with water under carefully controlled conditions has been initiated. Comparison of the scatter obtained with the known experimental uncertainty will provide a better idea as to whether or not the critical boiling process is fundamentally a random one.

An understanding of the heat-transfer and flow characteristics of alkali metals under boiling conditions is critical to the design of lightweight Rankine-cycle nuclear-power systems such as those being considered at ORNL and elsewhere for auxiliary space power application. Knowledge of burnout limits, heat-transfer coefficients, and flow stability criteria for potassium boiling near saturation conditions are among the items of immediate interest in support of the ORNL program; and experiments were undertaken to supply the necessary information for potassium boiling under a wide range of exit vapor quality, mass flow, and inlet subcooling conditions.

The first data reported for heat transfer coefficients and "burnout" heat fluxes with the forced-convection saturation boiling of potassium in vertical tubes were obtained from the program at ORNL. The general details of the system assembled for these studies are presented in the following schematic diagram. Liquid potassium was pumped from a cooled reservoir through the vertically mounted boiler to a liquid-vapor separator. An adjustable restriction (valve) upstream of the boiler provided secondary flow control. A tangential inlet to the separator generated the necessary centrifugal forces for separation of the entering vapor-liquid mixture; at low flows, gravity separation appeared effective. The flow rates of the separated streams of liquid and vapor (after condensation) were used to establish the boiler-exit quality. The photograph of the apparatus illustrates the general complexity of high-temperature forced-convection systems required in engineering-research studies.

Initial measurements were made with a simple boiler which consisted of a 6-foot-long, 1-inch-OD (0.87-inch-ID) type 347 stainless steel tube heated by clamshell heaters, and capable of operation at a maximum heat flux of 40,000 Btu hr^{-1} ft^{-2}. This low-flux boiler was replaced later by a high-flux boiler of unique design to enable operation at a maximum heat flux of 500,000 Btu hr^{-1} ft^{-2}. This boiler was formed by brazing a stack of twenty-one 5-inch-OD × 2-inch-thick OFHC copper disks to a 0.325-inch-ID × 0.028-inch-wall type 347 stainless steel tube. Heat was provided by a set of 21 clamshell heaters located external to the

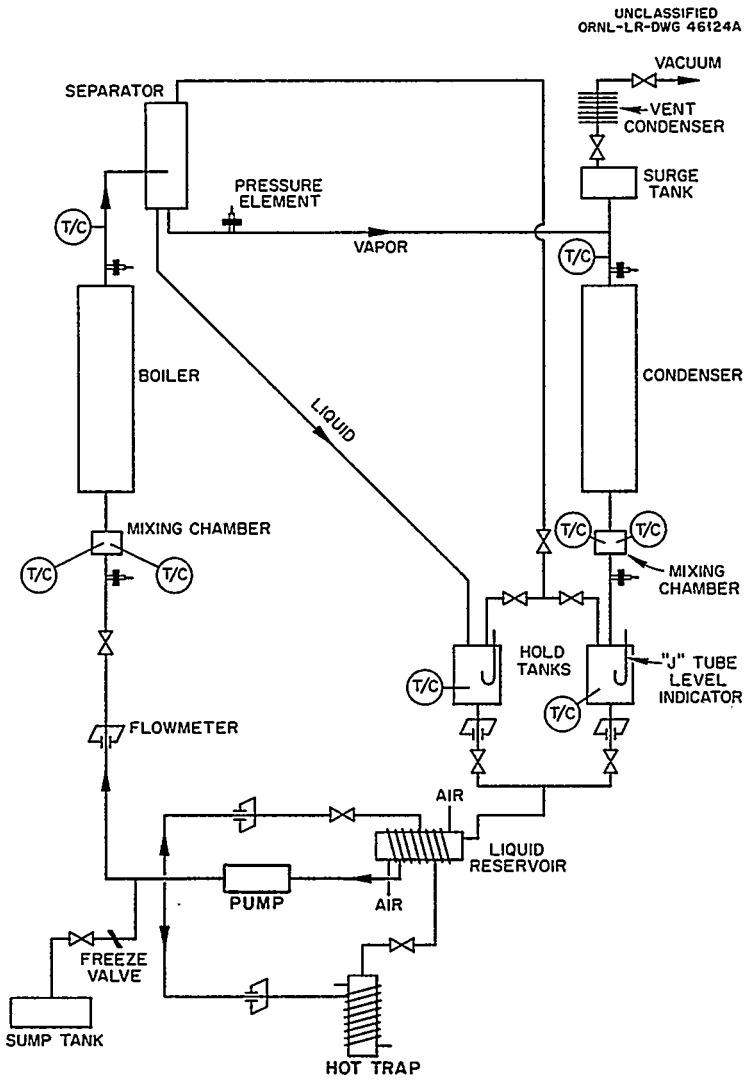

Schematic of system for study of saturation boiling with potassium. Liquid potassium is moved by an electrodynamic pump from a cooled reservoir to the vertical boiler; the boiler effluent mixture passes to a liquid-vapor separator, and the liquid and condensed-vapor streams are returned by gravity flow to the reservoir.

copper disks. The disks served a threefold purpose: (1) through the converging geometry, the heat flux was amplified, (2) thermocouples located radially within each disk allowed determination of the heat flux and, by extrapolation, the temperature at the boiling interface, and (3) burnout protection was afforded by the thermal capacity of the copper.

The critical heat-flux values obtained in these experiments are shown in the graph below. Comparison is made in each case to an extrapolation of the results in report NACA-TN-4382 for the forced-convection saturation boiling of water as adjusted to the specific geometries of the two potassium boilers. The agreement between the potassium experimental values and those predicted from water experience is quite good; since the thermal properties of steam and potassium vapor are not too dissimilar, this result is not unexpected.

The above data were obtained during periods of stable-flow operation for which tube-wall temperature oscillations were normally of the order of 2°F and attained significant magnitude (30 to 50°F) only as "burnout" was approached. However, for some conditions, stable fluctuations of very high amplitude (of the order of 250°F) occurred with the low-flux boiler; associated with these temperature fluctuations were related extreme variations in boiler pressure and flow. Under such circumstances, the critical heat fluxes observed were only 60% of those previously attained; this is shown by the "unstable-flow" curve in graph (*a*) for which the exit quality (weight percent

vaporized) was approximately 30% in contrast to the 85 to 95% vaporization achieved with stable flow. These low critical fluxes are believed to represent a film-boiling situation as opposed to the "dry-wall" condition for burnout with stable flow.

It was demonstrated in this study that heat fluxes at least as high as 267,000 Btu hr^{-1} ft^{-2} could be sustained with saturation boiling of potassium at 60% exit vapor quality, and that stable boiling could always be achieved by introducing the liquid feed to the boiler at saturation conditions. It is concluded that critical heat fluxes comparable to those observed for boiling water can be obtained with boiling potassium, at

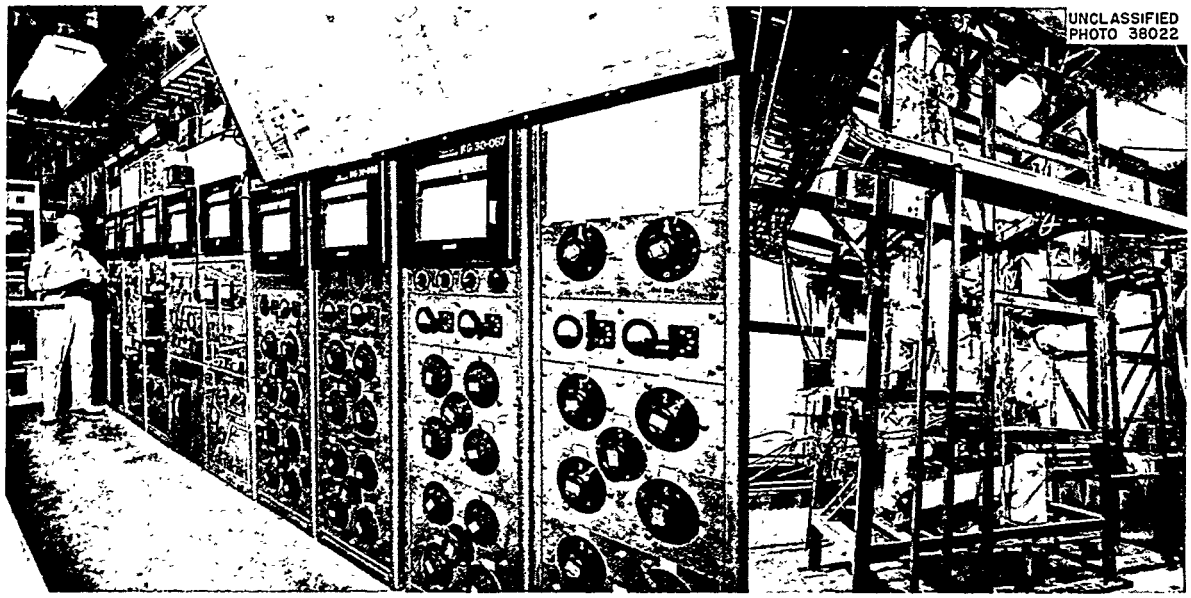

Boiling-potassium heat transfer apparatus. A portion of the instrumentation and control panel for power, temperature, pressure, and flow is shown at left; the loop, insulated for high temperature, is shown at the right.

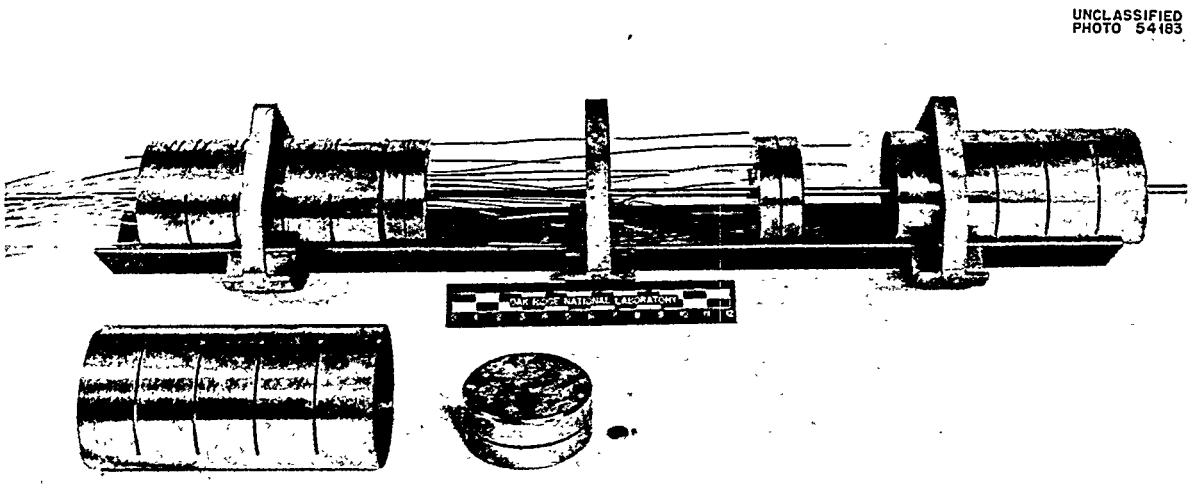

Partially assembled high-flux boiler for boiling potassium studies. The boiler consists of twenty-one 5-in.-OD × 2-in.-thick OFHC copper disks brazed to a 0.325-in.-ID × 0.028-in.-wall type 347 stainless steel tube and is shown positioned within brazing jig; a section of the outer jacket and a typical copper disk are shown in the foreground.

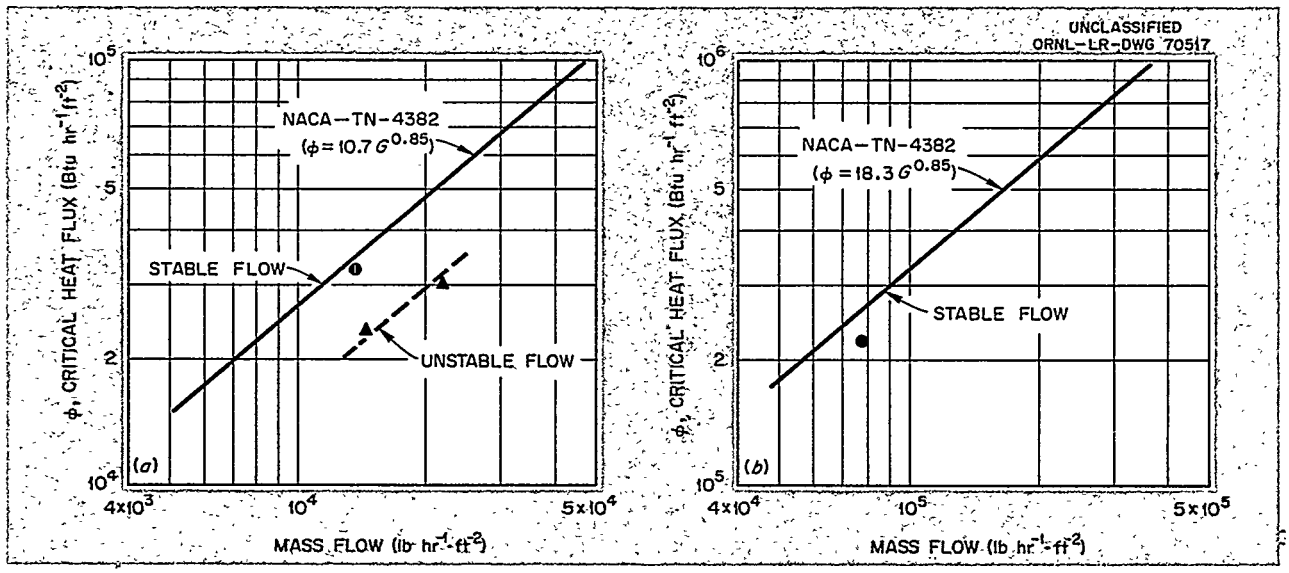

Critical heat flux as determined for the forced-convection saturation boiling of potassium in vertical tubes. (*a*) Low-flux boiler; (*b*) high-flux boiler. Comparison is made with the results from NACA-TN-4382 for water boiling under similar conditions as adjusted to the specific geometries of the two potassium boilers.

high exit vapor quality. Two of the initial objectives of the study have thus been achieved.

In continuing the study of forced-convection saturation boiling of potassium at near-atmospheric pressure, the immediate objectives are as follows: (1) the initiation of a series of experiments to define the temperature path of the fluid between inlet and exit in order to refine the calculation of heat-transfer coefficients, (2) the accumulation of further data on the critical heat flux, (3) the study of stability in the high-flux boiler as a function of inlet subcooling, and (4) the continued examination and correlation of the present data on critical fluxes, heat-transfer coefficients, and two-phase pressure losses during boiling.

The correlation and application of convective heat-transfer data depend on a precise knowledge of the thermophysical properties of the fluid being circulated and/or boiled. The experimental determination of these properties (e.g., viscosity, density, thermal conductivity, heat capacity, etc.) has comprised in the past an appreciable portion of the engineering-research effort at ORNL. While previous interest was directed toward molten-fluoride mixtures, the current orientation is to certain properties of some liquid metals. Since a significant program involving the properties of sodium, potassium, cesium, and rubidium already exists within the United States under the sponsorship of both the National Aeronautics and Space Administration and the Air Force, the work at ORNL has been restricted to those areas not covered by these studies. Thus the determination of the thermal conductivity of liquid lithium has been completed, and an investigation of the surface tensions of the liquid metals (primarily potassium) at the normal boiling temperature has been initiated.

Liquid lithium, by virtue of its wide liquid working range, high boiling temperature, and large volumetric thermal capacity, has received much attention as a reactor coolant. To aid in the evaluation of the suitability of lithium for high-temperature heat-transfer application, the thermal conductivity of this fluid was measured at temperatures up to 1550°F. The conductivity was determined by comparison with a standard material (type 347 stainless steel), utilizing an axial heat-flow apparatus (see diagram). Heat flowed downward from the main heater, through the upper heat meter, the sample region and the lower heat meter, and finally into the water-cooled heat sink. Radial heat flow was prevented by adjusting the guard heaters such as to match the axial temperature distribution in the guard cylinder to that of the test piece; the signals from coplanar Pt vs Pt–10%

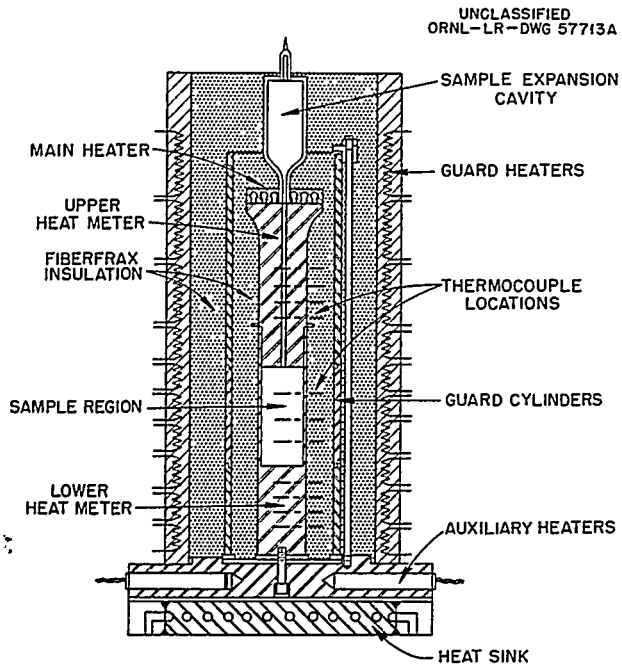

Lithium thermal conductivity apparatus. An axial heat-flow device in which the conductivity of the liquid sample is determined by comparison with a type 347 stainless steel standard (labeled upper and lower heat meters).

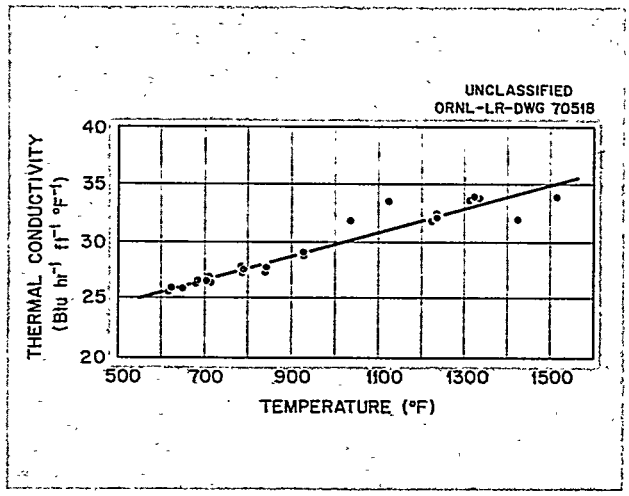

Experimental results for the thermal conductivity of liquid lithium. The data agree well (±10%) with limited earlier data and with theoretical predictions using recently obtained electrical resistivity values.

Rh thermocouples, located in the test piece and the guard cylinder at the indicated levels, were used in controlling the radial heat flow and in determining the axial gradient. Convection in the unoccupied regions central to the guard heaters was minimized by filling with Fiberfrax insulation. The entire apparatus was jacketed by an environmental heater (to establish temperature level) and contained within an evacuated (3×10^{-5} millimeter of mercury) bell jar.

The conductivity of the lithium specimen was calculated by combining the heat flux evaluated from the flow in the heat meters with the temperature gradient measured in the sample. Results for 99.82 weight percent lithium sample are shown in graph form below; the conductivity varied linearly from 25.6 (±7%) Btu hr^{-1} ft^{-1} $(°F)^{-1}$ at 600°F to 35.0 (±12%) Btu hr^{-1} ft^{-1} $(°F)^{-1}$ at 1500°F. Unpublished data obtained by Ewing and Miller at the Naval Research Laboratory over the temperature range 540 to 970°F lie 4% below the present results, while values predicted from theoretical equations (e.g., the Wiedemann-Franz-Lorenz-Sommerfeld equation) using recent electrical resistivity data fall 6 to 10% above the best line through the ORNL data.

An important factor in the correlation and evaluation of two-phase (boiling) data is the surface tension of the liquid against its vapor and against the heated surface. An experimental program to establish this property for the alkali metals at temperatures near their atmospheric boiling points has been initiated, using the maximum bubble-pressure technique. In this procedure an inert gas (or metal vapor) is supplied at extremely low flow to a capillary tube whose end is immersed just beneath the surface of a liquid pool. The pressure at which the slowly growing bubble disengages from the capillary tip is then related to the density and surface tension of the liquid; the density is obtained at the conditions of the experiment by varying slightly the depth of immersion and observing the change in maximum bubble pressure.

The design of an apparatus for extending the measurement of the thermal conductivity of lithium to higher temperatures (to about 2400°F) is being considered. Other work in the area of thermophysical-property determinations will depend on the outcome (i.e., availability and consistency of data) of the NASA and Air Force programs.

High-Flux Isotope Reactor

INTRODUCTION

Expansion of material studies into elements of very high atomic numbers represents a challenge to scientists in the fields of physics, chemistry, solid-state physics, and others. Research efforts to date have been strongly limited by the scarcity of transplutonium elements.

The primary purpose of the High-Flux Isotope Reactor (HFIR) is to produce research quantities of transplutonium isotopes. During the first year of full-power operation about 0.1 gram of californium-252 and much greater quantities of americium and curium will be produced. Appropriate recycling of curium could later raise the Cf^{252} production rate to 1.0 gram per year. These production rates are consistent with the availability of feed materials and are expected to satisfy minimum demand.

The HFIR reactor design employs a reflected cylindrical core with 93% enriched uranium fuel. Light water is used as moderator and coolant. The reflector is metallic beryllium. A central water-cooled duct is designed to house the target which will initially contain 300 grams of Pu^{242}. Provisions are made for insertion of other irradiation experiments to further exploit the high neutron fluxes generated in the reactor. The maximum unperturbed thermal-neutron flux in the center of the core is about 5×10^{15} *nv*. The corresponding average thermal-neutron flux in the plutonium target is about 2×10^{15} *nv*.

The amount of californium produced is proportional to about the cube of the thermal-neutron flux. Therefore every effort has been made in the design to achieve the maximum possible thermal-neutron flux in the target area. Some of the resulting unusual features include the concentric cylindrical arrangement of the central target area, fuel annulus, control region, and water-cooled beryllium reflector. The fuel plates are involute-shaped. The fuel loading is radially contoured, and burnable poisons are incorporated to minimize the peaking of power density and to maintain high neutron flux in the target region.

PROJECT STATUS

Specifications and drawings for the reactor building, reactor primary and secondary cooling systems, and most of the auxiliary equipment are complete, and construction and procurement are under way. With the exception of the core components the facility is scheduled for completion by late 1963. As of June 1962, the construction was about 20% complete.

The HFIR is scheduled to reach criticality early in 1964 and to achieve full power several months later.

The design of the reactor core components is progressing concurrently with critical experiments and a hydraulic mockup. Information yet to be obtained from these experiments is expected to result in only minor changes to the present design.

Construction of the full-scale hydraulic mockup is now virtually complete, and it is expected to be in operation about July 1962.

The somewhat unique design of the cylindrical fuel element for the HFIR has required a considerable development effort. To date, several elements have been fabricated satisfactorily, including a complete fueled element for the critical experiments and a nonfueled element to be used in the hydraulic mockup.

DESCRIPTION OF THE HFIR

Core Design Concept

The HFIR core will operate at higher steady-state average power density (~2 Mw/liter) than any other research and test reactor now in operation. Very high thermal-neutron flux density was achieved by optimizing the size of the central target region and by making the fuel region as compact as possible. The size of the fuel region is limited by heat-removal considerations. Significant factors affecting the design were practical limits on minimum fuel plate and coolant channel thickness and peak coolant velocity. These quantities are interrelated and were determined after thorough experimental and theoretical analysis of the associated mechanical, hydraulic, thermal, and metallurgical problems. Pertinent dimensions for this core and other related information are listed below:

Nuclear Characteristics	
Reactor power, Mw	100
Fuel-element power, Mw	97.5
Neutron fluxes, neutrons cm^{-2} sec^{-1}	
Peak thermal at center of core	5×10^{15}
Peak total nonthermal in fuel	4×10^{15}
Average thermal in target	2×10^{15}
Peak thermal in beryllium reflector	1×10^{15}
Fuel loading, kilograms of U^{235}	9
Length of fuel cycle, days	15

Heat Removal from Fuel Element	
Average power density, Mw/liter	2.0
Maximum power density, Mw/liter	4.5
Average heat flux, Btu hr^{-1} ft^{-2}	8.0×10^5
Maximum heat flux, Btu hr^{-1} ft^{-2}	2.1×10^6
Burnout heat flux at 900 psi operating pressure, Btu hr^{-1} ft^{-2}	3.1×10^6
Temperatures, °F	
Coolant inlet	120
Coolant outlet	181
Maximum plate surface	417
Maximum cladding surface	606
Coolant velocity, ft sec^{-1}	42
Pressure drop across core, psi	73
System design pressure, psi	1000

Core Design and Size	
Type of core	Cylindrical annulus; flux trap
Type of fuel plate	Aluminum-clad plates; involute geometry
Fuel plate thickness, inches	0.050
Coolant channel thickness, inches	0.050
Length of fuel plate, inches	24
Length of active core, inches	20
Inside diameter of fuel annulus, inches	5.068
Outside diameter of fuel annulus, inches	17.126
Active volume of core, liters	48.6
Outside diameter of beryllium reflector, inches	43.0
Thickness of control plates, inches	0.250
Active length of control plates, inches	
Inner plate	62.75
Outer plate	68.0

Core Materials	
Fuel	Enriched uranium (~93%)
Coolant	H_2O
Central moderator-reflector	H_2O
Control plates	Ag-Ni-Al
Reflector	Be + ~5% H_2O
Burnable poison	$B_4C + CdS$

The peak thermal-neutron flux in the central irradiation facility is much more dependent on the average power density than on the maximum power density. Therefore it was desirable to minimize the ratio of maximum to average power density which permitted an increase in power level and in peak thermal-neutron flux for the same maximum heat flux. In many reactors, rather large values of axial maximum to average power density ratios result from control rods being inserted into the fuel region from one end of the core. In the HFIR design this effect was minimized by inserting the control rods from both ends of the core and by locating them just outside the fuel region where they completely surround the fuel. A further improvement was made by dividing the length of the control rods into three regions, each containing a different amount of neutron absorber. One end region contains as much absorber as possible, while the opposite end contains as little as possible; the middle region is intermediate. With this control rod configuration, there is essentially no circumferential perturbation in the power distribution and very little in the longitudinal direction.

In reactors with a geometry like that of the HFIR the neutron flux distribution in the radial direction would cause a radial peak to average power density ratio of 3.4 in a clean core with uniform fuel distribution. The radial power curve, however, can be substantially flattened if the local fuel loading is varied inversely with the neutron flux. The involute-shaped fuel plates of the HFIR are designed with radially varying fuel and burnable-poison loading. The distribution is so specified that despite burnup of fuel and poisons and movement of the control rods the radial peak to average power density ratio remains about 1.13 during the entire fuel cycle. This permits maximum power and peak thermal-neutron flux operation for the life of each fuel loading.

Experimental Facilities

Facilities for irradiation experiments in the HFIR include a number of vertical through holes in the beryllium (ranging in diameters from 0.5 inch near the core to 3.0 inches near the outer diameter) and three 4.0-inch-diameter beam holes. The beam holes, which are located at the horizontal midplane of the core, have their point of closest approach to the core located about 3 inches out from the inner diameter of the beryllium reflector. One beam tube is oriented radially (for hard neutron spectrum), one has its projection tangent to the fuel (for a softer neutron spectrum), and the other is a through hole. Provisions have been made to extend the radial beam tube one-fourth mile for neutron time-of-flight experiments.

The central irradiation facility is to be used primarily for the production of transplutonium elements. The initial feed material loading is to be 300 grams of Pu^{242}. Powdered PuO_2 with aluminum filler will be compacted into pellets and loaded into $\frac{3}{8}$-inch-outside-diameter aluminum tubes. Thirty-one tubes surrounded by hexagonal flow-channeling shrouds form the target matrix. A cutaway view of the assembled target is shown in the figure below. As irradiation proceeds, individual rods will be periodically removed, processed, and replaced with new tubes containing recycle material. By the end of the second

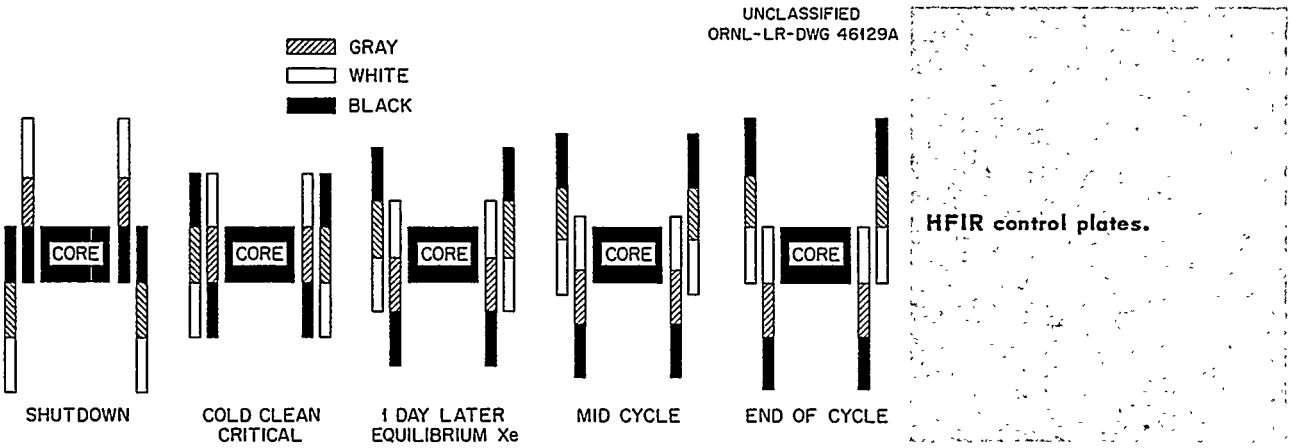

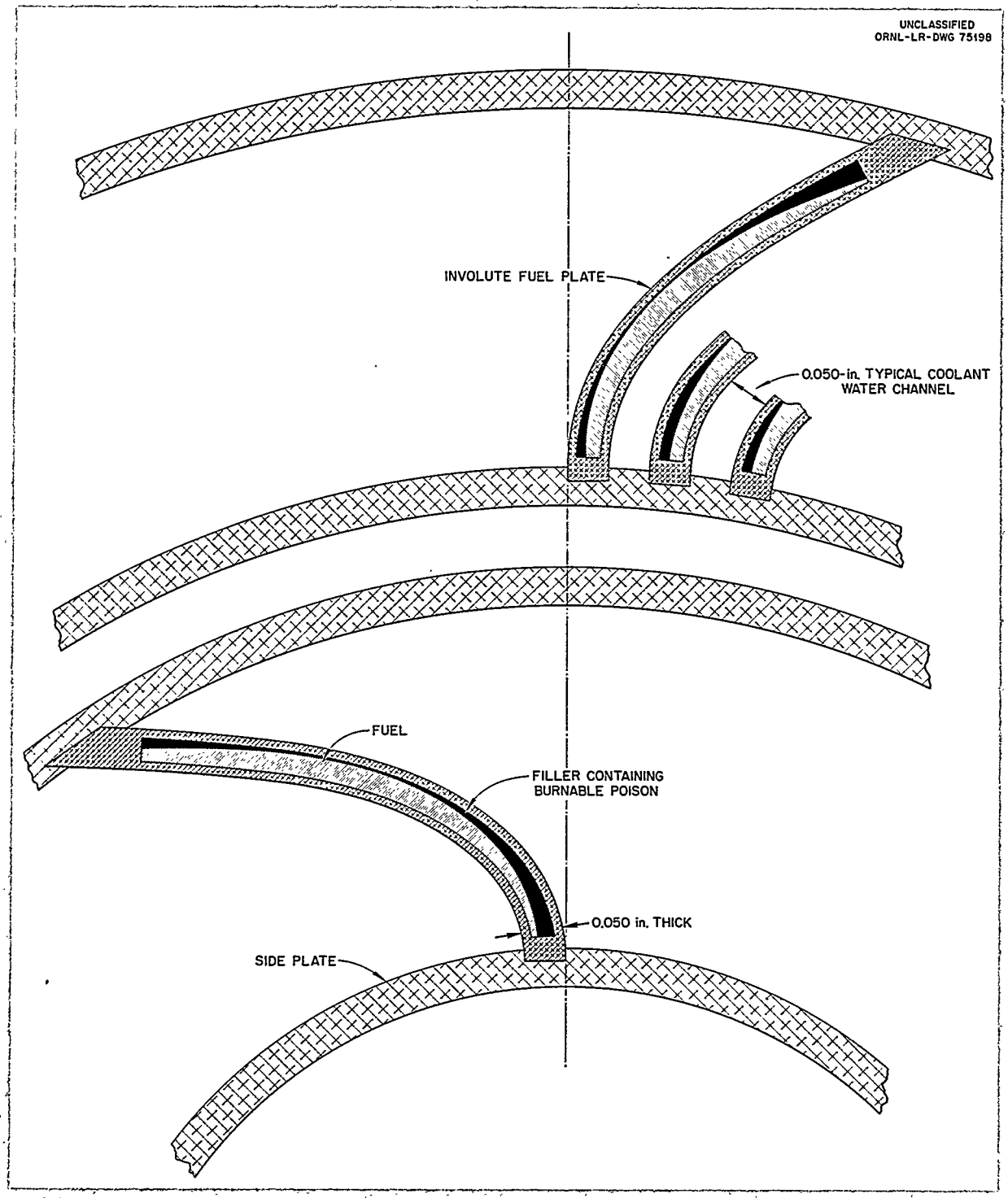

Schematic representation of the fuel and burnable-poison distribution in the HFIR involute fuel plate.

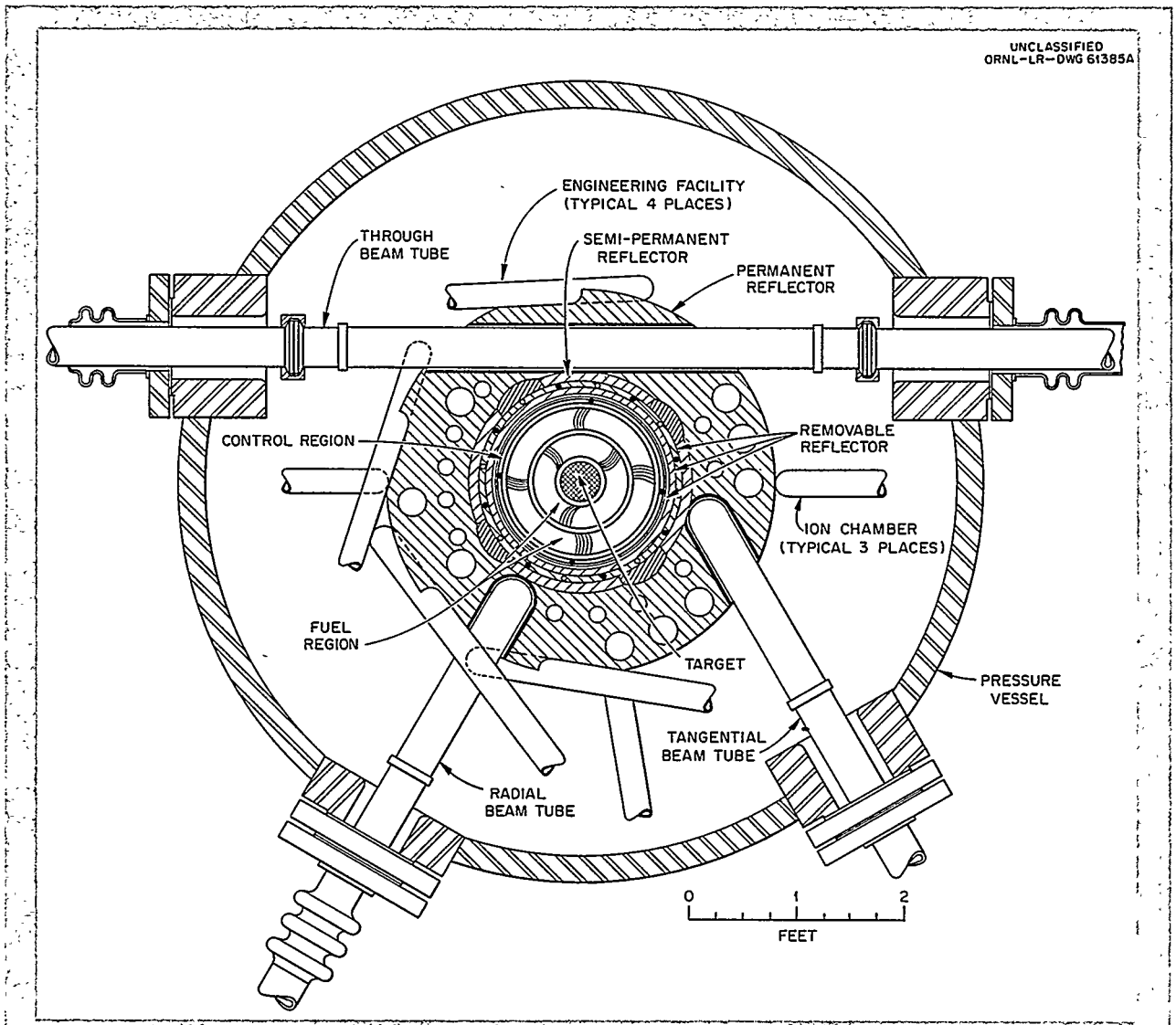

High-Flux Isotope Reactor. Horizontal section through pressure vessel.

year of full-power operation this technique should result in a Cf^{252} production rate of about 1 gram per year.

Reactor Building and Site

The HFIR is under construction at ORNL on a site between the main Laboratory area and the Clinch River. The structures in the accompanying photograph represent the status as of June 1962.

The building that houses the HFIR is a concrete structure that contains all of the high-pressure (1000 psi) primary cooling system. Three sets of heat exchangers and circulating pumps are located in individual cells, each cell having adequate shielding to permit maintenance during operation. The high-pressure piping from the reactor to these cells is also shielded; thus it was not necessary to provide a special nitrogen-16 decay tank.

The reactor core and vessel are located in one end of a water-filled pool that also has provisions for storing up to 27 irradiated fuel loadings and provides shielding for experiment and core component handling. The top of the pool is fitted with a light-weight cover that permits all gases that might emerge from the pool water to be carried by a continuous flow of air over the pool to an air

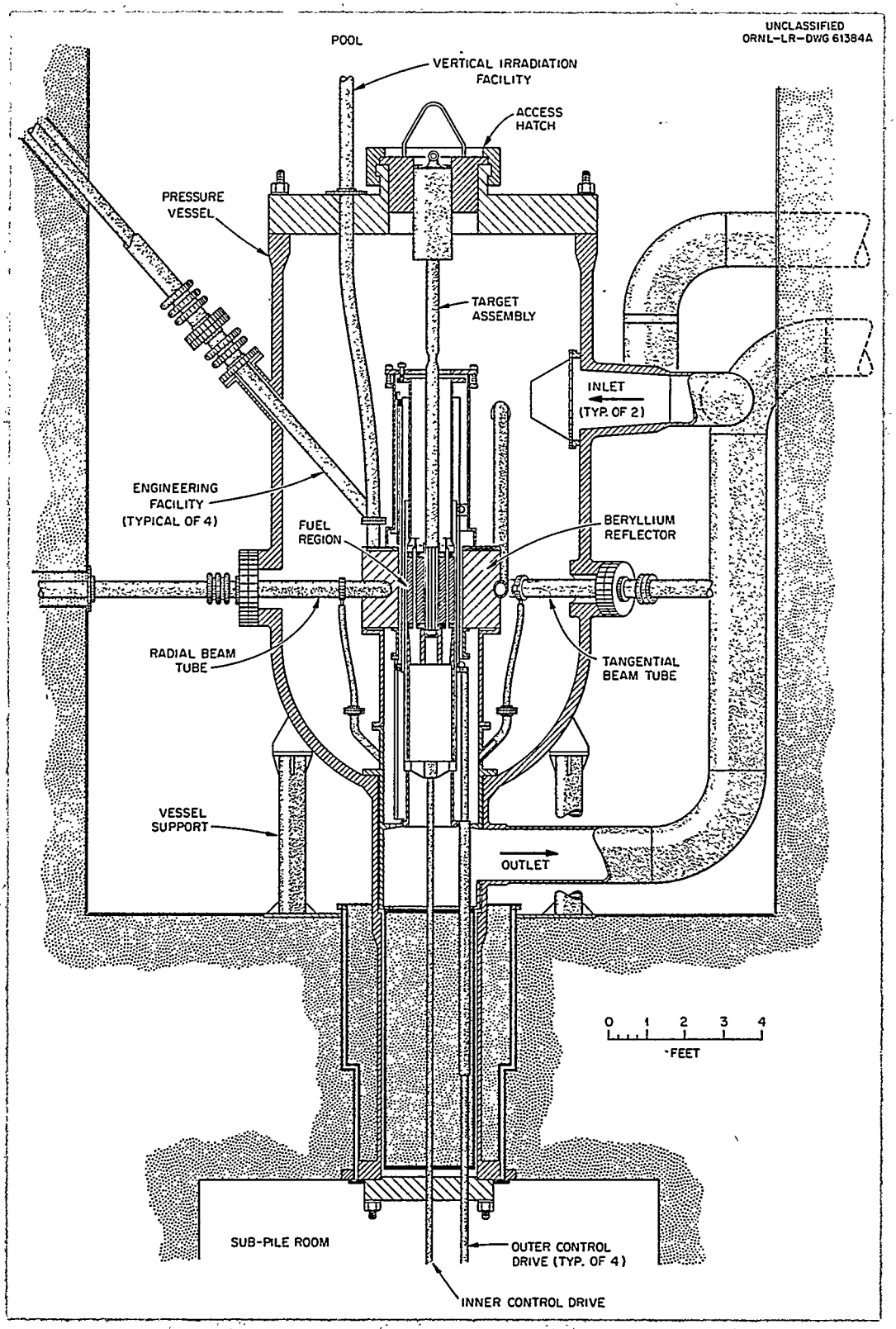

High-Flux Isotope Reactor. Vertical section through pressure vessel.

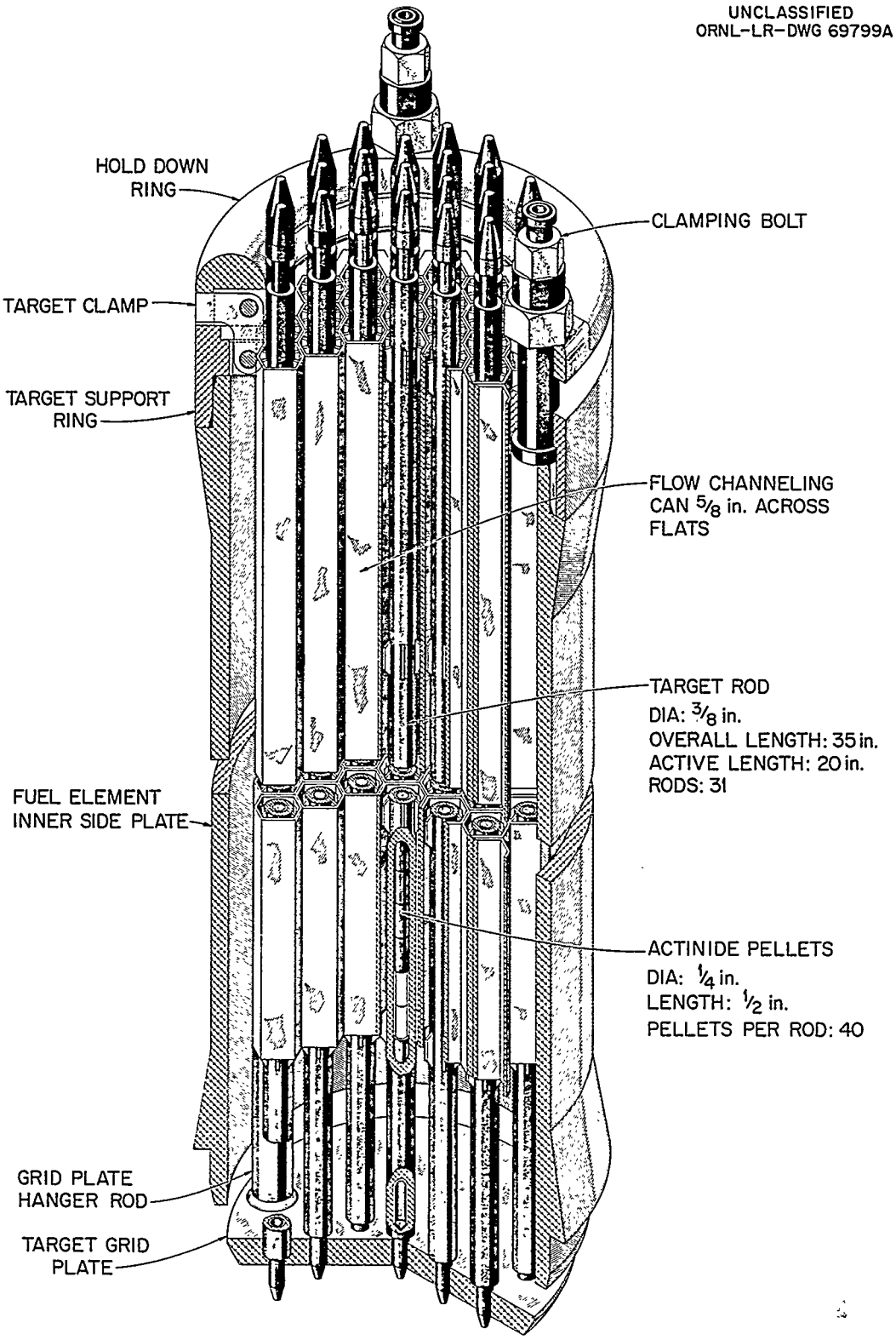

Proposed HFIR Target Assembly.

HFIR Reactor Site.

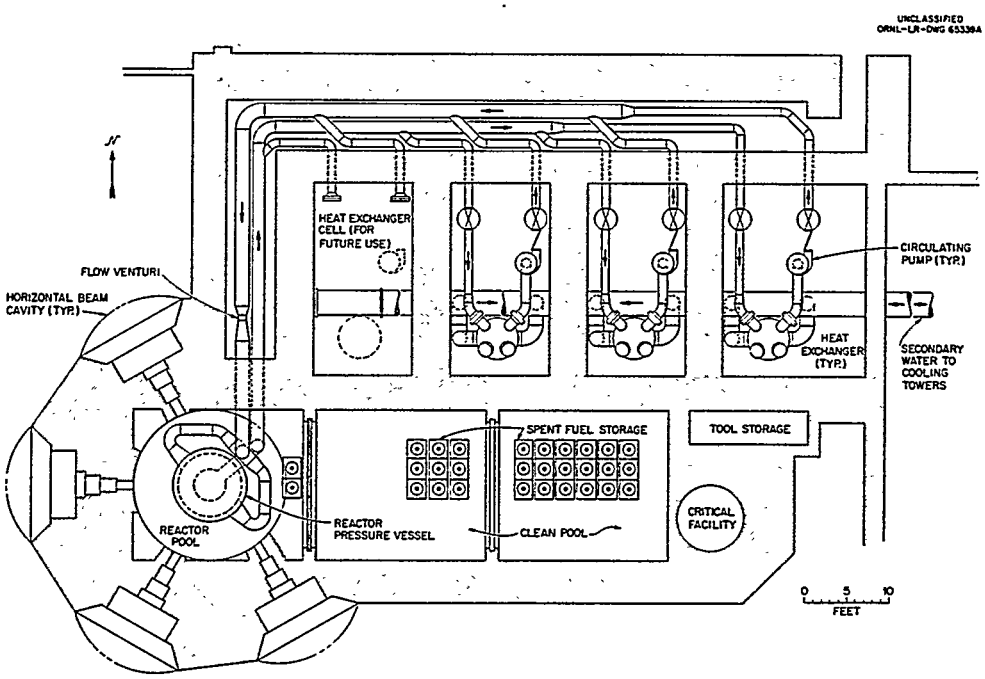

High-Flux Isotope Reactor. Reactor shield, heat exchanger cells, and pool structures (horizontal section).

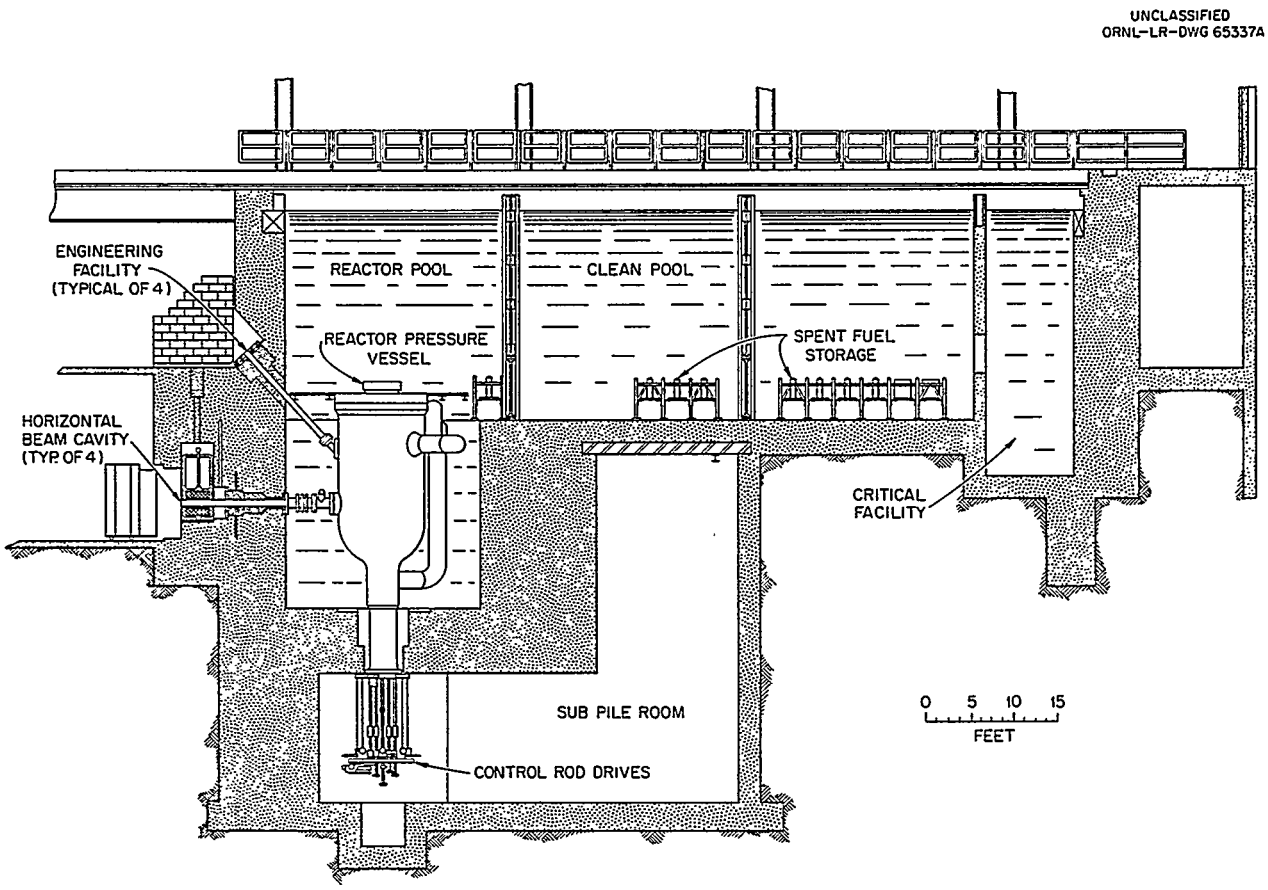

High-Flux Isotope Reactor.

cleanup system and then to the stack. Air pressure in the building is slightly less than atmospheric, and the pressure in the space between the pool and pool cover is less than elsewhere in the building. The pool cover is equipped with a small, easily movable opening through which components can be handled and transferred.

Construction work at the site is making good progress. Concrete work for the electrical building and the underground water storage tank is complete. Pouring of concrete for the exhaust stack is approximately 35% complete. The current schedule calls for completion of structure and services in September 1963. As of June 1, 1962, 20% completion was achieved.

EXPERIMENTAL PROGRAM

The design of the HFIR constitutes a very significant extrapolation beyond that of presently operating research and engineering test reactors. For this reason, a considerable amount of research and development has been conducted and is still in progress in connection with the HFIR project. During the early part of the program, extensive heat-transfer and corrosion tests were conducted on simulated HFIR fuel plates. Heat-transfer tests resulted in accurate correlations for both burnout heat flux and heat-transfer coefficients. Corrosion tests were designed to investigate the thermal resistance and the growth rate of an oxide film,

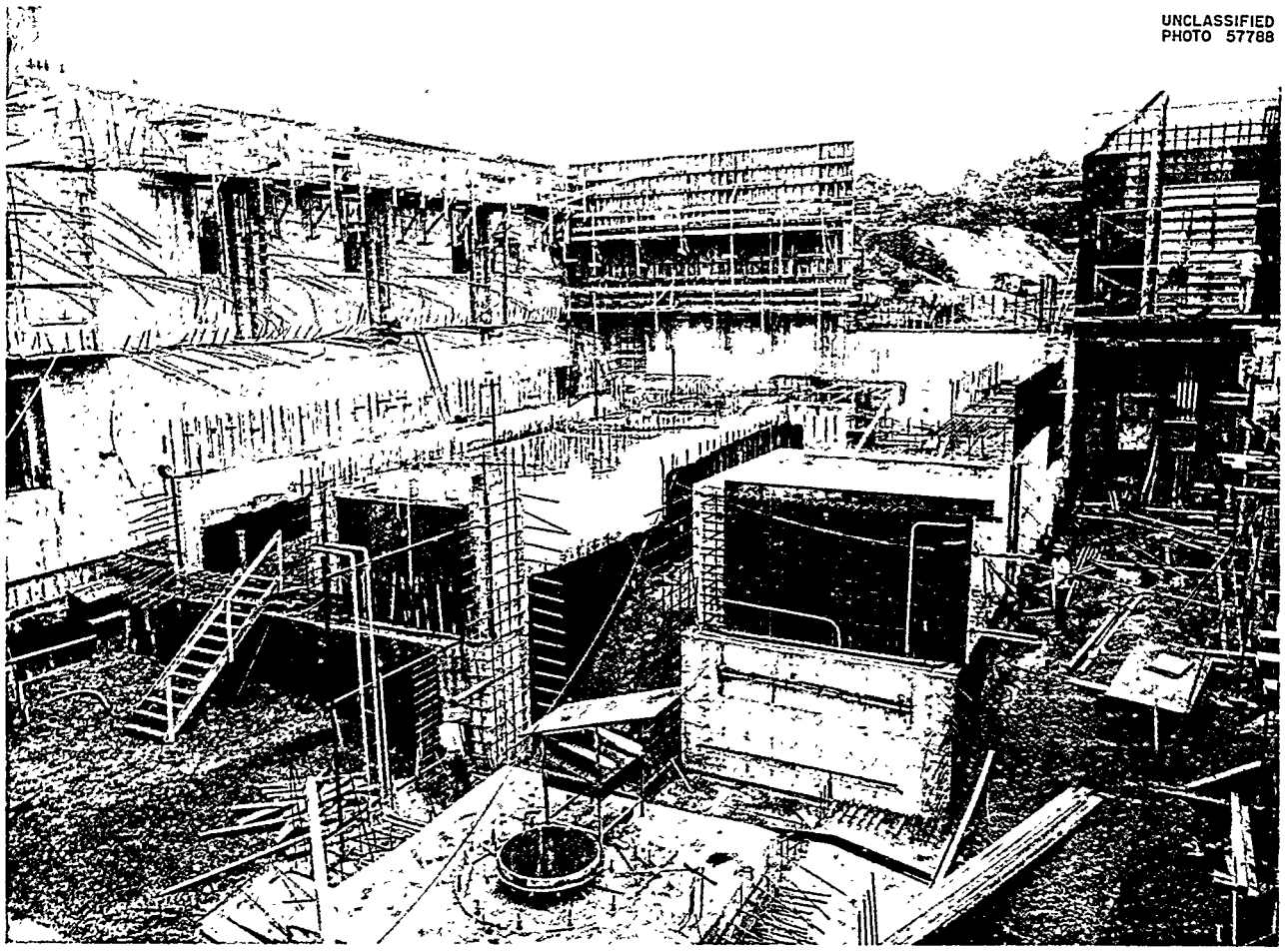

HFIR construction concrete work in reactor pool area looking east.

which in the HFIR contributes very significantly to the total thermal resistance between fuel and coolant. Results of this work, in addition to providing the necessary thermal design information, indicated that to minimize the oxide growth rate the pH of the coolant should be lowered to about 5. This is being achieved in the HFIR through the use of HNO_3 in the coolant. Corrosion tests on other core materials and combinations of materials are still in progress.

For reasons of geometry and process conditions the fuel elements are subject to severe hydraulic forces and thermal stresses that could lead to deflection of the fuel plates and restriction of coolant flow. To obtain a better understanding of the problem, actual plates were subjected to predicted temperatures, with pressure and temperature gradients simulating reactor conditions. These conditions were maintained long enough to furnish conclusive data about the creep behavior of the plates over the projected fuel-element life.

All the above experimental results obtained in connection with the fuel-element design, plus information concerning tolerances on dimensions and fuel loading and distribution, have been used in developing a method for predicting hot-spot and

burnout conditions during steady-state and transient operating conditions. Portions of the transient analysis are still in progress.

Heat generated by the unusually high gamma and neutron fluxes in the HFIR core could cause thermal deflections and create hydraulic problems in other adjacent components. A typical problem existed in the control region where hydraulic pressures normal to the control surfaces caused excessive control rod deflection. Experiments have demonstrated that a few small holes (~5% of the area) along the length of the control rods would reduce the hydraulic forces to acceptable values. Thus the design was modified to include the necessary holes.

Two somewhat unique design features of the HFIR, namely the continuous fuel gradation within a fuel plate and the overlapping-rod-reflector control, have placed heavy emphasis on the critical experiments for completion of the core design. The first fuel element suitable for use in the HFIR critical experiments was completed in May 1961, and since that time experiments have been in progress. During the past year nuclear design efforts have been primarily concerned with the utilization of the experimental data to finalize the core design.

Results of critical experiments and fuel-cycle analysis indicate that the uranium content of the fuel should be increased in order to assure a minimum fuel life of 10 days and an anticipated life of about 15 days.

The critical experiment program is being utilized to obtain further detailed information in connection with the reactivity worth of the control rods. Data from critical experiments and results from analog kinetic calculations indicate that minor modification of the present control rod

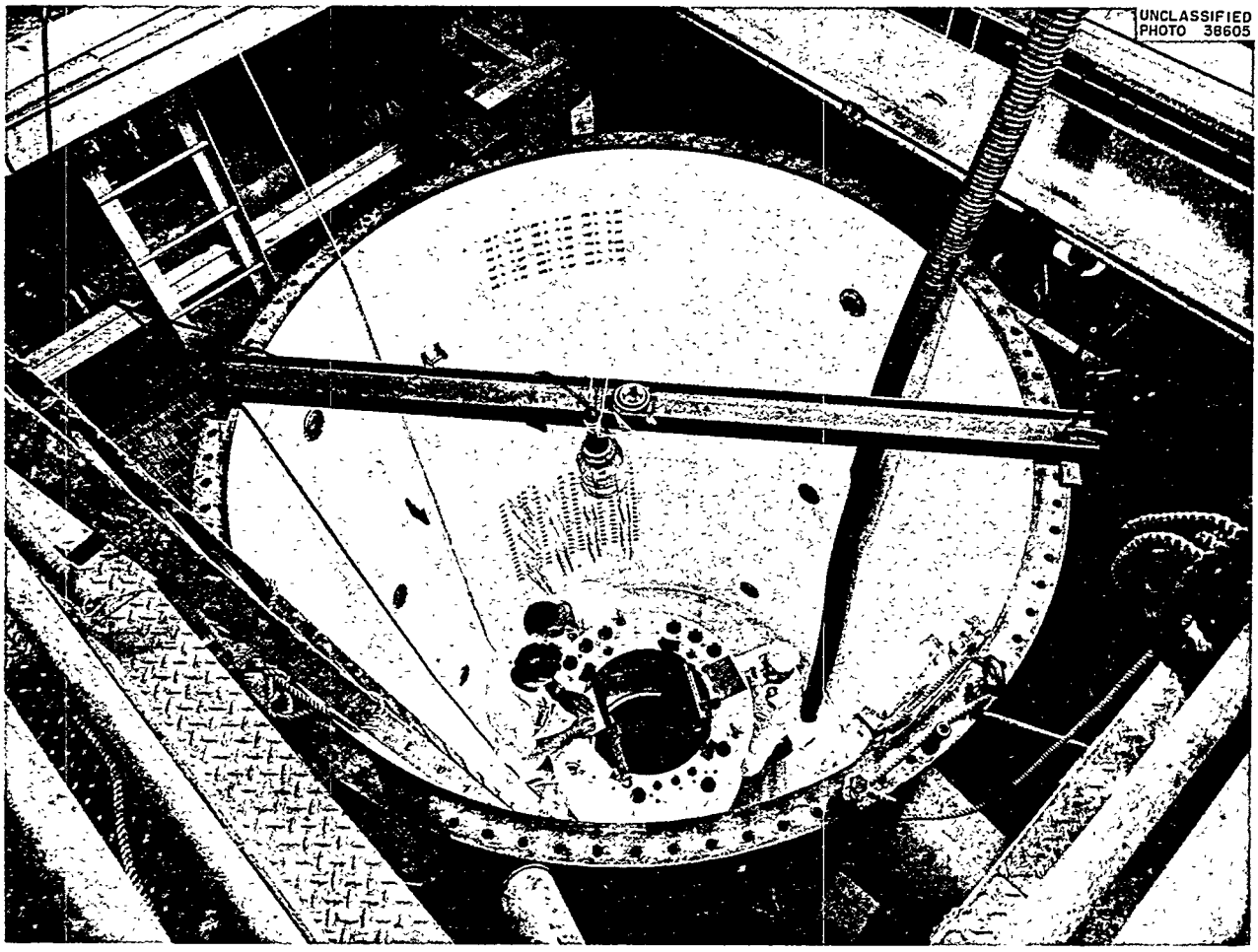

Aligning permanent reflector.

design may be necessary in order to satisfy the stringent criteria specified for response of the safety system.

HFIR Mockup

Core components of the HFIR are assembled into a close-fitting assembly that requires careful cooling achieved by high-velocity water flow. To ascertain that the assembly functions properly from the mechanical and hydraulic viewpoint, a mockup is being built consisting of a full-size core, reflector, and control system housed in a vessel having internal dimensions largely identical to those of the reactor vessel. This vessel is connected through a piping system to pumps that provide flow conditions presumably identical to those in the reactor.

The mockup parts are fabricated and installed in accordance with design tolerances in all critical areas, including control rod drives, reflector, and fuel support structure. Particular attention was given to the alignment of the parts with respect to each other. A photograph of a typical alignment operation is shown, which depicts the alignment of the reflector with respect to the center line of the reactor and control rod drives. A photograph of the partially complete installation of the rod drive and support platform is also included.

The usefulness of the mockup has already been demonstrated during the time of procurement and fabrication of various component parts. Experience gained in both phases has direct bearing on the work with the reactor parts.

Once completed, the mockup will serve to proof-test the core assembly for hydraulic behavior and stability. Extensive instrumentation is provided

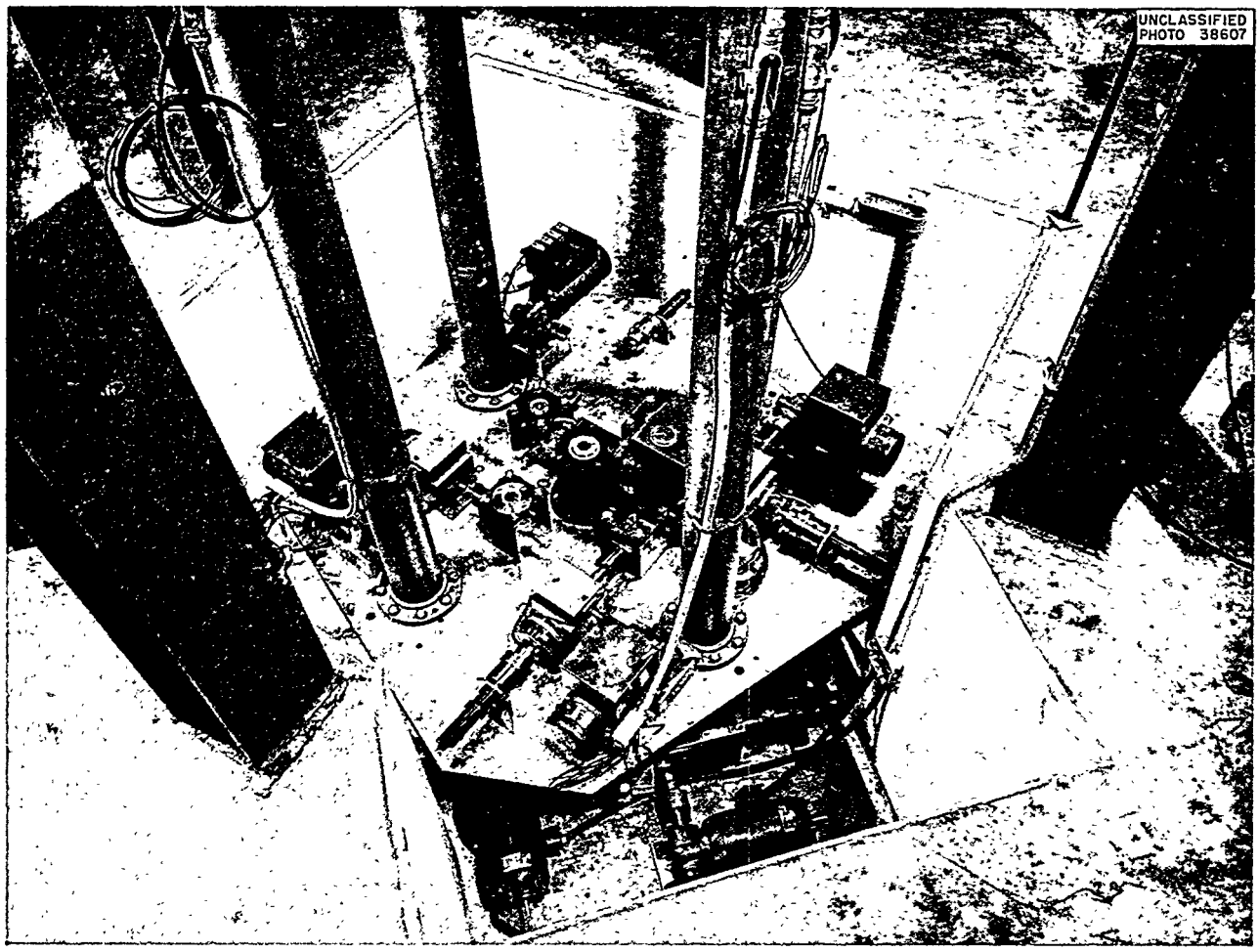

Partial installation on control rod drives.

to monitor flows and pressures at various points and to sense deflections. Strain-gage installations are provided to detect vibration in individual components.

The mockup will be available for development of special tools to handle the core and the target as well as those to be used in maintaining the reactor. Future uses include training of operating personnel and out-of-pile practice of more difficult maintenance operations.

The facility is now virtually complete and is expected to be in operation in July 1962.

Army Power Reactors

DISPERSION-FUEL-ELEMENT DEVELOPMENT

Mechanisms and Kinetics of Deboronization

Incorporation of small amounts of elemental boron in the matrix of stainless steel dispersion fuel elements has proved to be a useful means for gaining additional reactivity control, thereby permitting longer core lifetimes. To fully utilize this method, it is important to know and precisely control the amount of boron in the fuel matrix. The ability to do this has been hampered by boron losses which occur during elevated-temperature processing in the course of fabrication.

ORNL has investigated the mechanisms and kinetics of deboronization of stainless steel matrices during heating at 1135°C in various dynamic environments. When powder compacts of 5 weight percent elemental boron in various metals and oxides are heat treated in vacuum, argon, or helium, significant boron losses occur only when a supply of oxygen is available. The loss mechanism is believed to be oxidation of the boron and volatilization of the oxide, with the latter being the rate-controlling step. In a hydrogen environment, the synthesis of boron and hydrogen into a gaseous product is postulated to be the predominating loss mechanism. An increase in the rate of sintering of the powder compacts decreases the rate of boron loss. Deboronization of wrought specimens of 0.13 weight percent boron–stainless steel alloy occurs in either hydrogen or wet-helium environments. In this case the rate is controlled by the rate of solid-state diffusion of boron to the gas-metal interface.

Borosilicate-Glass Burnable Poison

Studies of means to avoid the loss of boron from UO_2–stainless steel dispersion fuel plates during fabrication showed that a refractory glass containing 4 weight percent B_2O_3 is an attractive material for the boron additive. This material in the form of spherical beads resists stringering in the fuel matrix at the fuel-plate rolling temperature and shows no reaction with the stainless steel or UO_2. Boron loss is undetectable within the accuracy of postfabrication chemical analysis.

Postirradiation Examination of SM-1 Fuel Elements

Although new fuel element designs are extensively tested prior to their use in an operating

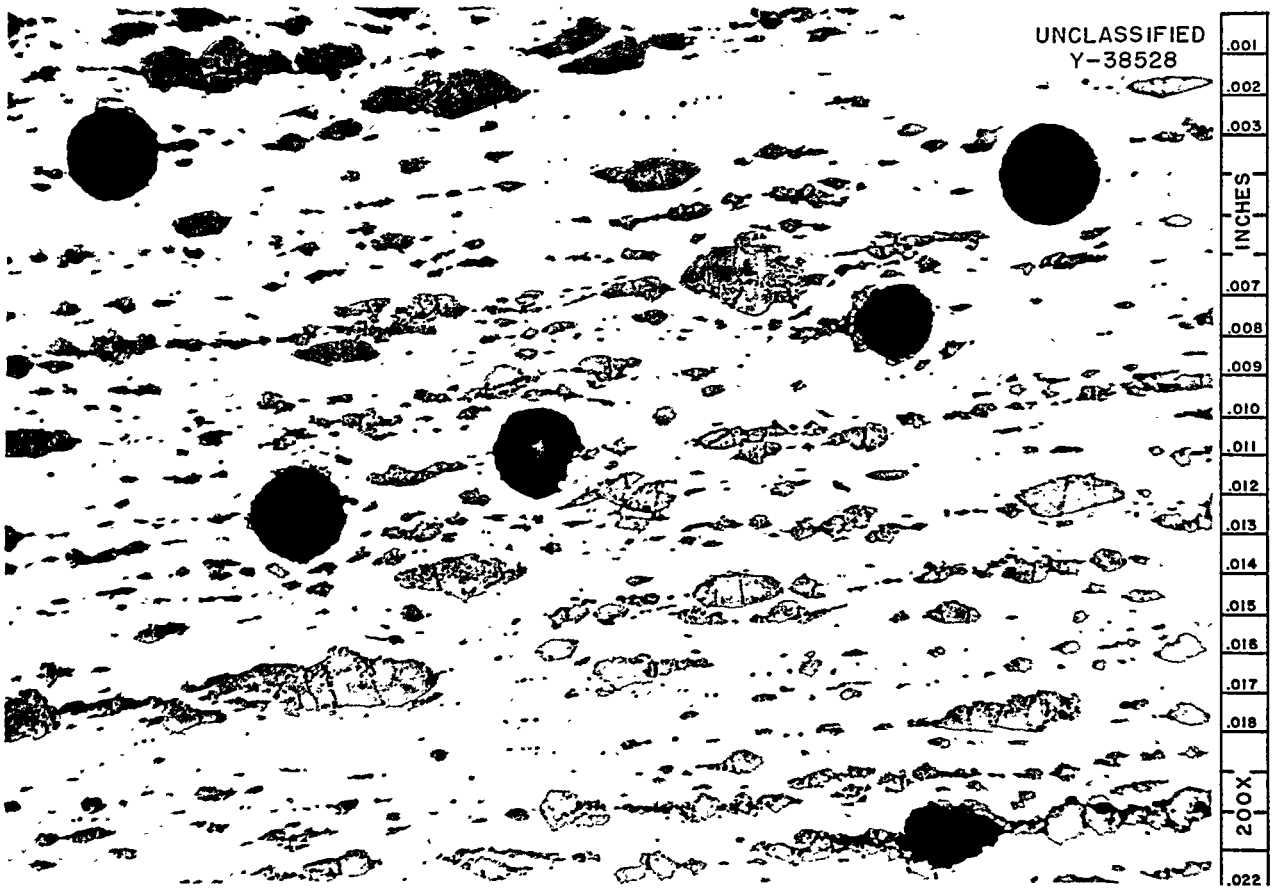

Core structure in annealed fuel plate containing boron-bearing glass beads, UO_2, and type 347 stainless steel. As polished. 200X.

reactor, full evaluation is possible only by observation of their behavior in service. The SM-1 reactor at Fort Belvoir, Virginia, began operation in 1957 fueled with a dispersion-type fuel element (stainless steel and enriched UO_2). These flat-plate fuel elements were developed by ORNL. This fuel element design has subsequently been utilized in other Army package power reactors. Periodically, fuel elements have been removed from the SM-1 reactor and destructively examined for evidences of deterioration in order to predict the imminence and probable mode of ultimate failure and to indicate areas wherein the design can be improved.

Fuel element No. 72 was examined after 10.5 megawatt-years of operation. The measured uranium-235 depletion was an average of 16% and a maximum of 30%. Fuel element No. 79 was examined after 16.4 megawatt-years of operation. The average uranium-235 depletion was 42%, and the peak depletion was 57%. Both elements were dimensionally stable except for rippling of the outer fuel plates. Significant brazed-joint corrosion by the pressurized-water environment was noted but did not appear to progress between 10.5 and 16.4 megawatt-years. Corrosion appeared to be confined to the brittle eutectic mixture in the braze-metal fillet. It is postulated that the deterioration shown may be due to the generation of cracks in this alloy by stresses induced during reactor operation, followed by acceleration of attack from a crevice corrosion process.

No sign of gross deterioration or cracking of the fuel matrix was noted. As expected, considerable porosity attributable to fission-gas precipitation was found in the UO_2.

A small number of intergranular cracks were observed in the cladding of some of the fuel plates

Typical microstructure of fuel-plate-to-side-plate brazed joint, showing corrosion of eutectic mixture. Specimen was in the SM-1 reactor about three years. Etchant: glycerol regia. 75X. Reduced 16%.

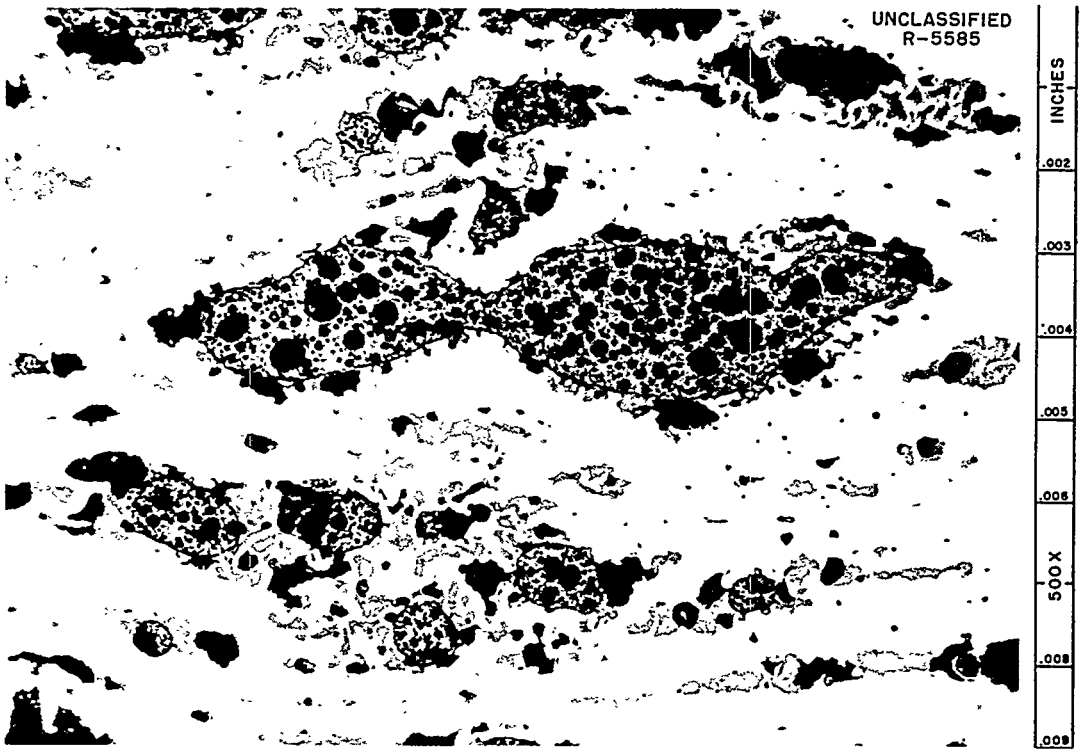

Typical microstructure of SM-1 fuel plate after 47% fission burnup of uranium-235 (22.5×10^{20} fissions per cubic centimeter). Etchant: H_2SO_4-H_2O_2-H_2O. 500X. Reduced 16%.

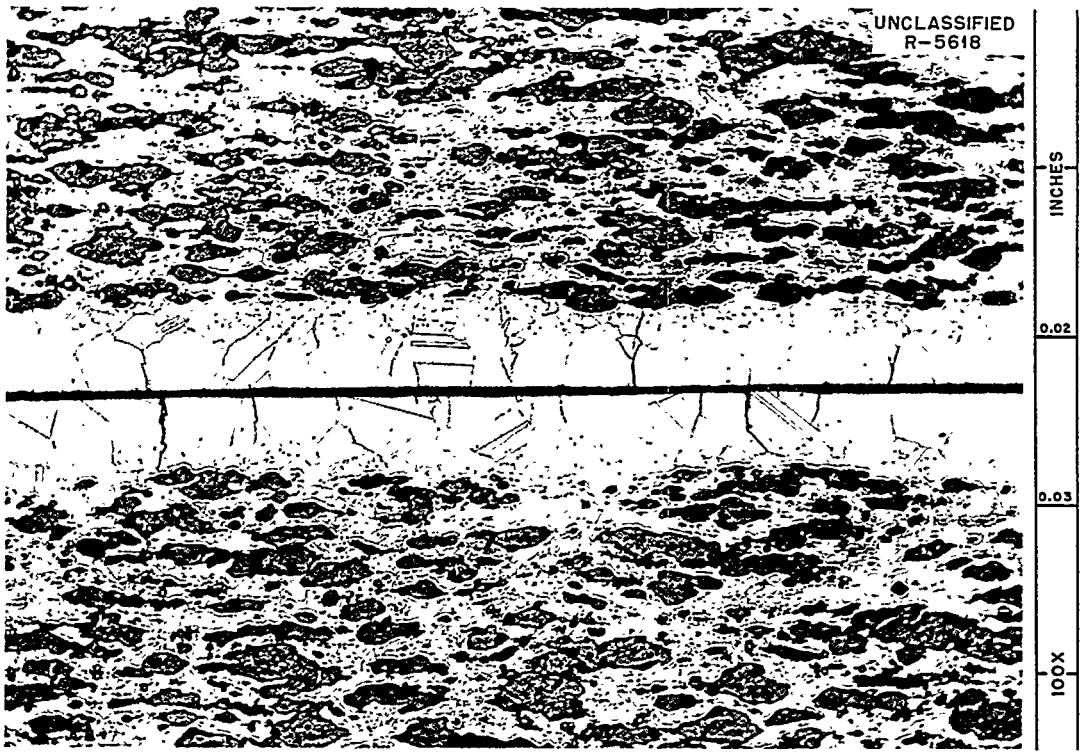

Cracking of fuel plate cladding in SM-1 fuel element after 16.4 megawatt-years of operation. Etchant: glycerol regia. 100X. Reduced 16%.

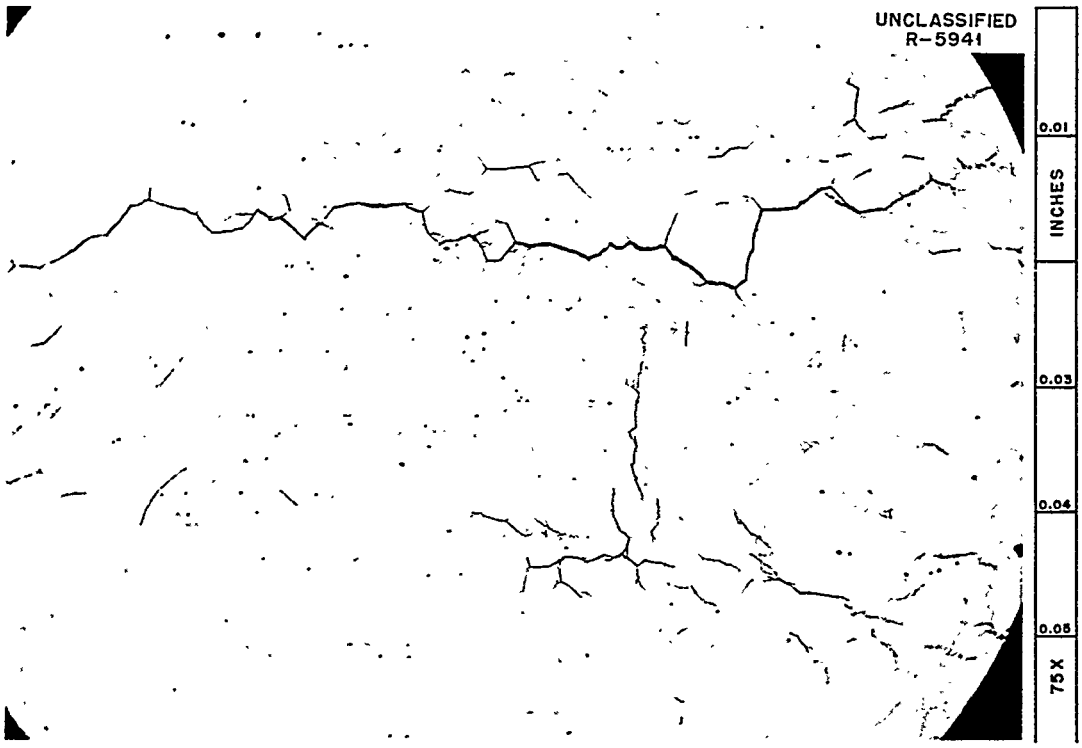

Cracking patterns in fuel plate cladding in SM-1 fuel element after 16.4 megawatt-years of operation. View shown is a polished and etched fuel plate surface. Etchant: glycerol regia. 75X. Reduced 16%.

of the 10.5-megawatt-year element. Both intergranular and transgranular cracking was observed in the cladding of the 16.4-megawatt-year element. Although some cracks penetrating to the surface of the fuel section can be seen, no penetrations into the matrix were found. The cause for the intergranular cracking may be related to the fact that the fabrication process results in carburization of the type 304L stainless steel cladding, and ultimately the material becomes sensitized as well as very coarse grained. The cause for the transgranular cracking is not yet known but may be due to a stress-corrosion phenomenon.

CONTROL-ROD DEVELOPMENT

Europium Oxide Studies

The first control rods used in the SM-1 reactor had neutron-absorber sections which consisted of stainless-steel-clad plates containing 3 weight percent enriched boron (90% boron-10) in iron. Accelerated irradiation tests of this material indicated that early failure of the SM-1 absorbers was likely to occur. Examination of two of the full-size rods exposed in the SM-1 reactor for two-thirds of a core life supported these findings, and the iron-boron neutron absorbers were replaced with absorbers containing 37 weight percent Eu_2O_3 in stainless steel.

One of the principal problems encountered in the development of the europium oxide–stainless steel absorbers was a reaction between the Eu_2O_3 and the silicon in the austenitic stainless steel. Use of low-silicon elemental metal powders circumvented the reaction problem, and 13 full-size SM-1–type absorbers were fabricated by ORNL without difficulty. Subsequently, however, other fabricators encountered a new swelling problem with the Eu_2O_3–stainless steel matrix during fabrication when the level of silicon appeared to be acceptable on the basis of previous work. Consequently, studies were undertaken by ORNL to explore the mechanism of this swelling problem.

The effects of variations in powder history and sintering environment on the dimensional behavior of Eu_2O_3 at 1350°C was investigated. Low-temperature-calcined (800°C) cubic Eu_2O_3 powder was found to be unsuitable because of large volume changes in compacts on heating to 1350°C and because of practical difficulties in blending the fluffy, cubic Eu_2O_3 with metallic powders. Volume changes of lesser magnitude accompanied by weight loss were exhibited by compacts of denser monoclinic powders. Considerable evidence indicates that the loss in weight and perhaps the dimensional changes were due to decomposition of a compound such as europium hydroxycarbonate. The presence of 0.4% carbonate was detected in the oxides which had been prepared several months previously. Freshly prepared Eu_2O_3 lost no weight in the temperature range of 1000 to 1400°C.

Another observation in these sintering studies points up the need for close control over all furnace equipment used in Eu_2O_3 processing. When pellets of Eu_2O_3 were heated in a molybdenum furnace to 1600°C for 2 hours in hydrogen, a silicon-rich, loosely adhering crust formed on the surface. The only apparent source for the silicon was silicate-base insulating materials which had previously been assumed to be not hot enough to allow silicon volatilization in a hydrogen environment.

Intentionally defected samples of Eu_2O_3–stainless steel control-rod materials were corrosion tested in 300°C water. Dispersions containing 30 and 40 weight percent Eu_2O_3 exhibited unsatisfactory corrosion behavior. Susceptibility to corrosion is increased by increased Eu_2O_3 content and by irradiation. The possibility of improving the corrosion properties of Eu_2O_3 compacts in high-temperature water is being investigated by ORNL.

Boron-Gradient Neutron Absorbers

Dimensional changes which occur in boron-iron dispersions under irradiation are attributed to helium pressure from the boron-10 (n, α) lithium-7 reaction leading to failure at the core-to-cladding interface. Microstructural examination of irradiated specimens has revealed that, because of self-shielding, boron in surface layers of the dispersion is burned to appreciably higher values than in the underlying material. For example, in specimens of 3 weight percent boron in iron which were subjected to an average boron-10 burnup of 11 atomic percent, the boron-10 burnup at the

surface was as high as 70 atomic percent. It thus appears that the useful life of the absorber can be increased if it can be designed so that the boron-10 burnup is uniform throughout the thickness.

ORNL has developed a neutron-absorber plate in which the boron distribution increases from the surface of the neutron-absorber plate to the interior in a step-wise fashion. The core section of the composite plate is made up of several layers. Each layer contains the desired amount of boron-10 dispersed in type 200 stainless steel by conventional powder-metallurgy methods. A full-size SM-1 absorber based on the boron-gradient

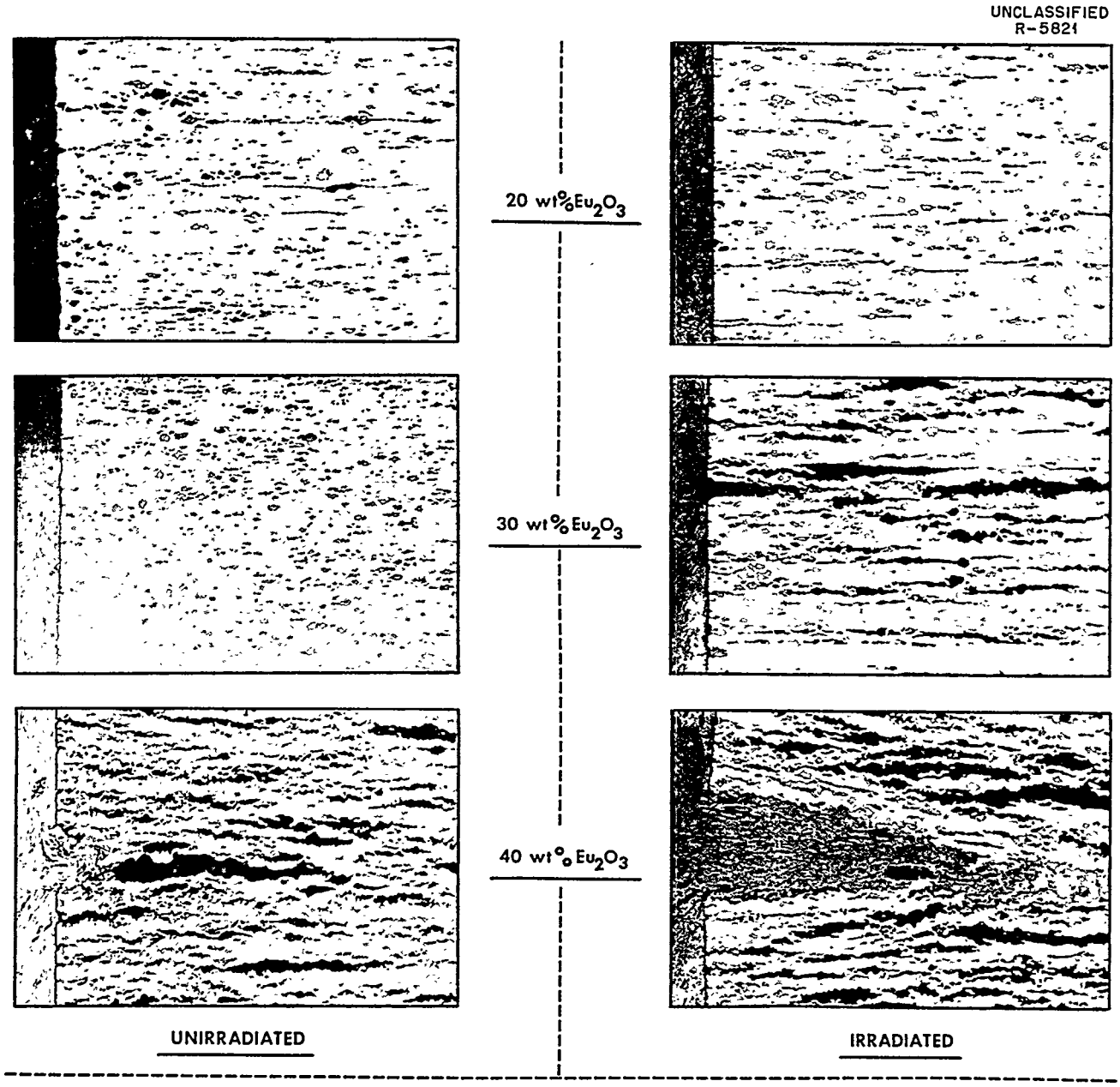

Structure of corrosion-tested Eu_2O_3-dispersion absorber specimens.

concept, with boron concentration varying from 1.14 to 3.44 weight percent, was fabricated and is currently being tested in the SM-1 reactor.

Another approach is also being investigated in an effort to increase control-rod life without incurring the comparatively high cost of the previously developed Eu_2O_3–stainless steel absorber. In this concept the irradiation-resistant but high-cost europium oxide is limited to the bottom third of the absorber section, where most of the neutron absorptions take place. The remainder of the absorber section contains a boron gradient of the type described above. The feasibility of fabricating the composite absorbers was demonstrated by the preparation of full-size sample plates of SM-1 design. A test of a complete control rod in the SM-1 reactor is planned.

Maritime Reactors Program

PRESSURIZED-WATER REACTOR CHEMISTRY

Water chemistry in the ORR pressurized-water in-pile loop is being studied (1) to provide chemical and radiochemical data on water conditions pertinent to loop operations, (2) to support this Laboratory's various commitments as consultant to a number of pressurized-water reactor programs, and (3) in general to increase the basic understanding of reactor water chemistry as an approach to more economical reactor operation. While much information on the chemistry of primary system water is presently available, relatively little in the way of a fundamental understanding of observed behavior has been gained, especially in connection with the important unsolved problems of the transport and deposition of corrosion products, "crud," and their associated radioactivity.

The relatively low levels of water-borne corrosion products and associated radioactivity in the ORR loop were composed of two distinct fractions: (1) a particulate or "crud" fraction which (from filtration tests and electron-microscopic and x-ray diffraction examination) had a sharp lower limit in particle size of ~0.5 micron and was well crystallized with the magnetite structure, and (2) a dissolved fraction which was not removed by the lowest-porosity filters (0.01 micron) and, from electromigration experiments, appeared to be present as simple ions (related to the bivalent metal hydroxides of Mn, Fe, Co, and Ni) at very low concentration (less than 10^{-6} *M*). The specific activities of these two fractions, as well as that of the "crud" found deposited on fuel-rod test assemblies removed from the in-pile section of the loop, were all comparable. This, as well as the well-crystallized appearance of the insoluble fraction, suggests that appreciable radiochemical exchange between the two fractions occurs and that this labile exchange equilibrium may be an important mechanism of activity transport in pressurized-water reactor systems at neutral pH.

A high-temperature filter unit was installed on a side stream of the loop to test the ion-exchange properties of magnetite as well as to determine its effectiveness as a high-temperature "crud" filter; preliminary results of tests with 80-mesh natural magnetite in this unit indicated 80–90%

removal of the dissolved (presumably ionic) water activity in a single pass at 400–425°F. It is planned to test synthetic magnetites of controlled purity and particle size as well as other inorganic materials. A suitable high-temperature-filter ion exchange system could be effective in reducing activity transport in pressurized-water reactor systems.

IN-PLACE TESTING OF NS "SAVANNAH" IODINE ADSORBERS

The containment vessel for the NS "Savannah" reactor system is located within a ventilated compartment which serves as a secondary containment for any radioactivity which might leak from the containment vessel. The reactor compartment is provided with two independent ventilation systems (normal and emergency), each equipped with a particulate filter and an iodine adsorber and capable of maintaining the compartment at negative pressure. Because of the importance of iodine removal in controlling the consequences of postulated accidents, ORNL was requested to develop procedures and techniques for in-place determination of iodine-removal efficiency, particularly of the charcoal unit in the emergency ventilation system.

Both laboratory tests and in-place tests were performed to determine the iodine-removal efficiency of the iodine adsorber in the reactor compartment emergency ventilation system. An in-place test was also conducted on the normal ventilation system.

Laboratory tests conducted with continuous iodine injection at 96 to 100°C with 80 to 90% saturated steam in air showed the iodine-removal efficiency of the charcoal unit alone to be 99.8 ± 0.1% at the 95% confidence level. These tests were conducted on 11-inch by 11-inch charcoal units fabricated by Flanders Filter Company in the same way and with the same materials used to make the units installed in the NS "Savannah." All the tests were of 12-hour duration, except one which was for 24 hours. No significant duration effect was noted. The results of these tests are shown in the accompanying table.

In-place tests were conducted on board the "Savannah" to determine whether the installation of the adsorber units in the reactor compartment

Iodine-Removal Efficiency Tests on 11- by 11-inch Charcoal Adsorbers

Run No.	Temperature (°C)	Face Velocity (ft/min)	Steam (% saturation)	Iodine-Removal Efficiency (%)
1	96	4.6	91.3	99.84
2	100	4.3	80.7	99.63
3	26	4.8		99.98
4	99	4.5	83.8	99.95
5	100	4.4	82.1	99.73
6	98	4.8	88.9	99.67
7	99	4.5	85.2	99.95
8	99	4.8	86.3	99.95
9	98	4.8	89.0	99.86
10	99	4.7	86.1	99.90
11[a]	100	4.7	83.4	99.90

[a]A 24-hour test; all others were for 12 hours.

emergency ventilation system was such that the efficiency of the adsorber medium itself actually could be realized. The charcoal adsorbers had been installed on December 14, 1961, and had been operated only intermittently for testing and system adjustment up to May 27, 1962, the time of the in-place tests. Prior to installation they had been subjected to two Freon penetration tests at the Edgewood Army Chemical Center and a stable-iodine penetration test at Armour Research Foundation. In the latter test 200 grams of iodine was adsorbed.

In the in-place tests elemental iodine labeled with I^{131} tracer was injected into the duct leading from the reactor compartment to the filter-adsorber assembly. Samples of air entering and leaving the filter assembly were radioassayed. The iodine was injected over a period of 15 minutes, and the test was continued for 2 hours at the ambient temperature of the reactor compartment. Earlier laboratory tests had shown that at room temperature in air no movement of iodine is observed after the initial injection. No radioiodine was found downstream from the adsorber within the limits of detection. Two tests were conducted with different amounts of tracer. The limits of sensitivities were such that 1/1,400 and 1/15,000, respectively, of the iodine collected upstream could have been detected in the downstream collector. The results of these tests, tabulated below, indicate that the charcoal adsorber assembly, as installed, is capable of realizing the iodine-removal efficiency observed in laboratory tests.

A similar in-place efficiency test was conducted on the reactor compartment normal ventilation system. The silver-copper mesh iodine adsorber was installed on December 14, 1961, and operated almost continuously up to the time of the in-place test June 2, 1962. In this test two downstream iodine collectors were used, one immediately following the air-cleaning assembly, and the other on the deck of the ship at the base of the stack. The amount of iodine was only negligibly lower in the air sample taken at the latter point. The observed iodine-removal efficiency was 95%. This result is consistent with laboratory tests on silver-plated mesh in air at room temperature.

NS "SAVANNAH" SHIELD EVALUATION

A Mobile Shielding Laboratory was developed for use in surveying the exterior of reactor shields to determine whether design dose levels have been achieved in actual operation. Six racks of laboratory-type scalers, electronic timers, and linear amplifiers were built into a Vanette truck. Specially designed neutron and gamma-ray detectors are coupled to the electronics by 250-foot lengths of cable. The Mobile Laboratory was prepared particularly for a survey of the "Savannah" reactor shield and has been used for this purpose. It has also proven to be generally useful, having been used for field surveys of other reactor shields.

The extremely low permissible levels of radiation specified for the "Savannah" (in some regions as low as 0.5 rem per year) required the development of more sensitive detectors than were previously available and careful calibration in a radiation field similar to that expected from

In-Place Iodine Tests of Reactor Compartment Ventilation Systems on NS "Savannah"

	Emergency	Emergency	Normal
Estimated system flow rate, cfm	200[a]	200[a]	4000
Duration of test, hr	2	2	2
I^{131} injected, mc	5	15	5
I^{127} injected, mg	1 to 2	1 to 2	10
Decontamination factor	>1400	>15,000	~20

[a]System under emergency mode of operation with maximum dilution.

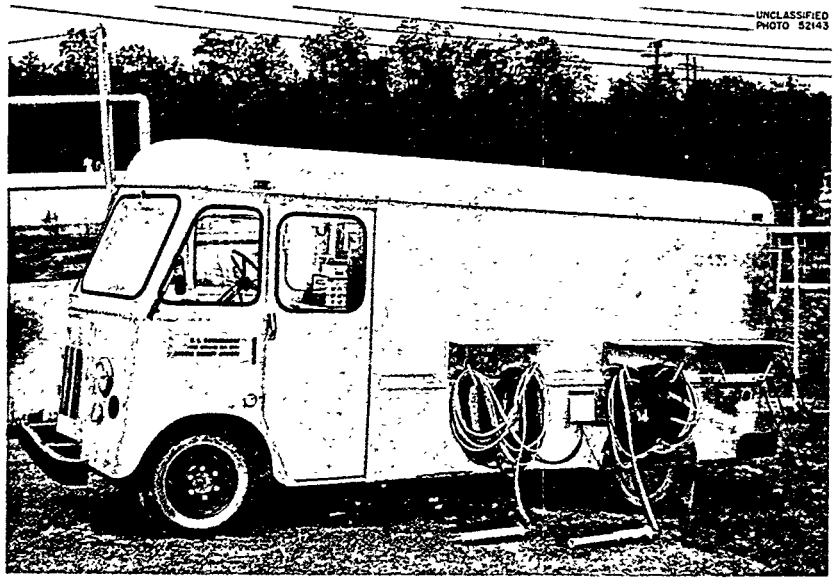

Mobile shielding laboratory.

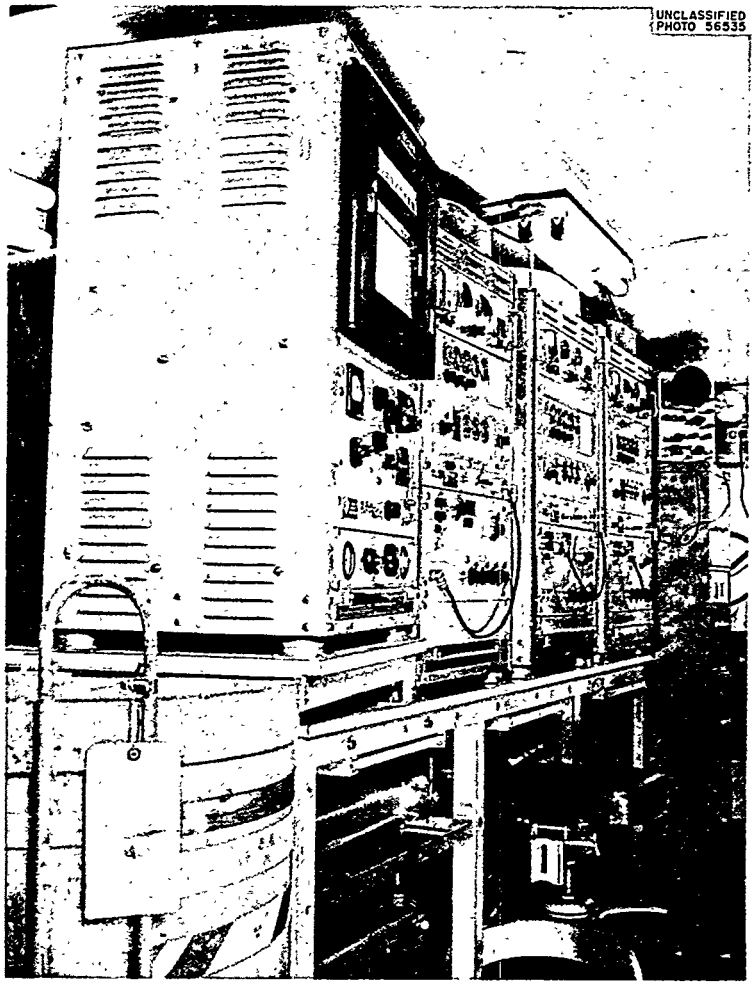

Interior view of mobile laboratory showing instruments on left side.

the "Savannah" shield. The primary gamma-ray instrument is an anthracene-crystal scintillation counter whose sensitivity has been increased by using a pulse-counting technique to permit measurement of dose rates as low as 0.01 milliroentgen per year. The pulse-counting method was made applicable by the development of a small, transistorized integrator which can be mounted within a standard A1D amplifier. The response of the integrator is linear to within ±5% over the entire pulse-height range of interest. Dose rates as high as 20 milliroentgens per hour can be measured before the anthracene crystal saturates; and the detector is insensitive to neutrons, sensing only about 2% of the actual dose from a polonium-beryllium source.

A highly sensitive BF_3 proportional counter is used for measuring thermal-neutron flux. The pressure of the BF_3 fill gas is several times that customarily used. This increases the sensitivity and also makes that counter better able to withstand accidental damage during field use. Response of the detector is approximately 7400 counts per minute per millirad per hour.

Fast-neutron dose rates for the NS "Savannah" are assumed to be only about one-tenth of the total permissible dose or about 0.05 rem per year. Although proton recoil proportional counters of the Hurst type have been widely used for fast-neutron detection, present techniques place a lower limit of about 1 millirad per hour on the measurable dose rate with such counters; and the lower energy bias level is approximately 0.2 million electron volts. In order to cover the energy range below this cutoff and to achieve greater sensitivity, a modified long counter was developed, consisting essentially of a high-pressure BF_3 counter enclosed in a cadmium-covered polyethylene cylinder. Two polyethylene cylinders were designed with the thicknesses tailored so that with one of the cylinders the counter response is proportional to the physical dose, and with the other the response is proportional to the biological dose. This instrument was calibrated with standard sources and was also shown to be capable of measuring fast-neutron dose rates as low as 0.05 millirad per hour from a mockup of the "Savannah" shield in the Bulk Shielding Reactor Facility.

The survey of the "Savannah" reactor shield was conducted May 20 to May 25, 1962, during a cruise of about 2800 miles. All measurements were made with the reactor at essentially full power.

Prior to the start of the survey, the secondary shield was marked in a 3-foot grid by the reactor operator. The general procedure consisted of making measurements at each of the grid points with both thermal-neutron and gamma-ray dosimeters. After each grid-point count, the detector was swept slowly over the shield surface between grid points to detect any small area of unusual leakage. The entire shield was covered in this manner for both thermal neutrons and gamma rays. Fast-neutron dose rates were measured at carefully chosen locations over the shield in sufficient quantity to permit a good map of the ratio of fast to thermal neutrons. By using these measured ratios, the thermal-neutron dose rates observed over the entire shield can be used to give a good estimate of the fast-neutron dose rate.

In addition, several special points were surveyed for which predicted dose rates were available from The Babcock and Wilcox Company shield design calculations. Finally, an experiment was performed for determining the effect of the accidental loss of water from the "deep tanks" beneath the reactor. In this experiment, fast-neutron, gamma-ray, and thermal-neutron detectors were positioned in three locations at tank-top level: fore and aft of the reactor shield on the vessel's center line and approximately amidship at one side of the shield. Counts were made at closely spaced, regularly timed intervals as the water was being pumped from the tanks. After the tanks were emptied, counters were interchanged, and the experiment was repeated while the tanks were being refilled.

Although reduction of the shielding survey data is not yet complete, it appears that the shield contains no significant voids or cracks and that the stringent dose-rate specifications have essentially been met. In addition, the data obtained by emptying the deep tanks indicate that no significant hazard will arise because of accidental emptying.

Nuclear Technology and General Support

RADIATION DAMAGE: ADVANCED ENGINEERING AND DEVELOPMENT

Alloy Research

The properties of some alloys are known to be strongly affected by diffusion-controlled reactions such as ordering or precipitation. Therefore the enhancement of such reactions by irradiation is of direct significance in the use of alloy materials in reactor environments. One particularly important point is how the rate of radiation-enhanced diffusion depends on the flux of the bombarding particles. This factor deserves special attention because the engineering testing of materials usually involves short-time high-flux irradiations in test reactors, whereas the components themselves are often subjected to long-time low-flux conditions in service.

Experiments at the Oak Ridge National Laboratory on the radiation enhancement of ordering in copper-aluminum alloys by neutron, electron, and gamma-ray bombardment have indicated that the reaction rate is proportional to the bombarding flux taken to a power less than unity. This observation implies that, for the same total dose, alloys irradiated at low fluxes undergo larger changes in properties than those irradiated at high fluxes, provided that diffusion in the alloy is the controlling factor.

Alloying by Transmutation

Recent experiments utilizing the high thermal-neutron flux available in the Oak Ridge Research Reactor have demonstrated that it may be possible to study the formation of alloys in a new and valuable way. For example, gold, which has a high thermal-neutron-absorption cross section, transmutes to mercury when irradiated with thermal neutrons. However, what was not realized previously is that during the irradiation the mercury (Hg), formed by transmutation, interacts with the gold (Au) to produce the intermetallic compound $Au_{0.8}Hg_{0.2}$, even though the temperature at which irradiation was performed was too low to permit these elements to interact thermally; that is, there was no melting. Experiments show that the intermetallic compound $Au_{0.8}Hg_{0.2}$ forms at 80°C, when formed in this way. Normally this compound forms at approximately 400°C when formed by melting the constituents together. (It may be that radiation-enhanced diffusion is the principal factor in causing the compound $Au_{0.8}Hg_{0.2}$ to form.) However, when shorter irradiation periods are employed and consequently smaller amounts of mercury are created, a random solid solution of mercury in gold is formed, and in this case diffusion need not play a role.

An important feature in these experiments is the necessity of irradiating extremely small, perfectly formed spheres of gold with diameters of the order of a few hundred microns to make certain that all portions of the gold are irradiated equally in order to introduce uniformly the mercury into the gold.

The possibility of introducing into a metal small amounts of a second element by controlling transmutation so that a few atoms at a time are affected may be most valuable in leading to a better understanding of the mechanism of alloy formation and behavior.

BASIC REACTOR PHYSICS

Coordinated with but separated from the various reactor projects at the Laboratory is the program of basic reactor physics. One phase of this program consists of experiments with integral multiplying assemblies which serve not only as a basis for establishing critical parameters but also as a means for studying basic fission properties. It

also includes experiments with nonmultiplying assemblies to study the slowing down and diffusion of neutrons in various moderating materials, specifically beryllium and water. In the latter measurements, particular emphasis is placed on the dependence upon temperature.

The integral experiments include an extension of the application of neutron-decay measurements, such as Rossi-α and pulsed-neutron techniques, to the investigation of basic properties of nuclear reactors. In these methods the time decay of the neutron population following a pulse is measured, yielding a value of the neutron decay constant. In the first method, pulses of fission neutrons are self-generated, while in the second the pulses of neutrons are generated externally by an appropriate nuclear reaction. A typical arrangement for the second method can be seen in the photograph, which shows a 150-kilovolt positive-ion accelerator, used to produce 14-million-electron-volt neutrons by bombarding a thick tritium target with deuterium ions. The two halves of the assembly mounted on the split table are blocks of a UF_4-paraffin mixture.

Another phase of the basic reactor physics program is the measurement of differential neutron cross sections, apart from those determined from the experiments with the integral assemblies. Currently, Van de Graaff accelerators are used for the measurement of α, the ratio of the capture cross section to the fission cross section, and for measurements of neutron inelastic and related elastic cross sections and angular distributions. Since the neutron-scattering data can never be obtained experimentally in the detail required, a very strong effort is also being made to develop a

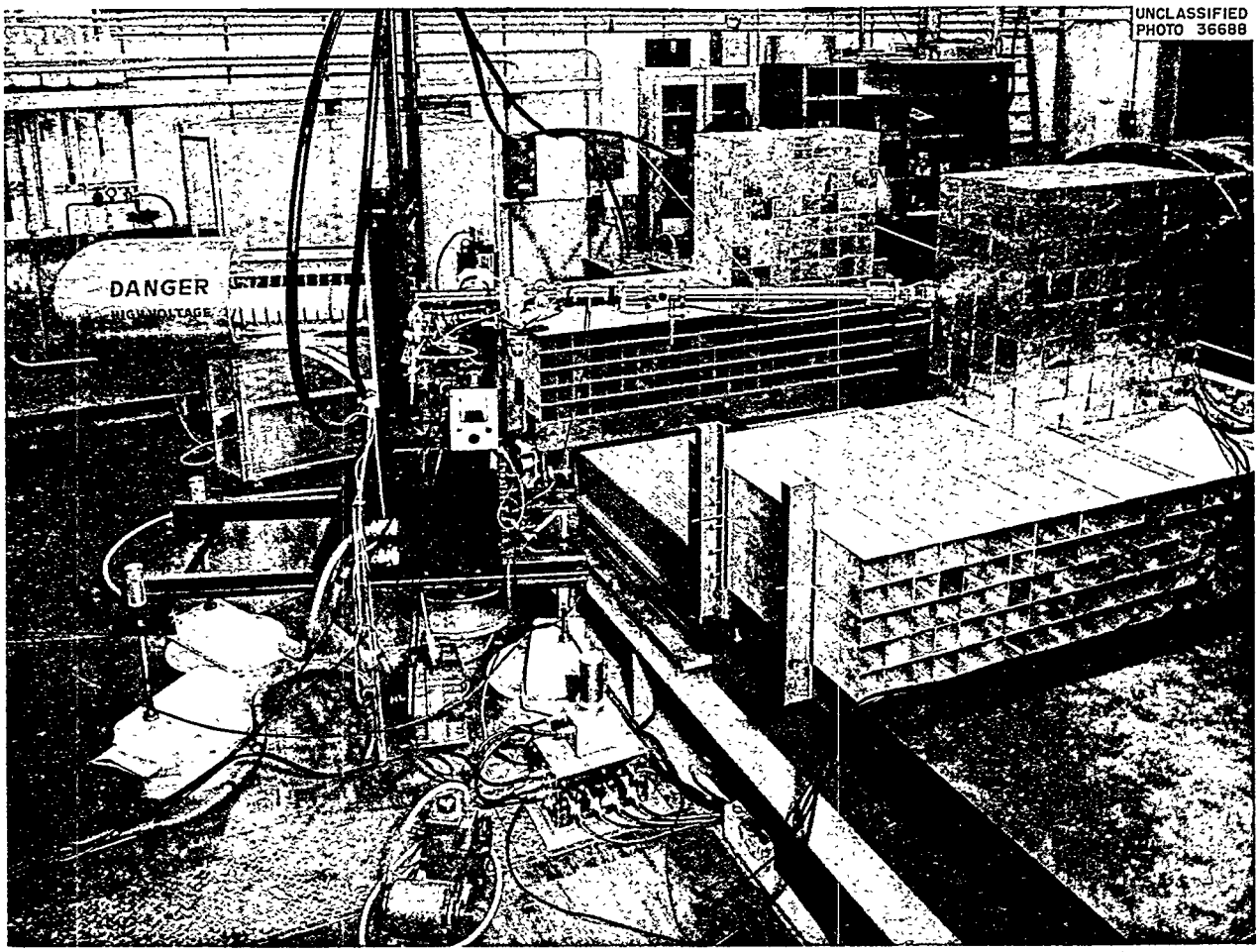

Typical experimental arrangement for time-dependent neutron studies.

theoretical model which will fit the experimental data and allow cross-section predictions to be made for a wide range of energies.

Representative studies from the reactor physics program are described in the following subsections.

Prompt-Neutron Lifetime in Hydrogen-Moderated 3% U^{235}-Enriched Uranium Critical Assemblies

During the past year the pulsed-neutron technique was used to obtain prompt-neutron decay constants for hydrogen-moderated uranium assemblies of low U^{235} enrichment. The resulting values, together with effective delayed-neutron fractions obtained from the more typical critical experiments, have allowed a determination of prompt-neutron lifetimes in equivalent spheres.

The assemblies used in the experiments consisted of reflected and unreflected delayed-critical parallelepipeds of a homogeneous mixture of UF_4 and paraffin. The fuel mixture had a density of 4.5 grams per cubic centimeter and contained 92 weight percent UF_4, in which the U^{235} enrichment was 3%. The $H:U^{235}$ atomic ratio was 133. The reflector was a 15-centimeter thickness of paraffin ($C_{25}H_{52}$), with a density of 0.93 grams per cubic centimeter.

The decay constants α were determined by (1) introducing into the assemblies bursts of neutrons produced by the 150-kilovolt Cockcroft-Walton generator shown in the photograph, (2) counting the resulting population of neutrons or prompt gamma rays, and (3) making a nonlinear least-squares fitting of the equation $y = B_1 + B_2 e^{-\alpha t}$ to the data. The resulting values of α are 344 ± 3 sec^{-1} and 258 ± 2 sec^{-1} for the unreflected and reflected assemblies respectively.

The effective delayed-neutron fractions β_{eff} in equivalent spheres were calculated by using the S_n transport method of Carlson [see *Proc. UN Intern. Conf. Peaceful Uses Atomic Energy, 2nd, Geneva, 1958,* **16**, *535–49,* (1959)] in the S_4 approximation; the 16-group cross sections of Hansen and Roach (see report LAMS-2543); experimentally determined values of the buckling (0.006413 cm^{-2}), extrapolation distance (2.5 centimeters), and reflector savings (5.7 centimeters). These calculations yielded values of k_{eff}, and the values of β_{eff} were determined from the difference in the k_{eff} values obtained with and without the delayed neutrons in four energy groups (3 through 6) being subtracted out of the calculation. This modification, for which the neutron energy distribution of Batchelor and McK. Hyder [see *Nuclear Energy* **3**, 7 (1956)] and the yields of Keepin *et al.* [*Phys. Rev.* **107**, 1044 (1957)] were used, included the subtraction of delayed neutrons from the fast fission of U^{238}. The resulting β_{eff} values were 0.00746 for an unreflected equivalent sphere with a 36.7-centimeter radius and 0.00744 for a reflected equivalent sphere with a 31.1-centimeter radius. The corresponding k_{eff} values were 0.991 and 0.999 respectively.

From the above results, the prompt-neutron mean lifetime was found to be 2.17×10^{-5} second for the unreflected sphere and 2.88×10^{-5} second for the reflected sphere.

Superprompt Critical Behavior of an Unreflected, Unmoderated Uranium-Molybdenum Alloy Assembly

The time-dependent behavior of the neutron population in an unreflected, unmoderated cylindrical assembly of a 90 weight percent uranium (93.2% U^{235})–10 weight percent molybdenum alloy following the rapid establishment of a superprompt critical condition with negligible initial neutron population was investigated to support the design of a reactor capable of producing bursts of 10^{17} fissions [*Nuclear Sci. and Eng.* **8**, 691 (1950)]. The assembly, called the ORNL Health Physics Research Reactor (see reports NDA-2136-1 and ORNL CF-61-8-71), is also designed to operate at a steady power of 1 kilowatt with natural convection cooling and at a power of 10 kilowatts for 10 minutes with forced air cooling.

The reactor is essentially a high cylinder of uranium-molybdenum alloy containing a total of 96.6 kilograms of U^{235}. It is 20.32 centimeters in diameter and 23 centimeters high. A steel rod, approximately 5 centimeters in diameter, supports 9.4 kilograms of U^{235} on the axis which, upon removal, reduces the reactivity of the assembly by 20 dollars. Three fuel rods are used to control the reactor and to provide the excess reactivity required for burst production.

Reactivities up to 11 cents above prompt critical have been rapidly introduced into the assembly, resulting in bursts yielding as many as 1.8×10^{17} fissions. The characteristics of such a burst are given in the figure.

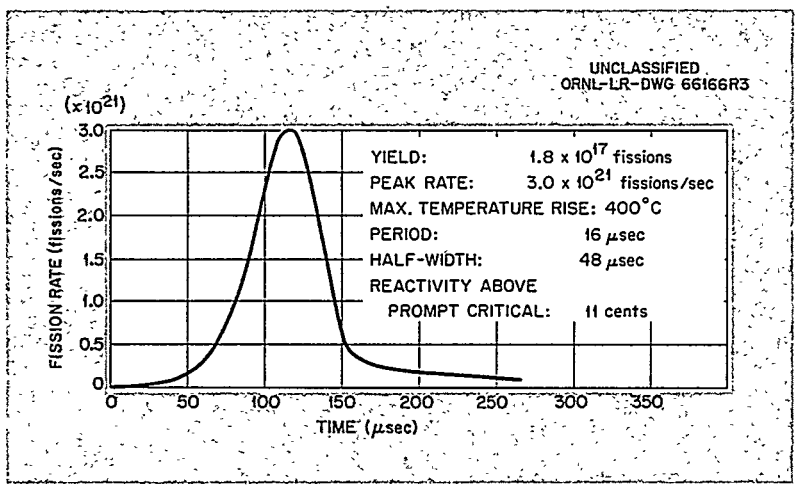

Burst characteristics of the ORNL Health Physics Research Reactor.

The number of fissions required to raise the peak temperature by 1°C obtained from these experiments is 4.6×10^{14}, while the value calculated from the specific heat of the uranium-molybdenum alloy (0.042 calorie per °C per gram) is 3.8×10^{14} fissions, assuming 178 million electron volts of heat energy deposited in the core per average fission.

The 9.4-kilogram U^{235} safety block is attached to the drive shaft of a motor by a magnet. Release of the magnet results in the safety block's falling out of the assembly. Pressure waves generated in the safety block by bursts yielding more than 6×10^{16} fissions caused it to disengage from the magnet about 225 microseconds after the peak of the burst. The removal of the safety block by this pressure wave terminates the low-amplitude "tail" which is sustained by delayed neutrons and results in a larger percentage of the fissions occurring in the peak of the burst. This phenomenon enhances the safety of operation of the system in the burst mode, since the reactor will scram itself before the scram instrumentation can cause shutdown.

The Measurement of α as a Function of Energy

One of the most important parameters required for reactor calculations is the value of α, the ratio of the capture cross section to the fission cross section. Values of this quantity have been given for the uranium isotopes in the thermal energy region [see HW-69342; *Nucleonics* **11**, 134 (1959); and *Nuclear Sci. and Eng.* **8**, 66 (1960)] and for U^{233}, U^{235}, and Pu^{239} at energies of 30, 65, and more than 150 kiloelectron volts [*Bull. Am. Phys. Soc.* **5**, 494 (1960)], but in the important energy region from 1 electron volt to 30 kiloelectron volts no reliable data exist. In an attempt to fill this gap, a series of experiments has been initiated to measure the value of α for U^{233}, U^{235}, and Pu^{239} over a wide energy range.

The experimental method being used throughout these experiments resembles that of Hopkins and Diven [*Bull. Am. Phys. Soc.* **5**, 494 (1960)], except that neutron energies are being determined by time-of-flight techniques. It consists of simultaneously measuring neutron absorptions and neutron-induced fissions within a sample, the absorptions being detected by the resulting gamma rays. If the gamma-ray detector and the fission counter both have efficiencies close to unity, then the ratio of the number of absorptions in anticoincidence with fission to those in coincidence with fission is equal to α, after proper correction for background.

Three groups of experiments will be performed. The first group, which is now under way, consists of measurements of α of U^{235} at 30 ± 10 kiloelectron volts and at 65 ± 20 kiloelectron volts. The neutron sources are, respectively, the Li^7 (p,n) and $T(p,n)$ reactions, the protons being provided by a 3.5-million-electron-volt Van de Graaff. The detector is a newly designed multiplate U^{235} fission chamber placed at the center of a 1.2-meter-diameter tank filled with a liquid scintillator,

as shown in the figure. The second group of experiments will consist of measurements of α for U^{233}, U^{235}, and Pu^{239} in the energy range from about 5 kiloelectron volts to 150 kiloelectron volts. Thick samples will be placed at the center of a 1.2-meter-diameter tank of liquid scintillator poisoned with gadolinium, the 3.5-million-electron-volt Van de Graaff again being used. Neutron energy will be measured by time of flight. Prompt-fission neutrons will be thermalized in the scintillation tank and subsequently captured in the gadolinium, resulting in a detectable gamma-ray pulse in the scintillator. The third group of experiments will be for the energy region from 1 electron volt to about 20 kiloelectron volts, again with a multiplate U^{235} fission chamber at the center of a large tank of liquid scintillator. The source will be neutrons from the Rensselaer Polytechnic Institute Electron Accelerator.

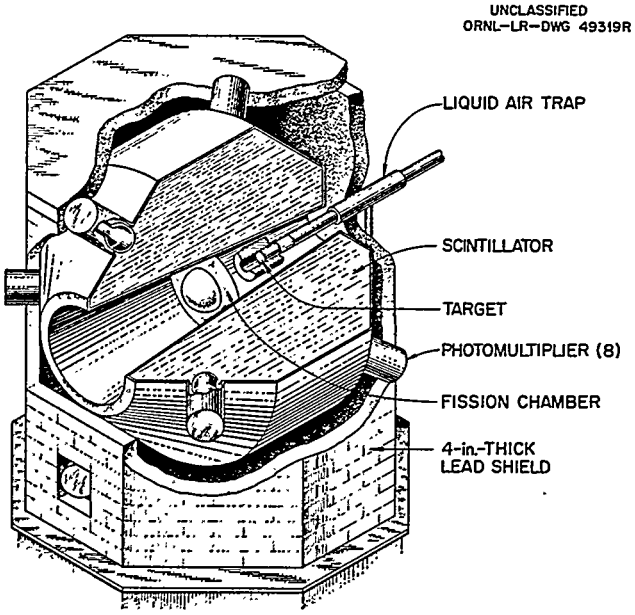

Experimental arrangement for measurement of α of U^{235} at 30 kiloelectron volts.

Thus far, only the U^{235} measurements at 30 ± 10 kiloelectron volts has been made. The resulting value is 0.375 ±0.053, which is in good agreement with the value reported by Hopkins and Diven [*Bull. Am. Phys. Soc.* 5, 494 (1960)]. This not only reaffirms their value but tests the validity of a method which has required the design and construction of a considerable amount of equipment, including fission chambers with up to 5 grams of U^{235} and electronics to permit discrimination against the concomitant large alpha-particle background.

Neutron Cross-Section Calculations

The improved accuracy of reactor calculations over the years has made it imperative that the accuracy of the neutron cross sections used in the calculations also be improved and that they be known in greater detail. For most energy regions the amount of information required is so enormous that all the cross sections can never be obtained from experiments. Thus it is essential that they be calculated on the basis of theoretical models which can produce the necessary detail. Toward this end, several theoretical models have been under development, which would not only aid reactor calculations but would also lead to a better understanding of low-energy physics.

One such model has been developed at this Laboratory. It is a nonlocal optical model which describes the total and differential cross sections for the scattering of nucleons (neutrons) by nuclei. This model is unique in that, although it depends on only a single set of parameters which are independent of the nucleon energy from 4- to 50-million electron volts, it fits the available experimental data very well.

With the nonlocal optical model it is now possible to predict total cross sections and the magnitude and angular distribution of the elastic (billiard ball) scattering for all elements heavier than magnesium for the 4- to 50-million-electron-volt energy range. The total cross sections are accurate to within 5% and the angular distributions to within 15%. Differential cross sections calculated for several elements with the model are compared with experimental results in the accompanying graph.

Work is continuing on the extension of the calculations to lighter materials and lower energies. In addition, a parallel effort is directed toward the study of nonelastic scattering – that is, neutron-induced reactions which lead to states of excitation in the target nucleus.

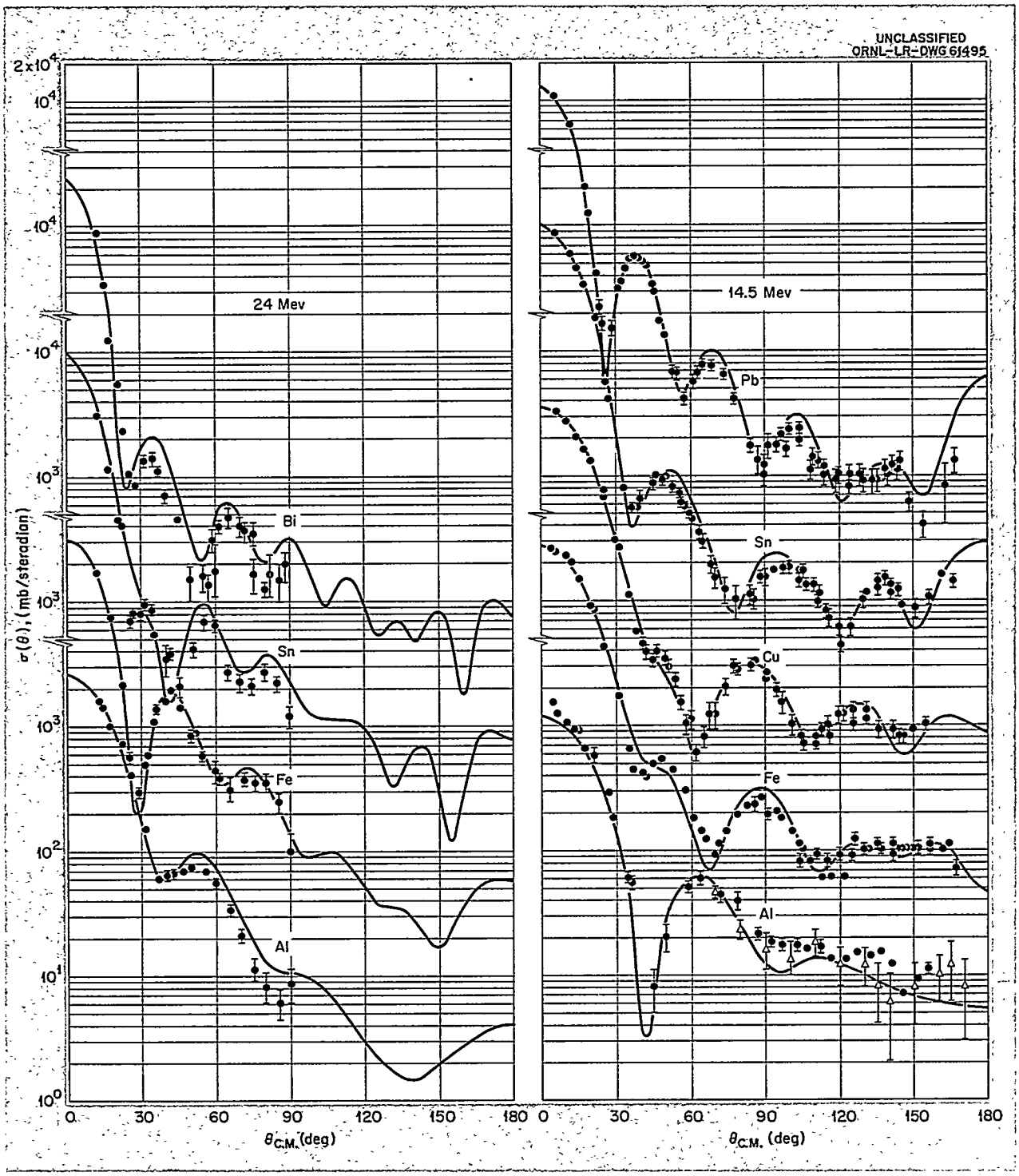

Comparison of predictions of the energy-independent nonlocal optical potential model calculations with experimental values of the differential elastic scattering cross section for 14.5- and 24-Mev neutrons incident on various elements. (Solid lines represent calculations.)

RADIATION SHIELDING

In recent years the radiation shielding program at the Laboratory has shifted from one devoted almost entirely to the study of shields for radiations from reactors to a program encompassing shielding studies for all types of nuclear radiations. As an example of the transition, the Tower Shielding Facility, which was originally constructed for shielding studies for reactor-powered aircraft, is now being used as an experimental facility to study the effectiveness of various structures against the radiation from nuclear weapons. It is also still being used for reactor shield studies, the current studies largely being associated with space nuclear auxiliary power (SNAP) reactor systems.

Another phase of the present shielding program consists of calculations of the interactions of high-energy particles with various materials of interest for the shielding of accelerators. Closely related to these are calculations and experiments investigating the interactions of high-energy radiations in space with materials proposed as shields for space vehicles.

During the past year a very important part of the shielding program has consisted of surveys of existing reactor shields to determine how well installed shields meet design specifications. This program was an outgrowth of a request by the Maritime Reactors Branch of the AEC for a survey of the NS "Savannah" shield (see the

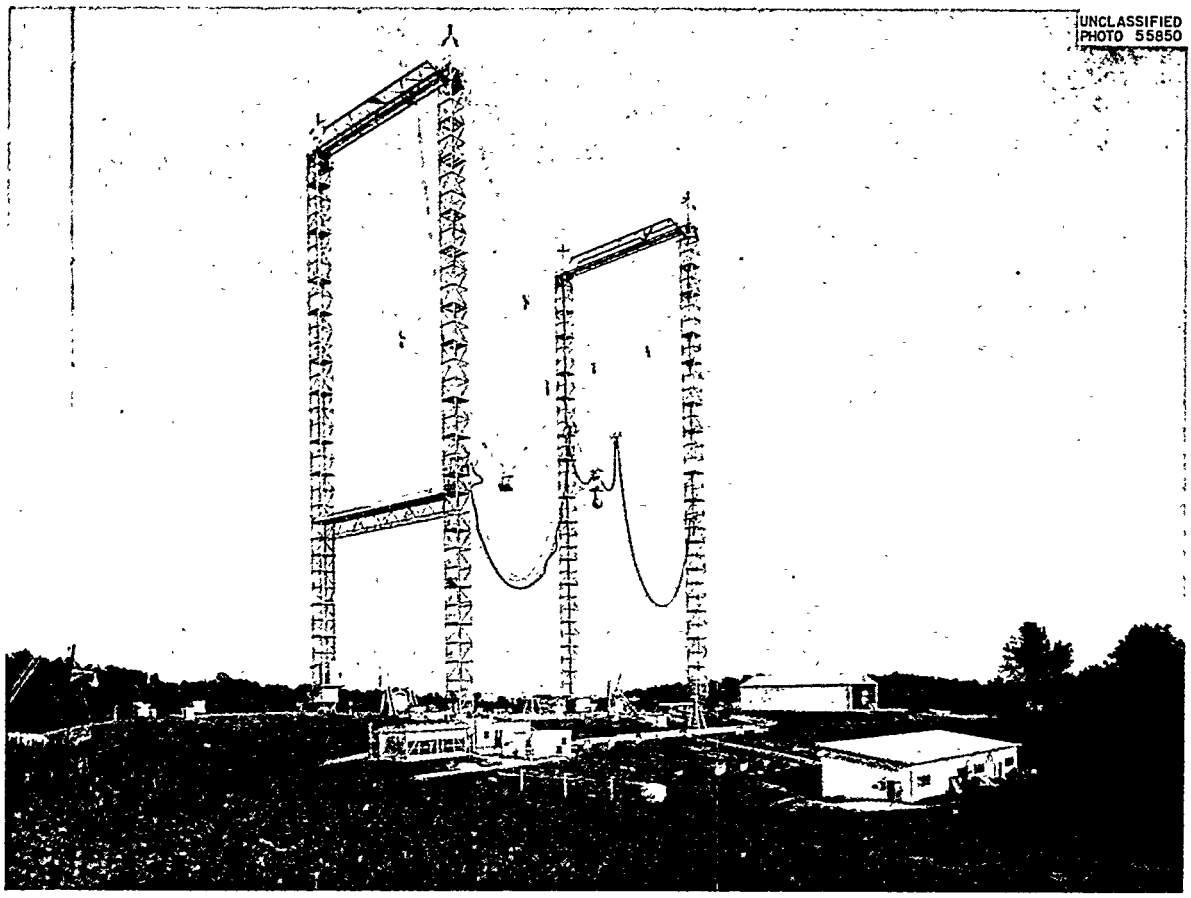

Tower Shielding Facility. The spherically shaped tank suspended between the two towers on the right houses the Tower Shielding Reactor II. The other tank houses radiation detectors. The reactor is operated remotely from an underground building to the left of the towers.

section, "Maritime Reactors Program"). In addition to the "Savannah" shield, a total of five shields were investigated.

Much of the overall shielding program consists of calculations and experiments to gather basic information for use in calculations for specific shields, the ultimate purpose being to reduce the necessity for expensive tests of shield mockups. Most of the papers given below, which are intended to be representative of the program, fall in this category.

Spectra of Low-Energy Neutrons in Lithium Hydride

Since lithium hydride is a material often proposed as a neutron shield, it is important that its radiation-attenuation characteristics be known in detail. In order to obtain the required information, a program was initiated several years ago for the purpose of determining the energy and angular distribution of neutrons both within a slab of lithium hydride and emerging from its surface. A wide range of energies is to be covered; however, during the past year the effort was concentrated on low-energy spectra and the effects of chemical binding. Spectral measurements were made at the General Atomic electron linear accelerator facility (measurements made in cooperation with J. Trimble and J. Young of General Atomic), and the results were compared with calculations.

The measurements employed time-of-flight techniques as described elsewhere (ORNL-3193, p 265; GA-1088). The source neutrons had a slightly hardened fission spectrum. Neutrons moderated in a 20-centimeter-thick LiH slab (0.75 gram per cubic centimeter) were sampled by means of a 1.25-centimeter-diameter reentrant hole partially penetrating the slab. The spectrum of forward-directed flux $\phi(\mu = 1,z,E)$ was thus obtained, where z is the distance from the bottom of the hole to the source side of the slab. $\phi(1,z,E)$ was constant in shape for z = 5, 7.5, and 10 centimeters. The scalar flux $\phi(z,E)$ was obtained from $\phi(1,z,E)$ with the Purohit transformation (ORNL-3005) derived for spectra in shields where high-flux gradients exist. $\phi(7.5\text{ cm}, E)$, as seen in the following figure, extends from about 0.025 to 300 electron volts.

Several calculations were performed. The NIOBE (Numerical Integration of the Boltzmann Equation) shielding code of United Nuclear Corporation (ARL

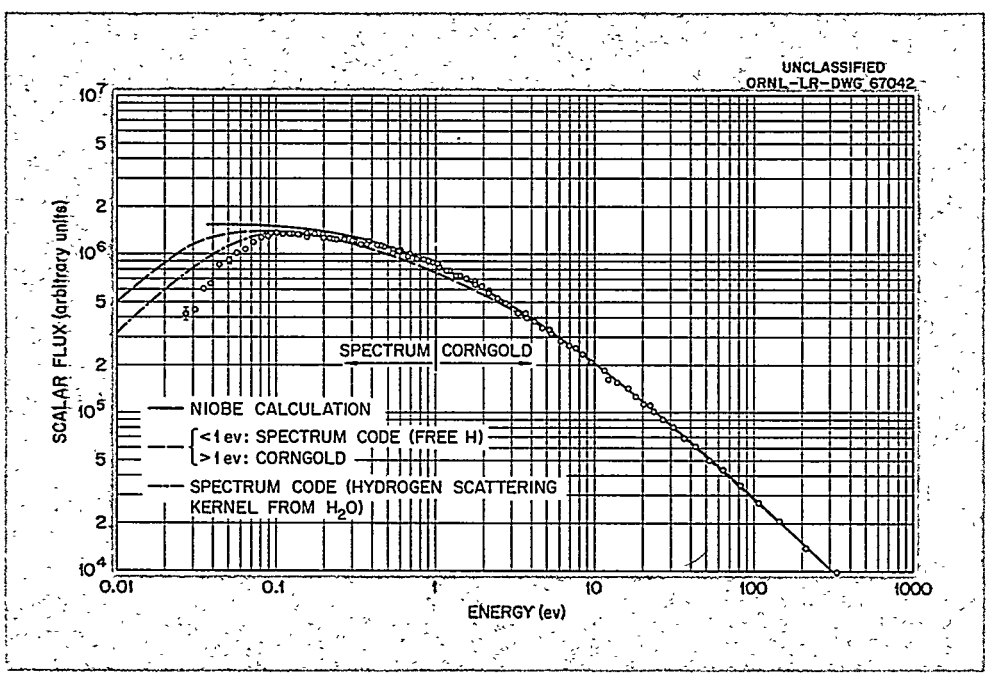

Comparison of measured and calculated scalar flux spectra for fast neutrons moderated in LiH.

Technical Report 60-134) applied to a 20-centimeter thickness of LiH (0.75 gram per cubic centimeter) and a fission source produced equilibrium spectra, $\phi(z, E)$, of constant shape in the range 5 to 15 centimeters. Purohit's transformation [ORNL-3005), $\phi(z, E)/\phi(\mu = 1, z, E)$] agreed at all energies with NIOBE predictions of this ratio (ORNL-3193, p 265). Above 0.4 electron volt, NIOBE and experiment are in excellent agreement. The measured spectrum falls off sharply from NIOBE predictions below 0.09 electron volt because of chemical binding. NIOBE employed free-atom cross sections.

The SPECTRUM thermalization code (GAMD-754) (below 1 electron volt) and the Corngold Asymptotic Expansion [*Ann. Phys.* **6**, 368 (1959)] (above 1 electron volt) were applied by General Atomic to an infinite-medium, constant-source-density calculation for LiH. The SPECTRUM code employed a free-hydrogen kernel and the scattering kernel for hydrogen bound in water as generated by the ROBESPIERRE code of General Atomic (GA-1803).

Although the water kernel gives better agreement with experiment, the remaining difference is large. It can arise from two sources now under investigation: the wrong kernel for LiH, and applying Purohit's transformation (ORNL-3005) below 0.1 electron volt with free-atom parameters. A LiH kernel is now being generated.

The neutron spectrum is very sensitive to chemical binding in a highly poisoned hydrogenous moderator [*Rev. Mod. Phys.* **22**, 254 (1950)], providing a rather sensitive check on the form of scattering kernel assumed. The measured spectrum should, however, be compared only with a transport calculation (finite gradient). But the mild disagreement between NIOBE and the thermalization codes above 0.1 electron volt implies that the gradient term in the Boltzmann equation has small effect on the spectral shape over one lethargy unit.

Fission Gamma-Ray Energy Release as a Function of Time After Fission

During the past several years a number of measurements have been made at the Laboratory of the energy spectra of gamma rays associated with fission [*Proc. U.N. Intern. Conf. Peaceful Uses Atomic Energy, 2nd, Geneva, 1958*, **15**, 366 (1959); ORNL-2852, p 93; ORNL-2609, p 45]. No recent experiments have been performed, but existing data have been summarized and combined with new and revised results from other laboratories. The results, in terms of gamma-ray energy release per unit time integrated over energy, are plotted in the accompanying figure. All the data except that of Walton (AFSWC-TR-61-10) pertain to the fission of U^{235} by thermal neutrons. At the shortest time interval is shown the yield obtained from the so-called "prompt" fission gamma-ray measurements of Peelle, Maienschein, and Love [*Proc. U.N. Intern. Conf. Peaceful Uses Atomic Energy, 2nd, Geneva 1958* **15**, 366 (1959)] measured with a resolving time of $\sim 5 \times 10^{-8}$ second. The actual time required for the fission process is, of course, much less. For the time interval between 6×10^{-8} and 1.1×10^{-6} second, the "short-lived isomer" data of the above-noted authors are shown. An integration over energy of the previously published spectral data for this time region agrees, to within ±25%, with integral experimental measurements of the time dependence for the energy range above 0.17 Mev. The time-dependent data were obtained with a single NaI(Tl) crystal, and thus the errors in the energy release are large. The factor-of-two limits shown, however, are surely conservative.

The noticeable gap in the data in the interval from 1×10^{-6} to 5×10^{-4} second after fission results from the breakdown, due to excessive background, of the method used to obtain the data for shorter times. It is hoped that this gap may eventually be filled by an extension of the method of Walton (AFSWC-TR-61-10) to this region.

For the time range from 5×10^{-4} to ~ 10 seconds, new data of Walton are shown. These were obtained with a pulsed gamma-ray source provided by an electron linear accelerator. The measurements were made with a plastic scintillator observing gamma rays following photofission in a U^{238} sample. The plastic scintillator, like the single NaI(Tl) crystal, does not permit a determination of the energy release, since it is a poor gamma-ray spectrometer. In order to calculate the results shown, Walton assumed: (a) that the energy spectra do not vary with time over the time region studied and (b) that the U^{238} photofission data could be normalized in the 1- to 10-second time region to that obtained from thermal fission of U^{235}. The detector efficiency was shown to be constant to within ±50% for gamma-ray energies

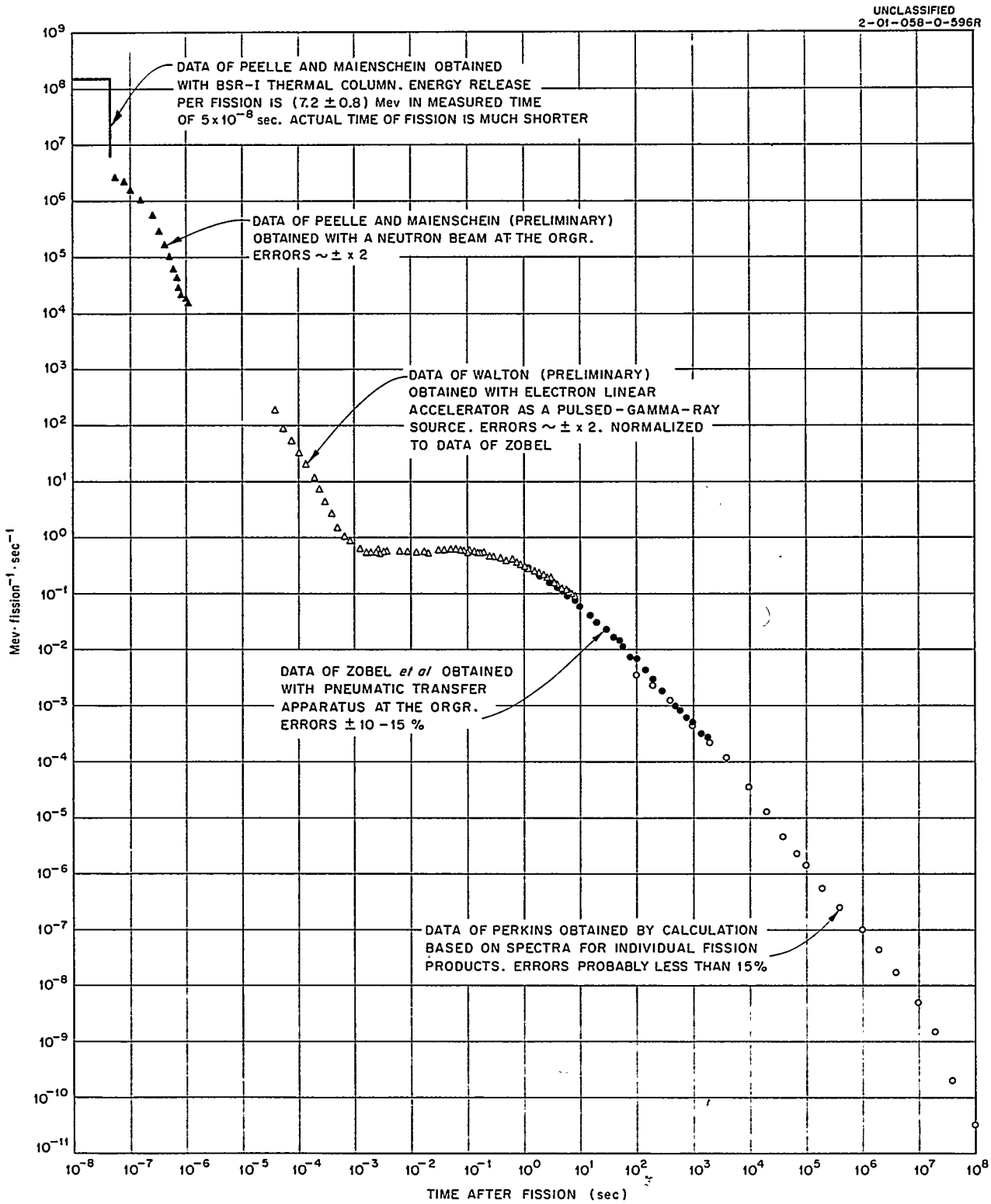

Fission gamma-ray energy release as a function of time after fission.

above ~0.3 Mev, and valid to within a factor of 2. If the assumption of a constant spectrum with time is tenable, the value for the energy release would also be valid to within a factor of 2.

Experimental Verification of a Geometrical Shielding Transformation

A geometrical transformation enabling dose rate obtained with a large disk to be inferred from data obtained with a smaller disk is being experimentally tested at the Lid Tank Shielding Facility (LTSF). Thermal-neutron fluxes from source disks with diameters of 7, 9.33, 14, and 19.80 inches, which were simulated by cadmium irises placed adjacent to the 28-inch-diameter LTSF source plate, are being measured and compared to predictions based on standard transformations. The experimental work is complete, and the analysis is in progress.

Shielding Codes

A number of subroutines and packages of subroutines have been written to handle various procedures frequently employed in shielding calculations.

The routine REDΦ5R (ORNL CF-61-1-2) was written in FAP language to allow the FORTRAN programmer to process more efficiently neutron histories generated by the Φ5R Monte Carlo code. The routine allows the machine to read magnetic tapes and compute simultaneously.

The routine TERPΦL (ORNL-3255) is used to generate a large table of values of a function by use of any of four interpolation schemes to interpolate between values given in a relatively small table with arbitrary entries. The values in the large table are at uniform intervals, allowing a simple, efficient table lookup.

The routine ENΦFX (ORNL CF-62-2-20) is a routine which evaluates the frequently occurring function,

$$E_n(x) = x^{n-1} \int_x^\infty \frac{e^{-y}}{y} dy \ .$$

The Gaussian integration package (ORNL-3263) accomplishes all the mechanics necessary to perform an up to fourfold numerical integration. Routines to evaluate the integrands must be supplied by the user.

The gamma-ray cross-section package (ORNL TM-234) is a system for generating the important gamma-ray cross sections for any array of multielement media and supplying these cross sections efficiently for any energy specified.

The code ΦGRE-P1 (ORNL TM-167) is a Monte Carlo program for computing gamma-ray transmission through laminated slabs. The source is an isotropic, cosine, or collimated monoenergetic source.

Intranuclear Cascade Calculation

A code for the calculation of intranuclear cascades has been completed. Cascade reactions for incident neutrons, protons, π^+, and π^- on all elements with atomic number greater than He^4 can be calculated. The energy range of incident particles for which the calculation is valid is from about 30 Mev to about 400 Mev. The details of the nuclear model that is used are described elsewhere (ORNL-3016, p 235). A wealth of information can be obtained from the cascade code and auxiliary analysis codes. This consists of data such as the momentum distribution, angular distribution, and excitation energy distribution of the residual nucleus; the angular distribution of the escaping cascade particles in various energy intervals; the energy spectra of the escaping cascade particles in various angular intervals, etc. In addition, an auxiliary code is available which permits the calculation of radiochemical data [i.e., (p,x,n) cross sections, etc.] by an evaporation calculation. This code incorporates the work of Dresner (ORNL CF-61-12-30) who used an evaporation model very similar to that of Dostrovsky *et al.* [*Phys. Rev.* **116**, 683 (1959)].

A Monte Carlo Calculation of Scattered Neutron Fluxes at an Air-Ground Interface Due to Point Isotropic Sources on the Interface

Scattered neutron fluxes on the interface between SiO_2 ground and air due to 1- to 19-Mev point isotropic monoenergetic sources located on the interface have been calculated by the Monte Carlo method at distances out to 4×10^5 centimeters from the source (ORNL-3287). The validity of the method was established by comparing Monte Carlo results for an infinite air medium with moments

method results. The two methods were found to yield fluxes that were in good agreement out to eight source mean free paths for a 2-Mev source. At higher source energies the treatment of inelastic scattering as isotropic elastic scattering overestimated the high-energy flux and underestimated the low-energy flux, while allowing only P_1 anisotropic elastic scattering overestimated the high-energy flux near the source and underestimated it far from the source. Scattered neutron fluxes at the interface of black ground and air, which is a useful limiting case, were also calculated.

Studies of the Longitudinal Development of High-Energy Electron-Photon Cascade Showers in Copper

Numerical results of the track lengths of photons and charged particles and the energy deposition as a function of depth out to ten radiation lengths in copper have been obtained for the case of electron-initiated electron-photon cascade showers (ORNL-3329). The incident energy varied from 50 to 45,000 Mev in these cases.

Monte Carlo methods were used to calculate the longitudinal development of the showers. The Bethe-Heitler cross sections which include screening and the correct energy dependence were used for bremsstrahlung and pair production events. The Klein-Nishina formula was used for Compton scattering. Energy losses by ionization collisions were treated as a continuous energy degradation process.

Nucleon-Meson Cascade Calculations

A straight-ahead approximation has been used to obtain a set of coupled integro-differential transport equations which describe a nucleon-meson cascade, and calculations have been carried out for several cases which are of interest in the design of the shield for the proposed 45-Gev Stanford accelerator (ORNL-3289). In order to carry out calculations, the necessary physical information concerning high-energy interactions has been extracted from cosmic-ray data by introducing many *ad hoc* assumptions. Because of the very crude nature of the input data, the results must be considered very approximate.

The equations and the IBM 7090 code which solves them numerically are not restricted to the Stanford problem, but may be used for other high-energy shielding calculations.

Calculation of the Attenuation of a Model Solar Flare and Monoenergetic Proton Beams by Aluminum Slab Shields

By use of the straight-ahead approximation, nucleon-meson penetration calculations have been carried out for a model proton flare spectrum incident on a shield and also for approximately monoenergetic incident proton beams (ORNL-3317). The shield material considered has approximately the properties of aluminum.

The results from the monoenergetic beams may be used to obtain shielding information for any incident proton spectrum.

Energy Removed from Primary Proton and Neutron Beams by Tissue

The energy removed from primary nucleon beams with energies between 10 and 1000 Mev as they pass through biological tissue has been calculated. It has been shown that for neutrons with energies above 15 Mev and for protons above 300 Mev the major energy removal mechanism is nuclear absorption of the primary nucleon and that the importance of this process increases with increasing nucleon energy. This investigation included a qualitative study of the biological importance of the secondary nucleons and of the nuclear recoils resulting from the absorption process. The results of the investigation have been published (ORNL-3260).

Shielding Calculations for SLAM Vehicle

Calculations of the radiation environment around the proposed nuclear-powered SLAM (Supersonic Low Altitude Missile) vehicle are being made. The calculations consider the radiation leakage from the reactor, the production of neutron-capture gamma rays in the air and structure, air scattering of gamma rays, and shadow shield penetration. From these data the total radiation intensity at the instruments will be determined. The entire calculation is being performed on an IBM 7090 computer.

Field Studies of Reactor Shields

The as-built characteristics of the biological shields of a variety of research, training, and testing reactors have been studied during 1961 and 1962. The investigations were made possible by the development of a mobile radiation measurement laboratory, consisting of gamma-ray and neutron counters of high sensitivity and wide range, housed in a vanette truck. Reactors studied during the program included the ORNL Graphite Reactor; the 100-kilowatt TRIGA Mk 11 Research Reactor of the University of Illinois, at Urbana, Illinois; the 60-megawatt Westinghouse Testing Reactor at Waltz Mill, Pennsylvania; the 10-kilowatt UTR-10 training reactor of the Virginia Polytechnic Institute, Blacksburg, Virginia; and the 1-megawatt "swimming pool" reactor of the University of Virginia at Charlottesville, Virginia. The equipment has most recently been used for a detailed survey of the shield of the NS "Savannah." In some cases the results of the studies have served to fortify confidence in the integrity of the shield; in others over-tolerance conditions have been disclosed.

Radiation Measurements in the Vicinity of the TSR-II

The use of the spherically shaped Tower Shielding Reactor II (TSR-II) as a source of radiation for a number of shielding studies requires a knowledge of the intensity and energy spectra of radiations at various distances from the reactor. This information has been obtained in a large number of so-called "free-field" measurements at the TSF. Two different reactor shields, differing theoretically only in the hardness of their fast-neutron leakage spectra, were employed; and measurements of the thermal-neutron fluxes, fast-neutron dose rates, and gamma-ray dose rates were made as a function of the slant range (50 to 1100 feet), reactor height (116.5 to 175 feet), and the detector height (40 inches to 145 feet). Spectral measurements were also made at a few positions. The results have been collected in an ORNL report (ORNL-3288).

Naval Vessel Shielding Studies

The necessity for determining the biological dose in the interior of naval vessels due to weapons burst has prompted the U.S. Naval Radiological Defense Laboratory to design a series of Tower Shielding Facility experiments. The TSR-II source is modified by a spherical shield designed to give neutron and gamma-ray leakage spectra similar to those from a weapon, the ratio of the doses also being similar to that from a weapon. The effects on the radiation dose of hollow cubical arrangements of steel plates simulating bulkheads and decks in a vessel are being measured at a distance of 100 feet from the reactor and far from the ground. The iron plates are 1 inch thick and 4 feet square. Radiation levels are measured internal to the cube with various arrangements of slabs designed to allow measurement of the scattered radiation contribution, as well as attenuation of the radiation, as a function of the angular orientation of the cube with respect to the source.

Shielding Studies for Civil Defense

A program to evaluate the effectiveness of various shelter configurations for protection from prompt weapons radiation is under way at the Tower Shielding Facility. The shelter investigated during the past year was a 2½-foot-wide by 6-foot-long tunnel which was approximately 10 feet below ground level and had a 4-foot-diameter vertical shaft connecting at one end.

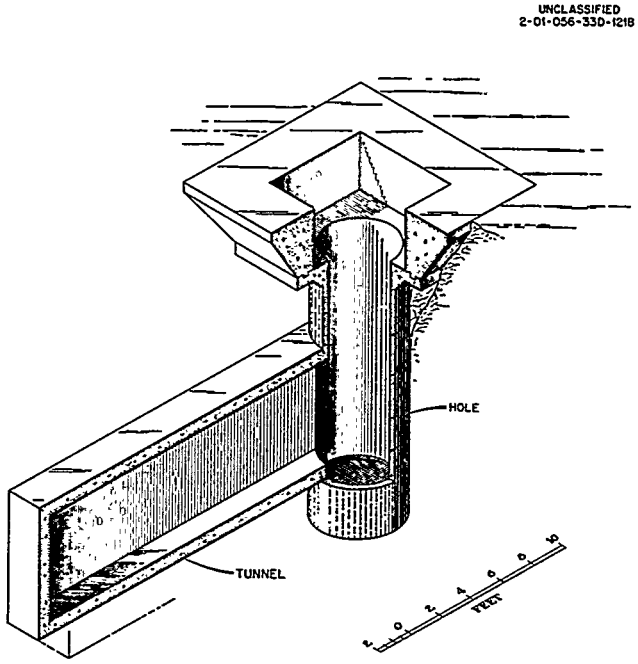

Shelter tunnel and vertical shaft.

Radiation levels within the tunnel and shaft were measured with the reactor at various angles of elevation, the "slant" range being maintained at 100 feet. Steel covers were placed over the top of the shaft in some configurations to simulate shields and blast-protective doors.

The program is continuing with investigations of other types of shelters.

ADVANCED TEST REACTOR CORROSION PROGRAM

The Advanced Test Reactor (ATR), which will be built in Idaho, has many features similar to those of the High Flux Isotope Reactor (HFIR), including fuel elements composed of thin uranium-bearing plates which will produce heat fluxes as high as 1.5×10^6 Btu hr^{-1} ft^{-2}. Present estimates indicate fuel-element surface temperatures as high as 360°F at the start of a 17-day reactor cycle. Economic considerations make aluminum the most desirable cladding material provided that adequate corrosion resistance and strength can be demonstrated.

The mechanical stability of the fuel plates depends indirectly on corrosion because corrosion leads to the formation of a layer of corrosion products with low thermal conductivity. Thus, as aluminum through which heat is being transferred corrodes, the temperature of the aluminum increases and the strength of the aluminum plates decreases. It is necessary, therefore, to minimize corrosion to prevent the penetration of the thin aluminum cladding as well as to ensure the mechanical stability of the fuel plates during reactor operation. Although aluminum appears to be suitable as cladding for the HFIR fuel plates, its use in the ATR is less certain because of the projected higher surface temperature (360°F vs 340°F) and the longer fuel cycle (17 days vs 10 to 15 days).

Tests conducted under simulated ATR operating conditions yielded results similar to results expected from an extrapolation of the HFIR test data; that is, at higher surface temperatures, higher rates of oxide formation were observed. In most tests, the thickness of oxide on the aluminum specimen was approximately proportional to time to the 0.75 power, with the proportionality constant dependent on the surface temperature (specimen-water interfacial temperature) and the pH of the coolant, and independent of the heat flux and flow rate within the rather narrow ranges investigated. In the pH range of 5 to 7, the rate of oxide buildup on the specimen was greater the higher the pH. Under identical conditions the rate of oxide accumulation on type 6061 and X-8001 aluminum alloys – the only two considered for use in the ATR – was practically the same. With both alloys, spontaneous spallation of some of the corrosion product occurred after oxide thicknesses of 0.002 to 0.003 of an inch had developed. Whenever oxide spalled from the type 6061 specimens, localized attack of the underlying metal was found; but, with X-8001 specimens, the attack of the aluminum was very uniform under all conditions.

The tests conducted to date indicate that the corrosion damage of either aluminum alloy under ATR operating conditions would probably not be sufficient to penetrate the cladding if the pH of the coolant were maintained at approximately 5 (with nitric acid). However, during an ATR reactor cycle sufficient oxide would accumulate to cause such high fuel-element temperatures near the end of a cycle that the fuel elements, as presently designed, may not have adequate mechanical stability. For this reason, means of reducing the rate of corrosion-product accumulation on aluminum by either modifying the water chemistry or forming protective coatings on the aluminum prior to test are presently being explored. In addition, it is necessary to conduct tests over a greater range of temperatures than has been employed so that the existing data can be correlated and used to predict rates of oxide growth at all temperatures of interest.

CONTRIBUTIONS OF METALS AND CERAMICS DIVISION TO REACTOR DEVELOPMENT

The contributions of the ORNL Metals and Ceramics Division to the Laboratory's reactor development program are discussed under the section, "Metallurgy and Materials Research." These contributions cover such areas as nondestructive test development, mechanical properties

research, zirconium metallurgy, solid reaction studies, materials compatibility studies, and fuel-element development.

POWER REACTOR FUEL PROCESSING

Low-cost processes are being developed for recovering source and fissionable material from spent reactor fuels of a form and composition that cannot be handled readily by previously developed technologies. Such fuels include the first-generation power reactor fuels composed of multitube stainless-steel- or zirconium-clad UO_2 or ThO_2-UO_2 assemblies and the second-generation graphite-base, uranium and thorium carbide, and BeO-UO_2 fuels. Both nonaqueous processes and head-end methods for preparing aqueous fuel solutions that may be processed by established solvent extraction technology have been investigated.

The most significant nonaqueous process is the fused salt—fluoride volatility process, which has been demonstrated on a pilot-plant scale. Development of the Sulfex and Darex head-end processes for stainless-steel-base fuels and the Zirflex process (invented at Hanford) for zirconium-base fuels was completed except for final large-scale testing with fully irradiated fuel.

The Sulfex process will be used in the Eurochemic plant in Mol, Belgium, and is being considered as the backup process to electrolytic dissolution at the Savannah River Plant. The Darex and the shear-leach processes are being considered as the prime methods for fuel processing by the planned Davison Chemical Company fuel processing plant. Design of pilot plants for these two processes was begun as a joint ORNL-ICPP effort. The pilot plants were to be installed at ICPP (Idaho Chemical Processing Plant), but both projects were canceled by the AEC in April 1962.

Remote decladding of stainless-steel-clad NaK-bonded uranium metal was demonstrated with the irradiated (675 Mwd/ton) first SRE core. The shear-leach process for all metal-clad oxide fuels is being evaluated on a full-size engineering scale with unirradiated prototype fuel.

Aqueous processes developed in the laboratory for zirconium-clad uranium-zirconium alloy fuels include the Neuflex, an alternative to the modified Zirflex process previously studied.

Fluoride Volatility Process

Volatilization of uranium and plutonium hexafluorides from fused salts is the basis of a nonaqueous chemical method being developed for processing nuclear reactor fuels. Dissolution of fuel in a fused salt (melting point, 650°C max) with anhydrous HF has been shown feasible for many materials for which aqueous methods are not feasible.

The volatilization of UF_6 from the resulting solution by reaction with elemental fluorine has been demonstrated on a pilot-plane scale. Volatilization of PuF_6 has been demonstrated at low concentrations on a laboratory scale. The uranium or plutonium fluoride is decontaminated from volatile fission products by selective sorption on and desorption from sodium fluoride. Other advantages of the process include disposal of essentially all fission product wastes as a water-insoluble solid and little need of criticality control with enriched uranium in the absence of water moderation. It is one of the few methods that can be used for processing certain advanced ceramic fuels. It can be used to process the refractory fuel-bearing ash that results from the combustion of graphite-base fuels and, with dissolvents of different compositions, may be able to process fuels clad in stainless steel and other metals. It can be used also with different head-end steps, such as chloride volatilization.

The uranium recovery process operability was demonstrated on a pilot plant scale in 10 runs with simulated fuel elements of Zircaloy-2 plate. Uranium recovery was demonstrated in 12 runs with nonirradiated fuel elements containing enriched uranium and in 4 runs with 6.5-year decayed uranium-zirconium and 5.2-year decayed uranium—Zircaloy-2 alloy fuel elements. Decontamination factors were, for example, 10^9 from Sr^{90} and about 10^8 from Ru^{106}. Fission product levels in all products were below the analytical limits of detection. The maximum total contaminants in the products were generally less than 900 ppm, with neptunium and molybdenum being the major impurities.

Uranium was recovered in laboratory experiments from Zircaloy-clad UO_2 pins that had decayed only 15 to 30 days, with overall decontamination factors varying from 10^2 for molybdenum gamma to 10^8 for strontium beta activity. The I^{131} gamma, tellurium beta, molybdenum beta, and ruthenium gamma activities tended to disappear during dissolution.

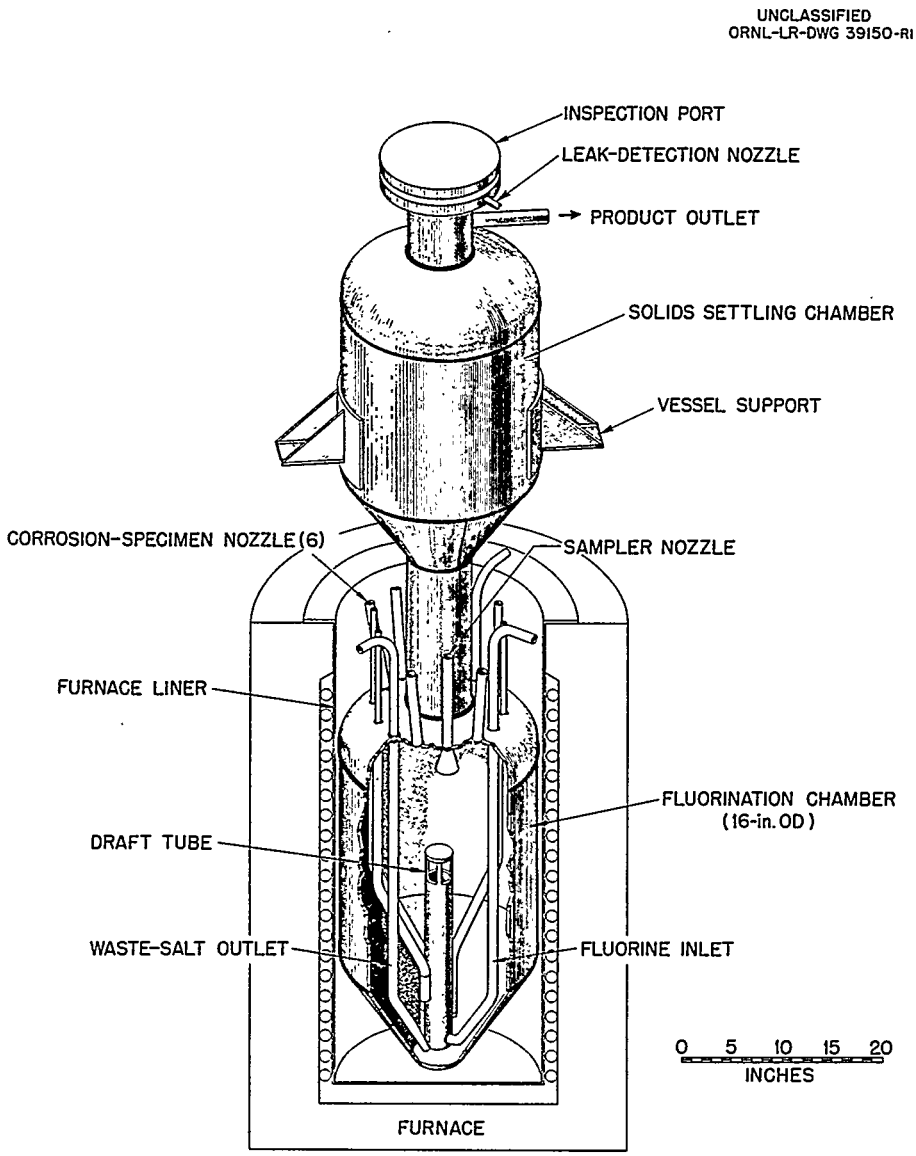

Fluoride volatility pilot plant fluorinator. Uranium tetrafluoride is converted to uranium hexafluoride in the nickel fluorination chamber. Elemental fluorine contacts uranium-bearing molten salt in the lower section of the vessel and forms volatile uranium hexafluoride, which leaves the vessel along with the unreacted fluorine at the product outlet. The normal salt level is 5 to 6 inches above the top of the draft tube. All flow lines and corrosion-specimen nozzles pass through the disk head of the bottom section. The top section of the fluorinator decreases the entrainment of salt and vessel-corrosion products in the outgoing gas. Salt samples for accountability and process control are withdrawn through the sampler nozzle.

Laboratory corrosion studies indicate that INOR-8 is a suitable material for the hydrofluorinator and either INOR-8 or an alloy of 79-4-17 wt % Ni-Mo-Fe for the fluorinator (see schematics). Off-gas solids downstream from the hydrofluorinator are largely eliminated by a recently developed HF condenser-scrubber.

The basic process is now being tested in the pilot plant with shorter-decayed fully irradiated Zircaloy-2—uranium fuel elements. Pilot plant experiments with stainless-steel-, BeO-, ThO_2-, and ZrO_2-containing fuels are planned.

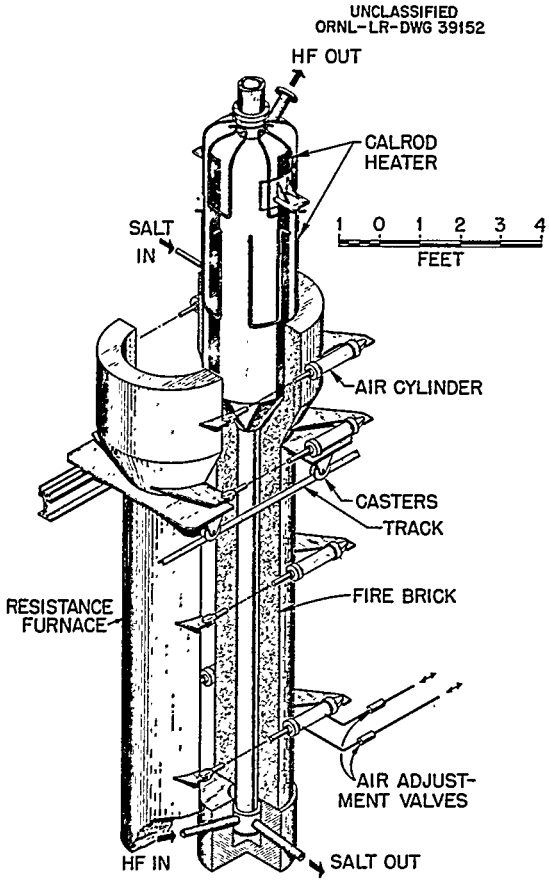

Fluoride volatility plant INOR-8 hydrofluorinator for dissolution of reactor fuels in molten salt with anhydrous hydrogen fluoride. Hydrogen fluoride enters the vessel at the bottom, a portion reacts with the fuel, converting uranium to uranium tetrafluoride, and the unreacted hydrogen fluoride leaves at the top for recycle. The vessel, normally operated at 500 to 650°C, is heated by the resistance furnace, which can be opened remotely for rapid vessel cooling. The bottom section (5 inches in inside diameter) of the hydrofluorinator accommodates fuel and salt; the top section (24 inches in inside diameter) decreases the entrainment of salt and reaction products in the outgoing gas.

Processes for Graphite-Base Fuels

Processes being developed (see ORNL-3186) on a cold laboratory and engineering scale for uranium- and/or thorium-graphite fuels include grind-leach and combustion-ash dissolution, both of which use 3 to 15 *M* HNO_3, 90% HNO_3 disintegration-leach, and chloride volatility. Only the grind-leach process appeared applicable to all graphite-bearing fuels.

More than 99% of the uranium and thorium was recovered from the High-Temperature Graphite Reactor by mechanical grinding to 16 mesh, followed by leaching with nitric acid or fluoride-catalyzed nitric acid. Coated-particle fuels had to be ground to −200 mesh to ensure rupture of the pyrolytic graphite or Al_2O_3 coatings. Uranium and thorium recoveries were more than 99% when the fuel was burned and the ash dissolved in an acid reagent, except from Al_2O_3-coated fuel particles, the chemical inertness of the sintered alumina precluding its dissolution in an aqueous reagent.

The ignition temperature of graphite was lowered from 700 to 300 to 400°C by presoaking in lead acetate, potassium permanganate, or copper nitrate solution.

Simultaneous disintegration and leaching with 90% HNO_3 recovered more than 99% of the uranium and thorium from fuels that did not contain coated particles. Both pyrolytic carbon and Al_2O_3 coatings were impervious to the reagent, but boiling 90% HNO_3 slowly oxidized graphite. Most of the carbon that was oxidized was converted to carbon oxides, but about 10% was converted to water-soluble organic acids, 60 to 80% of which was mellitic acid.

Uranium Carbide and Thorium Carbide Fuels

Details of the treatment of such fuels can be found in ORNL-3101 and the August 1962 issue of *Inorganic Chemistry*. Hydrolysis studies suggested that in heat-treating of $UC_{1.5}$ at 1600°C, any UC present disproportionates to uranium metal plus the sesquicarbide, although stoichiometric UC was stable under the same heat-treatment conditions.

Reaction of UC at temperatures between 25 and 100°C with water, 6 *N* HCl, or 20 *N* NaOH yielded principally methane, some hydrogen, and small quantities of saturated C_2 to C_8 hydrocarbons. With 4 or 16 *M* HNO_3, the major products were carbon oxides and water-soluble polycarboxylic acids, including mellitic and oxalic. Water hydrolysis of thorium monocarbide, as of UC, yielded principally methane. The primary hydrolysis product of U_2C_3 was saturated C_2 to C_8 hydrocarbons, but UC_2 yielded mostly nonvolatile hydrocarbons and some free hydrogen.

UO_2-BeO Fuels

GCRE-type fuel (70% UO_2–30% BeO pellets clad in Hastelloy-X) dissolved completely in about 8 hours in boiling 8 *M* HNO_3–0.5 *M* HF; the Hastelloy-X cladding was simultaneously attacked at a rate of only 0.3 mg min^{-1} cm^{-2}. In 2 to 3 *M* HNO_3 containing 3 to 4 *M* HCl the 30-mil cladding dissolved in 3 hours, and 99.6 to 99.8% of the uranium was leached with the resulting solution, which contained about 40 grams of Hastelloy-X per liter, in an additional 6 to 7 hours. (For details, see ORNL-3220.)

Fuels containing more than 90% BeO were best dissolved in boiling H_2SO_4 or HF-NH_4F solutions. The initial dissolution rates in 3 to 16 *M* H_2SO_4 can be represented by the equation: logarithm of (rate, mg min^{-1} cm^{-2}) = 0.223 (H_2SO_4, *M*) − 2.81. In HF solutions, the initial dissolution rate increased from 0 to 1.5 mg min^{-1} cm^{-2} as the HF concentration increased from 0 to 20 *M*.

Processes for Zirconium-Containing Fuels

The dissolution step of the Neuflex process (see flowsheet), a nitrate-free process for U-Zr-Sn alloy fuels containing up to about 10% U, was developed in small, cold, engineering-scale tests. The fuel is dissolved in NH_4F-H_2O_2, and uranium is recovered from the UO_2F_2 solution product by

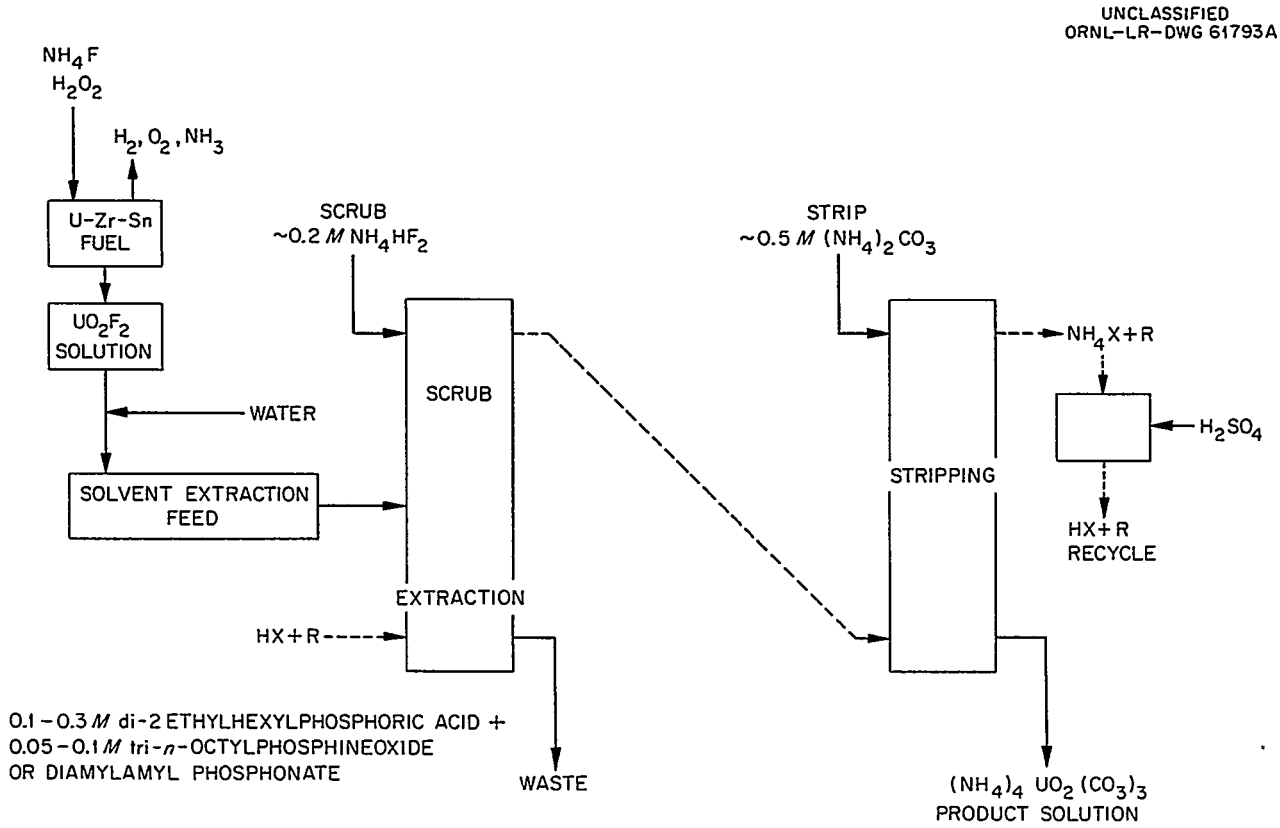

Neuflex head-end and solvent extracting process for the recovery of uranium from U-Zr-Sn fuels.

the Dapex process. In laboratory-scale tests, dissolution rates were 2 to 20 mg cm^{-2} min^{-1} at terminal free-fluoride/uranium ratios of 50 to 100. The dissolution off-gas consisted of 2 moles of H_2, 4 moles of NH_3, and traces of O_2, per mole of zirconium dissolved. Uranium is synergistically extracted from the diluted dissolver solution with di(2-ethylhexyl)phosphoric acid and a phosphine oxide or phosphonate ester, leaving a relatively noncorrosive waste. In laboratory-batch cascade extractions, uranium was satisfactorily recovered and was separated from zirconium by a factor of 10^4. Ammonium carbonate stripping of the organic yields a uranyl tricarbonate product.

The Zirflex decladding process was demonstrated at full-activity level in 22 laboratory-scale tests with PWR blanket (Zircaloy-clad UO_2) samples irradiated 182 to 17,700 Mwd per ton. Decladding in 6 *M* NH_4F–1 *M* NH_4NO_3 required 2.5 hours, and dissolution of the pellets in 4 *M* HNO_3–0.1 *M* $Al(NO_3)_3$, 5 hours. Little fracturing of high-density (96% of theoretical) pellets was noted [see photographs (*a*) and (*b*)]. Uranium and plutonium losses to the decladding solution were 0.01 and 0.09% respectively.

Laboratory studies indicated that zirconium tetrachloride may be removed from off-gas streams by hydrolysis during passage over boiling, near azeotropic, HCl solutions. This would eliminate the $ZrCl_4$ desublimation now required in the Zircex process.

Mechanical Processing

Mechanical dejacketing of the Core 1 fuel assemblies from the SRE, which had been irradiated to 675 Mwd per ton and decayed for 2 years, was successfully completed. The irradiated fuel cladding was highly hardened and much more difficult to handle than the ductile, unirradiated, assemblies. The cladding on about 7% of the fuel had to be stripped off with remotely operated hand tools. The slugs were satisfactorily steam-cleaned and recanned, and 18 liters of NaK was destroyed with steam.

Installation of the cold shear-leach facility (see photograph) in Building 4505 was completed, and the shear and leacher were completely tested hydraulically and mechanically with stainless-steel-clad porcelain-simulated fuel. The shear blade showed little wear after 3000 cuts, and particle size determinations indicated that small-size fines were predominantly porcelain and that the large pieces were mostly metal. Less than 0.1% of all particles were smaller than 0.25 micron. Fuel could not be sheared to lengths shorter than 0.5 inch without closing the tubing (see photograph). An assembly could be sheared to 1.5-inch lengths.

A cost estimate (see ORNL-3227) indicated that head-end and waste savings with the chop-leach process are appreciable but that overall plant savings are only 1 to 2%.

Solvent Extraction Studies

From solutions of UO_2 prepared in Zirflex tests, uranium and plutonium were almost quantitatively recovered (more than 99%) and were decontaminated from gamma-active fission products by factors of 2×10^4 and 7×10^3, respectively, in one cycle of 30% TBP extraction. In solvent recycle tests with these feeds, solvent diluted with *n*-dodecane was much less degraded than when diluted with Amsco 125-82. The amount of Nb^{95} in a form extractable by 30% TBP in *n*-dodecane from aqueous nitric acid decreased from about 30% in 4 *M* HNO_3 to less than 5% in 0.1 *N* acid-deficient solution (see ORNL-3285).

Protactinium Chemistry

Present chemical processing methods are not adequate for large quantities of Pa^{233} in thorium fuels. Studies on basic chemical data for use in future process development indicated a protactinium solubility of 0.12 to 0.20 milligram per milliliter in 27 to 33 *N* H_2SO_4, which increased to as much as 2.0 milligrams per milliliter in H_2SO_4 of concentrations less than 20 *N*. Protactinium hydrolyzed at H_2SO_4 concentrations below 10 *N*.

Organic amines extracted protactinium from H_2SO_4 solutions, the order of extraction being tertiary < secondary < primary. The extractability increased approximately linearly with amine concentration and rapidly with decreasing H_2SO_4 concentration. There was a single absorption peak at 2250 angstroms in sulfuric acid concentrations greater than 15 *N*, but below 7.5 *N* the peak was displaced to below 1950 angstroms, the limit of measurement.

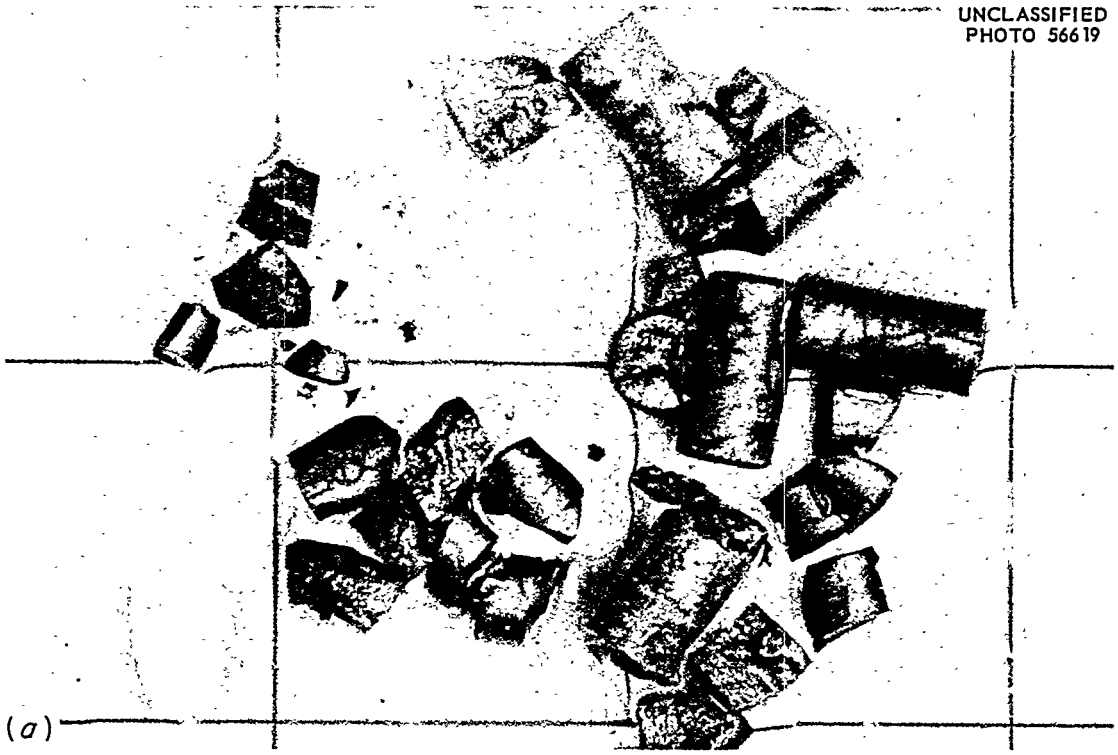

(*a*) Zirflex-declad high-density UO_2 pellets irradiated to 16,800 Mwd/ton. Density 93 to 95% of theoretical; photograph taken on 1-inch grid. (*b*) Zirflex-declad low-density UO_2 pellets irradiated to 6150 Mwd/ton. Density 93 to 95% of theoretical density; photograph taken on 1-inch grid.

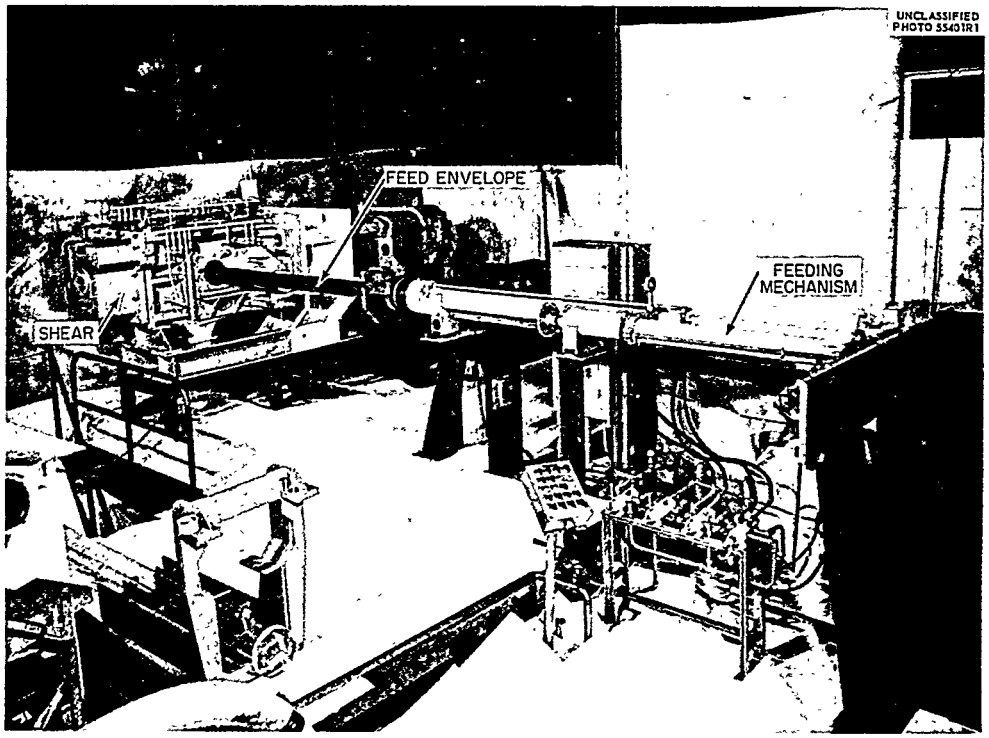

250-ton prototype shear and feed mechanism in building 4505.

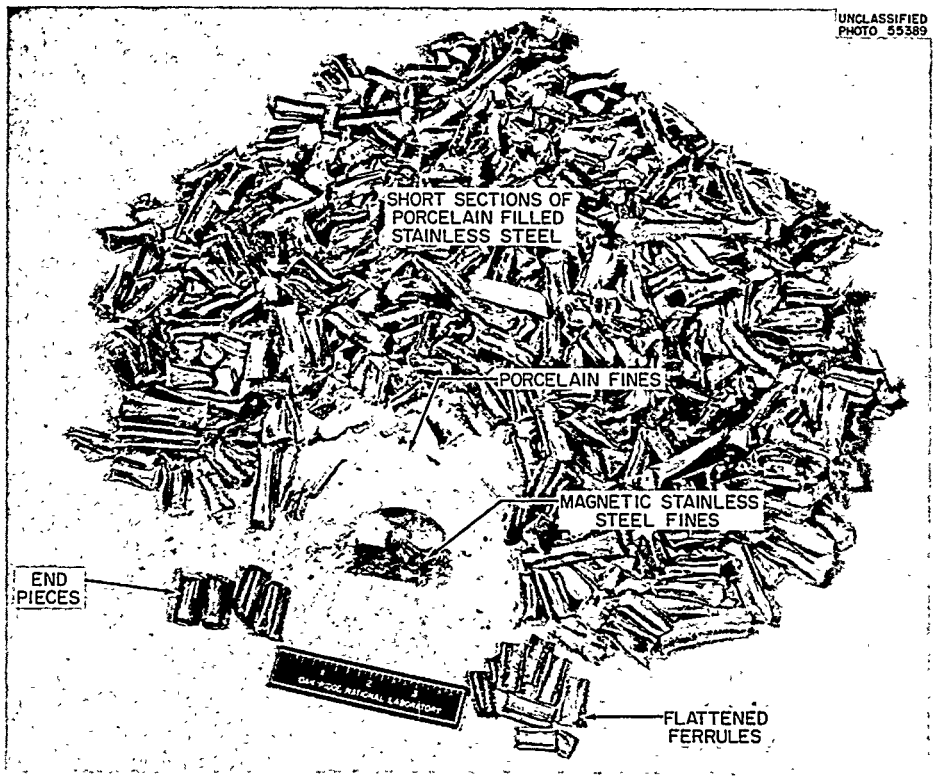

Composite material obtained from shearing of a porcelain-filled Mark I prototype fuel assembly.

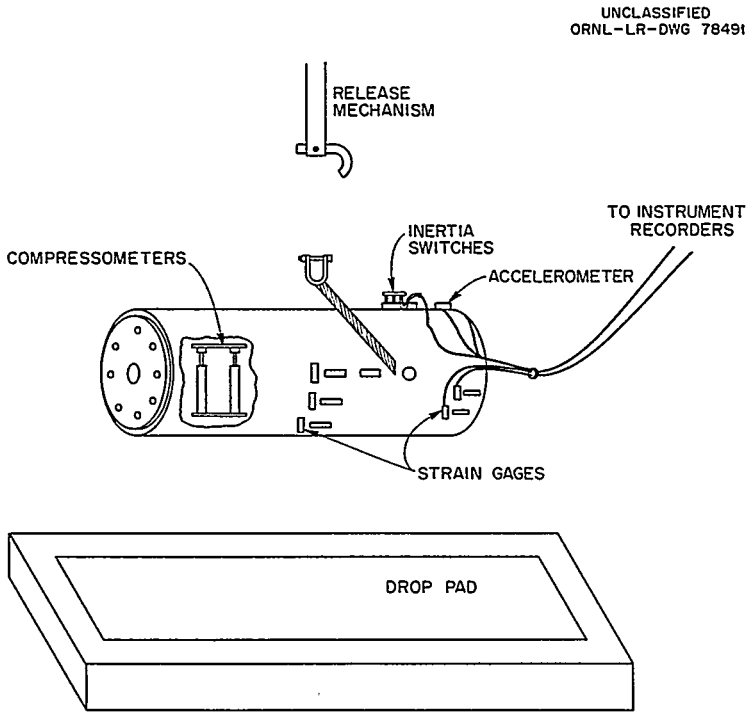

Cask drop-test apparatus and instrumentation. This represents the setup being used at ORNL for determining stress and damage to prototype fuel-shipping casks dropped from heights varying from 6 inches to 20 feet. The data are being analyzed to determine how best to predict what will happen to a 100-ton cask in a major transportation accident and to design large casks more resistant to accidental damage.

Fuel-Shipping Studies

The safety and conformance of shipments to proposed AEC fuel-shipping regulations (CFR Title 10, part 72) of highly radioactive spent fuel elements from reactors to processing facilities are being studied for improvement of cask design and to assist the AEC in improving the regulations. Mathematical models developed for predicting maximum temperatures of fuel in casks up to 300°C gave results to within 20°C of experimentally determined values. Strain, deceleration, and deformation data obtained from gages attached to prototype 1.5- to 6-ton shipping casks dropped from heights of 6 inches to 20 feet (see sketch) will be used in designing full-size casks.

DISSOLVER SOLUTION ANALYSIS

Highly accurate and precise analytical methods are required for the determination of the uranium and plutonium content of solutions resulting from the dissolution of reactor fuels. Accordingly, the Analytical Chemistry Division has continued to study the analytical problems associated with these fuel solutions with the aim of improving present methods and providing new methods for analysis of both existing and proposed fuel-dissolver solutions. These studies involved investigations of dissolution techniques, procedures for separating uranium and plutonium from the components of dissolver solutions, and methods for the final determination of uranium and plutonium (controlled-potential coulometric titrimetry).

During the past year, several controlled-potential coulometric titration methods were studied: the determination of Sb(III) and Sb(V); the determination of Np(III), Np(IV), and Np(VI); the determination of Pu(III), Pu(IV), and Pu(VI) separately and in mixtures; the direct determination of U(IV) and U(VI) in sodium tripolyphosphate medium; and the determination of both ionic and polymeric plutonium. The existing coulometric method for U(VI) determination was made considerably more tolerant to the presence of nitrates by the inclusion of sulfamic acid (to destroy nitrites) in the supporting electrolyte. Procedures and techniques were developed for determining the uranium content of ThO_2-UO_2 and Al-U fuel-element specimens, and similar studies are in progress on specimens of stainless steel–uranium, uranium carbide, and

molten-salt-reactor fuels. The determination of U(VI) by extraction into tri-*n*-octylphosphine oxide (TOPO) in cyclohexane, back-extraction, and coulometric titration is being studied and used for the analysis of various types of dissolver solutions. Preliminary work was also done on the application of this extraction to the separation and subsequent determination of plutonium. The determination of plutonium by adsorption on an anion exchange resin from 8 *M* HNO_3, elution, and coulometric titration was improved by using 0.35 *M* HNO_3–0.01 *M* HF as the eluting agent. A spectrophotometric study of the rate of disproportionation of Pu(IV) in nitric acid–aluminum nitrate solutions was completed. Finally, an instrument was designed and built specifically for the controlled-potential coulometric titration of elements of high equivalent weight. This instrument is expected to materially improve the precision and accuracy of determining both uranium and plutonium, particularly at the submilligram level.

Further work is planned to complete the studies of the TOPO extraction and coulometric titration method for uranium, and similar studies are needed to apply this separation to the determination of plutonium in the various types of dissolver solutions. Evaluation of the performance of these and other methods developed under this program will be made in the High Radiation Level Analytical Facility (HRLAF). Work is to be continued on the development of methods for the analysis of dissolver solutions of advanced fuels. New and promising methods for separating uranium and plutonium will be investigated as they present themselves. The performance of the high-sensitivity coulometric titrator will be thoroughly evaluated with specific application to the determination of uranium and plutonium.

POLAROGRAPHY IN ACIDIC FLUORIDE SYSTEMS

Acid fluoride systems have been widely used in nuclear reactor technology, particularly in the dissolution of reactor fuels, and efforts have been initiated to apply polarography to the analysis of such solutions. The use of this analytical method has been deterred, largely due to the lack of a suitable dropping-mercury electrode (DME). A Teflon DME was, for the first time, designed, fabricated, evaluated, and used successfully. The electrode is dimensionally stable, has a round, smooth-walled orifice that can be made to a specified diameter, a lapped face, and a lumen of shape that can be varied. Teflon DME's of orifice diameter in the range from 15 to 110 microns were made. Satisfactory geometric and performance characteristics were obtained in studying the polarographic reduction waves of some 26 reducible species.

In the course of the work, instrumentation was designed, built, and used for the automatic simultaneous measurement of drop rate m, drop time t, drop mass w, and drop count c of dropping electrodes. Descriptions of the Teflon DME and of this instrumentation are being prepared for publication in the open literature. The qualitative and quantitative results obtained to date with the Teflon DME indicate that the deterrent to polarographic work in glass-corroding media, particularly hydrofluoric acid, no longer exists. The possibilities for additional work with the Teflon DME are essentially unlimited because the whole area of polarography (both fundamental and applied) of redox systems in glass-corroding media is as yet essentially unexplored. The Teflon DME will also prove useful in determining the significance of certain geometric properties of any dropping-mercury electrode.

ABSORPTION SPECTROPHOTOMETRIC STUDIES OF THE POLYMERIZATION AND DEPOLYMERIZATION OF QUADRIVALENT PLUTONIUM

In the extraction and anion exchange processing and purification of solutions containing plutonium, the hydrolysis and subsequent polymerization of quadrivalent plutonium can cause serious difficulty because the colloidal, polymerized plutonium is not extractable nor does it sorb on anion exchange resins. The polymerized plutonium therefore passes into the raffinate of the extraction or ion exchange processes. In addition, solutions containing polymeric plutonium require drastic treatment before becoming suitable for further processing.

An absorption spectrophotometric study of these problems was undertaken to (1) determine the rate and extent of the polymerization of Pu^{4+} in HNO_3, $UO_2(NO_3)_2$-HNO_3, and $Al(NO_3)_3$-HNO_3 solutions at elevated temperatures and (2) to determine the rate and extent of the conversion of the polymerized Pu^{4+} to the ionic species under various conditions of acidity and temperature and by the use of degrading agents (i.e., NO_3^-, SO_4^{2-}, and F^-).

It has been established that polymeric plutonium is formed in solutions of low acidity and at high temperatures. The rate and extent of the polymerization increase very rapidly with a decrease in acidity and with an increase in temperature. At low acidities and high temperature, disproportionation and oxidation by nitrate of quadrivalent plutonium also occur. However, at low acidities, the trivalent and hexavalent plutonium, formed as a result of the disproportionation reaction, reproportionate to yield quadrivalent plutonium which then undergoes hydrolysis to yield polymer.

The polymerization process is irreversible in that the colloidal polymeric Pu^{4+} is not in true equilibrium with the ionic monomeric hydrolyzed species. Due to the irreversibility, drastic conditions of acidity are necessary to degrade or convert the polymer to the ionic species. When the temperature, plutonium concentration, acidity, or salt concentration exceeds that for a stable colloidal solution, the polymeric plutonium precipitates.

The experimental studies of the polymerization and depolymerization of plutonium have been completed. Digital computing techniques developed at ORNL are being used to resolve mathematically the absorption spectra of solutions that contain the ionic plutonium of the trivalent, quadrivalent, and hexavalent states, as well as the polymerized quadrivalent plutonium, in order to establish the valence distribution and to make other necessary types of analyses of the data. The results of these studies are being prepared for publication.

REACTOR CONTROLS DEVELOPMENT

Development is continuing on the new group of second-generation ORNL reactor control instruments (see ORNL-3191, pp 66–76), intended to meet the requirements of high-performance testing and power reactors and to exploit the characteristics of modern electronics techniques. The new systems are arranged in parallel independent channels of instrumentation, with a coincidence of two or more channels required for the initiation of control or safety action.

Safety System

The new reactor safety system, shown in the block diagram has as its coincidence element a special magnet with three electrically independent windings and a magnetic shunt (see ORNL-3191, pp 66–76). The safety element will be held if any two coils are energized and released if any two coils are de-energized. The advantage of this approach lies in the ability to apply a static test, preferably by locally perturbing the process variable as detected by the sensor, and confirming that as a result one coil in each magnet is de-energized. Thus the test encompasses the entire channel, excepting only the ability of the rod to drop.

A system was developed to test the water-temperature sensors, and thus the temperature control and safety channels, in the High-Flux Isotope Reactor (HFIR) and other water-cooled reactors. The in-process testing is accomplished by raising the water temperature at the sensors, one at a time. (Of course, the testing apparatus and procedure must not impair the ability of all sensors to detect a genuine danger condition at any time.)

The testing apparatus comprises a storage reservoir for hot water, a pump, and a special nozzle at each temperature sensor. The nozzles, which have throats $\frac{1}{16} \times \frac{1}{2}$ inch, are located $\frac{1}{8}$ inch from the sensor bulbs, on the downstream side of the bulbs in order to avoid the possibility of generating cavitation zones at the sensors.

A series of tests was performed in a test loop with a process water velocity of 21.5 fps, and temperature of 120°F, as in the HFIR. The hot water reservoir was at 180°F. The sensor was a commercial resistance thermometer with a stated response time of 1.7 sec. Analysis of data with various hot water injection velocities and orifice sizes indicates that the initial rate of rise of the sensor temperature is a function of the ratio of injection velocity to the process water velocity; the best response will be obtained when this ratio

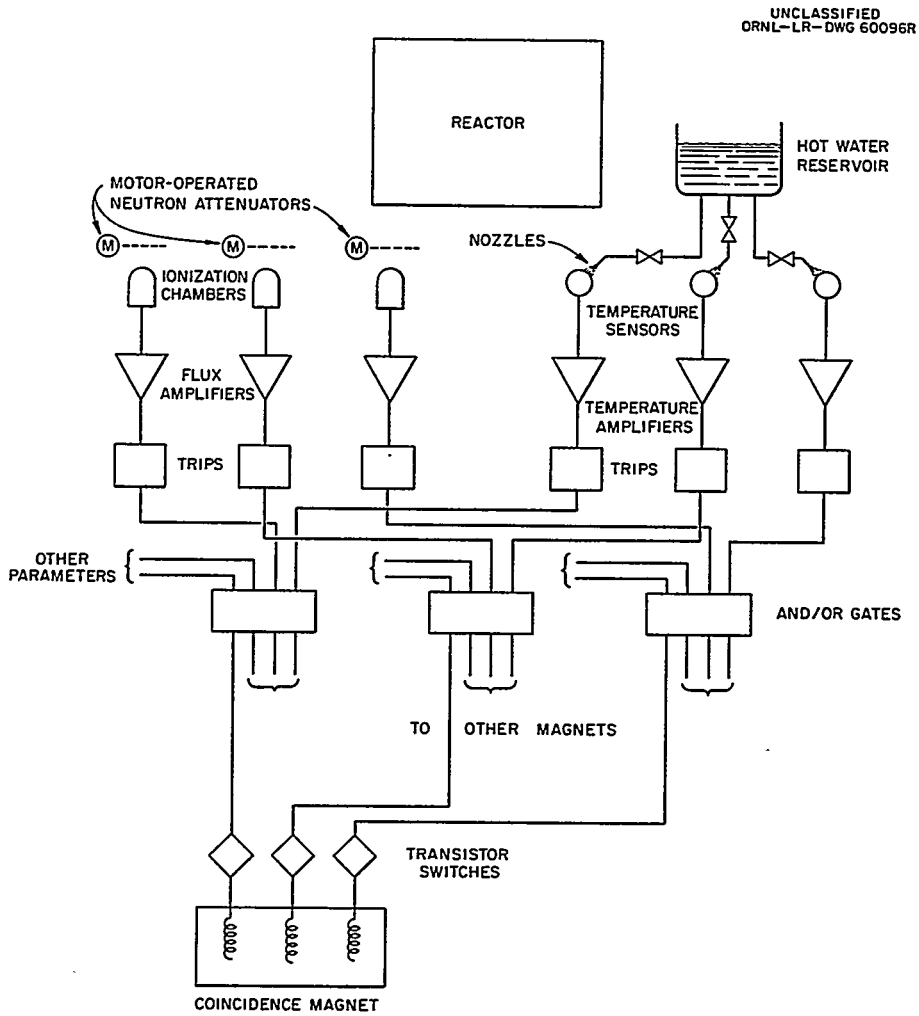

Block diagram of safety system with coincidence magnet and in-process testing.

is about 3. For the nozzle finally used, the injection velocity was 56 fps; the flow, 5.5 gpm at a nozzle ΔP = 56 psi. Under these conditions, the asymptotic temperature rise of the sensor was 40°F. The indicated sensor temperature rise reached 63% of this maximum 2.4 sec after the hot water injection was started; the sensor again read the process water temperature of 120°F 1.5 sec after the injection was stopped.

A figure of merit for such a system is the apparent reactor power increase seen by the sensor divided by the power input to the injection system; under the test conditions, the injector had a figure of merit of 1825.

Since the factors which influence the performance of the system are process water velocity and nozzle ΔP, the results of the tests at a system pressure of 27 psig can easily be extrapolated to the 900-psig operating pressure of the HFIR.

Analogous methods for in-process testing of instrumentation associated with process variables other than temperature, including neutron flux, are scheduled for development in the near future.

Development continued on the new electronic circuits required for the safety system. A transistor amplifier much simpler than the one reported earlier (ORNL-3191, pp 66–76) was devised for controlling the magnet current. Work was

begun on a transistor operational amplifier suitable for use with low input currents, as provided by ionization chambers. Development was started on a stable reliable trip circuit.

Analog computer studies using a very preliminary model of the HFIR were helpful in analyzing the performance of the reset flux amplifier (ORNL-3191, pp 66–76); predictions were confirmed as much as was possible with the crude reactor model used. In this amplifier, the gain is varied slowly by a servo system in order to recalibrate automatically the neutron-flux instrumentation so that it agrees with some absolute measure of reactor power such as heat power.

Regulating System

Development and testing continued on reactor controllers based on the multiple servo concept (E. R. Mann, private communication; and ORNL CF-61-1-82), wherein a multiplicity of independent servo systems (at least three) have their output velocities added algebraically in order to actuate a single control element. Failure of any one servo channel will not shut down the reactor, since the others will be able to overpower its saturated output in either direction. Simple tests and observations reveal easily which channel is in trouble.

The concept of the multiple servo was tested in a variety of configurations, using the analog computer to simulate some typical reactor systems. Both on-off and continuous velocity servos were assembled, using small motors and gears and transistor amplifiers. The calculations of Weaver (see ORNL CF-61-1-82) were confirmed. When one servo fails and stops, no perturbation of the regulated system is observed. When one servo fails by running away, however, some error in the controlled variable may be required to produce half the maximum velocity in the other two servos. For the case of on-off servos, the error is never greater than the servo deadband and is therefore negligible. For the case of continuous velocity servos, the error in the controlled variable depends on the servo gain; higher gain gives less error. On the other hand, the allowable gain is limited by stability considerations. For the examples studied, the maximum error in reactor power which could occur upon servo failure was less than 5%, which is acceptable for most plants.

The effect of a negative temperature coefficient of reactivity is to increase the allowable servo gain and thus to decrease the error in reactor power upon servo failure.

A model multiple servo system for the HFIR was built primarily to test mechanical components in this service, using $\frac{1}{4}$-hp dc motors and a triple-differential velocity adder. The motors were driven in the velodyne mode by transistor amplifiers. The performance of the servo was adequate at the design load; however, further development of the HFIR rods and drives required that the servos be redesigned to suit.

Startup and Wide-Range Instrumentation

A great deal of effort was expended in perfecting the design of the miniaturized flexible fission-chamber and preamplifier assembly [see ORNL-3191, pp 66–76 and *Trans. Am. Nucl. Soc.* 5, 185 (1962)]. This is part of an apparatus comprising a fission chamber, a preamplifier, and a drive mechanism. The movable assembly, which has a maximum outside diameter of 0.760 in., was made flexible so that a guide tube, curved as required, can be installed in the reactor shielding leading to the core. The assembly, shown in the photograph, is waterproof and is designed to operate continuously in an ambient temperature of 100°C.

Several developmental assemblies have been tested in a new guide tube installed in the Oak Ridge Reactor (ORR). The integral counting rate (see curve) shows a good plateau, and tests in a gamma-ray field of 1.8×10^6 r/hr demonstrated the negligible effect of gamma pileup.

Several minor circuit and layout changes were made in order to decrease the susceptibility of the system to electrical noise pickup. This problem is potentially very serious in pulse-counting systems; in many reactor installations, the counting-rate instrumentation is much too susceptible to spurious counting due to the operation of welders, crane motors, or even rod-drive motors. It is important that the counters should count only neutrons in order to make evident the presence of a source and that counts of extraneous origin can make a reactor startup very disorderly.

In a study of pickup noise in the laboratory, some aspects of observations made in the field were duplicated. Study of relay systems as noise sources showed that shock excitation of the interconnecting power wiring is responsible for a

substantial fraction of the pickup noise. Tests with different types of signal cables revealed, as expected, widely different susceptibilities to induced electrical noise. An experimental study of shielding and grounding demonstrated the value of complete double shielding. The grounding problem is complicated by capacitive coupling between grounds, leading to high-frequency ground loops; this work is continuing.

A complete transistor counting-rate instrument, comprising pulse amplifiers, pulse-height discriminator, logarithmic counting-rate meter, fission-chamber position servo, and reactor power and period computers, was developed to the breadboard stage, and is being tested. Together with the fission-chamber–preamplifier-drive assembly described above, this instrument will complete the new wide-range counting-rate channel (servo

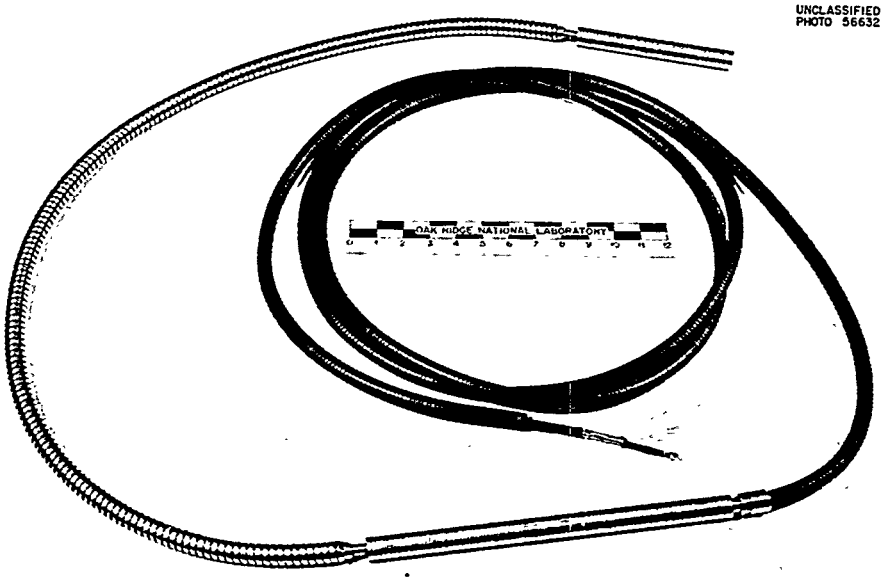

Flexible, radiation-resistant assembly of fission chamber, preamplifier, and interconnecting cables.

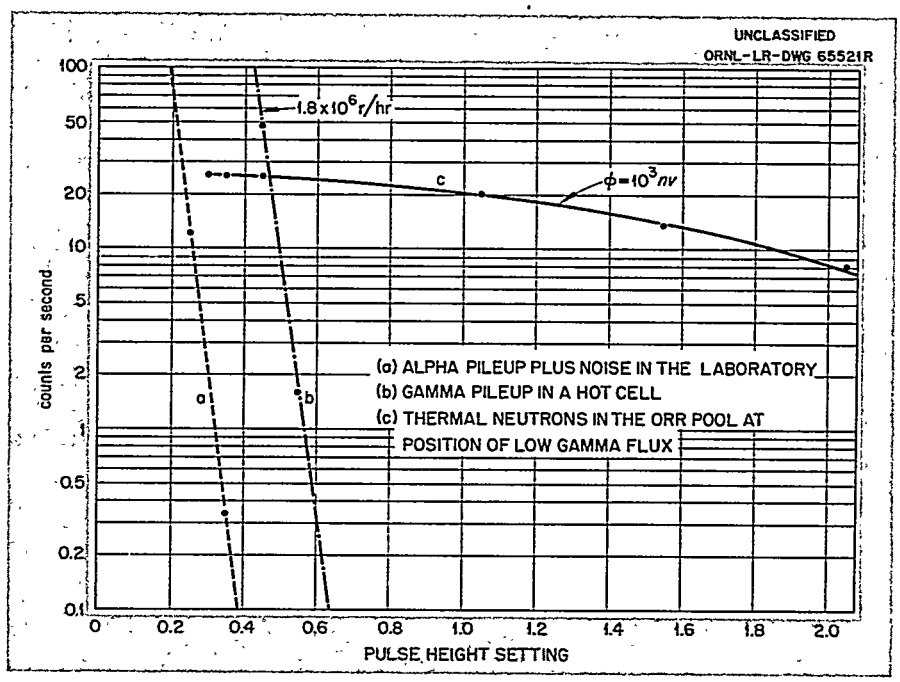

Integral counting-rate curves of the new startup channel.

fission chamber) for the second generation of ORNL reactor control instruments [see *Trans. Am. Nucl. Soc.* 3, 454 (1960)].

Ionization Chambers

Development and testing are continuing on the new series of ionization chambers (ORNL-3191, pp 66–76). Each chamber enclosure can contain up to three independent active sections, with differing characteristics. The electrode configuration of all sections is parallel circular plate, using aluminum or titanium coated with B^{10} or U^{235} for neutron-sensitive sections, and titanium, nickel, or tantalum for gamma-sensitive sections.

Development of a good method for coating boron on plates continues; present methods, while adequate, are expensive (evaporation coating) or hard to control (spraying of dispersion), and many of the coatings have marginal electrical conductivity.

A fission chamber using the same configuration was successfully assembled.

Preliminary tests in the Bulk Shielding Reactor of a gamma-compensated structure were very encouraging. The effective gamma-ray sensitivity was reduced by a factor of 80 by the compensation, which was found to be independent of chamber orientation in a region of high field gradient.

Three developmental three-section chambers are now in service in the Health Physics Research Reactor; their performance appears satisfactory.

A developmental two-section chamber was built for the ORR for use as a neutron- and gamma-sensitive safety chamber. The performance of the gamma-sensitive section has been excellent, with good sensitivity and saturation characteristics. The neutron-sensitive section will be rebuilt, with lower sensitivity to suit the proposed permanent location of the chamber.

PROCESS CONTROL

The pneumatic temperature probe (PTM) is a device for measuring gas temperatures by utilizing the dependency of the flow of gases through a restriction on the temperature and pressure conditions. The determination is made by measuring critical mass flow across a restrictive element such as a nozzle and by knowing the upstream pressure and other variables pertinent to the critical flow equation, computing the temperature at the entrance to the restrictive element. In practice it has been found useful to use two critical flow nozzles in series and to measure the ratio of the pressures at the nozzle inlets, together with the temperature at the downstream nozzle. The limitations of present thermocouple materials for long-term use at elevated temperatures make this device attractive for use on many installations.

The PTM system is being investigated at ORNL for use in the EGCR and for its general applicability to other temperature-measuring problems.

In order to determine the potentials of such a system and to intelligently apply it, it was necessary to get a fundamental understanding of sonic velocity flow through small bore nozzles.

The program being pursued is as follows: A variety of nozzle materials were tested, including sapphire, chrome-carbide, and types 304 and 321 stainless steel. The harder nozzle materials (sapphire and carbide) are more desirable but present some problems of mounting and sealing which require further development. The stainless steel nozzles showed a small shift in the first few hours of operation, but after that they proved to be stable. Stainless steel is not as desirable from the standpoint of erosion resistance, but only long-term tests (years) will determine performance.

Tests to date show that the PTM can be an accurate, predictable temperature sensing device, with good reproducibility (in nozzle sizes above 0.015 in. in diameter) for gas temperatures to 1800°F.

Future investigations will extend the upper temperature limit to 2000 to 2500°F and will concern the miniaturization of orifices, the abrasion resistance of orifice materials, and readout systems.

Waste Treatment and Disposal

WASTE TREATMENT

Pot Calcination of Highly Radioactive Wastes

High-activity wastes from reactor fuel processing may be converted to stable solids (prior to shipment and storage in a dry environment such as a concrete vault, limestone cave, or salt mine) by the pot calcination process. The liquid waste is evaporated to dryness, and the resulting solids are calcined in a stainless steel pot which, when sealed, could serve both as the shipping and the permanent storage vessel. Development work with synthetic Purex (nitric acid), Darex (dissolved stainless steel), and TBP-25 (aluminum nitrate) wastes was performed on both laboratory and engineering scales in order to provide design information for the construction of a pilot plant.

Design of a pilot plant for demonstration of the pot calcination process at the Idaho Chemical Processing Plant (ICPP) was carried through the preparation of engineering flowsheets in cooperation with personnel of the Phillips Petroleum Company. A recent decision by the AEC changed the intended location of the pilot plant from ICPP to Hanford, with the expectation that as much as possible of the original design would be retained.

The acidic waste is first evaporated to the desired concentration for feeding to the calciner. The evaporator vapor goes to an acid fractionation column, which produces concentrated acid for recycle to the fuel processing plant and a very dilute low-activity waste. The evaporator product, a concentrated solution or slurry, is fed to an electrically heated cylindrical pot for evaporation to dryness and calcination at temperatures near 900°C. Additives – for example, calcium salt and phosphorous acid – may be included to decrease sulfate and fission product volatilities and to produce glass. The calciner off-gases go through a condenser (where 85 to 95% of the nitrogen oxides are absorbed) and then are returned to the evaporator. The inert gases are separated in the reflux condenser of the acid rectifier, filtered, and released through a stack. When the pot is filled with calcined solids, connecting processing lines are broken, and the pot is sealed and removed from the furnace for shipment to a permanent disposal site.

The pots will be 6 to 24 inches in diameter and 8 to 15 feet high, the diameter being limited by decay-heat loss under storage conditions and the length by the size and weight of shipping casks permitted on public carriers.

Engineering-scale studies with simulated Purex, TBP-25, and Darex wastes demonstrated the operability of both continuous and batch evaporators in feeding 8-inch-diameter by 90-inch-high calciners at rates of 10 to 25 liters per hour. These rates are sufficient for processing the wastes from recovery of 1.8 tons per day of natural uranium fuel or 1 kilogram per day of enriched uranium fuel. The noncondensable off-gas was 15 to 50 cubic feet per hour. Solids, deposited radially in the calciner, contained a few tenths percent of nitrate ion and had bulk densities of 1.2 grams per cubic centimeter in the case of Purex and Darex and 0.7 grams per cubic centimeter in the case of TBP-25. Thermal conductivities of the solids at 800°C were 0.4 Btu hr^{-1} ft^{-1} $°F^{-1}$ for TBP-25 and 0.2 for Darex. The volume was about 10% of that of the liquid wastes. Sulfate volatilization in the calciner was limited to less than 1% by the addition of calcium nitrate solution; however, volatilization of both ruthenium and mercury was greater than 50%.

Simulated wastes from the TBP-25, Purex, and Darex processes were incorporated in glassy or microcrystalline solids by adding phosphite or hypophosphite and other fluxing agents and calcining. Volume reductions varied from 7 to 9.3 for TBP-25 and from 2.9 to 6.6 for Darex; corresponding densities were 2.35 to 2.84 and 2.2 to 3.8 grams per cubic centimeter, and softening points, 830 to 1000°C and 830 to 900°C. The addition of phosphite or hypophosphite to produce

a concentration 1.5 to 2.5 *M* (as a fluxing agent) decreased the ruthenium volatility to less than 0.1% in batch and in small semicontinuous experiments. Semiengineering-scale fixation of TBP-25 waste in a true glass incorporating 25 weight percent simulated waste oxides was accompanied by volatilization of 12.5% of the ruthenium present, with physical entrainment of 0.02% or less. The thermal conductivity of this glass varied from 1.05 to 1.60 Btu hr^{-1} ft^{-1} $°F^{-1}$ between 300 and 1050°C (softening point, about 1100°F).

Corrosion data indicate that stainless steel is a satisfactory material of construction for the calciner. Type 304L stainless steel was penetrated 0.14 and 4.5 mils in 19 to 24 hours of exposure to TBP-25 waste plus glass additives, and to Purex waste plus glass additives. This steel may be used for the calcination pot if sulfate volatility from Purex waste is properly controlled and if maximum fixation temperatures are kept below 900°C. Atmospheric corrosion in dry air at about 800°C was less than 5 mils per year.

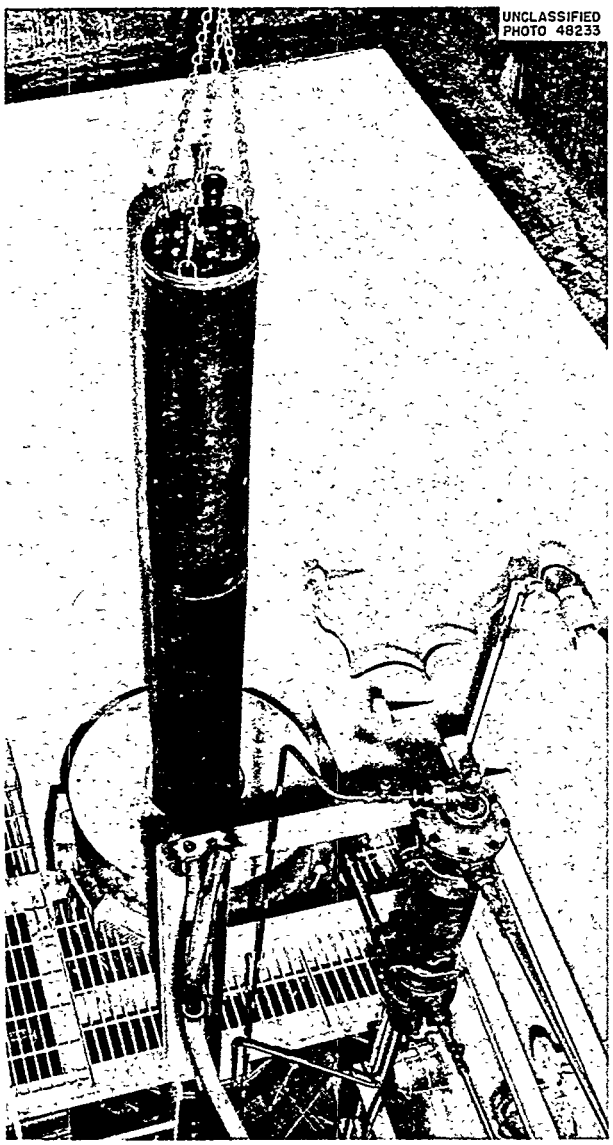

A pot being removed from a calcination furnace at Oak Ridge National Laboratory. The pot serves first as a part of the equipment that converts highly radioactive waste solutions to solids by evaporation to dryness and calcination of the resulting solids. Thereafter, the pot becomes the container for final storage of the waste in a dry place such as a concrete vault, limestone cave, or salt mine.

Chemical Scavenging and Ion Exchange Processing of Low-Activity Waste

Atomic energy laboratories and installations produce large volumes of low-activity waste whose chemical composition is not very different from tap water but which contains very small amounts

Cross section of glass made from synthetic TBP-25 waste.

of radioisotopes. This water originates from equipment cooling systems, floor drains, decontamination-pad drains, storage canals, laboratory sinks, purification systems on pressurized-water reactors, condensates from intermediate-activity waste evaporations, and discharges from low-radioactivity operations. A conceptual design and cost estimate for a 750,000-gallon-per-day plant for treating the total ORNL process waste stream indicated a capital cost of $511,000 and an estimated operating cost of 54 cents per 1000 gallons.

A scavenging–ion exchange process for removing trace amounts of fission products from process waste water was demonstrated with ORNL waste in a 600-gallon-per-hour pilot plant. The feed was adjusted to a pH of 11.6 with caustic in a flash mixer, and the precipitate, which scavenged part of the activity, was separated by a sludge blanket clarifier and polishing filter and was further concentrated for disposal by a sludge filter. A bed of Duolite CS-100 phenolic resin sorbed most of the remaining activity from the clarified liquid. After 2000 bed volumes had passed through the resin, the effluent contained less than 3% of the maximum permissible concentration of Sr^{90} and Cs^{137} in drinking water for continuous occupational exposure. Decontamination factors from Sr^{90} ranged from 2,047 to 12,160 (representing greater than a 99.9% removal) and from 77 to 3444 for Cs^{137}. The 50% Cs^{137} breakthrough point was at 2800 resin column volumes. Varying the length-to-diameter ratio of the column had no effect.

In laboratory studies with tap water, calcium hardness remaining in the clarifier effluent was decreased from 70 to less than 10 parts per million by the addition of 25 parts per million of lime at

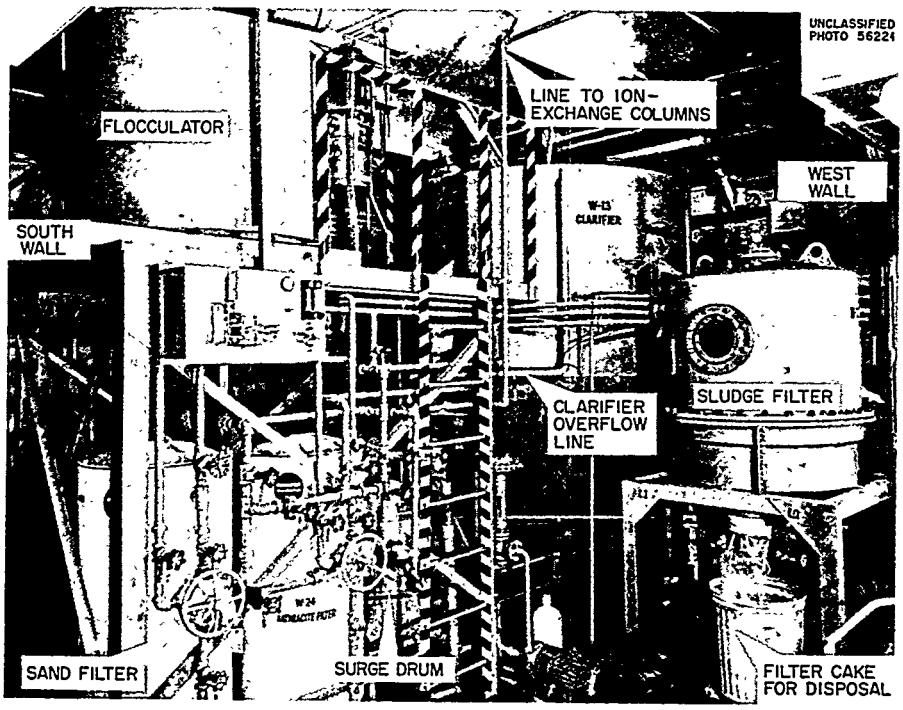

Precipitation-clarification equipment in the pilot-plant operation of the proposed ORNL low-level waste treatment prepares waste water for final decontamination by ion exchange. After the addition of chemicals to precipitate calcium carbonate, magnesium hydroxide, and ferric hydroxide, and to adjust the pH to 12, the waste flows through a flocculator, a sludge blanket clarifier, and through either a sand or an anthracite filter. The radioactive precipitate removed in the clarifier is reduced to a small volume by a sludge filter. The filtered waste water then flows to one of the ion exchange columns shown in the next photograph.

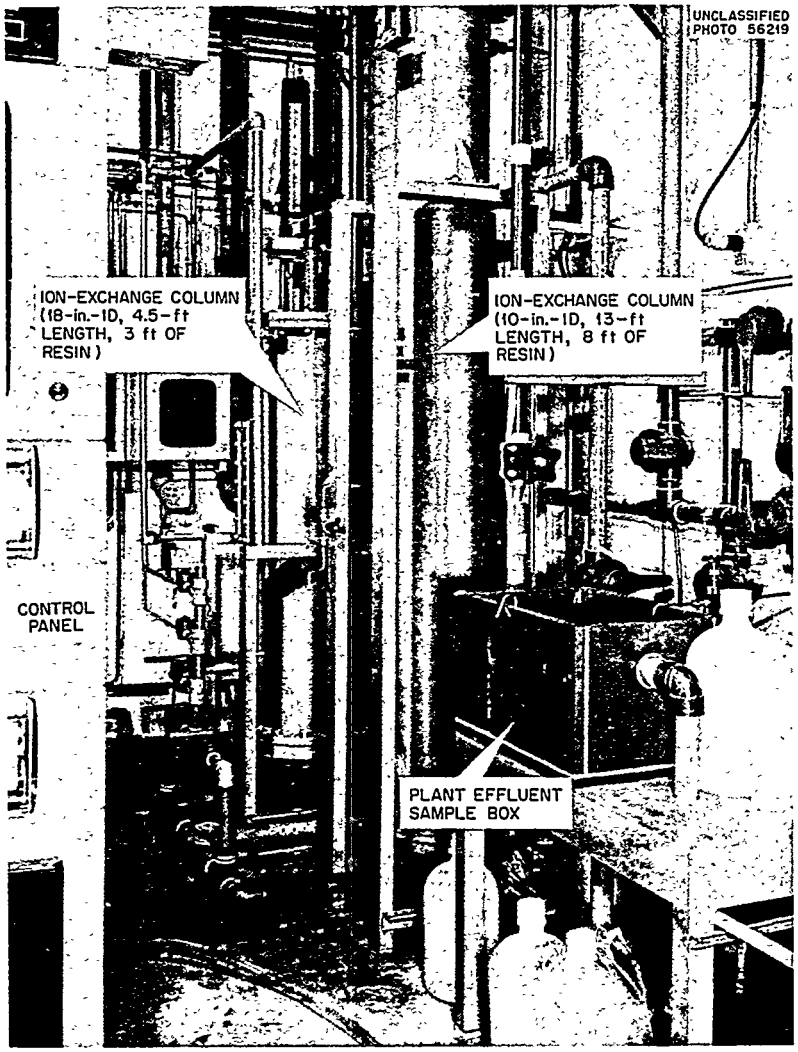

Two ion exchange columns are provided in the pilot plant of the proposed ORNL low-level waste-treatment method so that the effects of dimensions and configuration can be studied. After precipitation, clarification, and filtration in the equipment shown in the preceding photograph, the process water flows through one or the other of these ion exchange columns, which are filled with a phenolic-carboxylic cation exchange resin. This type of resin is unique in having a high capacity for the removal of strontium-90 and cesium-137 and in being easy to regenerate for re-use. Automatic instruments monitor and control the process.

25°C. Vermiculite was not suitable for use with the high-caustic head-end treatment of ORNL waste. Treatment of 20,000 bed volumes in a complete demineralization flowsheet should be possible before regeneration of the resin is required.

Foam Separation

Foam separation has shown considerable promise for removing metal ions, such as fission products, from radioactive waste solutions. After tests (see report RAI-100) with 107 commercial surfactants, the following were chosen for more extensive studies: aerosol OS, Igepon T 43, Igepon TC-42, Sipon LT-6, Tergitol 7, Veripon 4 C, and sodium dodecylbenzene sulfonate. Each of these could be used over a pH range of 4 to 10.

Studies with sodium dodecylbenzene sulfonate and ORNL tap water indicated that heights of theoretical transfer units for strontium removal are 1 to 2 centimeters of foam. Therefore only about 1 foot of foam height would be required for good decontamination (see ORNL-3314). When demineralized water instead of tap water was used, a decontamination factor from strontium of more than 1000 was obtained. Solution throughputs of 1.65 gal min^{-1} ft^{-3} of foam were achieved.

In a proposed process, low-activity waste is pretreated with grundite clay, and the clarified effluent is decontaminated in a foam column with sodium dodecylbenzene sulfonate as the surfactant (see flowsheet). In laboratory tests, tap water

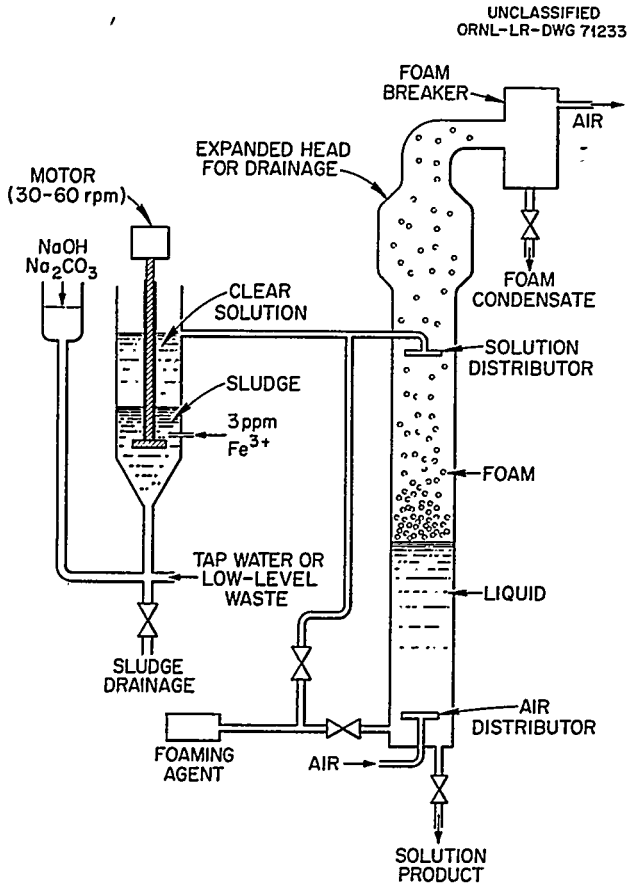

Schematic diagram of foam column for low-activity-waste treatment, with precipitator.

treated with 0.5 pound of 200-mesh grundite clay per 1000 gallons showed a preliminary decontamination factor from cesium of 10 to 40. Pretreatment of both tap water and low-activity waste with NaOH and Na_2CO_3 (to 5×10^{-3} *M*, each) decreased the total hardness from 40 to 2 parts per million and decontaminated the solution from strontium by factors of 100 and 10 respectively (see report RAI-101).

In brief studies on the foam separation of cesium from 6 *M* $NaNO_3$ solution, as a substitute for Hanford high-activity waste solution, copper ferrocyanide was added to precipitate cesium copper ferrocyanide, which was removed, with gelatin as a surfactant, by frothing or flotation. Volume reduction – that is, the ratio of the initial volume to the final cesium-rich solution volume – was greater than 300 in a nonoptimum test in which 96% of the cesium was recovered.

Analysis of the surface tension data for solutions of sodium dodecylbenzene sulfonate (see RAI-100) containing added H^+, Na^+, Ca^{2+}, or Ce^{3+} ions showed essentially the same value for all these cations for the parameter that measures the tendency of the surfactant to concentrate at the solution surface, 1.4×10^6 cubic centimeters per mole. This indicates that, at equivalent concentrations of the undissociated complex, the surfactant-cation complexes of these ions have the same degree of surface activity.

Engineering, Economic, and Hazards Evaluations of Waste-Disposal Methods

A study of long-term storage of neutralized wastes in tanks showed that this method of disposal is economically feasible (0.1 to 0.2 mill per kilowatt-hour of electricity delivered by the reactor) if the hazard is acceptable. Being studied is the temporary storage of acid or neutralized waste in tanks, followed by pot calcination to small volumes of thermally stable solids, the pots and contents to be shipped to an ultimate disposal site.

Costs for the storage of acid Purex and Thorex wastes in stainless steel tanks and of neutralized wastes in mild-steel tanks were minimum when the full time was 40 to 75% of the filling plus full time. For 0.5 to 30 years of storage, costs ranged from 2.0×10^{-3} to 9.3×10^{-3} mill per kilowatt-hour (electrical) for acid wastes and from 1.5×10^{-3} to 4.7×10^{-3} for alkaline wastes.

Estimated costs for converting acid and reacidified Purex and Thorex wastes to solids by pot calcination and for producing glass from acid Thorex wastes were \$500, \$855, and \$2515 in 6-, 12-, and 24-inch-diameter stainless steel pipes, 10 feet high. Aging had negligible effect on costs for processing in a vessel of a given size, because capital costs were only about 10% of vessel and operating costs.

Heat-transfer calculations of shipping containers for pot-calcined wastes of various ages showed that as many as thirty-six 6-inch-diameter pots of calcined, acid Purex waste can be shipped in a single-finned carrier after 2.4 years of decay without mechanical cooling en route. Four 24-inch-diameter pots of acid Purex waste can be

shipped, per carrier, after 11 years of decay. Costs for shipping pots up to 1000 miles ranged from 0.7×10^{-3} to 32×10^{-3} mill per kilowatt-hour (electrical).

A preliminary conceptual design and cost estimate for a solids disposal facility in salt indicated costs of 6×10^{-3} to 30×10^{-3} mill per kilowatt-hour (electrical), 60% to 85% of which was attributable to salt removal.

WASTE DISPOSAL

Introduction

The study of safe methods of radioactive waste disposal into geologic formations continues at an increasing pace. Two new tests of the hydrofracturing technique were made in the impermeable Oak Ridge formations. Cesium-137 and cobalt-60 were used to tag the grout. The tests successfully showed that hydrofracturing at 934 feet and 694 feet induced fractures that followed the bedding planes.

Laboratory work on the injection of low-level wastes into deep permeable layers has concentrated on the chromatographic dispersion of Sr^{90} and Cs^{137} in multicomponent exchange systems. The experiments showed that the normalized breakthrough curves are the same as the curves of the normalized dispersion of the solution front, but they lag behind by a factor related to the distribution coefficient.

The large-scale field study of the disposal of simulated high-level radioactive wastes in salt formations was successfully completed. Attention has now shifted to the study of the storage of solidified wastes in salt. For a 6-ton-per-day fuel reprocessing plant and with the salt temperature rise held to 125°F, 34 acres of mine area per year would be required to store 120-day-old waste.

Studies of the fate of radionuclides reaching the Clinch River showed that most of the major nuclides are in equilibrium with the river sediments and pass through the study reach undiminished. The time of movement in the river was tested with Au^{198} and showed to be 10% less than the predicted times at flows of 8,000 and 20,000 cubic feet per second.

Studies on the origin of radionuclides entering the White Oak Creek drainage system show that there are 21 sources of contamination in the basin. The Process Waste Water Treatment Plant continues to introduce the most Sr^{90} into the system, and the seepage pits introduce the most Ru^{106} into the system. At present there is a reservoir of over 1200 curies of Ru^{106} accumulated in the bed of White Oak Lake, and most of this is in the upper 2 feet of soil.

In the study of natural clay minerals to remove radionuclides, it was shown that heating illite and bentonite to 600°C for 15 minutes improves the efficiency of removal of cesium by collapsing the structure of the clay mineral. This treatment also increased the settleability of the clays. It was also shown that strontium is removed by cheap, quick-settling alumina nearly as well as by high-exchange-capacity minerals.

Disposal in Geologic Formations

Disposal in Natural Salt Formations. – Previous work at ORNL was concerned with the direct disposal of liquid wastes into cavities in salt; however, present studies are concerned with the disposal of high-level packaged solids produced by the various calcination processes now under development. When packaged solids are finally produced, some dry and safe repository must be available for ultimate disposal. Under study are the heat transfer between the solid-waste packages and the salt, the effect of temperature and radiation on the creep of rock salt, and the design and operation of a test facility in some salt mine.

The large-scale field experiments on the direct disposal of liquid wastes in salt cavities have been completed. Examination of the cavities showed that erosion occurred above the liquid level in the neutralized-waste cavity and below the liquid level in the acid-waste cavity. Laboratory studies showed that the major cause of this erosion is the alternate oversaturation and undersaturation of the waste solution at the vapor-liquid interface produced by the continuous evaporation of water followed by the return of unsaturated condensate. Temperature rises in the waste and the salt surrounding both cavities were close to those predicted. Thermal conductivity and diffusivity values for rock salt determined from the

temperature measurements were within 10 to 20% of the laboratory values for single salt crystals.

Prior to operating the field tests, the creep between the floor and the ceiling of the mine occurred at a constant rate. However, when the waste was heated, there was a rapid increase in the amount and rate of creep (thermal expansion and plastic flow), one-half inch in a year, but when the waste temperature stabilized, the creep slowly decreased until it was about the same as before the tests. The latest gage readings indicate that the total movement was greater than would have occurred if the salt had not been heated, but that the experiments did not disturb the stability of the mine room.

Calculations of the temperature rise in a uniform slab of waste in an infinite salt medium were performed for the case of disposal of liquid waste from a 6-ton-per-day fuel reprocessing plant. The new mine area required to limit the waste temperature rise to 125°F varied from 34 acres per year for 120-day-old wastes to 5 acres per year for 30-year-old waste. If the wastes are stored as solids above the mine floor, the acreage requirements are reduced by a factor of 2.3. Calculations of peak temperatures in the salt surrounding the pot-calcination cans stored in holes in the mine floor indicate that some space premium is paid for inserting cans having high heat-generation rates in the floor.

Previous studies showed that gamma doses greater than 5×10^8 roentgens produce a slight decrease in the compressive strength of rock salt. A computer program indicated that a gamma-radiation dose to the salt from cylinders containing pot-calcined waste buried in the floor would exceed the critical value only in areas close to the cylinders.

A feasibility study of the potential use of a salt mine for the disposal of low-activity solids was carried through a preliminary survey of the requirements and problems involved. Safety and engineering feasibility were promising, and costs (estimated by one of the salt companies) were competitive with the price schedule established by the AEC for regional burial grounds.

A study is also being made in order to determine the feasibility and approximate cost of carrying out a hot demonstration of the disposal of calcined radioactive material, using canned ETR fuel elements in lieu of actual calcined wastes.

Disposal in Permeable Formations by Well Injection. – The disposal of radioactive waste in deep permeable formations is a means for isolating large volumes of low-activity waste from flowing surface or ground water. The use of wells to dispose of brine in deep permeable formations is a current practice in the petroleum industry. The most significant additional factors, which must be considered before disposal of radioactive liquids becomes a reality, are those which concern the safety of the method and the additional costs imposed upon it by the safety requirements.

An advisory committee was established to review and coordinate the activities of several agencies participating in this development program. The Oak Ridge National Laboratory, the U.S. Bureau of Mines, the University of California, and the U.S. Geological Survey are represented on this committee.

In the disposal formation, the radionuclides move along the same pathways as the transporting solution but are retarded in movement due to the sorptive processes going on in the formation. Ion exchange is one of the complex phenomena important in retarding the movement of cationic radionuclides, but it is not completely adequate for describing the movement of many of the radionuclides in low- and intermediate-activity waste streams. The chemistry of the waste solution is altered continuously as it moves through the disposal formation by the buffering action of exchangeable hydrogen and the adsorption of stable components from the waste stream. These changes affect the ion exchange behavior of the radionuclides, but the effect on transition-element behavior (for example, ruthenium) may be much more pronounced, especially when there are changes in the oxidation-reduction states. The selective action of chelating agents in the waste stream or of minerals in the formation which form insoluble compounds with radionuclides of the waste stream provide additional complications to the ion-exchange system.

ORNL is studying the chromatographic dispersion of radionuclides in sandstones which represent possible disposal formations. The behavior of Sr^{90} and Cs^{137} in multicomponent exchange systems has been emphasized, and the results are being evaluated on the basis of the chemical, physical, and mineralogical properties of representative cores. For various clay systems investigated to date, the selectivity of strontium

compared with that of other divalent ions (that is, Ca^{2+}, Mg^{2+}, and Ba^{2+}) ranges from 1.0 to 1.5, while the sorption of divalent ions over sodium is favored by a factor of about 30 grams per milliliter. The normalized breakthrough curves obtained for radionuclides were coincident with the normalized dispersion of the solution front in the exchange columns, but the curves lagged behind the solution dispersion front by a factor related to K_d.

Further experiments are in progress to facilitate the prediction of fission-product movement in permeable formations and into the less-permeable boundary formations. A small-scale field test is expected to check the accuracy of the predicted movement and to provide a test demonstration of suitability of deep permeable formations for the actual disposal of radioactive wastes.

A committee of the American Association of Petroleum Geologists is assembling information on the sedimentary basins of the United States relevant to their possible use for disposal of radioactive wastes. Factors being considered are the known or probable presence of commercial reserves of oil or gas and the presence of deep permeable formations, shale, and salt for injection, hydraulic fracturing, and mined storage, respectively, of radioactive wastes. A preliminary survey of the country provisionally eliminated certain areas and directed attention toward a few which appear favorable and for which more detailed studies are projected.

Disposal in Impermeable Formations by Hydraulic Fracturing. – Hydraulic fracturing is extensively practiced in the petroleum industry to stimulate the production of oil wells. For this purpose the well casing is slotted opposite the producing formation, and a mixture of oil and sand is pumped down the well under sufficient pressure to force open and hold open the rock. Many thousands of oil wells are treated in this way every year in the United States. For waste disposal the well would be slotted at the bottom, the waste-cement mixture pumped in, the next few feet of the well tightly plugged, and then, after this waste-cement mixture had hardened, a new slot would be cut about 5 feet higher up the well and the next batch of waste-cement mixture injected. It is estimated that one well could take several million gallons of waste.

The pattern of the hydraulically produced fractures and, more particularly, the possibility of producing fractures which can be relied on to extend out between the beds of rock without turning and breaking upward toward the surface, has been the subject of much debate. The best opinion appears to be that the fracture pattern is very largely determined by local conditions and must, in each case, be determined experimentally for the particular site in question. Our first concern, therefore, was to test-fracture one of the more suitable local shale formations.

Three injections were made: the first of 27,000 gallons at a depth of 290 feet, the second of 92,000 gallons at 934 feet, and the third of 133,000 gallons at 694 feet. The material injected was a dilute cement-water grout to which were added tracer quantities of Cs^{137}. Core drillings, supplemented by gamma-ray logging of the core holes, permitted a delineation of the grout sheets and showed that they had indeed moved out parallel to the bedding, rather than upward toward the surface. The two deeper sheets at first appeared to have been offset upward in crossing what were taken for faults, but deviation surveys of the core holes showed that some core holes departed appreciably from vertical. It is quite apparent, however, that the local fracture pattern, at least under the conditions of the tests, favors the hope that considerable quantities of radioactive waste can be disposed of by hydraulic fracturing at Oak Ridge.

Certain features of the local geology, however, suggested an additional safety factor against vertical fracturing, with consequent vertical fluid movement, could be provided by drilling still deeper and fracturing in shales which lie below one of the major regional thrust faults. Therefore a test hole was drilled to a depth of 3263 feet. The thrust fault was found at 1360 feet, and well-bedded shale, presumably well suited to the formation of bedding-plane fractures, was found between 1642 and 1847 feet and also between 2648 and 2852 feet. We intend to use these two deeper shale zones for any future tests.

In addition to these field explorations and experiments, laboratory development of a suitable waste-cement mix has been undertaken by Westco, the research subsidiary of the Western Company, a company which does hydraulic fracturing for the petroleum industry. The problem was to formulate a mix with a low enough viscosity so that it can be pumped, but which will later set up and immobilize all the liquid. The problem is complicated

by the chemical composition of the waste concentrate, but a suitable mix was found, and plans are under way to field test it at shallow depths in the near future.

Preliminary design of the experimental test facility has been started, and the basic layout and method of operation have been determined.

Role of Soil Minerals in Waste Disposal

When radionuclides are released to the ground, whether by accident or through routine disposal of radioactive wastes, it is necessary to understand the retentive processes in the geologic formation which tend to restrict the movement of the radionuclides, particularly the complex ion-exchange properties of the host minerals. Knowledge of the fundamental properties of natural minerals is also important in developing practical uses of such materials for various waste-treatment applications. Studies at ORNL have emphasized definition of the mechanisms of sorption and retention of radiocesium and radiostrontium by soil minerals in order to provide a basis for more efficient utilization of these materials *in situ* or in treatment processes.

Cesium Removal. – About 90% of the cesium is removed from low-activity waste streams at ORNL by the addition of 200 parts of commercial illite per million parts of waste. However, improvement in cesium removal can be realized by appropriate treatment to promote selective sorption mechanisms. Tests with illite, heated at 600°C for 15 minutes, showed that its removal efficiency was increased by about 75%. The heat treatment also reduced the tendency of the clay to disperse and decreased the number of particles smaller than 10 microns by a factor of 1.5 to 2. Treatment of vermiculite with KCl or $BaCl_2$ nearly doubled the ability of this material to remove cesium from solution. Bentonite, a widely used drilling mud, was also made more effective for cesium removal by being heated for 15 minutes at 500 to 600°C in order to collapse the structure. The heat-treated bentonites not only gave higher cesium removals but also had vastly improved settling characteristics. The settleability of a clay is an important characteristic to be considered for use in the ORNL treatment plant, because approximately 50% of the activity in the effluent, following clay addition, is associated with suspended solids.

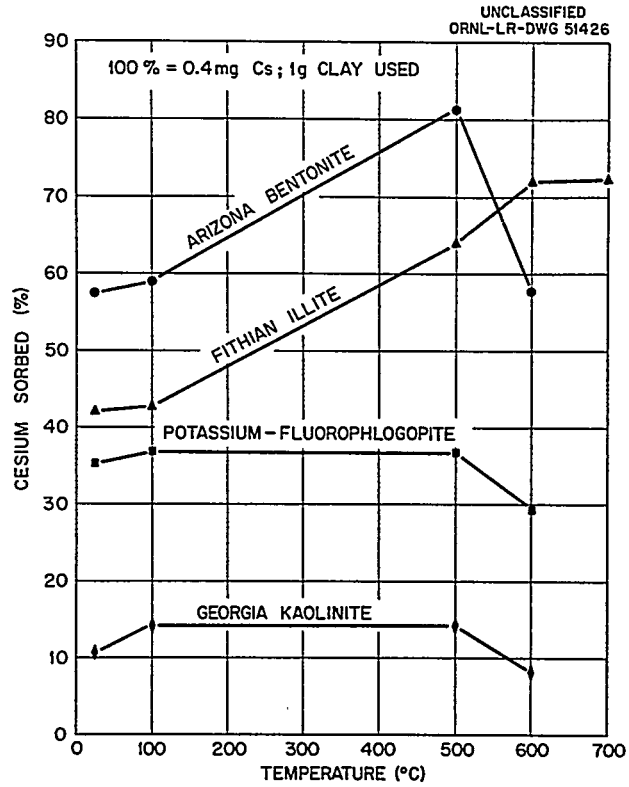

Sorption of cesium from 1.5 *M* $NaNO_3$ solution by several clays previously heated.

Although ion exchange reactions are usually reversible, vermiculite offers a unique system in which the crystal structure changes during the rapid forward exchange reaction, resulting in a very slow reverse reaction. This phenomenon involves conversion of the vermiculite to a mica-like structure when sufficient potassium, ammonium, rubidium, or cesium is sorbed by the mineral. The advantage of this process in waste disposal is that the radiocesium is sealed within the mineral and is released at an extremely slow rate. Tests, using potassium ions to induce this reaction, resulted in increasing the removal of cesium from solution by factors of 10 to 100 and resulted in much slower rates of desorption of the cesium. X-ray diffraction tests confirmed the structural changes coincident with improved cesium removal. Further experiments are being performed to characterize the sodium-potassium-calcium relationships in this reaction.

Strontium Removal. – Both inorganic and organic exchange materials are being investigated for

removing radiostrontium. Vermiculite, with calcium ions on the exchange sites, has shown improved strontium removals from wastes containing orthophosphates. Without orthophosphates, sodium ions on exchange sites offer less competition for strontium sorption.

With simulated low-activity wastes, rock phosphate columns have been capable of decontaminating up to 2000 bed volumes, with a decontamination factor of 1000. With 50 parts of orthophosphate per million parts of waste, the capacity increased to more than 3000 bed volumes.

The amount of calcium released from calcite and rock phosphate was higher in sodium nitrate solution. The concentration of calcium released from calcite in 1 *M* sodium nitrate was nearly four times the solubility of calcite in water. However, the calcium released by the rock phosphate is in competition with strontium for exchange sites, while the calcium removed from calcite combined with excess phosphate ion to form calcium (strontium) phosphate and, therefore, enhanced removal. Tests are being made in order to correlate strontium removals by calcite columns, with release of calcium from the calcite and the concentration of phosphate in the influent solution.

Alumina, despite its low exchange capacity, is capable of removing strontium nearly as well as the high-exchange-capacity minerals. Alumina removes strontium by adsorption (surface forces may be involved) rather than by absorption, which is usual for most other minerals.

Environmental Radiation Studies

Evaluation of Radionuclide Distribution and Movement in Clinch River. – The Clinch River Study is directed toward answering three basic questions: What is the ultimate fate of radioactive materials discharged to the stream? What is the total diluent capacity of the stream for continuous injection of low-level radioactive waste? What are the long-term consequences of continued use of the stream for this purpose?

At ORNL a comprehensive study of the Clinch River, downstream from Oak Ridge, has been continued, under the guidance of the Clinch River Study Steering Committee, which includes representatives of the U.S. Atomic Energy Commission, Oak Ridge National Laboratory, U.S. Public Health Service, U.S. Geological Survey, Tennessee Game and Fish Commission, Tennessee State Health Department, Tennessee Stream Pollution Control Board, and the Tennessee Valley Authority. For specific analyses and interpretation of results on various phases of the study, the Steering Committee has organized subcommittees on (1) water sampling and analysis, (2) bottom-sediment sampling and analysis, (3) aquatic biology, and (4) safety evaluation.

Dilution and Dispersion. – The dilution factors have been computed for discharge from White Oak Creek in relation to variable flow in the Clinch River. The mean and median daily dilution factors for 1950 to 1960 were about 450 and 570 respectively. Maximum and minimum daily dilution factors for the same period were 4330 and 5.

Time of travel in this highly regulated river is influenced by discharges from Norris Dam upstream, by Watts Bar reservoir levels downstream, by the rate of reservoir filling or emptying, and by the season of the year. Velocity-stage-discharge measurements and tracer tests with radioactive Au^{198} were made in order to verify predicted times of travel in the Clinch River. The tests indicate that observed time of travel is about 10% less than the computed time of travel for steady flows of 8,000 and 20,000 cubic feet per second. Times required for the tracer to reach the Gaseous Diffusion Plant, 6.3 miles downstream, and the mouth of the Emory River, 16.3 miles downstream, were 8 and 31 hours, respectively, for a steady flow of 8,000 cubic feet per second; and 2.8 and 9.3 hours, respectively, for a steady flow of 20,000 cubic feet per second. Further tests at higher and lower river flow rates are planned.

Dispersion tests with Au^{198}, made during periods of steady flow, indicated that waste water discharged from White Oak Creek is dispersed uniformly across the river within a distance of 4 to 6 miles downstream. The tests also showed that about a 500-fold reduction in radionuclide concentration occurs within this reach of the river.

Concentrations in River Water. – Daily samples of river water are collected from the Clinch River at four stations: one above, one at, and two below the outlet of White Oak Creek. Similar samples from the Tennessee River are collected at three stations; one of these is above the mouth of the Clinch River and one is 117 miles downstream at Chattanooga. Samples are composited in proportion to daily flow for weekly radiochemical determinations and for monthly analysis for stable-

chemical content. Radiochemical analyses showed that the predominant radionuclides discharged to the Clinch River were Ru^{106}, Cs^{137}, Co^{60}, and Sr^{90}. It was also found that of the nuclides moving downstream, about 20% of the cesium and more than 90% of the strontium, ruthenium, and cobalt were dissolved in the water, the remainder being associated with the suspended sediment and organic matter. Although the radioactivity levels in the water and suspended sediment were low, it was possible to estimate the total load of radionuclides passing each sampling station. The estimates indicated that there was little loss of Sr^{90} and Ru^{106} from the river water 117 miles downstream to Chattanooga. The stable-chemical analyses of Clinch River water included determinations of the stable isotopes of strontium, cesium, cobalt, and ruthenium, as well as other chemical elements, as an aid in interpreting the movement and accumulation of radionuclides.

Sediment Studies. – Studies by ORNL and the U.S. Public Health Service yielded additional information regarding accumulation of radioactivity in sediments of the Clinch River and factors influencing the deposition of sediments. A detailed survey of gamma activity at the surface of bottom sediments in the river showed that maximum activity downstream from the mouth of White Oak Creek (Mile 20.8) occurred at about Mile 12.0. The major radioactive constituent was cesium. Secondary constituents were cobalt, ruthenium, and rare earths. Core samples of sediments collected at five cross sections in the 20-mile study reach were analyzed to determine particle-size distribution, mineralogy, and exchange capacity. It was found that the sediments are a well-graded silty loam with fairly constant clay content. Sand content decreased in the downstream direction, and the minimum median particle size of 20 microns was found at River Mile 11.9.

With cooperation from the Tennessee Valley Authority, studies were made in order to improve the accuracy of sediment-volume determinations. From the results of a silt-range survey in 1961, it was concluded that accurate determinations of sediment volume may be based upon silt measurements at as few as four cross sections in the 20-mile stretch of the river.

The influence of bends on the deposition of sediments was studied by analyzing the relative curvatures of 15 bends in the Clinch River between Mile 4.7 and Mile 18.8. The relative curvature is the ratio of the radius of the bend to the width of river channel. The distribution of sediment deposits and of gross gamma counts of sediments *in situ* were studied in one of the sharpest bends of the river (relative curvature of 1.95). There is evidence that where the relative curvature is greater than 3.5 the distribution of sediment deposits in the bend is not different from that in a straight channel.

The annual survey of sediments in the Clinch and Tennessee Rivers, by use of a bottom-scanning gamma detector, was conducted again in 1961 and extended in the Tennessee River downstream through Kentucky Reservoir, 25 miles from the confluence of the Tennessee and Ohio Rivers. The number of curies of radioactive wastes, other than ruthenium, discharged into the Clinch River during the 12 months before the survey decreased to 72% of that discharged in the previous year. The gamma survey of sediments downstream also showed a similar decrease.

Evaluation of Radionuclide Distribution and Movement in White Oak Creek Drainage System. – The White Oak Creek drainage basin includes all ORNL facilities that contribute significant quantities of fission products to the environment. There are 23 known sources of contamination in the basin. The creek receives directly the discharges of partially treated process waste water, laundry water, sanitary sewage and reactor cooling-water effluents, and eventually seepage from the intermediate-level waste seepage pits and five solid waste burial grounds. Runoff from land surfaces subjected to local and general fallout also contributes some activity to the creek. In addition, some radionuclides enter the creek from the bed of former White Oak Lake.

The topographic, geologic, hydrologic, and meteorologic conditions at a site determine, to a large part, the fate of radioactive materials released to it. Radionuclides are released into the soil, atmosphere, and streams at ORNL. Thus, in order to determine their distribution and trace their movement, it is necessary to know in detail the geology, hydrology (surface and subsurface), topography, and meteorology of the environment into which they are released.

The most important mechanism in fixing or decreasing the mobility of activity released in the White Oak Creek drainage basin is the sorptive properties of the soil and rock on or through which the water flows. Silt suspended in the surface

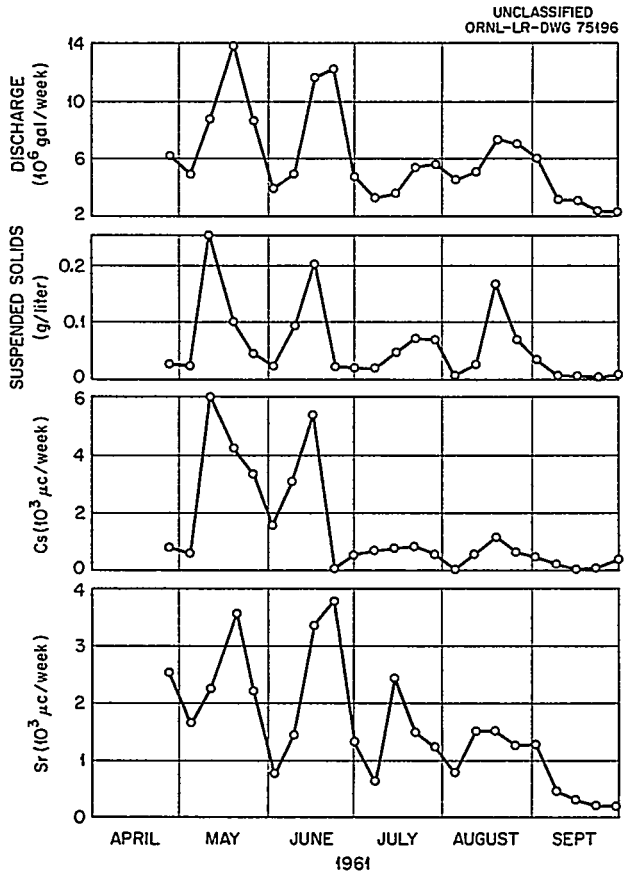

Stream discharge, strontium transport, suspended-solids concentration, and cesium transport at northwest tributary station in the White Oak Creek Basin.

streams also retards and modifies the downstream movement of contaminants.

A comprehensive study of fission-product accumulation and transport in the entire drainage area includes extensive stream monitoring and quantitative determinations of such physical and chemical factors as rainfall, surface runoff, extent of recharge, soil permeability, ground-water occurrence and movement, basal flow to surface streams, quality of water, turbidity loading and sediment transport in streams, and the sorption and retention of fission products in soils.

Temporary waste-sampling stations were installed along White Oak Creek and its tributaries to determine the amount and type of activity contributed to the system from fallout and other sources that could not be monitored directly. In addition, these stations provided information as to the chemical composition of creek water, transport of sediments, and flow in the creek. Representative samples of the effluent from the laundry and the sewage treatment plant were also taken.

Strontium-90 and cesium-137 were detected at all the stations; other radionuclides detected were Ru^{106}, Zr^{95}-Nb^{95}, Co^{60}, Zn^{65}, and the rare earths. The amount of strontium detected at the stream-sampling stations appears to vary with stream discharge, and an increase in the suspended solid load in the stream is generally followed by a corresponding increase in cesium transport. Thus, during periods of high stream discharge and/or heavy suspended-solids load, the transport of strontium and/or cesium is usually high. There is also a relation between the percentage of sorbed strontium in the creek water and the concentration of suspended solids in the water. The concentration of Sr^{90} in the creek, draining an area contaminated only by fallout, varied from 2.7×10^{-9} to 9.4×10^{-9} microcurie per cubic centimeter in weekly composite samples for a period of three months. The total transport for the period included 10 millicuries of $Sr^{89,90}$, 1.8 of the rare earths (exclusive of Y^{90}), 1.7 of Cs^{137}, and 1.5 millicuries of Ru^{106}. About 50 millicuries of gross activity was detected for a sampling period of six months at the laundry. Strontium-89,90 (7.8 millicuries), Ru^{106} (9.3), Cs^{137} (8.9), Co^{60} (5.0), and the rare earths (exclusive of Y^{90}) (12.9 millicuries) were the principal radionuclides detected. Analysis of samples from the effluent of the sewage treatment plant for a three-month period show a contribution of 79.1 millicuries of $Sr^{89,90}$, 49.1 of the rare earths (exclusive of Y^{90}), 14.5 of Cs^{137}, 3.0 of Ru^{106}, 2.9 of Co^{60}, and 0.2 millicurie of Zr^{95}-Nb^{95} to the creek. A mean concentration of 1.9×10^{-6} microcurie per cubic centimeter of Sr^{90} was observed for the sample period.

White Oak Lake formerly served as a final settling basin for low-level radioactive wastes discharged from ORNL. The lake extended about 1 mile upstream and covered an area of about 44 acres. The temporary holdup afforded some dilution and a period for the decay of short-lived radionuclides before release to the Clinch River; it also allowed the deposition and accumulation of contaminated sediments. The lake was drained in 1955.

Core samples taken along transects at the upper, middle, and lower parts of the former bed show

that, with the exception of the recent lacustrine deposit, there are no beds that persist vertically or horizontally. However, it appears that the amount of sand and gravel increases with depth, while silt and clay decrease.

The rate of ground-water movement in the bed of the lake was measured by the auger-hole method. Permeability values varied from 0.2 to 2.6 feet per day. The configuration of the water table determined by weekly water-level measurements showed a general movement normal to the flow of White Oak Creek. However, this pattern is modified over a large part of the lake bed by seepage from the intermediate-level waste pits.

Several thousand curies of Ru^{106} per year flow from the intermediate-level waste seepage pits onto the lake bed; however, less than half of the ruthenium finds its way into White Oak Creek. A series of core samples taken in the lake bed were radiochemically analyzed to determine the distribution of Ru^{106} in the soil. Results of the investigation show that (1) as of February 1962, there was approximately 1200 curies of Ru^{106} in the bed of former White Oak Lake; (2) the highest concentrations of Ru^{106} are found in the uppermost 2 inches of soil; (3) about 75% of the ruthenium found in the lake bed is associated with the first 2 feet of soil; and (4) although ruthenium is being transported by ground water through the lake bed soil, a relatively small amount of it is reaching the creek in this manner.

PHYSICAL RESEARCH

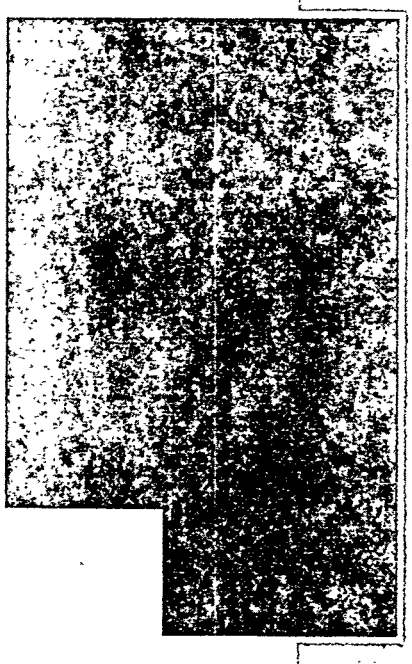

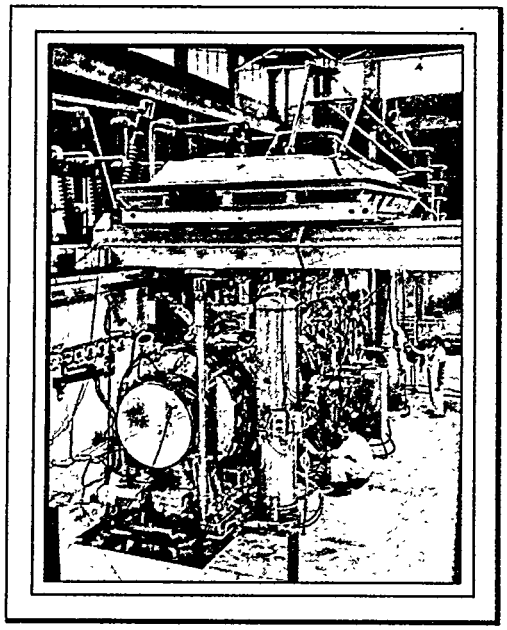

Physics and Mathematics Research

MAGNETIC PROPERTIES OF THE HEAVY RARE-EARTH METALS

The Commission's long-standing interest in and support of the development of methods for the production of pure rare-earth salts and pure rare-earth metals is well known and well documented in earlier reports. During the past year techniques for growing single crystals of rare-earth metals were perfected at Ames. With single-crystal specimens the magnetic properties of the heavy rare earths have been extensively studied: at Ames by means of classical methods and at Oak Ridge by neutron-diffraction methods. As a result of these two programs, each providing different but complementary information, considerable insight into the fundamental process of magnetism has been gained.

It has been found that below a certain critical temperature there is a transition from the paramagnetic state (in which the permanent magnetic moments of the rare-earth atoms are randomly oriented) to an ordered state (in which the moments form one or another type of magnetically ordered structure). At a still lower temperature, further transitions to other ordered structures have been detected. These magnetic structures, among them two novel types, have been deduced from the neutron-diffraction data.

In spite of the complexity of the magnetic properties of the rare-earth metals, which had heretofore resisted interpretation, the new data from the two laboratories allow a relatively simple interpretation in terms of a molecular field theory in which the effect of the anisotropy of the rare-earth atom is taken into account.

PROTON HELICITY EXPERIMENT

An experiment to measure the helicity of the lambda decay proton was performed by the liquid-helium bubble-chamber collaboration group. This cooperative effort involved physicists and students from four universities and scientists from the Oak Ridge National Laboratory. The experiment was performed by use of a separated K^- meson beam produced by the Bevatron high-energy accelerator at the Lawrence Radiation Laboratory at Berkeley, California.

Lambda particles were produced in the helium bubble chamber through the interaction of K^- mesons with helium. A lambda particle decays to a pion and a proton. The subsequent scattering of the proton by helium in the bubble chamber was measured. The proton helicity – that is, the alignment of its spin axis relative to the direction of its motion – was found to be positive. This finding was accomplished by measuring the polarization of the protons scattered by helium used as polarization analyzer. Several theories have made different predictions as to the sign of the asymmetry parameter, so that this experiment permits crucial verification or rejection of a theory. It is also to be noted that the lambda decay is a parity-nonconserving weak interaction similar to the beta decay, with the exception that the decay does not involve a neutrino. A nonvanishing asymmetry parameter is a result of parity nonconservation.

SUPERCONDUCTING MAGNETS

One of the most important recent developments in solid-state physics is the discovery at the Bell Telephone Laboratories of a class of superconducting alloys (that is, they have zero electrical resistance) at relatively high temperatures near 18°K and in remarkably high magnetic fields. With these substances and other related materials under development, one may expect to construct magnets producing fields in excess of 100,000 gauss of a

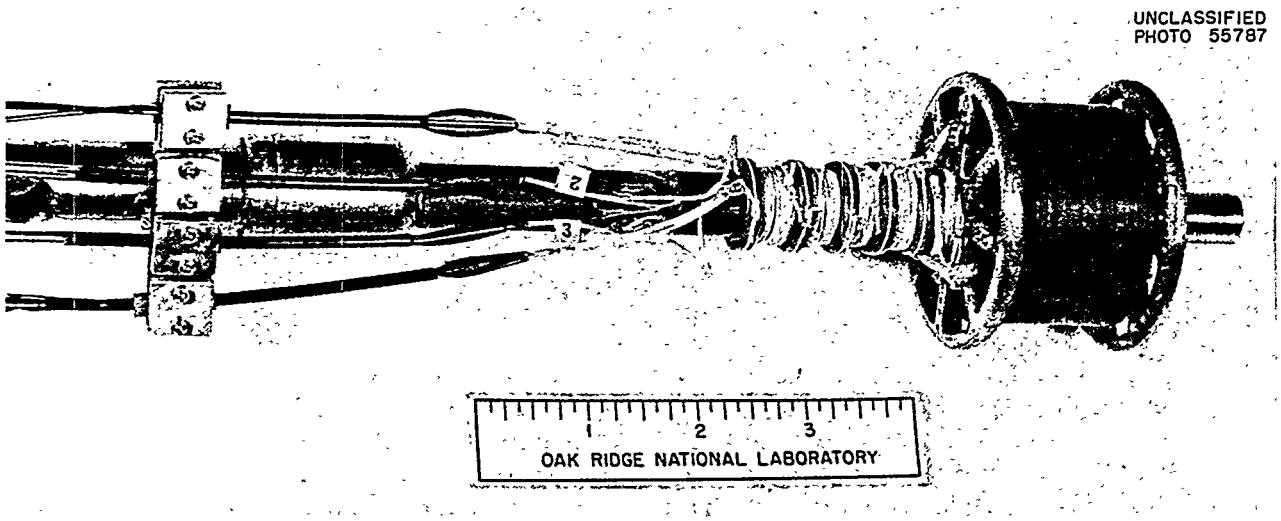

32,000-gauss superconducting magnet with 0.375-in. clear inside diameter.

sufficient size to be of importance, for example, to Project Sherwood and in accelerator construction.

These large devices would consume virtually no electric power, whereas similar equipment of the conventional type might require power in the range of hundreds to thousands of megawatts. The metallurgical and electromagnetic properties of these materials are being investigated at a number of laboratories, including the Oak Ridge National Laboratory, where a number of important metallurgical developments have been made and where several laboratory-scale magnets have been built and their properties studied.

THEORY OF NUCLEAR REACTIONS

There are several conceptually simple models of nuclear reactions – that is, of the scattering of one nucleus from another. Until recently, it has not been feasible to explore the predictions of these models in detail because of the lengthy numerical calculations involved. Calculations that have been made in recent years have almost always involved severe approximations, so that while comparison with experimental observations has been encouraging, it has not been decisive. However, the use of high-speed electronic computers now overcomes these difficulties, and a broad program of such calculations has been initiated at Oak Ridge National Laboratory.

The calculations will serve two purposes. Once the validity of these models has been established by comparison with experimental observations, it is possible to predict nuclear cross sections with reasonable certainty when measurements are not available. On the other hand, the analysis of experimental results in terms of these models gives valuable detailed information about the structure of the nuclei involved.

During the past year, particular success has attended the analysis of a certain class of nuclear reactions called inelastic scattering. The model used here assumes that a nucleus need not be spherical and that it either may be permanently deformed into an ellipsoid or it may undergo oscillations in shape in the way that a vibrating liquid drop does. The impact of a projectile may then set the nucleus rotating or oscillating; such inelastic scattering has been observed in many experiments, and in just the manner predicted by the model.

STABLE RARE-GAS ORGANIC MOLECULAR IONS

It is well known to scientists that the members of the group of elements known as the rare gases are all the same in their chemical behavior, or lack of behavior, for they are completely inert to

any chemical reaction. It was most interesting then to find that rather stable organic rare-gas ions could be formed. Not only were these ions rather stable, but the stabilities of the different rare gases were strikingly different from each other. For example, at ORNL studies were carried out on CH_3T and CH_3I^{131} in which the radioactive gases were allowed to decay in a specially designed mass spectrometer. Following the nuclear transformations it was found that while $(CH_3He)^+$ always decomposed, $(CH_3Xe)^+$ remained stable in 70% of the decays. These findings have been confirmed by studies on other radioactive molecules. Similar organic rare-gas ions have been recently discovered at ORNL and elsewhere by bombarding mixtures of rare gases and hydrocarbons with electrons.

CAPTURE CROSS SECTION OF TIN ISOTOPES

It has been recognized for many years that a detailed knowledge of the process of neutron capture is very important to the design of nuclear reactors. More recently it was proposed by cosmologists that certain stars ("fast reactors on a large scale") provide the mechanism by which one may account for the synthesis of heavy elements. These theories predict a definite relationship between capture cross sections for neutrons at a temperature near 10,000,000°C and the cosmic abundance of certain heavy nuclei.

The most sensitive experimental test of this effect has been accomplished at ORNL by measuring the capture cross section of the separated isotopes of tin for neutrons of energy corresponding to 10,000,000°C. This experiment was made possible only by using certain special techniques developed at ORNL over the past several years. These techniques involve the ability to produce fast bursts of 30-kev neutrons (less than 3 thousandths of a microsecond in duration) and a corresponding ability to quantitatively measure the capture event in an equally short time.

The results provided confirmation of the predicted relationship and also provided more quantitative information on the relative competition between red-giant and supernovae stars in the formation of elements heavier than iron.

Electronuclear Research

THE OAK RIDGE ISOCHRONOUS CYCLOTRON

The Oak Ridge Isochronous Cyclotron (ORIC) passed the preliminary testing stage and is being prepared for full-scale operation. ORIC is a versatile fixed-frequency cyclotron in which both the magnetic field and the frequency of the accelerating voltage can be varied. This makes it possible to accelerate a wide variety of particles to various energies, up to 75 Mev for protons.

Installation of the cyclotron, with a temporary radio-frequency power supply, was completed, and test operation began in March 1962. The performance clearly verified the theoretical calculations and detail design for this radically new

type of cyclotron. The three-sector azimuthally varying magnetic-field configuration provides the focusing forces required to continue fixed-frequency acceleration to much higher energy than is obtained in conventional cyclotrons. Fixed-frequency operation assures very intense beams.

A period of magnetic-field measurements preceded the cyclotron testing program. Many detailed measurements were required to determine the exact contribution of each of the 21 magnet circuits to the complex field configuration which gives the machine its versatility.

With the radio-frequency power supply limited during the testing stage, the proton energy was 8 Mev (million electron volts) at full radius. As predicted, a very low accelerating voltage is required, and the protons remain in focus and in phase during over 400 orbits. Detailed tests were made in order to determine the operating characteristics of the machine and the orbit dynamics of the ions. This information served as the basis for the design of the beam deflector system and other remaining components. After installation of these components and the final stage of the radio-frequency equipment is completed, the cyclotron will be brought up to its full energy range of 75-Mev protons, 40-Mev deuterons, 80-Mev alpha particles, and 100-Mev nitrogen ions, or operated at any intermediate energies desired below these values.

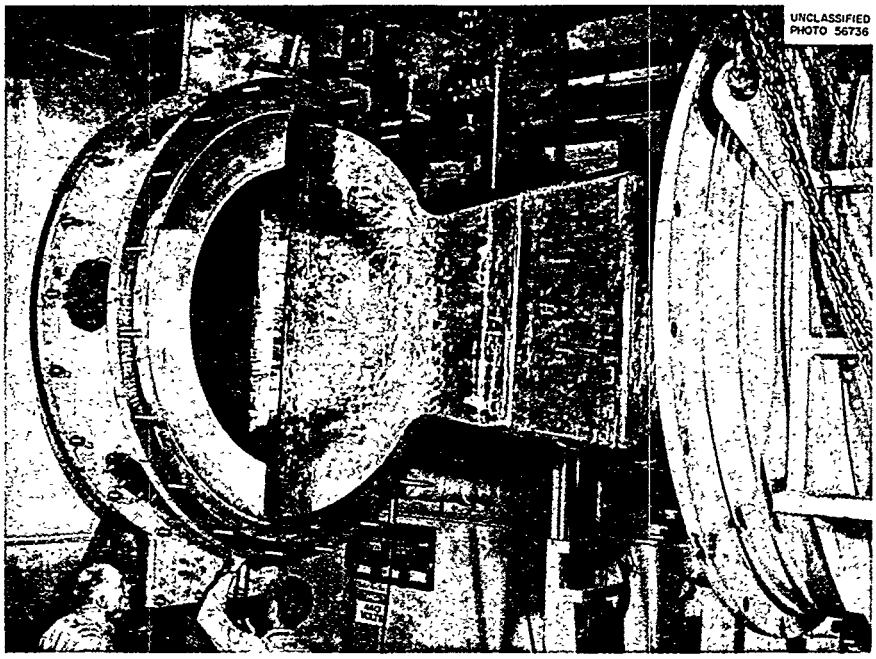

Oak Ridge Isochronous Cyclotron. The single dee of this new sector cyclotron is shown being inserted for test operation. The ORIC is designed to provide the highest fixed-frequency cyclotron operation available anywhere, giving proton energies up to 75 million electron volts. It also provides comparable energies for deuterons, alpha particles, and many heavy ions. Constant orbit frequency (isochronism) is made possible by arranging the magnet so that the average field increases with radius. Azimuthal variations in the magnetic field produced by the three pairs of sector pole tips provide the necessary focusing forces. The main coils of the magnet and 20 pairs of specially designed adjusting coils mounted between and on the pole-tip sectors are individually energized to allow optimization for a wide range of ion types and energies. The radio-frequency of the accelerating system is selected to obtain resonance. In anticipation of very intense beams, the cyclotron and experiment rooms are enclosed with heavy concrete shielding.

The three-sectored pole tips of the ORIC magnet, with valley coils and harmonic coils between the steel sectors, keep the ions focused toward the midplane.

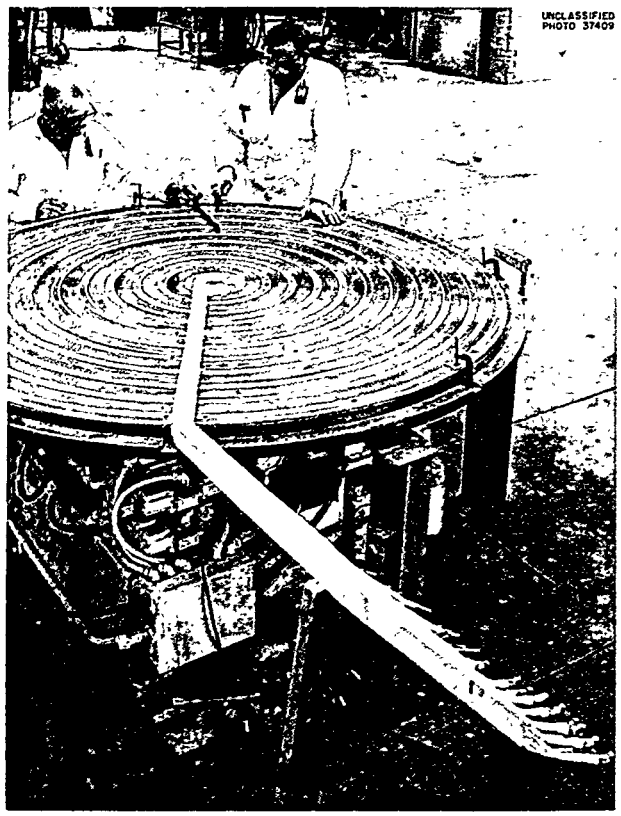

Ten pairs of concentric trimming coils mounted on the pole faces of the ORIC magnet are used for increasing the average magnetic field with radius to provide constant orbit frequency (isochronism) to energies far beyond the limits of conventional cyclotrons.

STUDIES OF NUCLEAR STRUCTURE

When an energetic proton strikes a nucleus and a deuteron comes out, the reaction can be pictured quite accurately as a neutron pickup; that is, the incoming proton attaches itself to a neutron in the nucleus and the coupled proton and neutron emerge as a deuteron. This kind of reaction is valuable for studying nuclear structure; it can be used to study how neutrons are bound in nuclei.

Experimentally it is found that the deuterons come out in sharply defined energy groups. This correlates with the well-known "shell" model of the nucleus; the energy groups correspond to the pickup of neutrons from different shells. The shell model assumes that the neutrons and protons which make up an atomic nucleus occupy discrete quantum-mechanical bound states, or shells.

For the model to "make good sense," the shell structure must be very nearly the same for nuclei which differ only slightly in the number of protons or neutrons. For example, a zirconium-90 nucleus, which contains 50 neutrons, differs from a zirconium-91 nucleus only in that the shell in which the fifty-first neutron belongs is empty in zirconium-90 but has one neutron in it in zirconium-91. That shell, called the $2d\ \frac{5}{2}$ shell, can hold six neutrons and is completely filled in a nucleus

of zirconium-96. This picture is only approximately correct, for the nuclear particles interact with each other through nuclear binding forces, which are especially strong between particles in the same shell. Thus, when a neutron is added to a nucleus, the shells are slightly disturbed.

The use of separated isotopes (prepared at ORNL) for targets in pickup reaction experiments has made it possible to study the changes in shell structure with neutron number. The shells are explored for each member of a sequence of isotopes. Experiments performed at the Oak Ridge National Laboratory 86-Inch Cyclotron show that the addition of a neutron to the nucleus of any zirconium isotope changes the shells only slightly but measurably. The addition of a neutron to a nucleus of an iron isotope, however, changes the shell structure so much that at first sight the shell model seems to have no meaning for these nuclei. If it is assumed, however, that a partly filled shell causes the whole nucleus to take on a nonspherical, football-like shape, then it is possible to restore meaning to the shell-model picture for iron nuclei.

NUCLEON TUNNELING

The heavy-ion cyclotron at the Oak Ridge National Laboratory has been used to study many aspects of heavy-particle physics. This specially designed accelerator produces a beam of 28-million-electron-volt nitrogen ions. One of the reaction mechanisms that has been singled out

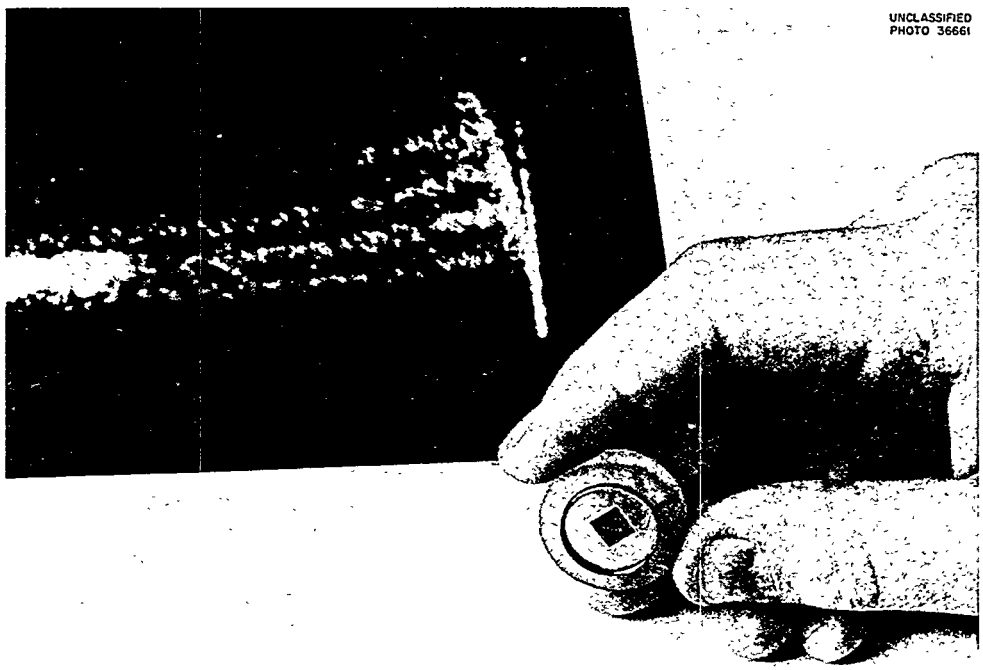

Solid-state (silicon-wafer) detector used for particle identification. The small square at the center of the circular plastic mounting is the silicon wafer, the sensitive part of the device. The photograph in the background is an example of data obtained with such a counter used in a particle-identifying scheme. Each dot corresponds to one particle emitted from a target bombarded by nitrogen ions accelerated in the ORNL 63-Inch Cyclotron. The dots cluster on several different lines according to the type of particle; the most prominent band is due to nitrogen atoms, the one below it is from carbon, while the two above are due to oxygen and fluorine.

for study is the transfer of a single nuclear particle.

To illustrate the reaction, the following picture may be used. As the bombarding nucleus passes the nucleus of a target atom, a single nucleon (proton or neutron) becomes detached from one nucleus and is transferred to the other. Although the nature of the interacting nuclei is not drastically changed, a reaction of this type can be recognized experimentally because the two residual atoms are no longer the same as the original pair. In many cases at least one of these reaction products is radioactive. This product is stopped in an array of suitably placed aluminum foil "catchers" that can be easily disassembled after the end of bombardment. The catchers are then quickly taken to radiation detectors, and the characteristic radioactivity of the stopped product is identified. Reactions in which the transferred particle is a proton can be identified by the use of a detection system that sorts the outgoing particles according to their nuclear charge and energy. This type of detection system consists of two silicon-diode barrier counters placed so as to record the simultaneous arrival of both reaction products. A third detector placed in front of one of the barrier counters identifies the nuclear charge of one of the outgoing particles.

Reactions have been investigated in which the neutron, or proton, is transferred from the bombarding ion to the target and from the target to the incident ion. These experiments demonstrate that transfer reactions occur when the two nuclei are on a near-collision course rather than on a

Conversion electron spectra. Electron lines photographed in a 63-gauss internal-conversion 180° spectrograph at ORNL are shown on the film strip. The lines are produced by a radioactive source deposited on a wire (0.025 × 2 centimeters) mounted on a holder as shown. Energy and relative intensity of electron lines are measured directly from the film strip. From these spectra several thousand of the more prominent gamma-ray transitions have been assigned to about 50 nuclei. This information is used in a systematic investigation of the processes of radioactive decay of rare-earth elements. The availability of calutrons for enriching isotopes of these elements and the high-current 22-million-electron-volt proton cyclotron, both operated by ORNL, makes possible the high intensity and resolution needed for these systematic studies. The observed properties of the low-energy nuclear levels are consistent with the predictions of the current nuclear model.

grazing contact or collision course. Since the transferring nucleon must "tunnel" through the space between the interacting nuclei, this type of reaction provides a sensitive means for probing the edge of the nuclear potential.

STUDIES OF DIRECT NUCLEAR REACTIONS

In conjunction with the Physics Division, several computer codes were written and are being used in the study of direct nuclear reactions. The purpose of this study is to gain some information on reaction mechanisms and to apply this knowledge to the analysis of the data, thereby deducing nuclear structure information.

The approach to these problems has been to make use of the Distorted-Wave Approximation. This theory assumes that the most important process is elastic scattering and that reactions can be described by a perturbation treatment if the distortion of the wave (in entrance and exit channels) by the nuclear potential is properly taken account of. In practice, use is made of the wave functions generated by the optical model. To this end an automatic search program is used to find optical-model parameters which fit measured elastic scattering. The wave functions thus found are used in the code Sally to compute reaction differential cross sections, angular correlations, and other measurable quantities.

Among the reactions being studied are deuteron stripping reactions [(d,p) and (d,n)] and pickup reactions [(p,d) and (n,d)]. Associated with this project is a detailed study of deuteron elastic scattering. Potentials were found which well-describe the scattering as a function of target mass and incident deuteron energy. Analyses of (p,d) experiments performed on the ORNL 86-Inch Cyclotron are in good agreement with the data, and spectroscopic factors deduced are "reasonable."

ORNL CYCLOTRON ANALOGUE

The successful operation of the Cyclotron Analogue demonstrated the practicability of a high-current proton cyclotron with a maximum energy of 800 to 1000 million electron volts. The Analogue, an eight-sector, spiral-pole cyclotron with an air-cored magnet structure, accelerates electrons to a kinetic energy in excess of the rest energy, 511 kiloelectron volts. This is a new record for isochronous cyclotrons. The Analogue was designed so that the particle motion closely models that expected in a high-current proton accelerator, the Mc^2 Cyclotron, now under study at the Laboratory.

The operation of the electron machine has been gratifying. Full design energy was achieved with only minor adjustments in the magnetic field. The orbit characteristics, such as radial and axial betatron frequencies, are almost exactly as predicted. The minimum dee voltage for acceleration of electrons to full energy is only 60 volts; this indicates that the electrons circulate at least 2600 turns. For the Mc^2 Cyclotron, in which protons will be accelerated one million volts per turn, less than 1000 turns will be required. The Analogue is being used primarily for the development of an efficient beam extraction system and to study allowable limits for imperfections in the magnetic field.

SUPERCONDUCTORS FOR MAGNETS

The availability of new alloys with unusual superconducting properties suggests new possibilities in the design and development of devices that use magnetic fields. At very low temperatures the electrical resistance of these superconductors is effectively zero. Potentially, large high-intensity magnets made with superconductors would require a negligible amount of electrical power. At certain critical-current densities and critical magnet-field intensities, however, superconductors lose their unusual property and regain their normal electrical resistance. The relationships of these critical currents, critical fields, and critical temperatures of the various superconductors are of immediate interest.

Critical factors in the physical structure of coils wound from superconductors are also being investigated at Oak Ridge National Laboratory.

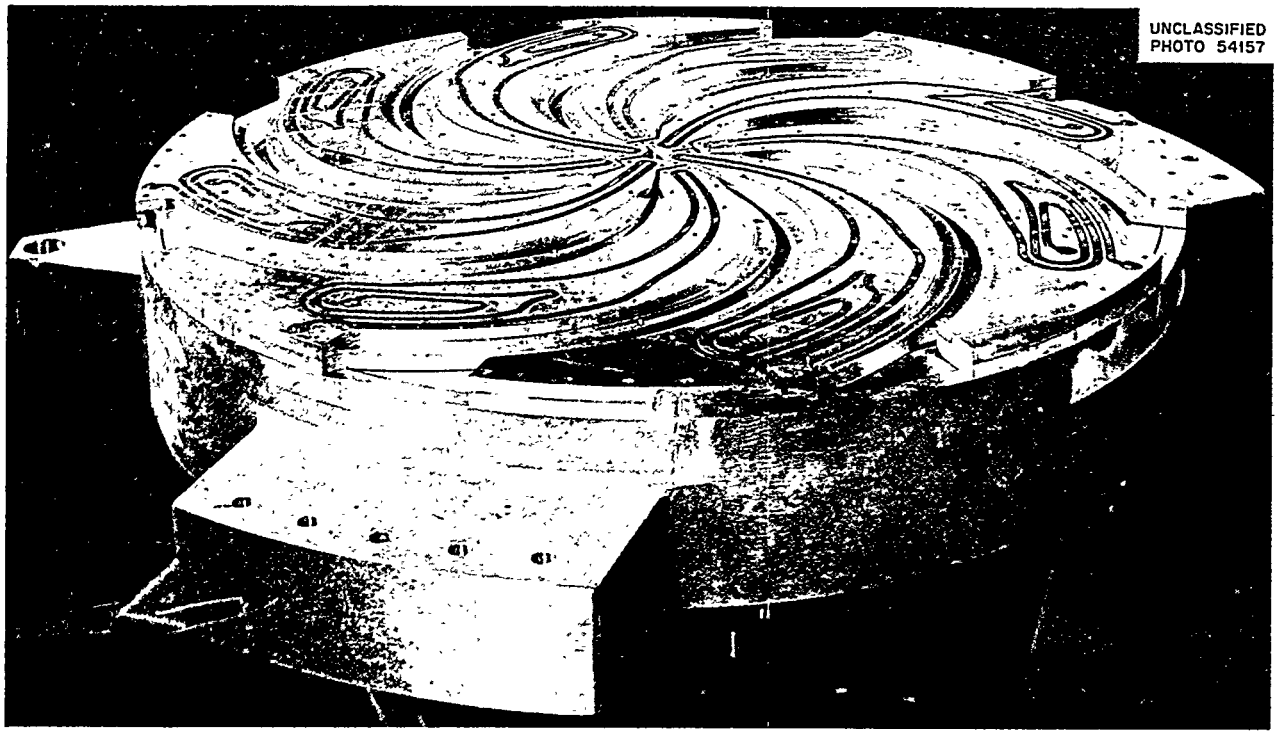

One of the two sets of 38-inch high-precision sector coils which provide the azimuthal variation in the magnetic field to focus electrons in the Cyclotron Analogue. The addition of these forces permits increasing the average magnetic field with radius in order to compensate the increase of mass with energy. Thus, the electrons are made to have the same period of revolution at all radii; that is, they are isochronous and can be accelerated with a fixed-frequency system. Applied to proton acceleration, this feature should provide a beam at least 100 times more intense than is obtainable in conventional proton accelerators in the 500- to 1000-Mev energy range.

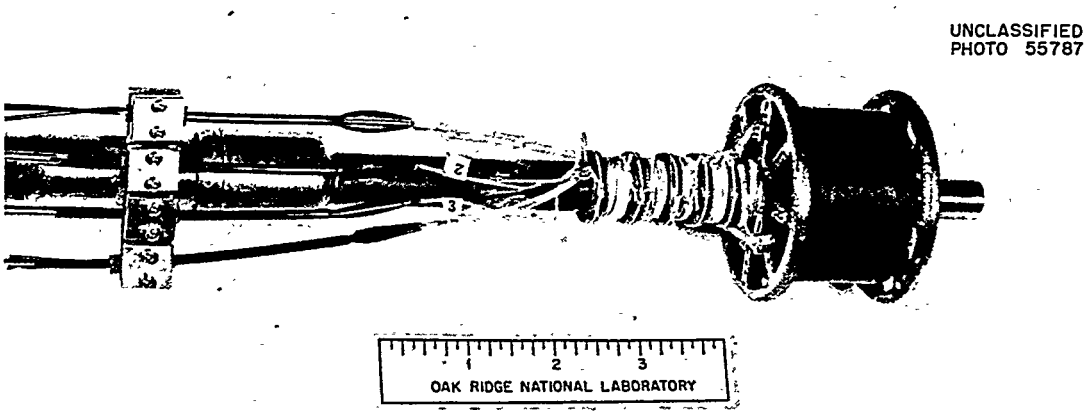

Superconducting model. This small but powerful magnet was wound at ORNL with 1800 feet of 10-mil-diameter niobium–25% zirconium alloy wire. In liquid helium (4.2°K) the wire remained superconducting at currents up to 18 amperes and produced a central magnetic field in excess of 30 kilogauss. When the winding, along with a closed copper secondary, is cast in epoxy resin, the same wire remains superconducting at currents up to 30 amperes. The small take-up coils lead to press joints developed at ORNL for joining the niobium-zirconium wire to heavy copper leads.

Short pieces of superconductors and small coils (100 feet of wire winding) are tested at liquid-helium temperature (4.2°K) in a high-field solenoid which is water-cooled for continuous operation at fields up to 117 kilogauss. Tests have been made for the niobium-zirconium alloys Nb–25% Zr, Nb–33% Zr, Nb–50% Zr, and Nb–75% Zr. In general, the critical field increases and the current capacity decreases with increasing zirconium content. In tests on 10-mil-diameter wire the 25% Zr is normal in a transverse magnetic field at 90 kilogauss while the 75% Zr still carries 5 amperes. In a longitudinal field the 25% Zr carries 400 amperes at 40 kilogauss, but only 185 at zero field.

Model magnets wound with the 10-mil Nb–25% Zr wire are being compared with the above tests. Short pieces of wire carry up to 75 amperes in a 30-kilogauss field. Under the same conditions a small 100-foot coil will carry only 30 amperes. In a large 1800-foot coil generating its own field of about 30 kilogauss, the critical current is only 18 amperes. When an 1800-foot coil is bifilarly interwound with 0.010-inch copper wire and cast in an epoxy resin, it carries up to 30 amperes with the copper secondary circuit closed. Whenever the superconductor goes "normal" and causes a field collapse, the field energy is deposited in the copper secondary circuit. Without a secondary all the field energy is deposited in the Nb-Zr circuit and can induce destructively high voltages as well as overheating the wire. Five such magnets have been tested and confirm the above observations.

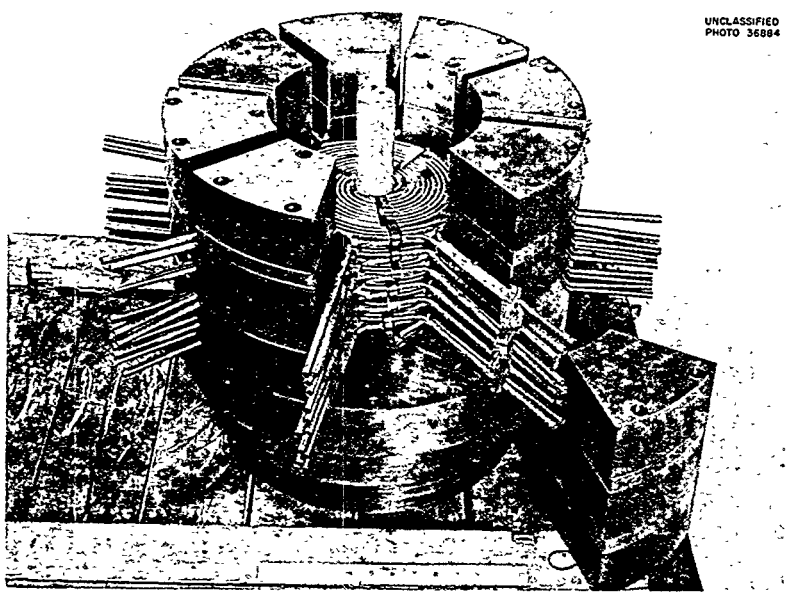

UNCLASSIFIED
PHOTO 36884

The ORNL high-field solenoid. The solenoid is shown partially assembled in its steel case. The positioning post at the center indicates the cavity (2 inches in internal diameter) available for high-field work. The 350 turns were formed from 112 strands of square copper tubing. The many separate water-cooling channels provide for the dissipation of 3250 kilowatts while the solenoid is in operation at constant magnetic fields up to 117 kilogauss. This solenoid is being used for studies of phenomena associated with superconductivity.

Chemistry Research

RADIATION CHEMISTRY OF ORGANIC MATERIALS: HIGH POLYMERS

It had been assumed, when assessing the effect of ionizing radiation on plastics and elastomers (elastic polymers), that radiation-induced changes are determined by the quantity of energy absorbed, without regard to the nature or type of the radiation. A careful comparison was therefore made of the rate of cross-linking in polystyrene in the mixed-radiation field of a nuclear reactor with the rate in a gamma radiation field. The results indicate that the fast neutrons of the reactor yield more cross links than gamma radiation does, for a given amount of energy absorbed in the sample. Then another question arose: Is the distribution of cross links produced by neutron bombardment different from that of cross links produced by gamma radiation? Since the methods of measuring cross links differ in their sensitivity to differences in distribution, this was resolved by using three methods for measurements of the amount of cross linking. For a given amount of energy deposited in the sample, it was found that fast neutrons are about three to four times as effective as gamma photons in producing cross links in polystyrene.

The energy absorbed from the radiation field of the reactor was established by calorimetric measurements. The total energy absorbed by the polymers was separated into components from the fast neutrons and from the gamma radiation by using materials of widely differing hydrogen content in the calorimeter, since fast neutrons transfer energy much more effectively to hydrogen than to elements of greater mass.

QUANTITATIVE DC DERIVATIVE CONTROLLED-POTENTIAL POLAROGRAPHY

The object of this program was to delineate the quantitative aspects of dc derivative controlled-potential polarography, including the development of procedures for the quantitative interpretation of derivative polarograms and comparison of the relative utilities of first- and second-derivative polarograms and regular polarograms.

Techniques for measuring resolved or overlapping derivative polarograms were developed. Equations were derived which, for simple, reversible, diffusion-controlled processes, respectively, express di/dt and d^2i/dt^2 as functions of i_d, dE/dt, n, F/RT, and $(E_{1/2} - E)$, in which it is shown that the peak height of a resolved derivative polarogram is directly proportional to i_d. The width of a peak at half height is an inverse function of n. If consecutive reductions take place, without chemical reaction with the products, the net polarogram is the sum of the polarograms for each constituent. Overlapping polarograms can be resolved mathematically by simultaneous equations, in which the proportionality constants can be evaluated by standard addition. Second-derivative polarograms overlap slightly less than the corresponding first derivative and considerably less than the corresponding regular polarograms, but, if interference exists, it is advantageous (because of more favorable signal-to-noise considerations) to resolve mathematically the overlapped first rather than the second derivative or regular polarograms. First derivative is superior to regular polarography if interference resulting from overlapping of waves is a problem. The use of operational amplifier systems for controlled-potential electrolysis and for computing the average value of current and its first or second derivative (at constant dE/dt) with respect to time has proved to be very advantageous in obtaining reproducible polarograms of good form, which can be interpreted quantitatively by means of theoretical relationships. In order to extend the lower concentration limit of derivative polarography, comparisons were made of the relative signal-to-noise ratios of various kinds of polarized electrodes.

Future work includes evaluating the use of DME capillaries having a drop time of about ½ second;

this enables changes to be made in the design of the current-averaging circuits, which allow higher scan rates to be used with negligible distortion of the forms of the polarograms.

SPECTROPHOTOMETRIC STUDY OF SOLUTIONS AT ELEVATED TEMPERATURES AND PRESSURES

Spectrophotometric techniques were developed for studying the fundamental chemistry of aqueous solutions of uranium, other transuranium elements, some of the lanthanides and fission products, and other elements of interest in aqueous solutions at temperatures higher than 100°C, and of various mixtures of these elements. A spectrophotometer system that can be operated with the samples at temperatures as high as 330°C and at pressures up to at least 3000 pounds per square inch with highly radioactive (alpha) solutions has been designed for ORNL by the Applied Physics Corporation, Monrovia, California, with installation expected early in 1963. It is anticipated that with this instrument system it will be possible to make spectrophotometric measurements up to near the critical point (about 372°C) in both water and deuterium oxide.

An ultimate goal of the program is to study the application of such an instrument suitably modified to provide an in-line analytical system for high-temperature, high-pressure fluid streams and for study of the chemistry of such systems. The technique will eliminate the complexities and uncertainties introduced by the withdrawal of samples from such systems because of the non-correspondence of equilibria (e.g., solubilities, valence states, adsorption, etc.) at high temperature with those at room temperature.

A study was initiated on the absorption spectral properties and related chemistry of light- and heavy-water solutions of UO_2SO_4, $UO_2(ClO_4)_2$, and $UO_2(NO_3)_2$ over the maximum temperature and pressure range possible with the present equipment, and the study will be extended into the higher temperature regions as the equipment construction and development permits.

The final cell system for this work, chosen from five possible and tested designs, is of the pressurized annulus type with a Poulter-Bridgeman type of window closure. It uses Haskel-seal metallic O-ring gaskets for metal-metal seals, single-crystal *c*-axis sapphire windows, and has a variable path length obtainable with one cell body. A full-scale titanium cell was built and was successfully tested at temperatures up to 350°C and pressures to 7500 pounds per square inch and is designed for 10,000. It will be used with a similar cell in the completed double-beam spectrophotometer system.

As an important and necessary adjunct to the program of spectrophotometry at high temperatures and pressures, an x-ray method was devised for measuring the densities of aqueous solutions at measured temperatures and pressures up to the solution critical points. A loop system for studying problems (gas-liquid equilibration, bubble separation, solid-liquid separation, etc.) associated with obtaining spectra of circulating fluids was constructed for use with a conventional Cary model 14R spectrophotometer and for operation up to about 170°C and up to about 200 psi.

Mathematical techniques which utilize high-speed digital computation have been developed to resolve seriously overlapping spectral bands and fine structure, and for other types of manipulations or calculations with spectral data. The visible and near-ultraviolet spectra of uranyl perchlorate and uranyl sulfate have been resolved completely into their individual components. These techniques may enable one to make a quantitative study of complex-ion formation, etc., in solution as a function of temperature and other variables. A fundamental program of study of the most appropriate mathematical functions for representing the shapes of spectral bands and of broadening factors, etc., is under way.

An automatic digital data read-out system has been designed, constructed, tested, and installed on a Cary model 14PM spectrophotometer. The system has an IBM-card output which simultaneously punches wavelength, absorbency, and other information. The system is entirely transistorized. The spectral data can be obtained at variable wavelength intervals as close as 1 angstrom; kinetic data (e.g., time vs absorbance at fixed wavelength) can also be obtained, using an integral digital clock system. This system can also be used, with no modification, with the high-temperature, high-pressure spectrophotometer system.

CHRONOPOTENTIOMETRY

An evaluation was made of chronopotentiometry with constant current and with mercury cathodes as a method for determining the concentration of a substance in an aqueous solution containing various concentrations of one or more electroactive species. Preliminary work was done by photographing chronopotentiograms on an oscilloscope. Because it was decided that this would be too tedious and imprecise for routine analysis and in order to direct attention to electrochemical limitations, a chronopotentiometer was designed. By use of operational amplifier circuits, the chronopotentiometer regulates the cell current to a chosen constant value, drives a timer which measures the transition time, and also can drive a chart recorder or an oscilloscope to record the entire chronopotentiogram. The performance of the chronopotentiometer is very satisfactory.

It was concluded that the principal limitation of chronopotentiometry as a method of measuring concentration arises from the nature of the electrochemical process: While the total cell current is held constant, the potential of the cathode is observed as a function of time. The usual equations relating transition time to concentration assume that all of the cell current is utilized for the primary faradaic process. In practice, even in the absence of kinetic complications, a variable fraction of the current is "stolen" by charging and surface processes and by faradaic processes other than that for the substance being determined. On the other hand, it is feasible to minimize errors from convection or from variable temperature, current, or cathode area. The analytical results are consistent with those reported by other workers. However, concentration determinations by constant current chronopotentiometry with a mercury cathode in aqueous solution did not have significant analytical advantages relative to polarograph concentration determinations. Best chronopotentiometric results are obtained at concentrations above millimolar, and the results become increasingly unsatisfactory below millimolar. This work has been completed. A paper is being prepared which will describe the chronopotentiometer and other results of this investigation.

COULOMETRIC INSTRUMENTATION

A direct-readout system has been installed on a model Q-2005 automatic, electronic, controlled-potential coulometric titrator such that the readout in volts is a power-of-ten multiple of the quantity titrated in grams. Also, a new coulometric titrator was designed which has greater sensitivity than that of the model Q-2005 titrator. Another modification of the model Q-2005 titrator was designed so that initial cell current can be as high as 3 amperes, which would be of value in making preparations of compounds at controlled potential.

FLAME SPECTROPHOTOMETER

A flame spectrophotometer was designed for high-sensitivity emission and atomic absorption flame photometry over a wavelength range from 270 to 870 millimicrons. A high dispersion, scanning, grating monochromator is used. Examples of anticipated applications of the instrument include the determination of magnesium in sea water, rubidium and cesium in river water and biological materials, and sodium, potassium, and lithium. The instrument will be evaluated initially for the atomic absorption flame photometric determination of elements such as zinc, cadmium, lead, magnesium, and mercury.

EFFECTS OF RADIATION ON ANALYTICAL METHODS

Past experience with the analysis of various materials under conditions of high radiation led to an empirical conclusion that many analytical methods suffer deleterious effects when used under such conditions. Very little work has been carried out to establish quantitatively either the source or degree of these effects. While the radiation chemists have published a great deal of work on the effect of radiation on specific materials, very few of their research findings

are specifically applicable to analytical chemistry problems.

Because of the need for such work on an analytical chemistry basis, work was initiated on measuring the effect of gamma radiation on some of the more commonly used analytical procedures. The effect of gamma radiation on several types of amperometric titrations with ethylenediaminetetraacetic acid (EDTA) were studied, and the results will be published. The chromium(VI)-diphenylcarbazide color reaction was also studied for gamma radiation effects, and these results are also being published. Future researches on the effects of various types of radiation on analytically used electrode systems, as well as gas-chromatography system components, are planned.

In the case of the EDTA amperometric titrations, it was found that the degree of degradation due to radiation is little affected by the titration conditions. The EDTA itself is resistant to radiation damage, and a correction factor can be calculated for any such damage. Investigation of the effects of gamma radiation on several of the organic end-point indicators commonly used in EDTA titrations showed that radiation levels of approximately 10^5 roentgens could be tolerated by these indicators before the end-point color change became invalid. The study of the chromium(VI)-diphenylcarbazide (DPC) reaction under high radiation conditions cleared up many of the questions concerning the reaction itself. The chromium-DPC color intermediate was observed to be sensitive to radiation at levels entirely different from those that affected the chromium or the DPC itself. The reaction is essentially an oxidation-reduction reaction.

MOLTEN-SALT SPECTROPHOTOMETRY

Spectrophotometric investigations of molten salts were continued. The main purpose of this study is to investigate the analytical usefulness of such spectra, particularly with respect to molten fluoride salts.

A marked improvement in the methods of preparing stable molten-salt solutions has been achieved. The high-temperature cell assembly is evacuated to a pressure of about 20 microns at a temperature of about 600°C prior to the insertion of a sample, which is accomplished without exposure of the cell or the sample to the atmosphere. Solutions of CoF_2 or UF_4 in LiF-NaF-KF, at 550°C, have been maintained up to 16 hours, with only a 10% loss of absorbance.

A new cell assembly is being designed which will eliminate all insulation material in the sample chamber. With the new apparatus it is expected that molten-salt solutions can be maintained for long times without any loss of color due to hydrolysis.

The preparation of solutions of UF_3 in molten fluoride salts has been of interest to evaluate the possible spectrophotometric determination of low concentrations of U(III) in the presence of U(IV) in fluoride salts. To date, the highest concentration of U(III) prepared contains 3.7 weight percent U(III) and a total uranium concentration of 4.0 weight percent in a solvent of LiF-NaF (60-40 mole percent). This solution is much too strongly colored, but it is hoped that the spectra can be obtained when the solution is diluted with more solvent. The results indicate that any residual HF in the fluoride salts will oxidize UF_3 to UF_4, possibly even below the melting point of the solvent.

A particularly significant advance was made in the method of confining corrosive liquids in a windowless container for spectrophotometric study. The liquid is held in a metal cylinder which has a hole, up to $\frac{3}{16}$ inch in diameter in a $\frac{1}{4}$-inch-OD cylinder, drilled through both side walls and centered on a line normal to the long axis of the cylinder. Light from the spectrophotometer passes through the cell by means of these apertures. The flow of liquid out of these holes is prevented by four to six smaller holes drilled in the side walls of the container in a plane immediately above the sample holes. (Surface-tension effects keep the liquid level in the plane of the small holes.) Much more light can be transmitted through the new cell than is the case with the pendent-drop technique, which is also used for confining corrosive liquids for spectrophotometric study. The cell is useful in the ultraviolet region of the spectrum to less than 200 millimicrons. Cursory data indicated that the eutectic of LiF-NaF-KF at 500°C is transparent down to at least 220 millimicrons.

NUCLEAR METHODS OF CHEMICAL ANALYSIS

The Nuclear Methods of Chemical Analysis program has as its broad purpose the application and evaluation of nuclear phenomena to analytical problems. Much of the initial work in this field has been devoted to the fabrication and use of alpha, gamma, and neutron sources using Am^{241} as the radioactive element. As a secondary effort, limited studies on fast-neutron reactions, neutron resonance, neutron-flux monitoring, and prompt-neutron capture gamma were carried out.

In the Am^{241} source program, alpha sources have been prepared and used in (1) trace beryllium analysis, using the (α,n) reaction; (2) compact and rugged timing devices which utilize the disintegration rate of Am^{241} as measured by a solid state detector; and (3) measurement of film thickness (up to 1 micron) of metals and organics by measurement of the alpha energy loss during transmission. Americium-241 gamma sources have been used to determine heavy-element concentrations in flowing streams, thickness gaging of metals, and in radiographic applications to determine the homogeneity of heavy-element dispersal in a low-molecular-weight matrix (i.e., Al_2O_3, graphite, etc.). The Am^{241} neutron sources (Am^{241}-Be and Am^{241}-B) have been used in activation analysis, neutron absorption, neutron transmission, and transistor radiation-damage studies. The extension of radioisotope source techniques will involve the preparation of sources of other transuranic elements (i.e., curium, californium, etc.) and their application to analytical instrumentation.

The feasibility of using an array of small neutron sources (each emitting 3×10^6 neutrons per second) to produce a homogeneous flux of thermal neutrons (1×10^5 neutrons per square centimeter per second) in a 183-cubic-centimeter volume was demonstrated. A small laboratory "activator" was built and is now being used in activation-analysis applications. The techniques of absorptiometry proved the value of low-intensity sources in the determination of isotopic ratios of uranium, lithium, and boron as an *in situ* application or in a flowing stream. Neutron-transmission studies with the same low-intensity neutron sources demonstrated the determination of boron loading of glasses, stainless steel, and plastics.

Significant advances have been made in neutron-flux monitoring, using threshold detectors. This work resulted in the increased utility of the reactor irradiation facilities by researchers.

SOLVENT EXTRACTION RESEARCH

The solvent extraction program has established uranium recovery processes now widely used in the uranium milling industry. Significant contributions have been made in the recovery and separation of fission product strontium, rare earths, and cesium from nitrate wastes; the recovery and separation of technetium, neptunium, and uranium from fluorination residues [see *Nucl. Sci. Eng.* 8, 907–14 (1960)]; recovery and separation of uranium and thorium (see ORNL-2993, p 149) and of plutonium and neptunium (ORNL-2993, p 155) from nitrate process solutions; the scavenging of plutonium and uranium from sulfate wastes (ORNL-2830); and the separation of trivalent actinides from lanthanides. Current investigations include studies of the fundamental nature of the extractants and the mechanisms of extractions as well as their applications.

Final-Cycle Plutonium Recovery by Amine Extraction

The extraction of plutonium with tertiary amines is attractive because of their high and nearly specific extraction power for tetravalent plutonium. The chemical and physical performance of a process (see flowsheet) for obtaining product plutonium in one step from a Purex 1BP plutonium stream was demonstrated in countercurrent runs with simulated feeds and with actual Purex plant solutions. Plutonium distributions confirmed previous equilibrium measurements, with satisfactory recoveries and concentration factors of 10 to 20. Decontamination factors from tracer Zr-Nb with the simulated solutions were near or above analytical limits, about 10,000, but those with the actual Purex process solutions were only about 100 to 500, much lower than expected and needed. The

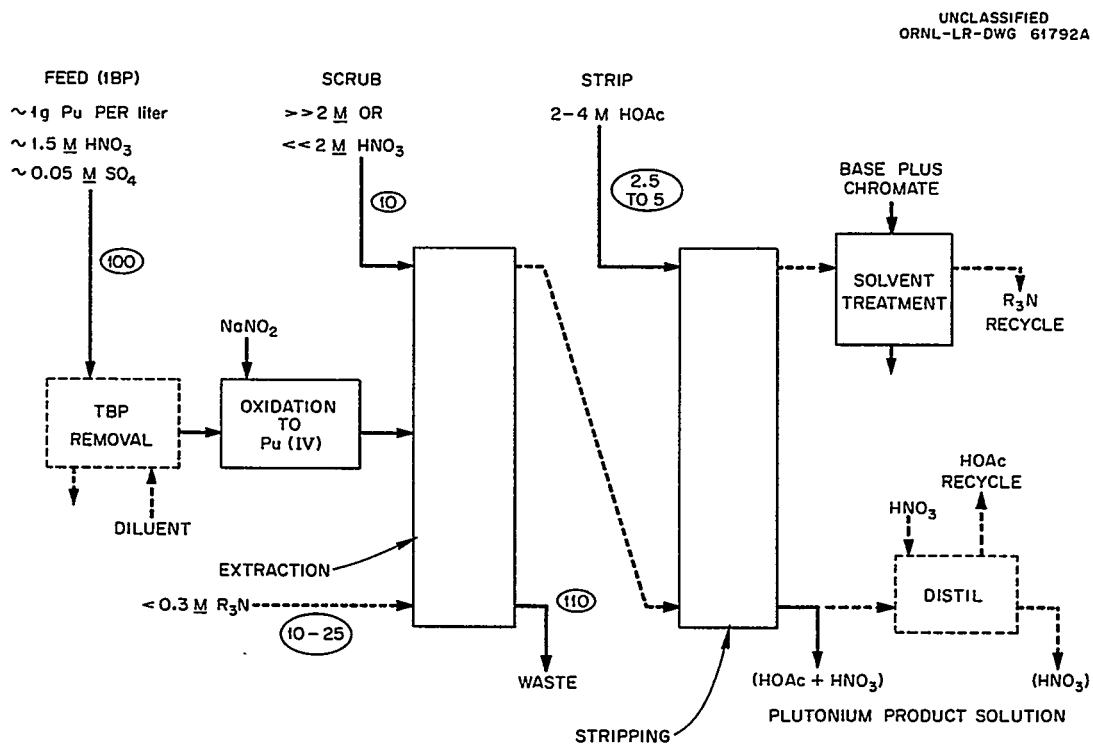

Amine extraction cycle for final plutonium recovery. The circled numbers indicate tentative relative volumes.

factors controlling decontamination in process solutions are now being studied in detail.

Metal Nitrate Extraction by Amines

A continuing investigation under subcontract at the Massachusetts Institute of Technology is determining extraction equilibria at macro concentrations of metal ions important as fission products or corrosion products in reactor fuel processing. Stainless steel metals and rare earths showed extraction coefficients generally equal to or less than 10^{-4} over the concentration ranges of interest; molybdenum extraction was high at low acidity but dropped below 10^{-4} at HNO_3 molarities equal to or less than 2. Zirconium extraction coefficients were low but increased with increasing nitrate concentration, approaching 0.01 at 8 *M* HNO_3 (0.5 *M* trilauryl-amine). Ruthenium extraction coefficients increased with decreasing acidity, approaching 1 at 0.5 *M* HNO_3.

Metal Chloride Extraction by Amines

The extraction of metal ions from hydrochloric acid and chloride salt solutions is being surveyed with typical primary, secondary, and tertiary amines and quarternary ammoniums. Extraction coefficients of iron(III), used in preliminary tests as a model, with the secondary amine Amberlite LA-1 were several times higher in diethylbenzene than in Amsco 125-82–alcohol diluent and were higher from lithium chloride than from other chloride salt solutions. With all the amines, extraction increased with increasing chloride concentration and in the order: Primene JM (primary amine) << Amberlite LA-1 (secondary amine) < Alamine 336 (tertiary amine) < Aliquat 336 (quaternary ammonium).

Acid Recovery by Amine Extraction

Preliminary tests indicated that sterically hindered amines may be used to remove sulfuric

acid from Sulfex process wastes in order to permit acid recycle and decrease waste volumes. A useful balance between acid extraction power and amenability to water stripping was obtained by proper choice of the degree of alkyl branching close to the nitrogen. The best compounds tested were tri(2-ethylhexyl)amine, di(2-ethylhexyl)hexylamine, and especially *N*-benzyl-di(2-ethylhexyl)amine, which extracted more than 90% of the sulfuric acid from simulated Sulfex waste and released it to the stripping solution at about 1 *M* H_2SO_4.

Extraction Performance and Cleanup of Degraded Solvents

Washing with sodium carbonate or sodium hydroxide of a TBP-aliphatic diluent solution that has been used in a radioactive environment removes the degradation products of TBP but not those of the diluent (e.g., Amsco 125-82). These products can act in combination with TBP to give strong, apparently synergistically enhanced, extraction of Zr-Nb. Enolizable nitroparaffins (RNO_2) are the most probable diluent degradation products responsible for the poor behavior of degraded solvent (ORNL-3153, p 109). Continued search for diluents more stable to nitration showed large variations in stability with structure of alkylbenzenes. Di- and cycloalkylbenzenes were less stable than simple monoalkylbenzenes, with indication that triethylbenzene was more stable than either and that monoalkylbenzenes were more stable when iso-branched than when either more branched or normal. These comparisons apply only to side-chain nitration; nitration of the benzene ring does not produce Zr-Nb extractants, although it must be considered for safety reasons (formation of nitrated benzenes).

The rate of Amsco 125-82 nitration more than doubled in the presence of TBP. The degradation, as measured by tracer Zr-Nb extraction or by the amount of nitroparaffin formed, or total organic nitrogen formed, was essentially the same from heating as from irradiation. For example, a 10-hour reflux with 2 *M* HNO_3 is equivalent to about 100 whr/liter of Co^{60} gamma irradiation. Amsco 125-82 was less susceptible to nitration after being scrubbed with concentrated H_2SO_4.

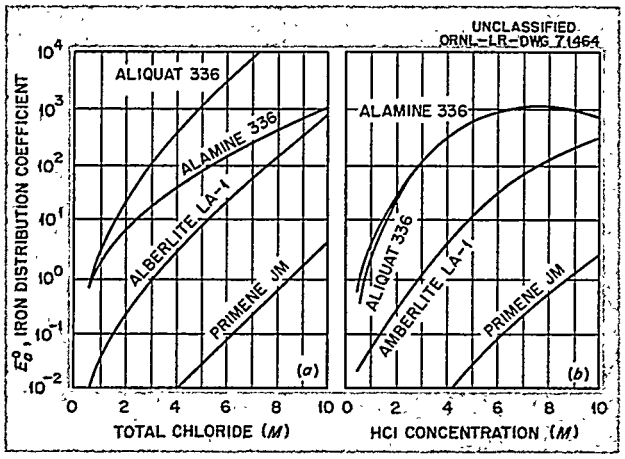

Extraction of Fe(III) from chloride solutions. Organic phase: 0.1 amine chloride in diethylbenzene (97% diethylbenzene–3% tridecanol, diluent for the Aliquat 336). Aqueous phase: 0.01 *M* Fe(III) in (a) LiCl–0.2 *M* HCl, and (b) in HCl. Contact time: 10 minutes at a phase ratio of 1 : 1.

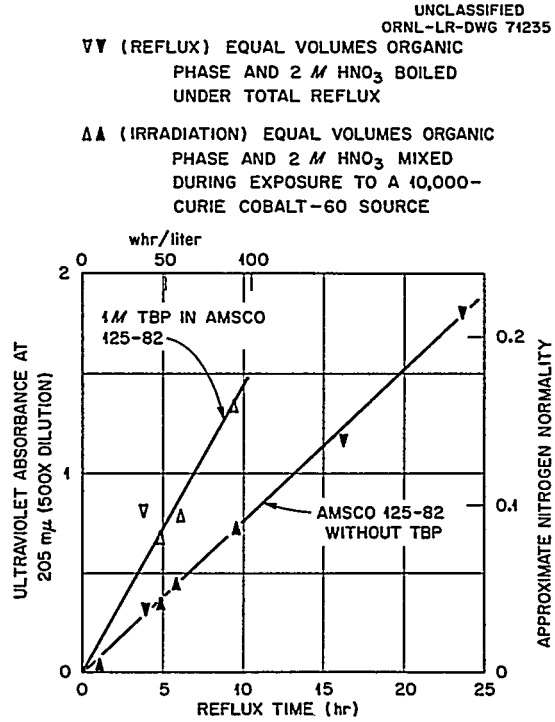

Radiation and chemical degradation of Amsco 125-82, alone and in the presence of 1 *M* tributyl phosphate (TBP).

Of many scrubbing agents tested, ethanolamine proved most effective in removing Zr-Nb extracting impurities from degraded solvent. However, the economic value appears marginal because of the appreciable loss of both TBP and ethanolamine and the relatively high price of the latter.

Suppression of Zr-Nb and Ruthenium Extraction by TBP-Amsco from Aqueous Feeds Pretreated with Oximinoketones and Oxalic Acid

Preliminary tests indicated that Zr-Nb and ruthenium extractions are significantly suppressed if the feed is treated with certain oximinoketones or oxalic acid. In countercurrent extraction of a solution of an irradiated fuel element by 30% TBP (tributyl phosphate), uranium decontamination from gross beta and alpha activity was improved three- to fourfold by pretreating the feed with 0.1 *M* diacetylmonoxime and 20- to 30-fold by pretreating with 0.05 *M* oxalic acid.

Separation of Elements in Concentrated Chloride Solutions

In the production of heavy transplutonium elements, the greatest separation yet achieved between trivalent actinides and lanthanides is by extraction with tertiary amine solutions from concentrated lithium chloride solutions. Curium is extracted about 100 times as well as europium by several amines in a variety of hydrocarbon diluents. Separations between the individual elements within the two groups are relatively small, the order of extractability and the separation varying with composition of amine, diluent, and aqueous solution. All the lanthanides are extracted preferentially to yttrium, which in most chemical systems is very similar to some of the heavier lanthanides. The maximum separation between europium and yttrium is about 10, and this is the only known system in which yttrium can be separated from all the lanthanides by a single extraction cycle.

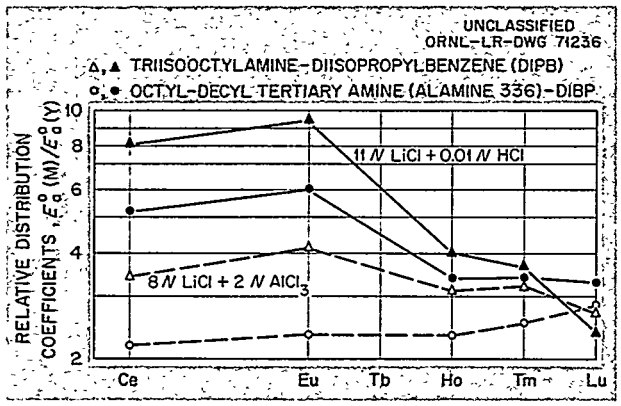

Tertiary amine extraction of lanthanides, compared with yttrium. Alamine 336–Amsco 125-82 plus 10% tridecanol, Alamine 336–diethylbenzene, and *n*-butyl didodecenylamine–DIBP mixtures behave similarly.

Gel-Liquid Extraction

Preliminary evaluations of the tertiary amine Alamine 336 absorbed in polystyrene-divinylbenzene beads, for use in the "gel-liquid extraction" method of obtaining multistage column contact with a liquid extractant, showed high separations but slow equilibration in the transplutonium–lanthanide–lithium chloride system, for example, the complete separation of Eu^{152} tracer (eluted first) from Am^{241} by slow elution with 13 *N* LiCl containing 0.005 *N* HCl. While this procedure does not appear competitive with the relatively easy separation by conventional solvent extraction in that system, the results indicate possible applications in other cases where separation factors are small or where useful extractants are limited by poor miscibility with common diluents.

Fundamental Studies of Solvent Extraction

In addition to and in support of the applied investigations described above, the fundamental nature of the extractants and the mechanisms of extraction are being studied. Results have been published previously on the extraction equilibria of sulfuric acid by amines [*J. Phys. Chem.* **60**, 239–45 and 943–46 (1956)]; of uranium and thorium sulfates by amines [*J. Phys. Chem.* **62**, 777–83 (1958); *ibid.*, **65**, 1358–61 (1961)]; and of uranium and iron perchlorates by dialkylphosphoric acid [*J. Phys. Chem.* **62**, 129–36 (1958); *ibid.*, **64**, 89–94 (1960)]; apparent dependence of equilibria on changing interfacial area

during extraction [*J. Phys. Chem.* 64, 877–80 (1960)]; dielectric and aggregation properties of amine extractants [*J. Phys. Chem.* 63, 747–49 (1959); *ibid.* 62, 363, 1119–23 (1958)]; interaction equilibria between reagents in a mixed extractant (*Journal of Inorganic Nuclear Chemistry*, in press); and aqueous metal complex formation constants determined by means of extraction equilibria [*J. Am. Chem. Soc.* 80, 4133–37 (1958); *J. Phys. Chem.* 64, 667–70 (1960)].

In current studies, alkali and alkaline-earth extractions by dialkylphosphoric acid from nitrate solutions showed the following series: alkaline earth > alkali and Li >> Na > K > Rb $\cong$ Cs. Strontium extraction was at a maximum near pH 5, with the extraction coefficient proportional to $(pH)^2$ below 4 and independent of pH above 7. Sodium extraction was accompanied by water extraction proportional to a linear function of the sodium loading. Direct manometric measurement of vapor-pressure differences showed that in wet benzene solution sodium di(2-ethylhexyl)phosphate is aggregated, while tricotylamine is ideal up to about 0.2 *M*. Transfer-rate measurements of S^{35}-tagged sulfate during amine sulfate extraction of uranium showed no evidence of exchange between $UO_2(SO_4)_2^{2-}$ and SO_4^{2-}, strengthening previous indications (see last two references given above) that neutral UO_2SO_4 is the species actually transferred under the conditions examined.

Contactor Development

A countercurrent pump-driven array of stacked hydroclones was developed for high-speed contacting in solvent extraction. Contact time and solvent holdup are minimized, which decreases solvent degradation by irradiation; less space and shielding are required than for conventional equipment; and decontamination from substances that reach chemical equilibrium slowly may be higher. In tests with 0.5-inch-diameter clones on the extraction of uranium from 1 *M* $NaNO_3$ by 18% TBP–Amsco, stage efficiency was 40 to 75% at a throughput rate of 1.2 to 2.0 liters per minute. The principal cause of the low efficiency was inadequate gross mixing rather than extensive backmixing.

PREPARATION OF RESEARCH MATERIALS

Uranium-232

A total of 32.9 milligrams of U^{232} for nuclear cross section measurements was prepared by neutron irradiation of Pa^{231} and chemical isolation of the uranium. The principal product solution contained 21.58 milligrams of uranium with an isotopic composition 98.9% U^{232}, 0.013% U^{233}, 0.010% U^{235}, and 1.08% U^{238}. The remainder of the uranium contains about 0.03% U^{233} and 0.003% U^{235}. Uranium-235 and U^{238} contamination resulted from about 7 parts per million of natural uranium in the Pa_2O_5 from which the U^{232} was produced and from traces of uranium in process reagents.

Six aluminum-Pa_2O_5 cermet targets containing a total of 48.1 grams of Pa^{231} were fabricated and irradiated. One target containing 7.35 grams of Pa^{231} was irradiated to 4.7×10^{18} *nvt* and processed for uranium recovery after 43 hours of decay and again after 91 hours of decay. The other five targets, containing a total of 40.6 grams of Pa^{231}, were irradiated to 4.1×10^{18} *nvt* and processed together for uranium recovery after 43 hours of decay and again after 77 hours of decay. The irradiated slugs were dissolved in HCl and HCl-HF, and the uranium was recovered by anion exchange and purified by a second anion exchange cycle and a TBP extraction.

Another gram of U^{232} containing about 1% U^{233} is being prepared by a longer reirradiation of the Pa^{231}.

Plutonium

As a part of the program to provide macro quantities of the heavier isotopes of plutonium and smaller quantities of americium and curium, 24 highly irradiated plutonium-aluminum alloy rods were successfully processed. The heavier isotopes of plutonium were desired for studies of their nuclear properties while the americium-curium would provide feed materials for process development. In completing the recovery of 675 grams of plutonium from these rods, a full-scale demonstration of a process based on anion exchange methods was possible.

Dissolution rates were satisfactory, averaging about 1 gram of plutonium per hour, in 6.5 *M* HNO_3–0.05 *M* Hg^{2+}–0.05 *M* F^+. Eighty percent of the plant losses, totaling 1% of the material processed, occurred during the scrubbing step in the first ion exchange cycle. The recovered plutonium was decontaminated from fission products by a factor of 10^6 in two ion exchange cycles; it met radiation specifications for further handling in subsequent isotope-separation steps. The useful life of Permutit SK anion exchange resin in the radiation fields characteristic of highly burned plutonium recovery processes was found to be limited to a total dose of 4×10^8 rads.

The wastes from the ion exchange system of the plutonium recovery process were stored for later development and demonstration at full level of the process for recovering americium and curium.

RADIATION EFFECTS ON CATALYSTS

A large radiation effect on catalysts reported in a series of Russian papers was not confirmed in a repetition of the work. On a unit surface area basis, the catalysts magnesium sulfate and magnesium sulfate–sodium sulfate in which radioactive S^{35} had been incorporated were less active than nonradioactive catalysts of the same composition in the dehydration of cyclohexanol. The decreased catalytic activity persisted even after the radioactivity had substantially decayed. In an extension of the work, neither x irradiation of the catalysts while in use nor preirradiation with Co^{60} gamma rays had any effect.

These results may possibly be explained by changes in the radioactive catalysts brought about by the emission of beta particles from S^{35} during the crystallization step of catalyst preparation. The reports of enhanced catalytic activity may be attributed to the failure to take into account the larger specific surface areas of the radioactive catalysts than their nonradioactive counterparts for a given set of preparation conditions.

CATION EXCHANGE AT ULTRAHIGH IONIC STRENGTH

Cation exchange, an important and well-established tool for separations, has been handicapped by fears that it would be ineffective at high ionic strength. It was shown at ORNL and at other laboratories that, contrary to theoretical expectations, some elements are strongly adsorbed at high ionic strength by cation exchangers. This observation complements an earlier one made a number of years ago at ORNL that, again contrary to expectations at that time, many elements are strongly adsorbed by anion exchangers at high ionic strength.

The usefulness of cation exchange at high ionic strength as a separations method was established at ORNL by studying the adsorption behavior of almost all the metallic cations in concentrated perchloric acid solutions, using principally radioactive tracer techniques. Very strong adsorption was found for the rare earths, scandium, most actinide elements, and some alkaline earths; a number of elements showed moderate, but significant, adsorption. Adsorption from concentrated hydrochloric acid solutions was also studied with nearly all the metallic elements and established as a valuable separations tool.

Over 50 elements were studied in mixed acid solutions which now appear of particular interest for separations because, with proper mixtures of acids, the adsorbabilities can be greatly modified. Thus, admixture of hydrofluoric acid with concentrated perchloric or hydrochloric solutions enormously decreases the adsorbabilities of elements which form strong fluoride complexes; in the case of uranium, admixture of chloride with concentrated perchloric acid solutions was very effective in controlling adsorbabilities and in providing unique isolation methods for this important element.

NEUTRON DIFFRACTION

A method for rapid photographic recording of neutrons has been developed at ORNL. The

UNCLASSIFIED
PHOTO 54665

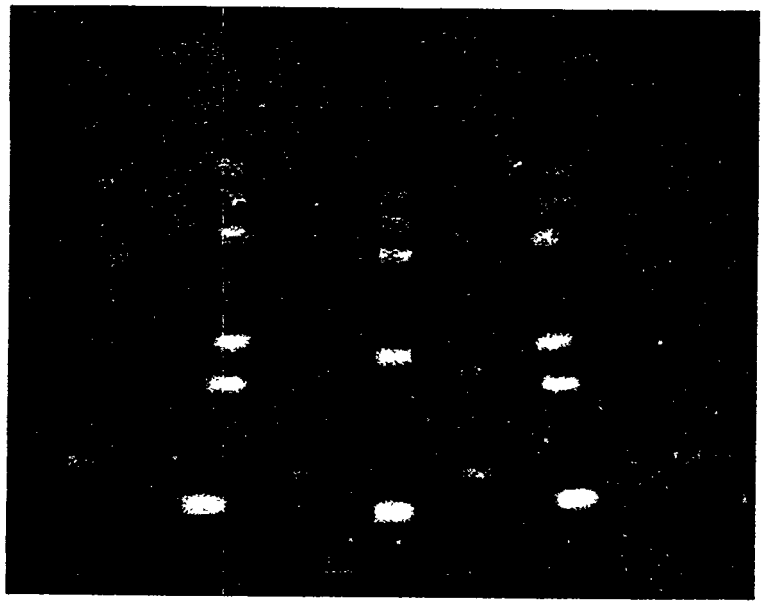

Neutron diffraction rotation photograph of sodium chloride; 30-minute exposure.

neutrons impinge on a special phosphor containing lithium-6, a high neutron absorbing isotope, in the form of lithium fluoride. The neutron energy is converted to visible light, which exposes a high-speed (ASA 3000) photographic film capable of being developed in 10 seconds. The method is especially useful in recording the patterns of neutrons scattered by crystals. Such a pattern is shown in the photograph.

A PRECISE MEASUREMENT OF THE LONGITUDINAL POLARIZATION OF BETA PARTICLES FOLLOWING THE DECAY OF PHOSPHORUS-32

About five years ago, one of the assumptions of nuclear theory, that parity is conserved in beta decay, was shown to be in error. If parity were conserved, then an electron emitted in beta decay would show no preference for right-handedness or left-handedness as determined by its direction of propagation (direction of the thumb along the line of flight) and the sense of its intrinsic spin (direction of curl of the fingers about the line of flight). A preponderance of one or the other (referred to as "longitudinal polarization") would result from nonconservation.

After the demonstration that parity was not conserved, Lee and Yang, the theorists who had suggested nonconservation, introduced a modified theory allowing for this, and other theorists introduced limitations which led to a quantitative prediction of the amount of longitudinal polarization to be expected in beta decay. It then became of interest to measure longitudinal polarization with sufficient precision to evaluate the parameters of the new theory.

Although longitudinal polarization of beta rays had been demonstrated soon after it was predicted to exist, the measurements were not sufficiently precise to use in a critical test of the quantitative theory. It was therefore decided to undertake at ORNL, as a cooperative venture by the Physics and Chemistry Divisions, a measurement adequate for this purpose.

The measurement (on phosphorus-32) has now been completed, using electrostatic rotation of the line of flight to convert longitudinal into transverse polarization, and Mott scattering from gold to convert the asymmetry in spin orientation into angular asymmetry of the scattered beam. The experiment was designed to minimize corrections for instrumental asymmetry, depolarization in the source, instrumental scattering, etc., and

these effects were in addition investigated experimentally. Large sources were used to give adequate counting rates, and multichannel recording was used to minimize various background effects. As a result of this combination of many facets of the Laboratory's experience in handling and measuring radioactivity, the value for the polarization is now known to better than 99%, an accuracy sufficient for quantitative comparison with theory.

The experimental value for the polarization, together with generally accepted theoretical assumptions, essentially eliminates the possibility of one kind of interaction between the particles participating in the beta decay and allows the calculation of the ratio of the contributions from two other kinds of interaction. The value of this ratio is in agreement with the currently accepted theory of beta decay.

CAPTURE-TO-FISSION RATIO IN URANIUM-233 FOR EPITHERMAL NEUTRONS

In any thermal nuclear reactor an inherent neutron loss results from the fact that some of the fissioning fuel atoms undergo neutron capture (being thereby transmuted into nonfissionable atoms), while the majority undergo the chain-propagating fission process. The ratio of these two reaction rates, which gives a measure of the loss, depends on the neutron energy: At thermal energies the capture-to-fission ratio is about 0.10 for uranium-233, the only feasible fuel for a thermal breeder reactor. While most of the neutrons are approximately in thermal equilibrium with the reactor medium, about 10% of the reactions occur at higher energies, where the capture-to-fission ratio could be appreciably higher than 0.10.

A measurement of this ratio, averaged over the higher-energy neutrons, has been made by analyzing for fission products and the nonfissioning uranium-234 produced in uranium-233 exposed only to higher-energy neutrons. The value of the capture-to-fission ratio obtained was 0.17, which, although higher than the thermal value, is not detrimentally important because only about 10% of the reactions occur at the higher energies. When this factor is taken into account, the effective ratio is only 0.107.

SOLUTIONS OF METALS IN MOLTEN SALTS

Studies of solutions of metals in molten salts at the Oak Ridge National Laboratory showed that in many cases, as with the alkali metals, a large fraction of the electric current passed through such solutions is carried by mobile electrons. In other systems, however, such as solutions of cadmium or bismuth in their molten chlorides, the electrons are not free but are trapped in lower-valence states of the metals. Most recently, it has been established that among the rare-earth metals, that group of elements closely resembling each other in most respects, both cases occur, with a dividing line at praseodymium.

Solutions of lanthanum and cerium metal in their molten trichlorides or triiodides exhibit relatively high electronic mobility, while a solution of neodymium metal in molten neodymium trichloride or triiodide is an almost purely ionic conductor. The neodymium solution contains a lower-valent neodymium ion, most probably having a double charge, which is infrequent in the rare-earth group of elements. On the other hand, each lanthanum or cerium atom dissolved, instead of forming such a divalent ion, appears to dissociate into a normal trivalent ion and three mobile electrons. These differences in behavior are explained by the position of the elements in the periodic system and the degree of filling of the *4f* group of orbitals in the electron shells of the atoms.

The case of the neodymium solutions is of additional interest. The conductivity of the neodymium trihalide-dihalide mixtures does not simply vary linearly with composition, but exhibits a strong positive deviation from additivity, which in the iodide system takes the form of a distinct maximum near 50 mole percent dihalide. This is interpretable in terms of a notable electronic contribution to the conductance, resulting from an electron exchange between dipositive and tripositive neodymium ions.

THE DIFFERENTIAL METHOD FOR MEASURING ISOTOPE EFFECTS

The rate of a particular chemical reaction is usually dependent on the isotopic content of the molecules reacting. For instance, formic acid in which the carbon atom is carbon-14 decomposes more slowly than ordinary formic acid, the molecules of which contain ordinary carbon (carbon-12). Knowledge of such differences is important, not only in the use of isotopes as tracers, where an unsuspected isotope effect can lead to mistakes, but in learning more about the mechanisms of reactions.

The area of greatest interest in isotope effects is organic chemistry, and much has been learned about the subject because of the availability of the radioactive isotope, carbon-14, which can be measured easily and precisely. During the past year such measurements have been remarkably improved by a combination of methods.

A standard method for measuring isotope effects is the method of competing reactions, in which the reactants are a mixture of two species, differing only in isotopic content. These species are then allowed to react competitively with an appropriate substance. Measurement of the isotopic content of the product reveals which isotopic species reacts faster. Obviously, the smaller the difference in rates, the more difficult the measurement.

The improvement was made possible by the availability of methods for the precise measurement of radioactivity and of a high-speed computer for the treatment of the data. This differential method requires that several samples be removed at frequent intervals throughout the reaction, in contrast to integral methods in which one composite sample is allowed to accumulate and its radioactivity to be measured after perhaps half-completion of the reaction. High-speed computation was necessary because the mathematical analysis of the problem showed that a separate curve of isotopic content versus the extent of reaction is obtained for each value assumed for the ratio of isotopic rates, and the computational problem is thus one of fitting points to a series of parametric curves.

The procedure can also be used for determining isotope effects due to stable isotopes, since mixtures of species containing both carbon-14 and deuterium have been allowed to react differentially, and the radioactivity measurements of the product fractions have been used as a measure of the change in deuterium content. This differential method has been used to measure isotope effects as small as 0.38%, with an error of 0.03%.

SEPARATION OF NITROGEN ISOTOPES

More than 70 grams of nitrogen-15, 95 to 99% pure, were separated and made available for use in research. The normal abundance of this rare isotope of nitrogen is 0.37%. By adding nitrogen-15 to ordinary nitrogenous materials, researchers can trace or follow the course of labeled material throughout an experiment and thus achieve an understanding of the mechanism which is involved. Since nitrogen is an important constituent of living matter, and since no other suitable tracer exists, the availability of nitrogen-15 is of great importance to those in the fields of biology, agriculture, chemistry, and physics.

EFFECTS OF REACTOR RADIATIONS ON ZIRCALOY-2 CORROSION IN HIGH-TEMPERATURE AQUEOUS ENVIRONMENTS

Zircaloy-2 exposed in-pile to fissioning solutions of oxygenated UO_2SO_4 at high temperatures corrodes at a steady rate, which depends upon the rate of fissioning near the surface and, at high rates of fissioning, upon the temperature. The detailed mechanism of this radiation corrosion is uncertain, but the corrosion is believed to result primarily from damage produced in the metal or oxide by the heavy fission-fragment recoils rather than from the ionizing effects of these and other types of radiations.

It has been recognized in the past that quantitative information on the effects of other types of heavy particles would be useful in evaluating the mechanism of the fission-recoil-induced

corrosion as well as in reactor development where Zircaloy-2 is commonly used as fuel plate cladding. Accordingly, experiments to determine the effects on Zircaloy-2 corrosion of reactor radiations alone, including fast neutrons, and of reactor radiations together with small amounts of fission-recoil irradiation were carried out as part of the program of Aqueous Homogeneous Reactor corrosion studies. These experiments were of the rocking-autoclave type. Oxygenated solutions of (1) UO_2SO_4 with uranium depleted of U^{235}, (2) D_2O, and (3) dilute acid were tested in the temperature range 250 to 300°C. Hydrogenated water was also tested in one experiment. Radiation exposures were performed in the Low Intensity Testing Reactor and the Materials Testing Reactor.

The results of these experiments were reexamined and reevaluated on the basis of presently available information regarding (1) neutron flux levels in the experiments, 1×10^{12} to 7.5×10^{12}, greater than 1 Mev; (2) probable effects of fissioning of residual U^{235} and of plutonium formed in the UO_2SO_4 experiments; and (3) the effects on nitrogen gas, initially present in some of the experiments, on the interpretation of gas-pressure-change measurements.

It was concluded that significant effects of reactor radiations alone occurred in all the experiments employing oxygenated solutions, with the amount of corrosion increasing approximately linearly with time. After allowance for the effects of low-intensity fission-recoil irradiations in the UO_2SO_4 experiments, it was found that the corrosion rates increased regularly with increasing fast neutron flux but were independent of temperature and solution composition. The rates ranged from about 0.5 to 3.0 mils per year. In the hydrogenated water experiment, the rate was less accurately determined, but it was probably substantially less than that in the oxygenated systems at a comparable radiation intensity. Most of the characteristics of the corrosion in oxygenated systems were similar to those previously observed for corrosion in fissioning solutions.

Beta and gamma radiations are assumed to be ineffective on the basis of the results of previously reported studies with fast electrons at high intensities; therefore the corrosive effects observed are ascribed to fast neutrons.

Several mechanisms, previously proposed to explain fission-recoil effects on Zircaloy-2 corrosion, postulate damage in the oxide of types which might be expected or are known to occur with fission-recoil irradiation but not with neutrons to any appreciable extent. Both types of radiations, however, produce interstitials and vacancies (displaced atoms), and damage by fast neutrons in solids is usually interpreted in terms of production of such defects. Estimates of rates of displacement of atoms in the surface layers of the metals and in the protective oxide show that neutrons and fission recoils produce comparable numbers of displacements at intensities yielding equivalent corrosion rates in the oxygenated solutions. This is considered indicative that the mechanism by which neutrons effect corrosion is the same as that for fission recoils and includes, as the initial step, the production of interstitials and vacancies.

ELECTROCHEMICAL STUDY OF ZIRCALOY-2 CORROSION AT ELEVATED TEMPERATURES

Electrochemical measurements have long been used to provide information about corrosion and its control at temperatures below 100°C in water or aqueous solutions. Unavailability of techniques and equipment for such measurements at higher temperatures (and pressures) has seriously deterred the use of this powerful method at temperatures of interest to nuclear-power reactors. Investigations of the electrochemistry of zirconium-alloy corrosion in high-temperature aqueous-solution environments are being made in a continuing study at ORNL. The studies are designed to provide basic information on the corrosion mechanisms of these materials which have widespread use in reactor systems. Attempts to correlate the data obtained with observed effects of radiation on corrosion and with alloy compositions are also projected.

An assembly, comprised of a high-pressure cell of titanium with provisions for continuous replacement of the test solution and with cooled Teflon seals for the necessary electrode penetrations, has been demonstrated at ORNL to yield satisfactory information at temperatures to 300°C. With this assembly, instantaneous measurements

of corrosion rates can be obtained by two independent methods, and the time dependence of the corrosion process can be established with a single specimen. The necessity of exposing and weighing of many specimens is obviated; moreover, the sensitivity of the measurement permits observations of corrosion rates and rate changes far smaller than those possible by cumbersome weight-change techniques. The results suggest that the mathematical relationships for current-potential behavior developed from low-temperature data apply equally well at the elevated temperatures. The equipment also includes a dc pulse system for determining the capacitance of the corroding electrode.

Previously, data were obtained on the time and temperature dependence of the open-circuit corrosion of Zircaloy-2 and crystal-bar zirconium in the temperature range 200 to 250°C in oxygenated, dilute sulfuric acid solution.

In recent investigations, measurements employing potentiostatic techniques were made on a Zircaloy-2 specimen following exposure in oxygenated 0.5 *m* H_2SO_4 at 293°C for several days. There were then only very small changes in rate with time at these conditions. The anodic and cathodic partial process reactions were studied separately over the temperature and potential range, 150 to 300°C and −1.400 to +0.300 volts vs platinum at about 40°C. The results showed an activation energy for the anodic partial process (oxidation of zirconium) of 31.1 kilocalories per mole independent of potential and temperature. The activation energy for the cathodic partial process (reduction of oxygen) was found to be a function of potential and temperature, 10.8 kilocalories per mole at −1.400 volts vs platinum between 220 and 300°C, changing to 5.4 kilocalories per mole at temperatures below 220°C. At −1.200 volts vs platinum, the activation energy was 5.4 kilocalories per mole over the entire temperature range. Postexposure examination of the specimen revealed some areas of white oxide, so that the mechanistic interpretations of the results are not yet clear. However, the feasibility of measurements of these types was demonstrated.

Additional experiments with Zircaloy-2 and with other alloys are planned in order to test previous results and to provide additional types of information on the corrosion characteristics.

BEHAVIOR OF MOLTEN-SALT MIXTURES

After continued application of the resources of chemistry and physics to studies of their behavior, the nature of the gaseous and the solid states of matter may be said to be reasonably well understood. The situation as regards the liquid state is less satisfactory. The nature and behavior of a special class of liquids, molten mixtures of ionic salts, is the subject of a continuing program of study in the Reactor Chemistry Division. Reciprocal systems (mixtures containing at least two cations and two anions) and systems with a common ion (mixtures of two different fluorides, for example) are under examination in this research program. The simple theories of molten-salt behavior, which consider purely electrostatic forces between the nearest-neighbor ions, have been modified to include the London dispersion forces between second nearest neighbors, the steric effects between nearest neighbors, and the terms for higher-order interactions. Association constants for formation of species within such melts, which are evaluated from electromotive-force measurements of suitable cells, show satisfactory agreement, over a considerable range of conditions, with those predicted from the extended theory. Evidence obtained from measurements of heats of mixing of simple salts and from measurements of freezing-point depression of one salt when a second is added is readily interpreted by extensions of this theory.

DENSITIES OF COMPLEX FLUORIDES

In the past it was frequently difficult to measure the densities of solid, complicated, fluoride compounds of interest to nuclear technology with the accuracy and precision required for unambiguous crystal-structure determinations. A very simple method for estimating these densities was tested in the Reactor Chemistry Division; it is based on the assumption that the volume of the complicated compound will be merely the sum of the known volumes of its simpler components. For instance, the volume of $NaYF_4$ would be calculated to be the sum of the volumes

of NaF and YF_3. This method has given estimates which agree on the average to within 5% of the measured density values; the availability of such estimates has greatly facilitated the assignment of the probable number of molecules per unit cell in crystals whose structures are currently under investigation.

CRYSTAL-STRUCTURE DETERMINATIONS

The availability of good single crystals of a new complex fluoride compound, $LiSbF_6$, from another program made it possible to undertake a challenging crystal-structure determination. Because the compound is composed of atoms of widely differing atomic numbers, the determination of its crystal structure by x-ray diffraction required that the diffracted x-ray intensities be measured very precisely with the use of scintillation-counter techniques. It proved possible to accomplish this with sufficient precision to determine the Sb-F bond length as 1.88 ± 0.01 angstrom. Previous attempts to estimate this distance in other Sb-F compounds or to determine it with less precise experimental techniques gave values differing from the present value by about 0.10 angstrom.

Two compounds, $LiCsF_2$ and $LiRbF_2$, prepared previously in phase studies of alkali fluorides, were also studied by x-ray diffraction. The crystal structure of $LiCsF_2$ was elucidated in detail and the $LiRbF_2$ shown to be isostructural with it. Crystals of these difluorides consist of fluoride tetrahedra surrounding Li^+ ions and sharing corners and edges in such a way as to form continuous sheets. These are held together by the larger cations which are coordinated by ten fluorides in an irregular configuration (six fluorides closer to the cation, four farther out). The adoption of this ionic arrangement limits the size which the larger cation can have, a possible indication of why this structure is not found for other 1 : 1 alkali-fluoride mixtures.

ELECTRICAL CONDUCTANCE OF AQUEOUS SOLUTIONS AT HIGH TEMPERATURES AND PRESSURES

The critical point of a material is the highest temperature and pressure at which it can exist as a liquid; at supercritical conditions, it exists as a dense fluid with many properties different from those observed under ordinary conditions. The measurement of the electrical conductance of aqueous solutions and supercritical aqueous fluids at high temperatures provides a powerful tool for fundamental study of solution behavior.

Such measurements of the electrical conductance of K_2SO_4 solutions varying in concentration from 0.0005 to 0.005 *m* were made up to temperatures of 750°C and up to pressures of 50,000 pounds per square inch. The measured equivalent conductance of the solutions reaches a maximum value of greater than 900 square centimeters per ohm at solution densities near 0.5 gram per cubic centimeter and then decreases slightly at higher densities. This maximum value is approximately six times greater than the equivalent conductance of K_2SO_4 at room temperature and indicates that the sulfate ion is nearly completely hydrolyzed to the bisulfate ion under these conditions.

PHASE EQUILIBRIA IN HIGH-TEMPERATURE AQUEOUS SYSTEMS

The solvent properties of supercritical aqueous fluids are being explored at temperatures up to 425°C and pressures up to 4000 pounds per square inch. In supercritical mixtures of water and sulfuric acid, remarkably high solubilities of a number of metallic oxides have been observed; concentrations as high as 7.2, 1.4, 1.3, and 0.59 weight percent of uranium, copper, lithium, and nickel oxides, respectively, were found, in separate experiments, with the use of gas mixtures containing approximately 9.0 weight percent sulfuric acid. The results of this study are of fundamental interest, but they also are relevant to studies of geochemical processes and to the long-range development of very high-temperature aqueous reactor-fuel systems.

At temperatures near 300°C aqueous solutions of uranyl sulfate are known to separate into two liquid phases. The effect of pressure in raising the phase-separation temperature was studied with the use of a new technique for visual observation of the point of separation. At pressures up to 5000 pounds per square inch the phase-separation temperature was elevated approximately 5.3°C per 1000 pounds per square inch of pressure for solutions containing from 5 to 60 weight percent of uranyl sulfate. This value corresponds approximately to the change of temperature with pressure over which H_2O is maintained at constant density; thus a first-order effect of solvent density on liquid-liquid immiscibility is indicated.

HIGH-TEMPERATURE ACIDITY MEASUREMENTS: U(VI) AND Th(IV) HYDROLYSIS

Direct measurement of equilibrium acidity at elevated temperatures by emf methods has thus far been little used in the study of high-temperature aqueous chemistry. In a continuing program in the Reactor Chemistry Division, methods for such measurements, employing the glass electrode and the hydrogen electrode, are being developed and applied in systems related to homogeneous reactor and pressurized-water reactor chemistry. Because of the importance to the AEC of the aqueous chemistry of U(VI) and Th(IV), studies of their hydrolysis have been chosen as the initial investigations in this program.

During the past year a study at 94°C and 25°C of U(VI) hydrolysis by means of precise measurements with the glass electrode was completed. Currently, a study at 94°C of Th(IV) hydrolysis, employing both the glass electrode and the hydrogen electrode, is nearly complete.

The results show that while U(VI) hydrolysis proceeds by the same mechanism at 94°C as at 25°C (i.e., the formation of species in which the ratio of $UO_2^{2+}:OH^-$ = 1:1, 2:2, and 3:5), the overall extent of hydrolysis is greater at the higher temperature, with the 1:1 product showing relatively increased stability. A similar effect was found in the hydrolysis of Th(IV).

Since a principal objective of this program is to relate the occurrence of chemical species in high-temperature solutions to the chemical and thermodynamic behavior of these solutions, the present results will be used in an attempt to interpret and extend knowledge of the high-temperature solubility behavior of UO_3 and ThO_2, previously studied in this division.

GAS-SOLUBILITY STUDIES

The solubilities of hydrogen in water and deuterium in heavy water are of interest to many research problems in the AEC reactor, chemical processing, and production programs. Studies in the Reactor Chemistry Division provided determinations of high precision and internal consistency for these solubilities at ten-degree intervals from room temperature to 300°C. The data for hydrogen and light water permitted a resolution of conflicting results in the literature; those for deuterium and heavy water had not previously been available over much of this temperature range.

CHEMICAL APPLICATIONS OF NUCLEAR EXPLOSIONS

The recovery of isotopes produced in a contained thermonuclear explosion is a possible method of obtaining inventories of such isotopes. Chemical studies on the dilution of tritium produced by a detonation in salt, such as in the Gnome underground explosion, indicated that it will probably be mixed with environmental water as HTO because of both isotopic exchange and oxidation by sulfate impurities.

In research on means of obtaining prompt samples of detonation products or irradiated target material from the detonation chamber, sampling procedures are in the conceptual design stage. Six of the seven chambers of a sequenced sampler designed to take gas samples over seven preselected millisecond time intervals, installed in a 12-inch-diameter pipe in the Gnome experiment, operated successfully. However, the sampling pipe was plugged and broken by the explosion

before any significant amount of detonation products reached the sampler. The sampler was undamaged and uncontaminated and may be used in future Plowshare experiments.

In preliminary tests on the use of hypervelocity jets, irradiation target materials (uranium and uranium-coated copper cones) were successfully jetted with high explosives. The tests were made at Frankford Arsenal. The uranium jets traveled at speeds of 10 to 100 kilometers per second, indicating that the target could be jetted from the detonation chamber ahead of the destructive shock wave.

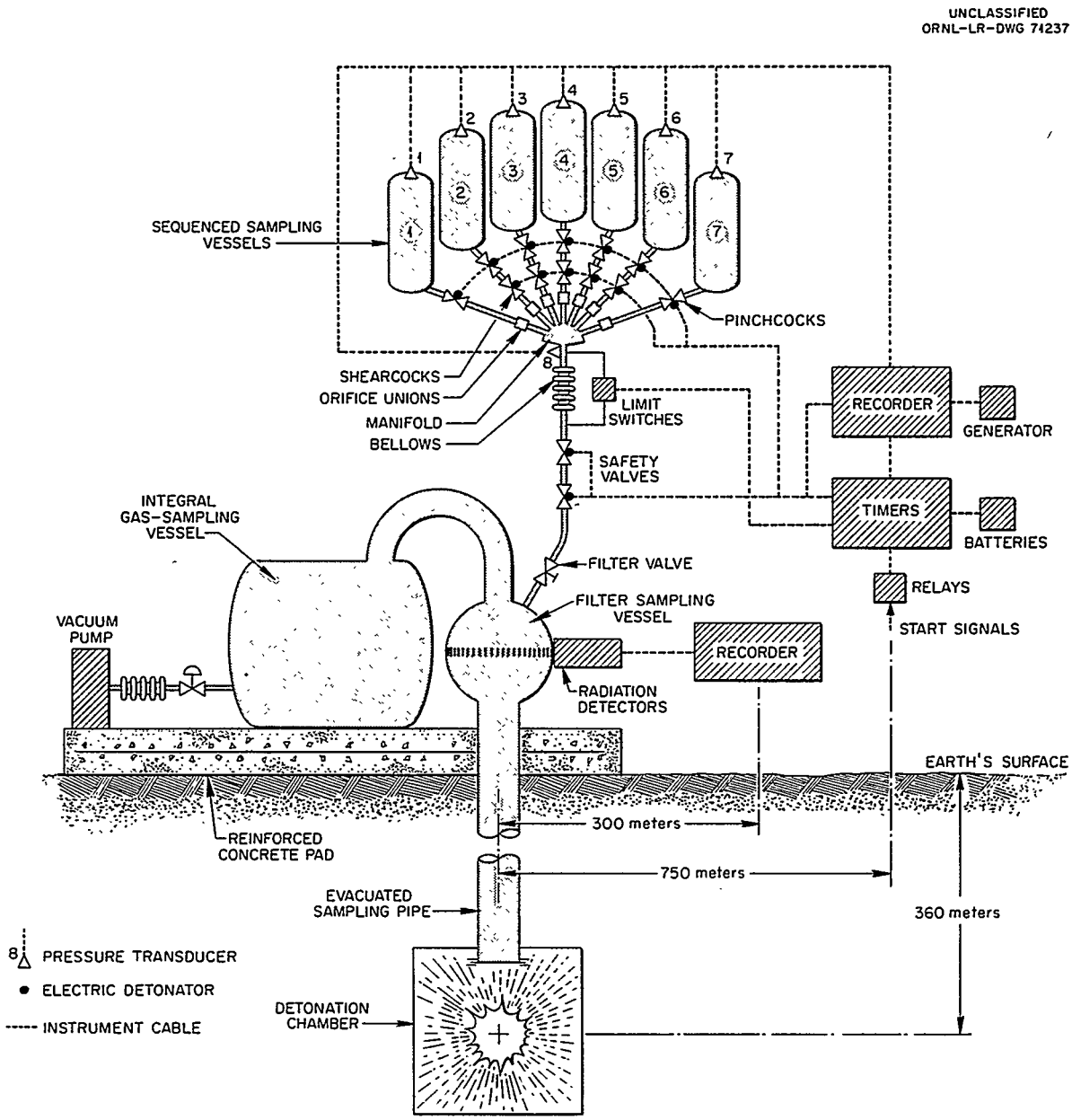

Sampling experiment in Project Gnome.

CHEMICAL PROCESSING OF TRANSURANIUM ELEMENTS

The Transuranium Processing Facility, TRU, is being built to produce, in conjunction with the High-Flux Isotope Reactor, gram quantities of the heavier transuranium elements for research uses. Development is continuing on chemical processes for isolating the transuranium elements and a method for making HFIR targets and process equipment. Corrosion studies were also made, and the conceptual design of the TRU facility was completed.

Separation Process Development

The solvent extraction systems to be used in decontaminating the actinides from fission products and separating them into specific fractions [(1) Am-Cm, (2) Bk, (3) Cf, Es, Fm] were studied in batch equipment and in countercurrent mixer-settler units.

In demonstration runs of the Tramex process (tertiary amine extraction process for separating actinides and lanthanides; see reports ORNL-3185 and -3244) with six extraction, six scrub, and six stripping stages, total americium losses were about 0.01%, and the decontamination factor from rare earths was more than 10^4. Ions extracted with the Am^{3+} were: Pd^{2+}, Fe^{3+}, Ti^{4+}, Ru^{4+}, TcO_4^-, Zr^{4+}, MoO_4^{2-} and Ni^{2+}, rare earths, Ru^{3+}, Y^{3+}, Ba^{2+}, and Sr^{2+} were not extracted.

The extracted contaminants except Ti^{4+} and Ni^{2+} remained in the organic phase when Am^{3+} was stripped with 5–10 *M* HCl. Ruthenium behavior is not completely predictable since it exists as both tri- and tetravalent ions in these solutions. Both actinide and lanthanide distribution coefficients increased rapidly with increasing nitrate contamination in the system. However, lanthanide extraction increased more rapidly, and the Am-Eu separation factor decreased from 100 at 0.01 *M* nitrate to 1 at about 0.7 *M* nitrate ion concentration.

In countercurrent demonstration runs of the phosphonate extraction process (see ORNL-3273; in press) for separating transcurium elements from americium and curium with four extraction, three scrub, and three stripping stages, total californium losses were about 0.1%, and the americium decontamination factor from californium was 1000. In runs made with europium as a substitute for berkelium, with eight extraction and eight scrub stages operating at about 50% efficiency, 99.9% of the europium was extracted, and the americium decontamination factor was 2000. The separation factor of 30 between berkelium and curium makes this an ideal system for separating the transcurium elements from americium and curium. However, separation factors for other adjacent actinides ranged from 1.3 to 3.3. Distribution coefficients were directly proportional to the cube of the phosphonate concentration and inversely proportional to the cube of the acidity over the range 0.5 to 4 *M* HCl. Extraction decreased to a minimum at 5.5 to 7 *M* HCl. Distribution coefficients were greater with aliphatic diluents than with aromatic diluents. The contaminant ions (Zr^{4+}, Ti^{3+}, Fe^{3+}, MoO_4^{2-}, and Pu^{4+}) were quantitatively extracted; Si^{2+}, Ru^{3+}, and Ni^{2+} remained with the americium and curium.

Berkelium can be separated from the heavier actinides (after oxidation in 8 *M* HNO_3 to Bk^{4+} with ozone or $KBrO_3$) by extraction with 30% di-2-ethylhexylphosphonic acid in decane or hexane diluent. Toluene, diethyl benzene, and Amsco 125-82 diluent reduced the berkelium back to unextractable Bk^{3+}. Americium was partially separated from curium by dissolving the hydroxides in 3 *M* K_2CO_3 and oxidizing the solution to form Am^{5+}; 80% of the americium but only 1% of the curium precipitated.

An anion exchange process (see ORNL-3291, to be issued) for recovery of americium, curium, and rare earths from plutonium process waste was developed and tested on a laboratory scale. With a feed containing 2.34 *M* $Al(NO_3)$, 1.5 grams of rare earths per liter, and tracer americium, the product contained 8.5 grams of rare earths per liter and was 0.05 *M* in aluminum. No americium losses were detectable, and decontamination from iron was essentially complete. Americium losses increased with increasing resin particle size, with decreasing resin cross linkage, and with increasing flow rates.

A chromatographic separation of californium, einsteinium, and fermium was demonstrated on

a small scale, but it was concluded that the procedure would be very difficult to operate on a large scale. When a column of Dowex 50-12X (200 to 400 mesh) resin loaded with 0.4 microgram of Cf^{252}, 0.26 nanogram of Es^{253}, and 0.3 picogram of Fm^{254} was eluted with 0.4 *M* ammonium α-hydroxyisobutyrate at pH 4.1, the first column cut contained 0.3% of the californium, 20% of the einsteinium, and 60% of the fermium. By the time 10% of the californium was eluted, 80% of the einsteinium and 90% of the fermium were also eluted. In a second test, a small amount of gassing disrupted the resin bed and gave poor separations.

Process Equipment Design and Development

Equipment was designed and is being constructed in cells 3 and 4 of Building 4507 to test the solvent extraction processes for transuranium element isolation at full activity levels.

A mixer-settler with improved impeller and interface weirs performed satisfactorily with the amine extraction flowsheet, and a stage height of 18 inches, with a capacity of 120 gal hr^{-1} ft^{-2} at 50°C, was obtained in a pulsed column with this same flowsheet.

A piping disconnect designed for remote operation was satisfactory, with less than 10^{-8} cubic centimeters of helium per second leakage after ten makes and breaks and after simulated mechanical damage or misalignment.

A pressurized-water fire-extinguishing system for glove-box fires was developed and demonstrated.

Conceptual design studies to determine the criteria to be followed in TRU equipment design were completed. Included were tentative irradiation and processing schedules and equipment flowsheets. Conceptual layouts of all TRU process equipment were completed, and detailed design of line penetration and disconnect wells was started.

HFIR Target Fabrication Process Development

The blending of actinide oxide and aluminum powder for pressing into pellets was successfully demonstrated, with small rods in the blending vessel to prevent agglomeration. Pellets having pressed densities 91% of theoretical were obtained at 33 tons per square inch. In tests of end-closure welds for HFIR target rods, direct-current fusion welding of a butt-joint design appeared to be a satisfactory method of producing the first closure with both types 1100 and X-8001 aluminum alloys. However, the problem of weld blowout in the second closure must be solved. Tubes were collapsed onto the pellets at an isostatic pressure of about 13,000 pounds per square inch but intimate contact between tube and pellets at all points was not obtained in these initial tests. Preliminary studies indicated that radiography could be used to inspect the end-closure welds. The remotely operable fabrication equipment for the TRU facility is being designed and some items are being fabricated or bought for future testing.

Transuranium Facility Design

Following several modifications to decrease the building size, complexity, and cost, the conceptual design and Title I engineering of the Transuranium Processing Facility on which final design will be based were completed. Title II engineering was started, and construction is scheduled to begin early in 1963. The facility has nine shielded cells for chemical processing and remote target fabrication. Rear access doors into the two analytical cells (8 and 9) provide for ease of operation and maintenance of equipment. Eight laboratories, four on each of two levels, will permit research and development support for the in-cell processing operations. The containment policy provides for four different ventilation systems at successively lower pressures: the building, which will be maintained continuously at −0.3 inch of water pressure; the cell bank at −1.0 inch; the cubicles within the cell bank at −1.3 inch; and the vessel off-gas system at −10 inch. In-cell operations and maintenance will be done with master-slave manipulators. Defective equipment will be removed without opening the cells to the atmosphere – by using a sealed, shielded caisson.

Corrosion Studies

In exploratory corrosion tests to select materials of construction for handling chloride solutions

in the TRU facility, six potential materials were selected: Hastelloys B and C, niobium, tantalum, titanium, and Zircaloy-2. Tests eliminated Hastelloy B and titanium and indicated possible hydrogen embrittlement with tantalum and niobium and severe corrosion of Hastelloy C in weld heat-effect zones. Heat-treated Hastelloy C appeared satisfactory for most components at low temperatures, but either tantalum or Zircaloy-2 must be used in some corrosive situations. The effect of alpha activity at the level of 2 watts per liter on corrosion of the above materials (see ORNL-3265) in chloride solutions was determined to be the same as that produced by H_2O_2 addition.

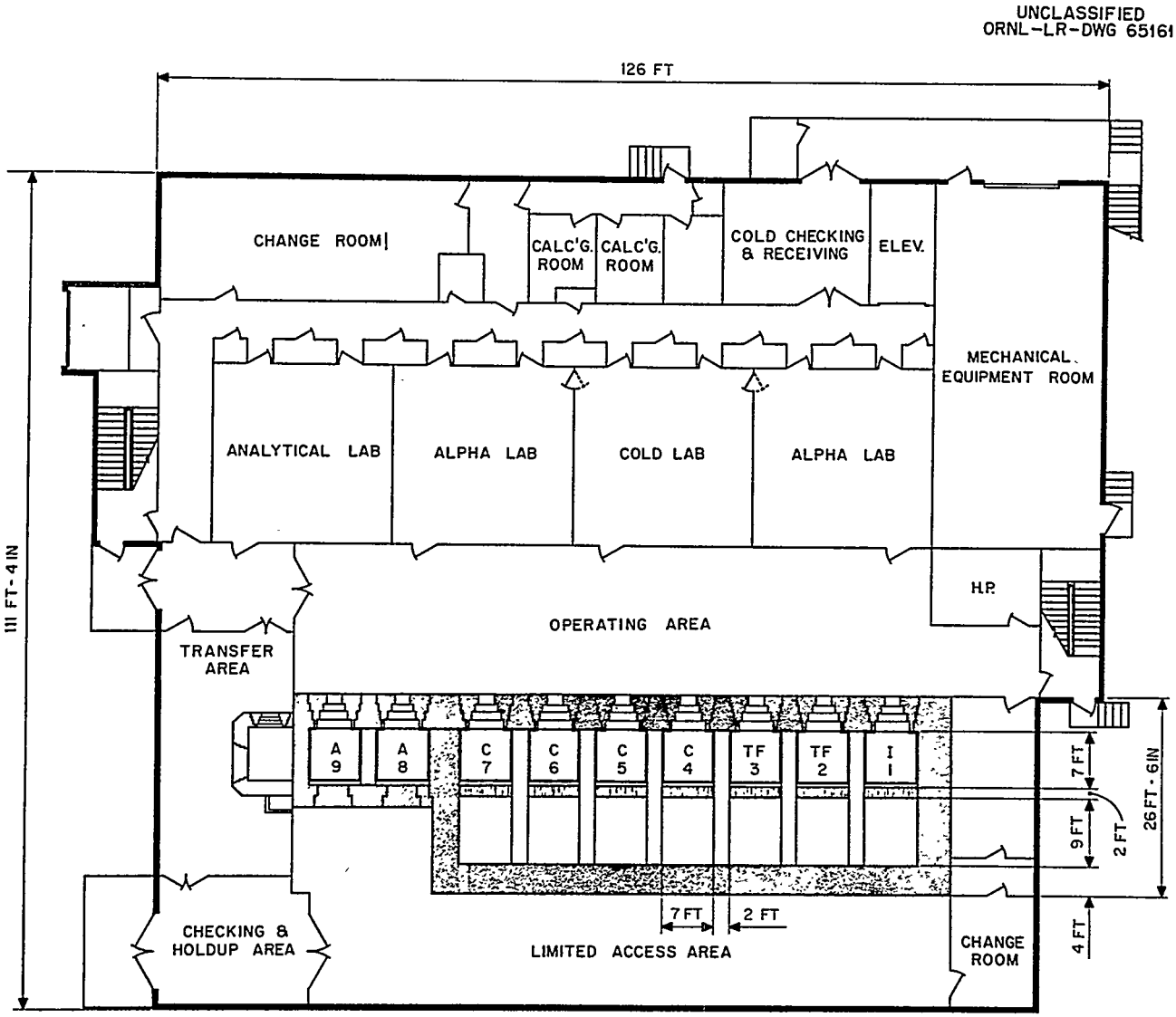

TRU facility – first-floor plan.

Metallurgy and Materials Research

INTRODUCTION

A broad program of research and development on materials for the present and future needs of nuclear energy is carried out by the Metals and Ceramics Division at the Oak Ridge National Laboratory. This Division comprises 131 technical personnel, including metallurgists, ceramists, chemists, physicists, and engineers, and 131 supporting personnel. During the past year, members of the Division published 40 research reports and 38 papers and presented 81 papers at national and international technical meetings.

SUPPORT FOR LABORATORY PROGRAMS

Procurement of Special Materials

Specifications and test procedures have been established by the Metals and Ceramics Division in order to enable the procurement of the ORNL-developed alloy INOR-8 of sufficiently high quality for the Molten-Salt Reactor Experiment.

Thermonuclear Research

A highly efficient getter-pumping technique was developed to help obtain the ultrahigh vacuum needed for thermonuclear experiments.

General Research Materials

Numerous problems concerning the selection and fabrication of materials arise in the ORNL shops that produce specialized equipment for the Laboratory's research programs. The Metals and Ceramics Division provides a full-time metallurgist to solve these problems. Noteworthy recent accomplishments include the development of materials fabrication methods for the circular trimming coils of the Oak Ridge Isochronous Cyclotron and for a parallel-plate fission chamber for the High Voltage Laboratory.

RESEARCH ON PROPERTIES OF MATERIALS

Crystal Research

Basic research on solid substances can be advanced considerably if single crystals, highly perfect and of controlled purity, are available. Crystals of beryllium oxide, thorium oxide, and ceric oxide have been successfully grown from molten lithium tungstate above 1000°C, and crystals of magnetite from lithium borate solution at 400°C under a pressure of 12,000 pounds per square inch. New high-temperature media and new techniques for growing crystals of many substances of importance in nuclear technology and research are under development. In particular, use of a newly developed plasma torch is being investigated for the growth of up-to-now unavailable single crystals of materials having melting points above 2500°C.

An electron-beam melting furnace, used for melting and purifying refractory metals, has been adapted to zone refining in order to obtain high-purity single crystals of these metals.

A useful way to manufacture reactor components such as fuel elements is through the consolidation of metal or ceramic powders by sintering at elevated temperatures. Experiments have recently shown that in the sintering of thorium oxide and other materials of similar crystal structure the transport of material is dominantly by plastic flow rather than by diffusion. In one demonstration of this, small crystals of calcium fluoride (isostructural with thorium oxide) were heated in contact with a large crystal. Chemical treatment of the surface revealed etch pits which develop where dislocations in the crystal intersect the surface. The very high density of dislocations at

Single crystals sectioned from niobium ingots zone melted in an electron-beam furnace.

the site of the small crystal is evidence for plastic flow. As further evidence for plastic flow, the rate of sintering of thorium oxide was found to increase with temperature too rapidly to be accounted for by diffusion.

Growing interest in detailed descriptions of radiation damage in a variety of materials has suggested the applications of x-ray diffraction techniques to this problem. Such techniques have been used in the Metals and Ceramics Division to evaluate the extent and character of damage in polycrystalline specimens of beryllium oxide that had been exposed to high (approximately 10^{21} neutrons per square centimeter) doses of reactor irradiation. Novel effects in diffraction patterns from the irradiated samples have been interpreted in terms of clusters of interstitial and vacancy defects, and information concerning the number and size of these clusters has been deduced. An x-ray diffraction study of the recovery of the damaged lattice during postirradiation annealing has also yielded significant insight into the dissolution of clustered defects and the possible generation of bubbles of helium gas.

Neutron-irradiated copper has been found to develop a different preferred orientation texture (alignment of crystalline grains) during subsequent fabrication operations than that developed by unirradiated copper.

Order-disorder reactions occur in many alloys of importance in nuclear technology. A clear understanding of processes that may occur and the reasons for their occurrence are desirable from both a fundamental and an applied point of view. A high-temperature x-ray diffraction study of such reactions in a 32 atomic percent gold-copper alloy

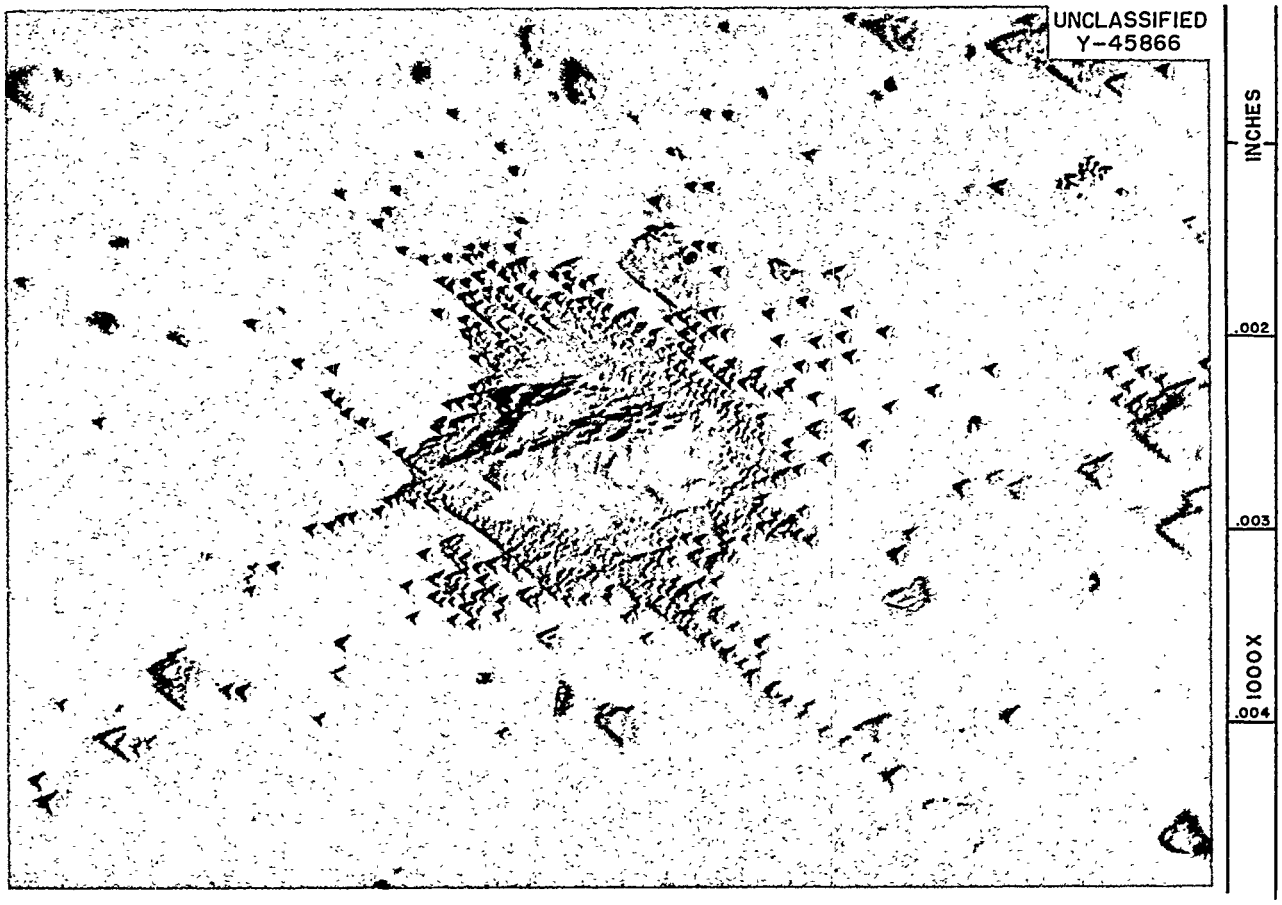

Cleaned surface of CaF_2 single crystal showing etch pits at point where smaller CaF_2 crystal had started to join surface. Heated 30 minutes at 1200°C. Sulfamic acid etch. 1000X.

has established the equilibrium nature of a new, antiphased structure. Transitions between the low-temperature ordered structure and the antiphased structure, and between the antiphased structure and the disordered structure, have been examined in detail. These results emphasize the importance of detailed descriptions of the atomic configurations in such studies.

Other x-ray diffraction studies at ORNL have been concerned with an analysis of the diffuse scattering from an alloy of copper with 15 atomic percent aluminum. An unexpected result was obtained which showed the aluminum atoms to be grouped in tetrahedral arrays, with each aluminum atom having only copper nearest neighbors. Such atomic groupings having an almost molecular character have not previously been observed in metallic systems.

Crystal physicists in the Metals and Ceramics Division have developed an improved lithium fluoride x-ray monochromator (device for isolating single wavelengths).

Research and Development on Pure Materials*

The purpose of the pure materials program is to produce research specimens (usually single crystals) of a composition, purity, perfection, or isotopic content that is not available commercially. The end products, which are required for basic solid-state researches, will be made available to other AEC laboratories as well as to ORNL.

*This section was contributed by the Reactor Chemistry Division.

Tests with pure crystals and with crystals containing known amounts of added impurities are important in determining the ultimate range of properties which can be made available in various solids. Single crystals are absolutely essential for the determination or utilization of characteristics which depend on crystallographic orientation. Primary emphasis is currently placed on the production of LiF crystals of selected isotopic ratios. During the last year, large (up to 260 grams) crystals of high-quality LiF (99.99% Li^7) were produced by the Stockbarger technique. These crystals were loaned to an AEC program at the Materials Science Center, Cornell University, for low-temperature thermal conductivity studies. The Cornell results showed the thermal conductivity of the ORNL crystals to be considerably higher than that of commercial LiF having the naturally occurring isotopic ratio. These crystals display no infrared absorption peaks for hydroxyl ion, which indicates that the important dehydration step of the purification process was successful. Smaller LiF crystals (typical size, $\frac{1}{10} \times \frac{1}{10} \times \frac{1}{2}$ millimeter) have been grown from the gaseous phase and found to be strain free by examination under polarized light, with highly perfect faces, all of the 100 type. These small crystals are now used as a standard for calibrating the shrinkage of x-ray film.

Solution growth of selected oxides from fluoride and oxide melts is being studied, with principal emphasis on MgO. The use of molten, nonaqueous, solvents allows significant crystal growth to occur at temperatures 1000 to 2000°C below the melting points of refractory oxides and thereby provides an impurity sink. Crystals of MgO, TiO_2, ZrO_2, and ThO_2, with maximum sizes, respectively, of $5 \times 2 \times 2$ millimeters, $5 \times 0.5 \times 0.5$, $1.5 \times 0.1 \times 0.1$, and $3 \times 1 \times 1$, have been grown from such melts.

Equilibrium in Ceramic Materials

Using their newly developed porous-collector technique, ORNL ceramists have obtained accurate and reproducible solid-liquid equilibrium information in the BeO-MgO-ZrO_2 ternary system and the associated binary systems at very high temperatures. The eutectic temperatures and compositions in the BeO-ZrO_2, BeO-MgO, and MgO-ZrO_2 systems are, respectively: 2045 ± 10°C, 59 ± 2 mole percent BeO; 1860 ± 10°C, 69 ± 2 mole percent BeO; 2080 ± 10°C, 65 ± 3 mole percent MgO. The eutectic plane in the ternary system occurs at 1720 ± 10°C.

When uranium dioxide containing added oxygen (UO_{2+x}) is heated in vacuum in the range 1200 to 1700°C, the approach to the formula UO_2 has been found to involve the volatilization of a uranium compound, probably UO_3.

Structure of Molten Media

Molten salts are a large class of liquids with many interesting and useful properties valuable in nuclear technology. Very little is yet understood of the structure of these materials. To determine molecular interactions in molten salts, the Metals and Ceramics Division developed high-temperature spectroscopic techniques and theoretical models to interpret the spectroscopic observations. These methods have been used to elucidate the nature of various molten-salt mixtures, including solutions of metals in salts, molten nitrates, and various molten mixtures containing transition-metal ions.

Measurement of Diffusion

Rates of diffusion have been determined for aluminum and manganese in aluminum, zirconium and niobium in zirconium, niobium in uranium dioxide, and thorium in thorium oxide, and measurements of diffusion of titanium in titanium have been started. Measurement of the self-diffusion of aluminum was possible for the first time because Al^{26} was obtained by use of the ORNL 86-Inch Cyclotron. The similar study of titanium is using Ti^{44} from the same source. This required a difficult separation from a scandium target. The self-diffusion of zirconium exhibited an unusual temperature dependence.

When diffusion takes place in polycrystalline materials, the simultaneous operation of two mechanisms sometimes leads to complicated results. A new method has been developed to analyze such results into grain-boundary diffusion in which atoms move along the surfaces between separate crystals or grains of the material and volume diffusion in which atoms move through the interior of the crystals. This method has been used to interpret the complex diffusion observed for thorium in thorium oxide and niobium in uranium dioxide.

Research on Mechanisms of Deformation

Metals suitable for service at very high temperatures are very strong and hence they are usually difficult to fabricate under ordinary metal-working conditions. Metallurgists at ORNL have shown that niobium and vanadium deform at room temperature by the formation of mechanical twins as well as by glide when these metals are sufficiently free of interstitial impurities. Among the impurities which prevent twinning at room temperature, carbon was found to be most effective, oxygen and nitrogen were moderately effective, and hydrogen least effective. These observations are being analyzed in terms of reactions between dislocations and impurity atoms.

Alloys of niobium with vanadium need not be as free of interstitial elements as either unalloyed element in order to undergo twinning at room temperature. Thus these alloys are fabricable at relatively low temperatures while retaining valuable high-temperature properties of the unalloyed metals. Twinning is ordinarily not observed in refractory metals except at very low temperatures.

By use of transmission electron microscopy ORNL metallographers have shown that the dislocations in severely cold-worked niobium are concentrated in arrays bounding areas free from such defects. Many of these arrays seem to be formed from short parallel segments of dislocations.

One quality which is responsible for the technical importance of metals is their ability to undergo large amounts of plastic deformation. During the deformation process, defects are formed on an atomic scale, and the material becomes

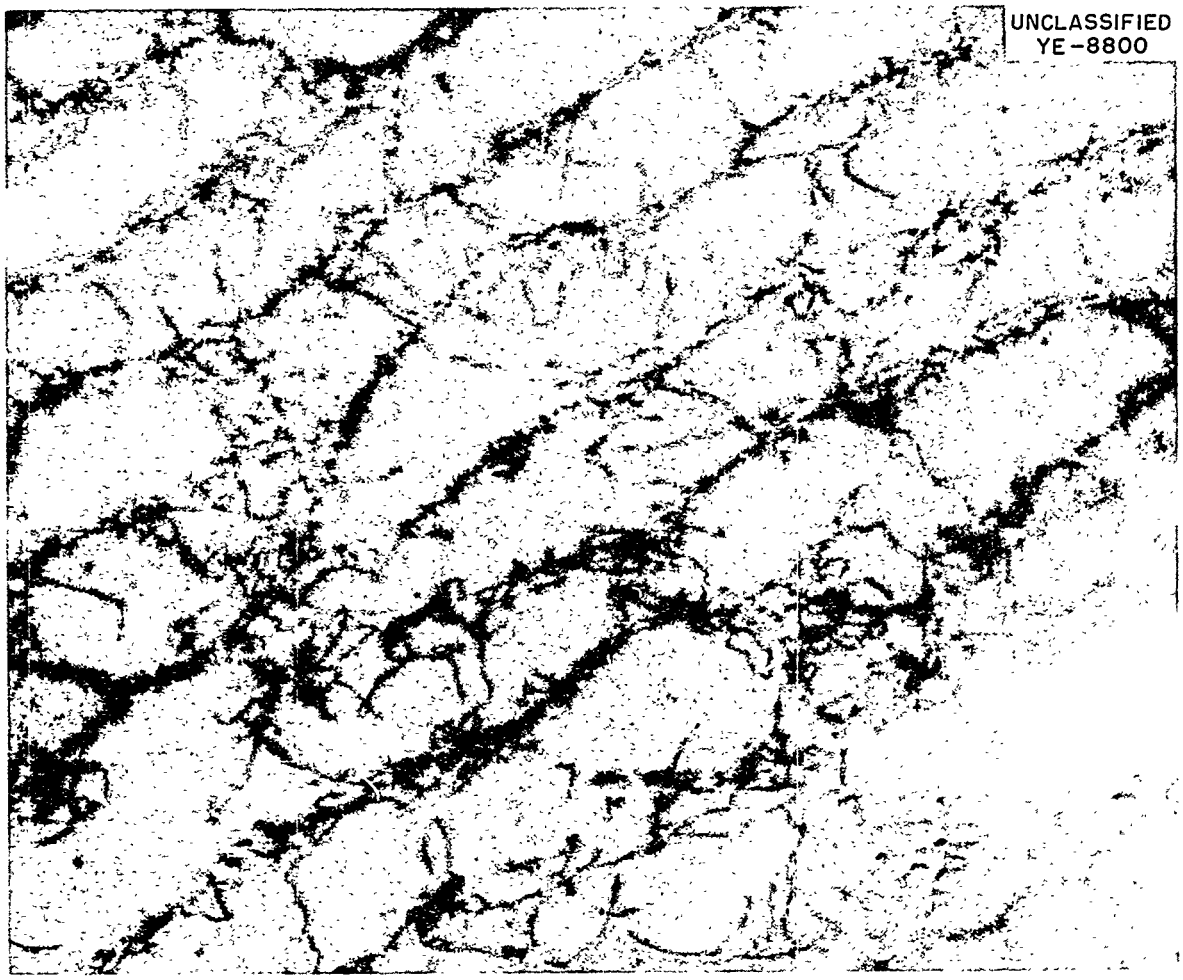

Transmission electron micrograph of cold-rolled niobium, showing cells formed by dislocation boundaries. 140,000X.

stronger and, in general, more brittle. Metallurgists at ORNL are studying the deformation processes by measuring the energy stored in metals during deformation. This energy will be related to the type and number of defects formed. A calorimeter has been built which measures the amount of mechanical work converted to heat during deformation. The energy stored is the difference between the mechanical work done and the heat liberated. Data on the effects of composition and temperature on the stored energy of two alloy systems show that alloying increases the amount of stored energy more than it does the strength.

Physics of the Early Transition Metals

Among the metals titanium, zirconium, hafnium, vanadium, niobium, tantalum, molybdenum, and tungsten are useful refractory metals, corrosion-resistant metals, metals with special nuclear applications, and useful superconductors. Metal scientists at ORNL are systematically studying the properties of these metals and their alloys to gain a better fundamental understanding of factors influencing metallic properties. The effects of concentration and metallic valence of several alloying metals on the physical properties of zirconium have given support to the broad theory of electron energy bands in metals, yet pointed up the need for refinement in some details of the theory. The Fermi surfaces of electrons in metals are being investigated by measurement of the low-temperature magnetoresistance (effect of magnetic field on electric conductivity); the first measurements revealed the nature of the conduction electrons in tungsten. The high magnetic field strengths needed for this study are obtained from a superconducting magnet.

Superconductivity Research

Superconductivity is a property of certain metals which are able at very low temperatures to carry electric currents with no resistance. Superconducting metals are characterized by interrelated critical temperatures, critical magnetic field strengths, and critical current densities, above which superconductivity is not possible. The

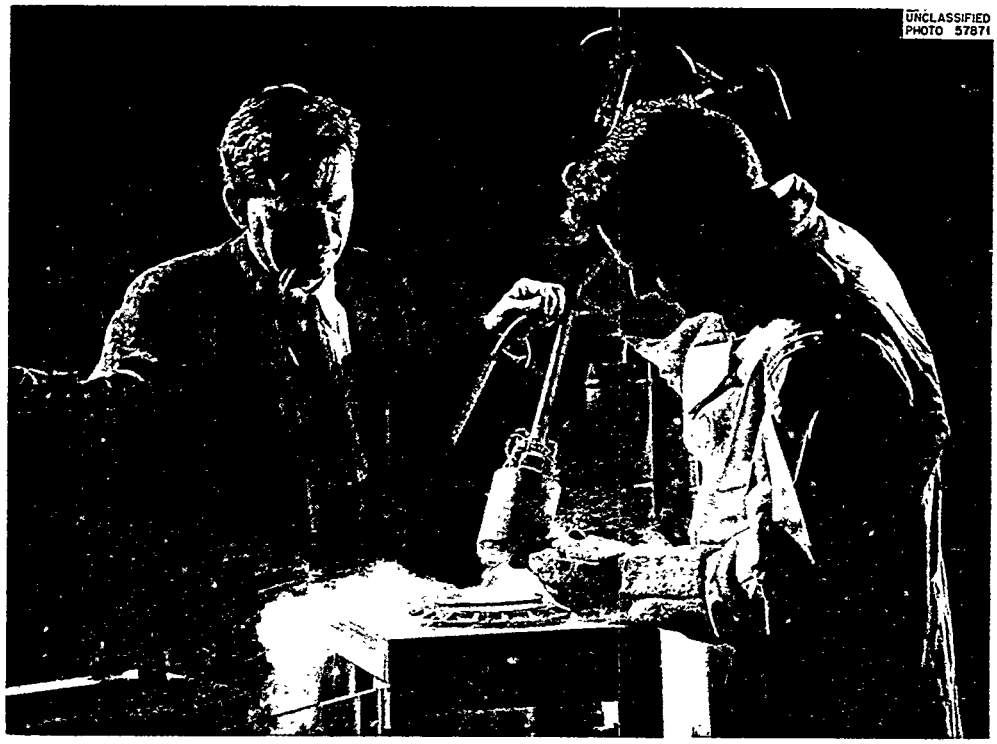

One of the first high-field superconducting magnets.

critical magnetic field strengths are especially high for certain alloys of niobium with tin and with zirconium.

Practical application of this property enables the construction and operation of magnets that produce high field strengths yet are small and require little power. One of the first superconducting magnets to use one of these alloys (Nb_3Sn) was built and used by ORNL metal scientists. This magnet attained a field strength of 25,000 gauss in April 1961. This pioneering effort is continuing to contribute to the usefulness and understanding of superconductivity. The critical current density of niobium-zirconium superconducting wire can be increased tenfold by heat treatments which depend on a small content of carbon or oxygen in the alloy. The critical current density of this same alloy was found to increase with decrease in wire size, showing that the current is carried principally on or near the surface of the wire. Superconducting magnets made with conventional electric insulation deteriorate with use; stable coils were found possible by the use of nonsuperconducting metals, such as Inconel, as insulation between the turns of the coil.

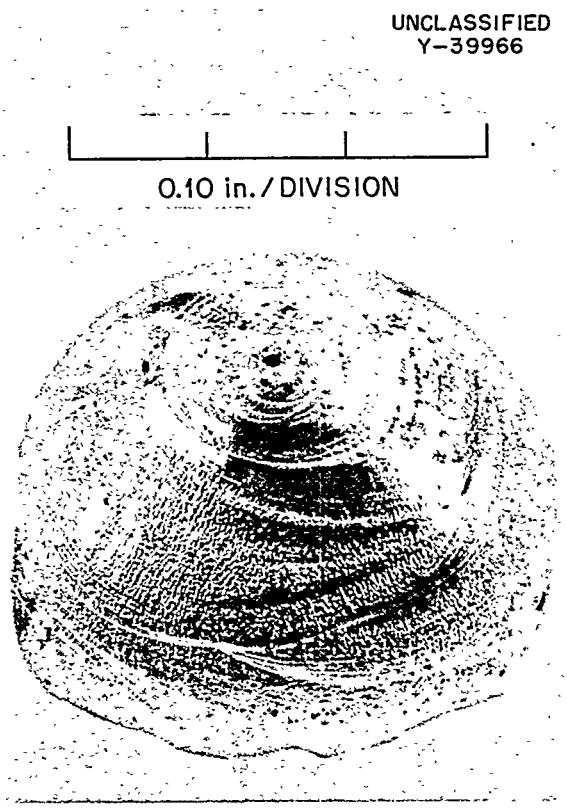

First gram-quantity ingot of technetium, a product of nuclear fission and not found in nature.

Important contributions have been made at ORNL to the metallurgy of the man-made element, technetium. This element does not occur in nature; it is obtained from the fission products produced in nuclear reactors. It is expected that some technetium alloys will be good superconductors. Technetium metal has been prepared in ingot form, methods for its fabrication have been developed, and studies are in progress on technetium-zirconium and technetium-molybdenum alloys.

FABRICATION RESEARCH AND DEVELOPMENT

Preparation of Ceramic Materials

As the operating temperatures sought for in nuclear reactors increase, the importance of ceramics as reactor materials increases. In the Metals and Ceramics Division, recent advances have been made in the fabrication of ceramic moderators, fuels, neutron absorbers, and other materials. These include beryllium oxide, beryllium oxide containing dispersed uranium oxide or thorium-uranium mixed oxide, uranium dioxide, thorium-uranium mixed oxide, thorium oxide, europium oxide, scandium oxide, and graphite containing dispersed pyrolytic-carbon-coated uranium carbide. For an irradiation study, 900 specimens of high-purity beryllium oxide, having controlled variations in density and grain size, were pressed and sintered to close tolerances (±0.002 inch).

While uranium carbide is a promising high-temperature reactor fuel, its fabrication from powder requires sintering at temperatures so high (1800 to 2000°C) that some uranium evaporates during formation of the compacts. Powder metallurgists at ORNL have succeeded in lowering the sintering temperature to 1300°C by mixing the intermetallic compound UAl_2 with the carbide before sintering. The aluminum escapes as vapor during the process, leaving a pure uranium carbide.

An important approach to the cutting of nuclear fuel cycle costs is the integration of remote fuel refabrication with chemical fuel-recovery processes,

so that the latter need not decontaminate recovered fuel to the high degree now required. The vibratory compaction method has been demonstrated feasible by ORNL ceramics engineers for the remote manufacture of thorium-uranium oxide fuel rods using thorium oxide powder made by the Chemical Technology Division's sol-gel process. A remotely operated pilot plant, now under construction, will manufacture 1000 fuel rods for a Brookhaven reactor.

Welding and Brazing Research

Nuclear systems often require newly developed materials, unusually sound connections, and intricate assemblies. Welding engineers at ORNL, therefore, maintain unceasing development of new welding and brazing techniques. Recent advances include methods for joining the new high-temperature metal niobium, alloys for brazing beryllium, methods for brazing graphite to graphite and to metals, methods for brazing ceramics to metals, and remote methods for use in maintenance of the Molten-Salt Reactor Experiment (MSRE). Austenitic stainless steels have been successfully welded to ferritic steels. Among the problems solved by ORNL welding engineers are penetrations in the thick pressure vessels of reactors with relatively thin-walled tubing for instrumentation. The accompanying photograph shows penetrations developed for the system for detecting defective fuel elements in the Experimental Gas-Cooled Reactor (EGCR).

Fuel Elements for the High-Flux Isotope Reactor

The fuel core of the High-Flux Isotope Reactor consists of 540 involute-shaped plates combined in only two fuel elements, sized to fit concentric with each other to form a 5.0-inch-ID × 17.0-inch-OD fuel annulus. (See the photograph, which shows the two unfueled fuel elements produced for the HFIR Flow Test Program.)

The plates are carefully assembled into the grooves of an inner tubular side piece, using Teflon strips to maintain spacing dimensions. All plates, except the last few, are mechanically joined to the side plate by peening. The last few are plug welded at 1-inch intervals along the length of the element. The plates are fastened at the periphery of the element by circumferential welds, again at 1-inch intervals along the length of the element. After carefully machining the outside diameter, an aluminum tube is shrunk-fit onto the assembly.

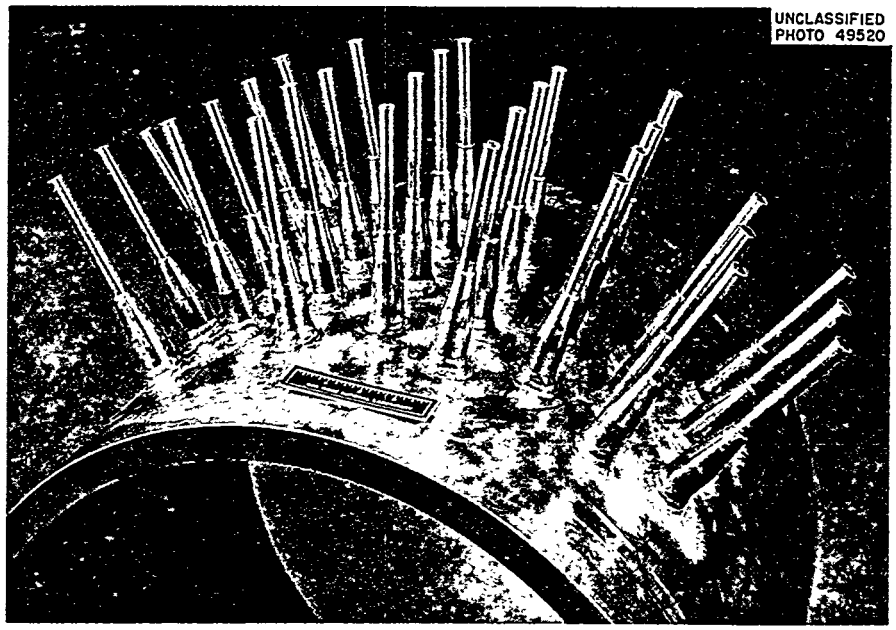

Quadrant of mockup of EGCR burst-slug-detection nozzle assembly.

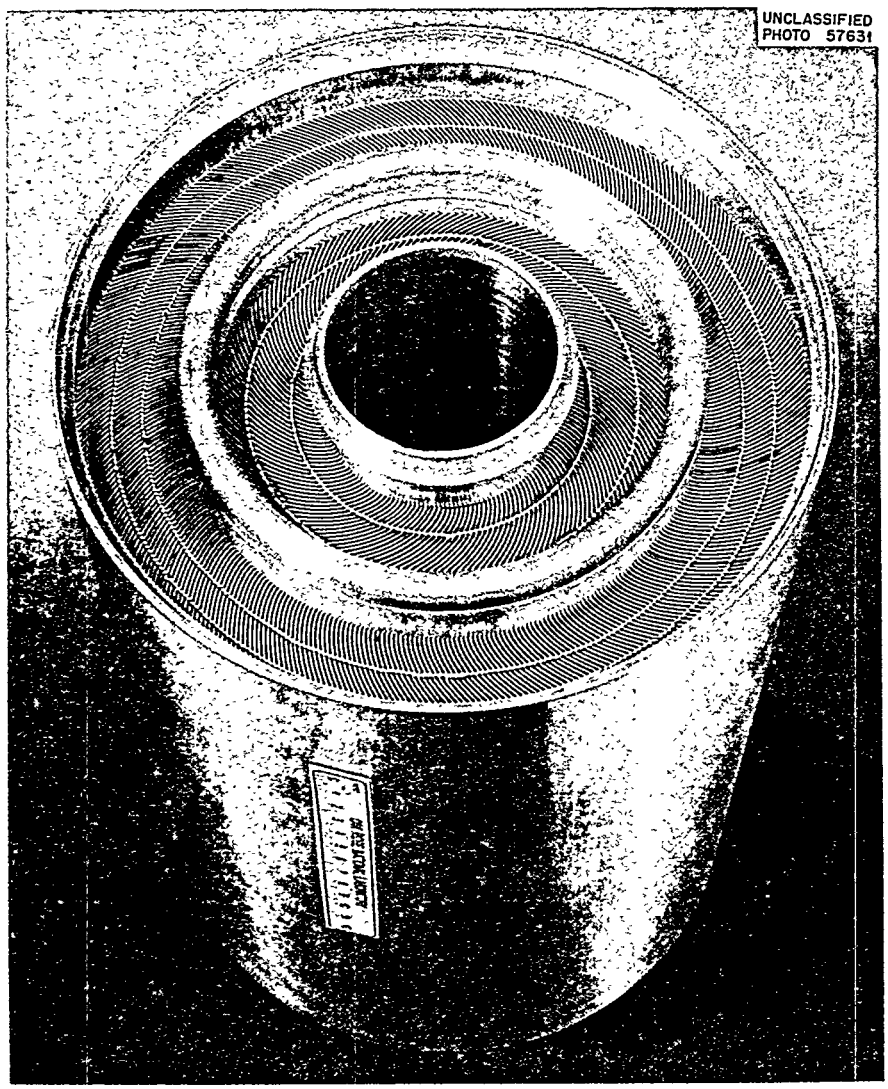

Core of the High-Flux Isotope Reactor.

This compact fuel core contains 9 kilograms of U^{235} and will operate at 100 megawatts for 15 days, with an unperturbed thermal-neutron flux of 5×10^{15} in the central trap region. The maximum power density is 4500 kilowatts per liter and requires a maximum heat-transfer rate from the fuel plate surfaces of 2.1×10^{6} Btu ft^{-2} hr^{-1}. The heat will be removed by water, which flows through the 0.050-inch coolant channel at 40 feet per second.

The fuel component has many features that pose challenging fabrication problems. The fuel contains a dispersion of U_3O_8 in aluminum, made by using powder metallurgy practices, and is contoured to flatten the power distribution in the radial direction. The contour must be held to very exact dimensions in order to control the fuel density to ±30% in areas as small as $\frac{5}{64}$ inch in diameter. This tolerance must be combined with an additional specification that nonbonds in the plate greater than $\frac{1}{16}$ inch in diameter are unacceptable. In addition, the burnable poisons, boron and cadmium, must be accurately and homogeneously incorporated in the inner-annulus plate in order to minimize reactivity variations during lifetime of the core.

Because of the requirement that the 0.050-inch spacing between plates be controlled to ±0.006 inch, the radii of the involute during forming of the plates must be controlled to ±0.002 inch. Deviations larger than this are out-of-specification.

Previous work demonstrated significant problems in these difficult areas. Many unbonded regions, for example, appeared while bonding the type 6061 aluminum cladding to the fuel section by hot rolling. The majority of these nonbonds had a blistered appearance. In studying this problem, it was found that an intolerable concentration of gas existed in the aluminum. Vacuum degassing alleviated this condition. Bonding of type 6061 to 6061 aluminum, more difficult to accomplish than bonding type 1100 to type 1100, was eliminated by first cladding the type 6061 with type 1100 and designing the plate fabrication so that the type 1100, and not the type 6061, aluminum surfaces were the mating surfaces being hot roll bonded. As a result of these two innovations the yield of blister-free plates increased from 50% to 85% for outer annulus plates and from 5% to 95% for the inner annulus plates.

Low-pressure marforming was shown to be a satisfactory method for forming unfueled plates to within the required tolerances. However, when composite fuel plates were formed under these conditions, a yield of only 26% was realized. This yield was more than doubled by controlling thickness deviations in the fabricated plate to less than 0.0004 inch. Although not completely solved, the problem is not insurmountable. It is fully anticipated that significantly higher yields can be realized by improved control of the variables associated with plate fabrication and forming techniques.

Another difficult area of development which has shown promise of resolution is the control and detection of inhomogeneities of fuel in small local areas. Destructive tests indicate that, in the majority of cases examined, local inhomogeneities can be controlled to within ±30%. Values which did not meet this specification appeared to be related to variations in the fuel section dimensions and not to segregation of the fuel per se. Considerable progress was made in detecting segregated regions nondestructively. X-ray-attenuation methods combined with gamma scintillation counting were selected, and equipment was designed and built. Examination of more than 50 fuel plates showed the selection of methods to be reasonable. Further improvements will be made in order to increase the scanning speed and develop the process for the examination of fuel plates on a production basis.

Additional development aimed at refinements will be conducted through FY 1963. However, the results during the current fiscal year have been sufficiently encouraging to initiate the procurement of fuel elements, with delivery of the first three anticipated by July 1963.

Target elements for the HFIR will be aluminum-clad dispersions in aluminum of Pu^{242} and of americium and curium. The background radiation of the target materials is so great that fabrication will have to be performed remotely in hot cells. Techniques and equipment have been devised with this in mind, and remote fabrication equipment is now being procured.

Metallurgists at ORNL are also contributing to fuel element development for the Advanced Test Reactor, the Enrico Fermi Fast Breeder, the Maritime Reactor Program, and the Army Reactor Program.

Damage by radiation limits the life of boron-containing control rods currently used in Army power reactors, and the rods are replaced at every refueling. Two successful approaches to long-lived control rods have been devised by ORNL metallurgists. Dispersions of europium oxide (which strongly absorbs neutrons) in stainless steel are remarkably resistant to radiation, and the lifetime of boron absorbers may be prolonged by varying the boron concentration along the absorber plate. Since most of the burnup of the absorber occurs in the first 6½ inches of the control rod, duplex absorbers having europium in the tips and the cheaper boron in graduated concentration in the rest of the rod have been fabricated for testing in the SM-1 reactor.

EVALUATION OF PROPERTIES OF MATERIALS

Evaluation Under Complex Conditions

The proper selection of current materials and the development of new materials to meet the demanding requirements in nuclear technology require knowledge and understanding of the mechanical properties of metals. While the Metals and Ceramics Division does extensive testing by conventional methods of numerous materials of importance in the Laboratory program, these

methods cannot accurately represent the complex conditions of actual service. This deficiency is being resolved by two approaches – by devising tests which duplicate the complex stress and thermal conditions in reactors and by developing models to enable evaluation of the resistance of materials to complex stresses from the results of simple tests.

Common methods of testing the durability of materials fall far short of duplicating the complex conditions in nuclear reactors, particularly the sharp temperature gradients. For two years, ORNL metallurgists have been evaluating gas-cooled reactor fuel elements in a highly instrumented test rig that closely duplicates service conditions. The annular fuel element separates a central heating rod and an outer cold wall. Gaps between fuel pellets and cracks developing in the pellets during testing are clearly evident in the photograph that shows a fuel element being tested. Current use of the rig is in the evaluation of fuel elements clad with finned beryllium tubing and with thin-walled stainless steel. Similar rigs are being built in England and France.

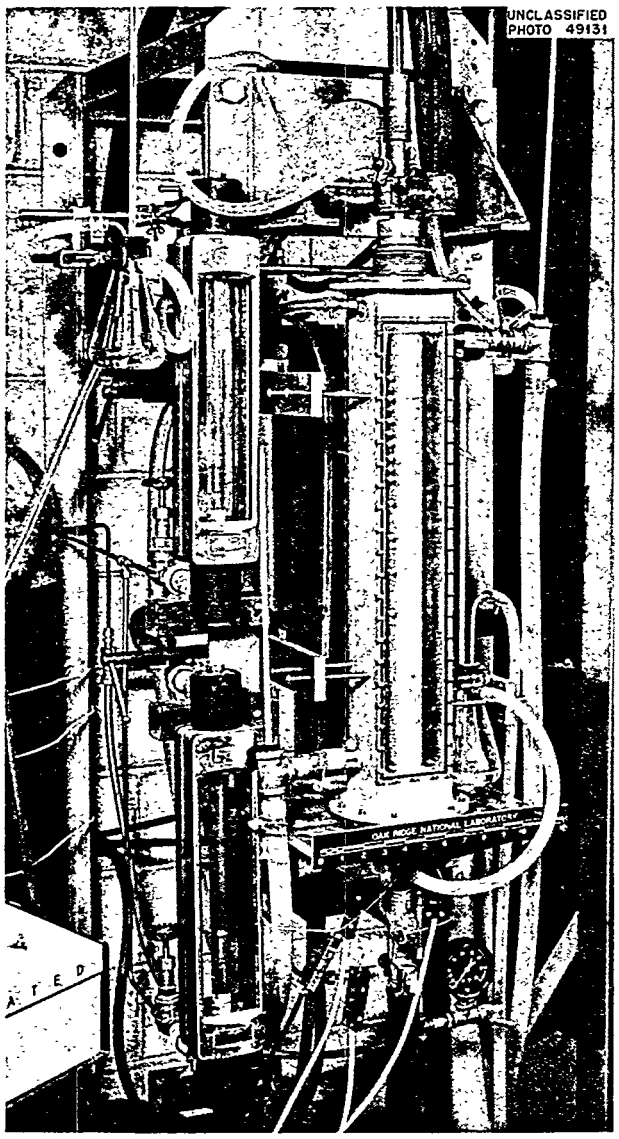

Experimental apparatus to simulate reactor fuel service conditions in gas-cooled reactors.

The service life of metals in stressed conditions at elevated temperatures is generally evaluated by "creep" testing, in which the deformation and eventual failure are measured at the desired service temperature under a constant load. In actual service, a metal is subjected to a variety of stresses, so there is a need to know the stress dependence of the lifetime. Metal technologists at ORNL have developed a test method in which the lifetime of a specimen is measured while the specimen is subjected to a load that increases at a constant rate. An analytical model has also been developed to treat the data from this test in order to obtain the effect of load on lifetime with far less testing than is required by the use of conventional creep testing. This analysis has been applied successfully to two types of stainless steel.

Creep testing and stress-rupture testing give the lifetimes of materials subjected to simple stress in one direction. Often the actual service conditions involve complex stresses. For example, tubing may be in compression or tension in the axial direction and at the same time tangentially stressed due to the pressure of contained fluid. ORNL metallurgists have successfully applied to Zircaloy-2 a method for analyzing creep under complex stresses in anisotropic materials (materials having different properties in different directions). This is an extension of their method developed previously for isotropic substances.

Hot-Hardness Testing

Measurement of the hardness of metals at high temperatures has been developed into a useful technique for evaluating metals under the actual conditions of heat treatment and high-temperature service. The conventional method, testing of

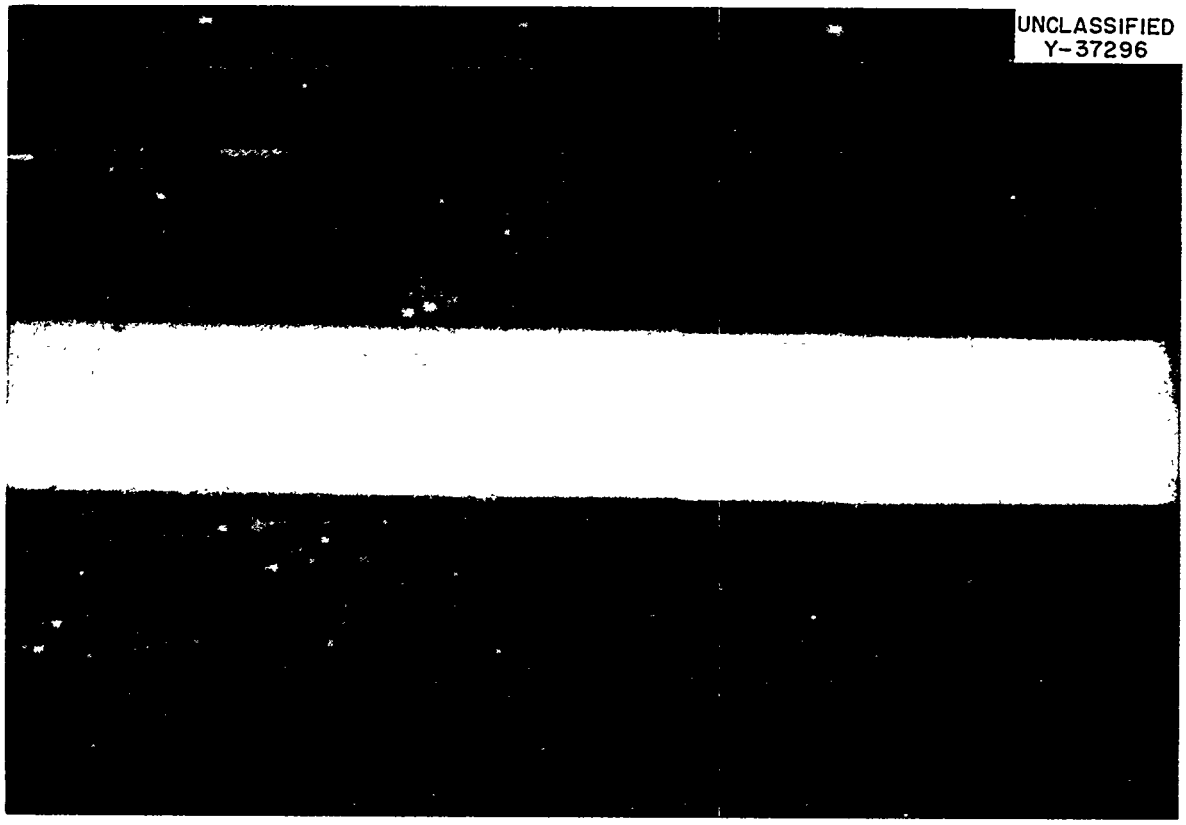

Fuel element being tested in thermal gradient, showing gaps between fuel pellets and radial cracks in the pellets.

a series of alloys after quenching to room temperature, often gives the incorrect indication of properties at service temperature.

Test for Uranium-Alloy Allotropy

The dimensional stability of uranium metal under irradiation may be improved by alloying with molybdenum, which stabilizes a high-temperature allotropic modification. A novel test has been devised for the determination of the stability of this modification, based on the fact that only the low-temperature form reacts with hydrogen. On the basis of this test and creep measurements, the alloy with 15% molybdenum has been recommended as the most serviceable alloy of a series tested for a particular reactor application.

Nondestructive-Test Development

Many of the inspection test methods currently used for quality control are not adequate for the nuclear industry. The service conditions associated with nuclear reactors have necessitated the establishment of more rigid acceptance standards on dimensional tolerance and permissible flaws. In addition, many new materials are being used which require the development of new inspection techniques. Efforts in the Metals and Ceramics Division have been directed toward the adaptation and improvement of existing techniques and the study of physical phenomena which offer promise for nondestructive testing.

A low-voltage radiographic technique has been perfected which will give useful radiographs on very thin sections of aluminum, steel, beryllium, and a variety of nonmetallic materials. The sensitivity of the technique is illustrated by the accompanying radiograph of roses, which shows details of the veins and the contrast between different numbers of petals. The microradiograph of UC_2 particles shows its application to the measurement of core and coating dimensions and to the detection of flaws in uranium carbide fuel particles coated with pyrolytic carbon.

Low-voltage radiograph of two American Beauty roses, showing contrast obtainable with new technique for examining low-density materials.

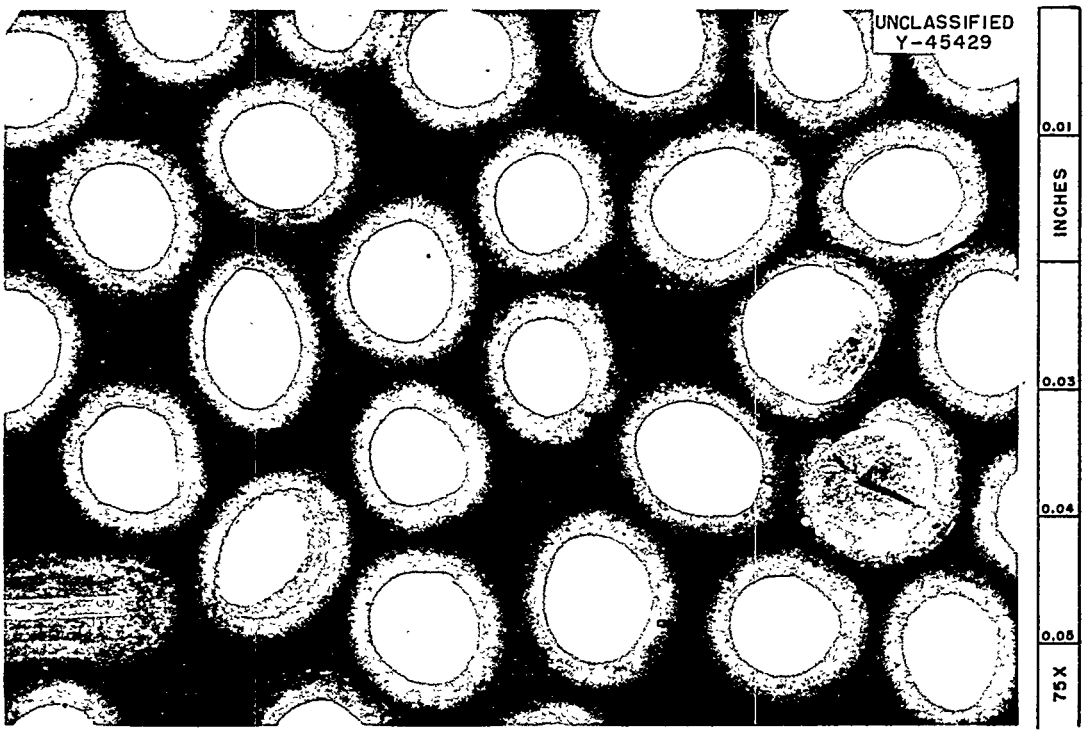

Microradiograph of UC_2 particles coated with pyrolytic carbon, showing possibility of measurement of dimensions and detection of flaws. Reduced 14.5%.

UNCLASSIFIED
PHOTO 50432

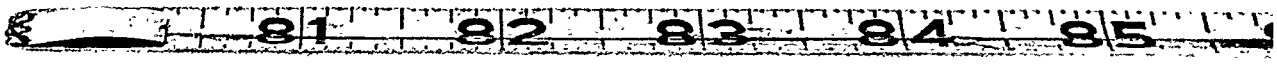

Probe containing eddy-current test coil for measuring small spacings between metal parts, such as coolant-channel spaces in a reactor fuel element.

An established technique for detecting flaws in metal components uses eddy currents which are induced into the metal by a small coil driven by an alternating-current electrical signal. It was shown at the Laboratory that this principle could be used as a basis for measuring the spacing between adjacent metal parts, such as fuel plates in a reactor fuel element, to a high degree of accuracy. The small size of some spacings, such as in the HFIR fuel element, necessitated probes which fit within a space of $\frac{1}{32}$ inch.

One type of defect which is difficult to detect is the lack of bonding between two pieces of metal (such as the cladding and core of a fuel element). Two techniques for the detection of such flaws were developed at ORNL which involve vibration of the specimen by ultrasonic waves. An improved, remotely operated ultrasonic test was devised for measuring the thicknesses of vessels in high radiation fields and was used on the core tank of the HRT.

Postirradiation Examination

A necessary aspect of the study of materials for nuclear energy is the examination and testing of the highly radioactive materials which have been exposed in nuclear reactors. Among the remotely operated devices being developed or recently developed by the Postirradiation Examination Group of the Metals and Ceramics Division are a micrometer, a hardness tester, an apparatus for the ultrasonic cleaning of specimens, a machine for canning specimens after inspection, an x-ray diffraction apparatus, and a complete set of equipment for the preparation and microscopic examination of metal specimens. A novel room-temperature technique for making replicas of radioactive specimens enables unshielded microscopic observations of the surface features of irradiated materials. For example, replicas made of a patch in the HRT core tank are shown in the accompanying photograph. Other irradiated ma-

UNCLASSIFIED
PIE-3043

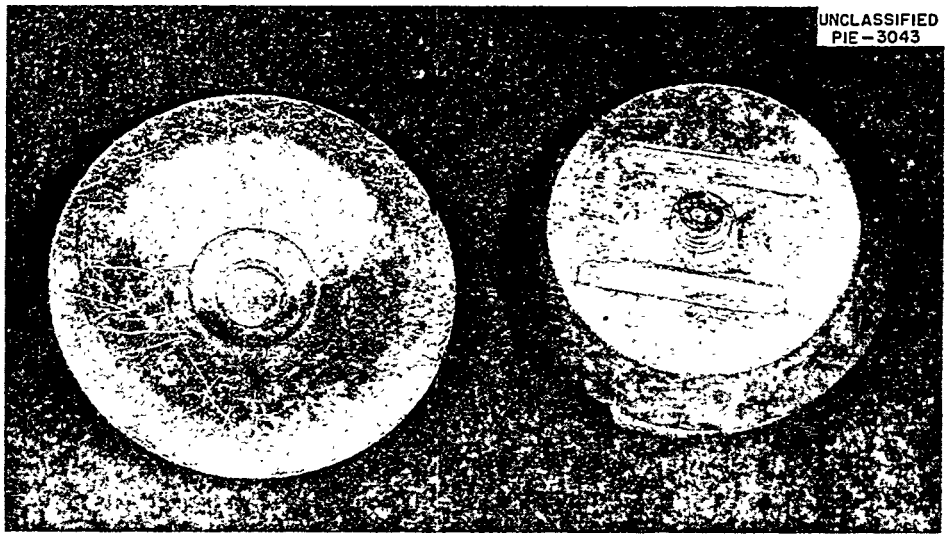

Positive replicas of HRE-2 upper core patch.

terials which have been recently examined include autoclaves from in-pile tests of slurry fuels, beryllium tubing that had burst in in-pile stress-rupture tests, and molten-salt reactor fuel.

Stability of Reactor Fuels

Reactor fuel elements are generally replaced after a very small fraction of the fissionable fuel is consumed, principally because the distortion of the element by radiation threatens to impair reactor operation. Metallurgists at ORNL have radiation tested high-concentration aluminum-base dispersion fuels to high burnup. A full-size reactor element fueled with 63% U_3O_8 (20% enriched in U^{235}) dispersed in aluminum was still in excellent condition after fission of 41% of the U^{235} and up to 57% in some plates. Specimens of the same fuel have been irradiated to 77% burnup with no appreciable dimensional change. At these high burnups, reaction between the uranium oxide and the aluminum matrix is observed, but this does not diminish the usefulness of the fuel.

Nuclear fuels are generally clad to prevent escape of fuel or fission products into the coolant stream, where excessive radiation would prevent maintenance of the reactor system. The operating conditions of the reactor are generally limited by the properties of the fuel cladding. A proposal to achieve higher reactor temperatures is the Pebble-Bed Reactor fueled with a bed of graphite spheres containing dispersed, coated uranium carbide particles. Metal scientists at ORNL, using neutron activation to measure the escape of fission products through pyrolytic carbon coatings on fuel particles, have discovered that under some conditions uranium migrates through the coating. This migration intensifies the problem of preventing excessive fission-product activity from entering the reactor coolant stream and limits the operating temperature of a reactor using coated-particle fuels at their present stage of development.

COMPATIBILITY OF MATERIALS AND ENVIRONMENT

It is well-known that metals and other materials interact to a certain extent with their environments. Therefore, the development and selection of materials require an evaluation of corrosion and other environmental effects. Consequently, a major part of the Metals and Ceramics Division program is the investigation of these processes, ranging from fundamental studies of reactions on metal surfaces to the determination of useful life expectancies under actual or simulated service conditions.

Metal-Surface Studies

Research on metal surfaces has as its objective a better understanding of the factors which determine the degree of corrosion resistance imparted to metals by oxide films formed on them. Chemists in the Metals and Ceramics Division have found that one important factor is the strain which develops in the oxide films as they grow and which can result in the mechanical destruction of the oxide films, with a resulting complete loss of oxidation resistance. During the past year, emphasis was placed on determining the origins of such strains. The initial stages of oxidation of tantalum were shown to involve the solution of oxygen, followed by the precipitation of an oxide phase in a manner describable in terms of a martensitic phase transformation. The stresses generated during this process actually exceed the yield strength of the metal.

The mechanism of the sulfidation of tantalum is analogous to that for oxidation and is also being investigated in a further effort to clarify the details of the oxidation process. Optical methods are being used to study the strains in films formed during oxidation of single crystals of copper.

Liquid Alkali Metal Systems

Liquid alkali metals are excellent coolants, particularly for high-temperature reactors. Their corrosive nature is partly due to the solubility of structural metals in them and partly due to the reaction of structural metals with impurities in the alkali liquid metals. The principal deleterious impurity is oxygen, which is difficult to remove from these very reactive metals. Gettering of oxygen with active metals such as titanium and zirconium has been found by ORNL corrosion scientists to be superior to conventional oxygen-removal methods. Although vanadium, zirconium, niobium, and tantalum have excellent resistance

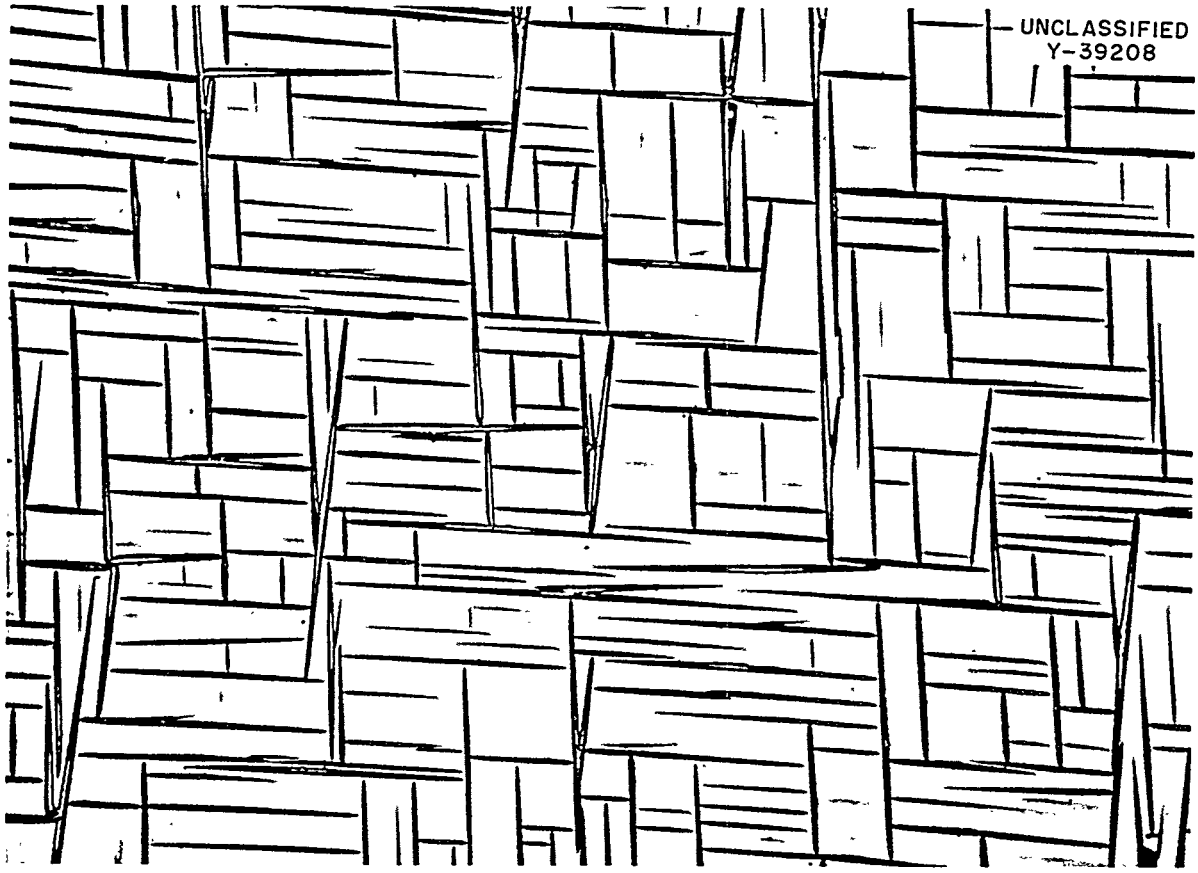

Oxide platelets formed on a tantalum single crystal, magnified 500 times. The precipitation of the oxide in such platelets was found to be an important step in the early stage of oxidation of tantalum.

to molten lithium, the latter two structural metals have been found to be severely penetrated by lithium when they are contaminated by oxygen; such contamination is often encountered in welds. Nitrogen and carbon in the metals have no such effect.

In present reactor use, alkali metal coolants transfer heat from the reactor to a secondary coolant, such as boiling water, which drives the power-producing turbine. For generating power in space vehicles, direct-cycle alkali metal systems appear attractive, in which the alkali vapor, generated by use of the reactor heat, drives the turbine. To define and solve the many new problems of corrosion and materials compatibility introduced by boiling alkali metals in reactor systems, ORNL metallurgists have designed and operated for thousands of hours experimental rigs containing these boiling metals. The accompanying photograph shows a forced-circulation loop operated with boiling potassium.

Corrosion in Molten Fluoride Reactor Systems

Molten fluoride salt mixtures have good properties for use as fluid reactor fuels and as a reactor-fuel reprocessing medium. In the past, extensive corrosion testing showed that the ORNL-developed alloy, INOR-8, is superior for service with these high-temperature liquids. Corrosion testing is continuing with studies of the effects of oxidizing impurities in the salts. Tensile specimens of INOR-8 were not appreciably affected by exposure at 500 to 705°C to the gaseous decomposition products of ammonium bifluoride, a gas mixture used to remove oxygen from the graphite moderator of molten-salt reactors. A room-temperature mercury-penetration test has been found to give a satisfactory measure of the penetration of graphite by molten-salt reactor fuel. To reverse the reactions of molten-salt fuels with graphite, carbon tetrafluoride must be present in the atmosphere of a molten-salt reactor. Graphite, INOR-8, and

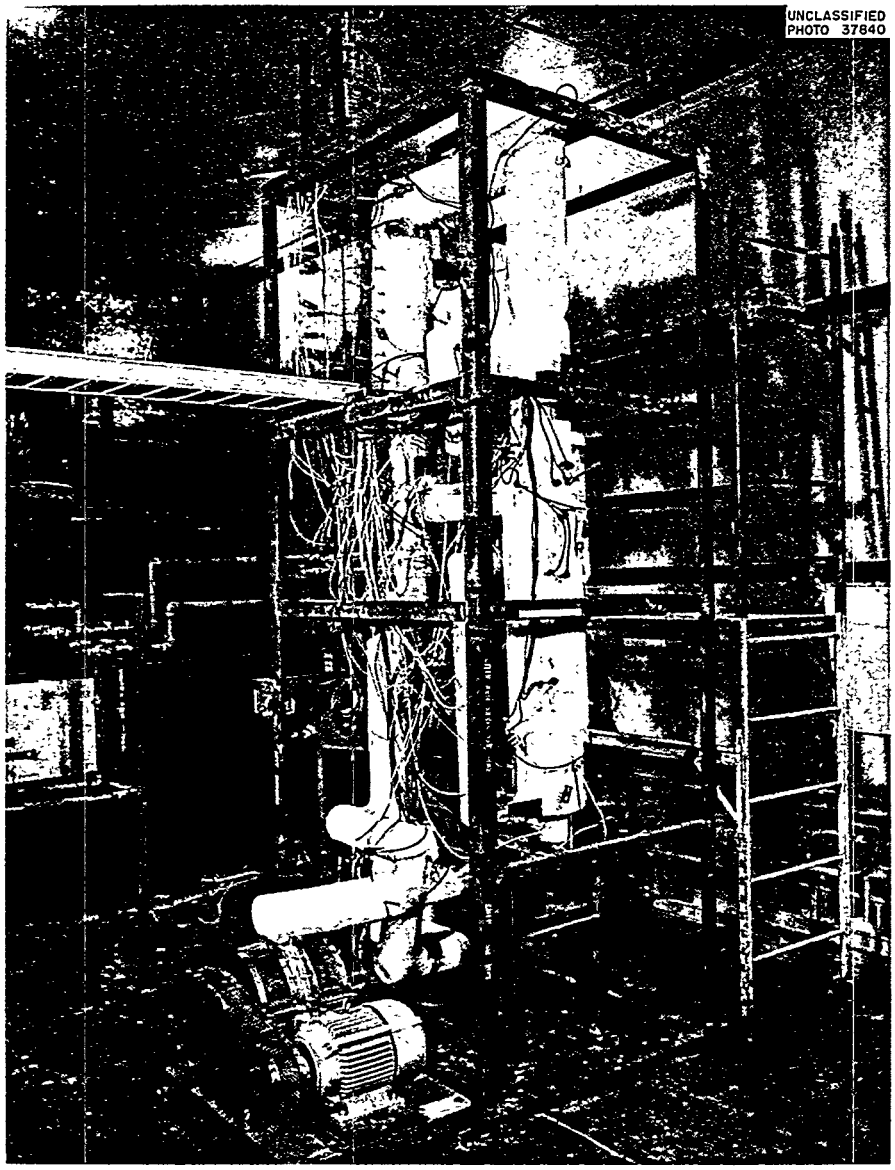

Boiling-potassium corrosion test loop.

nickel resist this gas, but stainless steel, molybdenum, and Inconel are severely attacked by it.

Compatibility of Materials with Gaseous Environments

Carbon dioxide is a widely used gaseous reactor coolant. Attack by carbon dioxide, particularly in the presence of water vapor, oxidizes and possibly carburizes beryllium which, because of its low neutron absorption, would be a desirable fuel cladding material. Alloying with barium did not improve the resistance of beryllium to low partial pressures of carbon dioxide. By exposing beryllium to carbon dioxide containing radioactive C^{14}, it was determined by autoradiography that the oxidation proceeds along inclusions, probably of impurities, and that the carbon is deposited in a surface-reaction layer of interdispersed oxide and metallic particles. The same technique applied to the reaction of iron- and nickel-base alloys with carbon dioxide showed that the carbon is deposited uniformly. Among these alloys, only those containing chromium are carburized by exposure to carbon dioxide. Creep and stress-rupture testing

of stainless steel in carbon dioxide revealed strengthening and embrittling effects which can be traced to carburization.

Because of its complete lack of reactivity, helium is the coolant of choice for high-temperature gas-cooled reactors, such as the Experimental Gas-Cooled Reactor (EGCR). By leakage and by outgassing of materials such as graphite, helium reactor coolant is expected to contain low concentrations of reactive gases; therefore, corrosion by impure helium is important. The action of low concentrations of carbon monoxide and carbon dioxide mixtures has been observed in static systems and circulating in loops containing both stainless steel and graphite to simulate the EGCR.

In both loop and capsule experiments simulating EGCR conditions, the nature of oxides formed on type 304 stainless steel was found to depend on the proportions of carbon monoxide and carbon dioxide in the gas desorbed from the graphite. Extensive studies have been made of the extent and mechanism of the oxidation and carburization processes taking place in stainless steel at low concentrations of these gases.

Interactions Between Solids

Graphite and stainless steel, two prominent materials in gas-cooled reactor systems, when in intimate contact above 600°C become firmly bonded, with considerable formation of carbide in the steel near the junction. This interaction is completely prevented by preoxidizing the stainless steel or by copper plating it.

The rate of the reaction between uranium monocarbide, a promising high-temperature reactor fuel, and beryllium, a reactor moderator and prospective fuel-cladding material, has been measured over the temperature range 700 to 1000°C.

Compatibility of Construction Materials with Conditions in Outer Space

Surprisingly, the very high vacuum of outer space may well be one of the severest media to which materials may be exposed. Metallurgists at ORNL have been evaluating the effects on metals of heating in the range from 1200 to 2000°F at pressures as low as 10^{-9} torr (about one trillionth of atmospheric pressure), and apparatus is being assembled to extend the studies to one hundredth of this pressure. In comparison with the same metals given similar heat treatments at atmospheric pressure, striking differences are found in such properties as strength and surface structure. The changes in properties result from changes in composition due to the selective evaporation of alloying components into the high vacuum. The rate of evaporation of a selection of iron- and nickel-base alloys at 1600 and 1800°F has been found to increase with an increase in the chromium content of the alloy.

FUNDAMENTAL INVESTIGATION OF RADIATION EFFECTS IN SOLIDS*

Theory Concerning Penetration Ranges of Energetic Atoms in Solids

One of the important problems in the investigation of radiation damage to solid materials is that of the physical extent of the damaged region caused by the introduction of an energetic atom.

Recently, both experiment and theory have been utilized in an attempt to determine, for example, the depth of penetration of such an energetic atom into the solid. In the theoretical approach the life history of an atom is calculated (approximately) as it moves through the solid, colliding frequently with atoms of the lattice structure, losing energy to these struck atoms (thus causing further damage), slowing down and finally coming to rest at some point in the material. The success of such calculations depends on the knowledge of the forces acting between atoms in such collisions in which the relative kinetic energy may vary from 100 to 100,000 electron volts. Very little is known at present about these forces, so that it is necessary to assume various forms for them and by comparison with experiment ascertain which is the most realistic. Results to date indicate that even so crude an approximation as treating the colliding atoms as if they were elastic balls may be adequate for many purposes. For more refined calculations it appears that the interatomic-force law derived from the screened Coulomb potential gives a very adequate fit to experimental data, though

*This section was contributed by the Solid State Division.

modification will certainly be required in some cases.

Sputtering

If a beam of ions strikes the surface of a solid, atoms of the solid are ejected, the yield of ejected material depending upon the nature of the ion, its energy, its angle of incidence upon the target, the nature of the solid, and other conditions. This phenomenon, referred to as "sputtering," is being studied because of its close relation to similar forms of radiation damage, which need to be better understood.

Argon ions in the energy range from 1 to 5 kilo-electron volts are used to bombard single crystals of copper (crystals that have only one crystal nucleus), perpendicularly to the surface. The sputtering yield (number of copper atoms removed per incident ion) is very strongly dependent upon the orientation of the single-crystal target. If the ejected atoms are collected on a glass plate, the deposit clusters in a small number of spots (1 to 5), showing that atoms leave the crystal in only a very few directions. The pattern of spots depends upon the orientation of the single crystal. The nature of the pattern suggests that the so-called "focusing-collision sequence" is responsible for the appearance of the spots and is probably a very important feature of the radiation damage process.

Electron-Microscope Studies of Radiation Effects in Thin Films and Foils

Electron-microscope studies of thin films and foils permit the direct observation of the damage structure induced by irradiation with energetic particles. Studies in progress in the Solid State Division on fission-fragment tracks in thin films have shown differences in structure between tracks in metals and nonmetals, differences which have been related to mechanisms of energy transport possible in the different materials. Studies on foils, which are believed to be more representative of bulk material, show defect structures induced by bombardment. The observation of tracks left by the passage of nitrogen ions (having 25 million electron volt energies) through thin films of platinum opens up the possibility of obtaining a more quantitative evaluation of the interaction of energetic particles with the matter they traverse.

Investigation of Metal Surfaces

The factors which affect crystal perfection in copper crystals grown from the melt are being studied. Single crystals are grown from high-purity copper in a graphite crucible. By use of an etch-pit technique, by which pits are formed by chemical dissolution at the intersections of dislocations in the crystal with the surface, the crystals are examined for dislocation content. It has been found that the crystals which grow such that the slip planes are oriented as far as possible from the growth direction are the most nearly perfect. Crystals with a dislocation density as low as 1000 per square centimeter have been grown. On subsequent annealing for long periods at temperatures near the melting point, the dislocation density decreased, and samples have been prepared with 100 dislocations per square centimeter. The dislocation density in these crystals is only a hundredth to a thousandth of that in copper crystals prepared previously.

Thermal-Neutron Damage in Metals

For most elements the absorption of a thermal (slow) neutron by the nucleus of an atom is accompanied by the immediate emission of one or more energetic gamma rays (the neutron-gamma reaction), which imparts a recoil energy to the atom. For many elements the recoil energy is large enough to displace the atom, which in turn may make other atomic displacements. Although this type of radiation damage had been predicted, recent experiments show that its relative importance to total radiation damage effects in reactors had been considerably underestimated.

Observation of changes in electrical resistivity at 4.5°K shows that the fraction of reactor damage caused by thermal neutrons is 19% in copper, 61% in silver, 65% in gold, 38% in platinum, and 88% in cadmium. (The samples were exposed to the radiation in the ORNL Graphite Reactor.) Use of this nuclear reaction for the study of fundamental processes in radiation damage looks highly promising.

Measurements of the Diffusion or Spread of Fast-Neutron-Produced Defects to Dislocations in the 270 to 370°K Range

Results obtained during the past year indicate that a lattice defect which can be characterized by a motion energy of approximately 1 electron volt and which travels over distances ranging up to about 1000 lattice spacings is primarily responsible for the dislocation pinning observed in the 270 to 370°K temperature interval in copper, as measured by internal-friction techniques. The defect best described by this motion energy in pure copper is the single vacancy, which is created in the lattice by neutron collisions and then migrates to the dislocations. Studies are also being conducted to ascertain the effects of temperature upon the equilibrium distribution of the resulting pinning points.

Radiation Damage in Semiconductors

It has long been assumed that radiation damage (electrical, chemical, optical, or mechanical-property changes) was primarily caused by the fast (damaging) neutrons in a reactor, whereas the main effect of thermal-energy neutrons was to produce radioactive elements that later transmuted to form new elements. It has just recently been established experimentally that (1) the recoil of unstable nuclei following thermal-neutron absorption and capture-gamma-ray emission can lead to atomic displacements in semiconducting materials and (2) that lattice defects are produced by the capture gamma rays that are emitted by the shielding materials often employed to shield against thermal neutrons. The above processes are comparable in magnitude and represent an appreciable fraction of the total amount of radiation damage that is produced in a semiconductor by reactor-produced radiation.

Defects in Ionic Crystals

Defects in the crystalline structure of solid materials are known to affect many of their physical properties. In order to be able to predict property changes resulting from defects introduced into materials by irradiation or other means, it is important to understand both the detailed structure of imperfections and the physical changes resulting from them.

A method of studying imperfections in insulators experimentally is that of observing changes in the absorption of light and of microwaves. Different imperfections will often manifest themselves in quite specific absorption bands. In certain cases the microwave absorption spectrum even permits the deduction of the detailed atomic structure of an imperfection center.

At ORNL such a program of study is in progress, with optical and microwave absorption measurements being used, as well as other related physical-property determinations, such as static magnetic susceptibility, ionic conductivity, and deformation measurements, that help in elucidating the effects of imperfections. Much of the work is done on fused silica and single crystals of potassium chloride, the latter as an example of a relatively simple crystalline solid, and the former as an amorphous or glass structure. Neutron and gamma irradiation and diffusion doping are methods used to create the imperfections.

A number of important results have already come out of this work. An imperfection center in potassium chloride that absorbs light near 8000 angstroms (the *M* center), and which for many years was thought to be a cluster of three vacancies containing one unpaired electron, has been confirmed to be two vacancies containing two electrons, the latter being paired. There is evidence that this center absorbs not only near 8000 angstroms but also near 5500 angstroms. However, the absorption at 5500 angstroms had not been discovered due to the interference of the optical absorption of another center, the *F* center. A study of the introduction of *F* and *M* centers showed that extremely small amounts of impurities (no more than is normally present in "pure" crystals) radically change the details of the introduction of the two centers.

In fused silica two imperfection centers, both of which absorb ultraviolet light, have been studied. It was shown that small amounts of impurities will radically change the rate of introduction of the two centers. Specific models for the centers have been proposed; however, it is more difficult to be sure of the exact structure of the imperfection centers in the more complicated silica structure than it is in simpler materials like the alkali halides. The centers in the fused silica are related to similar radiation-induced centers in crystalline quartz.

Controlled Thermonuclear Research

Work at ORNL on controlled thermonuclear research quickened its pace in 1961. Developments yielded in the period have placed at ORNL three major lines of effort toward controlled fusion. The first is the classic approach of DCX-1 (Direct-Current Experiment No. 1), the second is the extended DCX concept embodied in DCX-2, and the third is radio-frequency heating, which has thrust itself into prominence through preliminary experimental success. The period brought an increased emphasis on other plasma-physics studies, as well as continued development work in theory and computation, vacuum arc, plasma research and diagnostics, magnetics, vacuum technique, and materials problems.

DCX-1

In the continuing quest for controlled fusion, the three large-scale approaches used here – DCX-1, DCX-2, and the radio-frequency heating work – have all yielded valuable results. In the DCX-1 research, we now speak in terms of achieved confinement times of 37 seconds instead of milliseconds, albeit at the familiar, modest densities of a hundred million fast protons per cubic centimeter. This trapped, circulating population of protons is not a simple phenomenon, and measurements of its magnetic radiation and of its potential relative to ground contribute further to the knowledge of the stability of the DCX-1 plasma.

DCX-1 is a single-pass, small-trapping-volume, magnetic-mirror device presently being studied by injecting 600,000-electron-volt H_2^+ molecular ions in one pass through the machine, breaking up a fraction of the molecular ions on the background gas into 300,000-electron-volt H^+ atomic ions, which circulate in a circular orbit symmetrically located in the device. (Deuterium will have to be used in a fusion reactor; light hydrogen is used in present experiments to avoid the nuisance of neutron production.) In DCX-1 there is a serious attempt at present to reduce the background-gas density to that of the trapped plasma of ions, at which time the ion density may grow rapidly upon itself until other as-yet-unknown properties appear which set a new limit. This condition, exponentiation, is the preliminary goal of other experiments such as ALICE at Livermore, PHOENIX at Aldermaston, and OGRA in the USSR, as well as the DCX devices.

Advances in vacuum technology in DCX-1 have produced results about two orders of magnitude better than in the carbon-arc studies of previous years. The highest proton density achieved with gas breakup is now only slightly less than the background density. The mean lifetime of a trapped proton in DCX-1 has been increased from 0.01 second with carbon arc to more than half a minute without arc – a gain factor of over 1000 and hence strong indication of a much purer environment in the revised DCX-1.

The DCX-1 plasma is not a simple ring of protons behaving in a well-ordered pattern. At high background-gas pressures the plasma does indicate such character; that is to say, one observes a simple buildup after the H_2^+ beam is suddenly injected and a similar decay with the same time constant after the beam is suddenly turned off. As the pressure is lowered, the buildup process becomes more rapid and frequently is quite complex, whereas the decay process remains simple in character. Although these unusual buildup phenomena are not yet fully understood, they inherently affect the plasma exponential condition. A strong effort is being made to understand this effect more completely, as well as many associated plasma properties such as secondary slow ions, electrons, heat losses, radio-frequency radiation (the ions apparently bunch into one or more clusters that rotate at gyrofrequency or some multiple of it), plasma potentials, and oscillations as the various system parameters are changed. In spite of these phenomena, the sole loss mechanism for the trapped fast protons appears to arise from interactions with the background of gas in the vacuum tank; instabilities may develop, however, when the density of the trapped particles is increased.

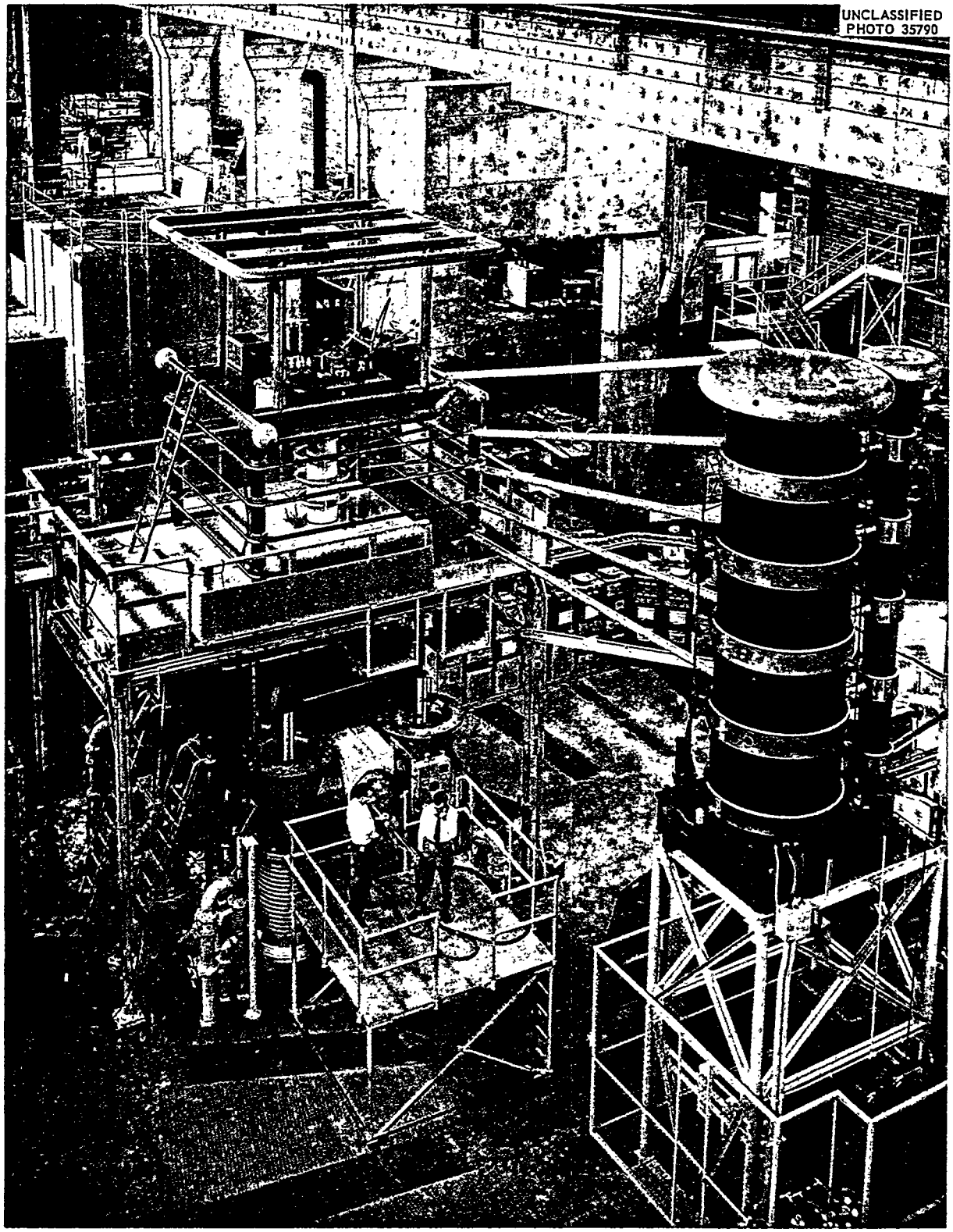

DCX-1.

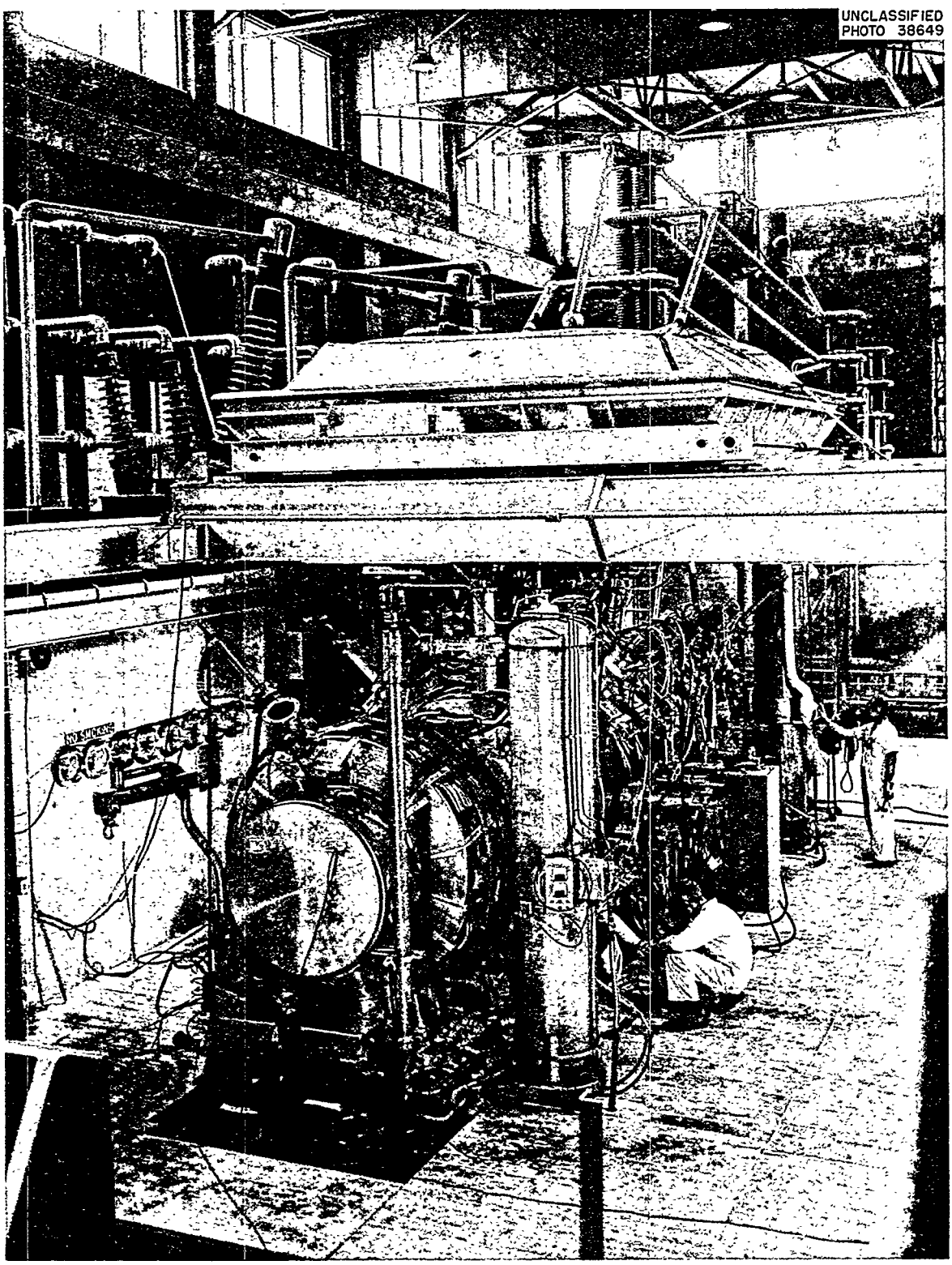

DCX-2.

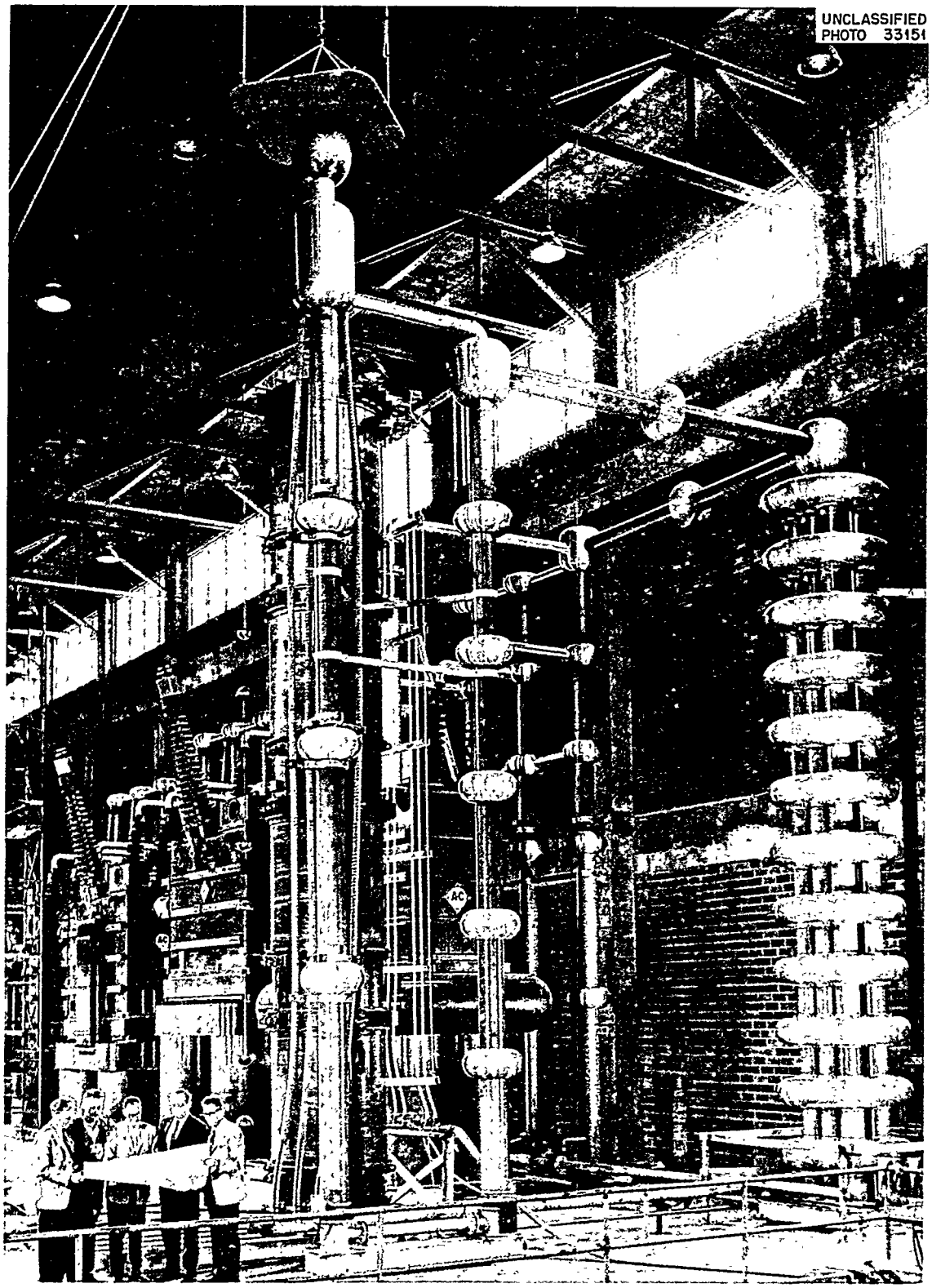

600-kilovolt, 1-ampere, dc power supply for DCX-2.

DCX-2

DCX-2 has been through a heavy phase of design and construction and is undergoing shakedown tests. In contrast to DCX-1, DCX-2 is a multiple-pass, large-volume, plasma-containment device somewhat similar to the Soviet OGRA except that injection takes place at a higher and more promising energy (600 kiloelectron volts vs 200 kiloelectron volts). Component testing has been encouraging; in particular, the generation of a hydrogen ion beam of 0.2 ampere at 600 kiloelectron volts should be noted.

The concept of the DCX-2 machine is to accumulate high-energy atomic ions resulting from the dissociation of injected high-energy molecular ions. In this it resembles DCX-1, but instead of allowing the molecular ions to escape quickly, in DCX-2 an effort is made to keep these molecular ions in the magnetic-mirror field as long as possible. This is accomplished by forming the injected beam into a tightly pitched helix. In order to achieve a maximum path length, a homogeneous magnetic field in a large volume of the apparatus is needed, with fluctuations on the axis not larger than 4 gauss out of 12,000 gauss. (In comparison, the earth's magnetic field is about $\frac{1}{2}$ gauss.) Inside the mirror coils a field strength of 36,000 gauss has to be produced, and finally a "field dip" of 1.5% is necessary at the transition zone between injected beam and helix. (For deuterium the field strengths mentioned will be increased to 17,000 and 50,000 gauss respectively.) Tests with the assembled DCX-2 magnets showed that the carefully calculated and designed coil system actually satisfies these extremely strict conditions. The final tailoring is being done by using the injected molecular ion beam itself as an indicator.

RADIO-FREQUENCY HEATING

The radio-frequency heating so far has been applied only as electron-cyclotron heating in a magnetic-mirror configuration. The results, however, are remarkable and produce a high-temperature, high-density, electron-heated plasma with a pronounced x-ray spectrum, diamagnetic effects, and supporting evidence for the theories of plasma pumping and burnout.

A plasma is produced in a magnetic trap by application of a radio-frequency electric field perpendicular to the steady magnetic field of the trap. The radio-frequency field oscillates in step with the natural electron gyrofrequency and accelerates the electrons to high energies. Because higher-energy electrons are less likely to be scattered, each electron is able to ionize at least one neutral gas atom before it is lost out of the trap, and a large number of ion pairs are accumulated to form a plasma.

The plasma has a high energy density, is highly ionized, and exhibits some extremely interesting characteristics. Measurements show a mean electron energy of 20,000 electron volts and an electron and ion density of about 3 million million per cubic centimeter. A considerable number of plasma electrons have energies in the million-volt range. Lifetime of the plasma in the trap is as long as $\frac{1}{4}$ second after the radio-frequency fields are turned off. The x-ray flux produced by electrons which leave the plasma and strike the container wall is several roentgens per hour.

A small fraction of the x rays come out in short bursts, indicating that some electrons are transported to the wall by small localized instabilities. The total amount of plasma lost in this way is inconsequential, but this is possibly because plasma pressure is only a few percent (about 10%) of magnetic field pressure. Instabilities of this sort are not unexpected in magnetic fields which decrease toward the periphery. In a second experiment, the plasma will be produced in a magnetic field which increases toward the periphery to see whether or not these instabilities depend on field shape.

In addition to its possible thermonuclear uses, mentioned in the first section of this report, this plasma will be used as an environment for the introduction of radio-frequency power to deuterium ions at their appropriate frequency.

PLASMA PHYSICS AND OTHER RESEARCH

In the realm of plasma physics other than these three large-scale approaches at ORNL, studies have been wide-ranging. Such studies may be

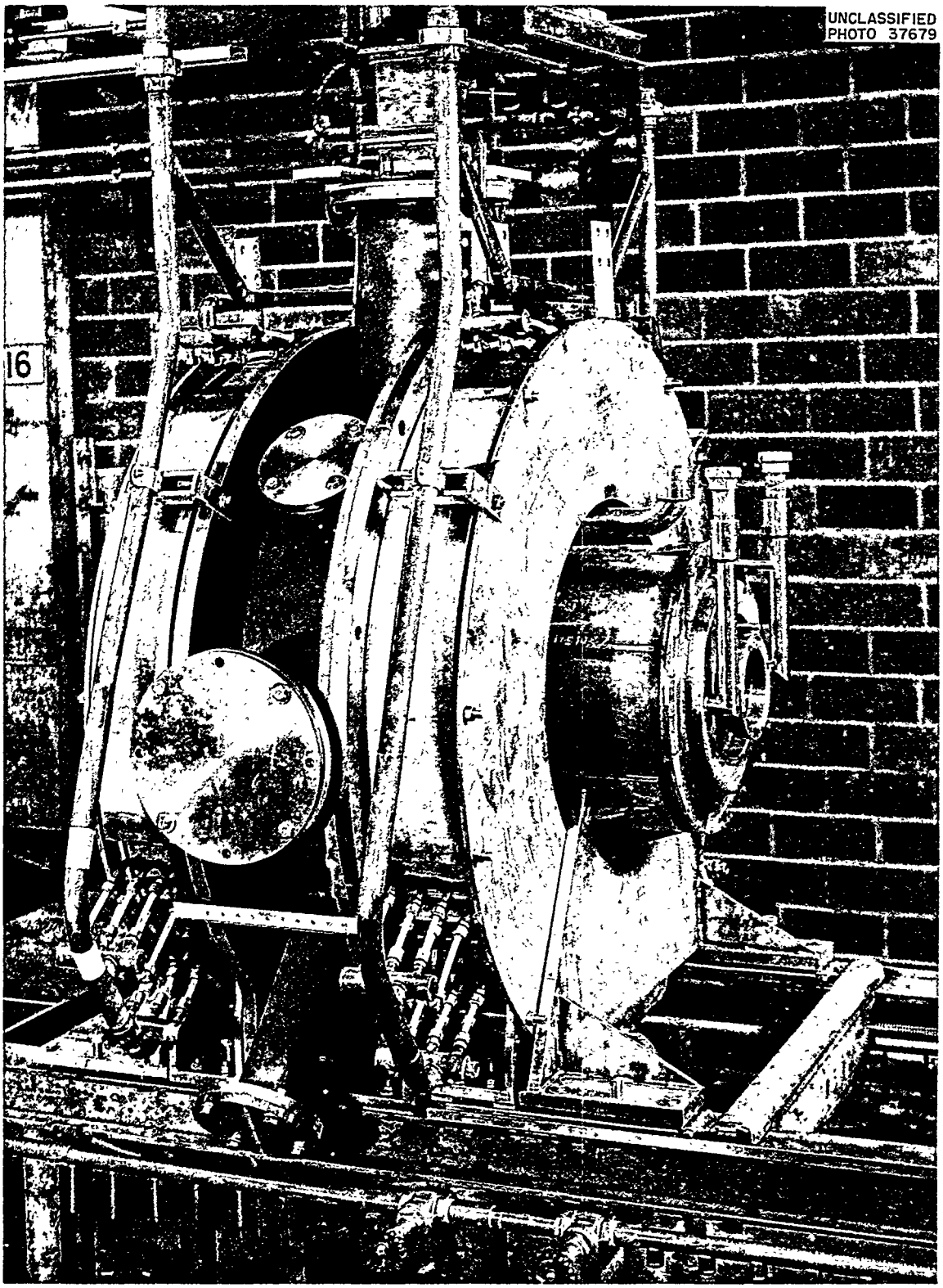

"Elmo," one of the devices used in the radio-frequency experiments.

viewed as constituting a fourth line of attack which might be labeled "plasma physics with emphasis on stability and containment." Plasmas, constituting as they do a "fourth state of matter," have some properties which are shared with liquids, solids, and gases. An example under investigation here is the generation and propagation of sound waves in plasmas – the vibration of the system of ions rather than of crystals, liquids, or molecules. This work has had an outgrowth in the development of a simple ballistic means of measuring plasma pressure. Methods have also been evolved for measuring ion densities and temperatures by sweeping the plasma along the magnetic field lines onto a collecting electrode. This technique makes use of qualities that distinguish plasmas from the other states of matter – the fact, for instance, that plasmas consist of electrons and ionized atoms at unusually high temperatures. The storminess or turbulence of plasmas can be graphically seen on repeated oscilloscope traces that show the collected current as a function of time; in the circumstances of the experiment the turbulence increased with magnetic field strength and in the presence of a magnetic mirror field.

Plasma Streams and Arcs

Research on high-density vacuum arcs, long a part of the ORNL development work, has included more studies on ion temperatures in the carbon arc. Lithium-arc work has concentrated on the part of the arc that streams past the cathode. Deuterium arcs have been analyzed rather comprehensively. Also, a hot-cathode arc in the particle density range of 10^{11} per cubic centimeter has been developed.

The use of the high-density high-current arcs (hydrogen, lithium, and carbon) in the DCX machines has ceased temporarily because of the discovery of serious losses (particle scattering and charge exchange events) when these arcs are used as high-efficiency "breaker-upper" targets for the injected H_2^+ ions. Experiments have been performed on low-density arcs and on plasma streams associated with electron beam plasmas using electron guns. Such arc plasmas have densities in the range of 10^{10} to 10^{12} electrons per cubic centimeter instead of the previously used 10^{14} densities and may prove useful for enhancing the trapped-proton densities in the DCX devices.

Significant features of some of the high-density arcs in magnetic fields from the standpoint of general plasma interest are: (1) the dc or steady-state nature of the system in the hundred-ampere range; (2) the operation of well-defined arcs up to 21 feet in length; (3) the feed of anode material along the arc toward the cathode (about 20% of the total arc current); (4) the gas-pumping action of the arcs; (5) the high ion temperatures achievable (up to 2.5 million degrees Fahrenheit in an 8-foot long carbon arc); (6) the damping or cooling of the arcs at elevated gas pressures; and (7) the "tornado" effect – a rotation of the plasma ions at speeds sometimes exceeding 100 times that in tornadoes.

Ion Sources

Ion beam development at ORNL has yielded improvement in techniques of handling high-energy ion beams of tenths of amperes (0.215 ampere at 600 kiloelectron volts). High-current beams of ions frequently spread due to self-repulsion of the positive ions. This space-charge spreading is tractable in at least two ways – by deliberate injection of electrons, or by trapping the electrons yielded by the residual gas between, for example, magnetic lenses.

Magnetics

Inasmuch as plasmas are contained by magnetic forces, magnetics development is another essential factor in a balanced plasma investigation program. Although much of the magnetics effort during the past period was in support of DCX-2, the development early in 1961 of superconducting materials (see *USAEC – Atomic Energy Research, 1961*, "Cryogenic Coils") which allow high magnetic-field intensities to be built up with quite low electrical requirements has had an impact on thinking here as well as elsewhere. Since these materials introduce a new aspect of volume optimization in coil windings while emphasizing the problem of current distribution, these matters have been studied on a rather general basis and applied as examples.

Superconducting solenoids are equivalent to powerful permanent magnets. Motivated by the possible application to thermonuclear research,

ORNL is doing developmental work on superconducting magnet coils. For instance, a small superconducting solenoid has been built which produced 42,000 gauss, operating at the temperature of liquid helium (−269°C).

Theory

Theoretical analysis of all phases of the work at ORNL is a vital part of the development program. In the theoretical work, several questions have been considered which are closely related to the DCX approach, but more general aspects of plasma physics are dealt with also. A notable contribution comes from the application of existing ORNL computing methods to the forward-looking problem of the breeding ratio in a fusion system. For example, for a two-region beryllium-containing blanket, it may be possible to produce 1.45 atoms of tritium for each tritium atom burned.

Vacuum and Materials Technology

For any continued development of plasma physics a vacuum-materials technology is essential since any neutral gas molecules can drain energy and cause a loss of ions from the plasma. At ORNL, in addition to the vacuum-equipment engineering associated with the main courses of approach to controlled thermonuclear fusion, useful vacuum-materials developments have been made. An example is that, under some circumstances, nearly all the gas molecules striking a titanium film stick.

The requirements of the lines of approach being followed at ORNL have led to a study of the use of evaporated metal coatings to act as pumps or getters for the gas which is present. Although this concept has been long used in many applications (vapor-deposited metal coatings maintain a vacuum in radio tubes, for example), needs for controlled thermonuclear research frequently require vacua which are thousands of times better. A new method was developed at ORNL in 1961 which eliminates many uncertainties in measurements of the pumping efficiency in the difficult range above 10%. This method was successfully used to study ways of improving the pumping efficiency for hydrogen on titanium films. Continued studies were carried out on ion gages and other pumping methods to meet the special needs of the project. A standard orifice-calibration method for ionization pressure gages extended the range of standardization to about 10^{-8} millimeter of mercury pressure (a thousand times lower than other absolute methods). A materials study of the effect of bombarding titanium with high-velocity deuterium ions indicated that the titanium was not eroded from the surface. Rather, it was found that the deuterium penetrated and diffused into the metal efficiently.

Reactor Operations

DETECTION OF BOILING IN THE ORR

An instrument capable of detecting boiling in a water-cooled reactor is needed to prevent fuel melting due to the local obstruction of coolant-water flow in the fuel elements. No instruments are normally present on water-cooled reactors to detect boiling, and several accidents have occurred where coolant-flow restriction resulted in fuel melting before the operators were aware of trouble.

The feasibility of such an instrument is being investigated, and a special heater was built in order to generate a controllable amount of boiling in the ORR and, therefore, to calibrate the detecting instruments. Two instruments are being developed, both based on frequency analysis. The first analyzes a signal in the acoustical frequency range, and the second analyzes a low-frequency signal produced by the reactor power fluctuations.

Encouraging partial results have already been obtained, as shown in the plotted data. The first graph shows the acoustical spectrum of the noise due to boiling in the absence of hydraulic-background noise, and the second graph shows the variation of the amplitude of the acoustical noise as a function of the power dissipated in the heater. The power at which the break occurs on this plot corresponds well with that obtained by a power-vs-temperature measurement, indicating that the acoustical method can "hear" boiling when it commences. Another set of measurements indicated that the acoustical boiling noise can be distinguished from the hydraulic-background noise.

The reactor power fluctuations analysis seems to indicate that this method could also be used to detect boiling, but the statistical accuracy obtained is not sufficient at present to permit an interpretation of the results.

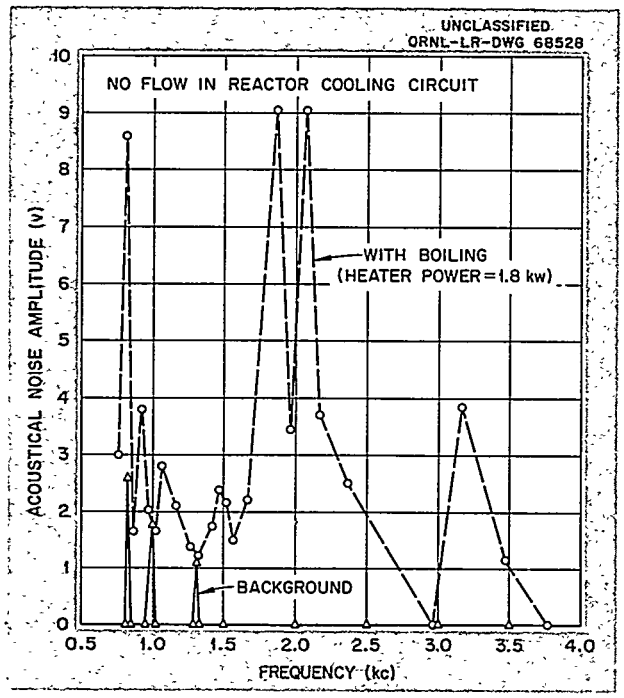

Acoustical noise spectrum; no reactor coolant flow.

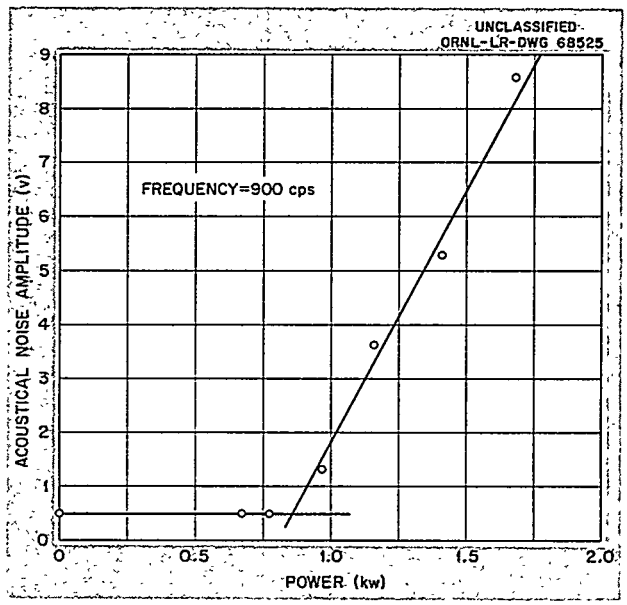

Acoustical noise amplitude as a function of heater power.

DEVELOPMENT OF A METHOD FOR ANNEALING THE ORNL GRAPHITE REACTOR

A unique method was developed for annealing the stored energy in the graphite of the ORNL Graphite Reactor. This method allows the energy release to be stopped at any time instead of proceeding to completion once it has been triggered. During normal operation, the cooling-air flow is from east to west so that the east half of the graphite remains below 140°C and the west half mostly above 140°C except in the periphery. Stored energy, therefore, accumulates in the east half of the graphite and in the periphery. By altering the air ducts to reverse the air flow and by protecting the uninsulated east concrete shield with water sprays, the temperature pattern was made reversible. This allows the east half of the graphite to be slowly heated (with nearly normal air flow being maintained) to or above 140°C except in the peripheral regions. A subsequent bakeout with the reactor shut down and the air flow greatly reduced allows much of the periphery to heat up to greater than 140°C. This procedure causes most of the stored energy to be released slowly and safely, with no abrupt temperature increases. (The temperature can be reduced at any time by increasing the air flow.) The graph below is a temperature-vs-time plot for fuel channel 1969, showing the temperature behavior during this release. The next graph shows temperature profiles through the same channel and also illustrates the way that reversing the air flow heats up the half of the central graphite containing stored energy above the specific heat curve.

The next step in the annealing development will be to orifice the peripheral fuel channels in order to elevate their temperatures both during normal operation (to reduce energy storage) and during annealing (to release stored energy). Orifices are being designed to be permanently installed.

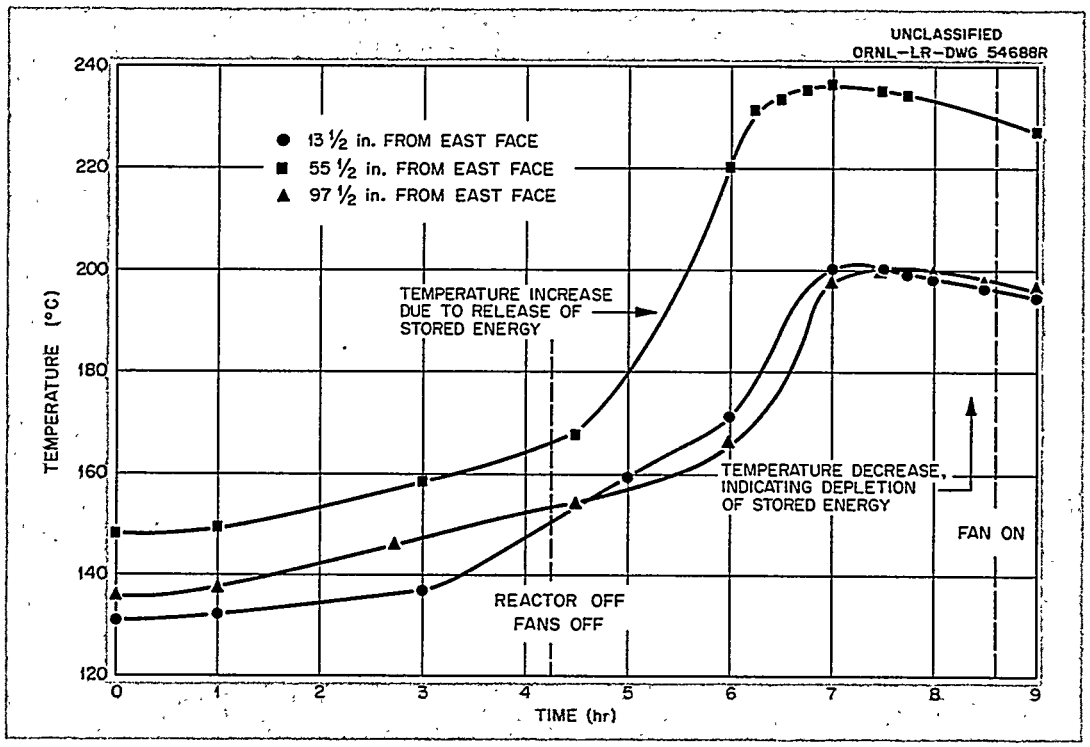

Time-temperature trace for channel 1969. Data taken Sept. 4, 1960.

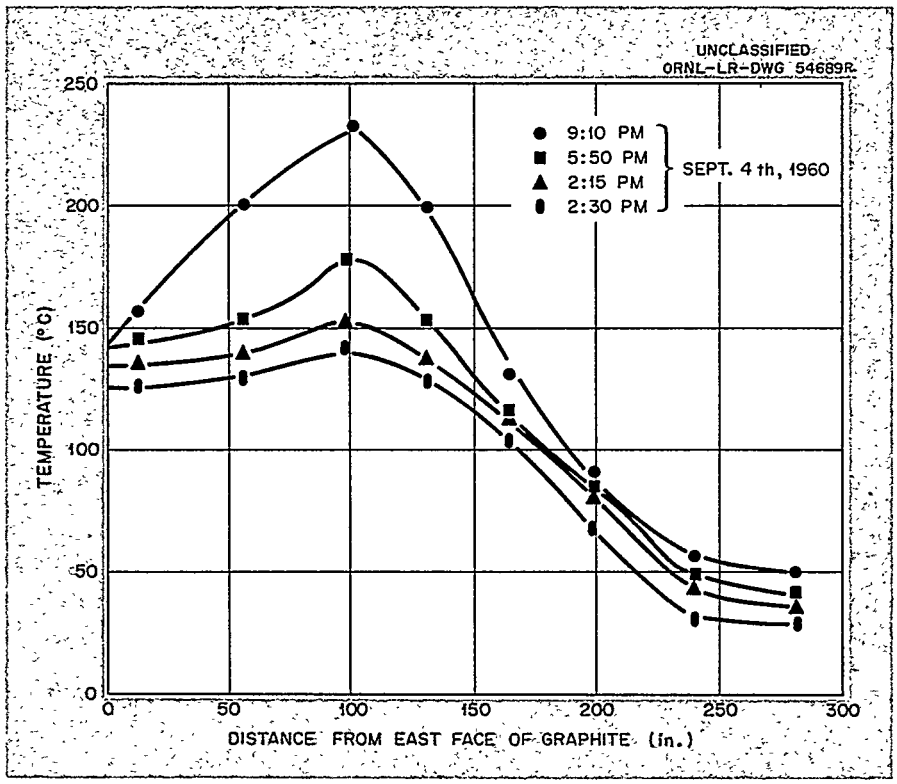

Temperature profiles for channel 1969.

TRAINING OF OFF-SITE PERSONNEL IN REACTOR OPERATIONS

There is an increasing demand for the training of reactor-operating crews in the actual operation of the reactors so that they can become familiar with practical procedures, safety precautions, and general operating methods.

The following table indicates the amount of such training given by the Operations Division during during calendar year 1961.

The training ranges widely. Shift workers are trained, startup crews are instructed, and day-to-day supervisory work is also taught.

Sponsoring Agency	Number of Trainees	Duration (man-months)
Republic of South Africa	7	56
TVA-EGCR	7	35
ORSORT	17	51
Picatinny Arsenal	1	16

BIOLOGY and MEDICINE

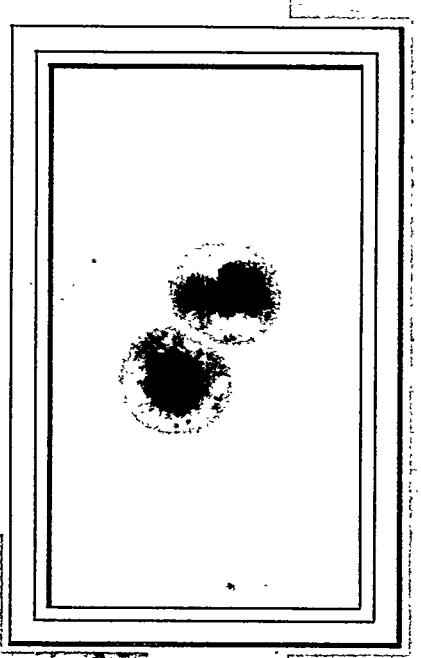

Biology

EDUCATIONAL AND TRAINING PROGRAMS OF THE ORNL BIOLOGY DIVISION, 1947–1961

From about the first year after the Biology Division of the Oak Ridge National Laboratory was established, there have been ever-increasing programs of pre- and postdoctoral training. Altogether, over the years 1947–61, 112 Fellows (U.S. citizens) were trained, plus a total of 56 (in "man-years") from 23 foreign countries. About 65% of the financial support for both of these programs came directly from our own budget; additional support has been provided in the form of fellowships awarded to individuals by the National Science Foundation, U.S. Public Health Service, American Cancer Society, International Cooperation Administration, Fulbright Program, and other U.S. and international agencies. In addition, many of our foreign postdoctoral trainees are supported by their own governments.

In addition, the Biology Division has trained a total of 119 college and university staff members (during the summers and also for longer periods) as well as 48 college undergraduates.

The level of these programs has steadily risen. In 1961 alone the Biology Division had five predoctorals, 24 U.S. postdoctorals, and 14 foreign trainees, for a total of 43 fellows in training. In addition, during the summer of 1961 there were 12 University Research Participants (university staff members) and 16 undergraduate college students in this Division for training.

Since about one-third of the Ph.D.'s and M.D.'s in this Division are recent postdoctorates on postdoctoral training programs, great pains are taken to ensure that these people become familiar with the new concepts in fields other than those of their specialty. There is an unusual opportunity to accomplish this in a research institution of this sort, which is housed in one very large building and covers disciplines which ordinarily are handled in six to ten different departments in most universities, where they would be scattered about on a large campus.

For example, a biochemist who comes here for specialized advanced training in enzymology or protein synthesis is quickly made aware of closely related work going on in the Division concerning, for example, coding problems in the transmission of genetic information. Cooperative projects which go across different disciplines are encouraged.

Besides the fairly extensive program in postdoctoral training, during the summer months there are about 15 college seniors spread among the the various laboratories who have come in either on Biology Division funds or on NSF-type fellowships. Other training programs operate at a different level, namely, one for college and university staff members who come in the summer, or for periods extending up to one year, for specialized training in the various disciplines available here.

GENETIC AND CYTOGENETIC STUDIES

Studies of the cell nucleus are of fundamental importance in radiation biology, since low-dose effects are often traceable to damage to this structure or its component parts, the chromosomes and genes. A number of investigations at Oak Ridge National Laboratory concern basic aspects of gene and chromosome structure and function and the ways in which radiation affects these entities.

Two sets of investigations are concerned directly with the various factors that affect the number of mutations and chromosome rearrangements produced by radiation. The large chromosomes of the broad bean, *Vicia*, are especially suitable for studies on chromosome rearrangements. The concept that there are only a few places in the nucleus where chromosomes are

close enough together to allow rearrangements to occur has been developed and explains a number of different findings, such as the differential radiation sensitivity of various cell types in both plants and animals. As a corollary of the limited number of places for rearrangement, most breaks must be repaired by restitutional reunion without detectable effect.

The protozoan, *Paramecium*, continues to provide a valuable material for studying the factors affecting the induction of lethal mutations. As for *Vicia*, there is evidence that a large fraction of the initial radiation damage is reparable, and this repair process is being investigated further. Less mutation is produced when the radiation is given at low dose rate than at high, and the relation between this phenomenon and repair is under study. Studies on the synthesis of major cellular components have been undertaken in both *Vicia* and *Paramecium* to obtain the knowledge that is needed to interpret the radiation effects.

A full understanding of the production of mutation will come only when the molecular alterations responsible for it are known and the consequences of these alterations for chromosome duplication and gene action are understood. One group is approaching this problem through the use of mutagens whose action on the hereditary

Biologist adjusting an ultraviolet monochromator.

material, deoxyribonucleic acid (DNA), can be inferred from biochemical and biophysical investigations on DNA and its constituent bases. Bacteriophage, which is largely DNA, is especially suitable for this purpose. Studies with chemical mutagens and with monochromatic ultraviolet light have allowed certain mutations to be tentatively identified as consequences of specific kinds of changes in the base pair composition of DNA.

Various analyses of mutation in a single genetic locus are being carried out at Oak Ridge in the mold *Neurospora*. Mutagens with known effects on DNA are being used to extend the findings with bacteriophage to genetic material with an organization more like that in higher plants and animals. A comparison is being made of the consequences of the mutations induced by various agents by studying the interaction between different altered gene products when they are together in a common cytoplasm. These interactions can be used to derive a "complementation map" of the gene product. Comparison of mutants with completely and partially inactive enzymes in such experiments shows that interaction can take place at different levels of organization. Work is also in progress to develop a system for precise measurement of forward mutation rates for both viable and lethal changes for use in radiation and space biology.

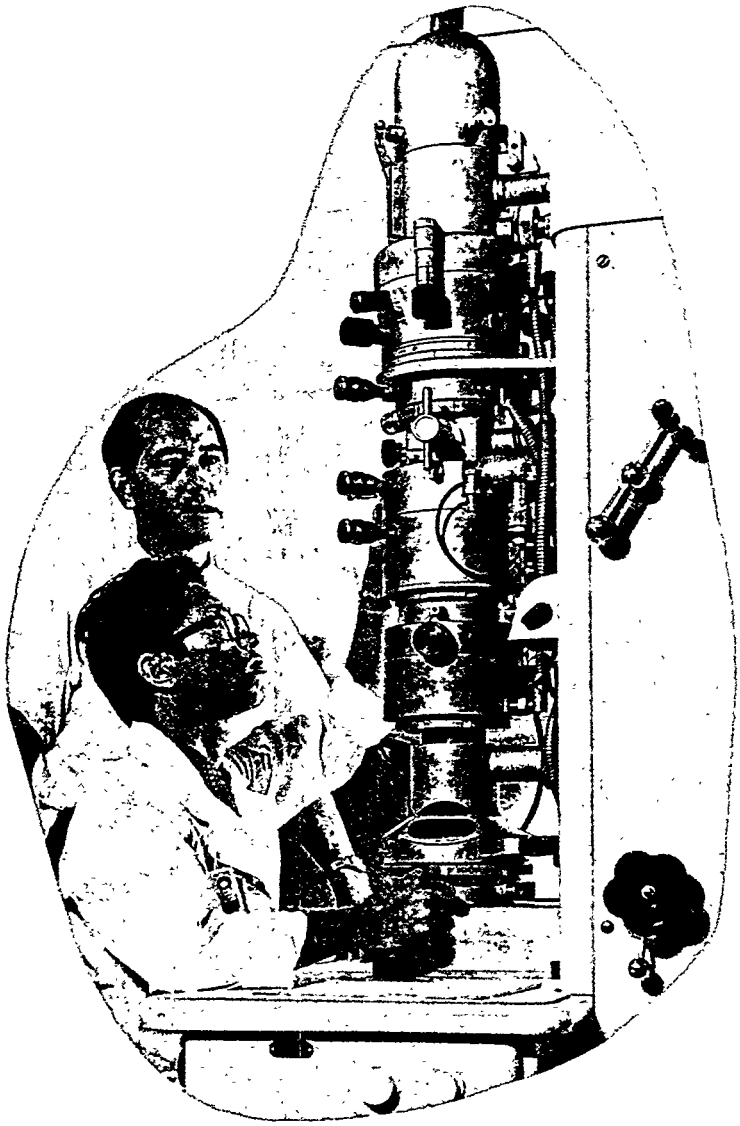

Investigator from abroad seated at the electron microscope, observed by distinguished Japanese embryologist who is now a staff member of the Biology Division.

The plant, maize, whose genetics has been studied extensively, is being used at Oak Ridge to attack one of the fundamental problems of gene action, the translation of the information carried in the genetic locus into the specificity of enzymatic proteins. It is widely accepted that this translation occurs through an intermediate messenger, probably a form of ribonucleic acid (RNA). The maize studies have concentrated on a combined genetic and biochemical analysis of a particular enzyme protein controlled by a single gene. The studies show that information from two allelic forms of this gene in a hybrid can interact to specify an enzyme with intermediate properties and that this probably occurs at the messenger level. The possibility of such a combination has important implications for theories of messenger action.

The fruit fly, *Drosophila*, has been studied by geneticists for over 50 years, and it is one of the best materials for many genetic studies. Two general lines of research are being pursued at Oak Ridge National Laboratory: the organization of the genetic information on the chromosome and the mechanics of transmission of this information from one generation to the next. Two studies on the organization of the genetic information may be cited. Detailed investigation of one genetic locus shows, contrary to some previous views, that the organization of the genetic information within this locus is much the same as in the better-analyzed loci in microorganisms, thus bringing more unity into our concepts of locus structure. A study of x-ray-induced male sterility has led to the view that there is a supragenic level of organization of the genetic information, since sterility is produced by interruptions in the continuity of the X (sex) chromosome and not just by alterations of specific loci. Studies on the transmission of chromosomes to the germ cells of the female (ovum) have given an important new concept, the existence of two kinds of pairing. One kind, *exchange pairing*, precedes exchange of genetic material between chromosomes; the second, *distributive pairing*, precedes disjunction of the chromosomes during germ-cell formation and is required for orderly distribution of the chromosomes to the offspring. Exchange and disjunction have been attributed in the past to a single kind of pairing; the concept of two kinds brings order to much that was previously puzzling.

MAMMALIAN CYTOGENETICS

A number of recent advances in cytological and cell-culture techniques have made possible new types of studies of mammalian cells and chromosomes and their radiosensitivity. At the Oak Ridge National Laboratory, cytogenetic investigations of human, monkey, and Chinese hamster materials are directed toward better measurement of human radiosensitivity and toward the understanding of the structure and function of mammalian chromosomes. As a measure of human radiosensitivity, chromosomal breakage induced in the blood-forming cells of a number of accidentally irradiated people is being investigated. Also, because it is impossible to irradiate human subjects for experimental purposes, a number of indirect measurements of the types and rates of chromosomal abnormalities induced by x rays and by neutrons are being made. For these experiments, human cells from blood and other tissues have been irradiated in culture, and similar cells from monkeys and hamsters are being irradiated both in culture and in the animal's body. Photograph (*a*) shows an example of a typical form of radiation damage, a dicentric chromosome produced by x irradiation of a human blood cell. These studies will make it possible to estimate induced aberration rates in cells in the human body. Knowledge of the radiosensitivity of human chromosomes will not only provide better estimates of human radiation hazards, but will make clinical evaluation of unknown radiation exposures possible by means of measurement of the chromosome aberration rate in the patient's blood cells.

Because of the selective absorption of various wavelengths by cell constituents, studies of the effects of ultraviolet (UV) radiation on mammalian chromosomes can provide important information about their structure. Ultraviolet irradiation penetrates only a few microns into tissue, making such studies impossible in whole animals. When cells are grown on a flat substrate in culture, however, they are very thin and are stretched out, presenting a very favorable geometry for the absorption of UV energy. Wavelengths of 2652 and 2804 angstroms are the most effective in inducing abnormal chromosomes, the latter wavelength frequently shattering most of the chromosome com-

plement of the cell. Photograph (*b*) shows an aberration in such a UV-treated Chinese hamster cell. These aberrations can be reversed by post-treating the cells with light of a longer wavelength (3300 to 4400 angstroms). Conversely, the amount of damage can be increased by inhibiting protein synthesis in the cells.

Chromosomal abnormalities induced by radiation of mammalian cells. (*a*) Dicentric chromosome in a cell from irradiated human blood. Arrows indicate aberration. (*b*) Aberrations in a Chinese hamster cell treated with ultraviolet radiation. Arrow indicates exchange between two chromosomes.

The study of killing of mammalian cells in culture by radiation yields information both on mammalian radiosensitivity and on the mechanism by which radiation brings about cell death. At Oak Ridge, cell killing is being studied in several ways; computer analyses of the shapes of dose-effect curves provide information about the possible role of chromosomal damage, as do studies of the action spectrum of UV killing. Lapse-time micro-cinematographic methods make it possible to follow the postirradiation histories of individual irradiated cells in culture, giving information about the manner in which they die.

A number of human congenital disorders are known to be associated with abnormalities of the chromosomes. The Laboratory is cooperating with several medical laboratories in the study of these abnormal chromosomal constitutions, particularly those present in various sexual disorders and in congenital mental deficiencies.

In collaboration with other institutions, studies of chromosome number and form and their relation to evolution in the Primates is being carried on. Small pieces of tissue, obtained by biopsy or necropsy of captive animals, are cultivated and used for examination of the chromosomes. Representative species of all the major primate groups have been studied cytologically, including anthropoid apes, Old and New World monkeys, and primitive prosimians. These studies reveal great diversity in the chromosomal constitution of Primates and permit conclusions to be drawn about the relationship between various species and about evolutionary patterns in this group. They also allow us to choose the best primate species for particular experimental purposes.

Mammalian cell-culture techniques are particularly well suited to investigations of the biological effects of the radiation encountered in human space flight. In collaboration with the NASA, the Oak Ridge National Laboratory is investigating the production of chromosomal abnormalities in human cells sent into space and subsequently returned to the earth for examination. In addition, the effects on human cells and chromosomes of some of the types of radiation expected to be important in space are being investigated by use of particle accelerators.

Geneticists in one of the animal rooms of the Mammalian Genetics Section of the Biology Division.

GENETIC AND DEVELOPMENTAL EFFECTS OF RADIATION IN MICE

Genetic effects of radiation in mammals, as well as a number of other biological effects, are being studied in a large-scale long-range program at Oak Ridge National Laboratory. These experiments not only provide urgently needed practical information for the estimation of the genetic hazards of radiation exposure of human beings, but also yield many results of basic biological importance.

In the radiation-genetics part of the above program, three lines of approach are being used. In one series of experiments, empirical measurements are being obtained on morphological defects, longevity, productivity, and other vital statistics in descendant populations of irradiated mice. In a second set of experiments, mutations at certain specific gene loci are being used to obtain data on the factors that influence both the frequency and the qualitative nature of the genetic changes induced. This includes comparisons of mutation induction in the various reproductive cell stages, from the earliest to the most mature, in both males and females. The relative effectiveness of different types of radiation and the relation of mutation frequency to total dose, dose rate, and dose fractionation are also being investigated. A third set of experiments is concerned with the study of radiation-induced chromosome aberrations, both for their own sake and as an index of radiation sensitivity to genetic effects.

One result of the first series of experiments (empirical measurements) obtained during the past year may be singled out for mention at this time. By using appropriate methods that distinguish naturally occurring from newly induced variability, it has been possible to demonstrate a slight but significant increase in skeletal abnormalities in first-generation offspring of mice irradiated either with x rays or neutrons. In general, the frequency of these abnormalities increases with the dose received by the father.

Along the second main line of approach (specific locus method), the work of the past year has concentrated on more detailed studies of the effects of dose protraction and dose fractionation. The range between the dose rates of 90 roentgens

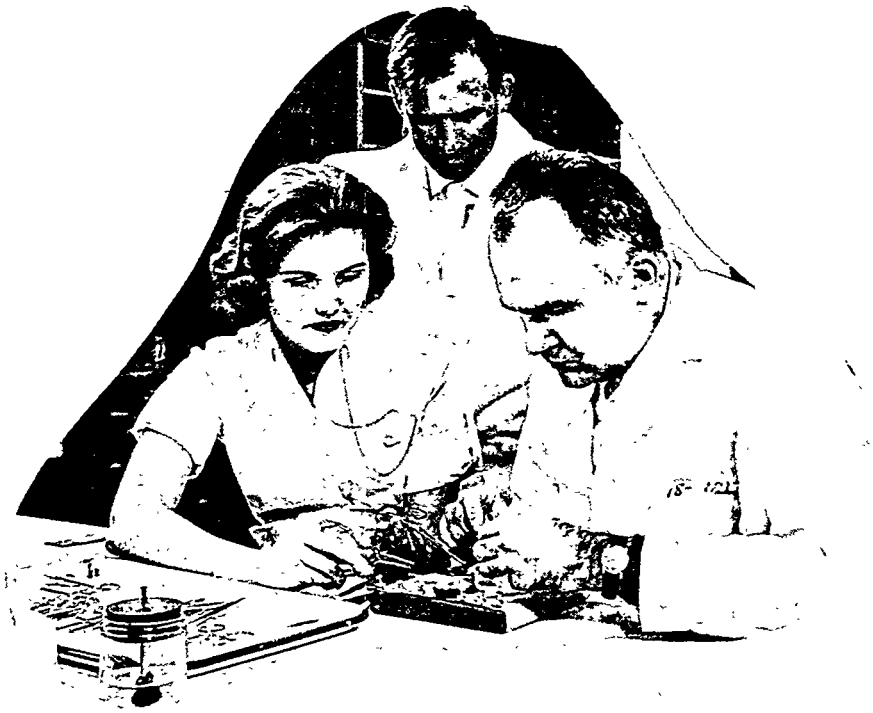

Consultant surgeon performing a splenectomy, assisted by technician.

per minute and 0.8 roentgens per minute, which were tested earlier, is being explored in an experiment at 9 roentgens per minute. The results are not yet conclusive, but at present they are showing an intermediate mutation frequency. Experiments with female mice have apparently uncovered a new complexity in the dependence of mutation rate on the state of the oocytes. This does not invalidate any earlier conclusions concerning dose-rate effects, but it must be studied further, because an unexpectedly high mutation rate was found following irradiation in a particular oocyte stage.

A series of experiments with different systems of dose fractionation of acute irradiation is being performed in an attempt to gain further understanding of both the dose-rate effect and the peculiar drop in the dose-mutation curve found at high acute doses. In the results obtained to date with total doses of 1000 roentgens, all systems of fractionation are giving mutation frequencies higher than that obtained with a single 1000-roentgen exposure.

One set of experiments in progress may be reported to illustrate the third line of approach in the mammalian genetics program at Oak Ridge National Laboratory. A new method is being used to compare the sensitivity of various cell stages to radiation-induced chromosome breakage. In the majority of cases, broken chromosomes are eliminated during subsequent cell divisions, and the loss of even a single chromosome is almost invariably lethal to the organism. However, as was established earlier at this laboratory, the loss of sex chromosome does not cause death in the female mouse and can be recognized by using appropriate marker genes, of which several have been developed at Oak Ridge. The frequency of such females obtained following irradiation of various cell stages is now being used as an index of the relative sensitivity of these stages to radiation-induced chromosome breakage. Animals with abnormal sex-chromosome constitutions are also studied for their own sake, since they provide important information on the effect of chromosome type on the expression of genes.

The bases for species differences in fertility of irradiated females are being studied at the Laboratory by comparing the histological response of mouse and guinea pig ovaries. Whereas 50 roentgens destroys almost all the oocytes in the earliest follicle stages in the mouse, about 40% of the oocytes in comparable follicle stages in the guinea pig survive 200 roentgens. A further species difference is that in the mouse, most late follicle stages survive doses as high as 500 roentgens, while in the guinea pig they are destroyed by 200 roentgens. In mammals the definitive number of oocytes is formed before birth; development of the oocyte is then arrested in meiotic prophase until shortly before ovulation. We have found that this arrest, however, occurs in a much earlier meiotic stage in the guinea pig than in the mouse. In view of the known importance of meiotic stage on radiation response, the above results suggest that variation in radiation response of diverse species may depend on the stage at which oocyte development is arrested.

Work on the effects of radiation on embryological development in mammals is continuing at Oak Ridge National Laboratory, mainly from the point of view of studying chromosome aberrations. It has been found that small variations in stage of development have large effects on the sensitivity to induced chromosome damage.

STUDIES OF LATE SOMATIC EFFECTS OF RADIATION

Irradiated mice in several large-scale experiments at Oak Ridge National Laboratory have been observed to die prematurely with diseases otherwise encountered in senescence, from which it has been inferred that radiation causes precocious aging. Not all age-dependent changes, however, have been found to be advanced to the same extent by a given radiation dose, nor have their frequencies been affected uniformly. Hence, although there may be an analogy between the effects of radiation and those of aging, the comparison is not a simple one.

The complexity of this relationship has been further illustrated by studies of the influence of the dose rate and quality of radiation on the induction of such late effects. These studies at Oak Ridge have demonstrated that densely ionizing radiations, such as fast neutrons, are generally several times as effective as sparsely ionizing radiations, such as gamma rays, in shortening the life span and causing associated diseases. Furthermore, the effectiveness of the former radiation does not diminish as greatly, if at all, with decreasing dose rate, as does that of the latter; for example, for a given total dose, protracted exposure to gamma radiation was generally 2 to 5 times less effective than an acute exposure. Not only, however, was the relative biologic effectiveness (RBE) of the two radiations found to differ with dose rate, but also with the type of effect. For example, the RBE of fast neutrons relative to gamma rays varied from about 2 to 20 in the induction of lens opacities, depending on the dose rate, but only from about 0.5 to 0.9 in the induction of ovarian tumors. The radiological significance of these variations remains to be determined, but their practical implications for human protection are obvious.

One of the most important late somatic effects of radiation is the induction of cancer, which has been studied in many strains of mice and rats exposed under varying conditions. Although the mechanism of cancer induction remains unknown, existing experiments have failed to provide a single unambiguous example of a linear relation between cancer incidence and radiation dose. In most instances the dose-response relationship has been curvilinear and complex, the frequency of tumors decreasing with increasing dose above a certain radiation level. No adequate information is available, however, concerning low-level irradiation; hence existing data are inappropriate for extrapolation to the usual human exposure situation.

Analysis of tumorigenesis is further complicated by the wide variation in susceptibility observed to result from constitutional and physiological variables (age, sex, genetic background, etc.). Although these factors have been observed to exert profound effects on the development of leukemias and other growths in mice and rats, their modes of action and significance for man remain to be determined. It is evident, nevertheless, that generalizations about dose-response relations in radiogenic cancer must remain highly speculative.

One of the most interesting developments in these studies is the growing evidence that a leukemia virus is involved in the pathogenesis

of radiation-induced leukemia in the mouse. Observations at Oak Ridge with the electron microscope have disclosed the presence of virus-like particles in a high proportion of mice with radiation-induced myeloid leukemia, and preliminary experiments suggest a strong correlation between the numbers of such particles and the leukemia-inducing potency of cell-free filtrates prepared from the affected tissues. Although these results are as yet inconclusive, they imply that radiation activates a latent leukemia virus in causing certain types of leukemia. Furthermore, the data suggest that the same viral agent may induce more than one hematologic form of leukemia, depending on the physiological condition of the host. The significance of these findings cannot be fully assessed as yet, but they compel reevaluation of radiogenic cancer in the light of microbiological and epidemiological considerations.

EXPERIMENTAL TREATMENT OF RADIATION INJURY AND THE PHYSIOLOGY OF BLOOD-FORMING ORGANS

Studies on the treatment of lethal radiation damage in mice and other small mammals by bone marrow transplantation have now been carried out for about ten years. The two major objectives of this work are quite clear. One is to develop for the small laboratory animal (large numbers of animals can be easily handled) a reliable experimental method of transplanting bone marrow that will prevent radiation death from hemorrhage, infection, and anemia. From these small-animal experiments, where it is also possible to test new ideas rather quickly, one can proceed to experiments on large animals and therapeutic trials in man.

The other objective of marrow transplantation research is now of major importance. It consists of the contributions to our understanding of the physiology of bone marrow and lymphatic tissues that are being developed through research of the marrow-transplantation type.

A research finding that fulfills both objectives is illustrated by the work at Oak Ridge National Laboratory on white-blood-cell transplantation in mice. It has been known for some time that the normal white blood cells can show immune functions as do cells from spleen or lymph nodes. New results obtained this past year at Oak Ridge show that normal white blood cells also can behave as bone marrow cells and, on transplantation in radiated mice, give rise to newly formed red blood cells and granulocytes. This work indicates that stem cells from lymphatic tissues and bone marrow are constantly present in the blood

Vials of frozen bone marrow are being placed in liquid nitrogen prior to long-term storage in liquid nitrogen refrigerators.

stream in the mouse and are not located only in the tissues and bone as was previously thought.

Since, under favorable genetic circumstances, white blood cells can be used in place of bone marrow transplants to keep the lethally irradiated mouse alive, the possibility now exists of using white-blood-cell preservation and injection in man to replace or aid autologous bone marrow transplantation.

Related studies at Oak Ridge on the physiology of blood platelets have revealed the existence of a humoral factor capable of increasing the level of circulating platelets in rats. This substance accumulates in the blood in response to artificial reduction of the platelet count or injection of foreign protein. Its chemical nature and mode of action remain to be elucidated, but preliminary data suggest that it may be a type of platelet-stimulating hormone analogous to erythropoietin. As such, its physiological implications would be far-reaching.

Attempts to explain the restorative effects of infused marrow on the recovery of the irradiated mouse thymus have indicated that the thymus is repopulated by elements derived from the grafted marrow. This conclusion was drawn from experiments in which the regenerated thymus revealed itself to be immunologically identical with the grafted bone marrow and not with the host. The results are of interest not only in elucidating the embryology and physiology of the thymus, but also in defining the mechanism by which marrow transplantation inhibits the induction of radiogenic thymic leukemia.

COMPARISON OF IONIZING RADIATION AND RADIOMIMETIC CHEMICALS

A variety of chemicals with radiomimetic activity have been compared with x rays in regard to their early and late effects in mice studied at Oak Ridge National Laboratory. These compounds included nitrogen mustard, triethylene melamine, myleran, and others. All of the drugs resembled x rays, in general, in their toxicity to dividing cells and in their shortening of the life span, induction of tumors, and opacification of the lens. None of the agents mimicked radiation consistently and quantitatively, however, in effects on different cells and tissues, whether through differences in mode of action or differences in concentration within the various organs and cells of the body. Furthermore, the chemicals differed greatly from one to another in the extent to which their effects were prevented by the radioprotective drug S,2-aminoethylisothiourea. It can be inferred, nevertheless, that these agents were qualitatively radiomimetic as a class and that they may be useful, therefore, in the further analysis of radiation injury at the molecular level.

GENETICS AND PHYSIOLOGY OF HEMOGLOBIN SYNTHESIS

The observation that transplanted homologous mouse bone marrow cells synthesized erythrocytes with hemoglobin of donor type rather than of recipient type prompted investigation of the genetics and physiology of hemoglobin synthesis. These studies at Oak Ridge National Laboratory have disclosed that the inheritance of hemoglobin is under the control of at least two genetic loci in the mouse. One of these loci (*Hb*) determines the electrophoretic mobility of the hemoglobin molecule, and the other (*Sol*) determines its solubility and crystallization properties. The *Hb* locus has been located in the first linkage group, but the location of *Sol* in the chromosome map remains to be determined. Examination of more than a score of genetically distinct strains of mice has led to the discovery of several different alleles at each locus. Further analysis of the mode of gene action at these loci has been carried out by fingerprinting the tryptic peptides of the α and β globin chains of different types of hemoglobin chains of different types of hemoglobin. Results to date implicate the influence of the *Hb* locus in the synthesis of peptides in the α chain. Further studies are expected to correlate the molecular configuration of both the α and β chains with their genetic determinants. Through this system, precise studies of gene action in mammalian protein synthesis are therefore envisaged.

RADIATION MICROBIOLOGY

As a result of the rapid advances being made in the understanding of basic biochemical and genetic mechanisms in bacteria, these organisms are becoming increasingly valuable for studying the details of radiobiological phenomena. Perhaps the most thoroughly studied bacterium, from a biochemical and genetic point of view, is *Escherichia coli*. Extensive use is made of various strains of this organism in radiobiological studies at Oak Ridge National Laboratory.

A detailed analysis of genetic factors affecting radiation sensitivity in *E. coli* is possible because of the existence of strains of different mating types. A study of the radiation sensitivity of the progeny from a cross involving a radiation-sensitive and radiation-resistant parent has revealed that radiation behavior can be influenced by many genes, each having a relatively small effect. At least some of these effects are cumulative. The genes that influence response to ionizing radiation can also influence response to nonionizing radiation. The available data indicate that these genes are not randomly distributed on the bacterial chromosome but seem to be clustered in a particular region. There is some evidence that these genes are involved in directing processes that lead to the repair of radiation-damaged essential cell constituents.

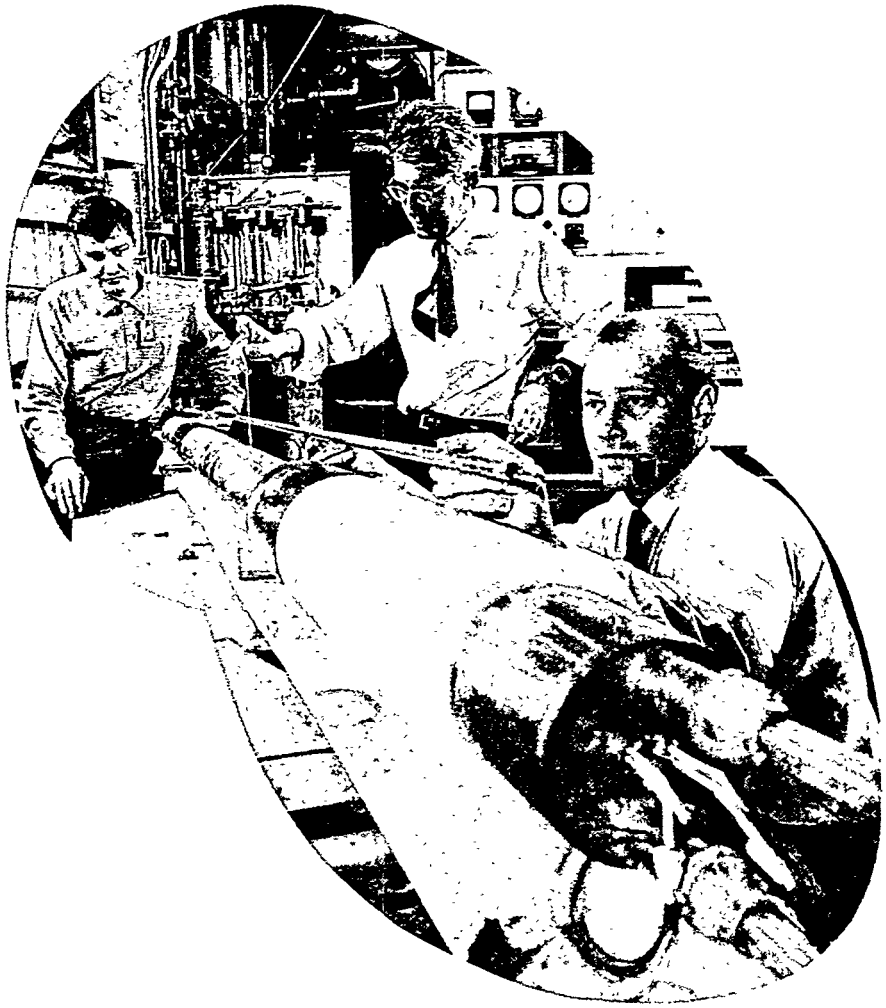

Thermal-neutron-exposure assembly before it was inserted in the Low-Intensity Test Reactor.

An understanding of the factors that determine radiosensitivity of living cells can be explored in microorganisms by use of modifications in the cultural medium in which the cells are grown before irradiation. Development of radioresistance can be experimentally controlled in the bacterium *E. coli*, and the changes in the physiological and genetic makeup which parallel the resistance changes can be examined. Development of resistance to radiation in all cases studied involves increase in cell sizes as well as increase in the deoxyribonucleic acid (DNA) content per cell. The increase in DNA per se is not the controlling factor, since a number of physiological processes appear to control the expression of resistance. It is of utmost importance to know the genetic-physiological interactions that bring about the expression of radiation resistance in these cells.

FUNCTION OF THE CELL NUCLEUS

In the Biology Division of the Oak Ridge National Laboratory, the synthesis of macromolecules is being studied in relation to the function and reproduction of the nucleus of growing cells. The genetic material deoxyribonucleic acid (DNA) must provide the information required for the synthesis of specific proteins, but must also function as a template for its own self-replication in the course of cell growth and reproduction. Our results support the well-known hypothesis that the ribonucleic acid (RNA) macromolecule is synthesized in the cell nucleus in a specific manner dictated by DNA, and that the RNA is transferred to the cytoplasm, where it, in turn, acts as a template for protein synthesis. We have found by the use of radioisotope tracers (1) that RNA is formed rapidly in the nucleus and appears to pass continuously into the cytoplasm and (2) that immediately following surgical removal of the nucleus from a cell, all RNA synthesis ceases. The experiments indicate that RNA synthesis takes place exclusively in the nucleus and that all cytoplasmic RNA must be derived from the nucleus.

We have also found that there are two periods in the life of a cell when DNA is apparently unable to support RNA synthesis, and, therefore, RNA synthesis stops. First, during the replication of the genetic code when DNA is presumably acting as a template for the synthesis of a new set of DNA, the RNA synthesis that is normally associated with this replicating DNA is completely absent. The experiment supports the idea that DNA acts as a template for both RNA and DNA synthesis and that these functions are mutually exclusive in a temporal sense. Second, when the cell enters division and the chromosomes are condensed into tight coils (as opposed to the highly dispersed state during the intermitotic, or growth, period), all RNA synthesis stops. The experiment is interpreted as evidence that DNA wrapped up into the highly condensed and compact form of the mitotic chromosome is unable to act as a template to guide the synthesis of either RNA or DNA. The absence of DNA synthesis in mitotically condensed chromosomes has been previously well established. Protein synthesis in the cytoplasm is not immediately affected by changes in nucleic acid synthesis in the nucleus, although any pronounced alteration in the rate of RNA synthesis in the nucleus is eventually reflected in the rate of protein synthesis in the cytoplasm. The latter finding is consistent with the hypothesis that RNA is the macromolecule by which the nucleus exerts control over synthetic activities in the cytoplasm.

PROTEIN SYNTHESIS

The problem of how amino acids are condensed into the large macromolecular proteins is being investigated at the molecular level in a number of cell-free systems. At the Oak Ridge National Laboratory one such system has been developed to the point where it is possible to observe the expression of a gene in a test tube. The synthesis of the induced enzyme β-galactosidase by a cell-free preparation from *Escherichia coli* requires the continual presence of the deoxyribonucleic acid (DNA) carrying the gene that determines the amino acid sequence in the enzyme protein. Studies are being conducted to determine the sequence of events occurring between the free amino acids and the fully formed protein and to determine the manner by which the amino acid sequence information in the gene is transmitted

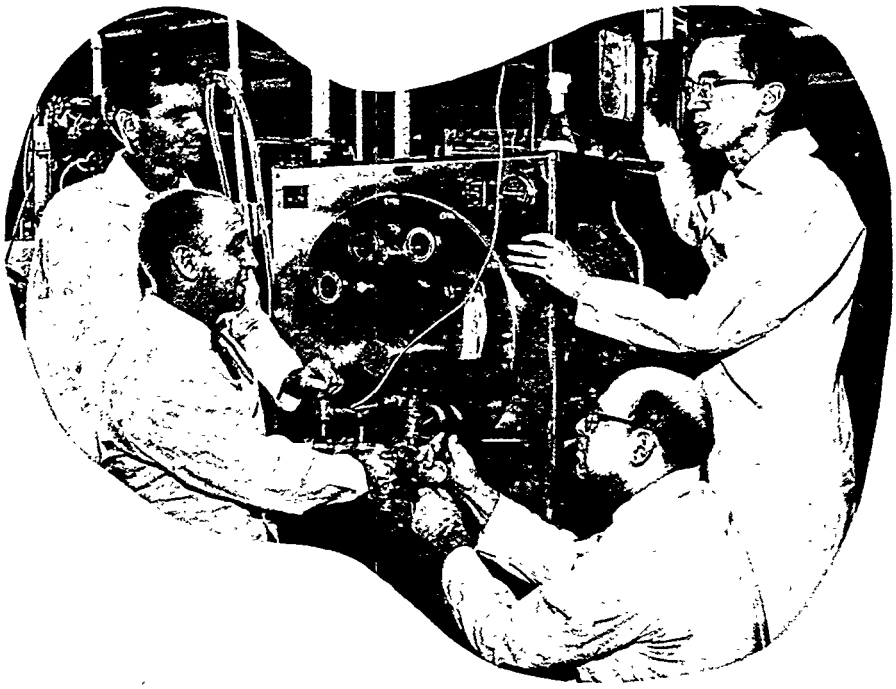

Biochemists observe operation of a Biogen, an apparatus for the continuous production of large quantities of bacteria used in a variety of enzymological studies.

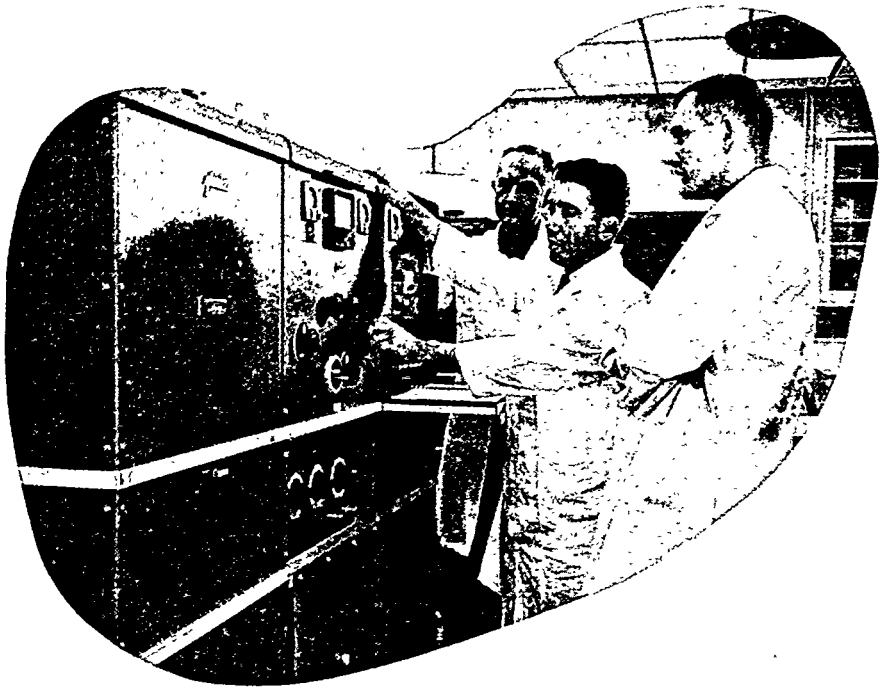

Biochemists observe final adjustments being made on the new Spinco Analytical Centrifuge in the Nucleic Acid Chemistry Section.

to the protein-synthesizing machinery. Preliminary experiments indicate that the genetic information is translated to a special kind of ribonucleic acid (RNA), called messenger RNA, and that the latter associates itself with ribosomes, thus becoming the specific template for the synthesis of this enzyme. One interesting observation is that the inducer of the enzyme must be present during the transcription of the genetic information from DNA to RNA. In the absence of inducer, although new RNA is made, such RNA does not contain information for the synthesis of this enzyme. This interesting phenomenon is being actively pursued because an understanding of the function of the inducer may help us understand how different genes in various cells are turned on and off at different stages of growth and metabolism. An understanding of these mechanisms is the key to an understanding of the regulation of normal growth and differentiation.

Similar studies are in progress with other microbial enzyme systems as well as systems from rat and mouse liver and germinating maize seeds.

NUCLEIC ACID RESEARCH

Nucleic acids and nucleoproteins are the important ingredients of the genetic apparatus, which is contained in the cell nuclei. The principal effects of radiations on living cells are caused by damage to the genetic structures in the cell nucleus. Hence, at the Oak Ridge National Laboratory there has been a long and intensive program of research on the chemistry and enzymology of nucleic acids and nucleoproteins.

From this work new constituents of ribonucleic acid have been discovered, and the chemical structures have been established, for example, that of pseudouridine. The important class of 2- and 3-prime nucleotides was elucidated in this project. Certain aspects of the detailed mechanism of biosynthesis of large polyribonucleotide polymers have been established. Mechanisms for the genetic transfer of information from one generation to the next are investigated here by comparing the chemical structure of the nucleic acids of bacterial cells and the viruses produced within the cells after infection.

MESSENGER RNA

The synthesis of a species of ribonucleic acid (RNA) that translates the genetic information in deoxyribonucleic acid to the sites of specific protein synthesis was discovered at the Oak Ridge National Laboratory in 1956. This discovery has now developed into one of the most active and important areas of research in biology; the tremendous recent effort of many laboratories may shortly lead to the solution of genetic specificity at the molecular level.

The universality of this "messenger" RNA in a variety of biologic sources has now been demonstrated in this laboratory, as well as in others. Independent techniques employed at the Pasteur Institute and at Oak Ridge National Laboratory arrive at the same probable mechanism of action of messenger RNA.

At present, efforts are in progress to isolate and purify this ribonucleic acid in order that its chemical, physical, and biologic properties can be elaborated.

THE PRIMARY ACTS IN PHOTOSYNTHESIS

The initial steps in photosynthesis involve conversion of energy from light quanta into some form which is available for utilization in the biochemical reduction of carbon dioxide to sugars. Since eight light quanta are needed to reduce one carbon dioxide molecule, and since the absorption cross section for photosynthesis is known to be the size of several hundred chlorophyll molecules, it appears that some type of cooperation exists between chlorophyll molecules in the photosynthetic apparatus.

Experiments at the Oak Ridge National Laboratory have shown that the photosynthetic apparatus of higher plants and photosynthetic bacteria, when dried, has electrical properties which are usually associated with organic semiconducting crystals. It has also been shown that upon illumination the photosynthetic apparatus (whether dried or in living cells) emits delayed light which has the characteristics of delayed-light emission due to untrapping of electrons in a semiconducting

crystal. The long lifetime of delayed-light emission could be explained if absorption of a light quanta results in an excited electron which may travel freely throughout a chlorophyll semiconducting system in a high-energy conduction band. The electron could be trapped, and upon untrapping would have some probability of falling back to the ground state and emitting the long-lifetime delayed light which is observed. The present experiments are concerned with the mechanism by which high-energy conduction-band electrons might be utilized in photosynthesis.

Recent studies of the delayed-light emission from living green algae have demonstrated that the dark decay curve of delayed light is dependent on the wavelength of exciting light. This result implies that the various colors of exciting light are not absorbed by the same photosynthetic pigment system and is consistent with other recent evidence that at least two photoreactions are present in higher-plant photosynthesis.

We have found that simultaneous excitation by wavelengths which cause enhancement (or "Emerson effect") of oxygen evolution results in a reduction of delayed-light emission. That is, the intensity of delayed light emitted after excitation with one wavelength is reduced when the plants are excited by both wavelengths. In the red region of the spectrum this negative enhancement of delayed light has the same action spectrum as the enhancement of oxygen evolution.

Chromatic transients similar to those reported for oxygen evolution have been observed in the delayed-light emission of living green algae. Under conditions where both wavelengths of exciting light result in equal amounts of delayed light, a shift from one exciting wavelength to another causes changes in the delayed-light emission, which then gradually returns to the steady-state value. The most effective wavelength combinations for producing chromatic transients are the same for oxygen evolution and delayed-light emission, and are also the most effective wavelengths for producing the Emerson effect and the negative enhancement of delayed-light emission.

It may be concluded that delayed light is emitted by the two pigment systems which are responsible for the Emerson effect and the chromatic transients in photosynthetic oxygen evolution. Since the function of each of the two pigment systems may be separated by the use of relatively precise delayed-light measurements, the investigation of the role of the two pigment systems in photosynthesis will be continued.

NEW GENETIC STRAINS OF PHOTOSYNTHETIC BACTERIA

Earlier work at the Oak Ridge National Laboratory has yielded several classes of mutants of *Rhodopseudomonas spheroides*: (a) forms showing hyperproduction of catalase, (b) forms lacking bacteriochlorophyll (BC), and (c) forms having abnormal carotenoid pigmentation. The third class includes types that accumulate (i) neurosporene, (ii) phytoene and phytofluene, (iii) phytoene only, and (iv) no identifiable polyene. These types demonstrate a block at almost every step of the currently accepted pathway for carotenoid biosynthesis (precursors → phytoene → → → spheroidenone). The missing link has been a mutant that accumulates zeta-carotene; a phenotype has now been isolated that accumulates phytoene, phytofluene, and zeta-carotene. The wild-type carotenoids prevent photooxidative injury sensitized by BC; they also cause a modification of the in vivo absorption spectrum of BC. Phytoene, phytofluene, and zeta-carotene appear not to show these signs of interaction with BC.

The traits listed above as (a), (b), and (c) have been combined in double mutants. Auxotrophic mutants incorporating these traits are now being sought, in order to provide material advantageous for genetic recombination studies. Two types of auxotroph have been isolated, one requiring histidine and the other apparently requiring a growth factor. These auxotrophs have, in turn, yielded forms lacking BC or carotenoids.

ULTRAVIOLET STUDIES

Studies of the action of ultraviolet (UV) radiation at the chemical and the cellular level constitute a most promising and fruitful approach to a better understanding of basic radiobiological processes. Such studies also yield important

information about the chemical structures and genetic apparatus of cells.

The effects of UV irradiation have been investigated at Oak Ridge National Laboratory along a number of different lines and have led to new and interesting results concerning the molecular changes produced by UV radiation.

Basic parts of the genetic apparatus of cells and viruses are nucleic acid polymers, which are polymers of four subunits: adenylic acid, guanylic acid, cytidylic acid, and thymidylic acid. The sequences of units (not known at present) presumably carry the information for protein synthesis and for their own duplication. A major effect of the UV irradiation of such polymers or of biological systems containing them is the formation of dimers between adjacent thymidylic acid units in a nucleic acid chain. This particular change in thymidylic acid probably accounts for over one-half the observed biological effect of UV radiation.

Chemical and optical techniques have been used to show that the dimers are formed by irradiation with 2800-angstrom light but are broken by 2400-angstrom irradiation. Subsequent irradiation with 2800-angstrom light forms them again. The presence of dimers in deoxyribonucleic acid (DNA) drastically affects the reactions between the nucleic acid polymer and various enzymes. The diesterases, which split off one unit at a time from a polynucleotide, cannot "chew" through a dimer. The dimer represents a block toward enzymatic degradation. Dimers also represent blocks to replication. DNA, which acts as a "primer" for DNA synthesis by a polymerizing enzyme obtained from calf thymus, when irradiated by UV light, is not a good primer. The decrease in priming activity is associated with an increase in the number of thymidylic acid dimers. Thus the presence of dimers in irradiated DNA can account for the observed changes in DNA synthesis produced by UV light in cellular and viral systems. If DNA synthesis in the neighborhood of a dimer is random rather than complementary, a mutant may be produced.

ELECTRON-SPIN AND NUCLEAR MAGNETIC RESONANCE STUDIES

As a means toward satisfying a continuing prime interest in studying radiobiological effects closely related to the initiating physical interaction of radiation with matter, a series of studies centered on the electron-spin resonance (ESR) measurements of chemical and biological systems has been in progress for several years. Investigations of this type lead to information concerning some of the primary basic physicochemical mechanisms involved in the action of radiation not obtainable by other methods. Studies conducted in the last year have extended our information on the kinetics of free radicals produced by ionizing radiation. A study was made of the free radicals produced by x-ray irradiation of succinic acid, disuccinoyl peroxide, and succinic peroxide, with the purpose of studying the role played by the free radicals of succinic acid in the formation of disuccinoyl peroxide or succinic peroxide. Preliminary studies were conducted on the natural and light-induced resonances in chloroplasts, chromatophores, and whole leaves at room temperature. Measurements for an international intercomparison of absolute number standards for ESR work have been made which reflect a continuing concern with measurement of numbers of spins present. Ultraviolet (UV) studies of amino acids at room and liquid-nitrogen temperatures revealed clear signals only at liquid-nitrogen temperature, and only with the aromatics, of which tryptophan seemed the most sensitive. The sensitivity to UV light per unit energy absorbed is much less than for ionizing radiation, unless local saturation effects greatly reduce the UV response. This suggests that little of the production of free radicals in amino acids by ionizing radiation can be due to low-energy excitations. Furthermore, it was found that the proteins bovine serum albumin and salmine showed far greater UV sensitivity at liquid-nitrogen temperature than did any amino acid. This suggests that disulfide and/or peptide bonds play a major part in the production of free radicals in proteins by UV light.

The nuclear magnetic resonance (NMR) technique offers a powerful method of attack on a

variety of problems in analytical and structural chemistry, in tracer studies, and in a number of more biophysical problems such as the physical state of biologically bound water. In collaboration with other groups in the Laboratory, the NMR approach is being used in problems of nulceotide structure and analysis as well as in polypeptide and protein chemistry. Work in the Biophysics Group has centered around the NMR spectroscopy of the radiation-protective compounds and in studies of the physical state of water in plant seeds.

Radiation-Protective Compounds

NMR spectra have been obtained under high resolution for S,2-aminoethylisothiourea (AET) and its various hydrolysis products and related compounds. With the determination of the spectra of the various pure compounds, it has been possible to easily follow the hydrolysis reactions of AET at different pH levels by examining the changing NMR spectra as the reactions proceed. This approach has been extended to studies of the formation of complexes of AET and its derivatives with serum proteins. Preliminary studies indicate that although AET does not readily complex, its hydrolysis product at normal blood pH, 2-mercaptoethylguanidine (MEG), does form a complex with serum protein. This observation thus supports the idea that the radiation-protection mechanism may involve transfer of energy or uncoupled electrons from a protein to the associated MEG molecule, where it can then be trapped.

Water Determination in Seeds

Electron-spin resonance studies of radiation-induced free radicals in seeds require quantitative knowledge of the amounts of water present in this material. By studies of the low-resolution proton NMR spectra of intact and ground seeds, it has been possible to make a rapid and nondestructive determination of this parameter. For wheat and barley seeds these calibration studies show that in the range of water content from 20% by weight to approximately 2%, the water is in a liquid form; that is, a sharp NMR line is observed, indicating that the water molecules are free to rotate and are in an essentially liquid or unbound state. Below 2% the removable water (by heat or desiccation) is "bound" in some loose chemical or physical manner, for in this range the NMR spectra show only the very broad resonance characteristics of the solid state.

AUXIN ACTIONS ON CELL DIVISION AND EXPANSION

Systems have been developed for studying (1) growth by expansion uncoupled from cell division and (2) cell division uncoupled from expansion in intact plants. At Oak Ridge National Laboratory, studies with the naturally occurring auxin, indoleacetic acid (IAA), have given clues concerning the mechanisms of auxin action as a growth hormone, as a herbicide, and as a causative agent in the production of plant tumors. A given IAA treatment can greatly stimulate growth of the coleorhiza and epiblast while greatly inhibiting growth of seminal roots in young wheat seedlings. IAA produces these same effects on these organs growing without deoxyribonucleic acid synthesis, mitosis, and cell division after gamma irradiation of the unsown grain. At different concentrations, IAA can either increase or decrease mitotic activity during appearance of the first mitoses in thermodormant lettuce seeds, in which there is no overall growth by expansion. IAA and the cell division factor kinetin exhibit a synergistic action on such mitotic activity, an action shown by the capacity of a given high concentration of IAA to inhibit mitotic activity in the absence of added kinetin and to increase mitotic activity in the presence of added kinetin. Thus IAA can have dual actions on growth in intact plants: it can influence (positively or negatively) growth by expansion apart from any possible actions on cell division, and it can influence (positively or negatively) mitotic activity apart from any possible actions on growth by expansion.

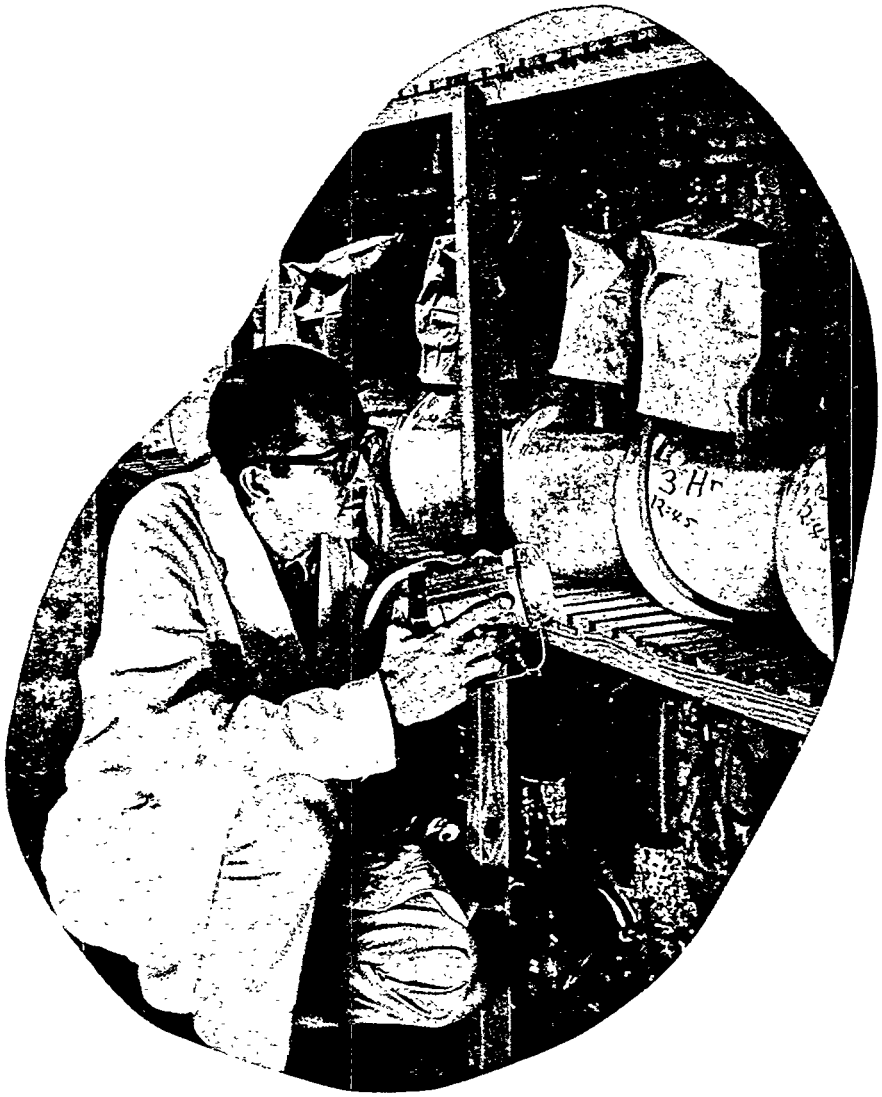

Geneticist examines colonies of the mold *Neurospora* in mutation study.

Environmental Research

RADIATION ECOLOGY

The ecology program at ORNL emphasizes three phases of radiation ecology: (1) development of quantitative information on biological accumulation and the movement of fission products and other radioisotopes in the plant and animal systems of terrestrial and fresh-water environments; (2) evaluation of the long-term effects on natural populations of plants and animals of chronic radiation resulting from radioactive materials introduced into the air, water, or soil; (3) use of radioisotopes as a research tool to better our knowledge of the delicate and little-understood balance of plants, animals, soils, and water, which together constitute natural ecological systems.

Research on Terrestrial Systems

Radioactive-tracer experiments and related supporting studies continued to provide fundamental information on the processes which maintain ecological systems such as forests. This work also provided a broader basis of experience for judging the problems of environmental contamination by radioisotopes.

A study of the behavior of Cs^{134}, a fission-product isotope, in white oak forests was completed during the past year. This was the first study of its kind in which the ecological cycle of an important radioelement was determined for one of the important hardwood species in this country. The purpose was to provide data for predicting the behavior of radiocesium which might enter a forest as fallout or as a product of atomic-waste-disposal operations. An average of about 40% of the radiocesium moved from the place of injection in tree trunks to foliage. Almost half of this foliage radiocesium was reabsorbed into the tree. Radiocesium transferred from trees via annual leaf fall was about two times greater than the quantity exported by rain. The annual loss of this radioisotope from inoculated trees was estimated at 19% of the original inoculation. Downward movement of radiocesium in soils under tagged trees was observed, and soils on wet sites had significantly greater percentages at lower depths down to 12 inches. However, 92% of the total soil radiocesium remained in the top 4 inches one year and seven months after tree inoculation. Transfers of radiocesium from litter to soil to plants were slight (0.3%) but started promptly, indicating that completion of a plant-to-soil-to-plant cycle may occur in a brief portion of a growing season.

The transition from behavior of a radioisotope inoculated in single trees to its ultimate distribution in a forest requires experiments in which large stands of vegetation are tagged in order to permit prolonged observation of the natural redistribution of tracers. Tracers experiments under field conditions on whole ecosystems are needed to help fill important gaps in the data needed for

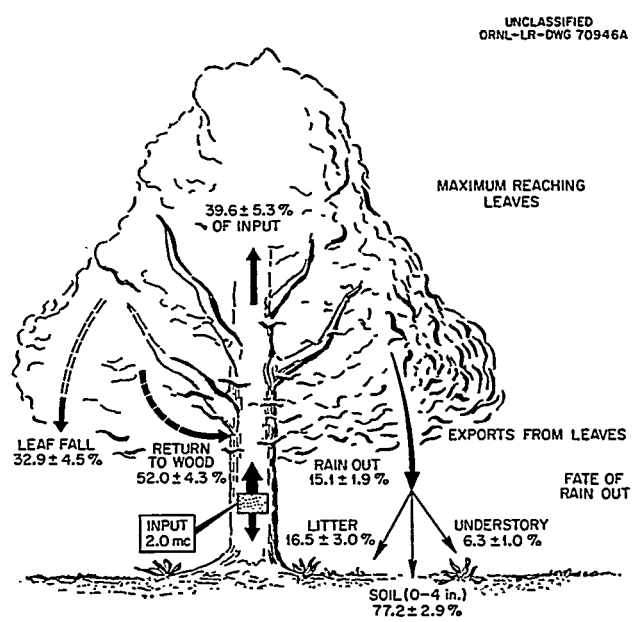

Cesium-134 cycle in white oak trees.

developing and evaluating theoretical ecological models for the circulation of elements. Results of the previous study on white oaks showed that cesium and presumably potassium circulate rapidly, through short-term cycles involving rain leaching from foliage, annual cycles involving foliage maturation, abscission and decay, and longer-term cycles involving tree mortality and root decay. Use of a long-lived tracer in an unusually productive and floristically and nutritionally rich forest of tulip poplar will provide a means for several concurrent and subsequent studies of the development, maintenance, and ecological interactions of a deciduous forest.

This experiment was started in the past year by tagging the overstory of a tulip poplar forest located in a protected flat-bottomed sinkhole area. A tower of scaffolding was constructed in order to provide a sampling and work area at several levels up to 40 feet above the ground. About 500 millicuries of Cs^{137} was introduced into the tulip poplars on this area. Some of the studies planned for this experiment include: (1) a comparison of the rapidity of the uptake of Cs^{137} and an estimation of the differential translocation and leachability of K^{42} for tulip poplar with previous results for other species; (2) determination of maximum radioactivity of the foliage and the subsequent

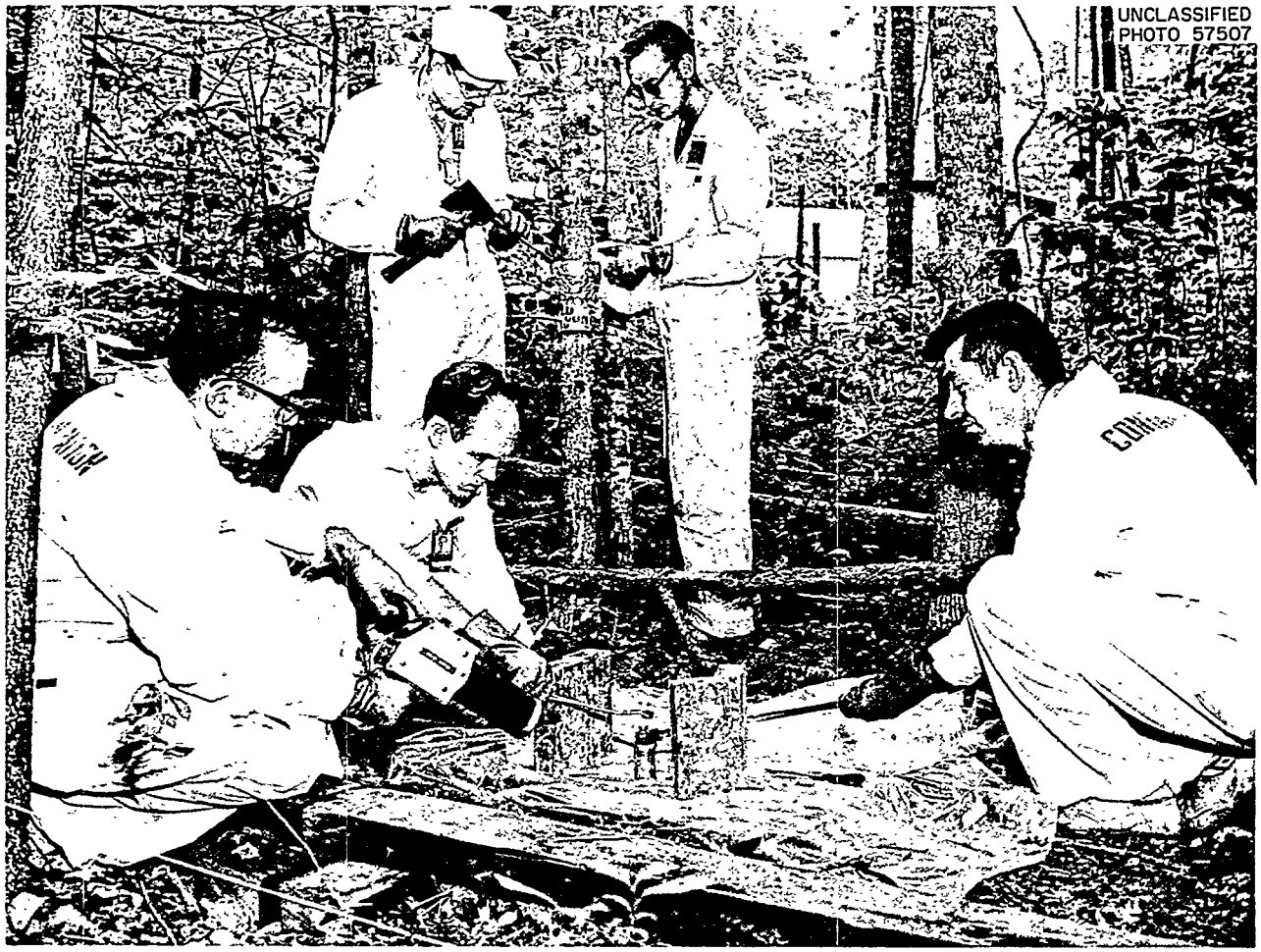

Tagging of a tulip poplar (*Liriodendron tulipifera*) forest with Cs^{137}. Scientists in center (rear) are readying a tree to receive the inoculation. Prior to adding the tag, water is added to a trough constructed around the tree and the bark is cut at equidistant points around the trunk. As water moves into the trunk, the isotope (being readied for dilution in foreground) is added to the trough with additional water for dilution.

decline due to leaching and reabsorption; (3) trapping of foliage-feeding insects in order to relate their activity to that of their food supply; (4) sampling of litter, soil, and soil moisture in order to indicate the rate and extent of infiltration into relatively homogeneous and permeable soil, which contrasts with the soils derived from Conasauga shales; (5) microbiological studies, in order to indicate the availability of radionuclides which have a high turnover rate through microbial populations; and (6) the measurement of radioisotope accumulation by invertebrate animals in leaf litter and soil.

Research in Radioactive Waste Areas

On the radioactive White Oak Lake bed at ORNL, ecological research on insects is providing information about the rates at which radioactive materials are passed from one type of organism to another. Insects feed upon the plants, accumulate radiostrontium and radiocesium from them, and eventually reach a state of equilibrium retention of radioactive chemicals. That is, the rate of feeding on the radioactive plants is balanced by the rate of excretion of radioactive materials from the insects. The rate of excretion provides important clues to the behavior of the radioisotopes in the plant-to-insect transfer. Measurement of the excretion rate of a radioisotope permits calculation of the rate of feeding of the insects, the total amount of radioisotope ingested by the insects, and the eventual concentration factor which may be expected. The excretion rate has been measured for strontium and cesium from different-sized insect species. Smaller insects excrete radioisotopes more rapidly than larger ones, so that larger insects build up higher body burdens. Immature stages of insects excrete radioisotopes more rapidly than do adults. Active insects excrete more rapidly than sedentary ones. Knowledge of these facts makes it possible to estimate the amounts of radioisotopes eaten by an entire community of insects.

Another way in which the excretion rates of radioisotopes provide information about the insect populations is in the detection of groups which behave differently metabolically. Newly emerged adults of the willow leaf beetles have slower excretion rates, since they are accumulating material to prepare for hibernation. Year-old beetles are actively mating, seeking oviposition sites, and laying eggs; these individuals have a more rapid excretion rate. This knowledge makes it possible to detect what part of the insect population is actually engaged in the business of reproduction – important information for estimating how rapidly insect populations may grow.

Clinch River Studies

Larvae of the midge *Chironomus tentans* Fab., a member of the fly family distantly related to *Drosophila,* live in the radioactive bottom sediments of White Oak Creek and the Clinch River below the Laboratory. The radioactivity adsorbed on the bottom silt results in a continuous dose of ionizing radiation to these larvae. This midge population has been subject to low-level ionizing radiation significantly higher than background since the first release of radioactive wastes to this area in 1943.

A preliminary investigation is now in progress to determine whether this 19-year natural experiment resulted in genetic changes in this population. A comparison was made of the salivary-gland chromosome slides prepared during October 1961. The 33 larvae collected from White Oak Creek had 43 aberrations of 12 types, and 29 larvae from the control area had 4 aberrations of 4 types.

There is a significant difference (P less than 0.001) between the number of aberrations observed in the contaminated and the control areas. If these preliminary results are substantiated during the ensuing year, an unusual opportunity will have been created for the study of the impact of radioactivity in nature on the population ecology and population genetics of a species. Since the irradiated population would differ from the non-irradiated populations by the frequency of occurrence of blocks of genes as indicated by chromosomal aberrations, there is an excellent occasion to study the flow of new gene combinations into surrounding populations, the fate of new mutations in the populations, and the effects of these mutations on the body structure. This information will provide a measure of the influence of localized radioactivity upon nearby populations.

Last year, staff ecologists demonstrated for the first time how clamshells may be used as biological indicators of the behavior of Sr^{90} over almost 500 miles of the Tennessee River. When Sr^{90} is

released to river water, a specific-activity ratio is established with the stable strontium in river water. Clams, which concentrate strontium up to 8500 times the concentration in the water, take up stable and radioactive atoms in the same proportion as they occur in the water.

The behavior of Sr^{90} was determined by comparing the specific-activity ratio in clamshells collected from locations 68, 164, and 489 river miles downstream from the release site with that of clams collected at the release site. The specific activity of Sr^{90} in the clams from the distant locations was equal to that expected on the basis of dilution of the contaminated water. Thus there was no significant loss of Sr^{90} from the Tennessee River water, indicating that Sr and Sr^{90} are in equilibrium with other components of the system such as organisms and bottom sediments.

These results indicate that low-level radioactive waste releases to the environment may be used as tracers to determine the fate of specific radionuclides in the wastes if the specific activity is determined in the organisms which concentrate these radioisotopes. The determination of nonradioactive strontium in natural water and organisms is of importance, because the presence of stable strontium governs the amount of radioactive Sr^{90} which may be taken up by organisms. A rapid and sensitive flame spectrophotometric method has been developed whereby trace concentrations of strontium can be determined in calcareous materials without the separation of strontium from calcium. This method, because of its speed and accuracy, not only will provide substantial savings in costs of environmental analyses but will contribute importantly to the understanding of the behavior of strontium in food chains leading to man.

Fish-tagging studies were conducted on the Clinch River in the vicinity of White Oak Creek to determine the movement of fish in this portion of the Clinch-Tennessee River system. Fish were caught in hoop nets, marked with numbered tags, and released at the point of capture. There have been 226 (4.31%) recoveries from 5244 fish tagged. Most of these recoveries were from white bass and white crappie. Particularly striking was the recovery of 142 (17.5%) tags from 812 marked white bass. Apparently, the white bass were originally captured as they made an upstream spawning run in the Clinch during April and May and then were recaptured by fishermen after returning to Watts Bar Reservoir. The distance between the point of tagging and recovery for white bass ranged from 14.2 to 60.1 river miles, and the average distance was 38 miles. The average time between tagging and recovery was 50 days. White crappie are more restricted in their movements, since the average distance between tagging and recovery is only 10 river miles and the average time the fish were at large was 89 days. It is evident that fish which

UNCLASSIFIED
PHOTO 38536

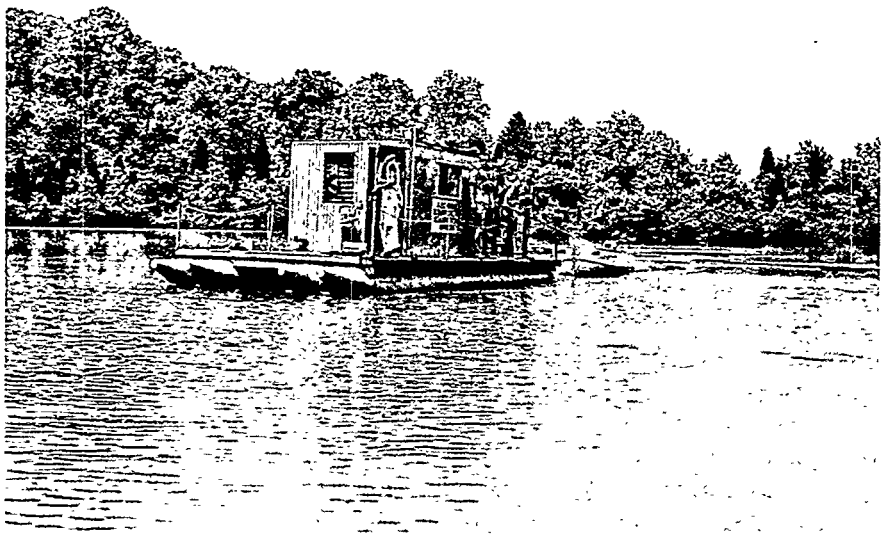

Setting hoop nets in the Clinch River. Movements of fish populations and their accumulation of radionuclides are studied by the use of netting techniques, electro fishing, and trapping. Operations are carried on from this laboratory houseboat, which is equipped for collecting and processing fish, and for conducting various types of physical and chemical measurements in water.

have been in the Clinch River in the vicinity of White Oak Creek move considerable distances in the Tennessee River system.

When the distribution of stable elements is known between water and fish, it should be possible to predict the concentrations of radioactive isotopes of those elements in the fish living in water receiving continuous releases of radionuclides. Fish-tagging studies showed that the white crappie tended to remain in the vicinity of capture. Consequently, individuals of this species from the Clinch River are being analyzed for Sr, Sr^{90}, Cs, and Cs^{138} to test the correlation between stable chemical and radiochemical analyses.

Initial results show 6.6×10^{-8} gram of strontium per gram of fish flesh (wet weight), which represents a concentration factor for strontium of 1.12 times. Bone samples contained 2.27×10^{-4} gram of strontium per gram of bone (dry weight), or a concentration of strontium that is 3850 times that in the water. The average Sr^{90} content of bone was 120 micromicrocuries per gram. This value in bone is equal to a water concentration which is 31% of the MPC of Sr^{90} in water in the neighborhood of atomic installations. These results agree quite well with monitoring data on river water. An analytical method for low concentrations of cesium has just been developed by the Analytical Chemistry Division for use on fish flesh and other biological samples. The preliminary analyses show that there is about 4.5×10^{-8} gram of cesium per gram of flesh (wet weight).

Health Physics and Instrumentation

CONTAMINATION CONTROL

A program was established at ORNL to study the basic and engineering aspects of deposition, retention, and redispersion of surface contamination. During the first year of the project, primary emphasis was directed toward evaluating standard methods of measuring "loose" contamination on various laboratory surfaces and toward examining the effects of surface pretreatment on the retention of deposited particulate contamination. A simple method was devised for assessing the potential reentrainment of deposited particulate matter into air currents impinging on the surface. Redistribution by air currents is greatly affected by surface pretreatment; thus, where air currents are the primary moving force, surface selection offers considerable promise toward promoting (or preventing) the retention of dust. On the other hand, particle removal by abrasion, as might be involved in contacting a surface with the hands or clothing, is affected only slightly by moderate differences in surface treatment.

ESTIMATION OF INTERNAL DOSE

Introduction

The Internal Dose Estimation Section attempts to establish safe guides and procedures which limit the intake of radioactive materials, thus holding the dose within acceptable limits. In addition to its continuing review of maximum permissible concentration (MPC) and body-burden values as recommended by the International Commission on Radiological Protection (ICRP) and the National Committee on Radiation Protection (NCRP), the Section has developed and improved two new interpretive tools during the past year which are reported below.

The first is represented by several statistical tests which permit objective conclusions to be drawn from the data on the concentrations of trace elements present in tissues of normal adults. These concentrations result from chronic (day-to-day) exposure and thus are typical of the concentrations of a radioactive contaminant which is present in the environment over long periods of time. It is to be expected that some individuals will have a higher concentration than others due to physiological differences as well as to differences in habits and tastes. This results in a distribution of dose values within the population. The present tests indicate with 95% confidence that the percentage of the population with doses exceeding three times the mean or median will not exceed 5% in most cases and may be even less, because it appears that the sample size is still a limiting factor in some of these cases.

The second procedure to be discussed provides a method of estimating an employee's bone burden of Pu^{239} on the basis of his urinalysis data. A computer code was written which carries out the calculations. This estimate seems to be within a factor of 2, generally, of estimates provided by other methods, but the accuracy of these is not known. In controlled situations – that is, in tests involving hospital patients where a known amount is injected and collection is complete – the code predicts the injected amount to within ±30% in all cases tested. The inaccuracy due to incomplete or sporadic sampling (in the occupational case) is probably much larger.

Estimation of Variability of Dose in a Population Under Conditions of Chronic Exposure

Maximum permissible concentration values are calculated for chronic low-level exposure by use of a "standard man" and thus, in general, do not take account of variations correlated with age, sex, weight, individual habits, etc. Under chronic low-level exposures, radioactive elements are expected to follow the same metabolic pathway as

that of the stable elements; that is to say, Sr^{90} follows stable strontium. Because large errors may be introduced by assuming that the excretion or deposition of chemicals in animals is similar to that in man, a study was initiated to determine the inorganic-element content of normal man. Tissue samples from 476 bodies of persons (ranging in age from 0 to 81 years) residing in 14 major cities of the United States and from foreign countries were analyzed by emission spectrography at ORNL.

These tissue-concentration values in themselves have only a limited meaning; therefore statistical tests were applied. The distribution of many isotopes in a variety of tissues was studied. The cases presented are chosen only to illustrate the methods and results.

One test was developed by Massey and determines the distribution of concentrations in the population with a certain confidence. In all cases, 95% confidence limits were determined, although others could have been determined. The second method, designed by Brunk, is used to determine with 95% confidence the percentage of a population above a particular concentration value. These two methods have been applied to obtain the curves shown in the figures for cadmium in kidneys and iron in the spleen. In the curves, the cumulative distribution of the sample is shown

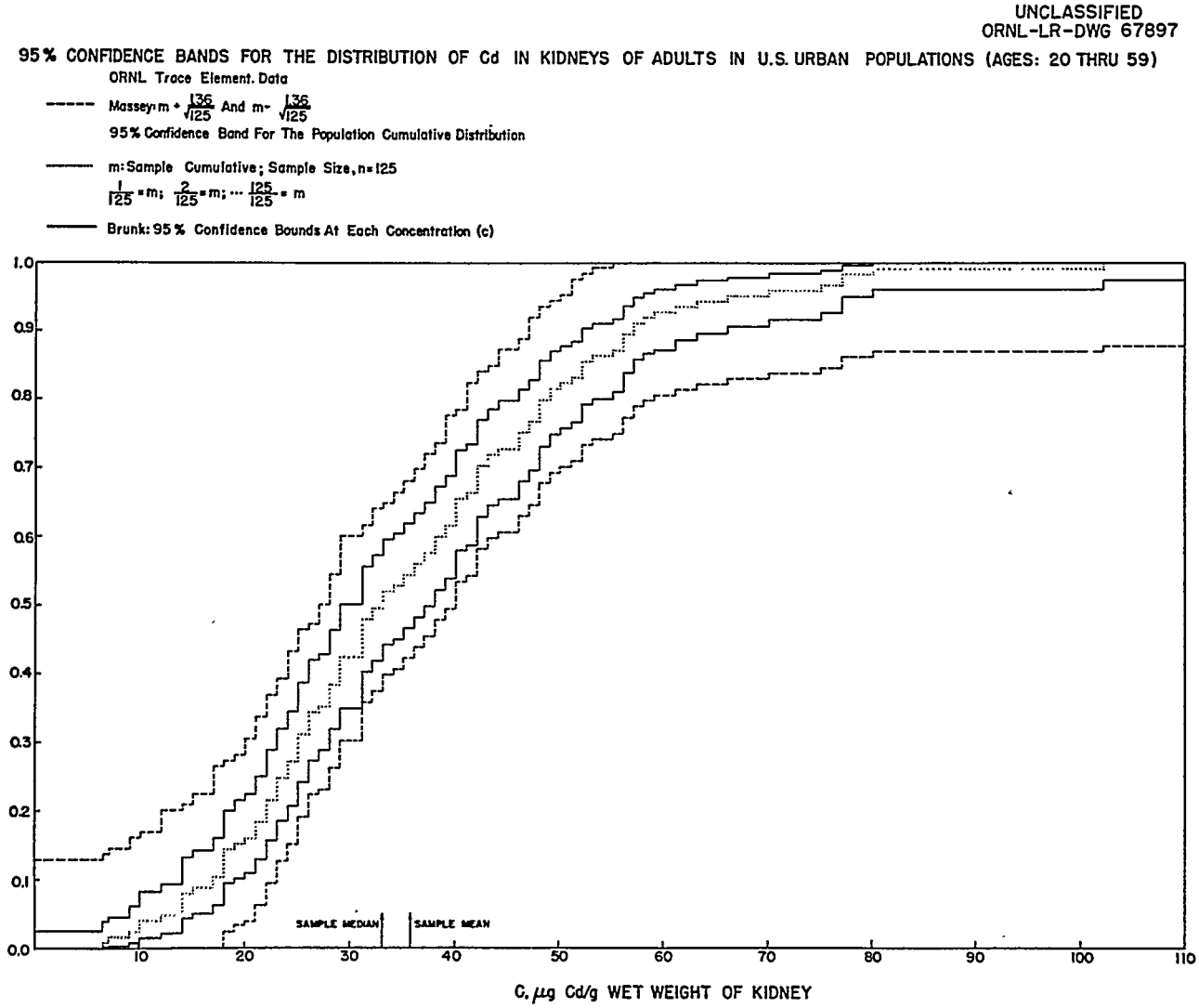

Ninety-five percent confidence bands for the distribution of cadmium in kidneys of adults in U.S. urban populations (ages, 20–59).

UNCLASSIFIED
ORNL-LR-DWG 69435

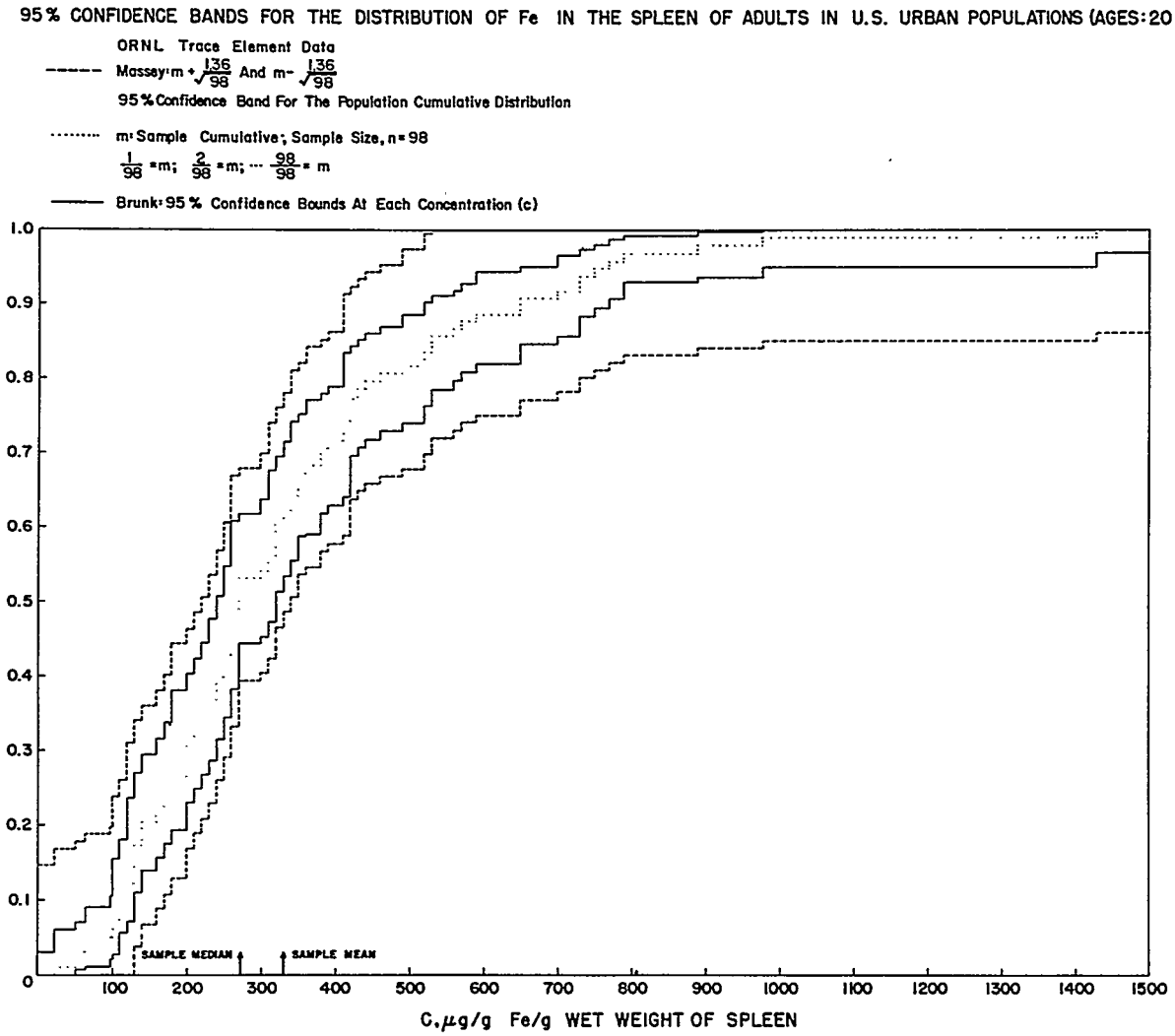

Ninety-five percent confidence bands for the distribution of iron in the spleen of adults in U.S. urban populations (ages, 20–59).

together with two bands about this distribution. The outer band, determined by the method of Massey, defines a region in which the entire cumulative distribution of the population will lie in 95% of the cases where this test is used; that is, it constitutes a 95% confidence region for the entire distribution curve of the population. The inner band defines a 95% confidence band for the percentage of the population above or below a given concentration value.

As stated above, the Federal Radiation Council and the ICRP estimated that the majority of the population will have a concentration not exceeding three times the mean value. From these curves one may assert with 95% confidence the percentage of the population which would be expected to exceed this value. From such statistical tests it is possible to estimate the dose variation of certain nuclides for the case of chronic low-level exposure.

Correlation Among the Metals Found in the Human Body

The chemicals Ca, Co, Cu, Fe, Mg, Mn, Mo, and Zn are called essential trace elements because they have known metabolic functions. An even

greater number of metals without known functions – that is, Ag, Al, Au, B, Ba, Bi, Cd, Cr, Ni, Pb, Sn, Sr, Ti, and V – occur in the human body in measurable amounts. Since very little is known about the metabolism of these nonessential metals, a study was made of the correlations between these and the essential elements. The correlation coefficient is a measure of the extent to which two variables vary alike and gives a quantitative estimate of the importance of factors which act alike on both variables. For a pair of elements, the correlation coefficient may have a value between +1 and −1. A value of +1 would indicate that for every individual a high value of one element is accompanied by a high value of the other, and a value of −1 would indicate that for every individual a high value of one element is accompanied by a low value of the other. Aluminum is highly correlated with other nonessential elements and appears to be a ubiquitous contaminant. Barium shows interesting correlations with both essential and nonessential elements. Cadmium is very highly correlated with zinc, as is strontium with calcium. In the brain, manganese is highly correlated with essential elements; in the lung, with nonessential. This is consistent with the observation that manganese poisoning results in a disturbance of the central nervous system. Chromium is correlated with zinc and copper in the liver and with nickel in most other tissues. Tin is correlated with zinc; lead with manganese and, to a lesser extent, with copper and zinc.

Interpretation of Excretion Data in Order to Estimate the Body Burden of Pu^{239}

Present procedures for working with Pu^{239} and other radioactive materials may result in some exposure of personnel. There is the ever-present possibility that small quantities may be ingested or inhaled. In the case of Pu^{239}, the radionuclide, once it has reached the blood, tends to deposit in the skeleton and in the liver. In such cases, the excretion rate is very low, and, once exposed, the individual will probably retain much of the material throughout life. Since animal studies indicated that a sufficiently large body burden of Pu^{239} may induce cancer, it is necessary to limit the body burden of Pu^{239} to levels well below those where damage might be expected. Since Pu^{239} in the body cannot be directly measured at these levels by present methods of monitoring the total body, it is necessary to base the estimate of body burden on the amount of Pu^{239} found in the urine or feces.

A code was written for the IBM 7090 computer, which interprets the urinary excretion of Pu^{239} (as given on the employee's record) in order to obtain an estimate of his body burden. This code is based on the known excretion pattern for man after a single injection of Pu^{239} into the blood.

The following table lists estimates of the body burden of Pu^{239} for 26 employees of Los Alamos Scientific Laboratory (LASL). Estimates of the body burden by W. H. Langham of LASL are shown, together with those determined by a computer program, PUQFUA, designed by J. N. P. Lawrence, also of LASL, and which embodies the same principles used by Langham in his personal evaluation of these cases. Since this method may reject some data as being inconsistent with the model, the number of samples rejected is shown. The estimates shown under PUQUAP and PUQUAE are those obtained by the present code, and they illustrate the effect of various assumptions concerning the time of the initial exposure. This effect is not of great significance. In general, the various methods seem to agree within a factor of about two, although occasional cases occur in which the disparity is greater.

The three related graphs show the sample values for employee E822; the effect of the three high urinary values, which the code PUQFUA rejected as inconsistent; and the effect of the rejection on the estimate. When the high values were rejected, it was assumed that the preceding value applied over the time interval between samples, but since no samples were taken, this is only a conjecture. In this case, the rejection of these values may be justified on other grounds, thereby resulting in an estimate more in line with the estimate based on the autopsy results for this case.

ELECTRON INTERACTIONS WITH WATER VAPOR

A study of the interaction of low-energy electrons with molecules in the gas phase can provide valuable data on elementary processes in radiation physics, radiation chemistry, and radiation biology.

COMPARISON OF PLUTONIUM BODY-BURDEN ESTIMATES

Code	Langham	PUQFUA	PUQFUA—Invalidated Samples	PUQUAP[a]	PUQUAP[b]	PUQUAE[a]	PUQUAE[b]
C135	0.08	0.1382	16	0.0882	0.1002	0.0758	0.0861
D334	0.07	0.1336	2	0.1002	0.1058	0.0872	0.0921
D711	0.07	0.1375	1	0.0901	0.1312	0.0785	0.1142
G717	0.06	0.0732	2	0.1340	0.1488	0.1168	0.1297
D63	0.06	0.1137	0	0.0702	0.0769	0.0611	0.0670
E36	0.06	0.0797	1	0.0739	0.0784	0.0644	0.0683
C397	0.05	0.0294	5	0.0454	0.0456	0.0390	0.0391
D501	0.04	0.0552	2	0.0376	0.0407	0.0328	0.0355
F664	0.04	0.0934	0	0.0511	0.0540	0.0445	0.0471
G716	0.04	0.0350	1	0.0242	0.0407	0.0211	0.0355
E742	0.03	0.0579	2	0.0490	0.0539	0.0427	0.0469
D775	0.02	0.0250	5	0.0231	0.0284	0.0210	0.0246
D182	0.02	0.0233	1	0.0179	0.0296	0.0156	0.0258
G524	0.02	0.0227	2	0.0177	0.0254	0.0154	0.0221
E629	0.02	0.0277	1	0.0165	0.0256	0.0144	0.0223
E390	0.02	0.0174	1	0.0173	0.0201	0.0151	0.0175
D791	0.02	0.0278	2	0.0205	0.0230	0.0178	0.0200
D591	0.02	0.0398	1	0.0213	0.0235	0.0186	0.0205
D205	0.02	0.0397	0	0.0156	0.0192	0.0136	0.0168
C137	0.02	0.0286	17	0.0350	0.0350	0.0300	0.0300
F634	0.01	0.0418	0	0.0478	0.0478	0.0413	0.0413
E252	0.01	0.0233	2	0.0173	0.0174	0.0150	0.0151
F412	0.006	0.0112	2	0.0103	0.0119	0.0090	0.0104
D670	0.006	0.0020	2	0.0179	0.0219	0.0156	0.0191
C365	0.006	0.0114	10	0.0090	0.0157	0.0077	0.0135
E822	0.032	0.0186	20	0.0296	0.0299	0.0255	0.0257
E822	0.0175[c]						

[a]Assumes exposure begins on date of first sample.
[b]Assumes exposure begins 15 days before date of first sample, with urine count predicted by excretion formula.
[c]Body-burden estimate from autopsy.

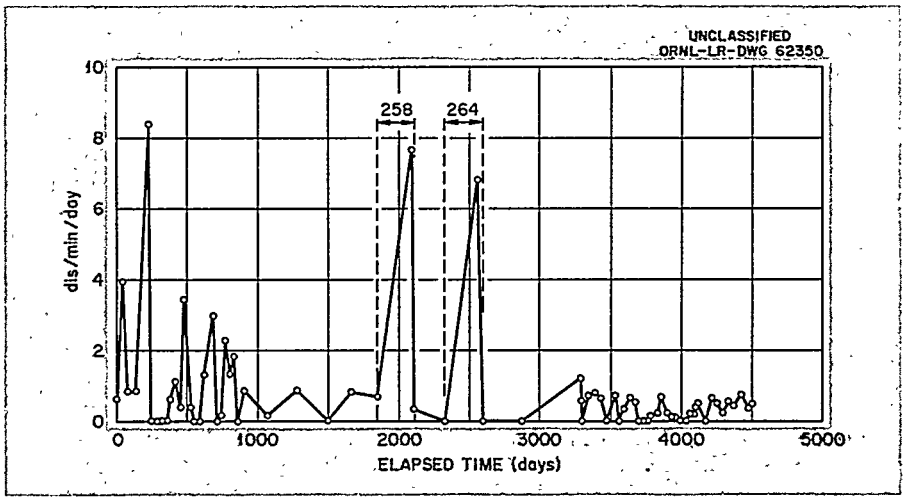

Urinalysis data of case E822.

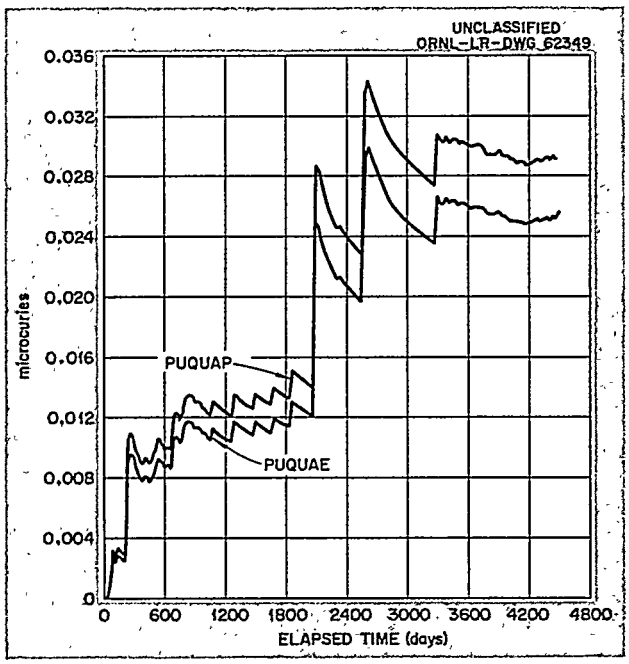

Estimated growth of body burden of case E822.

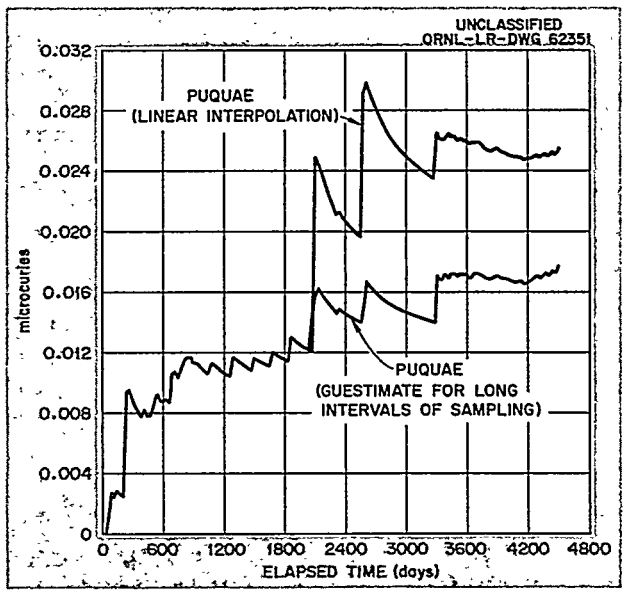

Two estimates of body burden of case E822.

A program is under way at ORNL to provide cross sections for low-energy-electron interactions and to clarify the basic mechanism by which electrons interact with molecules. In an electron-swarm experiment, it was found that electrons are captured by H_2O vapor in a resonance process peaking at 6.4 electron volts, with an energy-integrated cross section equal to 7.7×10^{-18} square centimeter per electron volt. At low electron energies (less than 1 electron volt), electron capture to H_2O vapor does not occur, suggesting that H_2O^- does not form as a stable ion. Electron transport times in gases (e.g., C_2H_4, CH_4, and CO_2) are greatly increased by the addition of small partial

pressures of water vapor. This suggests that long-duration collisions do take place and may arise from electron–permanent-electric-dipole interaction.

SIMULATED FALLOUT AREA

In the Frenchman Flat area of the Nevada Test Site, sources were arranged to simulate a plane source such as may be encountered in fallout. The array contained 441 equally spaced sources in the form of a square, 2000 feet on a side. Two sets of sources (Cs^{137} and Co^{60}) provided radiation of different gamma-ray energies. The radiation intensity at 3 feet above source distributions of 1 microcurie per square foot was about 0.2 milliroentgen per hour, which is about 20 times higher than the normal background radiation.

Aircraft equipped with scintillation counters and gamma-ray spectrometers measured the radiation intensity and spectra at various altitudes up to 1000 feet. Measurements of this type are vital to the interpretation of dose measurements made over fallout areas whether they are due to atom-bomb debris or radioiodine contamination from reactor accidents.

ABSORPTION AND REEMISSION OF ENERGY FROM ELECTRONS COLLECTIVELY EXCITED BY IONIZING RADIATION

For the last several years considerable experimental and theoretical work has been devoted to trying to estimate the importance of collective electron effects in the absorption of energy from ionizing radiation. Although certain energy losses experienced by an energetic charged particle in passing through various media have been attributed to the excitation of many interacting electrons simultaneously rather than to the excitation of a single electron, evidence has not been conclusive. It was postulated recently that any excited collective electron gas or plasma may loose its energy by emitting monochromatic light whose wavelength or color is characteristic of the energy of the excited plasma.

The observation of such light would constitute a strong argument in favor of the collective-interaction hypothesis advanced for explaining certain events that take place in biological systems and in metallic conductors. Experiments currently taking place at ORNL have so far failed to find any such light from thin films of silver, gold, copper, aluminum, sodium, and potassium. However, continuous spectra of light have been found, as postulated in 1945 by Russian physicists Frank and Ginsburg, who named such light "transition radiation" because it was expected whenever an energetic charged particle passed from vacuum into a solid, particularly into a metal. Experiments show that this light far exceeds in intensity the familiar visible part of the x-ray spectrum. Additional effort will be devoted to determining the dependence of the light on such things as the angle of observation with reference to the film, the film thickness and material, and the energy of the particle. Correlation of these observations with the optical properties of materials, such as the ability to reflect and transmit light, will improve understanding of those electronic energy states in solids that may be affected by radiation.

MODELS FOR THE STUDY OF RADIATION-INDUCED CANCERS

An attempt has been made to approach the problem of radiation-induced cancers through an analysis of natural or spontaneous carcinogenesis. The leukemias were chosen as the principal objectives for study because they are known to be induced by ionizing radiations and because there is a great wealth of evidence concerning them. That information was used in conjunction with a mathematical model in an effort to determine the etiological requirements for the different types of leukemia.

It is concluded that most childhood and adolescent leukemias develop from a cell containing three mutant genes, one of which is inherited. A condition of stress (for example, pneumonia) is an additional requirement. Many acute leukemias in adult life arise from a cell containing one inherited

and three somatic mutant genes. Chronic granulocytic leukemia usually involves a cell with three mutant genes and a defect known as the Philadelphia chromosome; occasionally, a mutant gene may substitute for the latter. Chronic lymphatic leukemia develops from a cell that has four mutant genes. It is tentatively concluded that most human cancers derive from a cell containing four mutant genes, one of which can sometimes be inherited. More complicated forms of inheritance are also possible. In certain cases, hormonal action can effectively substitute for a mutant gene. Although there is no sound evidence for a viral etiology in human cancers, on theoretical grounds a virus with the requisite specificity should be able to induce the malignant transformation in an appropriate cell.

Evidence of malignant neoplasms other than leukemias in Hiroshima survivors suggests that there was an increased incidence resulting from radiogenic simulation of the natural process. The situation with respect to radiogenic leukemias appears to be more complicated, and it is likely that at least three distinct mechanisms were effective at Hiroshima and Nagasaki.

HEALTH PHYSICS RESEARCH REACTOR AND THE JAPANESE DOSIMETRY PROBLEM

The Health Physics Research Reactor (a fast-burst reactor) was completed and will be used as an intense source of fast neutrons for health physics and biomedical research. The reactor is capable of delivering a burst of 10^{17} neutrons with a pulse width of about 38 microseconds and can be operated at a constant power up to 10 kilowatts. The first application of the reactor will be to obtain additional data on the penetration of neutrons and capture-gamma radiation, which are applicable to the problem of dose determinations for the Japanese survivors at Hiroshima and Nagasaki.

These experiments are in progress at the Nevada Test Site, where the reactor is suspended from a 1500-foot tower. Shielding structures, representing Japanese houses, are located at representative distances from the reactor tower. Neutron and gamma-ray spectra and neutron and gamma doses will be determined as a function of distance, and the radiation attenuation provided by the shielding structures will be measured. After completion of these tests, the reactor will be returned to ORNL and will be used as a neutron source, primarily for dosimetric and radiobiological studies.

BASIC INSTRUMENTATION: RESEARCH ON SEMICONDUCTORS AS DETECTORS OF NUCLEAR PARTICLES

The effectiveness of silicon surface-barrier detectors for energy measurements of heavy nuclear particles, such as alphas and protons, is well known. The need for detectors capable of analyzing the faster and more-penetrating beta particles stimulated a search for methods of producing detectors that have deeper sensitive volumes. This depth must exceed the maximum range of the incident particles if quantitative energy measurements are to be made.

One possible approach to the deeper-barrier requirement is simply to operate a surface-barrier detector at higher voltages, since the depth of penetration of the resulting electric field (and thus the sensitive depth) increases as the square root of the applied voltage. However, available detectors normally will not withstand the kilovolt potentials necessary to produce the required depths (1 to 1.5 millimeters).

Studies at ORNL showed that the breakdown voltage of a surface barrier can be greatly increased by appropriate control of the surface chemistry of the silicon. In essence, a surface barrier is a metal-to-semiconductor junction, which is formed by depositing a thin film of gold on one face of a silicon wafer. Also, the presence of certain chemical bonds (OH^-, I_2, CrO_4^{2-}, NH_3) can alter the normal surface charge on the silicon. By addition of controlled amounts of these substances, the charge distribution at the edge of the silicon-to-gold junction was modified so as to permit operation in the kilovolt range.

Such surfaces are sources of electrical noise, but it has been possible to suppress this edge noise by making use of a "guard ring" structure. This consists of separating the gold contact into two equipotential areas: a circular central spot (signal electrode); and a surrounding annular contact, which serves to isolate the noise.

With a modified silicon surface-barrier detector, sensitive depths up to 1.5 millimeters were produced by operating the detector at 2000 volts.

A second, also successful, approach to achieving sensitive depths of up to 2 millimeters was made by introducing lithium ions into the silicon lattice. The mobile lithium ions were drifted into the silicon in the presence of an electric field across the silicon diode. Lithium ions tended to distribute themselves in such a way as to produce intrinsic silicon.

These devices, called lithium-compensated *PIN* detectors, proved useful for high-resolution beta spectroscopy and low-energy x-ray and gamma-ray detection and spectroscopy. Spectra of the conversion electrons from the decay of bismuth-207 (1.050 Mev) exhibited 1% resolution, permitting an estimate of the ratio of not only $K/L + M + \ldots$, but also $L/M + N + \ldots$.

The improvements made in the silicon surface-barrier detector and in the lithium-compensated *PIN* detector now provide two new tools with comparable energy resolution capabilities which can now be used for the detection and energy measurement of nuclear radiation. A new field is now opened for low-energy gamma and beta spectroscopy, particularly of radionuclides having low specific activity. The energy resolution capabilities of these two new devices far surpasses the scintillation-counter capabilities.

ELECTRONICS

Two instruments were developed for the Office of Civil and Defense Mobilization at their request and according to their specifications. To date, two models of an aerial survey meter and one model of a shelter monitor have been developed and prototype versions fabricated. The aerial instrument is intended for use in a light airplane in order to make a survey after a nuclear event. The instrument is in two sections: a detector unit and an indicating unit. The detector unit can sit on the floor of the airplane, and the indicator unit is to be clamped to the control panel. Both accuracy and wide dynamic range are acquired by using three G-M tube detectors and three corresponding linear count-rate-meter circuits. The indicating unit has three meter readouts and color-coded lights to indicate the most significant reading. In addition, a tone is generated that corresponds to the count rate, and this signal permits the pilot to hear the rate or change of rate. A simulator has also been designed that replaces the detector unit for personnel training purposes. Full-scale values for the three ranges are 100 milliroentgens per hour and 1 and 10 roentgens per hour.

The shelter monitor is an ion chamber and linear electrometer with four ranges. The ion chamber has a 400-cubic-centimeter volume and is of simple but rugged construction. The electrometer circuit utilizes a single tube and is powered by two 6-volt lantern batteries. A transistorized dc-to-dc converter furnishes 500 volts regulated for the ion chamber. The ranges are 0 to 1, 10, 100 and 1000 roentgens per hour.

The Laboratory's entrance into the SNAP and Apollo programs resulted in requests from the Neutron Physics Division for engineering assistance in electronic-circuit development. Because of space and power requirements, most of the instrumentation must be transistorized. The experiments being performed have been with pulsed-type accelerators, which have resulted in a set of problems that are different from those encountered with reactor-type measurements. Photomultiplier gating circuits, timing pick-off circuits, time-to-pulse-height converters, fast-coincidence circuits, and fast-logic circuits have been developed as necessary building blocks of instrumentation for the experiments. Much of the work is in the time domain, and nanosecond pulse techniques are necessary for most of the design.

To date, two experiments have been performed at General Atomics in California and one at Harvard. Many such experiments are scheduled in order to cover the energy ranges of interest, and the instrumentation will continue to be modified and upgraded.

Isotope Development Program

Uses of Radioisotopes in Analytical Chemistry

A program on the application of radioisotopes in analytical chemistry was started during FY 1962. This program includes such applications as the testing of new analytical methods, isotope-dilution techniques, radioreagent methods, and the like. The intent is to solve analytical problems and to demonstrate the usefulness of tracer techniques, as part of the effort of the Division of Isotopes Development to further the use of radioisotopes for the public benefit.

Difficulties in the chemical determination of low concentrations of thorium in granite were solved by use of Th^{234} tracer. Details are given in report ORNL-3243 and in a forthcoming paper, *Determination of Thorium in Rocks by Radiotracer and by Gamma Spectrometry.* In searching for "gaps" in the analytical use of tracers, an extensive literature review was prepared, *Radioactive Tracers in Analytical Chemistry.*

Investigations by British and Russian workers of the photoneutron method for the determination of beryllium utilizing the $Be^9(\gamma,n)Be^8$ reaction suggest that this approach might be useful. Equipment was designed and is under construction; it uses Sb^{124} as the source of gamma radiation, and BF_3 counter tubes enriched in B^{10} to measure the neutron flux. The possibility of employing the photoneutron method in analyses in remote facilities will be investigated.

Isotope exchange reactions, which have been used extensively as a rapid and selective means of separating radioactive isotopes, are being studied to determine the concentrations of inactive isotopes by means of an active isotope. For example, inactive silver in solution can be determined by adding a known weight of AgCl that contains active silver and measuring the equilibrium distribution of the activity between the aqueous and solid phases. The rate of isotope exchange between solid and solution phases, however, usually depends critically on the method of preparation and the degree of aging of the solid. Consequently, studies were initiated concerning the possibility of utilizing isotope exchange reactions between immiscible liquid-liquid phases. A typical system might consist of a metal ion in an aqueous phase and a metal-reagent complex, containing an active isotope, dissolved in an organic solvent.

A survey of various metal-reagent compounds which might be suitable for isotope exchange reactions is in progress. It will be necessary to prepare the metal-reagent compound in a high degree of purity and then study its distribution between various aqueous and organic phases. At present, ion-association compounds formed between anionic metal complexes and tetraphenylarsonium ion are being investigated.

A new radiotracer technique was developed for the determination of trace amounts of fluoride. The fluoride is complexed with a radioactive metal and then extracted. The activity of the extract is proportional to the fluoride ion concentration. In this method, fluoride is complexed with Ta^{182} in a sulfuric acid system and the complex extracted with diisobutylketone. The extraction depends on the sulfuric acid concentration; the higher the sulfuric acid concentration, the more sensitive the extraction for fluoride.

Future work will involve testing the radiotracer technique for some common interferences and applying the method for the determination of fluoride ion in water and various industrial products. It is noteworthy that sulfate ion, a common interference in most fluoride procedures, is a requirement in this method.

Neutron-Activation-Analysis Research

The scope of the 1962 program was concerned with efforts in activation analysis applications, evaluations of activation analysis by use of various types of neutron sources, and in compiling a handbook on neutron-activation-analysis methods. Secondary efforts concerned with specific radiochemical separations and radioactivity measurement methods have also been pursued.

Many different applications of activation analysis were made in the physical and life sciences during this period. Ultrapure materials (metals, plastics, and the like), biological materials, water, geochemical specimens, petrochemicals, and foods are typical of the type of samples that were investigated. In particular, studies on biological specimens, such as blood, urine, and synovial fluids, were initiated in order to provide diagnostic evidence for trace-element effects in disease. Another significant study was directed to the use of activation analysis in forensic chemistry applications. Activation analysis was used to determine the origin of raw opium supplies and of illicit drugs. In these law-enforcement applications, activation analysis made it possible to afford a more specific identification of source areas than was possible by more-conventional analytical methods.

In the evaluation program, radioisotope-beryllium sources and reactor irradiation facilities have already been evaluated according to the practicability of their use in specific analysis problems. A low-voltage positive-ion accelerator of the Cockcroft-Walton type is now being installed for an extension of this evaluation. Source strength, type of neutrons involved, length of irradiation, sample size, etc., are being considered in these evaluations.

The handbook of activation analysis methods is now being readied for publication; many studies on radiochemical separations and radioactivity measurements have been made and will be reported. An extension of each of these efforts will be made for FY 1963.

Significant results were obtained from the use of a small Am^{241}-Be source system in activation analysis applications for determining macro concentrations of some elements in a variety of materials. Each analysis is made by a nondestructive method using gamma spectrometry.

Fission Product Recovery

Solvent extraction processes being developed to replace and extend the older precipitation methods for the recovery of fission products from reactor-fuel-processing high-activity waste concentrates (Purex 1WW) include the following:

1. A process to recover strontium and mixed rare earths by extraction with di(2-ethylhexyl)-phosphoric acid (D2EHPA). This was demonstrated in continuous countercurrent operation with actual Purex waste concentrate (see ORNL-3204 and ORNL TM-181). A modification of the ORNL strontium process was developed and used at the Hanford plant for the production of strontium from fission product concentrates derived from the waste.

2. Zirconium-niobium recovery with the same reagent, before the strontium extraction, was developed with tracers and simulated liquors (see ORNL CF-61-7-76).

3. Cesium recovery by extraction with substituted phenols from neutralized 1WW was demonstrated in batch countercurrent operation with tracers and simulated liquors (see ORNL TM-181, ORNL TM-107, and ORNL TM-265).

4. Feed pretreatment by amine extraction to remove nitric acid, sulfate, iron, zirconium-niobium, and ruthenium was developed with tracers and simulated liquors (ORNL TM-265). This may also serve for isolating zirconium-niobium and rare earths (ORNL TM-107).

5. These developments and the previously developed TBP process for rare-earth separation (ORNL-2863) are compatible and combine in a versatile integrated flowsheet (see drawing) for recovery and purification of all the fission products of principal importance.

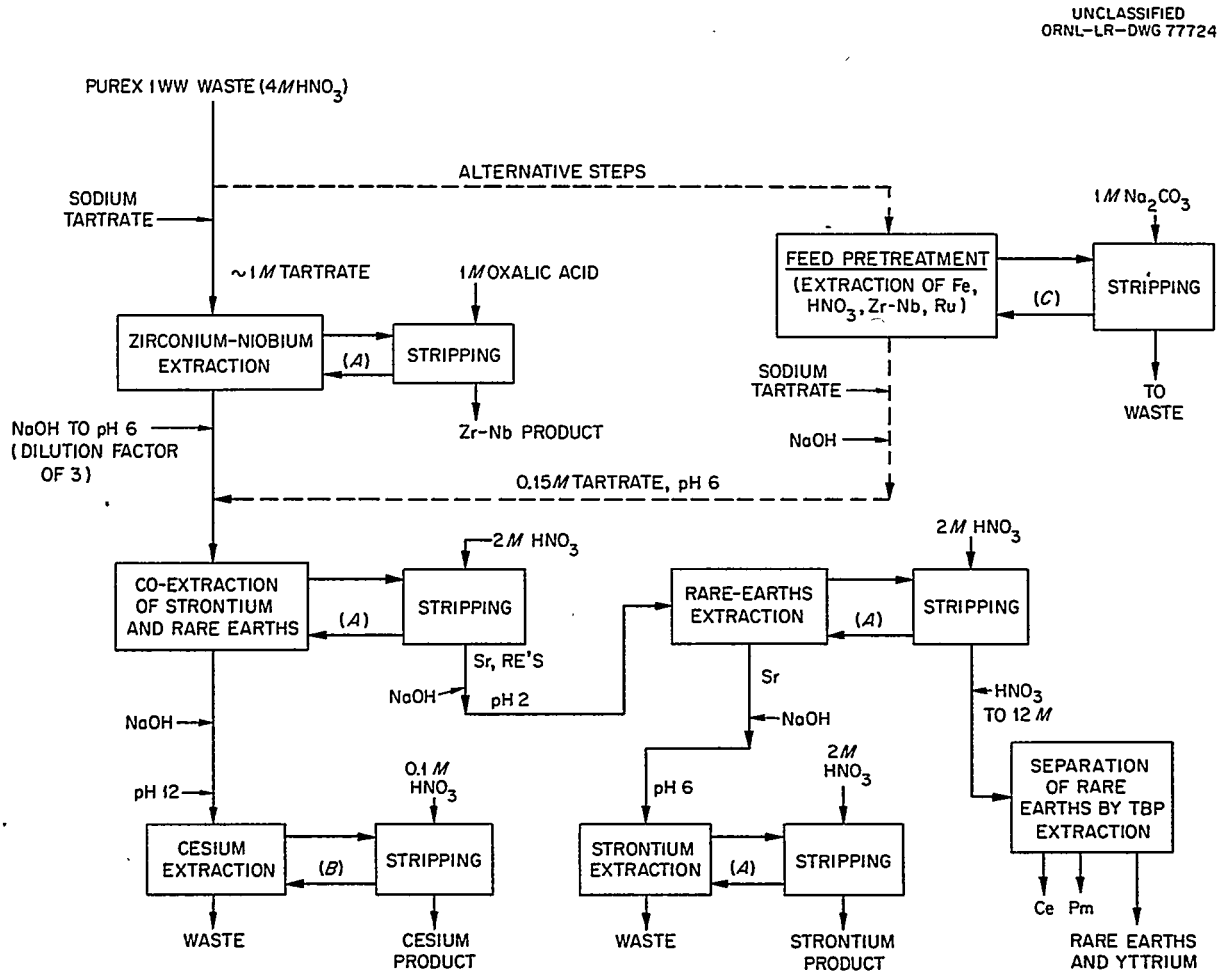

Tentative flowsheet for solvent extraction recovery of fission products from Purex waste concentrate. Solvents: (*A*), 0.3 *M* D2EHPA–0.15 *M* TBP in Amsco; (*B*), 1 *M* 4-*sec*-butyl-2-(α-methylbenzene)phenol in diisopropylbenzene; (*C*), 0.25 *M* Primene JM in Amsco.

Isotopes Development Center

INTRODUCTION

The work of the Isotopes Development Center is concerned with such activities as (1) the development of procedures such as those involved in the separation and purification of fission products; (2) the preparation and calibration of large radioactive sources; (3) the development of low-level radioactive sources; (4) the techniques for separating isotopes by thermal diffusion; (5) the preparation of thick and thin supported and self-supporting targets for accelerator and other types of research; (6) developing procedures for testing and evaluating sources and shipping containers; (7) the development of an inhomogeneous-field separator to improve calutron yields as well as the purity of stable isotopes; (8) studies of ion beams to improve calutron process efficiency; (9) ion-retention studies to increase the amount of separated material collected in the calutron

receiver; (10) development to improve charge material by internal chlorination and chemical techniques.

All these problems are related to the continuing responsibility of the Isotopes Development Center to provide large quantities of high-purity stable and radioactive isotopes in usable form.

RADIOISOTOPES

Solvent Extraction Recovery of Uranium

The decontamination and recovery of uranium is carried out very effectively by using two batch-solvent-extraction stages and by employing a differential extraction process (analogous to a Rayleigh distillation) in each stage. (A flowsheet for the first stage of this simple and practical arrangement is shown.) The extractant (e.g., 30% tributylphosphate in Amsco) enters the mixing vessel which contains an aqueous solution of uranium and fission products. After vigorous agitation, the mixed phases are rapidly circulated through the settler, where the extractant phase separates and leaves the stage, while the aqueous solvent phase returns to the mixing vessel. The concentration of uranium can be reduced to any desired level by continuing to pass extractant through the stage.

The second stage (not shown) simply reverses the process. The accumulated extractant from the first stage becomes the solvent phase, and the concentration of fission products can be reduced to any desired level by passing sufficient extractant (aqueous phase) through the stage.

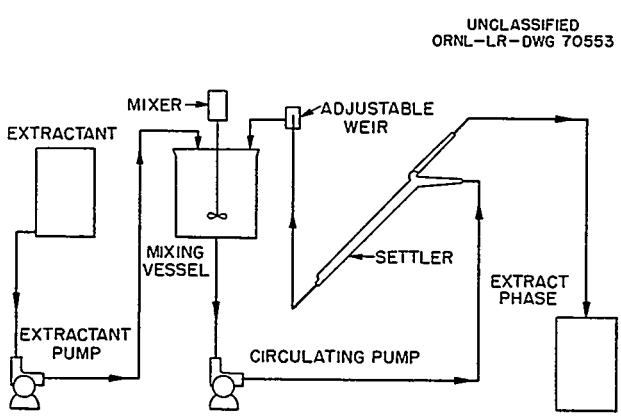

Extraction apparatus with light phase as extractant.

In the actual experiment for which this apparatus was designed, 15 kilograms of U^{235} was processed with an overall recovery of 99.5%; the decontamination factor for the fission products present was $>10^6$. The aqueous phase in the first stage was 3.6 *M* in HNO_3, 1 *M* in H_2SO_4, and contained 75 grams of uranium per liter. The second stage aqueous phase was 1 *M* in H_2SO_4 and 3 *M* in HNO_3.

Source Development and Fabrication

Preparation of Cesium Borosilicate Glass. – As a result of the need for an insoluble Cs^{137} compound to serve as a power source for an underwater generator, methods for preparing borosilicate glasses were investigated. The principal advantage of such a compound is its insolubility in water in case something happens to the containment system. However, the specific activity is lower than that for CsCl, commonly used in large sources.

The procedure used for a 27-kilocurie source to be employed by Lamont Geological Observatory for operating an underwater seismograph involved the following steps: (1) precipitation of cesium tetraphenylboron ($CsB\phi_4$) by the addition of sodium tetraphenyl boron ($NaB\phi_4$) to a solution of CsCl containing suspended fine-grain SiO_2; (2) filtration and drying of the $CsB\phi_4$-SiO_2 mixture; (3) calcining of the $CsB\phi_4$-SiO_2 mixture to drive off the organic and convert the cesium to Cs_2O and the boron to B_2O_3; (4) fusion of the residue at about 1200°C to form the $Cs_2O \cdot B_2O_3 \cdot XSiO_2$ glass.

The glass was fused into platinum dishes as it formed; six of these, each about 2.5 inches in diameter and 1 inch high, contained a total of 26.7 kilocuries of Cs^{137}, with a total heat output of 128 watts.

The volatility of the Cs_2O and the leach rate (solubility) of the cesium both vary considerably with the ratios of the constituents of the glass. Work is continuing to try to optimize the desirable characteristics. Also, other methods are being evaluated for converting cesium alum (the original product from the fission product separation process) directly to Cs_2CO_3 or Cs_2O.

Low-Level Radiation Sources. – There is an urgent demand for cheap, low-level alpha, beta,

and gamma sources which can be handled safely. One method for providing such sources involves fusing the activity in an insoluble form onto a suitable backing. A particularly fortuitous type of fusible substance would be an inorganic ion-exchange material which could first be used to adsorb the activity and then could be fused on the backing material.

Of several dozen potentially suitable ion exchangers which were tried, Decalso (a sodium aluminosilicate prepared by the Permutit Co.) proved to be the most suitable. It has a high exchange capacity, is efficient, and fuses very readily to give an adherent and insoluble layer of activity. The radiation level is readily controlled by varying the concentration of the solution being passed over the exchange bed.

Cesium-137, strontium-90, and other similar sources with activities as low as 0.01 microcurie have been prepared on 1-inch-square by ¼-inch-thick ceramic tiles by adsorbing the activity on Decalso and drying it, spreading a small amount on the tile, and then firing to give an insoluble nonsmearing glaze. It is also possible to incorporate the activity into various glasses, which are also insoluble and do not smear.

The Oak Ridge Gaseous Diffusion Plant has developed a method for coating, with thin metallic nickel layers, sources such as the glazed tiles just described. The coating provides further protection during handling and improves the appearance. Such sources can be prepared for about fifty cents each in large quantities.

Thermal Diffusion

Certain isotopic species, such as the inert gases, do not lend themselves to electromagnetic separation because of the difficulty in getting the atoms to "stick" in the calutron pockets, either physically or chemically. Hence it is fortunate that the thermal diffusion process can be used to separate these isotopes. It can also be used for any other isotopic separations where the gaseous state of the element or any of its compounds can be maintained.

Equipment has been designed and is in operation for the separation of research quantities of the low-abundance isotopes of neon, argon, and krypton. Columns have also been installed to investigate the separation of Xe^{124}, and large equipment is now operating for the separation of C^{13} by use of CH_4. The accompanying table shows the present status of the thermal diffusion program.

Isotope	Normal Abundance (%)	Enrichment of Present Product (%)	Expected Enrichment of Future Product (%)	Approximate Quantities of High Enrichment to be Available	Date Expected
Ne^{21}	0.26	2.3	30	0.5 g	1–63
Ne^{22}	8.82	99.97		2 g	In stock
Ar^{36}	0.34	99.5		2.5 g	In stock
Ar^{38}	0.06	2.2	30	0.5 g	1–63
Kr^{86}	17.37	>99.9		0.5 g	In stock
Xe^{124}	0.10	0.6	10	0.5 g	6–63
C^{12}	99.89		99.99	10 kg	1–64
C^{13}	0.11	~30	>85	250 g	25 g by 10–62

Target Information for Thin Self-Supporting Elemental Targets						
			Method of Preparation			
					Evaporation	
Elements	Approx Thickness of 0.001-in. Foil (mg/cm^2)	Thickness Typical Unsupported Thin Target ($\mu g/cm^2$)	Rolling	Electroplating	Resistance Heating	Electron Beam Furnace
Lithium	1.2	>1000	X			
Boron	6.2	20–300				X
Carbon	5.7	10–200			X[a]	
Magnesium	4.2	500–2000			X[b]	
Silicon	6.0	25–200			X	
Calcium	3.7	>1000	X			
Scandium	6.1	>1000	X			
Titanium	11.2	>1000	X[c]			
Vanadium	15.0	>1000	X			
Chromium[d]	18.0	600–2000		X	X	
Iron	20	>500	X			
Cobalt	22	>1000	X			
Nickel	22	>5			X	
Nickel	22	>300	X			
Copper	22	>1000	X	X		
Zinc	17	>1000	X			
Zirconium	16	>1000	X[c]			
Palladium	30	>1000	X			
Silver	23	>1000	X	X		
Cadmium	20	>1000	X	X		
Indium	18	>5000	X			
Tin	18	>3000	X			
Tantalum	42	>2000	X[c]			
Tungsten	48	>1000	X[e]			
Platinum	54	>2000	X			
Lead	27	>8000	X			
Lead	27	>1000			X	

[a]Carbon arc.
[b]Simultaneous thermochemical reduction and evaporation ($MgO + Al \rightarrow$).
[c]Rolled from "crystal bar."
[d]Subject to ductility of particular sample.
[e]Suspended in copper matrix.

Source and Cask Testing

In addition to making available high-purity radioisotopes, ORNL has the responsibility of seeing that those isotopes are suitably contained and properly shipped to the customers. Thus, both a source-evaluation and testing program and a shipping cask testing program were initiated. Criteria are being set up which will assure maximum safety of the encapsulated sources and maximum protection against spread of contamination during shipping. The sources and casks are subjected to leak tests, fire tests, physical and thermal stresses (including dropping, compressing, etc.), corrosion tests, and pressure tests. It is expected that, as a result of this program, a set of reliable fabrication standards, quality-control procedures, and evaluation methods will be made available to industry, to Commission facilities, and to the various states interested in regulatory practices.

Target Fabrication

The needs for targets for all types of research are numerous and varied. The Isotopes Development Center of ORNL is operating for the AEC a target fabrication center and is involved in the preparation of normal and isotopic targets of all kinds, including massive targets of metals and compounds, thin rolled foils, thin evaporated or electroplated self-supporting films, and supported (on backings) films of elements and compounds. The preceding table lists the types of targets currently being fabricated. In addition to these, development work is continuing to provide thinner and purer films of all kinds – particularly those which are required to be self-supporting.

ELECTROMAGNETIC SEPARATIONS

Inhomogeneous Field Separator

Limitations imposed on beam dispersion by the 24-inch radius in the calutron necessitated the investigation of a separator which would increase this dispersion yet retain the advantageous features of the calutron. In theory, a double-focusing isotope separator having an inhomogeneity of 0.5, a reference radius of 20 inches, and a deflection angle of 255° would increase beam dispersion by a factor of 1.6 over that experienced in the 24-inch-radius calutron.

A theoretical magnetic field was calculated which would eliminate radial aberrations to ion trajectories in the field $H = H_0(r_0/r)^n$ in all planes within 3 inches of the median. Shim contours required to produce this field were determined by a computer program that evaluated a series of approximations in which shim surfaces were considered to be magnetic equipotentials.

An experimental model was assembled with the shims as initially fabricated to the computer-determined specifications and with specially designed ion source and receiver components. Enriched samples processed from experimental runs of four elements were of higher isotopic purity than those previously obtained in either the 24-inch- or the 48-inch-radius calutrons.

Magnetic fields were measured in this system to determine deviation from theoretical values. Results show that present deviation from the field theoretically sought produces an image aberration of 0.065 inch for beams including ±8° divergence. In the standard beta calutron the aberration produced by similar beam spread is 0.075 inch. Thus, with the present shim system, the factor chiefly responsible for the increased purities obtained from the 255° separator is the 66% increase in separation between ion beams of corresponding isotopes.

It is anticipated that at least the first half of FY 1963 will be delegated to further investigations and experimental testing of this separator.

Ion-Beam Studies

A study is being made in order to determine the nature of the plasma associated with a calutron beam and to establish its effects on the primary ion beam (joint project with the Thermonuclear Division). Frequencies associated with intensity modulations of the primary beam entering a collector pocket and the resulting effect on focus have been observed. The growth of secondary plasma due to the primary beam and background neutrals has been studied.

Experiments show that the secondary plasma ion production rate increases linearly with pressure (as might be expected from charge exchange and

primary ionization) until a pressure of approximately 4×10^{-5} millimeter of mercury is reached; then the ion current rises sharply to an upper limit, with further increase in pressure.

Both arc conditions and residual gas pressures contribute to beam instabilities. Measurements indicate fluctuations in focal position ranging up to a maximum of 4 inches. These instabilities are not readily discernible when ion beam monitoring is dependent upon milliammeters; however, oscillations can be detected and continuously monitored with an oscilloscope connected to a conventional receiving pocket. Further studies concerning these instabilities will be made.

Ion Retention Studies

The retention of ions in receiver pockets that was achieved over the past two-year period averaged 80%, a 43% increase over the retention averaged from 1946–56. This increase is a result of equipment modifications that offset both the losses associated with the sputtering of receiver pocket walls and the low retention of isotopes on surfaces struck by ions.

A large and specially shaped collector pocket improves retention and provides a means of determining sputtering and saturation values under actual conditions encountered during the separation of large quantities of isotopic material. The ion beams strike a material having a low sputtering ratio, and the sputtered material collects in a well-cooled region protected from ion bombardment.

Measurements reveal that many target atoms are sputtered by a single impinging 35-kiloelectron-volt ion and that ionic saturation of target surfaces is in the order of milligrams per square centimeter. Data from collections indicate that percentage retention on the surface area struck is related to current density. Lower current density increases the percentage of retention on the target area.

Experiments performed with a Ca^{46} ion beam (0.22 microampere per square centimeter current density) on graphite, copper, and crystalline copper (with the 110 crystal face perpendicular to the beam) confirm that samples of higher isotopic purity can be obtained by selectively recovering material from the area struck by the ion beam.

In order to increase knowledge of sputtering and saturation values, other materials suited for use in receiver construction and target formation will be investigated.

Internal Chlorination

Chlorination of metal oxides by externally feeding chlorinating agents into the calutron was first used in Scandinavian separators to convert small quantities of oxide into separator charges. ORNL investigated this technique in order to determine its practical applications as well as the principles involved which determine its effect on the operation. The following schematic diagram illustrates the equipment used in the internal-chlorination process.

In a majority of cases, calutron operation with internal chlorination proved superior to that with the prepared chlorides; however, the basic reasons for such improvement are unknown. As soon as the new containment facility is available, the internal chlorination of plutonium feed material will be investigated. If the technique proves practical, the plutonium charge material would be used more efficiently, and a less complex procedure in chemistry would be required.

Decelerating Receiver

Increasing demands for accelerator targets of high isotopic purity for use in nuclear studies led to the investigation of a method for target preparation within the calutron. Such a procedure would permit a one-step process and would result in less contamination of the target. If an ion could be decelerated to an energy resulting in a self-sputtering ratio of less than one, a buildup that produces the target would occur in the area of impact.

A decelerating receiver was constructed so as to reduce ion energy by varying the potential from ground to receiving surface. Targets may be inserted into the receiver pocket so that direct deposition occurs or may be placed so that material is sputtered onto the target backing.

Research determinations to establish maximum permissible energy at impact will continue.

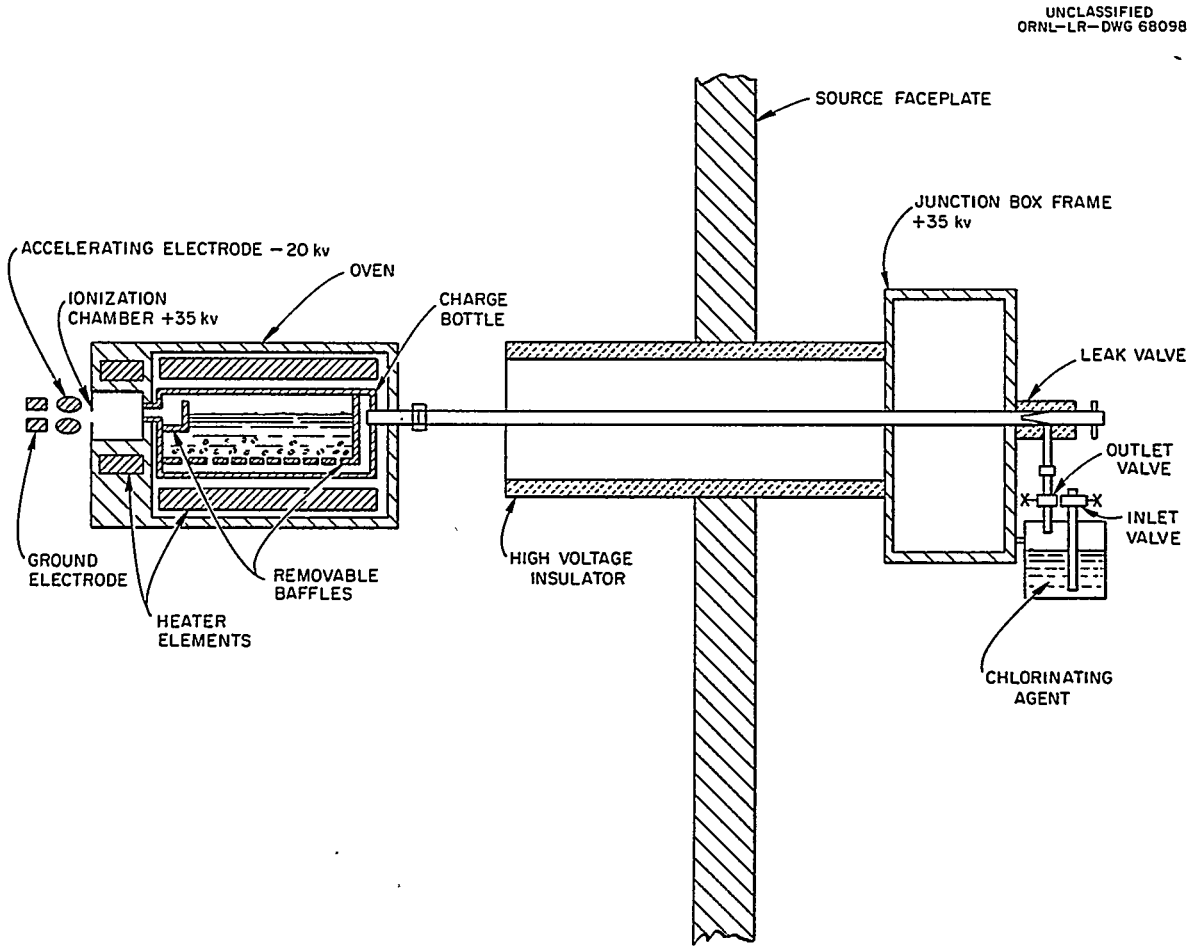

Schematic of internal chlorination process.

Developmental Chemistry

Advancement in achieving chemical purity was realized by applications of new techniques in refining isotopic samples of lead and the rare earths.

Special conversions of inventory samples included the formation of malleable, isotopically enriched zirconium and titanium metal in purities suitable for pressing and rolling into foils for cyclotron studies. The finely divided metal was reacted with elemental iodine, under vacuum, at a temperature of 225°C in the presence of a hot 7-mil tungsten wire; the metal was deposited in a pure form by thermal dissociation on the filament. The coated wire was pressed into a thin sheet and the tungsten filament removed. Repeated rolling results in foils of pure metal.

New techniques have been established to convert isotopically enriched barium from the inventory form of barium nitrate to barium oxide and to prepare anhydrous hydrogen chloride from isotopically enriched chlorine stored as sodium chloride.

Present developmental efforts are being directed toward forming special alloys from isotopically enriched samples and providing isotopically enriched rare earths as metals.

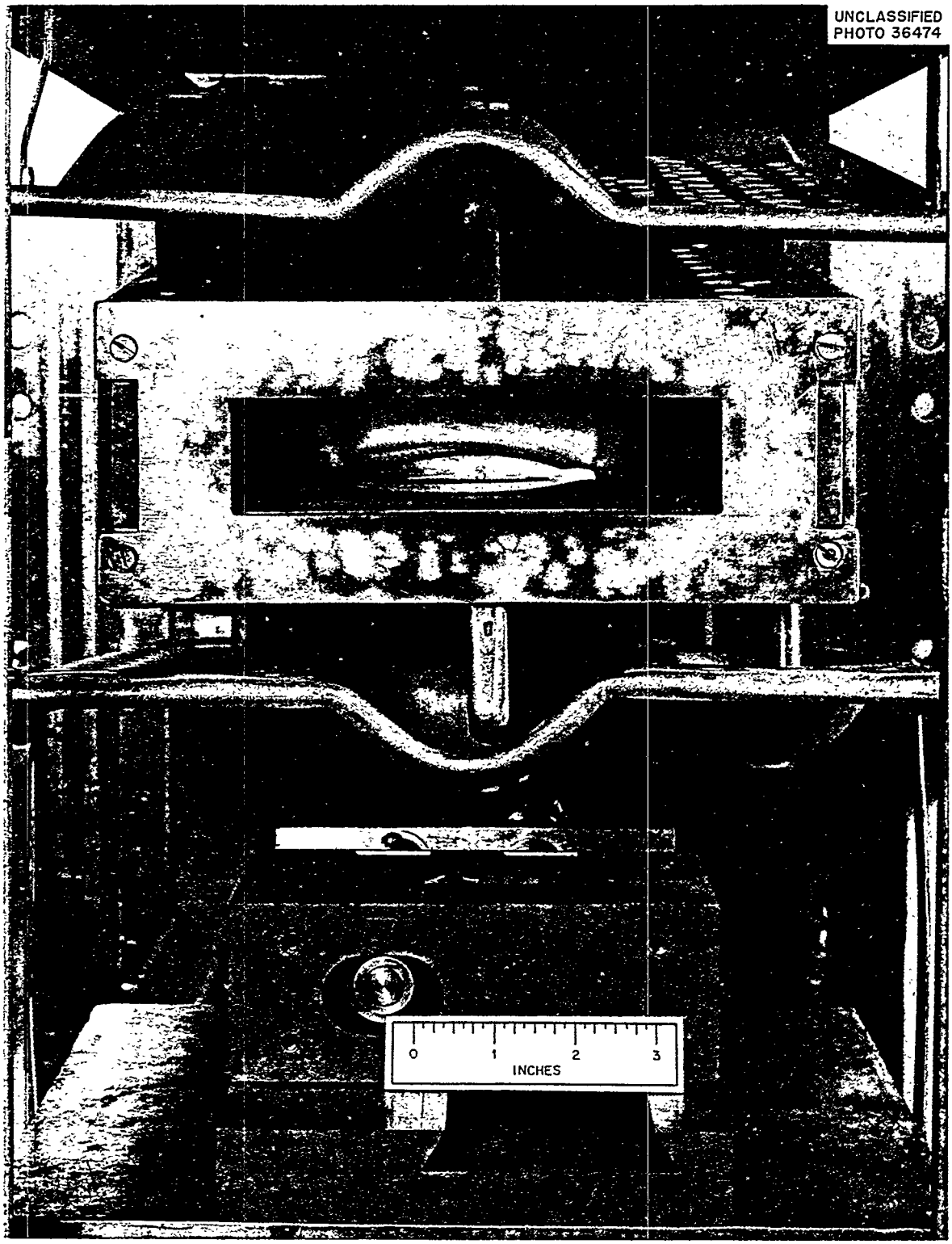

Decelerating receiver.

Training and Education Program

International Programs in Reactor Technology

The task of providing suitable training and experience in the fields of reactor operations supervision and in nuclear reactor safety, particularly with respect to selecting reactor sites and safe design, has become increasingly significant as the use of nuclear reactors has expanded.

Since 1959, the Reactor School of the Oak Ridge National Laboratory has offered two educational programs in order to provide this training: nuclear reactor operations supervision and nuclear reactor hazards evaluation. The programs represent a coordinated intense application of both lecture and laboratory training, which provides participants with the fundamental education required for reactor operations supervision and reactor hazards evaluation. The two programs directly support efforts of the U.S. Atomic Energy Commission to assist foreign countries in training their personnel, many of whom will eventually be responsible for establishing and guiding nuclear research and development programs in their own countries, particularly in connection with nuclear power stations.

The program of training at the Reactor School is also utilized by the AEC for the training of Commission and Commission contractor employees. With the increased emphasis on nuclear operational safety within the AEC and with its requirement for trained people, the programs, especially the Hazards Evaluation course, are quite applicable. Other government agencies make use of the programs for training in relation to their nuclear programs. These agencies include the Department of Health, Education, and Welfare, the Department of Defense, and the National Space Agency.

Eighty-nine students completed courses at the Reactor School during fiscal year 1962. Also, eighty-four students were enrolled for courses in the fourth session. Thirty-one students representing seven different countries completed eight months of their twelve-month program. Preparations were made for conducting a fifth session of International Reactor Programs in order to accommodate a moderate increase in the number of applications. The level of instruction is to remain the same.

Although basic nuclear technology courses relating to the reactor development field are available through several universities and colleges, specialized advanced courses generally are not offered. The instruction at the Reactor School is deliberately presented in such a way that the interrelationship of the various courses are emphasized in a manner not normally seen in university curricula. This close integration of subject matter is an important factor in achieving the objectives mentioned above within a one-year period.

Other Educational Programs

ASEE-AEC BASIC SUMMER INSTITUTE

Summer Institutes on Nuclear Energy for engineering-college faculty members are sponsored jointly by the American Society for Engineering Education and the Atomic Energy Commission. The 1961 ASEE-AEC Basic Summer Institute at North Carolina State College was given for the eight weeks from June 19 through August 11, 1961. Participants spent the last week of this period at the Reactor School of the Oak Ridge National Laboratory. The Reactor School work consisted of seven experiments in radiochemistry and physics (including a criticality experiment at the Pool Critical Assembly), tours, lectures, and preparation of reports covering their experiments. Twenty-eight participants completed the summer institute program and received certificates.

An evaluation committee, appointed by the ASEE, submitted the following conclusions in

their analysis of the 1961 program. "This program which has been offered for several years is well developed, efficiently organized, and the participants consider the program to be very worthwhile. The faculty at North Carolina are sold on the worthwhileness of the basic institute program but would like to see more homogeneity in the participants if possible. The faculty at Oak Ridge are not convinced that the basic institute is the best way to introduce a beginner to the field. They feel that it is not of sufficient length to develop a thoroughness of understanding in any part of the field. However, they indicated a willingness to cooperate with North Carolina on a program during the summer of 1962 if they are asked to do so."

SUMMER INSTITUTE FOR PHYSICS TEACHERS

In 1960 the Oak Ridge Institute of Nuclear Studies made a proposal for a joint ORNL-ORINS Summer Institute for Faculty Members from small liberal arts colleges. The primary purpose of the program would be to assist in the development of college courses, including laboratory experiments, devoted to the teaching of the principles and applications of nuclear energy. Participants would be selected from applications of teachers of courses in the physical sciences.

The first Summer Institute for Physics Teachers was conducted for eight weeks beginning June 26 and extending through August 18, 1961. The Laboratory conducted four weeks of the program, covering such subjects as quantum mechanics, neutron physics, subcritical assemblies, reactors, and plasma physics. Twenty participants completed the program and received certificates of completion.

TRAINING PROGRAM FOR REACTOR SAFEGUARD SPECIALISTS

In 1961 the Division of Personnel and the Division of Operational Safety of the AEC decided to establish a training program to help qualify more personnel for participation in their reactor safety inspection program. Since the Reactor School had a well-established program in reactor hazards evaluation, the Laboratory was requested to conduct a four-month training program, beginning March 5, 1962, for seven reactor safeguard specialists. The Reactor School program consisted of courses in health physics, instrumentation and controls, reactor physics, reactor hazards evaluation, reactor site evaluation, and reactor operations supervision. Although such a training program will not turn out proficient reactor safety specialists, graduates of the program can, with proper supervision or as part of inspector teams, make important contributions.

Service and Operating Divisions

SPECIAL PROJECTS AND NEW DEVELOPMENTS

Testing the Backflow Preventer

A reduced-pressure backflow preventer has been under test to determine its maximum protective effectiveness in water systems where radioactive contamination could occur. If such a device can be approved for installation, the Laboratory could improve its water distribution systems at a considerable saving. The behavior of the device was examined under simulated water-hammer, low-pressure fluctuations, ionic diffusion, and back-siphonage conditions.

The model investigated was tested and approved by the Research Foundation for Cross-Connection Control, University of Southern California, as being safe for installation in water systems for the prevention of backflow of sewage and industrial fluids or waste to a degree that significantly reduces the hazard to public health through chemical poisoning or the spread of disease.

A solution of manganese and potassium was placed in the discharge zone, and the degree of leakage, if any, is being determined by a neutron-activation method of analysis that has a detectable sensitivity of one part per billion.

Favorable results have been indicated to date, with the transfer of contaminants limited to not more than a few parts per billion. Further tests will define more precisely the protection against cross-contamination provided by this type valve.

Improvement to Waste Burials and Records

Substitution of auger holes (30 inches in diameter and 14 feet deep) for normal trench space for higher radioactivity levels (2 to 15 roentgens) of solid waste markedly reduced the probability of personnel exposure normally associated with operational duties at the Burial Ground. In effect, the radiation is immediately confined to a well-defined column as the waste is dumped from the shielded carrier into the hole. Another advantage of this type of confinement is economy of usable space available for burials. The holes are set in otherwise wasted areas, and the amount of earth required for adequate shielding is reduced by a factor of 6 or more. Thus an additional volume of 75,000 to 100,000 cubic feet per year is made available for solid waste burial.

The Burial Log (kept by the foremen) was replaced by an IBM record-keeping system, and a full record of waste burials is kept on IBM cards, with ensuing advantages. There are about 6,000 contaminated-waste burials each year.

Construction-Project Brochure

To better acquaint the customer with a major construction project and the planning services available to him for project planning, a brochure *(I have in mind a ... Construction Project)* was prepared and is available upon request. This brochure describes, in general terms, each phase required from the conception of a major construction project to the completed facility in full operation. The appendix contains a facility-planning check sheet to simulate the customer's planning and to aid the planning engineer in the development of a preliminary planning report on the proposed facility. The report and completed check sheet issued to the

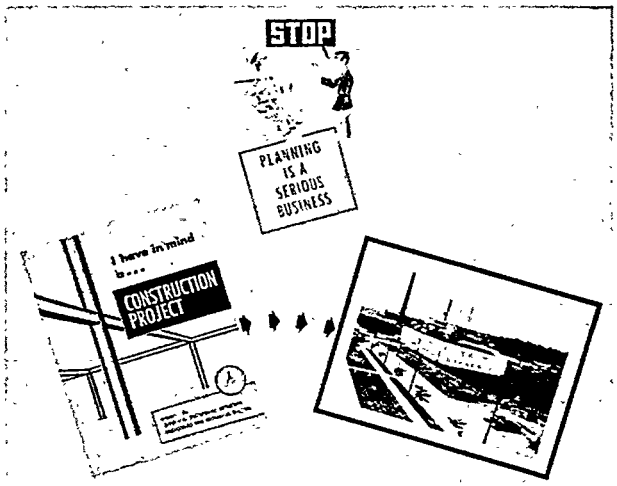

Construction-project brochure for helping the "customer" to save time and money.

requester upon completion are used by the program engineer during the conceptual-design phase.

Programmed Maintenance

In recognition of the growing complexity of the Laboratory's facilities and with the increasing number of systems and pieces of equipment in use, the Engineering and Mechanical Division has initiated the use of the IBM 7090 computer for scheduling repetitive maintenance activities.

During the last half of FY 1962, 500 pieces of equipment in the Isotopes and the Metals and Ceamics Divisions were inventoried for an analysis of maintenance requirements and service frequencies in order to establish the program. Service in accordance with established schedules was initiated, and weekly IBM Work-Request Schedule Cards will be in effect early in FY 1963.

The program is designed to relieve the operating, research, and service personnel of the need for personal tickler-file systems and to ensure consistency in the organization and administration of the wide range of repetitive maintenance functions that the Engineering and Mechanical Division performs. It has been estimated that there are 10,000 pieces of equipment at the Laboratory that require periodic maintenance and inspection.

Critical-Path Scheduling

A selected group has been trained in the use of the IBM 7090 computer in preparing schedules for major projects by the critical-path method (CPM). The CPM (see arrow diagram) is now being used in developing schedules for the Transuranium Processing Facility Project, the Curium Production Project, and the Molten-Salt Reactor Experiment. Work is expected to start soon on the Pebble-Bed Reactor Project.

Standard procedures are being developed for use of the CPM in controlling major projects. The Engineering and Mechanical Division will eventually be able to furnish complete critical-path scheduling service for any organization needing such assistance.

New Concepts and Methods in Design of Research Equipment

Orbital Shear. – The orbital shear device was designed for the remote removal of end caps from stainless-steel-jacketed spent fuel rods during mechanical dismantling operations. To shear through the jacket, a fuel rod is placed through aligned holes in two adjacent shearing plates. Hydraulic pressure offsets the plates and causes the hole edges to shear through the jacket at diametrically opposite joints. An eccentric motion imparted to the plates causes the shearing edges to move around the fuel rod, resulting in complete severance of the stainless steel jacket.

Remote Positioner. – A new design concept has been developed for accurately positioning a remote traversing device at predetermined locations by mechanical means (see photograph). Random selection of stop positions is possible, but the locating method eliminates all moving parts not accessible for maintenance. The principle is applied to the proposed intercell transfer conveyor at the Transuranium Facility.

Gamma-Ray Camera. – A lead-shielded pinhole camera was developed to locate unknown sources

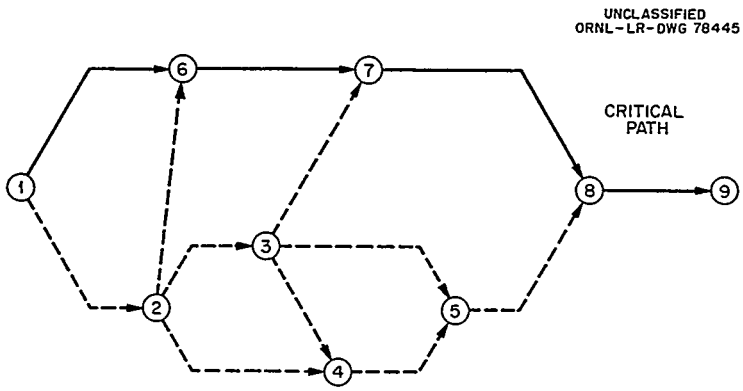

Typical arrow diagram.

78446

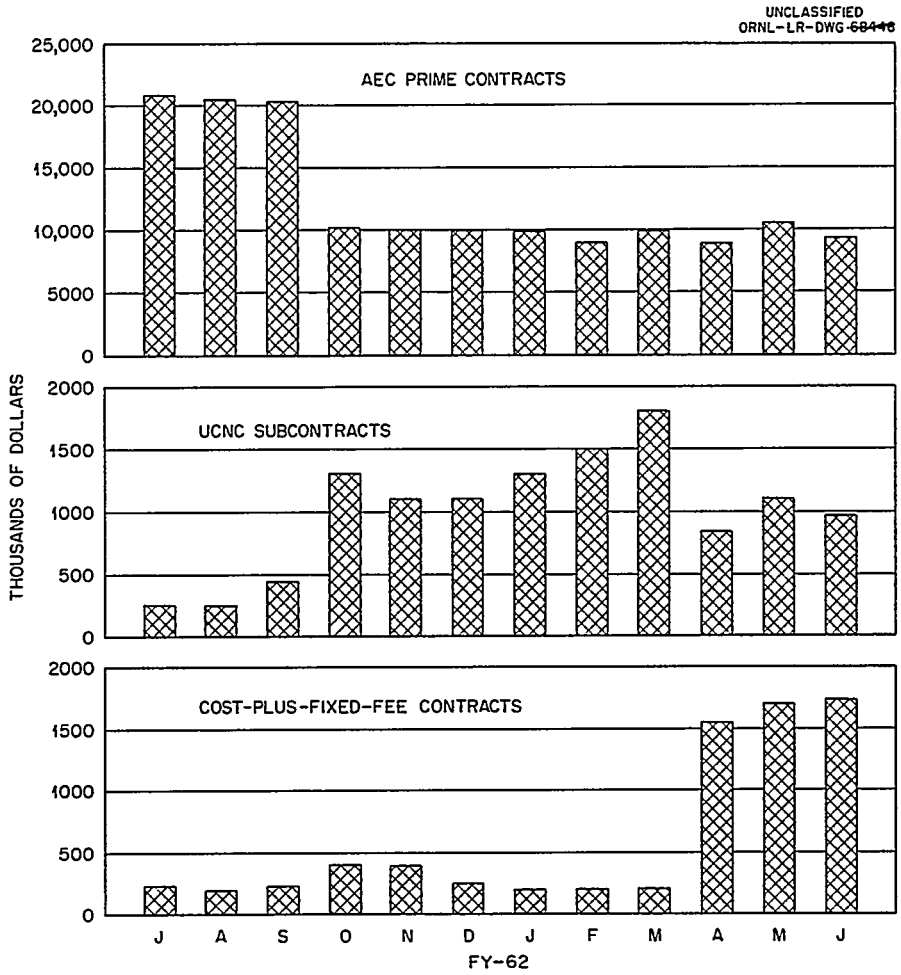

Total value of construction contracts in progress at ORNL.

of gamma radiation (see photograph). From a single setup, photographs are made on ordinary light-sensitive film and on x-ray film simultaneously. Developed negatives may then be superimposed to accurately locate sources of intense radiation.

The camera will provide 1.5 inches of lead shielding for the laminar-rolled film. Film advance and shutter operation may be automatically controlled from a remote location. This will enable the user to take several pictures from one setup without exposure to radiation. Mounting on a remotely operated stand will further increase the versatility of the camera.

Removable Alpha-Service Plugs. – Service plugs for gas, fluids, and electrical services were developed for alpha-gamma cells (see photograph). These plugs can be replaced or interchanged without breaking the alpha seal. The plugs are installed into sleeves which penetrate the cell shield wall.

The plug is made by molding 60% aluminum oxide, 36% epoxy resin, and 4% hardener. Quick-disconnect couplings are molded into each end of the plug for ease in breaking connections within the cell. The service line is molded through the plug. Double Neoprene O-rings are used to maintain an alpha seal when replacement is necessary. The plugs are designed to prevent accidental withdrawal of the plug into the operating area after initial installation. New plugs are inserted by ejecting the old plug into the cell area. Cylindrical lead gamma shields are placed in the sleeve behind the plug.

Manipulator Developments

Manipulator Boots. – A developmental program was conducted to find manipulator boot and gauntlet materials resistant to puncture, tears, and

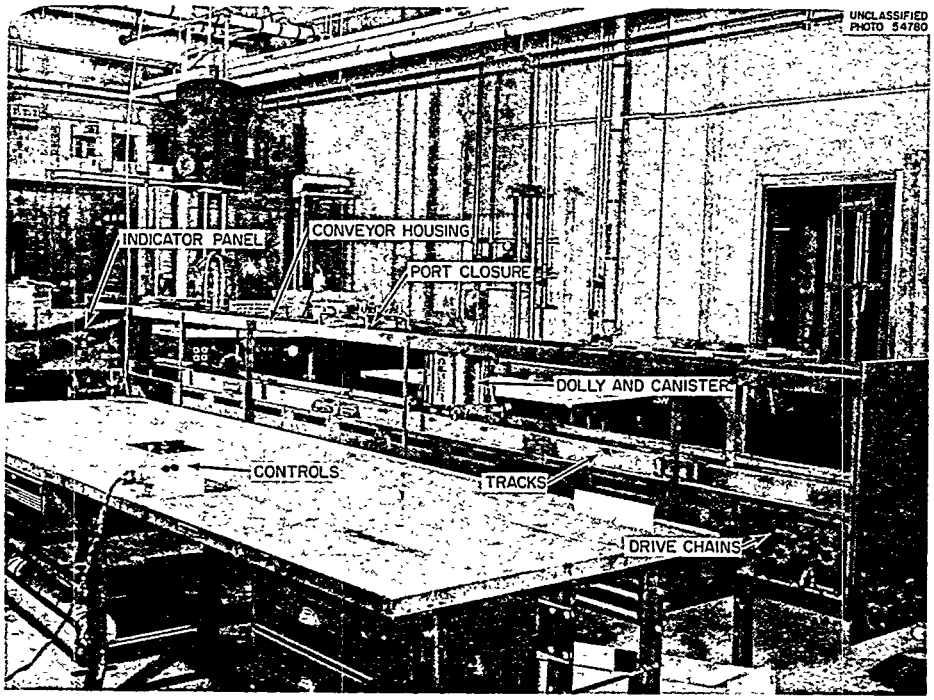

Model of intercell-transfer conveyor. An example of a new design concept for accurately positioning a remote traversing device.

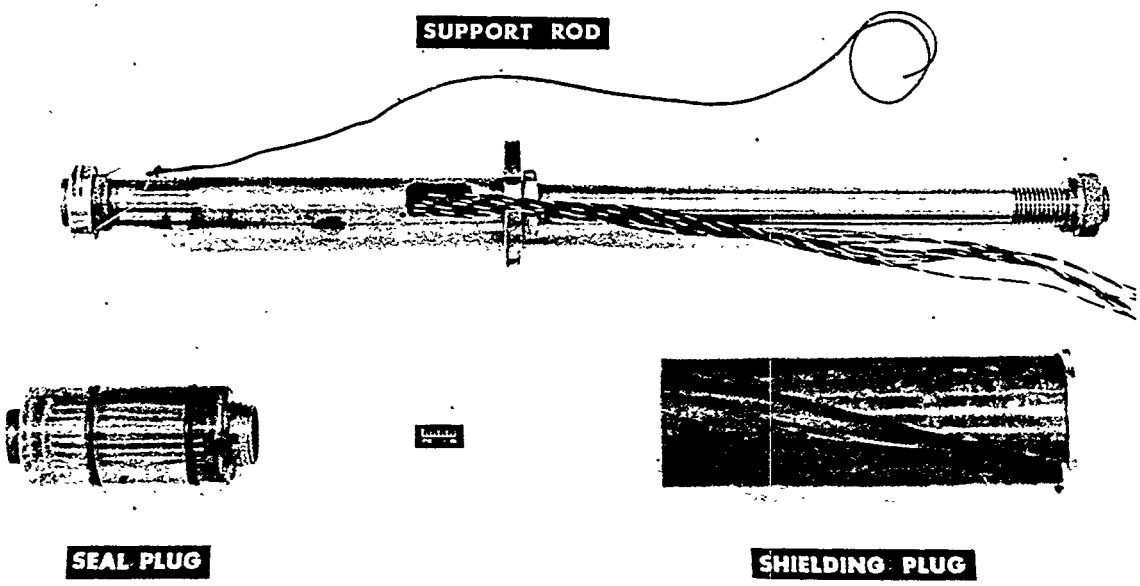

TYPICAL SERVICE PLUG ASSEMBLY

Removable alpha-service plugs.

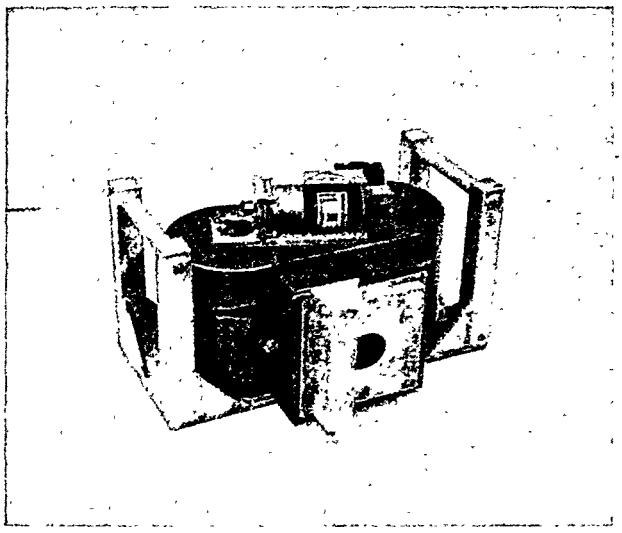

Gamma-ray camera.

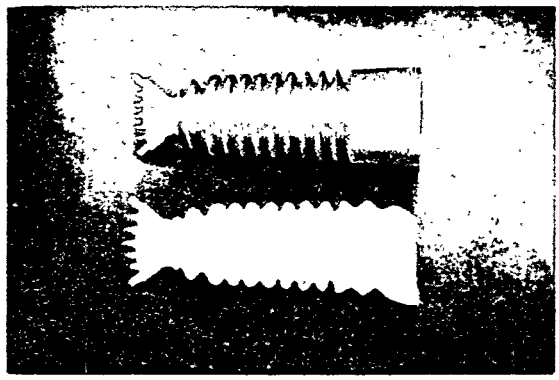

Mold and boot.

chemical and radiation exposure. Presently, the upper boot section is being made from 6-ounce nylon-reinforced vinyl; and by experimenting with several configurations and types of seams, a reasonable life expectancy has been achieved.

Since a majority of boot failures occur in the gauntlet section, more effort was expended in this area. In addition to being relatively expensive ($64 each), the commercial Neoprene gauntlets exhibit low puncture and tear resistance and only fair radiation resistance. As a possible replacement, a molded vinyl gauntlet was first developed. Although the cost of this material ($8 each) compares favorably, it provides less puncture, tear, and chemical and radiation resistance than Neoprene.

With assistance from the Ceramics and Plastics Department of the Y-12 Development Division, a method was developed for making gauntlets from liquid urethane rubber. These gauntlets exhibit excellent puncture, tear, and radiation resistance. Tests with various chemicals, however, show this material to have very little resistance to nitric acid. Considering the fact that very few of the Laboratory's manipulators come in contact with acid except during decontamination activities, this is not a major disadvantage. Made in the Manipulator Shop at a cost of approximately $6 each, this gauntlet should afford a considerable reduction in manipulator maintenance costs (see photograph). For a further possible cost reduction, an investigation is being made into the feasibility of using urethane rubber in place of the vinyl film for the upper boot section.

Wrist-Joint Yokes. – During the past eight months, numerous breakdowns have occurred due to failure of the model 8 wrist-joint yokes. Originally, these yokes were made from type 303 stainless steel, and failure was usually that of permanent deformation. To strengthen this part, the manufacturer changed the alloy to type 17-4PH. This alloy has a yield strength approximately $4\frac{1}{2}$ times that of the type 303 and an ultimate strength $2\frac{1}{2}$ times that of the 303. While this move eliminated the failures due to bending, the number of failures increased due to fractures. The hardness of the parts was changed from Rockwell C^{-41} to Rockwell C^{-35}. Eight of the softer yokes have been in service approximately six weeks, with no failures to date.

New Concepts and Methods in Fabrication of Research Equipment

Deep-Hole Drilling. – In the past, the use of deep holes in design meant that the special drills required must be purchased at a typical cost of $100 or more; therefore an English innovation of reversing the normal flow direction of cooling oil

and chips was adopted. A milling-machine head was mounted on a long-bed engine lathe to make a deep-hole machine. The method of making inexpensive drills by mounting carbide cutting edges on the end of pipes or tubes was mastered (see photographs). The lower cost and broad-application possibility resulted in the rapid increase of such work.

Parts for the ETR Moderator Experiment were drilled 40 inches deep, with hole diameters of $\frac{1}{4}$ and $1\frac{5}{8}$ inches. For the Thermonuclear Division, a special alloy steel rod was drilled to obtain a core section $\frac{7}{8}$ inch in diameter and 40 inches long for metallurgical analysis. A current job requirement includes a $\frac{1}{4}$-inch hole 20 feet long. Another machine is being adapted to increase the drill diameter capacity to several inches.

Reactor Fuel Elements. – Refinement of the tools and technique for roll-swaging fuel plates to side plates is nearing completion for the Advanced Test Reactor (ATR) fuel elements. A double roller locks both edges of a plate into the fuel elements assembly at one pass. Roll swaging is also being considered for the High-Flux Isotope Reactor (HFIR) fuel assembly. Another assembly method tested for the HFIR required development of a simple broach to cut tiny, semicircular grooves lengthwise, near the fuel plate edge and in the mounting groove. A method of locking these in assembly by inserting a wire was successfully demonstrated. Machining time for the sharp, square, inside corners of ATR fuel frames was reduced 87% and precision was increased by the development of a corner broach and guide. (See photographs showing roll-swaging method and broach.)

Flat Surfaces and Other Optics Studies. – An unusual application for flat optical surfaces now

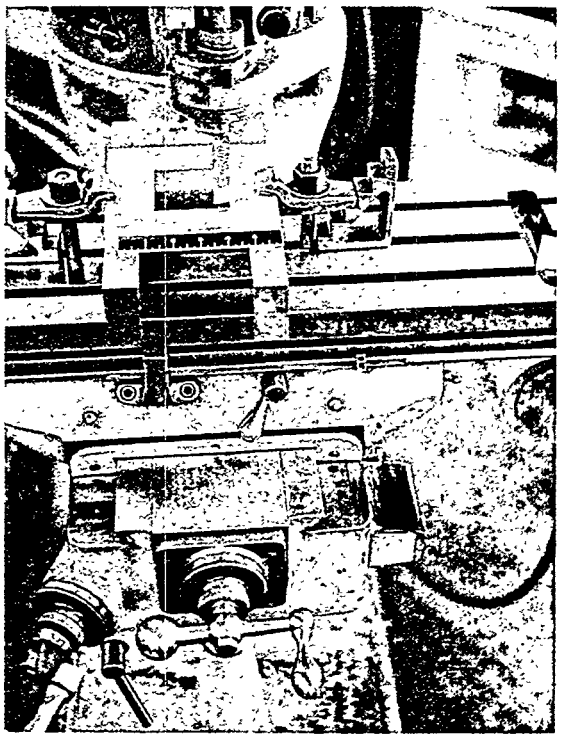

Broach for corners in fuel frames.

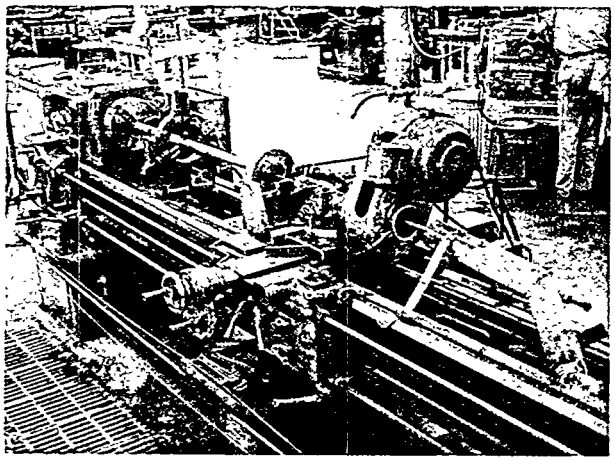

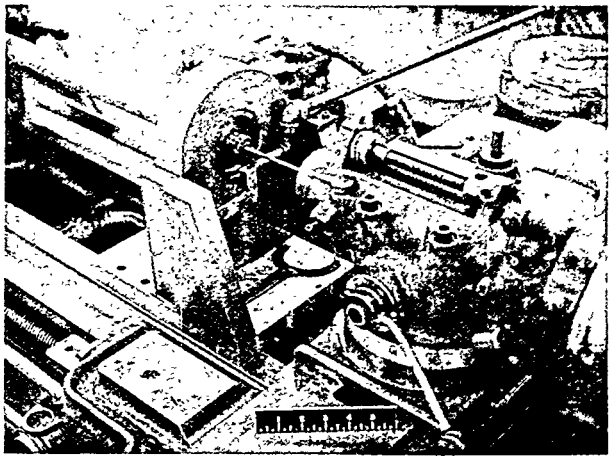

Modified long-bed engine lathe.

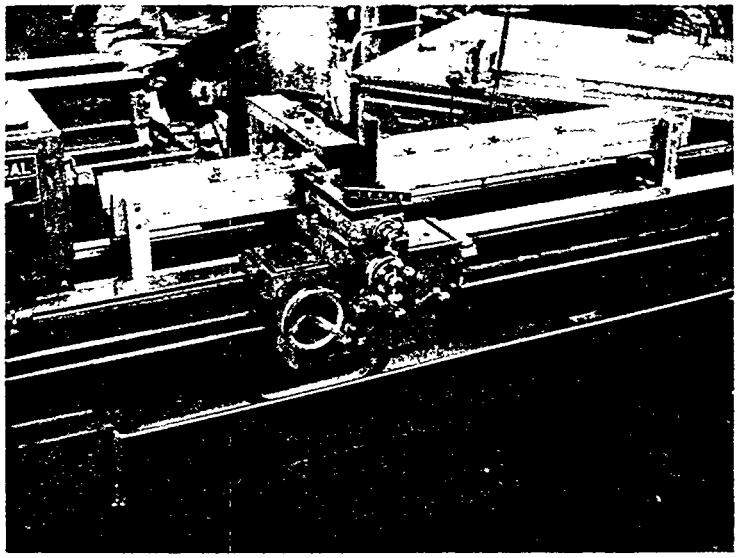

Roll-swaging method.

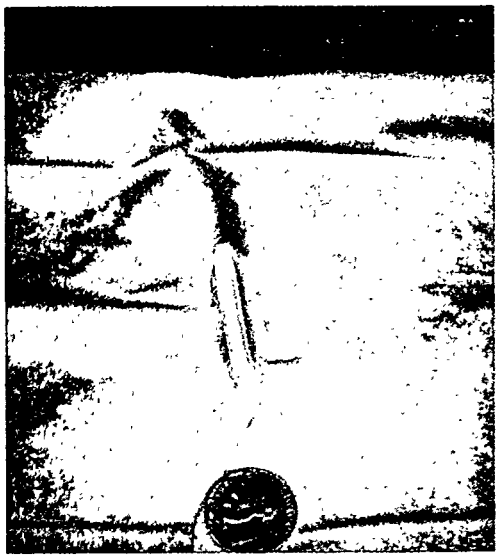

Quartz lens.

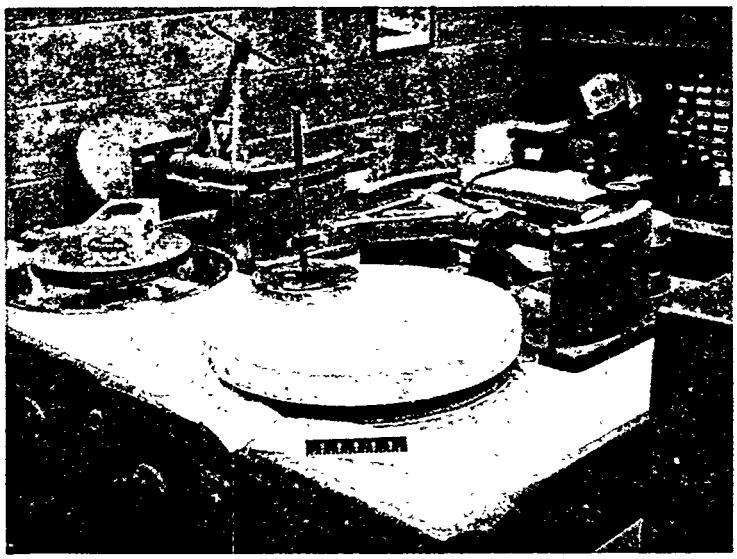

Flat-surface lapping machine.

under development is a transparent, ultracentrifuge sample cell (see photographs showing a biconcave quartz lens and a machine for lapping flat surfaces). The sample cavities and filling apertures are machined through one quartz disk. This and two other disks are ground and polished optically flat. Assembled under a 200-pound load in a titanium shell, the quartz flats must maintain a seal around the corrosive sample at 300°C and 1200 psi. An initial static leak test at lower temperature and pressure was successful.

A photographic periscope was developed and built for the Chemical Technology Division. A considerable improvement in techniques was realized in the grinding of lenses from unusual materials.

Optical alignment requirements have increased. Applications included the Oak Ridge Isochronous

Cyclotron magnet, an Oak Ridge Research Reactor experimental plug, and a fuel element inspection machine. A training seminar in the principles and use of optical alignment tooling (see photograph) multiplied the number of qualified personnel so that the method can be increasingly applied throughout the Laboratory.

New Joining Techniques. – Neutron bonding possibilities for materials of low neutron cross section with high-cross-section materials are being investigated. Teflon and aluminum with boron were chosen for the first experiment, soon to be completed.

Flame-spray application of brazing material was used successfully for furnace brazing (see photograph). Vacuum furnace techniques have been added to operations in the Engineering and Mechanical Division.

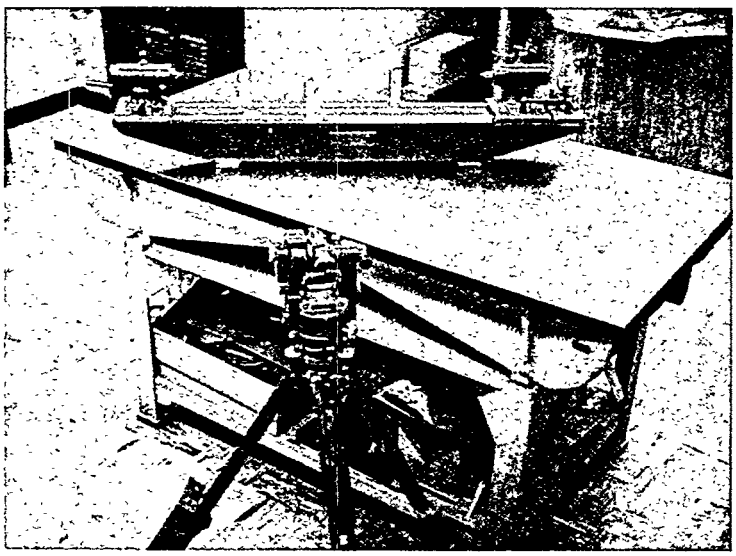

Optical-alignment tooling.

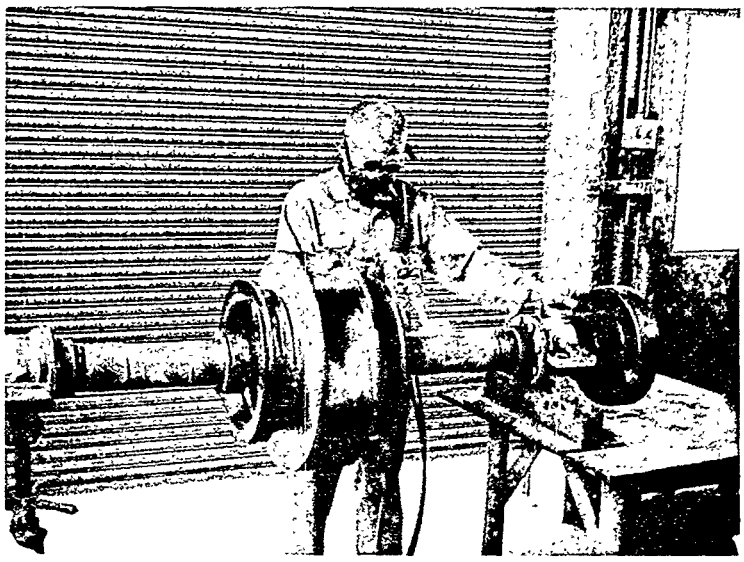

Flame-spraying of metal.

Glass-Working Techniques. – Various glasses with different grain sizes, as required for fritting and sintering or for slip-casting, have been tested. The techniques will be useful for more effective production of small precise parts, such as a semiconductor support ring.

Glass-to-metal seal requirements continued to become more complex. The largest and most unusual was the making and assembling of three Kovar seals 4 inches in diameter and bonded end-to-end within 0.005-inch alignment (see photograph). A quartz Dewar vessel with optical windows required a high degree of skill to maintain parallelism of the outer windows within 0.0003 inch. Glass-to-alumina seals are subject to random failure. Investigation of the cause and development of a more reliable technique are in progress.

Plastics, Elastomers, and Adhesives. – The large number of new materials demands continuous development. Shop methods receiving special attention are cold-casting, hot-forming, and vacuum-forming of plastics; casting and fabrication of silicones, epoxies, and vinyl resins; and the application of adhesives on these materials (see photographs). Several seal rings were molded on Viton, one of the best new materials for high-vacuum work.

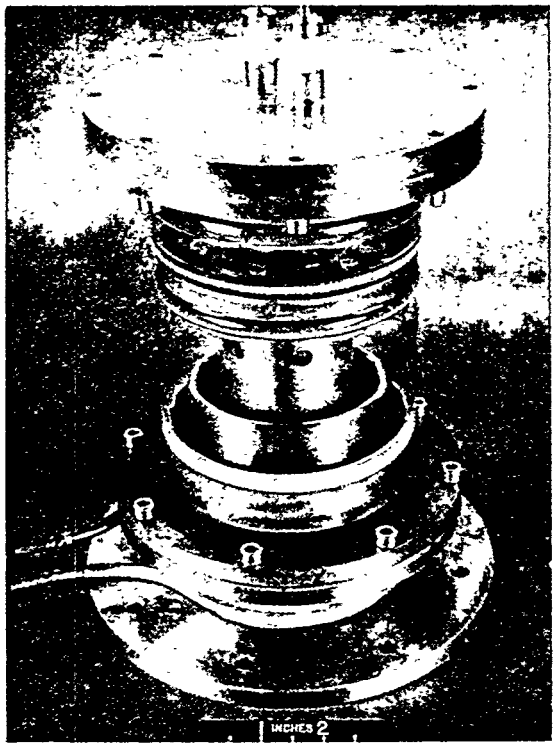

Stacked Kovar-seal assembly.

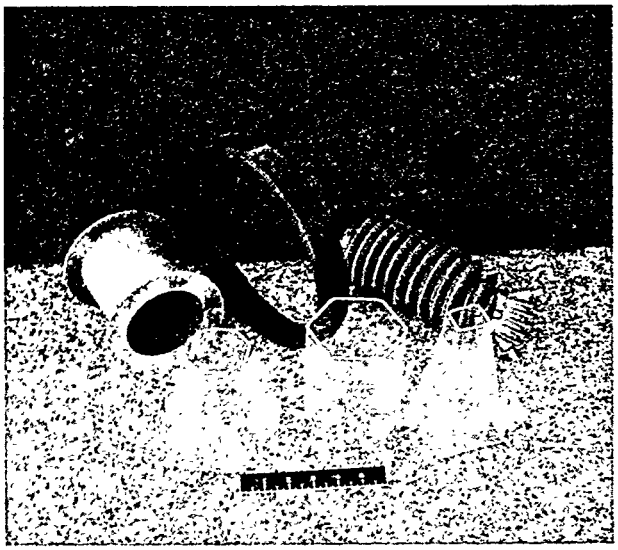

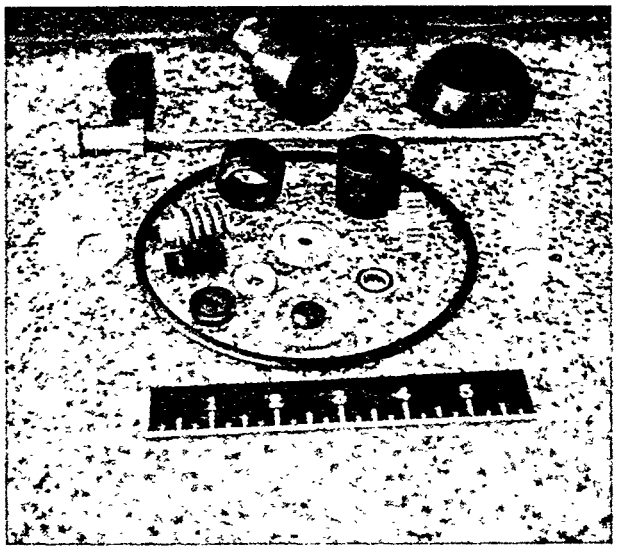

Molded and formed parts.

Inspection Engineering

The Inspection Engineering Department inspects purchased or fabricated items or systems and maintains standards of safety for pressure-containing or other special equipment within the intent of nationally recognized codes, standards, and regulations of ORNL and the AEC.

To carry out these functions in FY 1962, the Department's main efforts were directed toward inspection involving the following major Laboratory construction or assistance programs.

High-Flux Isotope Reactor
Molten-Salt Reactor Project
Fast-Burst Reactor
High-Radiation-Level Experimental Laboratory
Transuranium Laboratory
Radioisotopes Development Laboratory
NS "Savannah"
Experimental Gas-Cooled Reactor

In addition to inspections concerning the above list, periodic inspections of pressure-containing equipment, of reactor materials by special nondestructive test methods, of miscellaneous materials and equipment as requested, and of cranes and hoists have been continued. A high-efficiency particle-filter test program was developed and implemented.

Consultation services were provided to other divisions of the Laboratory and to the AEC in matters of specifications, materials, engineering, pressure-system designs, testing, inspection, and evaluation of pressure-containing integrity.

Department personnel participated actively in the development of internal and national codes, specifications, and standards for material and components in the nuclear industry.

Technical Information

PUBLICATIONS, REPORTS, AND PAPERS FOR CALENDAR YEARS 1961 AND 1962 FROM OAK RIDGE NATIONAL LABORATORY

Division	Books		Journals		Papers		Reports		Theses		Total	
	1961	1962	1961	1962	1961	1962	1961	1962	1961	1962	1961	1962
Analytical Chemistry	2	4	28	33	37	39	24	22	1		92	98
Biology	20	22	148	160	139	183	2	3		1	309	369
Chemical Technology	16	8	16	21	20	47	53	69	1	3	106	148
Chemistry	11	7	44	57	20	43	4	9		2	79	118
Directors				2								2
Electronuclear	9	4	7	20	24	37	5	5		2	45	68
Health Physics	21	6	34	26	34	47	18	24		5	107	108
Instrumentation	1	3	10	9	9	8	5	5		1	25	26
Mathematics	4	1	9	8	2	6	5	5			20	20
Metals and Ceramics	10	15	18	33	65	70	27	33	1	1	121	152
Neutron Physics	4	8	15	17	14	21	15	21		2	48	69
Physics	25	25	41	43	66	70	7	5	4	1	143	144
Reactor Chemistry	3	7	17	33	24	36	21	17			65	93
Reactor	10	7	14	20	21	43	19	57		4	64	131
Solid State	9	10	12	29	27	35	5	2	1		54	76
Thermonuclear	1	14	11	14	26	29	6	4	1		45	61
Radiation Safety								1				1
Engineering and Mechanical		1		1		2		2				6
Health				1		2						3
Inspection Engineering				1		2		2				5
Isotopes	2	4		2		9		3			2	18
Operations				1		13		14				28
Technical Information			4					1			4	1
Total	148	146	428	531	528	742	216	304	9	22	1329	1745

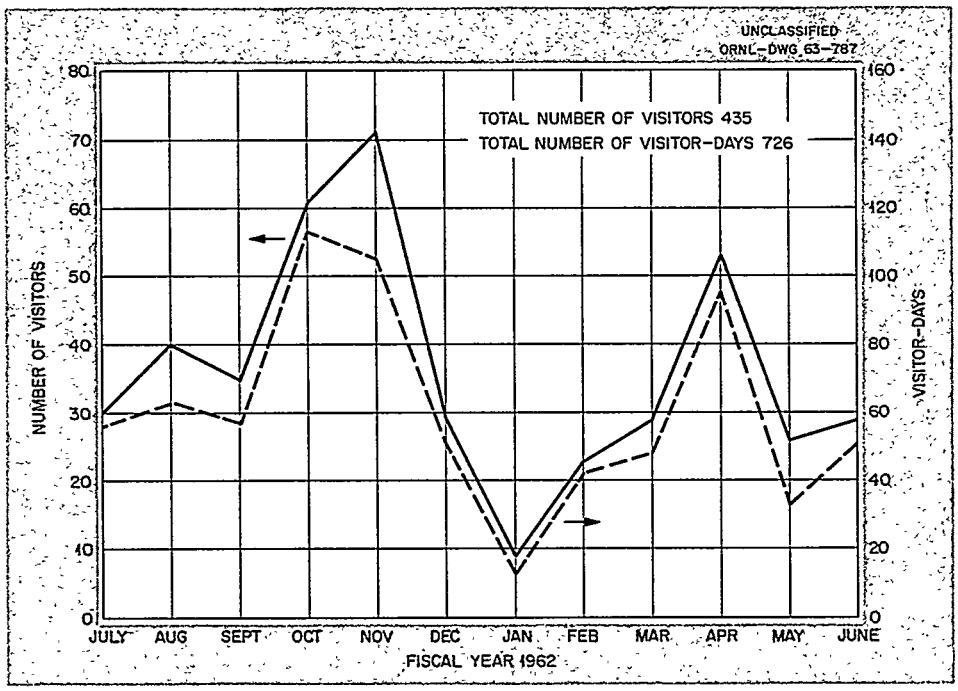

Noncitizen technical visitors coming to ORNL through the AEC in fiscal year 1962. Does not include visitors invited by ORNL research divisions.

TECHNICAL PUBLICATIONS DEPARTMENT, CALENDAR YEAR 1962

	No. of Publications	No. of Pages
Publications Edited, Typed, and Made Up		
Progress reports	29	7,732
Topical reports	14	1,978
Book chapters	34	1,301
Programs and abstracts of meetings	36	2,243
Papers, manuals, etc.	34	536
	147	13,790
Reports Processed for Cover, Distribution, and Figure Makeup		
Reports typed by Technical Publications	147	13,790
Reports typed by originating divisions		
ORNL formal reports	97	6,353
ORNL informal TM's and CF's	140	5,600
Slides		360
	384	26,103

REPRODUCTION DEPARTMENT, CALENDAR YEAR 1962

X-10 Administrative Shop		
Multilith Units Printed	6,270,600	
Xerox 914 units copied		
For Library ... 123,915		
For others 495,655		
Total Xerox units copied	619,570	
Multilith masters prepared by Xerox	15,000	
Total units printed in X-10 shop		6,905,170
K-25 Central Reproduction Services		
Multilith units printed		16,604,950
Total Units Printed for ORNL at X-10 and K-25		23,510,120

LABORATORY RECORDS DEPARTMENT, FISCAL YEAR 1962

Document Requests	
Number of requests received by Laboratory Records Department	17,576
Number of requests made by Laboratory Records Department	8,528
Total number of requests handled by Laboratory Records Department	26,104
Documents Originated at ORNL (Classified and Unclassified)	
ORNL Reports	
Numbers assigned	154
Reports issued	147
Total number of copies handled	100,008
ORNL-TM Memos (9-14-61 through 6-20-62)	
Numbers assigned	253
Memos issued	212
Total number of copies handled	15,015
CF Memos	
Numbers assigned	1,004
Memos issued	1,018
Total number of copies handled	39,058
Notebooks issued	382
Documents Received by ORNL (Classified and Unclassified)	
Documents received, including microcards (individual document identity)	14,213
Total number of copies	39,354
Documents Declassified	
Reports, memos, and notebooks	1,412
Total number of copies of reports, memos, and notebooks	5,772
Total number of copies of photographs and drawings (includes all prints, negatives, original drawings, and slides)	7,068
Number of Copies of Classified Documents Destroyed (Secret and Documented Confidential Only)	14,539
Number of Copies of Classified Documents Inventoried (Secret and Documented Confidential Reports and Memos)	70,497
Classified-Document Transfers Handled on Receipts	15,251
Drawings and Photographs Handled	
Drawing numbers issued	10,119
Photograph numbers issued	4,845
Prints and slides processed	62,466
Photographic work orders serviced	5,096
Photographs and drawings identified and retrieved	2,500
Records Center	
Volume of records in storage, ft^3	9,480
Volume of records destroyed, ft^3	1,979
Number of requests handled	2,695

SECURITY AND PATENT REVIEW

Technical papers and abstracts (for public release)	1490
Patent disclosures	64
Old documents (file clearance program)	2766
New ORNL formal reports	147
New ORNL CF's	1018
New ORNL TM's	212
KT Reports (MIT Practice School)	23
Old patent disclosures (file clearance)	~125

NUCLEAR DATA DEPARTMENT

Nuclear Data Collection	
Number of documents added to reprint file	~1200
Number of newly discovered nuclides entered in Data Collection	>30
Number of newly discovered isomers entered	~10
Number of visitors to Data Collection and requests for information	80
Trilinear Chart of Nuclides	
Fourth printing published by the Government Printing Office in September 1961	
Revision sheets:	
No. 9 (August 1961) distributed in February 1962	
No. 10 (June 1962) in process	
Status of third edition:	
Enlargement of panels (begun in 1957) completed	
Data for about 300 nuclides reviewed and revised	

ORNL LIBRARIES, FISCAL YEAR 1962

Major accomplishments of the library in FY-62 may be summarized briefly as follows:

1. The Health Physics, Metallurgy, and Ecology collections, totaling approximately 10,000 volumes, were merged during the year with the Central Research Library collection.
2. A monthly index to all Laboratory reports and memoranda was initiated, utilizing the 7090 computer and the keyword-in-context technique.
3. Manual transcribing of loan records was replaced by machine copying, enabling the Circulation section of the library to give much better service on the loan and recall of books.
4. Placing of Xerox copying machines in each of the libraries resulted in a total of approximately one-half million pages of copies from library books and journals.

	FY 61	FY 62
Volumes in library collections	98,708	101,473
Reports in library collections	177,625	190,000
Internal reports listed in key word index (half-year figure)		393
Reports received on special requests to ASTIA, NASA, etc.	557	519
Journals subscribed to by the libraries	2,289	2,377
Interlibrary loans to other libraries	558	845
Volumes borrowed from other libraries	487	619
Translations prepared at ORNL	47	44
Translations prepared under contract	42	74
Prepared translations purchased	115	138

GRAPHIC ARTS DEPARTMENT

The Graphic Arts Department prepares graphic representations of research data and engineering ideas developed at ORNL. Many types of drawings are made — cut-away, perspective, isometric, diametrics, charts, and graphs. During FY-1962, 7,874 illustrations, 90,462 photographs, and 12,120 slides were prepared. Many techniques were used — ink and pencil drawings, photographs, color renditions, and three-dimensional effects. Two brochures were completed (for the Isotopes and Biology Divisions), and more than one display was finished each month.

UNCLASSIFIED
ORNL-DWG 63-1651

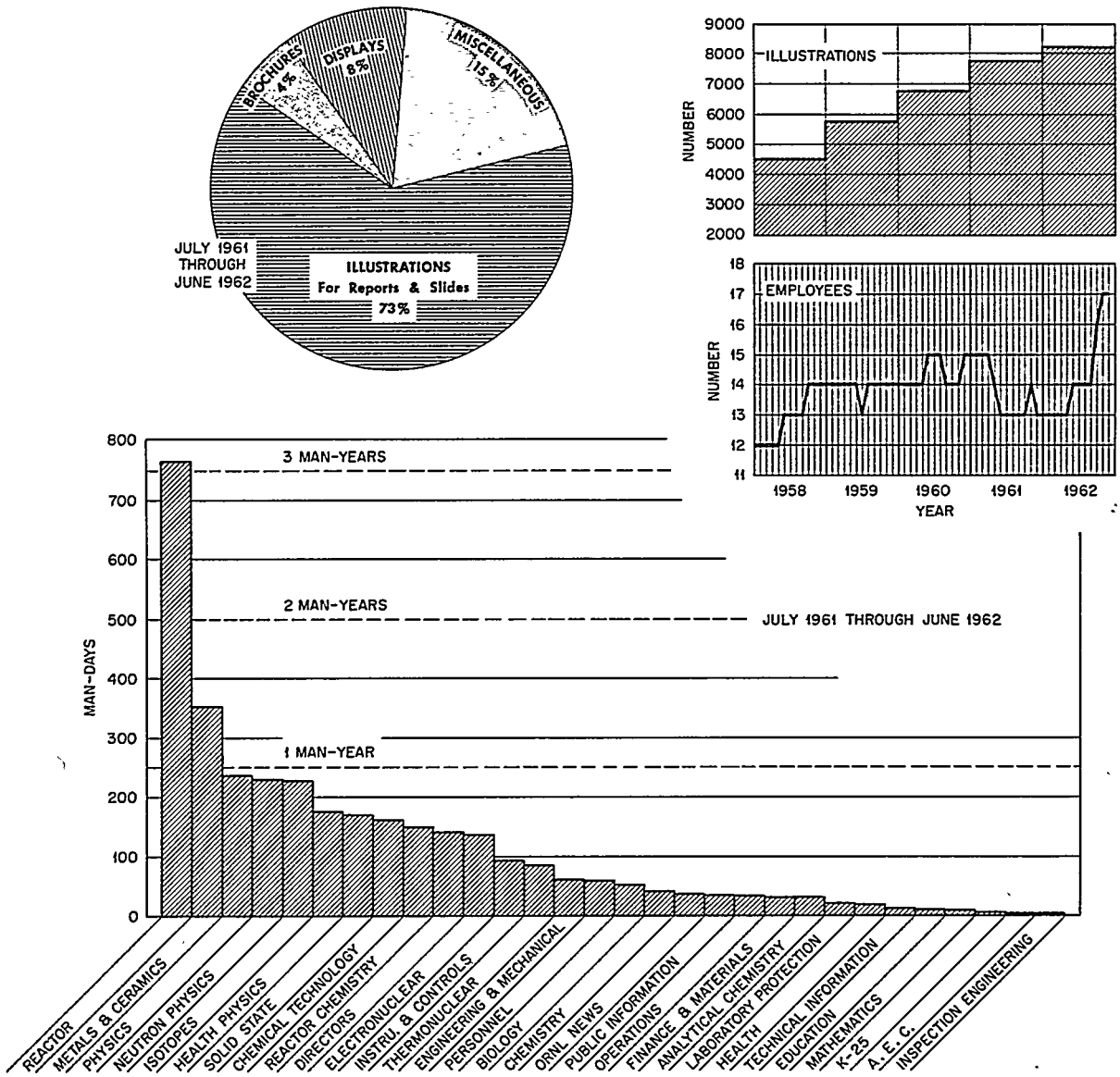

Technical illustration work of the Graphic Arts Department. *Bottom:* Distribution of technical illustration work by ORNL divisions. *Upper left:* Major categories of technical illustration services. *Upper right:* Comparison of the number of illustrations rendered and the number of employees for 1958 through 1962.

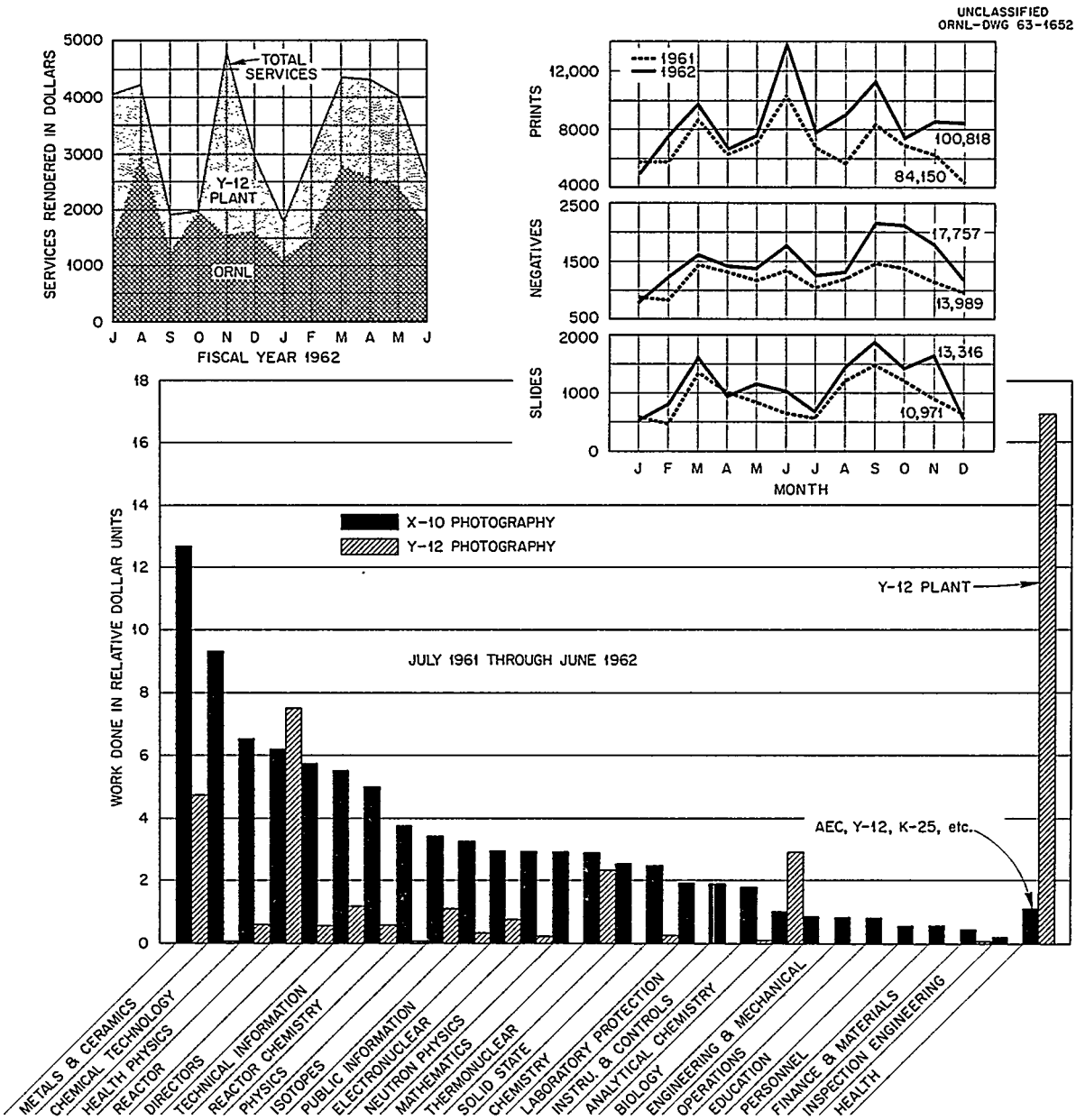

Photographic services of the Graphic Arts Department. *Bottom:* Distribution of work of the X-10 and Y-12 photographic groups by ORNL divisions. *Upper left:* Comparison of work done for Y-12 and ORNL by the Y-12 photographic group. *Upper right:* ORNL photographic production charts, showing a typical yearly production increase.

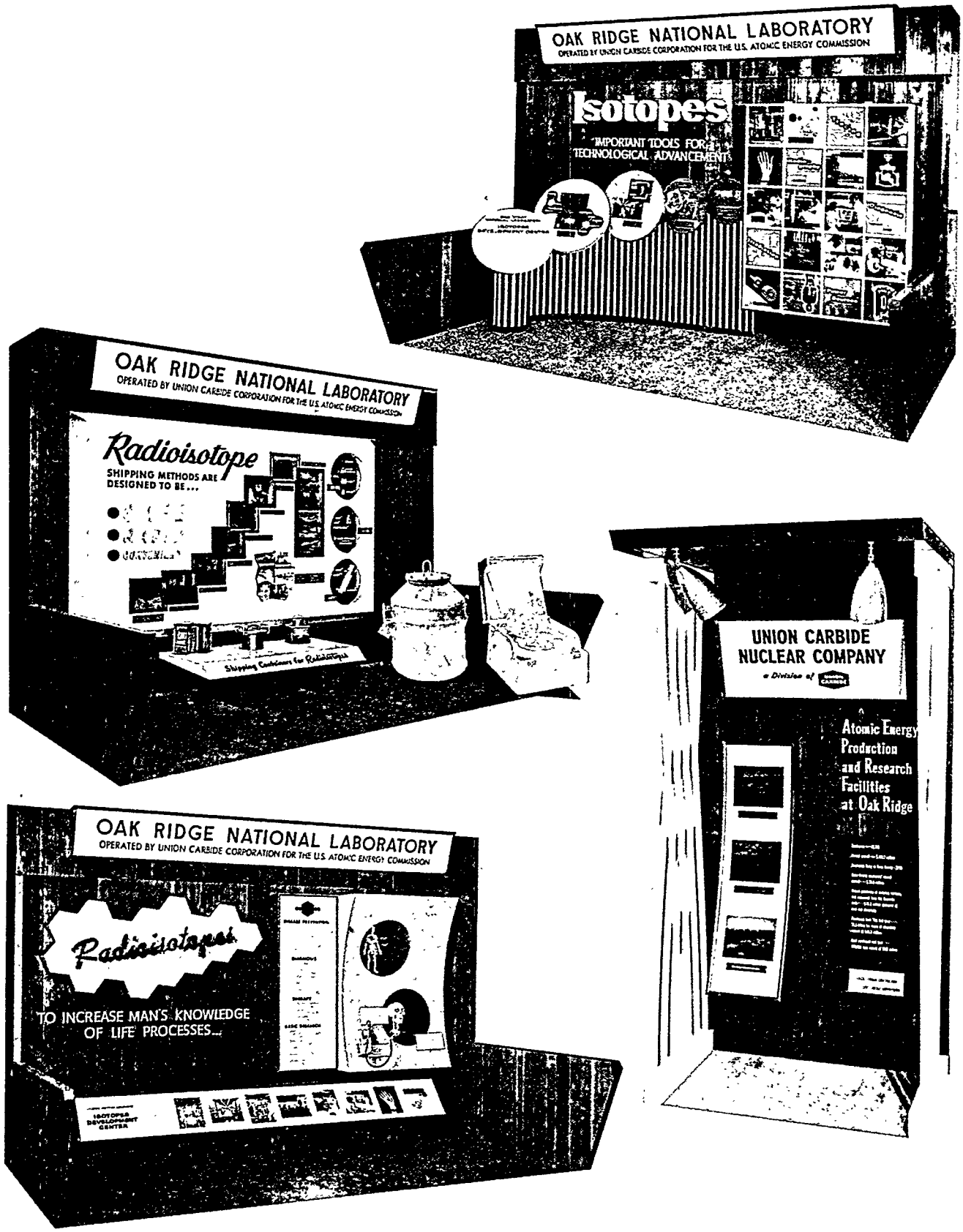

Some of the major displays completed in 1961 and 1962.

Health Services

In addition to dispensary visits for other purposes, each employee is invited about once a year (12 to 15 months) to come to the Health Division for certain basic clinical laboratory tests. The table below gives some idea of the amount of work done and the health services provided.

Selected Health Service Statistics, Calendar Year 1961

Dispensary total visits	56,869
Total visits rate per capita[a]	13.3
Percent occupational visits	31%
Complete physical examinations	3,278
Partial physical examinations	5,670
Absence frequency rate[b]	0.84
Absence severity rate[c]	4.5

[a]Based on 4275 employees.
[b]Frequency rate = (number of absences)/(number of employees) × 100.
[c]Severity rate = (number of days lost)/(number of employees) × 100.

ORNL-3350
Special

INTERNAL DISTRIBUTION

1. E. A. Bagley
2. P. S. Baker
3. L. H. Barker
4. S. E. Beall
5. D. S. Billington
6. R. E. Blanco
7. E. P. Blizard
8. A. L. Boch
9. E. G. Bohlmann
10. C. J. Borkowski
11. G. E. Boyd
12. M. A. Bredig
13. J. C. Bresee
14. R. B. Briggs
15. K. B. Brown
16. F. R. Bruce
17. G. C. Cain
18. A. D. Callihan
19. S. F. Carson
20. L. T. Corbin
21. D. D. Cowen
22. J. A. Cox
23. J. H. Crawford
24. F. L. Culler
25. J. E. Cunningham
26. A. C. Downing
27. D. E. Ferguson
28. J. L. Fowler
29. A. P. Fraas
30. J. H Frye, Jr.
31. J. H. Gillette
32. H. E. Goeller
33. A. T. Gresky
34. W. R. Grimes
35. C. S. Harrill
36. A. Hollaender
37. A. S. Householder
38. R. W. Johnson
39. W. H. Jordan
40. C. P. Keim
41. M. T. Kelley
42. B. H. Ketelle
43. E. Lamb
44. J. A. Lane
45. C. E. Larson
46. T. A. Lincoln
47. R. S. Livingston
48. L. O. Love
49. R. N. Lyon
50. H. F. McDuffie
51. R. A. McNees
52. H. G. MacPherson
53. F. C. Maienschein
54. W. D. Manly
55. A. J. Miller
56. E. C. Miller
57. K. Z. Morgan
58. M. L. Nelson
59. R. B. Parker
60. M. E. Ramsey
61. W. D. Reel
62. L. P. Riordan
63. A. F. Rupp
64. H. E. Seagren
65. E. D. Shipley
66. A. H. Snell
67. W. S. Snyder
68. E. G. Struxness
69. C. D. Susano
70. J. A. Swartout
71. E. H. Taylor
72. F. C. VonderLage
73. G. M. Watson
74. A. M. Weinberg
75. J. C. White
76. E. O. Wollan
77. R. G. Wymer
78. Gale Young
79. A. Zucker

80–82. Central Research Library
83. Reactor Division Library
84. Biology Library
85–86. ORNL – Y-12 Technical Library, Document Reference Section
87. ORNL Patent Office
88. Laboratory Records, ORNL R.C.
89–288. Laboratory Records Department